Behaviormetrics:
Quantitative Approaches to Human Behavior 5

Tadashi Imaizumi
Atsuho Nakayama
Satoru Yokoyama *Editors*

Advanced Studies in Behaviormetrics and Data Science

Essays in Honor of Akinori Okada

Springer

Behaviormetrics: Quantitative Approaches to Human Behavior

Volume 5

Series Editor

Akinori Okada, Professor Emeritus, Rikkyo University, Tokyo, Japan

This series covers in their entirety the elements of behaviormetrics, a term that encompasses all quantitative approaches of research to disclose and understand human behavior in the broadest sense. The term includes the concept, theory, model, algorithm, method, and application of quantitative approaches from theoretical or conceptual studies to empirical or practical application studies to comprehend human behavior. The Behaviormetrics series deals with a wide range of topics of data analysis and of developing new models, algorithms, and methods to analyze these data.

The characteristics featured in the series have four aspects. The first is the variety of the methods utilized in data analysis and a newly developed method that includes not only standard or general statistical methods or psychometric methods traditionally used in data analysis, but also includes cluster analysis, multidimensional scaling, machine learning, corresponding analysis, biplot, network analysis and graph theory, conjoint measurement, biclustering, visualization, and data and web mining. The second aspect is the variety of types of data including ranking, categorical, preference, functional, angle, contextual, nominal, multi-mode multi-way, contextual, continuous, discrete, high-dimensional, and sparse data. The third comprises the varied procedures by which the data are collected: by survey, experiment, sensor devices, and purchase records, and other means. The fourth aspect of the Behaviormetrics series is the diversity of fields from which the data are derived, including marketing and consumer behavior, sociology, psychology, education, archaeology, medicine, economics, political and policy science, cognitive science, public administration, pharmacy, engineering, urban planning, agriculture and forestry science, and brain science.

In essence, the purpose of this series is to describe the new horizons opening up in behaviormetrics—approaches to understanding and disclosing human behaviors both in the analyses of diverse data by a wide range of methods and in the development of new methods to analyze these data.

More information about this series at http://www.springer.com/series/16001

Tadashi Imaizumi · Atsuho Nakayama ·
Satoru Yokoyama
Editors

Advanced Studies in Behaviormetrics and Data Science

Essays in Honor of Akinori Okada

Springer

Editors
Tadashi Imaizumi
School of Management
and Information Sciences
Tama University
Tokyo, Japan

Satoru Yokoyama
School of Business
Aoyama Gakuin University
Tokyo, Japan

Atsuho Nakayama
Graduate School of Management
Tokyo Metropolitan University
Tokyo, Japan

ISSN 2524-4027 ISSN 2524-4035 (electronic)
Behaviormetrics: Quantitative Approaches to Human Behavior
ISBN 978-981-15-2699-2 ISBN 978-981-15-2700-5 (eBook)
https://doi.org/10.1007/978-981-15-2700-5

This Springer imprint is published by the registered company Springer Nature Singapore Pte Ltd.
The registered company address is: 152 Beach Road, #21-01/04 Gateway East, Singapore 189721, Singapore

Foreword

I am very pleased to write a foreword for the Festschrift of Prof. Akinori Okada. He was born in Tokyo in September 1943, and all his academic life has been active. Now he is 77-years old; it is the age of celebration, according to the traditional Japanese age system.

Professor Okada obtained a job at Chiba University in 1971 and moved to Rikkyo University in the next year to be a Senior Lecturer and then Associate Professor of statistics and operations research. He received his Ph.D. in Engineering from Keio University in 1979. He spent 35 years in Rikkyo University until he further moved to Tama University in 2007, where his best collaborator Prof. Tadashi Imaizumi serves.

Professor Okada has made significant contributions to the fields of multidimensional scaling and cluster analysis, especially the analysis of asymmetric relationships. His works on these fields are so influential that he edited more than 15 books in Japanese and English on multidimensional scaling, cluster analysis, statistics, linear algebra, operations research, data analysis, and marketing science. The book entitled 'Operations Research: Introduction to Management Science' [Operêshonzu Risâchi–Keieikagaku Nyumon–] written with Dr. Ken-ichi Goto, published in 1987, has been used as a standard textbook of operations research for more than 30 years in courses in the departments of social science schools in Japan.

I share a good memory with Prof. Okada; we hosted together the first International Meeting of the Psychometric Society (IMPS) in Osaka in Japan in 2001. Prior to that, Prof. Okada and the late Prof. Haruo Yanai participated in the council meeting of the Psychometric Society in the U.S. One of the main purposes for the visit was to propose we should host an annual meeting in Asia, particularly in Japan for the first time. As a result, the meeting was successfully held in July 2001, where Prof. Okada was the Vice President of the executive committee and I served as the chair of the local organizing committee. The meeting was a great success; more than 400 participants gathered and accordingly, the financial results were in a sound condition. The T-shirts with the IMPS logo shown by Prof. Heiser in the photo below was a gift for Prof. Jacqueline Meulman, as a small token of the members' appreciation; although she had seriously prepared for the meeting together with us, her sickness prevented her from attending the meeting in the end.

Photo 1 Professors Akinori Okada, Haruo Yanai, Willem Heiser, Kazuo Shigemasu and Yutaka Kano from the flush left. Photo taken on July 19, 2001, just after the IMPS2001

Professor Okada is the series editor in Springer named Behaviormetrics: Quantitative Approaches to Human Behavior. He launched the joint meeting of the German Classification Society and the Japanese Classification Society in corporation with German colleagues, and also organized the joint meeting with the Classification and Data Analysis Group of the Italian Statistical Society and the Japanese Classification Society in corporation with Italian colleagues. In addition to this, Prof. Okada served as the President of the International Federation of Classification Societies (2016–2017).

He led the Behaviormetric Society as the President (2012–2015), and has still been a member of the board of directors of the Society; his achievements have proven that he is one of the distinguished leaders of the behaviormetrics and classification societies.

In Japan, they say we should make a life plan for up to hundred years now, since the average life span continues to grow. Professor Okada still has a quarter of a century more of his life. We hope that he can continue to enjoy his life and remain active as an academician.

Osaka, Japan Yutaka Kano
November 2019

Preface

The year 2019 is the 40th anniversary of the doctorate degree of Akinori Okada, who is a Professor Emeritus at Rikkyo University, Japan. We are delighted to work as Editors for this 'Festschrift' of him. He received his Ph.D. in Engineering from Keio University, Tokyo in 1979. During the course of his long and distinguished career of more than 45 years, he has made significant research contributions to theory and applications in areas such as multidimensional scaling, cluster analysis, psychometrics, data analysis, operations research, data science, marketing research, consumer behavior, psychological, and social human relationships. Today these research contributions are essential constituents of the realm of 'behaviormetrics'. Akinori Okada has played an important role as a leader in developing behaviormetrics. Especially his research contribution toward the development and application of asymmetric multidimensional scaling and cluster analysis are significant. His work has been published in journals such as Advances in Data Analysis and Classification, Behaviormetrika, Journal of Classification, Psychonomic Science, Journal of Applied Psychology, Organizational Behavior and Human Performance, Japanese Journal of Behaviormetrics [Kôdo Keiryogaku], Japanese Psychological Review [Shinrigaku Hyôron], Sociological Theory and Methods [Riron to Hôhô], Communications of the Operations Research [Operêshionzu Risâchi], Japanese Journal of Applied Statistics [Ôyotôkeigaku], Japanese Review of Clinical Ophthalmology [Ganka Rinsho Ihô], The Journal of the Institute of Electronics and Communication Engineers of Japan [Denshi Jyôhô Tsushin Gakkaishi Shi] among other things, as well as in numerous refereed proceedings volumes.

He also played an important role as a scientific leader in behaviormetrics, and especially contributed his effort to introduce the quantitative concept in social sciences. He is the series editor of 'Behaviormetrics: Quantitative Approaches to Human Behavior', published by Springer, which covers all aspects of Behaviormetrics; theory, concept, method, and application in order to disclose and understand human behavior. He is one of the founding managing editors of the 'Advances in Data Analysis and Classification'. He also is the founding editor of the 'Bulletin of Data Analysis of Japanese Classification Society' or 'Dêta Bunseki no Riron to Ôyo' in Japanese. Akinori Okada was the President of the

International Federation of Classification Societies (2016–2017), the Behaviormetric Society (2012–2015), Japanese Classification Society (2005–2009), and chaired the program committee of numerous international conferences. He is a Research Fellow of the Operations Research Society of Japan. He has been an outside director of SHL-Japan Limited since 2002 as a statistician. Akinori Okada is a great mentor of many students. Three of his former students decided to honor him for his outstanding achievements in behaviormetrics and data science by inviting his colleagues and friends to contribute articles for this 'Festschrift', who sent us articles of high quality to us. Two of us wrote an article each as well. The present 'Festschrift' focuses on the latest developments in behaviormetrics and data science, and covers both theoretical aspect and applications to a wide range of areas including psychology, marketing science, sociology, social survey, operations research, etc. The contributions to this volume are intended for researchers and practitioners who are interested in the latest developments and applications in these fields. The present volume consists of two parts which express two aspects of the research of behavirometrics and data science by Akinori Okada: a theoretically-oriented part and an application-oriented part. Contributions are ordered alphabetically based on the corresponding authors' names within each of these two parts. We have to confess that there are several anomalies in the order of contributions due to the inattention of the first editor. We would like to express our deepest appreciation to authors for their contributions to the volume and cooperation while we edited the volume. We want to show our heartiest gratitude to Mr. Reginald Williams and Ms. Yasuko Hase for thoughtfully helping us in English for the e-mail of inviting authors and of the reminder to the authors. We cordially appreciate Mr. Yutaka Hirachi and Ms. Sridevi Purushothaman at Springer Nature for their assistance for publishing the present volume.

Tokyo, Japan
March 2020

Tadashi Imaizumi
Atsuho Nakayama
Satoru Yokoyama

Contents

Contributors

Daniel Baier Chair of Marketing and Innovation, Universitaetsstrasse 30, University of Bayreuth, Bayreuth, Germany

Fabian Ball Information Services and Electronic Markets, Institute of Information Systems and Marketing, Karlsruhe Institute of Technology (KIT), Karlsruhe, Germany

Eric J. Beh University of Newcastle, Callaghan, NSW, Australia

Hans-Hermann Bock Institute of Statistics, RWTH Aachen University, Aachen, Germany

Giuseppe Bove Dipartimento di Scienze della Formazione, Università degli Studi Roma Tre, Rome, Italy

Frank M. T. A. Busing Faculty of Social and Behavioral Sciences, Leiden University, Leiden, The Netherlands

Carlo Cavicchia University of Rome La Sapienza, Rome, Italy

Jeffry Chavarría-Molina School of Mathematics, Costa Rica Institute of Technology, Cartago, Costa Rica

Naohito Chino Aichi Gakuin University, Nagoya, Japan

Reinhold Decker Department of Business Administration and Economics, Bielefeld University, Bielefeld, Germany

Mark de Rooij Department of Methodology and Statistics, Institute of Psychology, Leiden University, Leiden, The Netherlands

Juan José Fallas-Monge School of Mathematics, Costa Rica Institute of Technology, Cartago, Costa Rica

Michael P. B. Gallaugher Department of Mathematics and Statistics, McMaster University, Hamilton, Canada

Wolfgang Gaul Karlsruhe Institute of Technology (KIT), Karlsruhe, Germany

Andreas Geyer-Schulz Information Services and Electronic Markets, Institute of Information Systems and Marketing, Karlsruhe Institute of Technology (KIT), Karlsruhe, Germany

P. J. F. Groenen Econometric Institute, Erasmus University, Rotterdam, The Netherlands

Willem J. Heiser Faculty of Social and Behavioral Sciences and Mathematical Institute, Leiden University, Leiden, The Netherlands

Christian Hennig Dipartimento di Scienze Statistiche "Paolo Fortunati", Bologna, Italy

Tadashi Imaizumi Tama University, Tama-shi, Tokyo, Japan

Alfonso Iodice D'Enza Department of Political Sciences, Università degli Studi di Napoli Federico II, Naples, Italy

Noriko Iwai JGSS Research Center, Osaka University of Commerce, Higashi-Osaka, Japan

Manabu Iwasaki Yokohama City University, Yokohama, Japan

Kunihiro Kimura Tohoku University, Sendai, Japan

Pieter M. Kroonenberg Faculty of Social and Behavioural Sciences, Leiden University, Leiden, The Netherlands;
The Three-Mode Company, Leiden, The Netherlands

Innar Liiv Tallinn University of Technology, Tallinn, Estonia

Michael Löffler Dr. Ing. h.c. F. Porsche AG, Stuttgart, Germany

Paul D. McNicholas Department of Mathematics and Statistics, McMaster University, Hamilton, Canada

Jacqueline J. Meulman Mathematical Institute, Leiden University, Leiden, The Netherlands;
Department of Statistics, Stanford University, Stanford, CA, USA

Hisao Miyano Chiba University, Chiba, Japan

Takashi Murakami Chukyo University, Nagoya, Japan

Miki Nakai Department of Social Sciences, College of Social Sciences, Ritsumeikan University, Kyoto, Japan

Keiko Nakao Tokyo Metropolitan University, Tokyo, Japan

Shizuhiko Nishisato University of Toronto, Toronto, Canada

Fulvia Pennoni Department of Statistics and Quantitative Methods, University of Milano-Bicocca, Milan, Italy

Alexandra Rese Chair of Marketing and Innovation, Universitaetsstrasse 30, University of Bayreuth, Bayreuth, Germany

Alessio Serafini Dipartimento di Economia, Università degli Studi di Perugia, Perugia, Italy

Javier Trejos-Zelaya CIMPA–School of Mathematics, University of Costa Rica, San José, Costa Rica

M. Van de Velden Econometric Institute, Erasmus University, Rotterdam, The Netherlands

Donatella Vicari Dipartimento di Scienze Statistiche, Sapienza Università di Roma, Rome, Italy

Maurizio Vichi University of Rome La Sapienza, Rome, Italy

Leo Vohandu Tallinn University of Technology, Tallinn, Estonia

Christoph Winkler Karlsruhe Institute of Technology (KIT), Karlsruhe, Germany

Satoru Yokoyama Department of Marketing, School of Business, Aoyama Gakuin University, Tokyo, Japan

Ryozo Yoshino Graduate School of Culture and Information Science, Doshisha University, Kyoto, Japan

Satomi Yoshino JGSS Research Center, Osaka University of Commerce, Higashi-Osaka, Japan

Giorgia Zaccaria University of Rome La Sapienza, Rome, Italy

Part I
Theoretically-Oriened

Co-Clustering for Object by Variable Data Matrices

Hans-Hermann Bock

Abstract Co-clustering means the simultaneous clustering of the rows and columns of a two-dimensional data table (biclustering, two-way clustering), in contrast to separately clustering the rows and the columns. Practical applications may be met, e.g., in economics, social sciences, bioinformatics, etc. Various co-clustering models, criteria, and algorithms have been proposed that differ with respect to the considered data types (real-valued, integers, binary data, contingency tables), and also the meaning of rows and columns (samples, variables, factors, time,...). This paper concentrates on the case where rows correspond to (independent) samples or objects, and columns to (typically dependent) variables. We emphasize that here, in general, different similarity or homogeneity concepts must be used for rows and columns. We propose two probabilistic co-clustering approaches: a situation where clusters of objects and of variables refer to two different distribution parameters, and a situation where clusters of 'highly correlated' variables (by regression to a latent class-specific factor) are crossed with object clusters that are distinguished by additive effects only. We emphasize here the classical 'classification approach', where maximum likelihood criteria are optimized by generalized alternating k-means type algorithms.

1 Co-Clustering

Clustering methods are well-known tools for analyzing and structuring data, intensively investigated in statistics, machine learning and data science, and broadly used in many application domains such as as market and consumer research, psychology and social sciences, microbiology and bioinformatics. The basic problem consists in grouping a given set of objects into homogeneous classes (clusters) on the basis of empirical data that allow to quantify the 'similarity' or 'dissimilarity' of the objects and so to define the homogeneity within, or the separation between, the classes. In the most simple case there is an $n \times p$ data matrix $X = (x_{ij})$, where values x_{ij}

H.-H. Bock (✉)
Institute of Statistics, RWTH Aachen University, Aachen, Germany
e-mail: bock@stochastik.rwth-aachen.de

T. Imaizumi et al. (eds.), *Advanced Studies in Behaviormetrics and Data Science*,
Behaviormetrics: Quantitative Approaches to Human Behavior 5,
https://doi.org/10.1007/978-981-15-2700-5_1

are recorded for n objects and p variables and we look for an appropriate partition $\mathcal{A} = (A_1, ..., A_k)$ of the set of objects $\mathcal{O} = \{1, ..., n\}$ (the rows of X) with classes $A_1, ..., A_k$ such that similar row vectors (objects) are united in the same class while row vectors from different classes are hopefully quite dissimilar. Depending on the context, the detected or constructed clusters will be interpreted as (personality) types, consumer groups, music styles, families of plants, gene clusters, etc. Since the early 1960s when clustering methods came up, a large variety of clustering models and clustering algorithms have been developed for different data types, see, e.g., Bock [7, 9], Jain and Dubes [26], Miyamoto, Ichihashi, and Honda [32], McLachlan and Krishnan [31], Basu, Davidson, and Wagstaff [5], Aggarwal and Reddy [1], and Hennig, Meila, Murtagh, and Rocci [25].

Co-clustering (biclustering, two-way clustering, block clustering) means the simultaneous (i.e., not separate) clustering of the rows and columns of a data matrix by determining an appropriate partition $\mathcal{A} = (A_1, ..., A_k)$ of the rows *together* with an appropriate partition $\mathcal{B} = (B_1, ..., B_\ell)$ of the set of columns $\mathcal{M} = \{1, ..., p\}$ such that both row and column clusters are 'homogeneous' and reflect the hidden interplay between row and column effects. Biclustering provides an aggregated view on the similarity structure within the sets $\mathcal{O}$ and $\mathcal{M}$ of objects and columns, respectively, and also can serve in order to reduce a large data table with $n \cdot p$ entries to a manageable size with only $k \cdot \ell$ blocks $A_k \times B_t$ together with their characterizations (data compression). Often the aggregated view on the blocks will provide a better insight into the latent relationships and interactions that may exist between objects and variables than a detailed analysis of the numerous entries x_{ij}. Many applications underline the usefulness of co-clustering methods, e.g., in marketing (Arabie, Schleutermann, Daws, & Hubert [3]; Gaul & Schader [18]; Baier, Gaul, & Schader [4]), psychology and social sciences (Kiers, Vicari, & Vichi [27]; Schepers, Bock, & Van Mechelen [38]), bioinformatics and gene analysis (Cheng & Church [16]; Madeira & Oliveira [28]; Turner, Bailey, Krzanowski, & Hemmingway [39]; Alfò, Martella, & Vichi [2]; Martella, Alfò, & Vichi [30]; Cho & Dhillon [17]; Martella & Vichi [29]; Pontes, Giràldez, & Aguilar-Ruiz [33]), and text mining (Dhillon [19]).

A range of co-clustering methods have been proposed in the past, see, e.g., the surveys in Van Mechelen, Bock, and De Boeck [40], Madeira and Oliveira [28], Charrad and Ben Ahmed [14], Govaert and Nadif [23, 24] and methodological articles such as Bock [8, 10–12], Govaert [20], Vichi [41], Govaert and Nadif [21, 22, 24], Rocci and Vichi [34], Salah and Nadif [35], Schepers, Bock, and Van Mechelen [38] and Schepers and Hofmans [36]. These methods differ, e.g.,

- By the type of observed data values x_{ij}, e.g., real-valued, integer, categorical, binary, mixed, etc.
- by the meaning of the entries x_{ij}, e.g., association values, measurements, frequencies, etc.
- by the classification structure, e.g., hierarchical versus nonhierarchical, hard versus fuzzy classifications, and mixtures.

– by the modeling approach using, e.g., probabilistic models, empirical concepts, optimization criteria, and algorithms, etc.
– by the practical meaning of the rows and columns.

Concerning this latter issue, we may distinguish between cases where rows and columns denote the categories of two given nominal factors (e.g., the crop variety i with the fertilizer j yields x_{ij} tons of cereals), and cases of the object $\times$ variable type mentioned in the first paragraph above (e.g., object i realizes the value x_{ij} for variable j). While the two-factor case is typically symmetric insofar as clustering of both rows and columns is (or may be) based on the nearness of corresponding entries in the rows and columns, respectively, this may be misleading in the second unsymmetric case since, differently from the objects (rows), the similarity of variables (columns) is typically expressed in terms of mutual dependencies or interrelationships. Insofar, in the object$\times$variable case, clustering of rows and columns should typically be based on different distance or similarity indices that must be integrated into a joint two-way clustering model.

In this paper, we consider two situations of this latter type and provide, as a paradigm for more complex situations, suitable probabilistic co-clustering models and corresponding k-means type algorithms: In Sect. 2 we describe a two-way two-parameter biclustering model where the row partition $\mathcal{A}$ refers to the first parameter (cluster means) while the column partition $\mathcal{B}$ is induced by the values of the second one (class-specific variances). A more sophisticated and novel co-clustering model is described in Sect. 4, where object classes are characterized by a class-specific *mean value* (main effect) while additionally each class of variables is characterized by a class-specific *latent factor* that is estimated together with the column partition. As a prelude for this latter two-way model we consider in Sect. 3 a (one-way) clustering algorithm for variables only, proposed by Vigneau and Qannari [43] that is related to correlation and latent factor concepts, and show that it can be derived from a probabilistic one-way clustering model. In Sect. 4 this model will be integrated in the two-way clustering case. Section 5 concludes with some remarks and possible extensions.

2 Co-clustering with Class-Specific Variances in the Variable Clusters

We have emphasized in Sect. 1 that for an object $\times$ variable matrix $X = (x_{ij})$, clustering of variables (columns of X) may be inspired by other purposes or characterizations than when clustering objects (rows of X). In this section, we consider a simple example for such a co-clustering problem and describe a model where object clusters are characterized by cluster means (main effects) while clusters of variables are distinguished by different variability of the data. More specifically, we consider the following probabilistic co-clustering model for independent normally distributed random variables X_{ij}:

$$X_{ij} \sim \mathcal{N}(\mu_s, \sigma_t^2) \quad \text{for} \quad i \in A_s, j \in B_t, s = 1, ..., k, t = 1, ..., \ell \tag{1}$$

with the k-partition $\mathcal{A} = (A_1, ..., A_k)$ of the n rows, the ℓ-partition $\mathcal{B} = (B_1, ..., B_\ell)$ of the p columns of the matrix $X = (X_{ij})$, where row clusters A_s are characterized by cluster-specific expectations μ_s while column classes B_t are characterized by class-specific variances σ_t^2. In this situation, maximum likelihood estimation of the unknown parameters $\mathcal{A}, \mathcal{B}, \mu = (\mu_1, ..., \mu_k)$, and $\sigma = (\sigma_1^2, ..., \sigma_\ell^2)$ (for fixed k and ℓ) is equivalent to the minimization of the co-clustering criterion

$$Q(\mathcal{A}, \mathcal{B}, \mu, \sigma; X) := \sum_{s=1}^{k} \sum_{t=1}^{\ell} \sum_{i \in A_s} \sum_{j \in B_t} \left[\frac{(x_{ij} - \mu_s)^2}{\sigma_t^2} + log\, \sigma_t^2 \right] \to \min_{\mathcal{A}, \mathcal{B}, \mu, \sigma}. \tag{2}$$

Equating to zero the partial derivatives w.r.t. μ_s and σ_t^2 yields the (implicit) formulas for the estimates $\hat{\mu}_s$ and $\hat{\sigma}_t^2$:

$$\mu_s = \left[\sum_{t=1}^{\ell} \frac{|B_t|}{\sigma_t^2} \bar{x}_{A_s, B_t} \right] / \left[\sum_{t=1}^{\ell} \frac{|B_t|}{\sigma_t^2} \right] \tag{3}$$

$$\begin{aligned} \sigma_t^2 &= \frac{1}{n \cdot |B_t|} \cdot \sum_{j \in B_t} \sum_{s=1}^{k} \sum_{i \in A_s} (x_{ij} - \mu_s)^2 \\ &= \frac{1}{n \cdot |B_t|} \cdot \sum_{j \in B_t} \sum_{s=1}^{k} \left[\sum_{i \in A_s} (x_{ij} - \bar{x}_{A_s, j})^2 + |A_s| \cdot (\bar{x}_{A_s, j} - \mu_s)^2 \right]. \end{aligned} \tag{4}$$

Here $|A_s|, |B_t|$ are the class sizes, and we use largely self-explanatory notations such as

$$\bar{x}_{A_s, j} := \sum_{i \in A_s} x_{ij} / |A_s|, \qquad \bar{x}_{i, B_t} := \sum_{j \in B_t} x_{ij} / |B_t|$$

$$\bar{x}_{A_s, B_t} := \sum_{i \in A_s} \sum_{j \in B_t} x_{ij} / (|A_s| \cdot |B_t|), \quad \bar{x}_{\cdot, \cdot} := \sum_{i=1}^{n} \sum_{j=1}^{n} x_{ij} / (n \cdot p).$$

So the estimate $\hat{\mu}_s = \mu_s$ is a weighted mean of the ℓ block means $\bar{x}_{A_s, B_t}$ (with weights inversely proportional to $\sigma_t^2 / |B_t|$, the variance of the mean $\bar{X}_{i, B_t}$ in the class B_t) and the estimate $\hat{\sigma}_t^2 = \sigma_t^2$ comprises terms that measure the variability within A_s (for the variables $j \in B_t$) and the distance between the individual means $\bar{x}_{A_s, j}$ from the class-specific estimated expectations μ_s.

Since it is impossible to obtain explicit formulas for both estimates we propose to resolve the co-clustering problem (2) by the following iterative algorithm of the k-means type:

1. Begin with two initial partitions $\mathcal{A}$ and $\mathcal{B}$ and an initial estimate for σ (e.g., with σ_t^2 the empirical variance of the data values in the $|B_t|$ columns of X corresponding to B_t);

2. Estimate the object-class-specific expectations μ_s by (3) (i.e., minimize Q w.r.t. μ);
3. Estimate the variable-class-specific variances σ_t^2 by (4) (i.e., minimize Q w.r.t. σ);
4. For given $\mathcal{B}$, μ, and σ minimize Q w.r.t. the k-partition $\mathcal{A}$ of the set of objects $\mathcal{O} = \{1, ..., n\}$. An elementary argumentation shows that the minimum is obtained by the *generalized minimum-distance partition* $\widetilde{\mathcal{A}}$ with object (row) clusters

$$\widetilde{A}_s := \{\, i \in \mathcal{O} \mid s = argmin_{s'=1,...,k}\, d(i, \mu_{s'}|\mathcal{B}, \sigma) \,\} \quad s = 1, ..., k,$$

where the distance d is defined by

$$d(i, \mu_{s'}|\mathcal{B}, \sigma) := \sum_{t=1}^{\ell} \sum_{j \in B_t} (x_{ij} - \mu_{s'})^2 / \sigma_t^2 \,.$$

5. Update the parameter estimates μ, σ by repeating Steps 2. and 3. for the current partitions $\widetilde{\mathcal{A}}$ and $\mathcal{B}$.
6. Given $\widetilde{\mathcal{A}}$, μ, and σ, minimize Q w.r.t. the ℓ-partition $\mathcal{B}$ of the set of variables $\mathcal{M} = \{1, ..., p\}$; the solution is given by the *generalized minimum-distance partition* $\widetilde{\mathcal{B}}$ with variable (column) clusters

$$\widetilde{B}_t := \{\, j \in \mathcal{M} \mid t = argmin_{t'=1,...,\ell}\, \delta(j, \sigma_{t'}^2|\widetilde{\mathcal{A}}, \mu) \,\} \quad t = 1, ..., \ell,$$

where the distance δ is defined by

$$\delta(j, \sigma_{t'}^2|\widetilde{\mathcal{A}}, \mu) := \sum_{s=1}^{k} \sum_{i \in \widetilde{A}_s} (x_{ij} - \mu_s)^2 / \sigma_{t'}^2 \;+\; n \cdot \log\, \sigma_{t'}^2 \,.$$

7. Iterate 2. to 6. until convergence.

Obviously this algorithm decreases successively the criterion Q, (2), and insofar approximates a solution to the stated co-clustering problem. Note that ties, empty classes, local optima, and oscillating partitions may be possible and must be considered or avoided in a corresponding computer program.

3 Clustering of Variables Around Latent Factors

In this section, we describe a method for one-way clustering of the p variables (columns) of a data matrix $X = (x_{ij})$ that has been proposed by Vigneau and Qannari [43] and uses squared correlations for measuring the similarity between two variables. In fact, we show that this method and the related clustering criterion can be derived, as a special case, from a relatively general probabilistic clustering

model that characterizes each cluster of variables by a class-specific latent factor. In the following Sect. 4 this model will be integrated in our co-clustering models (12) and (13) for the objects and variables of X.

In many practical contexts, the similarity of two random variables $Y_j, Y_{j'}$ is measured by their squared correlation $r^2(Y_j, Y_{j'}) := Corr^2(Y_j, Y_{j'})$. Similarly, in case of a $n \times p$ data matrix $X = (x_{ij}) = (y_1, ..., y_p)$, where the j-th column $y_j = (x_{1j}, ..., x_{nj})^\top$ represents the j-th variable, the similarity of y_j and $y_{j'}$ (or j and j') is measured by the square of the empirical correlation

$$r(y_j, y_{j'}) := \frac{s_{y_j, y_{j'}}}{\sqrt{s_{y_j, y_j} s_{y_{j'}, y_{j'}}}}$$

with

$$s_{y_j, y_{j'}} := (1/n) \sum_{i=1}^{n} (x_{i,j} - \bar{x}_{\cdot,j})(x_{i,j'} - \bar{x}_{\cdot,j'}) = (1/n)\, y_j^\top y_{j'},$$

where $\bar{x}_{\cdot,j} := (\sum_{i=1}^{n} x_{ij})/n$ is the mean of the n entries in the column j of X and the last equality sign holds for centered columns y_j (i.e., $\bar{x}_{\cdot,j} = 0$).

Vigneau and Qannari have integrated this similarity concept into the search for an optimal ℓ-partition $\mathcal{B} = (B_1, ..., B_\ell)$ of the set $\mathcal{M}$ of variables (columns of X). In order to formulate a corresponding clustering criterion, they define, for each class B_t, a suitable 'prototype variable' or 'class representative'. Instead of choosing one of the observed variables (columns) y_j from B_t (medoid approach), they construct a synthetic one, i.e., a virtual column $c \in \Re^n$ in X. More specifically (and for centered columns y_j), they define the prototype vector $c_{B_t} := (c_{t1}, ..., c_{tn})^\top \in \Re^n$ to be the vector $c \in \Re^n$ that is most 'similar' to the variables in B_t in the sense

$$S(c; B_t) := \sum_{j \in B_t} r^2(y_j, c) = (1/n)\, c^\top X_{B_t} X_{B_t}^\top c \quad \rightarrow \quad \max_{c \in \Re^n, ||c||=1}, \tag{5}$$

where X_{B_t} is the data matrix X restricted to the variables (columns) of B_t. Classical eigenvalue theory shows that the solution c_{B_t} is given by the standardized eigenvector v_t that belongs to the largest eigenvalue λ_t of $X_{B_t} X_{B_t}^\top$ (and also $X_{B_t}^\top X_{B_t}$), i.e., by the first principal component in B_t. Finally, Vigneau and Qannari formulate the following criterion for clustering variables:

$$g_3(\mathcal{B}; X) := \sum_{t=1}^{\ell} \sum_{j \in B_t} r^2(y_j, c_{B_t}) \quad \rightarrow \quad \max_{\mathcal{B}} \tag{6}$$

that is equivalent to the two-parameter *correlation clustering criterion*

$$g_4(\mathcal{B}, \mathcal{C}; X) := \sum_{t=1}^{\ell} \sum_{j \in B_t} r^2(y_j, c_t)^2 \quad \rightarrow \quad \max_{\mathcal{B},\mathcal{C}}, \tag{7}$$

where maximization is also with respect to the choice of the system $\mathcal{C} = \{c_1, ..., c_\ell\}$ of ℓ standardized class-specific prototype variables (vectors) $c_1, ..., c_\ell \in \Re^n$.

From its definition as a two-parameter optimization problems it is evident that for the variable clustering problem (7) a (sub-)optimum ℓ-partition $\mathcal{B}$ of variables can be obtained by a *generalized k-means algorithm*:

(1) Begin with an initial partition $\mathcal{B} = (B_1, ..., B_\ell)$ of $\mathcal{M} = \{1, ..., p\}$.
(2) Partially optimize the clustering criterion with respect to the class prototype system $\mathcal{C}$ for the classes B_t according to (5), thus yielding the class-specific eigenvector solutions c_{B_t} (class-specific principal components).
(3) Build a new ℓ-partition $\mathcal{B}$ of the variables by assigning each variable y_j to the 'most similar' c_{B_t}, i.e., the one with the largest value of $r^2(y_j, c_{B_t})$.
(4) Iterate (2) and (3) until convergence.

Defining the similarity of variables by a correlation coefficient involves implicitly the concept of a linear regression. In fact, the correlation clustering criterion (7) above can be obtained from a probabilistic clustering model in which any variable $y_j = (x_{1j}, ..., x_{nj})^\top$ of a class B_t is generated, up to a random normal error, from the same latent factor (prototype variable) $c_t = (c_{t1}, ..., c_{tn})^\top \in \Re^n$ by a linear regression. The corresponding regression-type variable clustering model is given by

$$X_{ij} = a_j + b_j c_{ti} + e_{ij} \quad \text{for} \quad i = 1, ..., n;\ j \in B_t \tag{8}$$

with variable-specific intercepts a_j, slopes b_j, and independent normal errors $e_{ij} \sim \mathcal{N}(0, \sigma^2)$. Estimating the unknown a_j, b_j, the prototype system $\mathcal{C} = (c_1, ..., c_\ell)$ and the ℓ-partition $\mathcal{B}$ by maximizing the likelihood of $X = (x_{ij})$ is equivalent to the optimization problem

$$g_5(\mathcal{B}, \mathcal{C}, a, b; X) := \sum_{t=1}^{\ell} \sum_{j \in B_t} \sum_{i=1}^{n} (x_{ij} - a_j - b_j c_{ti})^2 \quad \rightarrow \quad \min_{\mathcal{B},\mathcal{C},a,b}. \tag{9}$$

Partially optimizing the inner sum of g_5 with respect to a_j, b_j yields the classical regression estimates

$$\widehat{b}_j := \frac{s_{y_j c_t}}{s_{y_j y_j}} \quad \text{and} \quad \widehat{a}_j = \bar{x}_{\cdot,j} - \widehat{b}_j \bar{c}_{t,\cdot} \quad \text{for } j \in B_t \tag{10}$$

in B_t with, e.g., $\bar{c}_{t,\cdot} := \sum_{i=1}^{n} c_{ti}/n$, and the partial minimum of the two inner sums of (9) is given by

$$h(B_t, c_t) := \sum_{j \in B_t} \sum_{i=1}^{n} (x_{ij} - \widehat{a}_j - \widehat{b}_j c_{ti})^2 = \sum_{j \in B_t} n \cdot s_{y_j y_j}(1 - r^2(y_j, c_t))$$

and characterizes the homogeneity of B_t for a given prototype variable c_t. Finally, the multiparameter clustering problem (9) reduces to the two-parameter mixed continuous-discrete optimization problem for $(\mathcal{B}, \mathcal{C})$:

$$\begin{aligned} g_6(\mathcal{B}, \mathcal{C}; X) &:= min_{a,b}\, g_5(\mathcal{B}, \mathcal{C}, a, b; X) = \sum_{t=1}^{\ell} h(B_t, c_t) \\ &= \sum_{t=1}^{\ell} \sum_{j \in B_t} n \cdot s_{y_j y_j}(1 - r^2(y_j, c_t)) \quad \rightarrow \quad \min_{\mathcal{B},\mathcal{C}}. \end{aligned} \tag{11}$$

For the special case of standardized column variables y_j, i.e., for $x_{\cdot,j} = 0$ and $s_{y_j y_j} = ||y_j||^2/n = 1$, this criterion is equivalent to the criterion (6) proposed by Vigneau and Qannari [43]. Insofar we have shown that their criterion (6) can be derived from a probabilistic clustering model. A software program in R is given by Chavent, Liquet, Kuentz-Simonet, and Saracco [15]. In the next section, a similar model will be used for modeling the co-clustering problem.

4 Co-Clustering, Where Variable Clusters are Characterized by Class-Specific Factors

In this section, we propose a co-clustering model for an $n \times p$ object $\times$ variable data table $X = (x_{ij})$ with normally distributed entries where the clusters of objects (rows) are distinguished only by their levels (main effects) while each cluster of variables (columns) is, additionally, characterized by a cluster-specific factor with a high correlation to the variables within this class. Thereby we adopt the basic idea that has been followed in Sect. 3 when clustering the variables only. More specifically, with the notation of former sections and as an extension of the one-way clustering model (8), we consider the model

$$\begin{aligned} X_{ij} \;=\; \mu + \alpha_s + a_j + b_j c_{ti} + e_{ij} \qquad & \text{for } i \in A_s,\, j \in B_t, \\ & s = 1, ..., k, t = 1, ..., \ell, \end{aligned} \tag{12}$$

where $\mathcal{A} = (A_1, ..., A_k)$ and $\mathcal{B} = (B_1, ..., B_\ell)$ are the unknown partitions of rows and columns, respectively (with known k and ℓ), μ is a general effect and α_s the 'main effect' of row class A_s. In this model, the vector $c_t = (c_{t1}, ..., c_{tn})^\top$ represents a cluster-specific latent factor that acts, in cluster B_t, as an explicative variable in the regression model that explains the n observations of variable j in the j-th column $y_j = (x_{1j}, ..., x_{nj})^\top$ of X, up to the main effects, by a linear regression $a_j + b_j c_{ti}$

on the components of c_t with unknown variable-specific coefficients a_j and b_j. As before, e_{ij} are independent $\mathcal{N}(0, \sigma^2)$ errors.

The clustering problem then consists in finding estimates for the parameters μ, $\alpha = (\alpha_1, ..., \alpha_k)$, $a = (a_1, ..., a_p)$, $b = (b_1, ..., b_p)$, σ^2, the set of factors $\mathcal{C} = (c_1, ..., c_\ell)$, and the partitions $\mathcal{A}$ and $\mathcal{B}$ (under suitable norming constraints). In the model (12), the intercepts a_j of the linear regression part are specified separately for the variables j. In the following, we consider the more specialized co-clustering model where these intercepts are the same, β_t say, for all variables j from the same class B_t. This is described by the more specific co-clustering model

$$X_{ij} = \mu + \alpha_s + \beta_t + b_j c_{ti} + e_{ij} \quad \text{for } i \in A_s,\ j \in B_t,\ s = 1, ..., k,\ t = 1, ..., \ell \tag{13}$$

with the constraints

$$\widetilde{\alpha}_\cdot := \sum_{s=1}^{k} \frac{|A_s|}{n} \alpha_s = 0, \quad \widetilde{\beta}_\cdot := \sum_{t=1}^{\ell} \frac{|B_t|}{p} \beta_t = 0, \quad ||c_t||^2 = 1 \tag{14}$$

It describes a situation with additive class-specific main effects α_s and β_t while interactions are cell-specific with the product form $b_j c_{ti}$ (factor model).

Invoking the maximum likelihood approach for estimating the parameters in (13), we obtain the following factor-induced co-clustering problem:

$$Q(\mathcal{A},\mathcal{B}; \mu, \alpha, \beta, b, \mathcal{C}; X) := \sum_{s=1}^{k} \sum_{t=1}^{\ell} \sum_{i \in A_s} \sum_{j \in B_t} (x_{ij} - \mu - \alpha_s - \beta_t - b_j c_{ti})^2 \ \rightarrow \ \min \tag{15}$$

where minimization is over all parameters under the constraints (14) (the model (12) may be treated similarly). In the following, we propose a *generalized alternating k-means-type algorithm* for solving this problem where, in each step, we partially optimize the criterion Q, (15), with respect to the involved parameters in turn.

Step 1: Choose an initial configuration $(\mathcal{A}, \mathcal{B}, \mu, \alpha, \beta, \mathcal{C})$. A reasonable choice might be $\mu = \bar{x}_{\cdot,\cdot}$, $\alpha_s = \bar{x}_{A_s,\cdot} - \bar{x}_{\cdot,\cdot}$, $\beta_t = \bar{x}_{\cdot,B_t} - \bar{x}_{\cdot,\cdot}$, while $\mathcal{A}$ and $\mathcal{B}$ could be obtained by separately clustering the rows and columns of X, e.g., by the classical k-means algorithm. Moreover, the class-specific factors $c_1, ..., c_\ell$ might be chosen randomly from the unit sphere in $\Re^n$.

Step 2: For fixed $(\mathcal{A}, \mathcal{B}, \mu, \alpha, \beta, \mathcal{C})$, determine the optimum regression coefficients $b_1, ..., b_\ell$ that minimize the criterion Q, (15). For notational convenience, we introduce the 'adjusted' $n \times p$ data matrix $Z = (z_{ij}(\mathcal{A}, \mathcal{B}))$ with entries

$$z_{ij}(\mathcal{A},\mathcal{B}) := z_{ij}(\mathcal{A},\mathcal{B};\mu,\alpha,\beta) := x_{ij}-\mu-\alpha_s-\beta_t$$
$$\text{for } i\in A_s,\ j\in B_t,\ s=1,...,k,\ t=1,...,\ell$$

(where main effects are eliminated) such that this partial optimization problem takes the form

$$Q=\sum_{t=1}^{\ell}\sum_{j\in B_t}\sum_{i=1}^{n}(z_{ij}(\mathcal{A},\mathcal{B})-b_jc_{ti})^2=\sum_{t=1}^{\ell}\sum_{j\in B_t}Q_j\ \rightarrow\ \min_{b_1,...,b_\ell}. \tag{16}$$

Minimizing, separately for each $j\in B_t$, the inner sum Q_j yields the estimates:

$$\widehat{b}_j=\frac{\sum_{i=1}^{n}z_{ij}(\mathcal{A},\mathcal{B})c_{ti}}{\sum_{i=1}^{n}c_{ti}^2}=z_j(\mathcal{A},\mathcal{B})^\top c_t\qquad j\in B_t,\ t=1,...,\ell$$

(with $z_j(\mathcal{A},\mathcal{B})$ the j-th column of Z; note that $||c_t||^2=1$) and the partial minimum

$$\widetilde{Q}(\mathcal{C}):=\min_{b_1,...,b_\ell}Q=\sum_{t=1}^{\ell}\sum_{j\in B_t}\sum_{i=1}^{n}(z_{ij}(\mathcal{A},\mathcal{B})-\widehat{b}_jc_{ti})^2$$
$$=\sum_{t=1}^{\ell}\sum_{j\in B_t}\left(||(z_j(\mathcal{A},\mathcal{B})||^2-(z_j(\mathcal{A},\mathcal{B})^\top c_t)^2\right) \tag{17}$$

Step 3: Looking now for the factors c_t we have to minimize the criterion (17) with respect to $\mathcal{C}=(c_1,...,c_\ell)$. This amounts to maximize, separately for each class B_t, the criterion

$$\sum_{j\in B_t}(z_j(\mathcal{A},\mathcal{B})^\top c_t)^2=c_t^\top\underbrace{\left[\sum_{j\in B_t}z_j(\mathcal{A},\mathcal{B})z_j(\mathcal{A},\mathcal{B})^\top\right]}_{S_t}c_t=:c_t^\top S_tc_t$$

with respect to c_t under the constraint $||c_t||=1$. As in Sect. 3 the solution of this problem is given by the normalized eigenvector $\widehat{c}_t$ of the $n\times n$ matrix $S_t=S_t(\mathcal{A},\mathcal{B},\mu,\alpha,\beta)$ that belongs to the largest eigenvector of S_t (first principal component in B_t).

Step 4: After having obtained the coefficients $b_j=\hat{b}_j$ and the factors $c_t=\widehat{c}_t$ we substitute these estimates in the original co-clustering criterion Q, (15), and minimize it with respect to the global and main effects μ,α, and β under the norming constraints (14). A brief calculation yields the estimates:

$$\widehat{\mu} = \bar{x}_{\cdot,\cdot} - \sum_{t=1}^{\ell} \frac{|B_t|}{p}\, \bar{b}_{B_t} \bar{c}_{t,\cdot} \qquad \text{with } \bar{b}_{B_t} := \sum_{j \in B_t} \frac{b_t}{|B_t|}$$

$$\widehat{\alpha} = \bar{x}_{A_s,\cdot} - \bar{x}_{\cdot,\cdot} - \sum_{t=1}^{\ell} \frac{|B_t|}{p}\, (\bar{c}_{t,A_s} - \bar{c}_{t,\cdot})$$

$$\widehat{\beta}_t = \bar{x}_{\cdot,B_t} - \bar{x}_{\cdot,\cdot} - \bar{b}_{B_t} \bar{c}_{t,\cdot} + \sum_{\tau=1}^{\ell} \frac{|B_\tau|}{p}\, \bar{b}_{B_\tau} \bar{c}_{t,\cdot}$$

While in Steps 2.–4. we have obtained the estimates for the effects μ, α, β, the coefficients b_j and the factors c_t, i.e., the configuration $(\mathcal{A}, \mathcal{B}; \hat{\mu}, \hat{\alpha}, \hat{\beta}, \hat{b}, \hat{\mathcal{C}})$ for a fixed choice of the partitions $\mathcal{A} = (A_1, ..., A_k)$ of objects and $\mathcal{B} = (B_1, ..., B_\ell)$ of variables, we now update these partitions by consecutively minimizing the criterion Q, (15), with respect to $\mathcal{B}$ (Step 5.) and $\mathcal{A}$ (Step 6.).

Step 5: Concerning first the partition $\mathcal{B}$ of variables, the new and partially optimum ℓ-partition $\widehat{\mathcal{B}} = (\widehat{B}_1, ..., \widehat{B}_\ell)$ for Q is the *minimum-distance partition* of $\mathcal{M} = \{1, ..., p\}$ with the classes

$$\widehat{B}_t := \{j \in \mathcal{M}\} \mid t = argmin_{\tau=1,...,\ell}\, \delta(j, \tau; \mathcal{A}, \mathcal{B}, \hat{\mu}, \hat{\alpha}, \hat{\beta}, \hat{b}, \hat{\mathcal{C}})\} \tag{18}$$

for $t = 1, ..., \ell$ where the distance measure δ is defined by

$$\delta(j, \tau; \mathcal{A}, \mathcal{B}, \hat{\mu}, \hat{\alpha}, \hat{\beta}, \hat{b}, \hat{\mathcal{C}}) := ||(z_j(\mathcal{A}, \mathcal{B})||^2 - (z_j(\mathcal{A}, \mathcal{B})^\top c_\tau)^2 \tag{19}$$

for $j = 1, ..., p$, $\tau = 1, ..., \ell$ with $z_{ij}(\mathcal{A}, \mathcal{B}) = z_{ij}(\mathcal{A}, \mathcal{B}; \hat{\mu}, \hat{\alpha}, \hat{\beta}, \hat{b}, \hat{\mathcal{C}}))$. In fact, a look at (17) shows that the best partition $\widehat{\mathcal{B}}$ has to minimize the distance δ, (19), with respect to τ for all variables j. Note that it follows from the original formula (15) for Q that the same partition is obtained when using the expression

$$\widetilde{\delta}(j, \tau; \mathcal{A}, \mathcal{B}, \hat{\mu}, \hat{\alpha}, \hat{\beta}, \hat{b}, \hat{\mathcal{C}}) := \sum_{s=1}^{k} \sum_{i \in A_s} (x_{ij} - \hat{\mu} - \hat{\alpha}_s - \hat{\beta}_\tau - \hat{b}_j \hat{c}_{\tau i})^2$$

for $j = 1, ..., p$, $\tau = 1, ..., \ell$ instead of δ in (18).

Step 6: Starting with the partition pair $\mathcal{A}, \widehat{\mathcal{B}}$ and the current parameters $\hat{\mu}, \hat{\alpha}, \hat{\beta}, \hat{b}, \hat{\mathcal{C}}$, the estimation Steps 2.–4. are now repeated and will result in new estimates $\mu^*, \alpha^*, \beta^*, b^*, \mathcal{C}^*$. With these estimates and the partition $\widehat{\mathcal{B}}$ of variables, the k-partition $\mathcal{A}$ of the set of objects $\mathcal{O}$ is updated next: the new k-partition $\widehat{\mathcal{A}}$ that partially minimizes the criterion $Q(\mathcal{A}, \widehat{\mathcal{B}}; \mu^*, \alpha^*, \beta^*, b^*, \mathcal{C}^*; X)$, is the *minimum-distance partition* with classes

$$\widehat{A}_s := \{i \in \mathcal{O} \mid s = argmin_{\sigma=1,...,k}\, d(i, \sigma; \mathcal{A}, \hat{\mathcal{B}}, \mu^*, \alpha^*, \beta^*, b^*, \mathcal{C}^*)\} \tag{20}$$

for $s = 1, ..., k$, where the distance measure d is defined by

$$d(i, \sigma; \mathcal{A}, \hat{\mathcal{B}}, \mu^*, \alpha^*, \beta^*, b^*, \mathcal{C}^*) := \sum_{t=1}^{\ell} \sum_{j \in B_t} (x_{ij} - \mu^* - \alpha_\sigma^* - \beta_t^* - b_j^* c_{ti}^*)^2 \quad (21)$$

for $i = 1, ..., n, \sigma = 1, ..., k$.

Step 7: The Steps 2.–6. are repeated until convergence of the two partitions.

Finally, we have obtained the partitions $\mathcal{A}$ and $\mathcal{B}$ of objects and variables (rows and columns), together with their characterizations, i.e.,

- the main effects α_s of the classes A_s of objects;
- the main effects β_t of the classes B_t of variables together with the factors (prototype variables) $c_1, ..., c_\ell \in \Re^n$ of these classes.

The components of each factor c_t describe the contribution of the n objects to the composition of the column clusters B_t and the object×variable interaction terms $b_j c_{ti}$. For easily interpreting the numerical results we can, e.g.,

- display, for each variable j from class B_t, the n points (c_{ti}, y_{ij}), $i = 1, ..., n$, in $\Re^2$ that should be close to the corresponding regression line $\eta = \beta_t + b_j c$;
- display and compare the latent factors $c_1, ..., c_\ell$ with the discrete curves (i, c_{ti}), $i = 1, ..., n$, in $\Re^2$, where the object labels i are arranged such object classes form contiguous segments; and
- visualize the ℓ factors $c_1, ..., c_\ell \in \Re^n$ in a two-dimensional principal component display.

5 Discussion and Extensions

In this paper, we have proposed two probabilistic approaches for clustering simultaneously the objects (rows) and the variables (columns) of a data matrix. In contrast to other approaches where, e.g., ANOVA models or information distances are considered (see, e.g., Bock [8, 10–12]), our approach considers situations where the characterization of object clusters is different from the characterization of clusters of variables. In Sect. 2 this has been illustrated for the case when object clusters are characterized by class-specific means while variable clusters are characterized by class-specific variances. Moreover, in Sect. 4 we have introduced co-clustering models where object clusters were defined by main effects, and variable clusters by their main effects *and* a class-specific factor that explains the variables via a class-specific regression. This latter model was suggested after analyzing, in Sect. 3, a clustering method for variables only (proposed by Vigneau & Qannari [43]) and formulating a corresponding probabilistic model from which our new model can be derived.

For both co-clustering models, we have proposed an appropriate generalized k-means algorithm that proceeds by successively updating model parameters and partitions. These methods can be modified into various ways, e.g., by discussing the initial settings and the order of partial optimization steps. In this respect, this paper does not provide final results and lends itself to various investigations in the future. Basically, our models should be seen as a prototype for approaches that combine clustering of objects and clustering of variables in a simultaneous, probability-based framework. They can be extended to other two-parameter distributions, to the case of factor hyperplanes (involving higher principal components in each column class) and also to co-clustering models for three-way data similarly as in Bocci, Vicari, and Vichi [6], Schepers, Van Mechelen, and Ceulemans [37], Vichi, Rocci, and Kiers [42], or Wilderjans and Cariou [44], Wilderjans and Cariou [13].

References

1. Aggarwal, C. C., & Reddy, C. K. (2014). *Data clustering. Algorithms and applications*. Boca Raton, Florida: CRC Press, Taylor & Francis.
2. Alfò, M., Martella, F., & Vichi, M. (2008). Biclustering of gene expression data by an extension of mixtures of factor analyzers. *The International Journal of Biostatistics*, *4*(1), Article 3.
3. Arabie, P., Schleutermann, S., Daws, J., & Hubert, L. (1988). Marketing applications of sequencing and partitioning on nonsymmetric and/or two-mode matrices. In W. Gaul & M. Schader (Eds.), *Data, expert knowledge and decisions* (pp. 215–224). Heidelberg: Springer Verlag.
4. Baier, D., Gaul, W., & Schader, M. (1997). Two-mode overlapping clustering with applications to simultaneous benefit segmentation and market structuring. In R. Klar, & O. Opitz (Eds.), *Classification and knowledge organization*. Studies in Classification, Data Analysis, and Knowledge Organization (vol. 9, pp. 557–566). Berlin, Germany: Springer.
5. Basu, S., Davidson, I., & Wagstaff, K. L. (2009). *Constrained clustering*. Boca Raton, Florida: Chapman & Hall/CRC, Francis & Taylor.
6. Bocci, L., Vicari, D., & Vichi, M. (2006). A mixture model for the classification of three-way proximity data. *Computational Statistics and Data Analysis*, *50*, 1625–1654.
7. Bock, H.-H. (1974). *Automatische Klassifikation*. Göttingen: Vandenhoeck & Ruprecht.
8. Bock, H.-H. (1980). Simultaneous clustering of objects and variables. In R. Tomassone, M. Amirchahy, & D. Néel (Eds.), *Analyse de données et informatique* (pp. 187–203). Le Chesnay, France: INRIA.
9. Bock, H.-H. (1996). Probability models and hypothesis testing in partitioning cluster analysis. In P. Arabie, L. J. Hubert, & G. De Soete (Eds.), *Clustering and classification* (pp. 377–453). Singapore: World Scientific.
10. Bock, H.-H. (2003). Two-way clustering for contingency tables: Maximizing a dependence measure. In M. Schader, W. Gaul, M. Vichi (Eds.), *Between data science and applied data analysis*. Studies in Classification, Data Analysis, and Knowledge Organization (vol. 24, pp. 143–154). Berlin, Germany: Springer.
11. Bock, H.-H. (2004). Convexity-based clustering criteria: Theory, algorithms, and applications in statistics. *Statistical Methods & Applications*, *12*, 293–314.
12. Bock, H.-H. (2016). Probabilistic two-way clustering approaches with emphasis on the maximum interaction criterion. *Archives of Data Science, Series A*, *1*(1), 3–20.
13. Cariou, V., & Wilderjahns, T. (2019). Constrained three-way clustering around latent variables approach. *Paper presented at the 16th conference of the International Federation of Classification Societies (IFCS-2019)*, Thessaloniki, Greece, 28 August 2019.0

14. Charrad, M., & Ben Ahmed, M. (2011). Simultaneous clustering: A survey. In S. O. Kuznetsov, et al. (Eds.), *Pattern recognition and data mining*, LNCS 6744 (pp. 370–375). Heidelberg: Springer Verlag.
15. Chavent, M., Liquet, B., Kuentz-Simonet, V., & Saracco, J. (2012). ClustOfVar: An R package for the clustering of variables. *Journal of Statistical Software*, *50*, 1–16.
16. Cheng, Y., & Church, G. M. (2000). Biclustering of expression data. In *Proceedings 8th international conference on intelligent systems for molecular biology* (pp. 93–103).
17. Cho, H., & Dhillon, I. S. (2008). Co-clustering of human cancer microarrays using minimum sum-squared residue co-clustering. *IEEE/ACM Transactions on Computational Biology and Bioinformatics*, *5*(3), 385–400.
18. Gaul, W., & Schader, M. (1996). A new algorithm for two-mode clustering. In H. -H. Bock & W. Polasek (Eds.), *Data analysis and information systems. Statistical and conceptual approaches*. Studies in Classification, Data Analysis, and Knowledge Organization (vol. 7, pp. 15–23). Heidelberg, Germany: Springer.
19. Dhillon, I. S. (2001). Co-clustering documents and words using bipartite graph partitioning. In *Proceedings of 7th ACM SIGKDD international conference on knowledge discovery and data mining, KDD '01* (pp. 269–274). New York: ACM.
20. Govaert, G. (1995). Simultaneous clustering of rows and columns. *Control and Cybernetics*, *24*(4), 437–458.
21. Govaert, G., & Nadif, M. (2003). Clustering with block mixture models. *Pattern Recognition*, *36*(2), 463–473.
22. Govaert, G., & Nadif, M. (2008). Block clustering with Bernoulli mixture models: Comparison of different approaches. *Computational Statistics and Data Analysis*, *52*(6), 3233–3245.
23. Govaert, G., & Nadif, M. (2013). *Co-clustering*. Chichester, UK: Wiley.
24. Govaert, G., & Nadif, M. (2018). Mutual information, phi-squared and model-based co-clustering for contingency tables. *Advances in Data Analysis and Classification*, *12*, 455–488.
25. Hennig, C., Meila, M., Murtagh, F., & Rocci, R. (2016). *Handbook of cluster analysis*. Boca Raton, Florida: CRC Press, Taylor & Francis.
26. Jain, A. K., & Dubes, R. C. (1988). *Algorithms for clustering data*. Englewood Cliffs, New Jersey: Prentice Hall.
27. Kiers, H. A. L., Vicari, D., & Vichi, M. (2005). Simultaneous classification and multidimensional scaling with external information. *Psychometrika*, *70*, 433–460.
28. Madeira, S. C., & Oliveira, A. L. (2004). Biclustering algorithms for biological data analysis: A survey. *IEEE Transaction on Computational Biology and Bioinformatics*, *1*(1), 24–45.
29. Martella, F., & Vichi, M. (2012). Clustering microarray data using model-based double k-means. *Journal of Applied Statistics*, *39*(9), 1853–1869.
30. Martella, F., Alfò, M., & Vichi, M. (2010). Hierarchical mixture models for biclustering in microarray data. *Statistical Modelling*, *11*(6), 489–505.
31. McLachlan, G. J., & Krishnan, T. (2008). *The EM algorithm and extensions* (2nd ed.). Hoboken, New Jersey: Wiley.
32. Miyamoto, S., Ichihashi, H., & Honda, K. (2008). *Algorithms for fuzzy clustering*. Heidelberg: Springer Verlag.
33. Pontes, B., Giràldez, R., & Aguilar-Ruiz, J. S. (2015). Biclustering on expression data: A review. *ScienceDirect*, *57*, 163–180.
34. Rocci, R., & Vichi, M. (2008). Two-mode partitioning. *Computational Statistics and Data Analysis*, *52*, 1984–2003.
35. Salah, A., & Nadif, M. (2019). Directional co-clustering. *Advances in Data Analysis and Classification*, *13*(3), 591–620.
36. Schepers, J., & Hofmans, J. (2009). TwoMP: A MATLAB graphical user interface for two-mode partitioning. *Behavioral Research Methods*, *41*, 507–514.
37. Schepers, J., Van Mechelen, I., & Ceulemans, E. (2006). Three-mode partitioning. *Computational Statistics and Data Analysis*, *51*, 1623–1642.
38. Schepers, J., Bock, H.-H., & Van Mechelen, I. (2013). Maximal interaction two-mode clustering. *Journal of Classification*, *34*(1), 49–75.

39. Turner, H. L., Bailey, T. C., Krzanowski, W. J., & Hemmingway, C. A. (2005). Biclustering models for structured microarray data. *IEEE Tansactions on Computational Biology and Bioinformatics*, *2*(4), 316–329.
40. Van Mechelen, I., Bock, H.-H., & De Boeck, P. (2004). Two-mode clustering methods: A structured overview. *Statistical Methods in Medical Research*, *13*, 363–394.
41. Vichi, M. (2001). Double k-means clustering for simultaneous classification of objects and variables. In S. Borra, M. Rocci, M. Vichi, & M. Schader (Eds.), *Advances in classification and data analysis 19*, 43–52. Heidelberg: Springer.
42. Vichi, M., Rocci, R., & Kiers, H. A. L. (2007). Simultaneous component and clustering models for three way data: Within and between approaches. *Journal of Classification*, *24*, 71–98.
43. Vigneau, E., & Qannari, E. M. (2003). Clustering of variables around latent components. *Communications in Statistics, Simulation and Computation*, *32*(4), 1131–1150.
44. Wilderjans, T. F., & Cariou, C. (2016). CLV3W: A clustering around variables approach to detect panel disagreement in three-way conventional sensory profiling data. *Food Quality and Preference*, *47*, 45–53.

How to Use the Hermitian Form Model for Asymmetric MDS

Naohito Chino

Abstract In this paper, we shall first revisit the Hermitian form model (HFM) for the analysis of asymmetric similarity matrices (abbreviated as ASM) proposed by Chino and Shiraiwa [5] and show how to interpret the configuration of objects obtained by applying HFM to empirical and hypothetical ASMs. Finally, we shall discuss briefly how to apply HFM to ASM which changes as time proceeds through the mutual interactions among objects.

1 Introduction

In this section we shall introduce the Hermitian form model (hereafter, abbreviated as HFM) for the analysis of asymmetric (dis)similarity matrix, which was proposed by Chino and Shiraiwa [5]. Let us first suppose that we have an observed asymmetric similarity matrix $\mathbf{S} = \left[s_{jk}\right]$, whose element s_{jk} denotes the intensity of the similarity from object j to object k among N objects. Therefore, matrix $\mathbf{S}$ is N by N, and is in general asymmetric. We shall hereafter abbreviate the Asymmetric Similarity Matrix as ASM.

ASM can be found everywhere in our daily lives, in research laboratories, and so on. Sometimes researchers assume some ASM theoretically or hypothetically in order to explain a certain observed phenomenon. For example, one-sided love and hate among members of any informal group are typical examples which constitute such an ASM in daily lives. Trade data matrix among nations is another typical ASM. Amount of migration from one region to another is also such an example in geography.

In research laboratories, we may observe various pathways among voxels of neurons, biosynthetic pathways of nicotinamide adenine dinucleotide (NAD) (e.g., Imai & Guarente [11], Fig. 2), and so on. In field research we may observe, for example, the pecking order among a group of hens and cocks in biology (e.g., Rushen

N. Chino (✉)
Aichi Gakuin University, Nagoya, Japan
e-mail: chino@dpc.agu.ac.jp

T. Imaizumi et al. (eds.), *Advanced Studies in Behaviormetrics and Data Science*,
Behaviormetrics: Quantitative Approaches to Human Behavior 5,
https://doi.org/10.1007/978-981-15-2700-5_2

[15]). Suppose that the code is one in the case when there is a pathway or such an order, and otherwise it is zero. Then, we get an ASM whose elements are binary.

We sometimes assume some special ASM theoretically or hypothetically. For example, Sato, Akiyama, and Farmer [17] assume the payoff matrices of "rock-paper-scissors" in the context of the theory of the evolutionally stable strategy in biology. Equation (1) shows them.

$$\mathbf{A} = \begin{bmatrix} \varepsilon_x & -1 & 1 \\ 1 & \varepsilon_x & -1 \\ -1 & 1 & \varepsilon_x \end{bmatrix}, \mathbf{B} = \begin{bmatrix} \varepsilon_y & -1 & 1 \\ 1 & \varepsilon_y & -1 \\ -1 & 1 & \varepsilon_y \end{bmatrix}. \tag{1}$$

The weight matrix specifically assumed in the hidden layers is also considered as a typical ASM in recurrent neural networks (e.g., Goodfellow, Bengio, & Courville [8], Fig. 10.3). Usually, elements of the weight matrix are unknown parameters of some neural network model, and thus are estimated from data. From the psychometrical point of view, elements of ASM are measured at various levels. For example, these elements in the affinity data discussed above are measured at an *interval level*. Those in trade data are measured at a *ratio level*. Binary data frequently observed in research laboratories, which might be considered as count data, may be viewed as measured at a ratio level. This type of data can be sometimes said to be measured at an *absolute scale* level. Dummy variables, 1 and -1 in the payoff matrices might also be said to be measured at a ratio level.

For these elements of ASM, HFM assumes the *ratio level* of measurement. As a result, for example, affinity data matrices among members of any informal group discussed above should not be analyzed by HFM. In such a case, we may analyze such matrices using various asymmetric MDS methods which do not necessarily assume the ratio level of measurement (e.g., Okada & Imaizumi [13, 14]; Saburi & Chino [16]).

In this paper, we shall show how to interpret the configuration of objects obtained by applying HFM to theoretical or empirical ASMs, typical examples of which we listed above. In Sect. 2, we shall revisit HFM briefly. In Sect. 3, we shall explain how to interpret the configuration of objects obtained by HFM. In Sect. 4, we show some applications of HFM to empirical ASM, and interpret the configurations of objects obtained by HFM. In Sect. 5, we show some applications of HFM to theoretical or hypothetical ASM, and interpret these configurations obtained by HFM. In Sect. 6, we shall discuss the merit of HFM, and refer to a possibility of utilizing these configurations for future research. In Sect. 7 we shall discuss the ASM which changes as time proceeds through the mutual interactions among objects. We introduce a certain hypothetical force acting on the state spaces of some underlying dynamical system and discuss how to interpret such a force by utilizing the theory of HFM.

2 Revisit of HFM

In this section we shall summarize the HFM model proposed by Chino and Shiraiwa [5]. In HFM we first decompose N by N ASM, $\mathbf{S}$, into the symmetric part and the skew-symmetric part,

$$\mathbf{S} = \frac{\boldsymbol{S} + \boldsymbol{S}^t}{2} + \frac{\boldsymbol{S} - \boldsymbol{S}^t}{2} = \boldsymbol{S}_s + \boldsymbol{S}_{sk}, \tag{2}$$

and then construct a *Hermitian matrix* as follows:

$$\mathbf{H} = \boldsymbol{S}_s + i\ \boldsymbol{S}_{sk}, \tag{3}$$

where $i^2 = -1$. It is apparent from Eq. (3) that $\mathbf{S}$ is a *real matrix* while $\mathbf{H}$ is a special *complex matrix*. Since $\mathbf{H}$ is a Hermitian matrix, the conjugate transpose of $\mathbf{H}$ denoted by $\boldsymbol{H}^*$ is also $\mathbf{H}$. $\mathbf{H}$ is an N by N matrix.

In HFM we first consider the eigenvalue problem of $\mathbf{H}$, that is,

$$\mathbf{H}\boldsymbol{u}_i = \lambda_i \boldsymbol{u}_i,\ 1 \leq i \leq N, \tag{4}$$

where λ_i is the ith eigenvalue of $\mathbf{H}$, and $\boldsymbol{u}_i$ is the eigenvector associated with λ_i. It is well known that all the eigenvalues of $\mathbf{H}$ are *real*, since $\mathbf{H}$ is Hermitian. It is also well known that all of these eigenvectors are *unitary*, that is, mutually orthogonal in a complex space. Moreover, without loss of generality we can set $\lambda_i \neq 0$ $(1 \leq \mathrm{i} \leq \mathrm{n})$, and $\lambda_{n+1} = \lambda_{n+2} = \cdots = \lambda_N = 0$.

Then, let us define

$$\mathbf{U} = \left[\boldsymbol{u}_1, \ldots, \boldsymbol{u}_n, \boldsymbol{u}_{n+1}, \ldots, \boldsymbol{u}_N\right] = \left[\boldsymbol{U}_1, \boldsymbol{U}_2\right], \tag{5}$$

where $\boldsymbol{U}_1$ and $\boldsymbol{U}_2$ are composed of n column vectors, $\boldsymbol{u}_1, \ldots, \boldsymbol{u}_n$ and $N - n$ column vectors, $\boldsymbol{u}_{n+1}, \ldots, \boldsymbol{u}_N$, respectively. Moreover, let us define

$$\boldsymbol{\Lambda} = \mathrm{diag}\left[\lambda_1, \lambda_2, \ldots, \lambda_n\right]. \tag{6}$$

Using $\boldsymbol{U}_1$ and $\boldsymbol{\Lambda}$, we get

$$\mathbf{H} = \boldsymbol{U}_1 \boldsymbol{\Lambda} \boldsymbol{U}_1^*. \tag{7}$$

Here, $\boldsymbol{U}_1^*$ denotes the conjugate transpose of $\boldsymbol{U}_1$.
Let us further define

$$\boldsymbol{\Omega}_s = \begin{bmatrix} \boldsymbol{\Lambda} & \boldsymbol{O} \\ \boldsymbol{O} & \boldsymbol{\Lambda} \end{bmatrix}, \boldsymbol{\Omega}_{sk} = \begin{bmatrix} \boldsymbol{O} & -\boldsymbol{\Lambda} \\ \boldsymbol{\Lambda} & \boldsymbol{O} \end{bmatrix}, \tag{8}$$

and

$$\mathbf{X} = [\boldsymbol{U}_r, \boldsymbol{U}_c], \tag{9}$$

where $\boldsymbol{U}_r$ and $\boldsymbol{U}_c$ are such that $\boldsymbol{U}_1 = \boldsymbol{U}_r + i\boldsymbol{U}_c$. Here, $\boldsymbol{U}_r$ and $\boldsymbol{U}_c$ are, respectively, the real part and the imaginary part of the eigenvector matrix $\boldsymbol{U}_1$ of Eq. (7). Then, $\mathbf{H}$ in Eq. (7) can be rewritten as

$$\mathbf{H} = \mathbf{X}\boldsymbol{\Omega}_s\boldsymbol{X}^t + i\,\mathbf{X}\boldsymbol{\Omega}_{sk}\boldsymbol{X}^t. \tag{10}$$

Here, it should be noticed that the matrices $\mathbf{X}$, $\boldsymbol{\Omega}_s$, and $\boldsymbol{\Omega}_{sk}$ are all *real*.

In any case, if we write the (j,k) element of $\mathbf{H}$ in Eq. (7) as h_{jk}, this equation can be written in the form

$$h_{jk} = \Psi\left(\boldsymbol{v}_j, \boldsymbol{v}_k\right), \tag{11}$$

where Ψ is a *Hermitian form*, $\Psi\left(\boldsymbol{v}_j, \boldsymbol{v}_k\right) = \boldsymbol{v}_j\,\boldsymbol{\Lambda}\boldsymbol{v}_k^*$. This is the reason why we call our model the *Hermitian form model* (HFM) for the analysis of asymmetry. Chino and Shiraiwa [5] proved that a necessary and sufficient condition for this model to be expressible in terms of (complex) *Hilbert space* is the *positive semi-definiteness* (p.s.d) of $\mathbf{H}$. This means that all the eigenvalues of $\mathbf{H}$ are greater than or equal to zero and in this case we can embed objects in the Hilbert space.

If some of the eigenvalues are negative, we can embed objects in an *indefinite metric space*. However, if we restrict the dimension into one in the indefinite metric space, this space can be considered as a one-dimensional Hilbert space, and we can interpret the configuration of objects as if it were embedded in a Hilbert space even if the eigenvalue under consideration is negative. In this case, however, we must interpret the configuration of objects, noticing the sign of the eigenvalue. We shall show such an example in Sect. 3.

Next, if we use Eqs. (2), (3), and (10), then we get

$$\mathbf{S} = \mathbf{X}\boldsymbol{\Omega}_s\boldsymbol{X}^t + \mathbf{X}\boldsymbol{\Omega}_{sk}\boldsymbol{X}^t. \tag{12}$$

This equation can be rewritten, in scalar notation, as

$$s_{jk} = \sum_{l=1}^{n}\lambda_l\left(r_{jl}r_{kl} + c_{jl}c_{kl}\right) + \sum_{l=1}^{n}\lambda_l\left(c_{jl}r_{kl} - r_{jl}c_{kl}\right), \tag{13}$$

or

$$s_{jk} = \sum_{l=1}^{n}\lambda_l\left\{\left(r_{jl}r_{kl} + c_{jl}c_{kl}\right) + \left(c_{jl}r_{kl} - r_{jl}c_{kl}\right)\right\}, \tag{14}$$

where

$$\boldsymbol{U}_r = \left[r_{jl}\right], \boldsymbol{U}_c = \left[c_{jl}\right], \tag{15}$$

are the *real part* and the *imaginary part* of the eigenvector matrix $\boldsymbol{U}_1$, as introduced in defining the matrix $\mathbf{X}$ in Eq. (9). Therefore, both r_{jl} and c_{jl} are *real*. This means

that we may treat s_{jk} as if it were defined with *n two-dimensional Euclidean planes* notwithstanding the fact that HFM is a (complex) *Hilbert space model*. In general, one-dimensional complex plane can be identified with two-dimensional Euclidean plane.

Finally, we have an interesting identity in HFM (Chino & Shiraiwa [5]). Let $\Psi(\zeta, \tau)$ be a Hermitian form. Then, we have the following polar identity in the (complex) pre-Hilbert space (Cristescu [6]),

$$\Psi(\boldsymbol{\zeta}, \boldsymbol{\tau}) = \frac{1}{4}\left(\|\boldsymbol{\zeta} + \boldsymbol{\tau}\|^2 - \|\boldsymbol{\zeta} - \boldsymbol{\tau}\|^2\right) + \frac{1}{4}i\left(\|\boldsymbol{\zeta} + i\boldsymbol{\tau}\|^2 - \|\boldsymbol{\zeta} - i\boldsymbol{\tau}\|^2\right). \quad (16)$$

This equation also holds for the (complex) Hilbert space. Stated another way, we have

$$\Psi(\boldsymbol{\zeta}, \boldsymbol{\tau}) = \frac{1}{2}\left(\|\boldsymbol{\zeta}\|^2 + \|\boldsymbol{\tau}\|^2 - \|\boldsymbol{\zeta} - \boldsymbol{\tau}\|^2\right) + \frac{1}{2}i\left(\|\boldsymbol{\zeta}\|^2 + \|\boldsymbol{\tau}\|^2 - \|\boldsymbol{\zeta} - i\boldsymbol{\tau}\|^2\right). \quad (17)$$

Then, remembering Eq. (11), we have

$$h_{jk} = \frac{1}{2}\left(\|\boldsymbol{v}_j\|^2 + \|\boldsymbol{v}_k\|^2 - \|\boldsymbol{v}_j - \boldsymbol{v}_k\|^2\right) + \frac{1}{2}i\left(\|\boldsymbol{v}_j\|^2 + \|\boldsymbol{v}_k\|^2 - \|\boldsymbol{v}_j - i\boldsymbol{v}_k\|^2\right). \quad (18)$$

Remembering Eq. (3), we have

$$s_{jk} = \frac{1}{2}\left(\|\boldsymbol{v}_j\|^2 + \|\boldsymbol{v}_k\|^2 - \|\boldsymbol{v}_j - \boldsymbol{v}_k\|^2\right) + \frac{1}{2}\left(\|\boldsymbol{v}_j\|^2 + \|\boldsymbol{v}_k\|^2 - \|\boldsymbol{v}_j - i\boldsymbol{v}_k\|^2\right). \quad (19)$$

We can rewrite Eq. (19) as

$$s_{jk} = \|\boldsymbol{v}_j\|^2 + \|\boldsymbol{v}_k\|^2 - \frac{1}{2}\left(\|\boldsymbol{v}_j - \boldsymbol{v}_k\|^2 + \|\boldsymbol{v}_j - i\boldsymbol{v}_k\|^2\right). \quad (20)$$

This equation bridges the gap between observed asymmetric similarities, s_{jk}, which are real, and position vectors, $\boldsymbol{v}_j$ and $\boldsymbol{v}_k$, of objects, j and k, respectively, which are complex. As shown in the next section, it is utilized when we want to recover component asymmetric similarities from the configuration of objects embedded in the (complex) Hilbert space.

3 Interpretation of the Configuration of Objects by HFM

In this section, we shall explain how to interpret the configuration of objects embedded in a Hilbert space, which is obtained by applying HFM to any empirical or theoretical ASM. As discussed in the previous section, objects are embedded in either the Hilbert space or the indefinite metric space depending on the eigenvalues of the Hermitian matrix constructed from the ASM.

However, as also discussed in the previous section, both those spaces are considered as one-dimensional Hilbert spaces if we restrict the space in one dimension. As a result, we may interpret the n-dimensional configuration of objects in the whole space per one dimension as if it were a one-dimensional Hilbert space, that is, a complex plane. This means that we may think of the similarity, s_{jk}, in Eq. (13) as

$$s_{jk} = \lambda_l \left(r_{jl} r_{kl} + c_{jl} c_{kl}\right) + \lambda_l \left(c_{jl} r_{kl} - r_{jl} c_{kl}\right), \tag{21}$$

for the lth complex plane associated with the lth eigenvalue of $\mathbf{H}$. Here, r_{jl} and c_{jl} are, respectively, the real part and the imaginary part of the complex number, v_j, corresponding to the location of object, O_j, on the lth complex plane. Since the complex plane can be identified with the two-dimensional Euclidean plane, we can also consider r_{jl} and c_{jl}, respectively, as the abscissa and the ordinate of the position of O_j, on the lth Euclidean plane.

Then, let us rewrite r_{jl} and c_{jl} as x_{j1} and x_{j2}, respectively. Moreover, let us define, respectively, the position vectors, $\boldsymbol{x}_j = \left[x_{j1}, x_{j2}\right]$ and $\boldsymbol{x}_k = [x_{k1}, x_{k2}]$ of O_j and O_k. Then, Eq. (21) can be rewritten as follows, if we introduce trigonometric functions:

$$s_{jk} = \lambda \left|\boldsymbol{x}_j\right| \left|\boldsymbol{x}_k\right| \left(\cos\theta_{jk} - \sin\theta_{jk}\right), \tag{22}$$

where θ_{jk} is the *angle* from O_j to O_k.

If we identify, respectively, *real vectors*, $\boldsymbol{x}_j$ and $\boldsymbol{x}_k$, with *complex numbers*, $v_j = x_{j1} + i x_{j2}$ and $v_k = x_{k1} + i x_{k2}$, θ_{jk} is the difference in the *arguments* θ_j and θ_k of v_j and v_k, respectively, in a complex plane. Here, the argument of the complex number z, defined for $z \neq 0$, is the *angle* which the vector originating from 0 to z makes with the positive real axis *counterclockwise*. Figure 1 illustrates v_j and v_k in a complex plane, assuming that v_j is on the real axis. In this case, the argument of v_j happens to be zero, and thus θ_{jk} is equal to the argument of v_k.

However, in interpreting the configuration of objects obtained by HFM, it should be noticed that the positive direction of the configuration of objects must be measured *clockwise*, considering Eqs. (21) and (22). This means that the similarity from O_k associated with v_k to O_j associated with v_j is relatively greater than that from O_j to O_k in Fig. 1.

Remember here that the positive direction of the configuration of objects is *counterclockwise* in Chino's ASYMSCAL (Chino [1]), which is one of the asymmetric

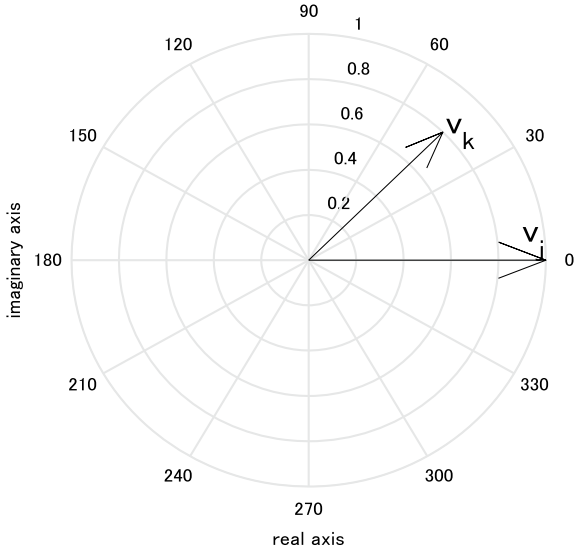

Fig. 1 Configuration of two objects, O_j and O_k in the complex plane, and the argument θ_{jk} measured counterclockwise from O_j

MDSs. This model is a Euclidean space model and embeds objects in the two-dimensional Euclidean space. The original model is written as

$$s_{jk} = \mathrm{a}\ \left(x_{j1}x_{k1} + x_{j2}x_{k2}\right) + \mathrm{b}\left(x_{j1}x_{k2} - x_{j2}x_{k1}\right) + c, \tag{23}$$

where a, b, and c are real constants.

If we identify real coordinate vector $\boldsymbol{x}_j = \left[x_{j1}, x_{j2}\right]$ with the complex number $z_j = r_{j1} + ic_{j1}$ and $\boldsymbol{x}_k = [x_{k1}, x_{k2}]$ with the complex number $z_k = r_{k1} + ic_{k1}$, Eq. (23) can be rewritten as

$$s_{jk} = \mathrm{a}\ \left(r_{j1}r_{k1} + r_{j2}r_{k2}\right) + \mathrm{b}\left(r_{j1}c_{k2} - c_{j2}r_{k1}\right) + c. \tag{24}$$

Now, let us set $a = b = \lambda$. Then, Eq. (24) is written as

$$s_{jk} = \lambda\ \left(r_{j1}r_{k1} + r_{j2}r_{k2}\right) + \lambda\ \left(r_{j1}c_{k2} - c_{j2}r_{k1}\right) + c. \tag{25}$$

If we further rewrite Eq. (25) as

$$s_{jk} = \lambda\ \left(r_{j1}r_{k1} + r_{j2}r_{k2}\right) - \lambda\ \left(c_{j2}r_{k1} - r_{j1}c_{k2}\right) + c, \tag{26}$$

and compare it with Eq. (21) of HFM, we see that the positive direction of the configuration of objects is opposite in the case of Chino's ASYMSCAL.

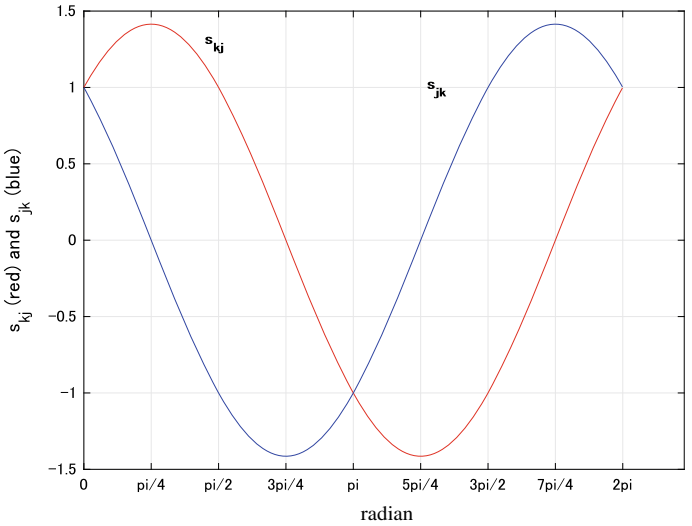

Fig. 2 Values of s_{jk} (blue curve) and s_{kj} (red curve) plotted against θ_{jk} when the eigenvalue of $\mathbf{H}$ is *positive*

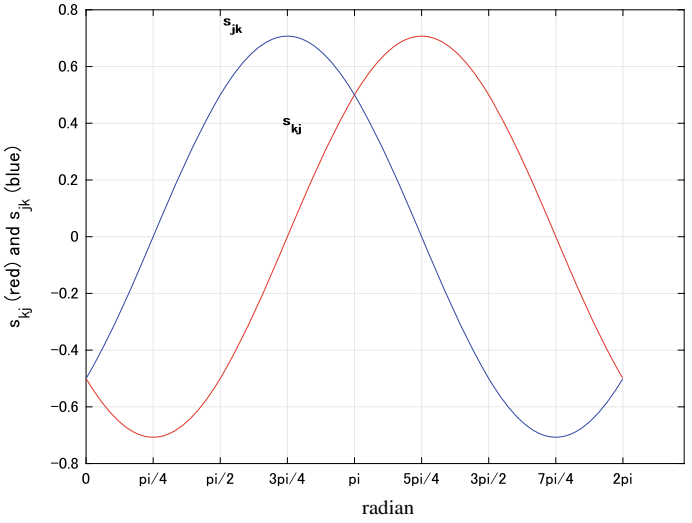

Fig. 3 Values of s_{jk} (blue curve) and s_{kj} (red curve) plotted against θ_{jk} when the eigenvalue of $\mathbf{H}$ is *negative*

Table 1 Summary of signs of s_{jk} and s_{kj} which depend on θ_{jk}

θ_{jk}	$(0, \frac{\pi}{4})$	$(\frac{\pi}{4}, \frac{\pi}{2})$	$(\frac{\pi}{2}, \frac{3\pi}{4})$	$(\frac{3\pi}{4}, \pi)$	$(\pi, \frac{5\pi}{4})$	$(\frac{5\pi}{4}, \frac{3\pi}{2})$	$(\frac{3\pi}{2}, \frac{7\pi}{4})$	$(\frac{7\pi}{4}, 2\pi)$
s_{jk}	+	−	−	−	−	+	+	+
s_{kj}	+	+	+	−	−	−	−	+

Table 2 Summary of signs of s_{jk} and s_{kj} which depend on θ_{jk}

θ_{jk}	$(0, \frac{\pi}{4})$	$(\frac{\pi}{4}, \frac{\pi}{2})$	$(\frac{\pi}{2}, \frac{3\pi}{4})$	$(\frac{3\pi}{4}, \pi)$	$(\pi, \frac{5\pi}{4})$	$(\frac{5\pi}{4}, \frac{3\pi}{2})$	$(\frac{3\pi}{2}, \frac{7\pi}{4})$	$(\frac{7\pi}{4}, 2\pi)$
s_{jk}	−	+	+	+	+	−	−	−
s_{kj}	−	−	−	+	+	+	+	−

In any case, s_{jk} in Eq. (22) of HFM depends on θ_{jk} discussed there. Figures 2 and 3 illustrate the details of s_{jk} as a function of θ_{jk}. In these figures, we set $|\boldsymbol{x}_j|\,|\boldsymbol{x}_k|$ in Eq. (22) equal to 1 for simplicity. Moreover, we set λ equal to 1 and -1 for Figs. 2 and 3, respectively. These correspond to the cases when the eigenvalues of $\mathbf{H}$ are positive and negative, respectively.

It is apparent from Fig. 2 that s_{kj} is greater than s_{jk} within the range, $0<\theta_{jk}<\pi$, while s_{jk} is greater than s_{kj} within the range, $\pi<\theta_{jk}<2\pi$. Moreover, signs of s_{jk} and s_{kj} depend on θ_{jk}, as summarized in Table 1.

In contrast, it is apparent from Fig. 3 that s_{jk} is greater than s_{kj} within the range, $0<\theta_{jk}<\pi$, while s_{kj} is greater than s_{jk} within the range, $\pi<\theta_{jk}<2\pi$. Moreover, signs of s_{jk} and s_{kj} depend on θ_{jk}, as summarized in Table 2.

Finally, we shall consider a bit about the skewness between s_{jk} and s_{kj}. It is easy to show that from Eq. (22) we have

$$s_{jk}-s_{kj} = -\lambda\,|\boldsymbol{x}_j|\,|\boldsymbol{x}_k|\,\sin\theta_{jk}\,. \tag{27}$$

Therefore, if we set $\lambda\,|\boldsymbol{x}_j|\,|\boldsymbol{x}_k|$ equal to 1, we have

$$s_{jk}-s_{kj} = -\sin\theta_{jk}, \tag{28}$$

and

$$|s_{jk}-s_{kj}| = |\sin\theta_{jk}\,|\,. \tag{29}$$

The green curve in Fig. 4 is the very amount of the skewness between the similarities, s_{jk} and s_{kj}. From this figure, it is apparent that the skewness between them takes the maximum values when θ_{jk} is $\frac{\pi}{2}$ or $3\frac{\pi}{2}$.

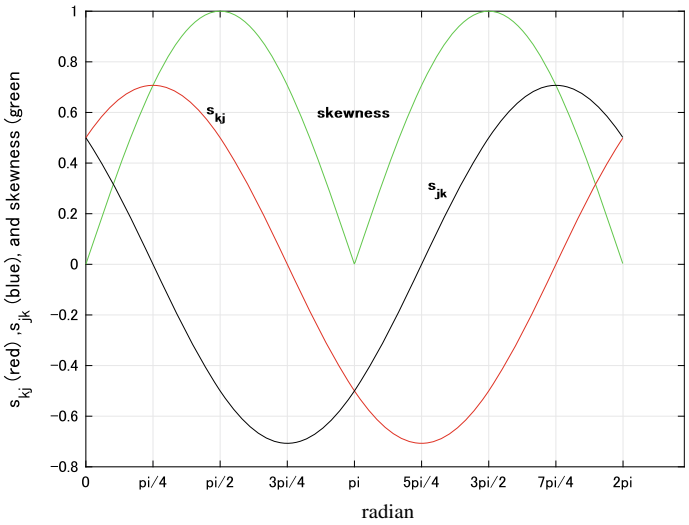

Fig. 4 Skewness curves (green) between s_{jk} (black curve) and s_{kj} (red curve) plotted against θ_{jk}

4 Applications of HFM to Empirical Asymmetric Relational Matrices

In this section we show two applications of HFM to empirical asymmetric relational data matrices. One is the international trade data among Japan, America, China, and Russia in 2015, which appeared in The Asahi News Paper in Japan. Table 3 shows this.

According to convention, we administered a log transformation to each element of this ASM prior to the analysis via HFM. Eigenvalues of the Hermitian matrix constructed from the transformed ASM were 29.9714, 6.1145, 4.4377, and 3.5309. This means that the trade data has a *Hilbert space structure as a whole*. Of course, each of the configurations of nations on the complex planes associated with these eigenvalues is considered as embedded in a *one-dimensional Hilbert space*, as indicated in the previous section. Moreover, these configurations embedded in one-dimensional

Table 3 The international trade data among Japan, America, China, and Russia in 2015

	1. Japan	2. USA	3. China	4. Russia
1. Japan	43,480	1,382	1,200	55
2. USA	736	189,592	1,161	71
3. China	1,764	4,832	119,684	348
4. Russia	173	164	333	13,755

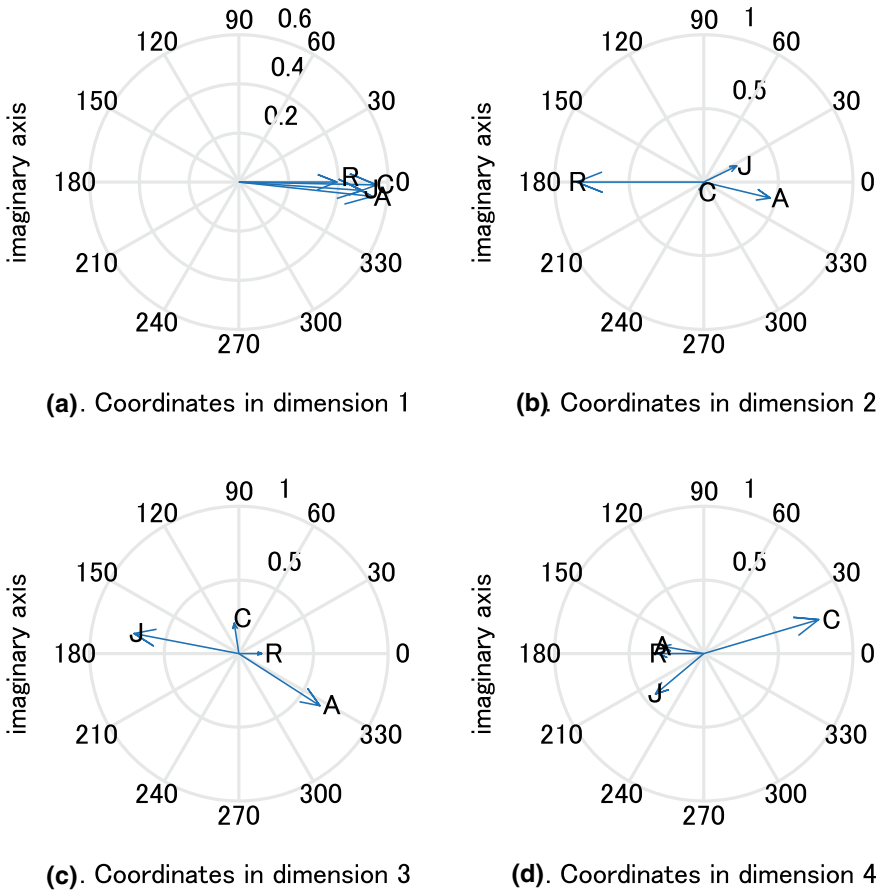

Fig. 5 Four configurations of nations corresponding to the one-dimensional Hilbert space. In this figure, alphabets, A, C, J, and R, indicate USA, China, Japan, and Russia

Hilbert spaces are mutually orthogonal (to be precise, *unitary*) in the whole space with the complex Hilbert space structure.

Figure 5 shows four configurations of nations corresponding to these one-dimensional Hilbert spaces. Of course, these four configurations are associated with the four eigenvalues of the Hermitian matrix discussed above.

Figure 5a, which is the configuration associated with the maximum eigenvalue of the Hermitian matrix, suggests that this dimension looks like a *size-factor* in PCA because four nations are compressed in a narrow region. However, if we enlarge this region, we see that major asymmetric relationships among nations observed in the ASM are reproduced in the enlarged configuration. Here, in interpreting this configuration, it should be noticed that the positive direction of this figure is *clockwise* because the eigenvalue is positive in this case. It should also be noticed that angles

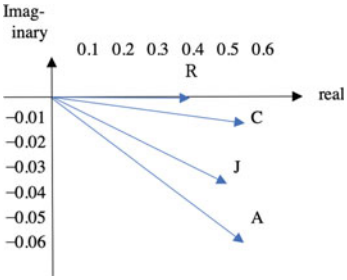

Fig. 6 The enlarged configuration of four nations. Here, the positive direction of this figure is clockwise because the eigenvalue is positive in this case

θ_{jk} between two nations all fall within $\pi/3$ (30°), as is apparent from Fig. 5a. Then, looking at Fig. 2, we see that $s_{kj} > s_{jk}$.

As a result, applying this relation to nations in Fig. 6, the amount of export from C (China) to A (USA) is greater than that from A to C. Similar trade imbalances are indicated from C to J, and from J to A. Finally, it should be noticed that the magnitude of the skewness between s_{jk} and s_{kj}, which is defined by Eq. (29), increases as θ_{jk} increases within $\pi/3$, as shown in Fig. 4. Since this magnitude is also proportional to $\left|\boldsymbol{x}_j\right| |\boldsymbol{x}_k|$ in Eq. (27), the magnitude of skewness between A and C might be the greatest of all the dyadic relations shown in Fig. 6.

The other application is concerned with the biosynthetic pathways of proteins in mammals (e.g., Imai [10]; Imai & Guarente [11]), an example of which appears in Fig. 2 of Imai and Guarente [11]. We reconstruct an ASM from this figure in such a way that the similarity is 1 if the directional arc exists from an element to another element of 11 substances, and otherwise it is 0. These substances are composed of tryptophan (an α-amino acid), NAD (nicotinamide adenine dinucleotide, a non-protein chemical compound), NIC (nicotinamide, an organic molecule), and so on.

Table 4 Biosynthetic pathways of proteins in mammals which was reconstructed from Fig. 2 of Imai and Guarente [11]

	1	2	3	4	5	6	7	8	9	10	11
1	0	1	0	0	0	0	0	0	0	0	0
2	0	0	0	1	0	0	0	0	0	0	0
3	0	0	0	1	0	0	0	0	0	0	0
4	0	0	0	0	1	0	0	0	0	0	0
5	0	0	0	0	0	1	0	0	0	0	0
6	0	0	0	0	0	0	1	0	1	0	0
7	0	0	0	0	0	0	0	0	0	0	0
8	0	0	0	0	0	0	0	0	0	0	0
9	0	0	0	0	0	0	0	1	0	0	0
10	0	0	0	0	0	1	0	0	0	0	1
11	0	0	0	0	0	0	0	0	0	1	0

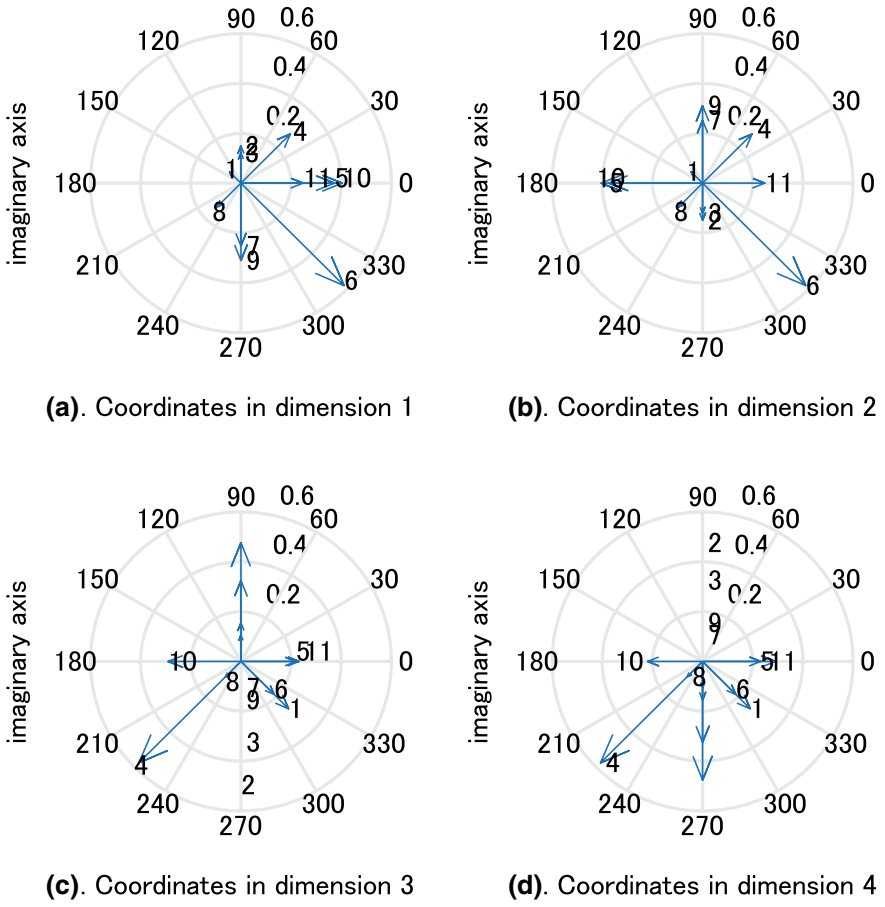

Fig. 7 Four configurations of the biosynthetic pathways corresponding to one-dimensional Hilbert spaces, which constitute a part of the holistic 11-dimensional Hilbert space

Table 4 shows this. Here, it should be noticed that in general such a pathway can be considered as a weighted digraph (directed graph) in graph theory.

Since the weighted digraph accompanies a weight matrix, we say that a unique ASM is associated with any weighted digraph.

Eigenvalues of the Hermitian matrix constructed from this ASM were 1.6302, −1.6302, −1.2534, 1.2534, −0.8706, 0.8706, ... These eigenvalues mean that this data has a *holistic indefinite metric structure*. Of course, each of the configurations of the biosynthetic pathways of proteins in mammals on the complex planes associated with these eigenvalues can be embedded in a *one-dimensional Hilbert space*, as discussed previously.

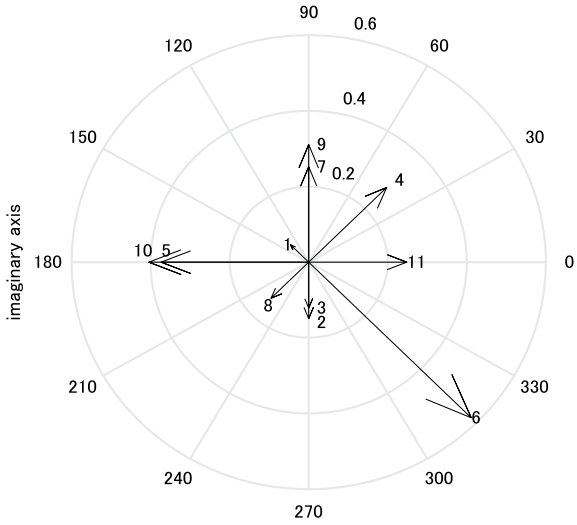

Fig. 8 An enlarged configuration of Fig. 7b

Figure 7 shows four configurations of the biosynthetic pathways composed of these one-dimensional Hilbert spaces. These four configurations are associated with the first four eigenvalues of the Hermitian matrix discussed above.

Figure 7a, is the configuration associated with the maximum eigenvalue of the Hermitian matrix. Although this configuration recovers the major pathways contained in the original data matrix, it does not include the important cyclic pathways, starting from O_6 (NAD) to come back to it through O_9 (NIC) and O_{10} (NMN). In contrast, Fig. 7b, which is the configuration corresponding to the maximum eigenvalue but with negative sign, recovers almost all the pathways contained in the original matrix. Figure 8 is an enlarged configuration of Fig. 7b. In interpreting this configuration, it should be noticed that its positive direction is *counterclockwise* because the eigenvalue associated with it is negative. Noticing this point, we can find the following pathways in Fig. 8 by following an object to another object *counterclockwise* within π radian, referring to Fig. 2 of Imai and Guarente [11]:

1. O_1 (Tryptophan) $\rightarrow$ O_2 (Quinolinic acid) $\rightarrow$ O_4 (NaMN) $\rightarrow$ O_5 (deamido-NAD) $\rightarrow$ O_6 (NAD) $\rightarrow$ O_9 (NIC) $\rightarrow$ O_{10} (NMN) $\rightarrow$ O_6 (NAD)
2. O_3 (NA) $\rightarrow$ O_4 (NaMN)
3. O_9 (NIC) $\rightarrow$ O_8 (1-methyl-nicotinamide)
4. O_6 (NAD) $\rightarrow$ O_7 (O-acetyl-ADP-ribose)

The first pathway includes a cycle starting from O_6 and returning to itself. The second pathway runs into the first pathway at O_4 (NaMN). The third pathway gets away from the first pathway at O_9 (NIC). The fourth pathway also gets away from the first pathway at O_6 (NAD).

5 Applications of HFM to Theoretical or Hypothetical Asymmetric Relational Data Matrices

In this section, we show two applications of HFM to theoretical or hypothetical asymmetric relational data matrices. Sato et al. [17] investigated the problem of learning to play the game of rock-paper-scissors, using the following set of nonlinear differential equations.

$$\begin{bmatrix} \dot{x}_i \\ \dot{y}_j \end{bmatrix} = \begin{bmatrix} x_i \left((\boldsymbol{A}\boldsymbol{y})_i - \boldsymbol{x}^t \boldsymbol{A}\boldsymbol{y} \right) \\ y_j \left((\boldsymbol{B}\boldsymbol{x})_j - \boldsymbol{y}^t \boldsymbol{A}\boldsymbol{x} \right) \end{bmatrix}, i = 1, \cdots, n, j = 1, \cdots, m, \tag{30}$$

where $\boldsymbol{x} = (x_1, \ldots, x_n)^t$ is the relative frequency vector for one population, while $\boldsymbol{y} = (y_1, \ldots, y_m)^t$ is that for the second population. This approach is based on the theory of games and the notion of *evolutionarily stable strategy* (abbreviated as ESS), of which theory was introduced by Maynard and Price [12].

In any case, in Eq. (30) **A** is the payoff matrix for one population, while **B** is the payoff matrix for the second population, and these two matrices are denoted as

$$\mathbf{A} = \begin{bmatrix} \varepsilon_x & -1 & 1 \\ 1 & \varepsilon_x & -1 \\ -1 & 1 & \varepsilon_x \end{bmatrix}, \mathbf{B} = \begin{bmatrix} \varepsilon_y & -1 & 1 \\ 1 & \varepsilon_y & -1 \\ -1 & 1 & \varepsilon_y \end{bmatrix}, \tag{31}$$

where $-1 < \varepsilon_x < 1$ and $-1 < \varepsilon_y < 1$. Here, columns of these matrices are placed in the order of "rock", "paper", and "scissors". If $\varepsilon_x = -\varepsilon_y = \varepsilon$, this game is called a *zero sum game.* In matrix notation, this condition is denoted as $\mathbf{A} = -\boldsymbol{B}^t$. Matrices, **A** and **B**, are nothing but *theoretical* examples of ASM, in that these ASMs cannot be observed and are hypothesized a priori.

Although Sato et al. [17] discusses these matrices from the viewpoint of a dynamical system, they do not discuss the *metric structure* of these matrices. Such a structure can be examined by applying HFM to them. Let us now examine the structure of **A** in the case when $\varepsilon_x = 0.25$, which is one of the cases in which ε_x and ε_y are treated as a bifurcation parameter of the dynamical system described by Eq. (30). The eigenvalues of the Hermitian matrix constructed from this ASM were 1.9821, −1.4821, 0.2500. These eigenvalues mean that this data has a *holistic indefinite metric structure*. Figure 9 shows this structure. Each of the configurations shows the positions of the three elements, i.e., "1. rock", "2. paper", and "3. scissors", in a one-dimensional Hilbert space. Again, these configurations are complex orthogonal (unitary) in the holistic indefinite metric space.

Figure 10 shows the enlarged configuration of Fig. 9a. It should be noticed that the eigenvalue corresponding to it is positive. This means that the positive direction of this configuration is *clockwise*. Considering this point, we can conclude that 1 (rock) defeats 3 (scissors), 3 defeats 2 (paper), and 2 defeats 1. These relations completely reproduce the triadic relations assumed in the rock-paper-scissors game.

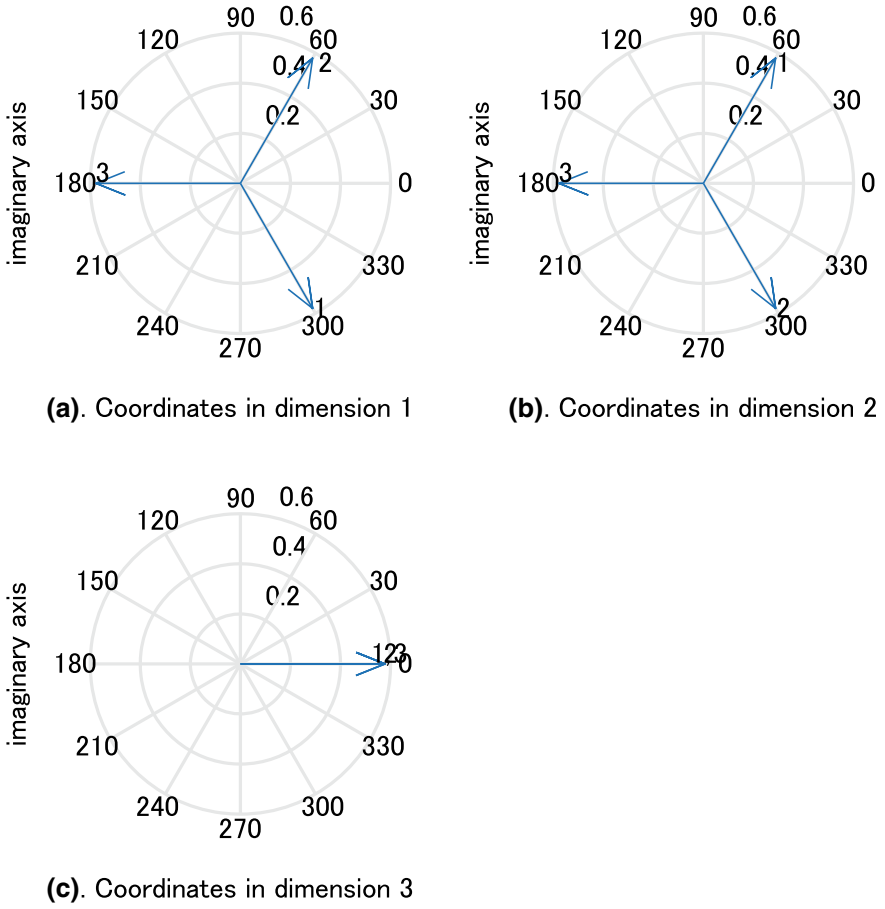

Fig. 9 Three configurations of the payoff matrix **A** corresponding to one-dimensional Hilbert spaces, which constitute the holistic 3-dimensional Hilbert space

Figure 11 shows the enlarged configuration of Fig. 9b. It should be noticed that the eigenvalue corresponding to it is *negative*. This means that the positive direction of this configuration is *counterclockwise*. Considering this point, we see that the same triadic relations as in Fig. 10 are reproduced.

Figure 9c is the configuration whose associated eigenvalue is *positive*. As a result, the positive direction of this configuration is *clockwise*. However, regardless of this information, the configuration reveals the collapse of the triadic relations.

Another application of the theoretical ASM is the following matrix,

$$\mathbf{C} = \begin{bmatrix} 1 & -1 & 1 \\ 1 & 1 & -1 \\ -1 & 1 & 1 \end{bmatrix}. \tag{32}$$

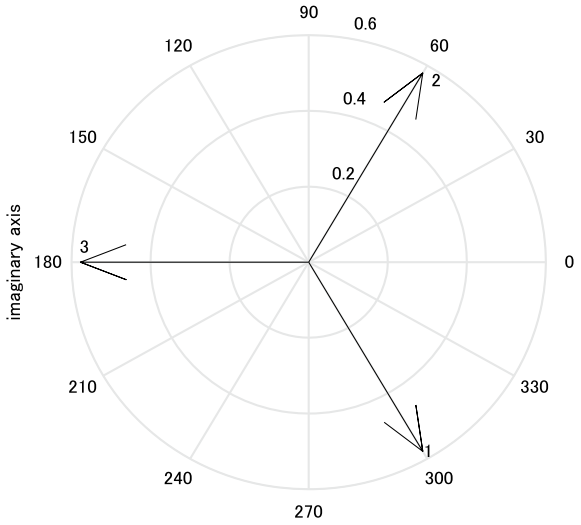

Fig. 10 Configuration of elements (1. Rock, 2. Paper, 3. Scissors) in the one-dimensional Hilbert space, which corresponds to the largest eigenvalue of **H** (the enlarged configuration of Fig. 9a

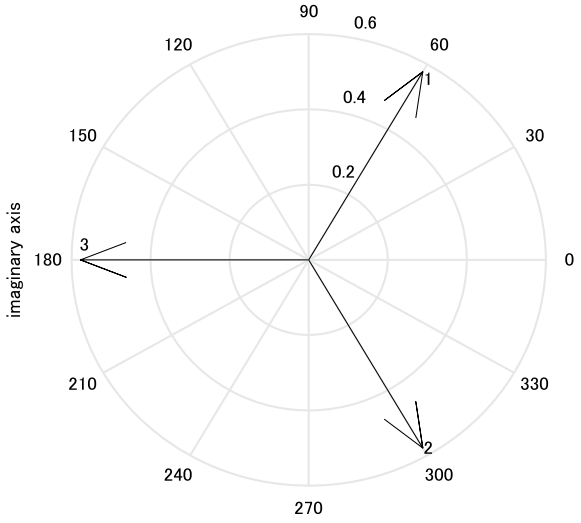

Fig. 11 Configuration of elements (1. Rock, 2. Paper, 3. Scissors) in the one-dimensional Hilbert space, which corresponds to the second largest eigenvalue of **H** (the enlarged configurations of Fig. 9b)

According to the rock-paper-scissors game, **C** is not the payoff matrix, because ε in Eq. (31) is out of the range defined in the payoff matrices. However, such a matrix is plausible as a general ASM, and has already been analyzed elsewhere (e.g., Chino [2]).

In fact, eigenvalues of the Hermitian matrix constructed from this ASM were 2.7321, 1.000, and −0.7321. These eigenvalues mean that this data has a *holistic indefinite metric structure*. Figure 12 shows this structure. Each of the configurations shows the positions of the three elements, i.e., "1. rock", "2. paper", and "3. scissors", in a one-dimensional Hilbert space.

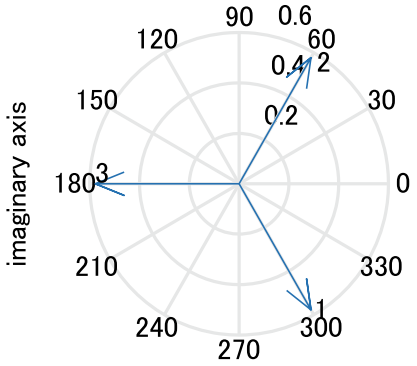

(a). Coordinates in dimension 1

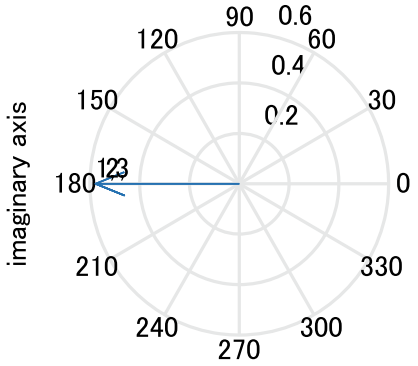

(b). Coordinates in dimension 2

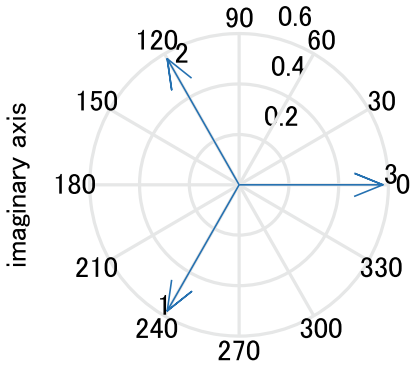

(c). Coordinates in dimension 3

Fig. 12 Three configurations of the matrix **C** in Eq. (32) corresponding to one-dimensional Hilbert spaces, which constitute the holistic 3-dimensional Hilbert space

Figure 13 shows the enlarged configuration of Fig. 12a. At a glance, this configuration is completely different from that of Fig. 12. However, the sign of the eigenvalue corresponding to the configuration of Fig. 11 is *negative*, while that of Fig. 13 is *positive*. This means that these two configurations indicate the same information about the asymmetric relations among elements.

Similarly, we see that Figs. 9c and 12b convey the same information about the asymmetric relations among elements, considering the signs of the eigenvalues corresponding to these configurations. We also find that Figs. 9b and 12c convey the same information. However, it should be noticed that the sizes of the eigenvalues for these pairs of figures are different from one another. This means that the contributions of one-dimensional Hilbert space structures to the holistic space structure depend on the diagonal elements, i.e., ε in Eq. (31), in the case of tripartite deadlock relation.

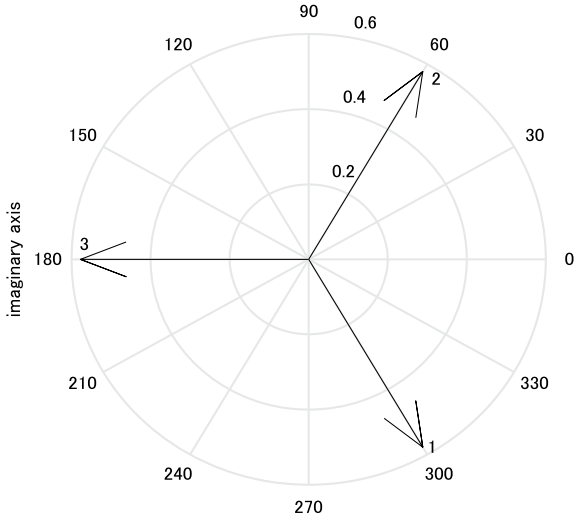

Fig. 13 Configuration of elements (1. Rock, 2. Paper, 3. Scissors) in the one-dimensional Hilbert space, which corresponds to the largest eigenvalue of **H** associated with **C** (the enlarged configuration of Fig. 12a)

6 Decomposition of ASM to Elementary ASMs via HFM

In the application sections we have seen that HFM enables us to get *multiple configurations* of objects which are *mutually complex orthogonal* (i.e., unitary), given any empirical ASM or theoretical ASM. Moreover, we can recover *real* component ASMs' from these configurations of objects embedded in a *complex* space (i.e., Hilbert space or indefinite space), using Eq. (20) of HFM.

For example, the theoretical ASM defined by Eq. (32) has three configurations of objects in the complex space, as shown in Fig. 12 in the previous section. If we compute *component ASMs* from these configurations using Eq. (20), we have

$$\boldsymbol{C}_1 = \begin{bmatrix} 0.333 & -0.455 & 0.122 \\ 0.122 & 0.333 & -0.455 \\ -0.455 & 0.122 & 0.333 \end{bmatrix}, \boldsymbol{C}_2 = \begin{bmatrix} 0.333 & -0.455 & 0.122 \\ 0.122 & 0.333 & -0.455 \\ -0.455 & 0.122 & 0.333 \end{bmatrix},$$

$$\text{and } \boldsymbol{C}_3 = \begin{bmatrix} -0.333 & -0.122 & 0.455 \\ 0.455 & -0.333 & -0.122 \\ -0.122 & 0.455 & -0.333 \end{bmatrix}. \tag{33}$$

Since these component ASMs are associated with the three configurations of which eigenvectors are mutually complex orthogonal, these component ASMs convey unrelated information about objects with one another. Therefore, if we apply HFM to some empirical ASM as in Table 4, and if we find a component configuration which is not congruent with the previous results of the experiment, it might be worthwhile to examine theoretically and/or experimentally whether such a configuration exists or not substantively.

7 Hypothetical Force Acting on the Hilbert Space and Its Interpretation

The ASMs we have dealt in the previous sections are matrices observed at some instant of time, or those assumed theoretically or hypothetically. However, in actual situations an ASM frequently changes as time proceeds through the *mutual interactions* among objects. In such a case, configuration spaces obtained by HFM can be thought of as *state spaces* of some underlying *dynamical system*. The state space understudy is, of course, the Hilbert space or indefinite metric space.

Then, we can naturally introduce some *forces* acting on these state spaces by which objects move as time proceeds (e.g., Elaydi [7]; Hirsch & Smale [9]). As a result, the configuration of objects changes as time proceeds. If we take a snapshot of such a process at some instant in time, we can compute the *longitudinal ASMs* using Eq. (20) of HFM. Figure 14 shows an illustration of forces exerting on the configuration space in Fig. 6. In fact, trade imbalance changes year after year by the political and economic interactions among nations.

In Fig. 14, blue arrows denote the *position vectors* of the four nations, while red arrows indicate *usual vectors* denoting here the *forces* acting on the two nations, A (USA) and J (Japan). According to these forces, USA approaches Japan, while Japan does not necessarily approach America. These forces can be defined as the *mutual interaction matrix* as follows. In this case its order is four, which corresponds to the number of nations.

$$\mathbf{M} = \begin{bmatrix} m_{11} & m_{12} & m_{13} & m_{14} \\ m_{21} & m_{22} & m_{23} & m_{24} \\ m_{31} & m_{32} & m_{33} & m_{34} \\ m_{41} & m_{42} & m_{43} & m_{44} \end{bmatrix}. \tag{33}$$

Here, each element of this matrix is a *complex number*. Moreover, subscript numbers, 1, 2, 3, and 4, denote J (Japan), A (USA), C (China), and R (Russia), respectively, as in Table 3. Therefore, the force emanating from USA to Japan can be expressed as, say, $m_{21} = 0.07 + 0.1i$, and that issuing from Japan to USA can be expressed as, say, $m_{12} = 0.1 - 0.01i$. We assume that the matrix $\mathbf{M}$ is defined *theoretically* or *hypothetically*, although it is also an ASM. Moreover, we assume that its elements are all *constant*.

The mutual interaction matrix is sometimes used in dynamical system models. For example, the payoff matrices hypothesized by Sato et al. [17] which was discussed in Sect. 5 are considered as such mutual interaction matrices. The weight matrix representing hidden-to-hidden recurrent connections assumed in *recurrent neural network models* is thought of as another example (e.g., Goodfellow et al. [8]). In this case, however, the weight matrix is *real*. Chino [3, 4] has recently been developing a *dynamic weighted digraph model* using a set of *nonlinear complex difference equations*, in which a mutual interaction matrix is hypothesized to explain changes in the

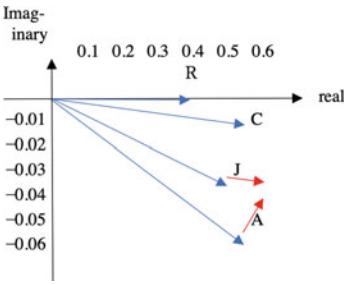

Fig. 14 An illustration of forces exerting on the configuration space in Fig. 6. Red arrows indicate the forces acting on the two nations, America and Japan. Here, the positive direction of this figure is clockwise because the eigenvalue is positive in this case

observed ASM over time. In this case, the elements of the interaction matrix are *not real but complex*, one example of which is the matrix **M** defined in Eq. (33).

8 Conclusions

HFM is one of the MDS models which is specifically designed to analyze asymmetric (dis)similarity matrix (abbreviated as ASM), and was proposed by Chino and Shiraiwa [5]. Among various asymmetric MDS models which have been proposed up to now, HFM is a special one in that embedded spaces are *complex*, especially, a (complex) Hilbert space or an indefinite space, although original ASMs are always *real*. This property might sometimes be a barrier for users' understanding of HFM. Therefore, we explained in this paper how to use HFM to various ASMs which are observed in our daily lives, in research laboratories, and so on.

In the introductory section, we gave some typical examples of ASMs and point out that the ratio level of measurement is required for the elements of ASM to which we apply HFM. In Sect. 2, we revisited HFM and explained the reason why it is promising to introduce a complex space in order to summarize the real asymmetric relationships among objects. The keyword for introducing complex spaces is the *Hermitian form* defined in the complex space. Formulae which play important roles in relating any ASM, **S**, with this form are obtained by considering the two elementary equations, i.e., Eqs. (2) and (3) in that section. On the way to deducing the HFM, we also get an important formula, Eq. (20). This equation builds a bridge between the similarity from O_j to O_k (*real*) and coordinate vectors of the two objects (*complex*).

If we apply HFM to any ASM, then we get multiple configurations of objects embedded in a (complex) Hilbert space or an indefinite metric space, depending on the signs of the eigenvalues of the Hermitian matrix **H** in Eq. (3). If the nonzero eigenvalues are all positive, we may adopt a Hilbert space as a holistic configuration space. Otherwise we may adopt an indefinite metric space as a holistic space. Moreover, we may interpret these configurations separately per dimension, because these configurations, which are associated with the eigenvectors corresponding to these eigenvalues, are *unitary*, i.e., complex orthogonal. Furthermore, each of these configurations can be thought of as embedded in a one-dimensional Hilbert space,

which can be regarded as a (real) Euclidean two-dimensional space, except the sign of the corresponding eigenvalue. If the sign is positive, we may consider that the positive direction of the configuration is *clockwise*, and if the sign is negative, we may regard it as *counterclockwise*. In Sects. 4 and 5, we pointed out two empirical ASMs and two theoretical or hypothetical ASMs, and explained how to interpret the obtained configurations of objects via HFM.

In Sect. 6, we focused on a theoretical or hypothetical ASM, and explained how to recover the component ASMs from the multiple configurations of objects. In Sect. 7, we discussed the cases in which ASM changes as time proceeds. In such cases, it will be appropriate and natural to introduce some *forces acting on the complex spaces* by which objects move as time proceeds. Then, it may be appropriate and natural to introduce a *dynamical system model* in which some *mutual interaction matrix* is assumed.

Acknowledgements The author is indebted to Gregory L. Rohe for proofreading of an earlier version of this paper.

References

1. Chino, N. (1978). A graphical technique for representing the asymmetric relationships between N objects. *Behaviormetrika*, *5*, 23–40.
2. Chino, N. (2017). Dynamical scenarios of changes in asymmetric relationships on a Hilbert space. *Handout Presented at the 45th annual meeting of the behaviormetric society of Japan* (pp. 1–29).
3. Chino, N. (2018). An elementary theory of a dynamic weighted digraph. In *Proceedings of the 46th annual meeting of the behaviormetric society of Japan* (pp. 26–29).
4. Chino, N. (2019). An elementary theory of a dynamic weighted digraph (1). In *Proceedings of the 47th annual meeting of the behaviormetric society of Japan* (pp. 56–59).
5. Chino, N., & Shiraiwa, K. (1993). A brief survey of asymmetric MDS and open problems. *Behaviormetrika*, *39*, 127–165.
6. Cristescu, R. (1977). *Topological vector spaces*. Leyden: Noordhoff International Publishing.
7. Elaydi, S. N. (1999). *An introduction to differential equations*. New York: Springer.
8. Goodfellow, I., Bengio, Y., & Courville, A. (2016). *Deep learning*. Cambridge: The MIT Press.
9. Hirsch, M. W., & Smale, S. (1974). *Differential equations, dynamical systems, and linear algebra*. New York: Academic Press.
10. Imai, S. (2011). Dissecting systematic control of metabolism and aging in the NAD World: The importance of SIRT1 and NAMPT-mediated NAD biosynthesis. *FEBS Letters*, *585*, 1657–1662.
11. Imai, S., & Guarente, L. (2014). NAD^+ and sirtuins in aging and disease. *Trends in Cell Biology*, *24*, 464–471.
12. Maynard Smith, J., & Price, G. R. (1973). The logic of animal conflict. *Nature*, *246*, 15–18.
13. Okada, A. & Imaizumi, T. (1984). Geometric models for asymmetric similarity. *Research Reports of School of Social Relations*, *Rikkyo (St. Paul's) University*.
14. Okada, A., & Imaizumi, T. (1987). Nonmetric multidimensional scaling of two-mode, three-way proximities. *Journal of Classification*, *14*, 195–224.
15. Rushen, J. (1982). The peck orders of chickens: How do they develop and why are they linear? *Animal Behavior*, *30*, 1129–1137.

16. Saburi, S., & Chino, N. (2008). A maximum likelihood method for an asymmetric MDS model. *Computational Statistics and Data Analysis*, *52*, 4673–4684.
17. Sato, Y., Akiyama, E., & Farmer, J. D. (2002). Chaos in learning a simple two-person game. *Proceedings of the National Academy of Science of the United States of America*, *99*, 4748–4751.

Asymmetric Scaling Models for Square Contingency Tables: Points, Circles, Arrows and Odds Ratios

Mark de Rooij

Abstract We study two asymmetric scaling methods within the context of loglinear modelling of square contingency tables: the distance-radius model and the slide-vector model. The usual association parameters of a loglinear model are replaced by a distance term. We are specifically interested in whether and how the asymmetry in these methods translates to odds ratio structures, as the latter is a primary measure of association for contingency tables. We define models in terms of distances and squared distances. We show that the distance-radius model with distances and the slide-vector model with squared distances do not represent asymmetry in the odds ratios. Finally, we also study models without main effects, where the distances directly represent the observed frequencies. We show that in that case the distance-radius model perfectly represents marginal heterogeneity.

1 Introduction

Professor Okada was a member of the committee that evaluated my Ph.D. thesis. In that time (2001) Leiden University had a system where first a main reviewer (called a referent) evaluated the thesis and after approval of this referent the thesis went to a committee for approval. Professor Okada was the referent of my thesis entitled *Distance models for transition frequency data*. Afterwards Professor Okada and I met oftentimes in conferences of various classification societies as well as the psychometric society.

My first memory of meeting Professor Okada goes back to the European meeting of the Psychometric Society in Lueneburg (Germany 1999). Okada gave a presentation about his and Professor Imaizumi's asymmetric multidimensional scaling

M. de Rooij (✉)
Department of Methodology and Statistics, Institute of Psychology, Leiden University, Leiden, The Netherlands
e-mail: rooijm@fsw.leidenuniv.nl

T. Imaizumi et al. (eds.), *Advanced Studies in Behaviormetrics and Data Science*,
Behaviormetrics: Quantitative Approaches to Human Behavior 5,
https://doi.org/10.1007/978-981-15-2700-5_3

method for three-way two-mode data (Okada & Imaizumi [7]), because as he told the audience 'several people asked me to present again this scaling procedure' while the program gave another topic.

I recently asked Professor Okada about his remembrance of first meeting me. Akinori indicated that we first met at the European Meeting of the Psychometric Society in Santiago de Compostela (Spain 1997). This meeting was my first conference as a young Ph.D student and I was quite overwhelmed by so many new ideas and all kinds of other impressions.

Nevertheless, we see that there is *asymmetry* in our memories. Asymmetry is also the research topic of mutual interest, more specifically the representation of asymmetric data using distance-based graphs. Asymmetric data are collected in many areas of science, for example in psychology where memories are often asymmetric (as shown above), in political science where voters change their vote from one political party to another, or in marketing science where certain products become more popular, or in demographic studies where from generation to generation changes occur in the distribution over occupational classes.

In this paper, we will focus on the analysis of square contingency tables in a loglinear modelling framework, similar to the work of De Rooij and Heiser [4]. That is, we define a model for the expected frequencies of a contingency table and fit it by maximizing the Poisson likelihood. In the models the association term of a loglinear model for a two-way contingency table is replaced by a distance term. The distance formulations we consider are the Euclidean distance, the distance-radius model and the slide-vector model. Furthermore, we will distinguish between distances and squared distances. The squared Euclidean distance was also used in De Rooij and Heiser, where they coined this model the symmetric distance-association model.

The distance-radius model was proposed by Okada and Imaizumi [6] for two-way matrices and later extended to three-way two-mode data in Okada and Imaizumi [7]. The model uses the radius of circles to represent asymmetry (for more details see Sect. 3).

The slide-vector model was proposed by Zielman and Heiser [9]. The slide-vector model uses a vector or arrow, to point out the direction of asymmetry (for more details see Sect. 3). The distance-radius model and the slide-vector model were proposed together with least squares algorithms. To apply the models to square contingency tables the frequencies have to be transformed to (dis)similarities. Such a transformation can be performed in different ways, making the relationship between the original data and the data analysis sometimes a bit vague. Okada and Imaizumi [6], for example, write

> The original car switching data represent large differences in the size of the frequencies which reflect the large differences in market share. These size differences should be removed in order to distinctively unveil the factors which control the car switches. Hence the size differences were taken away by means of multiplying each row and column by rescaling coefficients.

Zielman and Heiser [9] use the same data in their paper. They write

> The raw brand switching matrix is not appropriate as input for the scaling program. The matrix has to be adjusted for differences in market share and the data have to be converted from similarities to dissimilarities. These two steps can be performed by applying the gravity model, which amounts to first dividing the raw frequencies y_{ij} by their row and column sum; and secondly, inverting the standardized frequencies. These inverted numbers yield squared distances according to the gravity model, so as a last step the square root of the quantities is taken.

These different transformations make the comparison between the outcomes of the two analyses difficult: is the difference due to the models or due to the preprocessing? Even if those preprocessing steps would be the same, we could still wonder how to combine the preprocessing and the model into a final conclusion about the data. When we combine the preprocessing and the distances into a single model one is forced to think in terms of the data. Moreover, it becomes clear which aspects of the data are represented by which part of the analysis (Timmerman [8]).

The modelling framework we develop in the next sections enables us to have a closer look at differences and similarities between the models. By putting different distance formulations in the same framework for the analysis of frequency data directly, we obtain a clearer picture. We will be specifically interested in how the different distance formulations represent the association structure as defined by the odds ratio. The odds ratio is independent of the marginal distribution of the variables and therefore an important statistic for the analysis of contingency tables.

In the next section we will outline the general modelling framework. In Sect. 3 we present three distance formulations. In Sect. 4 we derive the representation of the odds given the three distance formulations. In Sect. 5 we analyse an empirical data set, which will be introduced in the next section. Section 6 concludes with a discussion.

2 Modelling of Square Contingency Tables

We will be interested in the analysis of square contingency tables, i.e. tables where the row and column variables have the same categories and the entries represent a frequency. An example is given in Table 1, where a 10×10 table is presented within the rows occupational categories for the father and in the columns the same categories for their sons (Ganzeboom & Luijkx [5]; De Rooij [3]). The occupational categories are (1) Large proprietors, higher professionals and managers; (2) Lower professionals and managers; (3) Routine nonmanual workers; (4) Small proprietors with employees; (5) Small proprietors without employees; (6) Lower grade technicians and manual supervisors; (7) Skilled manual workers; (8) Unskilled and semiskilled manual workers; (9) Self-employed farmers and (10) (Unskilled) agricultural workers. Although not strict, overall a lower number represents a higher social status category.

The entries in the table represent how often the combination of a row and column entry is observed simultaneously, i.e. the number 52 represents fifty-two fathers in occupational category 1 whose sons were also employed in this category. The

Table 1 Occupational mobility data within the rows occupational categories for the father and in the columns the same categories for their sons

Fathers	Sons										+
	1	2	3	4	5	6	7	8	9	10	
1	52	94	43	4	7	5	11	17	2	1	236
2	50	121	42	3	6	9	37	26	2	5	301
3	36	65	40	7	4	5	23	20	3	1	204
4	21	31	17	18	2	1	9	12	0	0	111
5	8	23	11	6	1	2	14	12	0	1	78
6	14	19	11	2	2	6	8	10	0	1	73
7	32	76	48	5	1	12	80	65	2	1	322
8	21	45	39	3	7	11	63	59	5	3	256
9	23	52	14	3	3	7	33	32	61	10	238
10	5	10	10	1	0	3	19	13	2	2	65
+	262	536	275	52	33	61	297	266	77	25	1884

numbers are denoted by y_{ij}, for $i, j = 1, \ldots, I$, which are the observed frequencies representing fathers in category i and their sons in category j.

Similar tables can be observed in longitudinal research with a categorical variable. In that case, a cross-tabulation of the categories of interest at time point 1 against time point 2 can be made. Also in citation research, we can make a contingency table, where in the rows and columns we have journals and the entries denote how often a row journal cites a column journal.

In all these examples, the diagonal entries of the table are usually large compared to the off-diagonal entries. In Table 1 for example, there are 440 father–son pairs who have the same occupational category, while there are 1444 pairs who differ in occupational category. Most often, the interest in the analysis of such data is in change, that is, in the off-diagonal entries of such a table. Therefore, weights w_{ij} can be used, which are equal to one if $i \neq j$ and 0 otherwise.

2.1 Poisson Model

We will define models for square contingency tables with observed counts y_{ij}. Given the model, expected values are denoted by μ_{ij}. Different models put different structures on these expected values. In what follows, all models are defined as follows:

$$\log(\mu_{ij}) = \lambda + \lambda_i^R + \lambda_j^C - \delta_{ij}, \tag{1}$$

where λ_i^R and λ_j^C are the main effects that model the marginal distributions of the table (i.e. the market share in the quotes of Sect. 1), λ is a constant ensuring that

the sum of expected frequencies equals the sum of observed frequencies, and δ_{ij} represents a (squared) distance function. The distance is inversely related to the expected frequencies: the larger the distance the smaller the expected frequency, the smaller the distance the larger the expected frequency. We will consider different distance functions and compare the models, more details will follow in the next sections.

To estimate the parameters we will minimize the Poisson deviance as defined by

$$D = -2 \sum_{i,j=1}^{I} y_{ij} \log(\mu_{ij}) - \mu_{ij}.$$

As argued above for square contingency tables, the diagonal values are often very large compared to the off-diagonal values while the interest is not so much in these entries. Therefore, in the analysis of such tables the diagonal entries receive a weight of zero or the model is extended with an extra set of parameters for the diagonal cells. We will use the weighted Poisson deviance, which is defined as

$$D_w = -2 \sum_{i,j=1}^{I} w_{ij} \left(y_{ij} \log(\mu_{ij}) - \mu_{ij} \right),$$

where $w_{ij} = 0$ when $i = j$, otherwise $w_{ij} = 1$.

2.2 Model Fit

To assess model fit we will use two chi-square distributed statistics, the Pearson chi-square test and the Likelihood ratio test. The Pearson chi-square statistic is defined as

$$X^2 = \sum_{i,j} w_{ij} \left(\frac{(y_{ij} - \mu_{ij})^2}{\mu_{ij}} \right),$$

and the Likelihood ratio chi-square statistic as

$$G^2 = 2 \sum_{i,j} w_{ij} \left(y_{ij} \log \frac{y_{ij}}{\mu_{ij}} \right).$$

Both statistics are chi-square distributed given a number of degrees of freedom (*df*) which depend on the specific model structure. For comparison of different model structures we will use Akaike's Information Criterion, which is defined as

$$AIC = G^2 - 2df.$$

2.3 Marginal Heterogeneity and Association

Having a square contingency table, the interest often focusses on two facets: (1) changes in marginal distributions and (2) the association pattern. For the data in Table 1 the marginal distribution for the fathers is presented in the last column (labelled '+') while that of the sons is presented in the last row. We see that occupational classes 1 (+26), 2 (+235), 3 (+71) and 8 (+10) became larger while 4 (−59), 5 (−45), 6 (−12), 7 (−25), 9 (−161) and 10 (−40) became smaller. In our generic model (Eq. 1), the marginal distributions are modelled using the main effect terms, the λ_i^R and λ_j^C.

An important tool for understanding association patterns for contingency tables is the odds ratio

$$\frac{y_{ij}\,y_{i'j'}}{y_{i'j}\,y_{ij'}} = \frac{p_{ij}\,p_{i'j'}}{p_{i'j}\,p_{ij'}},$$

where p_{ij} denotes the cell proportion ($y_{ij} = np_{ij}$). The odds ratio is an important tool because it is independent from the marginal distributions.

For a $I \times 2$ table the odds of category 1 for row i is the probability of category 1 divided by the probability category 2, i.e. p_{i1}/p_{i2}, where a value larger than 1 indicates that the probability for category 1 is larger than the probability for category 2. The odds ratio compares the odds for two different rows i and i'

$$\frac{p_{i1}/p_{i2}}{p_{i'1}/p_{i'2}} = \frac{p_{i1}\,p_{i'2}}{p_{i'1}/p_{i2}}.$$

The odds ratio is a nonnegative number and equal to 1 when the odds in the two rows are equal, meaning no association. Values larger than 1 indicate that the odds in row i are larger than the odds in row i'. The further the value is away from 1 the stronger the association, where an odds ratio of $\frac{1}{4}$ indicates a similar strength as an odds ratio of 4. See Agresti [1] for further properties of the odds ratio. Often we take a log-transform of the odds ratio, which makes the statistic symmetric around zero, $\log(\frac{1}{4}) = -\log(4)$.

The log of the odds ratio can also be defined in terms of the expected frequencies (or probabilities) and then be expressed in terms of the model parameters. For our generic model (Eq. 1) we have

$$\theta_{ii'jj'} = \log\left[\frac{\mu_{ij}\mu_{i'j'}}{\mu_{i'j}\mu_{ij'}}\right] = -\delta_{ij} - \delta_{i'j'} + \delta_{i'j} + \delta_{ij'}.$$

In the next sections we will work out the model implied log odds ratio for different definitions of δ_{ij}.

We will be specifically interested in symmetric and asymmetric odds ratio structures. We call the odds ratio symmetric when $\theta_{ii'jj'} = \theta_{jj'ii'}$. For example, from the data we can compute

1. the observed odds that a son of a father who is a in category 5 (small proprietor without employees) falls in category 1 (large proprietor/higher professional/manager) instead of category 2 (lower professional and manager) is half those same odds for a father in category 6 (lower grade technician and manual supervisors), i.e. $\exp(\theta_{5612}) = \frac{8/23}{14/19} = 0.47$, the log of this odds ratio equals $\theta_{5612} = -0.75$.
2. the observed odds that a son of a father who is a in category 1 falls in category 5 instead of category 6 is twice those same odds for a father in category 2, i.e. $\exp(\theta_{1256}) = \frac{7/5}{6/9} = 2.1$, the log of this odds ratio equals $\theta_{1256} = 0.74$.

We see that these log odds ratios are not equal, i.e. they are asymmetric. We expect asymmetric models to represent asymmetric odds ratio structures.

3 Three Distance Formulations

In our generic model we have the term δ_{ij}. We will in this section consider specifications for this term. For example, in Sect. 3.1 we use the distance-radius model and define $\delta_{ij} = d_{ij}^p(\mathbf{X}, \mathbf{r})$ for $p \in \{1, 2\}$ and in Sect. 3.2 we use the slide-vector model and define $\delta_{ij} = d_{ij}^p(\mathbf{X}, \mathbf{z})$.

3.1 Distance-Radius Model

The first asymmetric multidimensional scaling model we consider is the one proposed by Okada and Imaizumi [6] which is a distance-radius model. Their distance measure is defined as

$$d_{ij}(\mathbf{X}, \mathbf{r}) = d_{ij}(\mathbf{X}) - r_i + r_j,$$

where $\mathbf{X}$ is a $I \times M$-matrix with coordinates (x_{im} of the points representing the categories (i) of the contingency table in the M-dimensional space ($m = 1, \ldots, M$). The r_i represent the radius of a circle for each category, the centre of which is defined as the point representing that category. The r_i are constrained to be larger than zero, and identified by setting the smallest equal to zero.

In a graphical representation (see Fig. 1) the objects are depicted as points with coordinates $\mathbf{x}_i$ in a Euclidean space each having a circle with radius r_i. In the plot we show two points labelled 1 and 2 with radii 0.75 and 0.25. The distance from point 1 to 2 following the definition, $d_{12}(\mathbf{X}, \mathbf{r}) = 2 - 0.75 + 0.25$, is given by the red dotted line, the distance from 2 to 1 is given by the blue dashed line ($d_{21}(\mathbf{X}, \mathbf{r}) = 2 - 0.25 + 0.75$). The blue line is longer (2.5) compared to the red line (1.5), i.e. there is asymmetry. The asymmetry is readily interpretable from the graph, i.e. the distance from a point with a large radius towards a point with a small radius is smaller than the other way around.

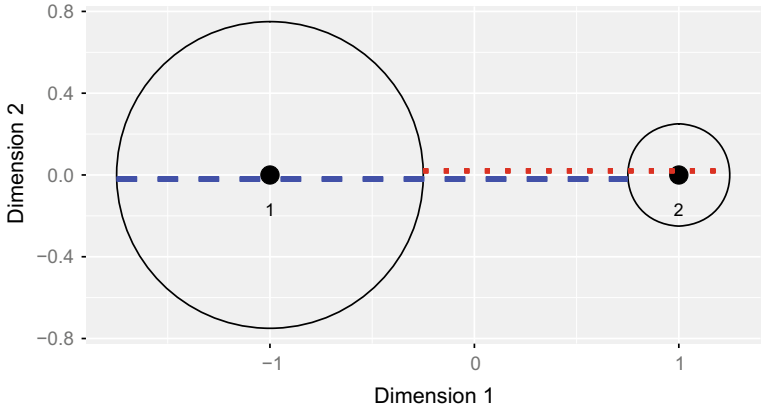

Fig. 1 The distance-radius model for two points with different sizes of radii. The distance between 1 and 2 is represented by the red dotted line, whereas the distance between 2 and 1 is represented by the blue dashed line

When we use $\delta_{ij} = d_{ij}^2(\mathbf{X}, \mathbf{r})$, with

$$d_{ij}^2(\mathbf{X}, \mathbf{r}) = \left(d_{ij}(\mathbf{X}) - r_i + r_j\right)^2,$$

the asymmetric effect is more pronounced, i.e. the squared distances are $2.5^2 = 6.25$ and $1.5^2 = 2.25$.

The number of parameters equals 1 for the λ parameter, $2(I-1)$ for the main effects of rows and columns, $I-1$ for the radius parameters (r), and $IM - M(M+1)/2$ for the coordinates. We solve the translational and rotational freedom indeterminacy by setting the upper diagonal entries in $\mathbf{X}$ equal to zero. The number of observations equals $I^2 - I$, so that the degrees of freedom for this model are $I^2 - I - 1 - 3(I-1) - (IM - M(M+1)/2) = I^2 - (M+4)I + M(M+1)/2 + 2$.

3.2 Slide-Vector Model

The slide-vector model was proposed by Zielman and Heiser [9] and is based on a configuration of points and a vector, representing a shift of the column points in the opposite direction (or a shift of the row points along the direction). In our framework we define

$$\delta_{ij} = d_{ij}^p(\mathbf{X}, \mathbf{z}))$$

with $p = \{1, 2\}$ and

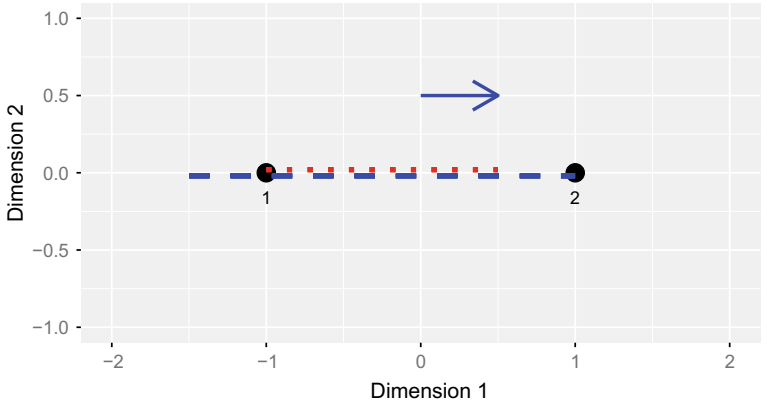

Fig. 2 The slide-vector model. The distance between 1 and 2 is represented by the red dotted line, whereas the distance between 2 and 1 is represented by the blue dashed line

$$d_{ij}(\mathbf{X}, \mathbf{z}) = \sqrt{\sum_m (x_{im} - x_{jm} + z_m)^2}.$$

In the slide-vector model we again have coordinates for the points representing the categories. Moreover, we have a vector of length M representing the slide-vector. If we define $y_{jm} = x_{jm} - z_m$ we see that the distance equals $\sqrt{\sum_m (x_{im} - y_{jm})^2}$, which is a so-called unfolding or two-mode distance. So, simply subtracting the slide-vector from the points and then inspecting the distance between the original points and the newly derived points (y_{jm}) reveals the asymmetry.

In a graphical representation (Fig. 2) the objects are depicted as points with coordinates $\mathbf{x}_i$ in a Euclidean space. Besides that there is an arrow representing the slide-vector. In the plot we show two points labelled 1 and 2. The distance from point 1 to 2 following the definition is given by the red line ($d_{12}(\mathbf{X}, \mathbf{z}) = \sqrt{(-1 - 1 + 0.5)^2}$), the distance from 2 to 1 is given by the blue line ($d_{21}(\mathbf{X}, \mathbf{z}) = \sqrt{(1 + 1 + 0.5)^2}$). The blue line is longer (2.5) compared to the red line (1.5), i.e. there is asymmetry. The asymmetry is readily interpretable from the graph, i.e. the distance from one point towards another in the direction of the slide-vector is smaller than the reverse distance. Note that when the slide-vector is orthogonal to the line connecting two objects, there is no asymmetry for these two points. The longer the slide-vector, the more asymmetry.

The number of parameters in the distance part of the slide-vector model is $(I + 1)M - M(M + 1)/2$, therefore the degrees of freedom for modelling a square contingency table excluding the diagonal equals $I^2 - I - 1 - 2(I - 1) - (I + 1)M + M(M + 1)/2 = I^2 - (M + 3)I + 1 + M(M - 1)/2)$.

3.3 Symmetric Distance-Association Model

In De Rooij and Heiser [4] we developed distance-association models. In the current paper, we will be specifically interested in the symmetric distance-association model as it will serve as a reference for the asymmetric models. In the symmetric distance-association model the only asymmetry that is modelled is marginal asymmetry, i.e. the model is a special case of the quasi-symmetry model (Caussinus [2]), where geometric constraints are placed on the symmetric association parameters. In the symmetric distance-association model δ_{ij} is defined by

$$\delta_{ij} = d_{ij}^p(\mathbf{X}) = \left(\sqrt{\sum_{m=1}^{M} (x_{im} - x_{jm})^2} \right)^p .$$

This is simply the Euclidean distance when $p = 1$ or the squared Euclidean distance when $p = 2$. These distances are symmetric, i.e. $d_{ij}^p(\mathbf{X}) = d_{ji}^p(\mathbf{X})$.

The number of parameters in this model is equal to 1 for the general λ-term, two times $I - 1$ for the main effects and $IM - M(M+1)/2$ for the coordinates. Note that in the distance part we have rotational and translational freedom, which are taken into account in the computation of the number of parameters. The degrees of freedom for this model are the number of observations $(I^2 - I)$ minus the number of parameters, which is $I^2 - I - 1 - 2(I-1) - IM + M(M+1)/2 = I^2 - I(M+3) + M(M+1)/2 + 1$.

4 Odds Ratio Structures

In this section we discuss odds ratio structures as implied by the three distance formulations, each for $p = 1, 2$. We like to show the difference between the two asymmetric models compared to the symmetric distance-association model. Therefore, we start with the latter, after which we discuss the distance-radius model and the slide-vector model.

4.1 Symmetric Distance-Association Model

Because $d_{ij}^p(\mathbf{X}) = d_{ji}^p(\mathbf{X})$ $(p = 1, 2)$, the symmetric distance-association model implies a symmetric association structure, i.e. $\theta_{ii'jj'} = \theta_{jj'ii'}$, i.e.

$$\begin{aligned} \theta_{ii'jj'} &= -d_{ij}^p(\mathbf{X}) - d_{i'j'}^p(\mathbf{X}) + d_{i'j}^p(\mathbf{X}) + d_{ij'}^p(\mathbf{X}) \\ &= -d_{ji}^p(\mathbf{X}) - d_{j'i'}^p(\mathbf{X}) + d_{ji'}^p(\mathbf{X}) + d_{j'i}^p(\mathbf{X}) = \theta_{jj'ii'}. \end{aligned}$$

4.2 The Distance-Radius Model

Let us start with the model using distances ($p = 1$), i.e.

$$\delta_{ij} = d_{ij}(\mathbf{X}, \mathbf{r})).$$

If we work out the logarithm of the odds ratio given by this model structure we have

$$\begin{aligned}
\theta_{ii'jj'} &= -d_{ij}(\mathbf{X}, \mathbf{r}) - d_{i'j'}(\mathbf{X}, \mathbf{r}) + d_{i'j}(\mathbf{X}, \mathbf{r}) + d_{ij'}(\mathbf{X}, \mathbf{r}) \\
&= -(d_{ij}(\mathbf{X}) - r_i + r_j) - (d_{i'j'}(\mathbf{X}) - r_{i'} + r_{j'}) \\
&\quad +(d_{i'j}(\mathbf{X}) - r_{i'} + r_j) + (d_{ij}(\mathbf{X}) - r_i + r_{j'}) \\
&= -d_{ij}(\mathbf{X}) - d_{i'j'}(\mathbf{X}) + d_{i'j}(\mathbf{X}) + d_{ij'}(\mathbf{X}) + r_i - r_j + r_{i'} - r_{j'} - r_{i'} + r_j - r_i + r_{j'} \\
&= -d_{ij}(\mathbf{X}) - d_{i'j'}(\mathbf{X}) + d_{i'j}(\mathbf{X}) + d_{ij'}(\mathbf{X}) \\
&= \theta_{jj'ii'},
\end{aligned}$$

i.e. no asymmetry beyond the margins is modelled anymore; the effect of the radii is absorbed by the main effects. Since the main effect parameters already model the marginal distributions perfectly, the addition of the circles is superfluous. As a result, the fit of the distance-association model ($p = 1$) and the distance-radius model ($p = 1$) will be the same.

For the distance-radius model with squared distances ($p = 2$) the logarithm of the odds ratio becomes

$$\theta_{ii'jj'} = -d^2_{ij}(\mathbf{X}, \mathbf{r}) - d^2_{i'j'}(\mathbf{X}, \mathbf{r}) + d^2_{i'j}(\mathbf{X}, \mathbf{r}) + d^2_{ij'}(\mathbf{X}, \mathbf{r}),$$

which can be further worked out into

$$\begin{aligned}
\theta_{ii'jj'} = &-d^2_{ij}(\mathbf{X}) - d^2_{i'j'}(\mathbf{X}) + d^2_{i'j}(\mathbf{X}) + d^2_{ij'}(\mathbf{X}) \\
&+2\left(d_{ij}(\mathbf{X}) - d_{ij'}(\mathbf{X})\right) r_i + 2\left(d_{i'j'}(\mathbf{X}) - d_{i'j}(\mathbf{X})\right) r_{i'} \\
&+2\left(d_{i'j}(\mathbf{X}) - d_{ij}(\mathbf{X})\right) r_j + 2\left(d_{ij'}(\mathbf{X}) - d_{i'j'}(\mathbf{X})\right) r_{j'} \\
&+2(r_i - r_{i'})(r_j - r_{j'}).
\end{aligned}$$

This is a quite difficult structure for interpretation. However, we see that on the first line the symmetric pattern is given, whereas the last three lines present asymmetry in the association structure. So, the distance-radius model with squared distances is modelling an asymmetric association pattern, while the same model based on distances does not.

4.3 The Slide-Vector Model

The logarithm of the odds ratio for the slide-vector model based on distances ($p = 1$) is

$$\begin{aligned}\theta_{ii'jj'} &= -d_{ij}(\mathbf{X},\mathbf{z}) - d_{i'j'}(\mathbf{X},\mathbf{z}) + d_{i'j}(\mathbf{X},\mathbf{z}) + d_{ij'}(\mathbf{X},\mathbf{z}),\\ &= -\sqrt{\sum_m (x_{im} - x_{jm} + z_m)^2} - \sqrt{\sum_m (x_{i'm} - x_{j'm} + z_m)^2}\\ &\quad + \sqrt{\sum_m (x_{i'm} - x_{jm} + z_m)^2} + \sqrt{\sum_m (x_{im} - x_{j'm} + z_m)^2},\end{aligned}$$

which cannot be further simplified. This shows that the odds ratio structure is asymmetric, $\theta_{ii'jj'} \neq \theta_{jj'ii'}$.

The logarithm of the odds ratio for the slide-vector model with squared distances ($p = 2$) is

$$\begin{aligned}\theta_{ii'jj'} &= -d^2_{ij}(\mathbf{X},\mathbf{z}) - d^2_{i'j'}(\mathbf{X},\mathbf{z}) + d^2_{i'j}(\mathbf{X},\mathbf{z}) + d^2_{ij'}(\mathbf{X},\mathbf{z}),\\ &= -(\sum_m (x_{im} - x_{jm} + z_m)^2) - (\sum_m (x_{i'm} - x_{j'm} + z_m)^2)\\ &\quad + (\sum_m (x_{i'm} - x_{jm} + z_m)^2) + (\sum_m (x_{im} - x_{j'm} + z_m)^2)\\ &= -(\sum_m x^2_{im} + x^2_{jm} - 2x_{im}x_{jm} + z^2_m + 2x_{im}z_m - 2x_{jm}z_m)\\ &\quad -(\sum_m x^2_{i'm} + x^2_{j'm} - 2x_{i'm}x_{j'm} + z^2_m + 2x_{i'm}z_m - 2x_{j'm}z_m)\\ &\quad +(\sum_m x^2_{i'm} + x^2_{jm} - 2x_{i'm}x_{jm} + z^2_m + 2x_{i'm}z_m - 2x_{jm}z_m)\\ &\quad +(\sum_m x^2_{im} + x^2_{j'm} - 2x_{im}x_{j'm} + z^2_m + 2x_{im}z_m - 2x_{j'm}z_m),\\ &= -d^2_{ij}(\mathbf{X}) - d^2_{i'j'}(\mathbf{X}) + d^2_{i'j}(\mathbf{X}) + d^2_{ij'}(\mathbf{X})\\ &= \theta_{jj'ii'},\end{aligned}$$

which shows that in this case ($p = 2$) the slide-vector ($\mathbf{z}$) only represents marginal heterogeneity: the association structure is symmetric. When fitted to data this model will have the same fit as the symmetric distance-association model with squared distances, i.e. there is no additional value of the slide-vector.

5 Data Analysis

In Table 2 the chi-square statistics, degrees of freedom and *AIC* statistics for the four models in two dimensions are given. We also give the Mean Squared Error of the local log odds ratio

$$\text{MSE}(\theta) = \frac{1}{(I-1)^2}\sum_{ij}(\theta_{ii'jj'} - \hat{\theta}_{ii'jj'})^2,$$

where $i' = i + 1$ and $j' = j + 1$. This measure can be interpreted as an overall measure of how well the observed log odds ratios are represented. Note that the observed log odds ratios were computed based on $y_{ij} + 0.5$.

5.1 Symmetric Distance-Association Model

We applied the distance-association models to the occupational mobility data, where we gave zero weight to the diagonal entries.

The two-dimensional model with distances ($p = 1$) had a chi-square statistic 60.9 and a likelihood ratio statistic of 64.8, both with 54 degrees of freedom. The *AIC* equals −43.18 and the MSE(θ) is 0.53. The estimated distances, main effect parameters and overall λ are given in Table 3. From this table we can derive that the estimated log odds ratio θ_{5612} equals

$$\begin{aligned}\hat{\theta}_{5612} &= -d_{51} - d_{62} + d_{61} + d_{52}\\ &= -1.03 - 0.49 + 0.81 + 1.11\\ &= 0.40\end{aligned}$$

which equals the estimated log odds ratio θ_{1256}. The observed equivalents of these two log odds ratios were −0.75 and 0.74. So, these particular log odds ratios are not good represented by the symmetric distance-association model.

Table 2 Fit statistics for the four models. DA is the symmetric distance-association model; DR is the distance-radius model; SV is the slide-vector model. $p = \{1, 2\}$ represent distances and squared distances, respectively

	X^2	G^2	*df*	*AIC*	MSE(θ)
DA ($p = 1$)	60.88	64.82	54	−43.18	0.53
DA ($p = 2$)	60.89	64.47	54	−43.53	0.54
DR ($p = 2$)	42.51	44.65	45	−45.35	0.38
SV ($p = 1$)	56.54	62.08	52	−41.92	0.54

Table 3 Estimated distances and main effect parameters for distance-association model ($p = 1$)

	1	2	3	4	5	6	7	8	9	10	$\hat{\lambda}_i^R$
1	0.00	0.38	0.53	0.71	1.03	0.81	1.21	1.78	6.40	1.83	−0.26
2	0.38	0.00	0.43	0.93	1.11	0.49	0.90	1.55	6.08	1.45	−0.16
3	0.53	0.43	0.00	0.64	0.69	0.45	0.76	1.26	6.37	1.53	−0.51
4	0.71	0.93	0.64	0.00	0.46	1.08	1.34	1.63	6.99	2.16	−0.88
5	1.03	1.11	0.69	0.46	0.00	1.05	1.16	1.27	7.00	2.04	−1.03
6	0.81	0.49	0.45	1.08	1.05	0.00	0.42	1.10	5.96	1.09	−1.56
7	1.21	0.90	0.76	1.34	1.16	0.42	0.00	0.73	5.89	0.88	0.07
8	1.78	1.55	1.26	1.63	1.27	1.10	0.73	0.00	6.27	1.30	0.37
9	6.40	6.08	6.37	6.99	7.00	5.96	5.89	6.27	0.00	5.03	4.90
10	1.83	1.45	1.53	2.16	2.04	1.09	0.88	1.30	5.03	0.00	−0.94
$\hat{\lambda}_j^C$	0.44	1.01	0.32	−1.32	−1.40	−1.27	0.37	0.74	2.94	−1.83	4.12

The two-dimensional model with squared distances had a chi-square statistic 60.9 and a likelihood ratio statistic of 64.5 with the same number of degrees of freedom. The *AIC* equals −43.18 and the MSE(θ) is 0.53. The fit statistics for the two symmetric distance-association models are almost equal. The estimated squared distances, main effect parameters and overall λ are given in Table 4. From this table we can derive that the estimated log odds ratio θ_{5612} equals

$$\begin{aligned}\hat{\theta}_{5612} &= -d_{51}^2 - d_{62}^2 + d_{61}^2 + d_{52}^2 \\ &= -0.61 - 0.12 + 0.43 + 0.35 \\ &= 0.04\end{aligned}$$

Table 4 Estimated squared distances and main effect parameters for distance-association model ($p = 2$)

	1	2	3	4	5	6	7	8	9	10	$\hat{\lambda}_i^R$
1	0.00	0.10	0.23	0.46	0.61	0.43	0.98	1.44	1.33	1.83	0.41
2	0.10	0.00	0.06	0.36	0.35	0.12	0.46	0.80	0.86	1.22	0.32
3	0.23	0.06	0.00	0.17	0.12	0.11	0.33	0.57	1.08	1.38	−0.00
4	0.46	0.36	0.17	0.00	0.08	0.52	0.76	0.94	2.08	2.46	−0.44
5	0.61	0.35	0.12	0.08	0.00	0.31	0.38	0.48	1.62	1.87	−0.75
6	0.43	0.12	0.11	0.52	0.31	0.00	0.12	0.33	0.53	0.72	−1.05
7	0.98	0.46	0.33	0.76	0.38	0.12	0.00	0.05	0.60	0.64	0.56
8	1.44	0.80	0.57	0.94	0.48	0.33	0.05	0.00	0.87	0.82	0.61
9	1.33	0.86	1.08	2.08	1.62	0.53	0.60	0.87	0.00	0.06	0.59
10	1.83	1.22	1.38	2.46	1.87	0.72	0.64	0.82	0.06	0.00	−0.24
$\hat{\lambda}_j^C$	1.10	1.47	0.82	−0.84	−1.09	−0.80	0.84	0.99	−1.37	−1.11	2.71

which equals the estimated odds ratio θ_{1256}. These estimated log odds ratios are the mean of the two observed log odds ratios. Given that the model implies a symmetric structure this is optimal for these specific log odds ratios.

5.2 Distance-Radius Model

We apply the distance-radius model to the occupational mobility data. The two-dimensional model with squared distances had a chi-square statistic 42.5, a likelihood ratio statistic of 44.7 with 45 degrees of freedom. The *AIC* equals −45.35 and the MSE(θ) equals 0.38. The model fits better than the two symmetric distance-association models.

The estimated squared distances, main effect parameters and overall parameter are given in Table 5. The estimated radii of the ten occupational classes are

`1.31, 1.1, 1.04, 1.16, 1.15, 0.95, 0, 0.72, 1.11` and `1.15`

showing category 7 has the smallest radius, while category 1 the largest. Therefore, the distance from category 1 to another is smaller than the other way around, implying that the frequency towards category 1 is larger than other way around (taking into account the main effect parameters). Furthermore, category 7 has the smallest radius, meaning that the distance from category 7 to the others is larger than the other way around, implying that the frequency towards category 7 is smaller than the other way around (taking into account the main effect parameters).

From the table with estimated squared distances we can derive that the estimated log odds ratio θ_{5612} equals

Table 5 Estimated squared distances and main effect parameters for distance-radius model ($p = 2$)

	1	2	3	4	5	6	7	8	9	10	$\hat{\lambda}_i^R$
1	0.00	0.01	0.00	0.04	0.27	0.00	1.00	0.00	0.49	1.05	−0.12
2	0.28	0.00	0.24	0.51	1.10	0.28	0.37	0.23	0.96	1.75	0.33
3	0.24	0.36	0.00	0.06	0.32	0.05	0.44	0.04	1.04	1.75	−0.11
4	0.24	0.36	0.00	0.00	0.11	0.04	0.43	0.02	1.01	1.69	−0.86
5	0.70	0.90	0.12	0.13	0.00	0.12	0.16	0.05	1.35	1.97	−0.80
6	0.57	0.68	0.17	0.36	0.55	0.00	0.50	0.00	0.69	1.23	−0.97
7	2.61	2.53	2.03	2.76	3.62	1.44	0.00	1.22	2.89	4.10	2.18
8	1.46	1.58	0.75	1.07	1.18	0.21	0.11	0.00	0.92	1.42	0.69
9	1.20	0.94	0.79	1.22	1.55	0.27	0.27	0.03	0.00	0.12	0.21
10	1.82	1.52	1.25	1.75	2.00	0.53	0.07	0.11	0.07	0.00	−0.55
$\hat{\lambda}_j^C$	1.07	1.80	0.81	−0.93	−0.67	−1.01	0.72	0.34	−1.40	−0.72	2.87

$$\begin{aligned}\hat{\theta}_{5612} &= -d_{51} - d_{62} + d_{61} + d_{52} \\ &= -0.70 - 0.68 + 0.57 + 0.90 \\ &= 0.08,\end{aligned}$$

whereas θ_{1256} is estimated by

$$\begin{aligned}\hat{\theta}_{1256} &= -d_{15} - d_{26} + d_{16} + d_{25} \\ &= -0.27 - 0.28 + 0.00 + 1.10 \\ &= 0.54.\end{aligned}$$

The model shows asymmetry in the odds ratio structure. For these specific odds ratios the asymmetry is in the correct direction; however, the estimates are still a bit off. Overall, this model best represents the odds ratio structure, i.e. the MSE(θ) equals 0.38 which is much smaller than the MSE for the other models.

5.3 Slide-Vector Model

Finally, we also applied the slide-vector model to the occupational mobility data. The two-dimensional model had a chi-square statistic 56.5 and a likelihood ratio statistic of 62.1, both with 52 degrees of freedom. The *AIC* equals −41.92, worse than the symmetric distance-association models.

The slide-vector points into the direction of categories 1 and 2 and away from 7 and 8, showing that the distance towards categories 1, 2 and away from 7, 8 is smaller than the other way around. The expected frequency towards categories 1 and 2 will, therefore, be larger than the frequencies from categories 1 and 2, taking into account the difference in main effects. Similarly, the expected frequency away from categories 7 and 8 will be larger than the expected frequency towards categories 7 and 8.

In Table 6 the estimated distances, main effect parameters and the overall λ are given. From the table, and following the same computations as before we can derive that the implied log odds ratio θ_{5612} equals 0.2 while the implied log odds ratio θ_{1256} equals 0.1. The direction of asymmetry for these two odds ratios is opposite to that of the observed data. Overall, the MSE(θ) equals 0.54 which is very similar to the distance-association models, i.e. the slide-vector does not represent the asymmetry in the odds ratios very well for this specific data set.

5.4 Models Without Main Effects

We saw that for the slide-vector model based on squared distances and the distance-radius model with distances the asymmetry that the distances represent is absorbed

Table 6 Estimated distances and main effect parameters for slide-vector model ($p = 1$)

	1	2	3	4	5	6	7	8	9	10	$\hat{\lambda}_i^R$
1	2.48	2.48	2.91	3.68	4.96	3.05	5.44	5.68	4.35	5.07	1.09
2	2.48	2.48	2.91	3.72	5.03	3.01	5.43	5.67	4.29	4.96	1.32
3	2.04	2.05	2.48	3.26	4.57	2.64	5.01	5.26	3.98	4.77	0.52
4	1.66	1.75	2.03	2.48	3.62	2.56	4.58	4.83	4.02	5.12	−0.58
5	2.04	2.19	2.17	1.85	2.48	3.01	4.26	4.49	4.39	5.76	−0.65
6	2.23	2.17	2.63	3.61	5.02	2.48	4.97	5.20	3.60	4.14	−0.43
7	0.79	0.67	0.65	1.68	3.10	0.25	2.48	2.71	1.65	2.98	−0.87
8	0.99	0.89	0.76	1.67	3.05	0.30	2.24	2.48	1.47	2.86	−1.05
9	2.28	2.15	2.52	3.63	5.10	1.89	4.24	4.44	2.48	2.71	0.22
10	3.79	3.64	3.96	5.06	6.50	3.19	5.15	5.31	3.13	2.48	0.40
$\hat{\lambda}_j^C$	−0.22	0.47	0.06	−1.15	0.18	−1.63	2.14	2.34	−1.61	−0.59	5.34

in the marginal terms, or in other words the asymmetry in the distances models marginal heterogeneity. This raises the question what happens if the main effects in the generic model are deleted. In this section we are therefore interested in the model

$$\log(\mu_{ij}) = \lambda - \delta_{ij}$$

with $\delta_{ij} = d_{ij}(\mathbf{X}, \mathbf{r})$ or $\delta_{ij} = d_{ij}^2(\mathbf{X}, \mathbf{z})$. The odds ratio structure remains the same as before; however, the asymmetry in the distances now also has to model both marginal distributions and therefore the change in marginal distributions.

5.4.1 Distance-Radius Model

The two-dimensional model had a chi-square statistic of 131 and a likelihood ratio statistic of 130.3, both with 63 degrees of freedom. The *AIC* statistic for this model equals 4.3. We see that this model fits significantly worse due to the omission of the main effect parameters. This model has a symmetric association structure. The question arises how well the model represents the marginal heterogeneity, because the margins itself are not perfectly represented (as a model including the main effects would).

In Table 7 we present the observed and estimated marginal frequencies, and also the change in marginal distributions $\hat{\mu}_{+i} - \hat{\mu}_{i+}$ or $y_{+i} - y_{i+}$. We see that although the distance-radius model does not perfectly estimate the marginal distributions (as a model including main effects would) but nevertheless represents the change in marginal distributions perfectly.

Table 7 Observed and estimated marginal distributions and marginal change. DR is the distance-radius model; SV is the slide-vector model

		1	2	3	4	5	6	7	8	9	10
Observed	y_{i+}	236	301	204	111	78	73	322	256	238	65
	y_{+i}	262	536	275	52	33	61	297	266	77	25
	$y_{+i} - y_{i+}$	26	235	71	−59	−45	−12	−25	10	−161	−40
DR	μ_{i+}	197.7	140.8	177.5	94.5	79.1	69.1	238.7	202.3	180.1	64.2
	μ_{+i}	223.7	375.8	248.5	35.5	34.1	57.1	213.7	212.3	19.1	24.2
	$\mu_{+i} - \mu_{i+}$	26.0	235.0	71.0	−59.0	−45.0	−12.0	−25.0	10.0	−161.0	−40.0
SV	μ_{i+}	170.2	186.3	168.3	64.3	106.9	46.2	230.4	232.3	166.8	72.5
	μ_{+i}	239.3	241.6	244.2	88.6	36.9	101.1	206.2	201.0	53.3	31.8
	$\mu_{+i} - \mu_{i+}$	69.2	55.3	76.0	24.3	−70.0	54.9	−24.2	−31.2	−113.5	−40.7

5.4.2 Slide-Vector Model

The two-dimensional model had a chi-square statistic 549.1 and a likelihood ratio statistic of 445.1, both with 70 degrees of freedom. The *AIC* statistic for this model equals 305.1. This model fits very badly compared to all our previous models.

Table 7 also gives the estimated marginal distributions and change in marginal distributions for this slide-vector model. We see that the slide-vector model has difficulties with the representation of the marginal heterogeneity, i.e. the two parameters cannot deal with the heterogeneity and possible more dimensions are needed. In full dimensionality the model probably represents the marginal heterogeneity perfectly.

6 Discussion and Conclusion

We considered the distance-radius model and slide-vector model in comparison with the Euclidean distance in a loglinear framework. Such a framework allows for the comparison between models in terms of marginal heterogeneity (often dealt with using preprocessing) and association (often modelled on the resulting data from the preprocessing). The advantage of putting the different steps in a single framework is that we obtain a more precise idea what the asymmetric scaling models are actually achieving.

We worked out the odds ratio structures given different asymmetric scaling models and found that some implementations do not model any asymmetry in the odds ratio structure. More precisely, the distance-radius model with standard distances ($p = 1$) and the slide-vector model with squared distances ($p = 2$) result in a symmetric odds ratio structure.

In contrast, the distance-radius model with squared distances and the slide-vector model with distances do imply an asymmetric odds ratio structure. Because the distance-radius model uses more parameters to represent the asymmetry, it gives a more accurate representation of the asymmetry. The slide-vector model has a very simple representation of asymmetry, and therefore hardly performs better than any symmetric model (at least in our example).

References

1. Agresti, A. (2002). *Categorical data analysis*. New York: Wiley.
2. Caussinus, H. (1965). Contribution á l'analyse statistique des tableaux de corrélation [contributions to the statistical analysis of correlation matrices]. *Annals of the faculty of Science, University of Toulouse*, *29*, 715–720.
3. De Rooij, M. (2001). Distance-association model for the analysis of repeated transition frequency tables. *Statistica Neerlandica*, *55*, 156–180.
4. De Rooij, M., & Heiser, W. J. (2005). Graphical representations and odds ratios in a distance-association model for the analysis of cross-classified data. *Psychometrika*, *70*, 99–122.
5. Ganzeboom, H. B. G., & Luijkx, R. (1995). Intergenerationele beroepsmobiliteit in Nederland: patronen en historische veranderingen. In J. Dronkers & W. C. Ultee (Eds.), *Verschuivende ongelijkheid in Nederland* (pp. 14–30). Assen: Van Gorcum.
6. Okada, A., & Imaizumi, T. (1987). Nonmetric multidimensional scaling of asymmetric proximities. *Behaviormetrika*, *21*, 81–96.
7. Okada, A., & Imaizumi, T. (1997). Asymmetric multidimensional scaling of two-mode three-way proximities. *Journal of Classification*, *14*, 195–224.
8. Timmerman, M. E. (2014). Aim at doing the wash in one go. In M. de Rooij & C. M. van Putten (Eds.), *Psychology and Statistics: Ready for the future* (pp. 21–24). Leiden University.
9. Zielman, B., & Heiser, W. J. (1993). The analysis of asymmetry by a slide-vector. *Psychometrika*, *58*, 101–114.

Flight Passenger Behavior and Airline Fleet Assignment

Wolfgang Gaul and Christoph Winkler

Abstract Flight passenger behavior comprises, for example, booking requests as well as cancelations and the no-show phenomenon before the departure of an airplane while airline fleet assignment describes the task of putting together among other things—but above all—an attractive schedule of origin–destination flight connections with corresponding takeoff and landing times. We propose an approach that takes into account the interrelations between flight passenger behavior and airline fleet assignment and integrates aircraft-type allocation to flight legs, the treatment of different booking classes, the offering of specific as well as flexible products to flight passengers, and overbooking decisions to avoid empty seats in airplanes. An exemplary description of how the new approach reacts to alterations of the underlying situation is added to show the flexibility and advantages of our model formulation.

Keywords Flight passenger behavior · Airline fleet assignment · Refleeting · Class-dependent (over) booking · Flexible products · Deterministic linear programming

1 Introduction

Contributions concerning applications of operations research techniques in the air transport industry are known for quite some time (see, e.g., Gopalan & Talluri [12]; Barnhart, Belobaba, & Odoni [2] for earlier overviews) where an important part of the scientific literature describes so-called network problems because in aviation, an itinerary between two airports may consist of more than one flight leg with transfers on the ground (see, e.g., Lapp & Weatherford [20]; Vossen & Zhang [29]; Barz & Gartner [4] for some more recent papers).

W. Gaul (✉) · C. Winkler
Karlsruhe Institute of Technology (KIT), Karlsruhe, Germany
e-mail: wolfgang.gaul@kit.edu

C. Winkler
e-mail: christoph.winkler12@web.de

T. Imaizumi et al. (eds.), *Advanced Studies in Behaviormetrics and Data Science*,
Behaviormetrics: Quantitative Approaches to Human Behavior 5,
https://doi.org/10.1007/978-981-15-2700-5_4

From a mathematical perspective the determination of booking limits (see, e.g., Bertsimas & de Boer [6]) and bid prices (see, e.g., Talluri & van Ryzin [25]; Adelman [1]; Klein [16]; Kunnumkal & Topaloglu [19]) to control the seat capacities in airplanes, sometimes formulated with the help of (randomized) linear programming (see, e.g., Talluri & van Ryzin [26]; Topaloglu [27]; Kunnumkal, Talluri, & Topaloglu [18]), and also applied in simulation experiments (see, e.g., Bertsimas & de Boer [6]; Gosavi, Ozkaya, & Kahraman [13]; Van Ryzin & Vulcano [28]) have been tackled.

In order to compensate cancelations during the booking process and no-shows just before the departure of an airplane overbooking—as acceptance of booking requests that exceed the physical capacities of available resources—has a long history (see, e.g., Beckmann [5] for an early contribution and Wannakrairot & Phumchusri [30] for a more recent paper).

Another aspect is the consideration of booking classes, which takes into account constraints concerning the seats in airplanes or in which different price settings can be charged due to buying restrictions and marketing strategies.

The distinction between specific and flexible products (see Gallego, Iyengar, Phillips, & Dubey [8]; Gallego & Phillips [9] who introduced this concept and Petrick, Goensch, Steinhardt, & Klein [21]; Petrick, Steinhardt, Goensch, & Klein [22]; Koch, Goensch, & Steinhardt [17] for more recent publications) is of interest as it allows to give seats, which could not be sold as specific offers, to flexible flight passengers who can do without some of the predefined restrictions such as fixed flight leg(s), booking class, and utilization time, by which specific products are characterized.

Because of the underlying complexity of the overall problem situation in air transport optimization, a comprehensive solution (which combines subproblems as, e.g., airline fleet assignment and maintenance, scheduling and routing of flights, crew rostering, incorporation of flexible products within the offering of an airline, as well as class-dependent (over) booking w.r.t. available seat capacities of airplanes) is a challenge. Some papers explicitly attempt to integrate two or more subproblems, e.g., airline fleet assignment and crew rostering (see, e.g., Sandhu & Klabjan [23]; Gao, Johnson, & Smith [10]), airline fleet assignment and routing decisions (see, e.g., Barnhart et al. [3]; Haouari, Aissaoui, & Mansour [14]) or airline fleet assignment and schedule design (see, e.g., Sherali, Bae, & Haouari [24]; Kenan, Jebali, & Diabat [15]).

In this paper we present a new approach in which aircraft-type allocation to flight legs, overbooking, incorporation of flexible products as an additional offering of an airline, and the treatment of different booking classes are combined within an integrated formulation for which a properly adapted Deterministic Linear Programming (DLP) description is used (see, e.g., Gaul & Winkler [11] for the historical development of DLP adaptions to overbooking and the consideration of flexible products as well as further applications).

Against this background, basic notations with respect to airline fleet assignment and flight passenger behavior are presented in Sect. 2 before in Sect. 3 a new approach—formulated as modified DLP—is described, which simultaneously can handle the aforementioned aspects. Section 4 presents an example designed to clar-

ify how the DLP approach reacts to changing situations. Finally, in Sect. 5 concluding remarks are provided.

2 Notation

2.1 Airline Fleet Assignment

With $|M|$ as notation of the cardinality of a set M, assume that an airline operates a set of aircraft-types $\tilde{T} = \left\{1, \ldots, |\tilde{T}|\right\}$ where c_τ denotes the number of aircrafts of type $\tau \in \tilde{T}$.

Airports as set of nodes $N = \{1, \ldots, |N|\}$ of an air transport network and a set of activities A associated with the airports and divided into a set G of ground operations (e.g., (dis)embarkation of passengers and luggage, refueling, maintenance, and other services in connection with aircrafts on the ground) as well as a set F of flight operations (landings and takeoffs) are needed for the description of the underlying situation.

A distinction between a planning and a realization period is advised where the realization period corresponds to a properly defined time interval at the end of the planning period.

Costs that arise from performing activity a with aircraft-type τ are denoted by $cost_{a\tau}, a \in A, \tau \in \tilde{T}$, where only activities are considered that end within the realization period.

The subset $B \subset A = F \cup G$ of activities that start before the beginning of the realization period and end within this period are called cross-border activities w.r.t. the realization period. Finally, for the model description in the next section the sets $In\,(n) = \{\ a \in A \mid \text{ ending of } a \text{ takes place within the realization period at airport } n\}$, $Out\,(n) = \{\ a \in A \mid \text{ beginning of } a \text{ takes place within the realization period at airport } n\}$, $n \in N$ have to be specified.

Notice, that after a certain time-point t^* aircraft-type allocation to flight legs cannot be performed any longer due to organizational restrictions w.r.t. the underlying situation.

As an important feature within the offering of an airline the set $K = \{1, \ldots, |K|\}$ indicates physically available classes of seat capacities in aircraft-types (e.g., first, business, and economy) as well as booking classes in which different price settings are charged due to marketing considerations. $cap_{\tau k}$ denotes the capacity of class $k \in K$ on aircraft-type $\tau \in \tilde{T}$.

Additionally, the distinction into specific and flexible products is of interest. Specific products are described by a set $I = \{1, \ldots, |I|\}$ of origin–destination itineraries and the assigned class $k \in K$ with revenue r_{ik}, while a set $J = \{1, \ldots, |J|\}$ with revenue s_j, $j \in J$ indicates flexible products where an execution-mode set $M_j \subseteq I$ fixes a possible allocation of $j \in J$ to a subset of appropriate origin–destination itineraries

(remember that a flexible offering can be assigned to whatever specific product that fulfills the constraints by which the flexible product is described).

We use $F = \{1, \ldots, |F|\}$ as set of flight legs by which origin–destination itineraries are composed (the same notation as already described earlier when explaining flight operations) and a matrix V (with entries v_{fi} equal to 1 if origin–destination itinerary i needs flight leg f, and equal to 0 otherwise, for $f \in F$ and $i \in I$, respectively, v_{fm} equal to 1 if execution-mode m uses flight leg f, and equal to 0 otherwise, for $f \in F$ and $m \in M_j$). The class-matrix W (with w_{ik} equal to 1 if the origin–destination itinerary i offers class k, and equal to 0 otherwise, respectively, w_{mk} equal to 1 if exection-mode m provides class k, and equal to 0 otherwise) indicates the class which is of importance for seat capacity allocation.

2.2 Flight Passenger Behavior

Flight passenger behavior is not known in advance but can be influenced by the airline management via, e.g., attractive flight schedules, ticket prices, and the shape of execution-mode sets M_j. As available seat capacities should be sold within a given time horizon which is discretized into T time-points or intervals (which are numbered backward from T to 1 (time of departure)), let D_{ikt}^{spec} denote the random variable which describes the aggregated demand for the specific product i in class k up to time-point t and d_{ikt}^{spec} the realization of D_{ikt}^{spec}, respectively, D_{jt}^{flex} and d_{jt}^{flex} in the flexible case. In former applications of DLP the expected values $E\left(D_{ikt}^{spec}\right)$, respectively, $E\left(D_{jt}^{flex}\right)$, were used as bounds for seat allocations. Here, we suggest $D_{ikt}^{*spec} = d_{ikt}^{spec} + adjust_{ikt}$, respectively $D_{jt}^{*flex} = d_{jt}^{flex} + adjust_{jt}$, where it is assumed that the experience of the management of the airline helps to assign $adjust$ values which describe demand still to come up until departure. This could be supported by computer routines which consider—among others—the actual realization of flight passenger demand, additional information about the development of future demand, available seat capacities, and the time to departure. The pragmatic use of $adjust$ values has several reasons. In early phases of the planning period, assumptions about probability distributions for flight passenger demand at takeoff time may not be profound enough while $adjust$ values can easily be adapted, even to (unforeseen) events that may influence future developments of the underlying situation. Although stochastic programming, which is known for quite some time, is an option where stochastic programming with discrete probability distributions would even lead to linear programs (see, e.g., Cleef and Gaul [7] for a paper in which network flow theory is applied for the solution of a stochastic problem formulation), we have decided to use the just mentioned $adjust$ values to avoid assumptions concerning probability distributions and penalty costs which compensate for the nonconformity between finally realized flight passenger demand and seat capacity allocation. Additionally, the $adjust$ values tend to decrease when t approaches takeoff time.

The situation that refleeting is no longer possible after time-point t^* leads to a two-stage procedure. In the first stage, aircraft-type allocation to flight legs and seat determination are simultaneously considered in the airline fleet assignment. In the second stage, when aircraft-type allocation is no longer possible, the task of seat determination (together with class-dependent (over)bookings and incorporation of flexible products) is the main objective. While in the first stage $x_{ik}^{old} \geq 0$, $i \in I, k \in K$, describes specific demand that, e.g., originates from cancelations in earlier periods and has to be considered in the actual realization period, in the second stage x_{ik}^{old} describes already confirmed seat allocations for flight passengers with specific demand. At some (as late as possible) time-point t^{flex} before departure also flight passengers with flexible demand are informed about their now confirmed seat allocations.

To consider overbooking, the situation has to be modeled, that flight passengers don't show up or that too many seats were sold before the departure of an airplane. Here, p_{fk}^{spec} and p_{fk}^{flex} denote the expected show-probabilities (divided into specific and flexible bookings). Additionally, a parameter ρ_{fk} indicates the share of flexible flight customers and d_{fk} the costs for a denied service concerning flight leg f and class k.

3 Model

Now, the following Deterministic Linear Programming (DLP) adaption can be formulated that describes an integrated approach in which airline fleet assignment combines several aspects as, e.g., aircraft-type allocation to flight legs, seat determination, overbooking, the incorporation of flexible products, and the consideration of different booking classes:

$$max \quad \sum_{i \in I} \sum_{k \in K} r_{ik} \cdot x_{ik} + \sum_{j \in J} s_j \cdot \sum_{m \in M_j} \sum_{k \in K} y_{jmk}$$

$$- \sum_{f \in F} \sum_{k \in K} d_{fk} \cdot u_{fk} - \sum_{a \in A} \sum_{\tau \in \tilde{T}} cost_{a\tau} \cdot l_{a\tau}$$

$$s.t. \sum_{i \in I} v_{fi} \cdot w_{ik} \cdot x_{ik} + \sum_{j \in J} \sum_{m \in M_j} v_{fm} \cdot w_{mk} \cdot y_{jmk} \leq z_{fk} \quad \forall f \in F, k \in K \qquad (1)$$

$$\sum_{j \in J} \sum_{m \in M_j} v_{fm} \cdot w_{mk} \cdot y_{jmk} \leq \rho_{fk} \cdot z_{fk} \quad \forall f \in F, k \in K \qquad (2)$$

$$x_{ik} \geq x_{ik}^{old} \quad \forall i \in I, k \in K \qquad (3)$$

$$x_{ik} \leq D_{ikt}^{*spec} \quad \forall i \in I, k \in K \qquad (4)$$

$$x_{ik} \in \mathbb{Z}_+ \quad \forall i \in I, k \in K \tag{5}$$

$$\sum_{m \in M_j} \sum_{k \in K} y_{jmk} \leq D_{jt}^{*flex} \quad \forall j \in J \tag{6}$$

$$y_{jmk} \in \mathbb{Z}_+ \quad \forall j \in J, k \in K, \; m \in M_j \tag{7}$$

$$z_{fk} \in \mathbb{Z}_+ \quad \forall f \in F, k \in K \tag{8}$$

$$u_{fk} \geq z_{fk} \cdot \left(\rho_{fk} \cdot p_{fk}^{flex} + \left(1 - \rho_{fk}\right) p_{fk}^{spec} \right) - \sum_{\tau \in \tilde{T}} l_{f\tau} \cdot cap_{\tau k} \quad \forall f \in F, k \in K \tag{9}$$

$$z_{fk} \geq \sum_{\tau \in \tilde{T}} l_{f\tau} \cdot cap_{\tau k} \quad \forall f \in F, k \in K \tag{10}$$

$$u_{fk} \in \mathbb{Z}_+ \quad \forall f \in F, k \in K \tag{11}$$

$$\sum_{\tau \in \tilde{T}} l_{a\tau} = 1 \quad \forall a \in A \tag{12}$$

$$\sum_{a \in B} l_{a\tau} \leq c_\tau \quad \forall \tau \in \tilde{T} \tag{13}$$

$$\sum_{a \in In(n)} l_{a\tau} = \sum_{a \in Out(n)} l_{a\tau} \quad \forall n \in N, \tau \in \tilde{T} \tag{14}$$

$$l_{a\tau} \in \{0, 1\} \quad \forall a \in A, \tau \in \tilde{T} \tag{15}$$

where $\mathbb{Z}_+$ denotes the nonnegative integers.

The decision variables of this model are $l_{a\tau}$, u_{fk}, x_{ik}, y_{jmk}, and z_{fk} which are all dependent on the time-point t when the calculations are performed. The binary variables $l_{a\tau}$ indicate which aircraft-type $\tau \in \tilde{T}$ is allocated to which activity $a \in A$. u_{fk} collects the number of denied boardings on flight leg f and class k. x_{ik} (specific) and y_{jmk} (flexible) denote the numbers of seats (within execution-mode $m \in M_j$ in the case of flexible products) assigned to passengers w.r.t. the offering of specific and flexible products. The overbooking-limits z_{fk}, for which ρ_{fk} (share of flexible flight passengers in class k of flight leg f) and p_{fk}^{spec}, p_{fk}^{flex} (show-probabilities divided into specific and flexible customers) have to be taken into consideration, are also calculated. After time-point t^* the $l_{a\tau}$ values have to be fixed and interest can be concentrated on the overbooking-limits (calculated within the model) and, e.g., alterations of the shares of flexible flight passengers or show-probabilities (provided by the management of the airline).

The objective function maximizes the revenues of specific and flexible products, from which the costs for denied services as well as the costs for the allocation of aircraft-types to flight and ground activities are subtracted. The constraints (1) secure that the sum of flexible and specific products does not exceed the overbooking-limits which are bounded from below by the capacities of the aircraft-types (constraints (10)). Conditions (2) state that only predefined parts of the overbooking-limits can be allocated to flexible flight passengers. Constraints

(3) consider already confirmed seat allocations. Restrictions of type (4) and (6) use the adjusted aggregated demand for specific and flexible products up to time-point t as additional bounds. Notice, that also other model descriptors (e.g., flight legs, number of aircraft-types, costs, revenues, and show-probabilities) can undergo alterations when the time-point t changes. For simplicity, however, the index t is omitted except for the most important flight passenger demand values. Constraints (5), (7), and (8) restrict the numbers of allocated specific and flexible products as well as the overbooking-limits to nonnegative integers.

Conditions (9)–(11) delineate overbooking: Constraints (9) provide lower bounds for denied boardings as difference of flight passengers who show up (the overbooking-limits weighted with the show-probabilities (divided into flexible and specific bookings and multiplied by the shares of flexible and specific passengers)) minus the capacity of the aircraft-type used. Constraints (10) secure that the overbooking-limits exceed the capacities of the allocated aircraft-types (already mentioned) while restrictions (11) are self-explanatory.

Finally, the integration of aircraft-type allocation to flight legs is described by means of the conditions (12)–(15). Constraints (12) assign the underlying set of aircraft-types to flight and ground activities while constraints (13) consider the numbers c_τ of aircrafts of type τ which enter the realization period in connection with the cross-border activities w.r.t. the realization period already mentioned earlier. Restrictions (14) describe some kind of generalized flow constraints as all ingoing activities of aircraft-types $\tau \in \tilde{T}$ into airports $n \in N$ must go out, again. Constraints (15) secure that binary variables are used for the allocation task.

Earlier descriptions of airline fleet assignment have appeared in the literature (see, e.g., Gaul & Winkler [11]) but this approach possesses some features which merit attention, for example:

- Overbooking and the incorporation of flexible products are jointly treated.
- The consideration of different booking classes allows to specify class-dependent revenues and denied boarding costs and to work with different show-probabilities as well as shares of flexible flight passengers for selected classes. As a result, class-dependent overbooking-limits can be calculated which are of importance for the decisions of the management of an airline.
- The recalculation of solutions dependent on time-points t at which aggregated demand data are explicitly updated also allows to check and adapt other model parameters (e.g., the shares of flexible flight passengers or the show-probabilities).
- The use of adjusted flight passenger demand values on the basis of management experience leads to straightforward computations.
- The allocation of flight legs to available aircraft-types with different seat capacity classes and the choice of suited execution-mode sets M_j can be used to better balance overbooking and avoid empty seats.

4 Example

The example is kept small on purpose but large enough to allow a first impression concerning the complexity of the model, to demonstrate how starting conditions could look like, which kinds of data are taken into consideration, which results can be expected, and how the management of an airline is able to model flight and ground activities and can react to changings of the data that describe the underlying situation.

4.1 Starting Situation and Data

Based on management experience and historical data, the following starting situation for the application of approach (1)–(15) is assumed for an airline as depicted in Fig. 1 in which $|F| = 17$ flight legs connect $|N| = 3$ airports P, Q, and R with $|G| = 20$ ground operations in a realization period of two days (although not needed for the calculations concerning the realization period, some activities before as well as after the realization period are also shown for clarity of description, see, e.g., g_{20} as ground operation which starts before the beginning of the realization period and ends in a subsequent period). Four different routes, each served by a certain aircraft-type, are marked: for longer distance flights between airports P and R continuous arrows (flight legs $f_1, \ldots, f_5$), for shorter distance flights with intermediate landings in airport Q waved arrows (flight legs $f_6, \ldots, f_9$), dashed arrows (flight legs $f_{10}, \ldots, f_{13}$), and double-drawn arrows (flight legs $f_{14}, \ldots, f_{17}$) are used. Additionally, accompanying ground activities at the corresponding airports are shown.

As the management of an airline can restrict the offering of packages of flight connections, we assume for simplicity that return tickets for longer distance flights are only sold if an overnight stay between landing and return flight takes place. Additionally, on shorter distance flights no round trips within the realization period are offered and no itineraries which allow an overnight stay in P, Q, or R in the realization period (of course, flight passengers can buy single tickets and put together their own routes).

With these restrictions, still, the following origin–destination itineraries have to be considered: P $\rightarrow$ Q: f_6; f_{12}; f_{14}, P $\rightarrow$ Q $\rightarrow$ R: $f_6 \rightarrow f_7$; $f_6 \rightarrow f_{15}$; $f_{14} \rightarrow f_{15}$; $f_{12} \rightarrow f_{13}$ (numbered as $i = 19, 20, 21, 26$), P $\rightarrow$ R: f_2; f_4, Q $\rightarrow$ P: f_9; f_{11}; f_{17}, Q $\rightarrow$ R: f_7; f_{13}; f_{15}, R $\rightarrow$ Q: f_8; f_{10}; f_{16}, R $\rightarrow$ Q $\rightarrow$ P: $f_8 \rightarrow f_9$; $f_8 \rightarrow f_{17}$; $f_{16} \rightarrow f_{17}$; $f_{10} \rightarrow f_{11}$ (numbered as $i = 22, 23, 24, 25$), and R $\rightarrow$ P: f_1; f_3; f_5 (notice, that the ending of f_5 takes place in the subsequent period). Finally, a round trip R $\rightarrow$ P $\rightarrow$ R with itinerary $f_1 \rightarrow f_4$ (numbered as $i = 18$) is offered for travelers with an overnight stay at P. A round trip P $\rightarrow$ R $\rightarrow$ P with overnight stay at R using $f_2 \rightarrow f_5$, although possible, will not be considered as the ending of f_5 does not take place in the realization period. With three booking classes (e.g., first, business, economy) per origin–destination itinerary, there are 75 specific products. As flight leg f_5 and ground operations g_9, g_{14}, and g_{19} end after the realization period, revenues and costs

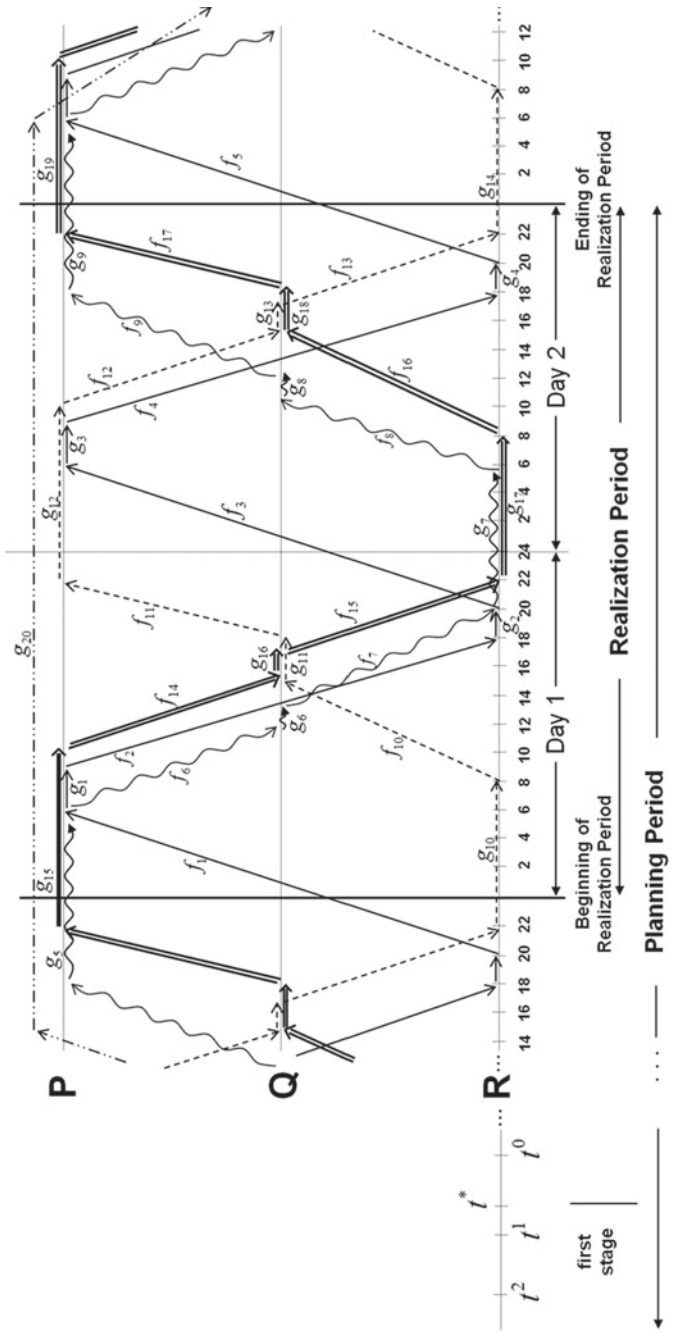

Fig. 1 Airline fleet assignment example

resulting from these activities are not included in the optimization w.r.t. the underlying realization period but the activities appear in the generalized flow constraints (14). On the other side, the set B of cross-border activities w.r.t. the realization period (known as operations which start before and end in the actual realization period) is considered which comprises f_1, g_5, g_{10}, and g_{15}, i.e., four airplanes enter the underlying realization period. $|\tilde{T}| = 3$ aircraft-types with $c_1 = 1$ (small: 200 seats), $c_2 = 2$ (medium: 300 seats), and $c_3 = 1$ (large: 400 seats) are assumed for which shares of 5%/10%/85% for first/business/economy are used for the separation of the overall capacities.

Additionally, two flexible products $j = 1$ (from P to R with execution-mode set $M_1 = \{2, 19, 20, 21\}$) and $j = 2$ (from R to P with $M_2 = \{22, 23, 24\}$) are considered at a time-point t^2 in the planning period some time before time-point t^* after which refleeting is no longer possible. Notice, that the management of the airline decides which specific itineraries and which booking classes are assigned to flexible offerings. Here, M_1 and M_2 are subsets of the sets of all itineraries that could be selected.

To allow an as simple as possible description, direct longer distance flight legs from P to R and from R to P, respectively, have revenues of 1200, 600, and 300 mu (monetary units) depending on the three booking classes (assumed independent (for simplicity) of the specific product) with a discount (30%) if flight passengers accept a transfer in Q. For shorter distance flight legs 720, 360, and 180 mu are the revenues, the round trip R $\rightarrow$ P $\rightarrow$ R is priced with 1800, 900, and 450 mu, again, for the three booking classes. The revenues for the flexible products are 175 mu, in each case.

The assignment of aircraft-type τ to flight leg f induces costs with $cost_{f1} = 18.000$, $cost_{f2} = 30.000$, and $cost_{f3} = 42.000$ mu (assumed independent (for simplicity) of flight leg f). Costs for ground activities after longer distance inbound flight legs $(g_1, \ldots, g_4)$ are $cost_{g1} = 1.500$, $cost_{g2} = 2.000$, and $cost_{g3} = 5.000$ mu, costs for ground activities after shorter distance inbound flight legs $(g_5, \ldots, g_{19})$ are $cost_{g1} = 1.000$, $cost_{g2} = 1.500$, and $cost_{g3} = 3.500$ mu (notice, again, that costs for g_9, g_{14}, g_{19}, (and g_{20}) are considered in the subsequent period).

Concerning the overbooking situation the compensation costs for denied services in classes $k = 1, 2, 3$ are $d_{f1} = 1500$, $d_{f2} = 750$, and $d_{f3} = 400$ mu for longer distance flight legs $(f_1, \ldots, f_4)$, respectively, $d_{f1} = 900$, $d_{f2} = 500$, and $d_{f3} = 300$ mu for shorter distance flight legs $(f_6, \ldots, f_{17})$.

Further, the expected show-probabilities, divided into flexible and specific bookings, have to be specified: For the show-probabilities of flexible flight passengers p_{fk}^{flex}, we take a value of 1.0 for all flight legs and all classes (because we argue, that if someone can make a flexible booking s(he) is such flexible that s(he) can always come to departure). For the show-probabilities of specific flight passengers p_{fk}^{spec} we deliberately take values smaller than 1.0 as explained in the discussion of the solution of this example.

Finally, flight passengers' demand values have to be specified. We consider three demand situations at time-points t^2 and t^1 in the first stage, and t^0 in the second stage ($t^2 > t^1 \geq t^* > t^0$) (remember that after time-point t^* refleeting is no longer possible).

Table 1 Changes of the demand situation in the first stage and corresponding optimal airline fleet assignment, respectively, refleeting

	demand $D^{*spec}_{ikt^2}$ at time point t^2				optimal fleet assignment	
i \ k	1	2	3	show-prob.	τ values	number of seats
1	15	33	315	0,99	3	400
2	17	32	326	0,95	3	400
3	15	23	305	0,94	3	400
4	15	41	322	0,95	3	400
5	16	28	315	0.93	3	400
6	10	20	115	0,99	2	300
7	11	25	115	0,95	2	300
8	10	28	190	0,95	2	300
9	10	24	200	0,95	2	300
10	7	22	125	0,95	1	200
11	6	20	115	0,95	(1)	200
12	8	16	141	0,95	(1)	200
13	5	17	99	0,95	1	200
14	7	22	125	0,9	2	300
15	6	20	115	0,9	(2)	300
16	8	18	141	0,95	(2)	300
17	5	17	99	0,95	2	300
18 (1,4)	2	3	28		(3,3)	400
19 (6,7)	3	10	130		(2,2)	300
20 (6,15)	3	5	115		(2,2)	300
21 (14,15)	8	20	125		(2,2)	300
22 (8,9)	4	10	95		(2,2)	300
23 (8,17)	2	5	90		(2,2)	300
24 (16,17)	4	8	102		(2,2)	300
25 (10,11)	2	8	92		(1,1)	200
26 (12,13)	2	8	50		(1,1)	200

	demand $D^{*spec}_{ikt^1}$ at time point t^1				optimal refleeting	
i \ k	1	2	3	show-prob.	τ values	number of seats
1						
2						
3						
4						
5						
6						
7						
8						
9						
10						
11	11	36	225		(2)	300
12	14	30	266		(2)	300
13						
14						
15					(1)	200
16					(1)	200
17						
18 (1,4)						
19 (6,7)						
20 (6,15)					(2,1)	200
21 (14,15)	10	24	150		(2,1)	200
22 (8,9)						
23 (8,17)						
24 (16,17)					(1,2)	200
25 (10,11)						
26 (12,13)						

Table 1 shows the values D^{*spec}_{ikt} for specific products i, classes k, and the time-points t^2 and t^1 together with the show-probabilities for specific flight passengers. On the right-hand part of Table 1 only those values, that have changed compared to the information depicted at the left-hand part, are given. Additionally, $D^{*flex}_{1t^2} = 80$ and $D^{*flex}_{2t^2} = 70$ are the numbers of flight passengers interested in the flexible products with the shares of flexible passengers ρ_{fk} as $\rho_{f1} = 0$, $\rho_{f2} = 0.1$, and $\rho_{f3} = 0.2$ for all flight legs which are considered in the execution-mode sets of the flexible offerings M_1 and M_2 (notice that we have chosen $\rho_{f1} = 0$ for all flight legs to avoid that first class passengers and flight passengers with flexible demand are jointly seated).

As one of the important messages concerning flight passenger demand situations in the first stage, the optimal airline fleet assignments (see also Tables 2, 3) are already contained in Table 1. Consider that, when an aircraft-type serving a certain flight leg changes, all itineraries which contain this flight leg are affected. This is shown in the last two columns of the left-hand and the right-hand parts of Table 1. In particular in itineraries composed by more than one flight leg, the number of seats is determined by the minimum seat capacities of the corresponding aircraft-types used which might change as well. Given the complexity of the situation described up to now we

have—on purpose—selected only three successive time-points t^2, t^1, and t^0 in which the demand values for $i = 11$, 12, and 21 (between time-points t^2 and t^1 in the first stage) and for $i = 3$ (at time-point t^0 in the second stage) with $D^{*spec}_{ikt^0} = 18/39/325$ are assumed to have changed to be better able to explain whether and how such alterations have an effect on the model solutions.

4.2 Results

Tables 2, 3, and 4 illustrate results of the application of model (1)–(15).

In the first and second column of Tables 2, 3, and 4, the numbers of assigned specific demand x_{ik} (with and without transfer) and of assigned flexible demand y_{jmk} are depicted. In the third column, the denied boardings u_{fk} are given. Besides the calculated overbooking-limits z_{fk} in the fourth column, the aircraft-types τ allocated to flight legs f are indicated.

Table 2 Results for the demand situation at time-point t^2 with execution-mode sets M_1, M_2

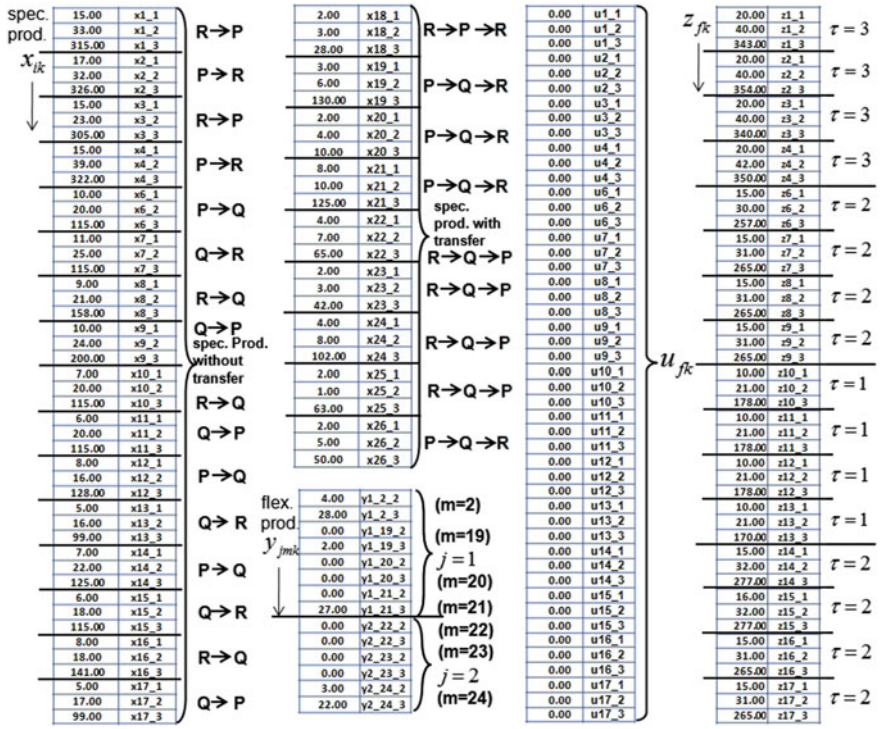

Table 3 Results for the demand situation at time-point t^1 with execution-mode sets M_1, $\tilde{M}_2$

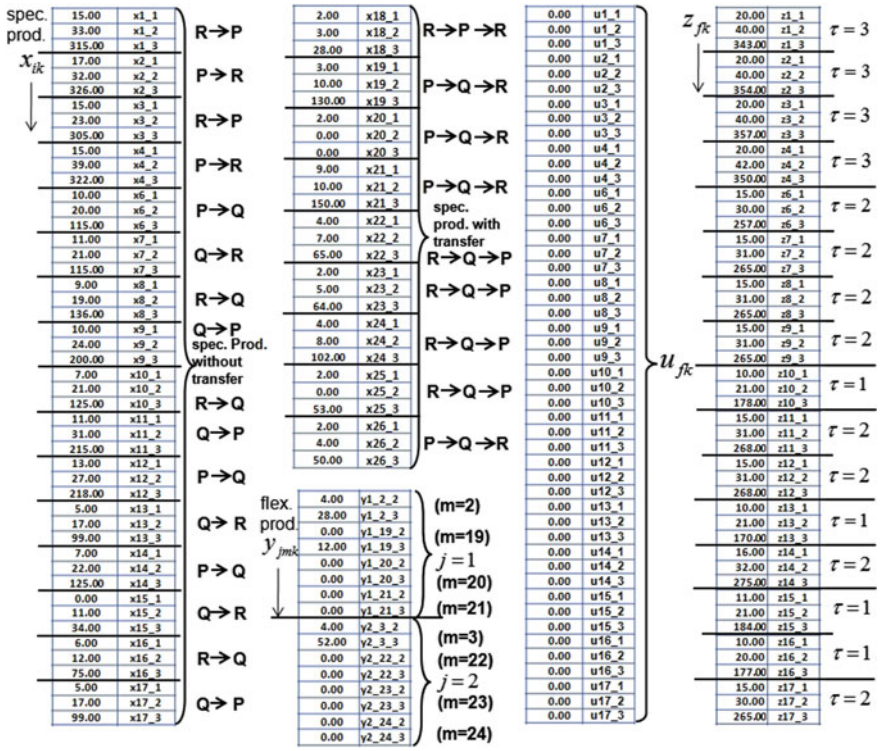

Table 2 reveals, e.g., that the seat capacity for specific product 3 is not exploited (because 400 $(20 + 40 + 340)$ seats are available) so that the management could change the execution-mode set M_2 to $\tilde{M}_2 := M_2 \cup \{3\}$ to incorporate more additional flexible flight passengers, who are interested in a connection from R to P. In addition to this alteration, remarkable differences between Tables 2 and 3 are related to the alteration of aircraft-type allocation between time-points t^2 and t^1, i.e., refleeting takes place. At time-point t^2 the route $f_1 \to f_2 \to f_3 \to f_4$ is operated by aircraft-type $\tau = 3$ (large: 400 seats), for the two routes $f_6 \to f_7 \to f_8 \to f_9$ and $f_{14} \to f_{15} \to f_{16} \to f_{17}$ aircraft-type $\tau = 2$ (medium: 300 seats) is used with two airplanes, and the route $f_{10} \to f_{11} \to f_{12} \to f_{13}$ is served by aircraft-type $\tau = 1$ (small: 200 seats). At time-point t^1, however, the aircraft-type allocations change. With the updated demand values at t^1, one aircraft of type $\tau = 2$ operates the route $f_{14} \to f_{11} \to f_{12} \to f_{17}$ while the aircraft-type $\tau = 1$ was allocated to route $f_{10} \to f_{15} \to f_{16} \to f_{13}$.

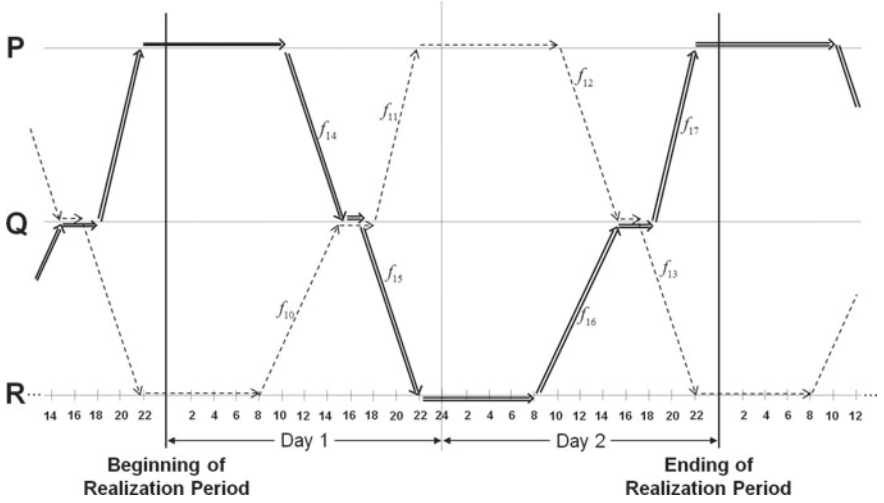

Fig. 2 Airline fleet assignment (demand situation at time-point t^2)

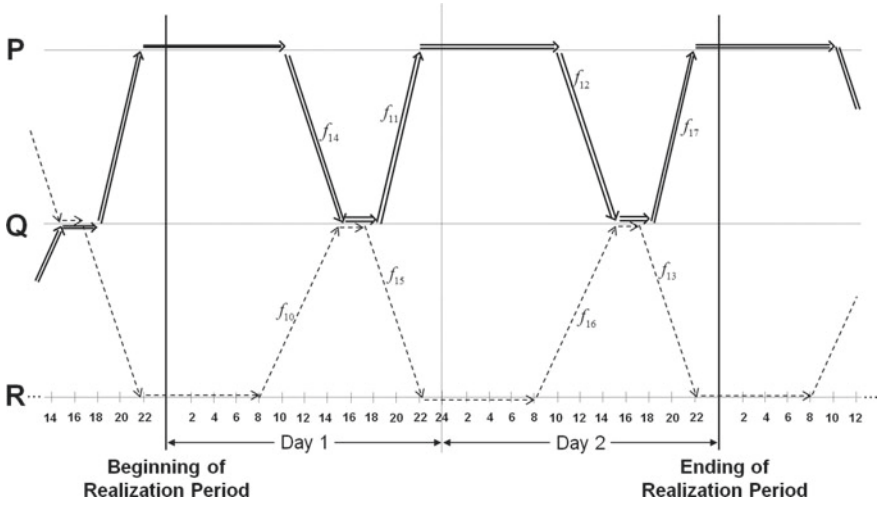

Fig. 3 Airline fleet assignment after refleeting (demand situation at time-point t^1)

Figures 2 and 3 show only those routes in the underlying example in which aircraft-types are reallocated (double-drawn arrows for type $\tau = 2$, dashed arrows for type $\tau = 1$) to meet the airline fleet assignment constraints.

In Table 2 the sum of overbooking-limits exceeds the sum of available seat capacities (in total 4800 seats on all flight legs in the underlying realization period) by 163 (1 first / 15 business / 147 economy) but no denied boardings are marked. 86 flexible

Table 4 Results for the demand situation at time-point t^0 with execution-mode sets M_1, $\tilde{M}_2$, and M_3

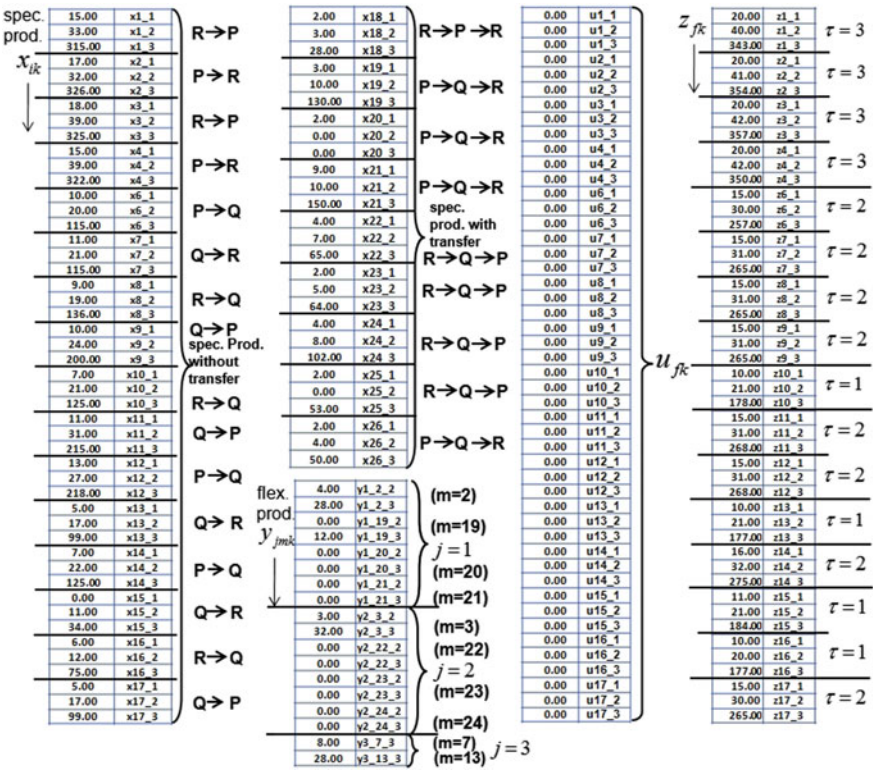

customers (61 to the flexible product $j = 1$ and 25 to the flexible product $j = 2$) are assigned (remember that flexible demand was not allowed in class 1).

Table 3 reveals that the available seat capacities are now exceeded by 175 (2 first / 12 business / 161 economy) possible overbookings but, again, no denied boardings appear. This time, 44 flexible flight passengers (flexible product $j = 1$) and 56 flexible customers ($j = 2$) are assigned (remember that $i = 3$ was added to the execution-mode set for the flexible product $j = 2$ ($\tilde{M}_2 = M_2 \cup \{3\}$)). From Table 3 the management of the airline can deduce (see the descriptions in Tables 6 and 7 for situation t^1) that seats are still available for flight legs 7 and 13 in class $k = 3$. Therefore, the management can decide to offer an additional flexible product $j = 3$ from Q to R with $s_3 = 100$ mu and execution-mode set $M_3 = \{7, 13\}$ because for this flexible offer flight passenger demand of $D_{3t^0}^{*flex} = 50$ seems reasonable.

Let us assume that $t^1 = t^*$ so that refleeting is no longer possible after time-point t^1. Now, Table 4 shows for time-point t^0 and execution-mode sets M_1, $\tilde{M}_2$, and M_3 the corresponding results. This time, the sum of overbooking-limits exceeds the sum

Table 5 Comparison of seat allocations of flight leg 3

		situation t^2			situation t^1			situation t^0		
	k	1	2	3	1	2	3	1	2	3
specific product (3)	x_{3k}	15	23	305	15	23	305	18	39	325
	y_{23k}	–	–	–	–	4	52	–	3	32
$x_{3k}+y_{23k}$		15	23	305	15	27	357	18	42	357
overbooking-limits	z_{3k}	20	40	340	20	40	357	20	42	357
seat capacities of aircraft-type used		20	40	340	20	40	340	20	40	340

Table 6 Comparison of seat allocations of flight leg 7

		situation t^2			situation t^1			situation t^0		
	k	1	2	3	1	2	3	1	2	3
specific product (7)	x_{7k}	11	25	115	11	21	115	11	21	115
(19): (6)→(7)	x_{19k}	3	6	130	3	10	130	3	10	130
	$y_{1,19k}$	–	0	2	–	0	12	–	0	12
	y_{37k}	–	–	–	–	–	–	–	–	8
$\sum_{i\in\{7,19\}} x_{ik}+y_{1,19k}+y_{37k}$		14	31	247	14	31	257	14	31	265
overbooking-limits	z_{7k}	15	31	265	15	31	265	15	31	265
seat capacities of aircraft-type used		15	30	255	15	30	255	15	30	255

of available seat capacities by 185 possible overbookings (2 first / 15 business / 168 economy). While, again, 44 flexible flight passengers are assigned to the flexible product $j = 1$, now, the number of flexible passengers assigned to $j = 2$ decreases to 33 (the reason is that the increased specific demand values for $i = 3$ (remember, $D_{ikt^0}^{*spec} = 18/39/325$) are more attractive than the assignment of flexible demand). On the other hand, altogether 36 flexible flight passengers are assigned to the new execution-mode set M_3 (8 to $i = 7$ and 28 to $i = 13$).

Except for flight legs 3, 7, and 13 (see Tables 5, 6, and 7), we leave it to the interested reader to check the numbers of flight passengers (with specific and flexible demand) assigned to the origin–destination itineraries of the underlying example, to add these numbers in those cases where different itineraries use the same flight leg and/or different types of flight passengers are jointly seated in a certain class, and to compare the results obtained with the demand values of Table 1, the available seat capacities in the classes of the aircraft-types used, and the overbooking-limits calculated by the program.

Table 7 Comparison of seat allocations of flight leg 13

		situation t^2			situation t^1			situation t^0		
	k	1	2	3	1	2	3	1	2	3
specific product (13)	x_{13k}	5	16	99	5	17	99	5	17	99
(26): (12)→(13)	x_{26k}	2	5	50	2	4	50	2	4	50
	$y_{3,13k}$	--	--	--	--	--	--	--	--	28
	$\sum_{t\in\{13,26\}} x_{tk} + y_{3,13k}$	7	21	149	7	21	149	7	21	177
overbooking-limits	z_{13k}	10	21	170	10	21	170	10	21	177
seat capacities of aircraft-type used		10	20	170	10	20	170	10	20	170

When flight passengers demand values w.r.t. origin–destination itineraries exceed the corresponding overbooking-limits, waiting lists or rejections with hints for alternative offerings can be used.

For the calculation of overbooking-limits, the assessment of the expected show-probabilities and the shares of allocated flexible customers are crucial.

Although—to make the description of the underlying situation easier—in some cases model parameters ($cap_{\tau k}, cost_{a\tau}, d_{fk}, r_{ik}, s_j, \ldots$) have been simplified and assumed to be independent of aircraft-types, classes, flight legs, or ground activities, and the chosen values were arbitrarily selected to establish a frame for the computations, the possibilities, how the management of an airline can adapt airline fleet assignment to changes in the underlying data and influence flight passenger behavior should have become clear.

5 Concluding Remarks

An approach has been presented in which the concepts of airline fleet assignment with aircraft-type allocation to flight legs, overbooking, incorporation of flexible products as additional offering of an airline, and class-dependent seat determination are combined within an integrated formulation for which a properly adapted Deterministic Linear Programming (DLP) description is used.

An example has been discussed which allows an elaborated impression with regard to the complexity of the underlying problem situation. Questions concerning, e.g., which kinds of data have to be provided, which results can be expected, and how the management of an airline is able to influence flight passengers and can react to changes in the situation are tackled. As the decision variables of the approach are dependent on the time-point when the calculations are performed, repeated applications of the approach can reveal how airline fleet assignment can be used to better balance booking requests and avoid empty seats. To keep the example simple, only

alterations of selected flight passenger demand values and executions-mode sets for flexible passengers were considered.

References

1. Adelman, D. (2007). Dynamic bid-prices in revenue management. *Operations Research*, *55*(4), 647–661.
2. Barnhart, C., Belobaba, P., & Odoni, A. (2003). Applications of operations research in the air transport industry. *Transportation Science*, *37*(4), 368–391.
3. Barnhart, C., Boland, N. L., Clarke, L. W., Johnson, E. L., Nemhauser, G. L., & Shenoi, R. G. (1998). Flight string models for aircraft fleeting and routing. *Transportation Science*, *32*(3), 208–220.
4. Barz, C., & Gartner, D. (2016). Air cargo network revenue management. *Transportation Science*, *50*(4), 1206–1222.
5. Beckmann, M. J. (1958). Decision and team problems in airline reservations. *Econometrica*, *26*(1), 134–145.
6. Bertsimas, D., & de Boer, S. V., (2005). Simulation-based booking limits for airline revenue management. *Operations Research*, *53*(1), 90–106.
7. Cleef, H. J., & Gaul, W. (1982). Project scheduling via stochastic programming. *Mathematische Operationsforschung und Statistik, Series Optimization*, *13*(3), 449–468.
8. Gallego, G., Iyengar, G., Phillips, R., & Dubey, A. (2004). *Managing Flexible Products on a Network* (CORC Technical Rep. TR-2004-01). IEOR Department, University of Columbia.
9. Gallego, G., & Phillips, R. (2004). Revenue management of flexible products. *Manufacturing & Service Operations Management*, *6*(4), 321–337.
10. Gao, C., Johnson, E., & Smith, B. (2009). Integrated airline fleet and crew robust planning. *Transportation Science*, *43*(1), 2–16.
11. Gaul, W., & Winkler, Ch. (2019). Aviation Data Analysis by Linear Programming in Airline Network Revenue Management. To appear in *Studies in Classification, Data Analysis, and Knowledge Organization*.
12. Gopalan, R., & Talluri, K. T. (1998). Mathematical models in airline schedule planning: A survey. *Annals of Operations Research*, *76*(1), 155–185.
13. Gosavi, A., Ozkaya, E., & Kahraman, A. F. (2007). Simulation optimization for revenue management of airlines with cancellations and overbooking. *OR Spectrum*, *29*(1), 21–38.
14. Haouari, M., Aissaoui, N., & Mansour, F. Z. (2009). Network flow-based approaches for integrated aircraft fleeting and routing. *European Journal of Operational Research*, *193*(2), 591–599.
15. Kenan, N., Jebali, A., & Diabat, A. (2018). An integrated flight scheduling and fleet assignment problem under uncertainty. *Computers & Operations Research*, *100*(2), 333–342.
16. Klein, R. (2007). Network capacity control using self-adjusting bid prices. *OR Spectrum*, *29*(1), 39–60.
17. Koch, S., Goensch, J., & Steinhardt, C. (2017). Dynamic programming decomposition for choice-based revenue management with flexible products. *Transportation Science*, *51*(4), 1031–1386.
18. Kunnumkal, S., Talluri, K., & Topaloglu, H. (2012). A randomized linear programming method for network revenue management with product-specific no-shows. *Transportation Science*, *46*(1), 90–108.
19. Kunnumkal, S., & Topaloglu, H. (2010). Computing time-dependent bid prices in network revenue management problems. *Transportation Science*, *44*(1), 38–62.
20. Lapp, M., & Weatherford, L. (2014). Airline network revenue management: Considerations for implementation. *Journal of Revenue and Pricing Management*, *13*(2), 83–112.

21. Petrick, A., Goensch, J., Steinhardt, C., & Klein, R. (2010). Dynamic control mechanisms for revenue management with flexible products. *Computers & Operations Management*, *37*(11), 2027–2039.
22. Petrick, A., Steinhardt, C., Goensch, J., & Klein, R. (2012). Using flexible products to cope with demand uncertainty in revenue management. *OR Spectrum*, *34*(1), 215–242.
23. Sandhu, R., & Klabjan, D. (2007). Integrated airline fleeting and crew-pairing decisions. *Operations Research*, *55*(3), 439–456.
24. Sherali, H. D., Bae, K.-H., & Haouari, M. (2010). Integrated airline schedule design and fleet assignment: Polyhedral analysis and Benders' decomposition approach. *Informs Journal on Computing*, *22*(4), 500–513.
25. Talluri, K. T., & van Ryzin, G. J. (1998). An analysis of bid-price controls for network revenue management. *Management Science*, *44*(11), 1577–1593.
26. Talluri, K. T., & van Ryzin, G. J. (1999). A randomized linear programming method for computing network bid prices. *Transportation Science*, *33*(2), 207–216.
27. Topaloglu, H. (2009). On the asymptotic optimality of the randomized linear program for network revenue management. *European Journal of Operational Research*, *197*(3), 884–896.
28. Van Ryzin, G. J., & Vulcano, G. (2008). Simulation-based optimization of virtual nesting controls for network revenue management. *Operations Research*, *56*(4), 865–880.
29. Vossen, T., & Zhang, D. (2015). Reductions of approximate linear programs for network revenue management. *Operations Research*, *63*(6), 1352–1371.
30. Wannakrairot, A., & Phumchusri, N. (2016). Two-dimensional air cargo overbooking models under stochastic booking request level, showup rate and booking request density. *Computers & Industrial Engineering*, *100*, 1–12.

Comparing Partitions of the Petersen Graph

Andreas Geyer-Schulz and Fabian Ball

Abstract The Petersen graph has been of long term interest to many graph theorists because of its appearance as counterexample in many places. In this contribution we use the Petersen graph—because of its transitivity and its large, but not too large automorphism group—as a show piece for invariant partition comparison measures. We show that we can decompose distances between partitions of the Petersen graph in an (invariant) structural part and a (variable) part caused by an automorphism. In addition, we study the effects caused by subgroups of the automorphism group and their interpretation.

1 Motivation

The Petersen graph, shown in Fig. 1, received its name from Julius Petersen (1839–1910), who first used it as a counterexample to a theorem of Tait on the 4-colour problem (Petersen [18]). For readers interested in a biography of Julius Petersen, we recommend Lützen, Sabidussi, and Toft [16]. However, the Petersen graph first appeared in Kempe [15] as the graph of the Desargues' configuration.

With graph theorists the Petersen graph soon achieved star status for two reasons:

- The Petersen graph is and continues to be a yardstick to assess conjectures, and it serves as a rich source of counterexamples to theorems. It is the most often referenced graph in Capobianco and Molluzo's book on counterexamples in graph theory (Capobianco & Molluzzo [6]).
- The Petersen graph has a lot of interesting properties. In fact, Holton and Sheehan devoted a whole book with several hundred references to exploring different properties of the Petersen graph (Holton & Sheehan [13]).

A. Geyer-Schulz (✉) · F. Ball
Information Services and Electronic Markets, Institute of Information Systems and Marketing, Karlsruhe Institute of Technology (KIT), 76131 Karlsruhe, Germany
e-mail: andreas.geyer-schulz@kit.edu

F. Ball
e-mail: ball@kit.edu

T. Imaizumi et al. (eds.), *Advanced Studies in Behaviormetrics and Data Science*, Behaviormetrics: Quantitative Approaches to Human Behavior 5,
https://doi.org/10.1007/978-981-15-2700-5_5

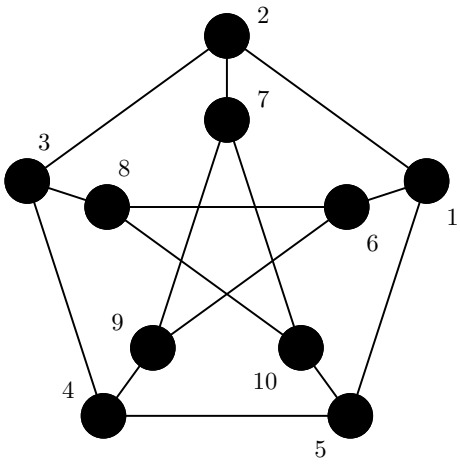

Fig. 1 The Petersen graph PG with the edge list {1, 6}, {2, 7}, {3, 8}, {4, 9}, {5, 10}, {1, 2}, {2, 3}, {3, 4}, {4, 5}, {5, 1}, {6, 8}, {7, 9}, {8, 10}, {9, 6}, {10, 7}

Our interest in the Petersen graph started by using it as a symmetric graph for a modularity maximizing graph clustering algorithm (Geyer-Schulz, Ovelgönne, & Stein [10]) to illustrate the effect of symmetry on the stability of the cluster solution. In the conference presentation the first author also became a victim of the Petersen graph: After showing three isomorphic, modularity optimal solutions (Newman & Girvan [17]) of the Petersen graph (see Fig. 2), he was asked how many modularity optimal solutions are there? He boldly conjectured *five* and added "As one can easily see". Clearly, at that point in time, he was overconfident and unaware of the true automorphism group of the Petersen graph. And the answer *five* is true if we consider only a single action (g_1 in Table 1) of the automorphism group of the graph. We hope, it is clear now why the Petersen graph never made it into the final version of the paper cited above.

For people in molecular biology, the two partitions of the Petersen graph shown in Fig. 3 also make sense if they accept rings of nucleobases: The five pairs in the left partition correspond to five base pairs (either adenine with thymine or cytosine with guanine or reverse), the two rings in the right partition to rings of nucleobases. The

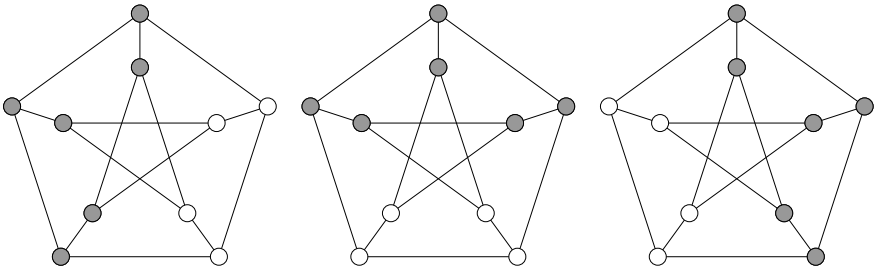

Fig. 2 How many modularity optimal partitions are there?

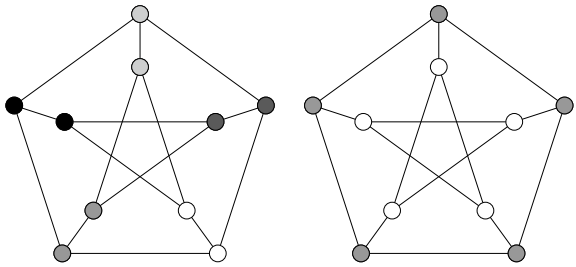

Fig. 3 How many optimal partitions are there for pairs and rings?

cluster criterion of maximizing modularity can be used to generate these solutions by appropriately increasing the edge weight of each pair (left graph in Fig. 3) or the weights of the five edges of each ring (right graph in Fig. 3)

In the rest of this paper we use the Petersen graph and the three different clustering solutions shown in Figs. 2 and 3 as a show case of how clustering of completely transitive graphs works and what is needed to properly diagnose such solutions.

In Sect. 2 we introduce the automorphism group of the Petersen graph and we show how the number and the set of equivalent optimal solutions for each of the three clustering criteria can be computed. Last, but not least, in Sect. 4 we show the construction of three classes of invariant partition comparison measures and we compute the structural distance between solutions of the three cluster criteria by a decomposition of the classic partition comparison measures for the Petersen graph.

2 The Automorphism Group of the Petersen Graph

A finite, undirected, unweighted graph $G = (V, E)$ with nodes $V = \{1, \ldots, n\}$ and edges $E = \{\{u, v\} \mid u, v \in V, u \neq v\}$ (uv is short hand for $\{u, v\}$) has graph partitions $\mathcal{P}, \mathcal{Q}$. A partition $\mathcal{P} = \{C_1, \ldots C_k\}$ has the usual properties of a partition: non-empty subsets, completeness under union, and disjointness of subsets.

Graph symmetry is expressed by permutation functions, where a permutation function p is a bijection $p : V \to V$ on the nodes V. The image of p on u is $u^p : u \mapsto u^p$. We extend this notation for sets, partitions, and graphs by pointwise application of p to the elements of V which are contained in sets, partitions, and graphs in a natural way, e.g., for the set of edges: $E^p = \{u^p v^p \mid uv \in E\}$.

A permutation group H on a finite set V with cardinality n consists of a set of permutation functions which fulfills the group axioms (closedness, identity, inverse, and associativity) under the group operation of function composition. For two permutation functions $p, q \in H$, their composition pq is defined as the successive application of the functions from left to right: $u^{pq} = (u^p)^q$. Repeated composition of p is denoted by $p^i, i \in N_0$. We define $p^0 = id$ as the identity permutation and by p^+ we denote the closure of the composition operation. This means, we repeat the composition until the resulting set of permutation functions remains constant. A classic text on permutation groups is Wielandt [22]. The largest permutation group on n symbols

is called the symmetric group $Sym(n)$ and its explicit representation consists of $n!$ permutation functions. A generator S of a permutation group is a set of permutation functions from which the explicit representation of the group is computed by successively applying the group operation until no further permutation functions can be generated (Coxeter & Moser [7]). We denote this by the closure operation S^+. The cardinality of a generator S is usually much smaller than the cardinality of the explicit representation of a permutation group, e.g. for $Sym(n)$, $|S_{Sym(n)}| = 2$ instead of $n!$.

The study of graph symmetry requires the computation of the automorphism group $Aut(G)$ of a graph G, which consists of all permutation functions on V which are graph automorphisms:

Definition 1 A permutation function p is an automorphism of a graph G iff $G^p = G$.

The condition $E^p = E$ provides a computable and constructive test that p is a graph automorphism. A brute force approach for solving the graph automorphism problem for a graph with n nodes consists in testing for $n!$ permutations that $E^p = E$ holds. For the Petersen graph, this means testing 3628800 (= 10!) permutation functions to extract its automorphism group.

Kemp [14, pp. 26–28] introduces five representations for a permutation function p (the standard, linear, graph, matrix, and cycle representations). In this contribution we use three of these representation:

Standard representation. $p_1 \in Sym(n)$ is written in two lines: The elements of V appear in the top row, and the elements under the mapping p_1 in the row below.

$$p_1 = \begin{pmatrix} 1\,2\,3\,4\,5\,6\,7\,8\,9\,10 \\ 2\,3\,4\,5\,6\,7\,8\,9\,10\,1 \end{pmatrix}$$

Linear representation. The linear notation of the permutation $p \in Sym(n)$ is the sequence of $1^p, 2^p, \ldots, n^p$. It requires a fixed ordering of the elements of V. This corresponds to the second line of the standard representation with elements sorted in increasing order. We use this representation in the rest of the paper for the (machine generated) presentation of results on the Petersen graph.

$$p_2 = 2, 1, 3, 4, 5, 6, 7, 8, 9, 10$$

Cycle representation. Let $p \in Sym(n)$ and $i_1 \in V$. The sequence $i_1, i_2, \ldots$ with $i_j = i_{j-1}^p$, $j = 2, 3, \ldots$ has the property that an element is generated which already exists in the sequence. This element must be i_1, because otherwise for some $j \in V : j = i_k^p = i_t^p$ with $i_k \neq i_t$ (which violates the bijection property of p). The sequence $i_1, \ldots i_l$ is called a cycle of p generated by i_1. (A cycle is uniquely determined by each of its elements which makes this notation not unique.) A permutation p is in cycle notation if

$$p = (i_{11}, \ldots, i_{1r_1})(i_{21}, \ldots, i_{2r_2}) \ldots (i_{k1}, \ldots, i_{1r_k})$$

where the $(i_{j1}, i_{j2}, \ldots, i_{jr_ji})$, $1 \leq j \leq k$ are the cycles of p. Trivial cycles are omitted. The identity permutation id has only trivial cycles and is represented as (). The permutations $p_1 = (1\,2\,\ldots\,n)$ and $p_2 = (1\,2)$ form a generator $S_{Sym(n)}$ of $Sym(n)$.

Note that the closure operations also define the set of isomorphic partitions of a graph G under $Aut(G)$. For example, for an arbitrary partition $\mathcal{P}$ of a fully connected graph (a clique of size n), the set of isomorphic partitions of $\mathcal{P}$ is $EC_{\mathcal{P}} = \mathcal{P}^{S^+_{Sym(n)}}$, because the automorphism group of such a clique is $Sym(n)$.

The Petersen graph PG is a representative of several special graph classes: A Moore-graph, a (3, 5)-cage, a Kneser (5, 2)-graph, … Since the automorphism group of the Petersen graph is isomorphic to S_5 (Wood [23]), the order of $Aut(PG)$ of the Petersen graph is $|Aut(PG)| = 5! = 120$. The Petersen graph is node and edge transitive. Transitive means that each node or edge can be mapped onto each other node or edge. It is 3-transitive, which means it contains exactly 120 paths of length 3 that are isomorphic.

Given the popularity of the Petersen graph, one would expect to find a generator of the automorphism group of the Petersen graph either in Holton's book or in modern text books on graph theory. In Holton and Sheehan [13, p. 23] one finds only two automorphisms of the Petersen graph which we show in Table 1: g_1 formalizes a rotation of the 5 pairs of PG, whereas g_2 moves the nodes of the inner ring to the outer ring while preserving the pairs, but not their circular arrangement. They do not suffice to generate the full automorphism group of the Petersen graph ($|\{g_1, g_2\}^+| = 20$).

After an extended literature search we uncovered a more recent source for generators of the automorphism group of the generalized Petersen graph $GP(10, 3)$, which is isomorphic to the Desargues configuration (Pisanski & Servatius [19, p. 177]). Pisanski and Servatius present the four automorphisms shown in Table 2 which generate the automorphism group of $GP(10, 3)$, which is of order 120, too. In addition, it is shown that $Sym(5)$ is isomorphic to the automorphism group of the Desargues configuration (Pisanski & Servatius [19, pp. 178–179]). Unfortunately, however, the standard Petersen graph PG (denoted as a generalized Petersen graph $GP(5, 2)$) only has the three generators g_1, g_2, and g_3 of Table 2 in common with the generalized Petersen graph $GP(10, 3)$, while g_4 is not on automorphism of the Petersen graph PG at all. A proper replacement of the last generator for the standard Petersen graph, however, is not easy to find.

The generator of the automorphism group of the Petersen graph shown in Table 3 has been computed by `saucy` (see Darga, Sakallah, & Markov [8]) and verified

Table 1 Two automorphisms of the Petersen graph (Holton & Sheehan [13, p. 23]). i is the index of p_i in Table 4

Cycle representation	Linear representation	i
$g_1 = (1\,2\,3\,4\,5)(6\,7\,8\,9\,10)$	2, 3, 4, 5, 1, 7, 8, 9, 10, 6	17
$g_2 = (1\,6)(2\,9\,5\,8)(3\,7\,4\,10)$	6, 9, 7, 10, 8, 1, 4, 2, 5, 3	72

Table 2 Three automorphisms of the Petersen graph (g_1, g_2, g_3). g_4 is not an automorphism (Pisanski & Servatius [19, p. 177]). i is the index of p_i in Table 4

Cycle representation	Linear representation	i
$g_1 = (1\,2\,3\,4\,5)(6\,7\,8\,9\,10)$	2 3 4 5 1 7 8 9 10 6	17
$g_2 = (1\,9\,3\,10)(2\,7)(5\,6\,4\,8)$	9 7 10 8 6 4 2 5 3 1	108
$g_3 = (2\,5)(3\,4)(7\,10)(9\,8)$	1 5 4 3 2 6 10 9 8 7	5
$g_4 = (2\,7)(4\,6)(5\,8)(9\,10)$	1 7 3 6 8 4 2 5 10 9	NA

Table 3 The generator of the Petersen graph computed by `saucy`. i is the index of p_i in Table 4

Cycle representation	Linear representation	i
$g_1 = (4\,8)(5\,6)(9\,10)$	1, 2, 3, 8, 6, 5, 7, 4, 10, 9	2
$g_2 = (2\,6)(3\,8)(4\,10)(7\,9)$	1, 6, 8, 10, 5, 2, 9, 3, 7, 4	10
$g_3 = (1\,3)(4\,5)(6\,8)(9\,10)$	3, 2, 1, 5, 4, 8, 7, 6, 10, 9	25

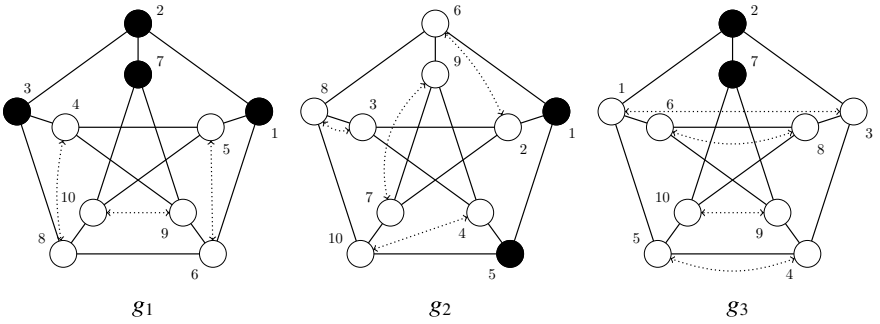

Fig. 4 The group actions g_1, g_2, g_3 of the `saucy` generator from Table 3. Black nodes are fixed

by the authors by the brute force approach described above. Figure 4 illustrates the effects of the group actions of the generator found by `saucy`.

However, this is not the end of the story. Because $Aut(PG)$ is isomorphic to $Sym(5)$ (by replacing the five edges which link the ring with the pentagram of the PG with five single nodes, we obtain a clique with five nodes), we expect that a minimal generator with two permutations exists. By brute force search, we discovered the generator of the Petersen graph shown in Table 5 which is one out of 3420 minimal generators. The set of permutations {2, 17} which combines Holton's and `saucy's` first generator is also a minimal generator.

Table 4 provides the base for a compact representation of generators of $Aut(PG)$ as a set of at least two indices. For example, the `saucy` generator shown in Table 3 is denoted as {2, 10, 25}. p_6 completes Holton's automorphisms to the generator {6, 17, 72}, and the three sets of permutations {3, 17, 108}, {5, 16, 108}, or {4, 5, 17}, which are all generators of $Aut(PG)$, are adaptations of the generator of Pisanski

Table 4 The full automorphism group $Aut(PG)$ of the Petersen graph in linear notation. Node labels are presented in Fig. 1. Holton's two automorphisms are {17, 72}, the three automorphisms of Pisanski and Servatius are {17, 108, 5}, the generator computed by `saucy` is {2, 10, 25}, and a minimal generator is e.g. {71, 118}

i	Permutation	i	Permutation	i	Permutation
1	1, 2, 3, 4, 5, 6, 7, 8, 9, 10	41	4, 5, 1, 2, 3, 9, 10, 6, 7, 8	81	7, 10, 5, 1, 2, 9, 8, 4, 6, 3
2	1, 2, 3, 8, 6, 5, 7, 4, 10, 9	42	4, 5, 1, 6, 9, 3, 10, 2, 8, 7	82	7, 10, 5, 4, 9, 2, 8, 1, 3, 6
3	1, 2, 7, 9, 6, 5, 3, 10, 4, 8	43	4, 5, 10, 7, 9, 3, 1, 8, 2, 6	83	7, 10, 8, 3, 2, 9, 5, 6, 4, 1
4	1, 2, 7, 10, 5, 6, 3, 9, 8, 4	44	4, 5, 10, 8, 3, 9, 1, 7, 6, 2	84	7, 10, 8, 6, 9, 2, 5, 3, 1, 4
5	1, 5, 4, 3, 2, 6, 10, 9, 8, 7	45	4, 9, 6, 1, 5, 3, 7, 8, 2, 10	85	8, 3, 2, 1, 6, 10, 4, 7, 5, 9
6	1, 5, 4, 9, 6, 2, 10, 3, 7, 8	46	4, 9, 6, 8, 3, 5, 7, 1, 10, 2	86	8, 3, 2, 7, 10, 6, 4, 1, 9, 5
7	1, 5, 10, 7, 2, 6, 4, 8, 9, 3	47	4, 9, 7, 2, 3, 5, 6, 10, 1, 8	87	8, 3, 4, 5, 10, 6, 2, 9, 1, 7
8	1, 5, 10, 8, 6, 2, 4, 7, 3, 9	48	4, 9, 7, 10, 5, 3, 6, 2, 8, 1	88	8, 3, 4, 9, 6, 10, 2, 5, 7, 1
9	1, 6, 8, 3, 2, 5, 9, 10, 4, 7	49	5, 1, 2, 3, 4, 10, 6, 7, 8, 9	89	8, 6, 1, 2, 3, 10, 9, 5, 7, 4
10	1, 6, 8, 10, 5, 2, 9, 3, 7, 4	50	5, 1, 2, 7, 10, 4, 6, 3, 9, 8	90	8, 6, 1, 5, 10, 3, 9, 2, 4, 7
11	1, 6, 9, 4, 5, 2, 8, 7, 3, 10	51	5, 1, 6, 8, 10, 4, 2, 9, 3, 7	91	8, 6, 9, 4, 3, 10, 1, 7, 5, 2
12	1, 6, 9, 7, 2, 5, 8, 4, 10, 3	52	5, 1, 6, 9, 4, 10, 2, 8, 7, 3	92	8, 6, 9, 7, 10, 3, 1, 4, 2, 5
13	2, 1, 5, 4, 3, 7, 6, 10, 9, 8	53	5, 4, 3, 2, 1, 10, 9, 8, 7, 6	93	8, 10, 5, 1, 6, 3, 7, 4, 2, 9
14	2, 1, 5, 10, 7, 3, 6, 4, 8, 9	54	5, 4, 3, 8, 10, 1, 9, 2, 6, 7	94	8, 10, 5, 4, 3, 6, 7, 1, 9, 2
15	2, 1, 6, 8, 3, 7, 5, 9, 10, 4	55	5, 4, 9, 6, 1, 10, 3, 7, 8, 2	95	8, 10, 7, 2, 3, 6, 5, 9, 1, 4
16	2, 1, 6, 9, 7, 3, 5, 8, 4, 10	56	5, 4, 9, 7, 10, 1, 3, 6, 2, 8	96	8, 10, 7, 9, 6, 3, 5, 2, 4, 1
17	2, 3, 4, 5, 1, 7, 8, 9, 10, 6	57	5, 10, 7, 2, 1, 4, 8, 9, 3, 6	97	9, 4, 3, 2, 7, 6, 5, 8, 1, 10
18	2, 3, 4, 9, 7, 1, 8, 5, 6, 10	58	5, 10, 7, 9, 4, 1, 8, 2, 6, 3	98	9, 4, 3, 8, 6, 7, 5, 2, 10, 1
19	2, 3, 8, 6, 1, 7, 4, 10, 9, 5	59	5, 10, 8, 3, 4, 1, 7, 6, 2, 9	99	9, 4, 5, 1, 6, 7, 3, 10, 2, 8
20	2, 3, 8, 10, 7, 1, 4, 6, 5, 9	60	5, 10, 8, 6, 1, 4, 7, 3, 9, 2	100	9, 4, 5, 10, 7, 6, 3, 1, 8, 2
21	2, 7, 9, 4, 3, 1, 10, 6, 5, 8	61	6, 1, 2, 3, 8, 9, 5, 7, 4, 10	101	9, 6, 1, 2, 7, 4, 8, 5, 3, 10
22	2, 7, 9, 6, 1, 3, 10, 4, 8, 5	62	6, 1, 2, 7, 9, 8, 5, 3, 10, 4	102	9, 6, 1, 5, 4, 7, 8, 2, 10, 3
23	2, 7, 10, 5, 1, 3, 9, 8, 4, 6	63	6, 1, 5, 4, 9, 8, 2, 10, 3, 7	103	9, 6, 8, 3, 4, 7, 1, 10, 2, 5
24	2, 7, 10, 8, 3, 1, 9, 5, 6, 4	64	6, 1, 5, 10, 8, 9, 2, 4, 7, 3	104	9, 6, 8, 10, 7, 4, 1, 3, 5, 2
25	3, 2, 1, 5, 4, 8, 7, 6, 10, 9	65	6, 8, 3, 2, 1, 9, 10, 4, 7, 5	105	9, 7, 2, 1, 6, 4, 10, 3, 5, 8
26	3, 2, 1, 6, 8, 4, 7, 5, 9, 10	66	6, 8, 3, 4, 9, 1, 10, 2, 5, 7	106	9, 7, 2, 3, 4, 6, 10, 1, 8, 5
27	3, 2, 7, 9, 4, 8, 1, 10, 6, 5	67	6, 8, 10, 5, 1, 9, 3, 7, 4, 2	107	9, 7, 10, 5, 4, 6, 2, 8, 1, 3
28	3, 2, 7, 10, 8, 4, 1, 9, 5, 6	68	6, 8, 10, 7, 9, 1, 3, 5, 2, 4	108	9, 7, 10, 8, 6, 4, 2, 5, 3, 1
29	3, 4, 5, 1, 2, 8, 9, 10, 6, 7	69	6, 9, 4, 3, 8, 1, 7, 5, 2, 10	109	10, 5, 1, 2, 7, 8, 4, 6, 3, 9
30	3, 4, 5, 10, 8, 2, 9, 1, 7, 6	70	6, 9, 4, 5, 1, 8, 7, 3, 10, 2	110	10, 5, 1, 6, 8, 7, 4, 2, 9, 3
31	3, 4, 9, 6, 8, 2, 5, 7, 1, 10	71	6, 9, 7, 2, 1, 8, 4, 10, 3, 5	111	10, 5, 4, 3, 8, 7, 1, 9, 2, 6
32	3, 4, 9, 7, 2, 8, 5, 6, 10, 1	72	6, 9, 7, 10, 8, 1, 4, 2, 5, 3	112	10, 5, 4, 9, 7, 8, 1, 3, 6, 2
33	3, 8, 6, 1, 2, 4, 10, 9, 5, 7	73	7, 2, 1, 5, 10, 9, 3, 6, 4, 8	113	10, 7, 2, 1, 5, 8, 9, 3, 6, 4
34	3, 8, 6, 9, 4, 2, 10, 1, 7, 5	74	7, 2, 1, 6, 9, 10, 3, 5, 8, 4	114	10, 7, 2, 3, 8, 5, 9, 1, 4, 6
35	3, 8, 10, 5, 4, 2, 6, 7, 1, 9	75	7, 2, 3, 4, 9, 10, 1, 8, 5, 6	115	10, 7, 9, 4, 5, 8, 2, 6, 3, 1
36	3, 8, 10, 7, 2, 4, 6, 5, 9, 1	76	7, 2, 3, 8, 10, 9, 1, 4, 6, 5	116	10, 7, 9, 6, 8, 5, 2, 4, 1, 3
37	4, 3, 2, 1, 5, 9, 8, 7, 6, 10	77	7, 9, 4, 3, 2, 10, 6, 5, 8, 1	117	10, 8, 3, 2, 7, 5, 6, 4, 1, 9
38	4, 3, 2, 7, 9, 5, 8, 1, 10, 6	78	7, 9, 4, 5, 10, 2, 6, 3, 1, 8	118	10, 8, 3, 4, 5, 7, 6, 2, 9, 1
39	4, 3, 8, 6, 9, 5, 2, 10, 1, 7	79	7, 9, 6, 1, 2, 10, 4, 8, 5, 3	119	10, 8, 6, 1, 5, 7, 3, 9, 2, 4
40	4, 3, 8, 10, 5, 9, 2, 6, 7, 1	80	7, 9, 6, 8, 10, 2, 4, 1, 3, 5	120	10, 8, 6, 9, 7, 5, 3, 1, 4, 2

Table 5 A minimal generator of the Petersen graph. i is the index of p_i in Table 4

Cycle representation	Linear representation	i
$g_1 = (1\,6\,8\,10\,5)(2\,9\,3\,7\,4)$	6, 9, 7, 2, 1, 8, 4, 10, 3, 5	71
$g_2 = (1\,10)(2\,8)(6\,7)$	10, 8, 3, 4, 5, 7, 6, 2, 9, 10	118

and Servatius [19, p. 177] for $GP(10, 3)$ to PG. Each set of generators represents a certain structural symmetry of PG. We leave a detailed analysis of the geometry of the group actions of the automorphism group of the Petersen graph for further research.

3 Multiple Isomorphic Solutions of Graph Clustering Algorithms

Multiple equivalent solutions of graph clustering algorithms all have the same value of the clustering criterion. They can be divided in two subsets:

1. The set of isomorphic solutions generated by $Aut(G)$.
2. The set of non-isomorphic solutions which have the same value of the cluster criterion. This group of solutions is left for further research.

First, what do we mean by an *optimal* solution of a graph clustering algorithm? Since most graph clustering algorithms are only heuristics with no guarantee to find a globally optimal partition, we refer to the best paritition a graph clustering algorithm finds as "optimal". Let $\mathcal{P}$ be an "optimal" graph partition in this sense. With the help of $Aut(G)$ it is possible to generate the set of isomorphic partitions $EC_{\mathcal{P}}$ by

$$EC_{\mathcal{P}} = \mathcal{P}^{Aut(G)}. \tag{1}$$

A partition is called stable iff $|EC_{\mathcal{P}}| = 1$ else it is called unstable. The transitivity of the Petersen graph implies that the only stable partitions are the trivial partitions: the 1-cluster and the singleton partition. All other partitions are unstable. This means that a set of partitions isomorphic under $Aut(PG)$ and of cardinality greater than 1 exists for all other partitions of the Petersen graph.

The set representation of a partition consists of a set of sets, whereas the linear representation of a partition is an n-element vector $\mathbf{v}$ of cluster labels. $v_i = c$ simply means that node i is element of cluster c with $c \in 1, \ldots, k$. The linear representation specifies a partition up to label isomorphism, e.g.:

$$(1, 2, 2, 1, 1, 1, 2, 2, 1, 1) \simeq (2, 1, 1, 2, 2, 2, 1, 1, 2, 2).$$

Table 6 Number of optimal solutions under $Aut(PG)$

	$\mathcal{P}_{Modularity}$	$\mathcal{P}_{2Rings}$	$\mathcal{P}_{5Pairs}$
Number of partitions (up to label isomorphism)	60	12	120
Number of partitions (with canonical labelling)	60	6	6

Table 7 The set of six isomorphic partitions for $\mathcal{P}_{2Rings}$ computed by $\mathcal{P}_{2Rings}^{Aut(PG)}$

	Representation of Partitions		
	Up to label isomorphism	Canonical labels	Set of sets
1.	(1, 1, 1, 1, 1, 2, 2, 2, 2, 2)	(1, 1, 1, 1, 1, 2, 2, 2, 2, 2)	{{1, 2, 3, 4, 5}, {6, 7, 8, 9, 10}}
2.	(2, 2, 2, 2, 2, 1, 1, 1, 1, 1)		
3.	(1, 2, 1, 2, 2, 1, 1, 1, 2, 2)	(1, 2, 1, 2, 2, 1, 1, 1, 2, 2)	{{1, 3, 6, 7, 8}, {2, 4, 5, 9, 10}}
4.	(2, 1, 2, 1, 1, 2, 2, 2, 1, 1)		
6.	(1, 2, 1, 2, 1, 1, 2, 2, 2, 1)	(1, 2, 1, 2, 1, 1, 2, 2, 2, 1)	{{1, 3, 5, 6, 10}, {2, 4, 7, 8, 8}}
9.	(2, 1, 2, 1, 2, 2, 1, 1, 1, 2)		
7.	(1, 2, 2, 1, 2, 1, 2, 2, 1, 1)	(1, 2, 2, 1, 2, 1, 2, 2, 1, 1)	{{1, 4, 6, 9, 10}, {2, 3, 5, 7, 8}}
10.	(2, 1, 1, 2, 1, 2, 1, 1, 2, 2)		
8.	(1, 2, 1, 1, 2, 2, 2, 1, 1, 2)	(1, 2, 1, 1, 2, 2, 2, 1, 1, 2)	{{1, 3, 4, 8, 9}, {2, 5, 6, 7, 10}}
5.	(2, 1, 2, 2, 1, 1, 1, 2, 2, 1)		
11.	(1, 1, 2, 1, 2, 1, 1, 2, 2, 2)	(1, 1, 2, 1, 2, 1, 1, 2, 2, 2)	{{1, 2, 4, 6, 7}, {3, 5, 8, 9, 10}}
12.	(2, 2, 1, 2, 1, 2, 2, 1, 1, 1)		

Table 8 The set of six isomorphic partitions of $\mathcal{P}_{5Pairs}^{Aut(PG)}$

{{1, 6}{2, 7}{3, 8}{4, 9}{5, 10}}	{{1, 2}{3, 8}{4, 5}{6, 9}{7, 10}}
{{1, 6}{2, 3}{4, 5}{7, 9}{8, 10}}	{{1, 5}{2, 7}{3, 4}{6, 9}{8, 10}}
{{1, 2}{3, 4}{5, 10}{6, 8}{7, 9}}	{{1, 5}{2, 3}{4, 9}{6, 8}{7, 10}}

The three optimal partitions for the three cluster criteria shown in Figs. 2 and 3 are in set (and linear) representation:

$\mathcal{P}_{Modularity} = \mathcal{P}_M = \{\{1, 4, 5, 6, 9, 10\}, \{2, 3, 7, 8\}\} = (1, 2, 2, 1, 1, 1, 2, 2, 1, 1)$

$\mathcal{P}_{2Rings} = \mathcal{P}_R\{\{1, 2, 3, 4, 5\}, \{6, 7, 8, 9, 10\}\} = (1, 1, 1, 1, 1, 2, 2, 2, 2, 2)$

$\mathcal{P}_{5Pairs} = \mathcal{P}_P\{\{1, 6\}, \{2, 7\}, \{3, 8\}, \{4, 9\}, \{5, 10\}\} = (1, 2, 3, 4, 5, 1, 2, 3, 4, 5)$

We show the number of isomorphic optimal solutions with and without elimination of label isomorphism for these partitions in Table 6 to show the variation in the effect of this transformation. For $\mathcal{P}_{2Rings}$, we illustrate the elimination of label isomorphisms in Table 7. The set of isomorphic solutions for $\mathcal{P}_{5Pairs}$ is presented in Table 8 and, last but not least, the set of isomorphic solutions for $\mathcal{P}_{Modularity}$ is shown in Table 9.

Table 9 The set of 60 isomorphic partitions of $\mathcal{P}^{Aut(PG)}_{Modularity}$

{{1, 4, 5, 6, 9, 10}{2, 3, 7, 8}}	{{1, 2, 3, 7, 8, 10}{4, 5, 6, 9}}
{{1, 2, 3, 4, 5, 9}{6, 7, 8, 10}}	{{1, 5, 6, 8, 9, 10}{2, 3, 4, 7}}
{{1, 5, 7, 10}{2, 3, 4, 6, 8, 9}}	{{1, 4, 5, 6, 8, 10}{2, 3, 7, 9}}
{{1, 2, 4, 5, 7, 10}{3, 6, 8, 9}}	{{1, 2, 3, 8}{4, 5, 6, 7, 9, 10}}
{{1, 2, 3, 4, 6, 8}{5, 7, 9, 10}}	{{1, 2, 6, 7}{3, 4, 5, 8, 9, 10}}
{{1, 2, 3, 5}{4, 6, 7, 8, 9, 10}}	{{1, 2, 6, 8}{3, 4, 5, 7, 9, 10}}
{{1, 2, 3, 4, 5, 7}{6, 8, 9, 10}}	{{1, 4, 5, 6}{2, 3, 7, 8, 9, 10}}
{{1, 6, 7, 8, 9, 10}{2, 3, 4, 5}}	{{1, 2, 5, 7}{3, 4, 6, 8, 9, 10}}
{{1, 5, 6, 7, 8, 10}{2, 3, 4, 9}}	{{1, 2, 4, 5, 6, 9}{3, 7, 8, 10}}
{{1, 2, 6, 7, 8, 9}{3, 4, 5, 10}}	{{1, 2, 5, 7, 9, 10}{3, 4, 6, 8}}
{{1, 2, 7, 9}{3, 4, 5, 6, 8, 10}}	{{1, 6, 8, 10}{2, 3, 4, 5, 7, 9}}
{{1, 2, 3, 4, 5, 10}{6, 7, 8, 9}}	{{1, 3, 4, 5, 8, 10}{2, 6, 7, 9}}
{{1, 2, 6, 9}{3, 4, 5, 7, 8, 10}}	{{1, 2, 3, 6, 8, 10}{4, 5, 7, 9}}
{{1, 3, 5, 6, 8, 10}{2, 4, 7, 9}}	{{1, 2, 3, 6, 7, 8}{4, 5, 9, 10}}
{{1, 2, 4, 5}{3, 6, 7, 8, 9, 10}}	{{1, 2, 3, 4, 5, 6}{7, 8, 9, 10}}
{{1, 5, 6, 9}{2, 3, 4, 7, 8, 10}}	{{1, 2, 5, 6, 7, 10}{3, 4, 8, 9}}
{{1, 3, 4, 5}{2, 6, 7, 8, 9, 10}}	{{1, 2, 3, 6, 7, 9}{4, 5, 8, 10}}
{{1, 4, 5, 6, 8, 9}{2, 3, 7, 10}}	{{1, 2, 4, 6, 7, 9}{3, 5, 8, 10}}
{{1, 4, 5, 9}{2, 3, 6, 7, 8, 10}}	{{1, 2, 3, 4, 7, 9}{5, 6, 8, 10}}
{{1, 2, 7, 10}{3, 4, 5, 6, 8, 9}}	{{1, 2, 3, 4}{5, 6, 7, 8, 9, 10}}
{{1, 3, 4, 6, 8, 9}{2, 5, 7, 10}}	{{1, 2, 3, 4, 5, 8}{6, 7, 9, 10}}
{{1, 2, 5, 10}{3, 4, 6, 7, 8, 9}}	{{1, 6, 7, 9}{2, 3, 4, 5, 8, 10}}
{{1, 2, 3, 5, 6, 8}{4, 7, 9, 10}}	{{1, 4, 5, 6, 7, 9}{2, 3, 8, 10}}
{{1, 2, 5, 6, 8, 10}{3, 4, 7, 9}}	{{1, 4, 5, 7, 9, 10}{2, 3, 6, 8}}
{{1, 2, 3, 6, 8, 9}{4, 5, 7, 10}}	{{1, 3, 6, 8}{2, 4, 5, 7, 9, 10}}
{{1, 3, 4, 5, 6, 9}{2, 7, 8, 10}}	{{1, 5, 6, 10}{2, 3, 4, 7, 8, 9}}
{{1, 2, 3, 6}{4, 5, 7, 8, 9, 10}}	{{1, 5, 8, 10}{2, 3, 4, 6, 7, 9}}
{{1, 2, 5, 6, 7, 9}{3, 4, 8, 10}}	{{1, 5, 6, 8}{2, 3, 4, 7, 9, 10}}
{{1, 2, 5, 7, 8, 10}{3, 4, 6, 9}}	{{1, 2, 3, 5, 7, 10}{4, 6, 8, 9}}
{{1, 2, 6, 7, 9, 10}{3, 4, 5, 8}}	{{1, 4, 6, 9}{2, 3, 5, 7, 8, 10}}

4 Measures for Comparing Partitions and for Comparing Isomorphic Sets of Partitions

As a motivating example for this section we compare the isomorphic modularity optimal partitions $\mathcal{P}_1 = \{\{1, 4, 5, 6, 9, 10\}\{2, 3, 7, 8\}\}$, $\mathcal{P}_2 = \{\{1, 5, 6, 8, 9, 10\}\{2, 3, 4, 7\}\}$, $\mathcal{P}_3 = \{\{1, 2, 4, 5, 7, 10\}\{3, 6, 8, 9\}\}$, and $\mathcal{P}_4 = \{\{1, 2, 3, 7, 8, 10\}\{4, 5, 6, 9\}\}$ from Table 9 with five well-known partition comparison measures. Table 10 shows the results. It is obvious that none of these measures is suitable for identifying

Table 10 Comparison of Partitions from Set of Isomorphic Modularity Optimal Partitions. Computed with R-Package `partitionComparison` (Ball & Geyer-Schulz [2])

Measure	$m(\mathcal{P}_1, \mathcal{P}_1)$	$m(\mathcal{P}_1, \mathcal{P}_2)$	$m(\mathcal{P}_1, \mathcal{P}_3)$	$m(\mathcal{P}_1, \mathcal{P}_4)$
jaccardCoefficient	1.000	0.448	0.2727	0.448
randIndex	1.000	0.644	0.4667	0.644
minkowskiMeasure	0.000	0.873	1.0690	0.873
larsenAone	1.000	0.792	0.5833	0.800
mutualInformation	0.673	0.178	0.0138	0.291
variationOfInformation	0.000	0.991	1.3183	0.764

partitions which are structurally identical. What we need for comparing partitions of the Petersen graph is a class of partition comparison measures which are designed for the comparison of sets of isomorphic partitions.

We start with the formal definition of an invariant partition comparison measure:

Definition 2 A partition comparison measure $m : P(V) \times P(V) \rightarrow \mathbb{R}$, for which a suitable identity axiom holds, is invariant under automorphism if

$$m(\mathcal{P}, \mathcal{Q}) = m(\tilde{\mathcal{P}}, \tilde{\mathcal{Q}})$$

for all $\mathcal{P}, \mathcal{Q} \in P(V)$ and $\tilde{\mathcal{P}} \in \mathcal{P}^{Aut(G)}$, $\tilde{\mathcal{Q}} \in \mathcal{Q}^{Aut(G)}$. $P(V)$ denotes the set of all partitions of V.

The term *suitable identity axiom* simply means that the identity must be properly formulated for the partition comparison measure used. For the similarity measures (`jaccardCoefficient`, the `randIndex`, and the `larsenAone`) the identity axiom is $m(\mathcal{P}, \mathcal{Q}) = 1$, if $\mathcal{P} = \mathcal{Q}$. For the distance measures (`minkowskiMeasure` and `variationOfInformation`), it is $m(\mathcal{P}, \mathcal{Q}) = 0$, if $\mathcal{P} = \mathcal{Q}$. And, last but not least, for the `mutualInformation` measure $m(\mathcal{P}, \mathcal{Q}) = \max$, if $\mathcal{P} = \mathcal{Q}$.

Theorem 1 *Invariant partition comparison measures do not exist.*

Proof First, we note that a partition $\mathcal{P} \in P(V)$ is

1. either stable ($1 = |\mathcal{P}^{Aut(G)}|$) or
2. unstable ($1 < |\mathcal{P}^{Aut(G)}|$).

Let the identity axiom be $m(\mathcal{P}, \mathcal{Q}) = 0$, if $\mathcal{P} = \mathcal{Q}$ and set $c = 0$. Let $\mathcal{P} \neq \mathcal{Q}$. From the identity axiom follows that $m(\mathcal{P}, \mathcal{Q}) \neq c$. Let $\mathcal{P}$ and $\mathcal{Q}$ be on the same orbit of $Aut(G)$ with $1 < |\mathcal{P}^{Aut(G)}|$ and $\mathcal{P} \neq \mathcal{Q}$. From the invariance axiom we know that $m(\mathcal{P}, \mathcal{Q}) = c$, because the group action is an isomorphism. By combining the invariance and the identity axiom, we get

$$c = m(\mathcal{P}, \mathcal{Q}) \neq c$$

which is a contradiction. (Based on Aumann & Shapley [1]). □

Theorem 1 demonstrates the incompatibility of the identity and the invariance axiom in a metric space. An implication of this incompatibility is that a single measure either respects the identity or the invariance axiom.

For the analysis and comparison of several optimal partitions computed by graph clustering algorithms for graphs with symmetries, we actually need the combination of a measure and its invariants and an understanding of their relations:

1. We want a measure that measures the distance between partitions. The classic partition comparison measures which respect the identity axiom but not the invariance axiom serve this purpose. We denote such a measure by d. For a survey and references to the seminal papers of these measures, see Ball and Geyer-Schulz [4, pp. 18–21].
2. We want a measure that identifies isomorphic partitions as isomorphic and measures the distance between non-isomorphic partitions (each of which is an element of a set of isomorphic partitions), or, to phrase it in the language of Haar [11], a measure which is invariant to the group transformations of the symmetry group of the graph. We refer to such a measure as d^*. This is the purpose of invariant partition comparison measures introduced by Ball and Geyer-Schulz [4].
3. We want to be able to decompose a classic measure in its structural and its transformation part (a measure decomposition) and we want to assess the size of the structural part and the actual, minimal, average, and maximal potential size of the transformation part. See Ball and Geyer-Schulz [4].

In the following we will, without loss of generality, consider only distance functions. All similarity functions for which $s(\mathcal{P}, \mathcal{P}) = 1$ holds can be converted to a distance function by $d(\mathcal{P}, \mathcal{Q}) = 1 - s(\mathcal{P}, \mathcal{Q})$. As the example of the `mutualInformation` measure shows, such a transformation can be found: For nonnormalized similarity functions with an identity $m(\mathcal{P}, \mathcal{Q}) = \max$, the transformation is $d(\mathcal{P}, \mathcal{P}) = \max - m(\mathcal{P}, \mathcal{Q})$.

A metric for a space S (with $s, t, u \in S$) has a distance function $d : S \times S \rightarrow \mathbb{R}^+$ for which the following holds:

1. Symmetry: $d(s, t) = d(t, s)$.
2. Identity: $d(s, t) = 0$ if and only if $s = t$.
3. Triangle inequality: $d(s, u) \leq d(s, t) + d(t, u)$.

The metric space $(P(V), d)$ has as elements the set of finite node partitions $P(V)$, the metric space $(P(V)^{Aut(G)}, d^*)$ has as elements sets of equivalent partitions of $P(V)$.

A pseudometric space has equivalence classes denoted as $[s]$ as elements. In a pseudometric space (S, d^*) the identity condition is replaced by the invariance condition $d^*(s_1, s_2) = 0$, if $s_1, s_2 \in [s]$. In addition, for the distance function $d^*(s, t)$ the symmetry axiom and the triangle inequality hold. Note that in a pseudometric space, $d^*(s_1, s_2) = 0$ does not allow to infer that $s_1 = s_2$.

We consider in the following the pseudometric space $(P(V), d^*)$, which we get with the help of the transformation $t : P(V) \rightarrow P(V)^{Aut(G)}$, which maps a partition

to its equivalence class under the automorphism group of the graph. As a result, we have endowed the space $P(V)$ with the metric d to recognize identical partitions and the pseudometric d^* to recognize isomorphic partitions.

The construction of an invariant measure d^* is based on the ideas of Hausdorff [12, p. 166] and von Neumann [20, 21]: We simply compute the set of all distances d between pairs of partitions for the direct product of the two equivalence classes of the partition, and we compute the minimum, the maximum, and the average of this set of distances, all of which are invariant with regard to the finite automorphism group of the graph and thus can be used for d^*:

$$d_L^*(\mathcal{P}, \mathcal{Q}) = \min_{\substack{\tilde{\mathcal{P}} \in \mathcal{P}^{Aut(G)}, \\ \tilde{\mathcal{Q}} \in \mathcal{Q}^{Aut(G)}}} d(\tilde{\mathcal{P}}, \tilde{\mathcal{Q}}) \tag{2}$$

$$d_U^*(\mathcal{P}, \mathcal{Q}) = \begin{cases} 0 & \text{if } \mathcal{P}^{Aut(G)} = \mathcal{Q}^{Aut(G)} \\ \max_{\substack{\tilde{\mathcal{P}} \in \mathcal{P}^{Aut(G)}, \\ \tilde{\mathcal{Q}} \in \mathcal{Q}^{Aut(G)}}} d(\tilde{\mathcal{P}}, \tilde{\mathcal{Q}}) & \text{else} \end{cases} \tag{3}$$

$$d_{av}^*(\mathcal{P}, \mathcal{Q}) = \begin{cases} 0 & \text{if } \mathcal{P}^{Aut(G)} = \mathcal{Q}^{Aut(G)} \\ \frac{1}{|\mathcal{P}^{Aut(G)}| \cdot |\mathcal{Q}^{Aut(G)}|} \sum_{\substack{\tilde{\mathcal{P}} \in \mathcal{P}^{Aut(G)}, \\ \tilde{\mathcal{Q}} \in \mathcal{Q}^{Aut(G)}}} d(\tilde{\mathcal{P}}, \tilde{\mathcal{Q}}) & \text{else} \end{cases} \tag{4}$$

The proof that all three constructions are pseudometrics is in Ball and Geyer-Schulz [4, pp. 12–13]. The diameter $dia(\mathcal{P})$ of the equivalence class of a partition is defined by:

$$dia(\mathcal{P}) = \max_{\substack{\tilde{\mathcal{P}} \in \mathcal{P}^{Aut(G)}, \\ \tilde{\mathcal{Q}} \in \mathcal{P}^{Aut(G)}}} d(\tilde{\mathcal{P}}, \tilde{\mathcal{Q}}) \tag{5}$$

Note that a direct (naive) implementation of these three variants of d^* has a computational complexity $O(n^2)$, where n is of the order of $Aut(G)$, which makes the computation of an invariant partition comparison measure quite expensive.

However, Ball and Geyer-Schulz [4] have found a way to reduce the complexity of computation of an invariant partition comparison measure to $O(n)$ if both partitions are unstable and to $O(1)$ if one partition is stable. They exploit the fact that both partitions are subject to the actions of the same graph automorphism group. This implies that $Aut(G)$ establishes identities on distances between partitions

$$d(\tilde{\mathcal{P}}, \tilde{\mathcal{Q}}) = d(\mathcal{P}^h, \mathcal{Q}^g) = d(\mathcal{P}, \mathcal{Q}^{gh^{-1}}) = d(\mathcal{P}^{hg^{-1}}, \mathcal{Q}) \tag{6}$$

with $\mathcal{P}, \mathcal{Q} \in P(V)$ and $g, h \in Aut(G)$. These identities set up a relative measurement system and they show that we only have to choose one partition, say $\mathcal{P}$, as a reference point to measure the n distances to each of the partitions in $\mathcal{Q}^{Aut(G)}$. Since the choice of a reference point should not affect the distance we measure, we

may always choose the partition with the equivalence class of higher cardinality as a reference point. In the case of a stable partition the complexity reduces to $O(1)$. For a complete proof for all three variants of invariant measures, we refer the reader to Ball and Geyer-Schulz [4, pp. 11–12].

$P(V)$ has the metric d and the three invariant pseudometrics d_L^*, d_U^*, and d_{av}^*. With these distances we can decompose the distance d in a structural part and a part induced by the group-action:

$$d(\mathcal{P},\mathcal{Q}) = \underbrace{d_L^*(\mathcal{P},\mathcal{Q})}_{d_{L,struct}} + \underbrace{\left(d(\mathcal{P},\mathcal{Q}) - d_L^*(\mathcal{P},\mathcal{Q})\right)}_{d_{L,Aut(G)}} \tag{7}$$

$$= \underbrace{d_U^*(\mathcal{P},\mathcal{Q})}_{d_{U,struct}} - \underbrace{\left(d_U^*(\mathcal{P},\mathcal{Q}) - d(\mathcal{P},\mathcal{Q})\right)}_{d_{U,Aut(G)}} \tag{8}$$

$$= \underbrace{d_{av}^*(\mathcal{P},\mathcal{Q})}_{d_{av,struct}} - \underbrace{\left(d_{av}^*(\mathcal{P},\mathcal{Q}) - d(\mathcal{P},\mathcal{Q})\right)}_{d_{av,Aut(G)}} \tag{9}$$

$dia(\mathcal{P})$ measures the maximal effect of the automorphism group $Aut(G)$ on a single equivalence class $\mathcal{P}^{Aut(G)}$. In addition, $e_{Max}^{Aut(G)}$ is an upper bound of the automorphism effect on the distance of two partitions $\mathcal{P}$ and $\mathcal{Q}$:

$$e_{Max}^{Aut(G)} = \min(dia(\mathcal{P}), dia(\mathcal{Q})). \tag{10}$$

Additionally, $e_{Max}^{Aut(G)} \geq d_U^* - d_L^*$ holds.

The three families of invariant measures have been implemented in R for all partition comparison measures in the R-Package partitionComparison by Ball and Geyer-Schulz [2].

5 Comparing Partitions of the Petersen Graph

In this section we present a detailed analysis of the properties and a comparison of the optimal partitions shown in Figs. 2 and 3 (and tabulated in Tables 7, 8 and 9) for the three different clustering criteria with regard to the Rand distance d_{1-RI} and to the variation of information distance d_{VI}. First, we show some properties of these partitions and their distances from the singleton and the 1-cluster partition in Table 11. Because the singleton and the 1-cluster partition are stable, no automorphism effects occur and d_L^*, d_U^*, and d_{av}^* correspond to d. (The variation of information measure establishes a complete and consistent order on the distances of optimal partitions to the trivial partitions of PG.)

Our next example shows the decomposition of the distance measure into an invariant structural and an automorphic part. From the equivalence classes of the optimal partitions, we pick a second partition to show the effect of $Aut(PG)$ on the measure:

Table 11 Properties of the three optimal partitions

Measure	$\mathcal{X} = \mathcal{M}$	$\mathcal{X} = \mathcal{R}$	$\mathcal{X} = \mathcal{P}$
Partition type	(6, 4)	(5, 5)	(2, 2, 2, 2, 2)
Number in type	210	126	945
Number of partitions $\lvert\mathcal{X}^{Aut(G)}\rvert$	60	6	6
Stable?	False	False	False
Diameter $dia(\mathcal{X}, d_{1-RI})$	0.533	0.533	0.178
Diameter $dia(\mathcal{X}, d_{VI})$	1.32	1.35	1.11
d_{1-RI} to {{1}{2}{3}{4}{5}{6}{7}{8}{9}{10}} (singeton)	0.467	0.444	0.111
d_{VI} to {{1}{2}{3}{4}{5}{6}{7}{8}{9}{10}} (singleton)	1.630	1.609	0.693
d_{1-RI} to {{1, 2, 3, 4, 5, 6, 7, 8, 9, 10}} (1-cluster)	0.533	0.556	0.889
d_{VI} to {{1, 2, 3, 4, 5, 6, 7, 8, 9, 10}} (1-cluster)	0.673	0.693	1.609

$$\mathcal{P}_{M1} = \{\{1, 2, 4, 5, 7, 10\}\{3, 6, 8, 9\}\}$$
$$\mathcal{P}_{R1} = \{\{1, 5, 6, 8, 10\}\{2, 3, 4, 7, 9\}\}$$
$$\mathcal{P}_{P1} = \{\{1, 2\}\{3, 8\}\{4, 5\}\{6, 9\}\{7, 10\}\}$$

In Table 12 we show the results of the comparison of optimal partitions. The structural part of the variation of information measure d_{VI} for $d^*_{L,VI}$ between $\mathcal{P}_M$ and $\mathcal{P}_R$ is 0.521, between $\mathcal{P}_M$ and $\mathcal{P}_P$ it is 0.936 and between $\mathcal{P}_R$ and $\mathcal{P}_P$ it is 1.194. For some comparisons (e.g. between $\mathcal{P}_M$ and $\mathcal{P}_R$), the automorphism effect $Aut(d, d^*)$ dominates the structural effect d^*. This implies that the structural order is disguised by the automorphism effect. Note, that the choice of the invariant measure class has an influence on the order of partitions. The second part of Table 12 allows a comparison of the Rand distance d_{1-RI} with the variation of information distance. For the lower invariant measure, the Rand distance leads to the same order of distances as the variation of information distance: From Table 12 we observe $d^*_{L,1-RI}(\mathcal{P}_M, \mathcal{P}_R) = 0.20$, $d^*_{L,1-RI}(\mathcal{P}_M, \mathcal{P}_P) = 0.356$, and $d^*_{L,1-RI}(\mathcal{P}_R, \mathcal{P}_P) = 0.378$ which leads to the following order:

$$d^*_{L,1-RI}(\mathcal{P}_M, \mathcal{P}_R) < d^*_{L,1-RI}(\mathcal{P}_M, \mathcal{P}_P) < d^*_{L,1-RI}(\mathcal{P}_R, \mathcal{P}_P)$$

Next, we study the automorphism effects within the three sets of multiple equivalent solutions (see Tables 7, 8 and 9). Obviously, for all three classes, $d^*_L = 0$ for the Rand distance and the variation of information distance.

We observe for the pair and ring set of solutions, that d takes only two values: $d(\mathcal{P}i, \mathcal{P}_i) = 0$, and for $i \neq j$)

Table 12 Measure decomposition for distances between optimal partitions

$\mathcal{P}, \mathcal{Q}$	$d = d_{VI}$	d_L^*	$Aut(d, d_L^*)$	d_U^*	$Aut(d, d_U^*)$	d_{av}^*	$Aut(d, d_{av}^*)$
$\mathcal{P}_M, \mathcal{P}_R$	1.366	0.521	0.846	1.366	0.000	1.168	−0.198
$\mathcal{P}_{M1}, \mathcal{P}_R$	1.194	0.521	0.673	1.366	0.173	1.168	−0.026
$\mathcal{P}_M, \mathcal{P}_P$	0.936	0.936	0.000	2.045	1.109	1.491	0.555
$\mathcal{P}_{M1}, \mathcal{P}_P$	1.491	0.936	0.555	2.045	0.555	1.491	−0.000
$\mathcal{P}_R, \mathcal{P}_P$	2.303	1.194	1.109	2.303	0.000	1.378	−0.924
$\mathcal{P}_{R1}, \mathcal{P}_P$	1.194	1.194	0.000	2.303	1.109	1.378	0.185
$\mathcal{P}, \mathcal{Q}$	$d = d_{1-RI}$	d_L^*	$Aut(d, d_L^*)$	d_U^*	$Aut(d, d_U^*)$	d_{av}^*	$Aut(d, d_{av}^*)$
$\mathcal{P}_M, \mathcal{P}_R$	0.556	0.200	0.356	0.556	0.000	0.467	−0.089
$\mathcal{P}_{M1}, \mathcal{P}_R$	0.467	0.200	0.267	0.556	0.089	0.467	0.000
$\mathcal{P}_M, \mathcal{P}_P$	0.356	0.356	0.000	0.533	0.178	0.444	0.089
$\mathcal{P}_{M1}, \mathcal{P}_P$	0.444	0.356	0.089	0.533	0.089	0.444	0.000
$\mathcal{P}_R, \mathcal{P}_P$	0.556	0.378	0.178	0.556	0.000	0.407	−0.148
$\mathcal{P}_{R1}, \mathcal{P}_P$	0.378	0.378	0.000	0.556	0.178	0.407	0.030

1. $d_{1-RI}(\mathcal{P}_i, \mathcal{P}_j) = 0.178$ and $d_{VI}(i, j) = 1.109$ for partitions $\mathcal{P}_i, \mathcal{P}_j$ from the pair set of multiple equivalent solutions.
2. $d_{1-RI}(\mathcal{P}_i, \mathcal{P}_j) = 0.533$ and $d_{VI}(i, j) = 1.1346$ for partitions $\mathcal{P}_i, \mathcal{P}_j$ from the ring set of multiple equivalent solutions.

That the distribution of the automorphism effects is structurally similar for the ring and pair solutions for the Petersen graph PG is unexpected given that the cluster size of in the ring set is considerably larger than in the pair set.

The automorphism effects between the partitions of the modularity optimal partitions are more complex and the structure of the effects depends on the partition comparison measure selected. $Aut(d_{1-RI}, d_{L,1-RI}^*) \in \{0.000, 0.356, 0.533\}$ and $Aut(d_{VI}, d_{L,VI}^*) \in \{0.000, 0.764, 0.991, 1.282, 1.318\}$. We show the distribution of distances of the pairwise distance matrix of this set in Table 13 for both distances considered. Note, that because of the identities shown in Eq. 6 the complete structure of the distances are contained in a single row or column of the pairwise distance matrix. In addition, the automorphism effect does not follow a normal distribution, because $d_{av,RI}^* = 0.48$ and $d_{av,VI}^* = 1.1757$. Last, but not least, Table 13 shows that the variation of information distance is a finer measure than the Rand distance.

We already know from Table 11 that partitions of the same partition types as the three optimal solution sets shown in Tables 9, 7, and 8 exist which are not optimal. In Table 14 we show, that a structural difference exists between an optimal and a non-optimal partition of the same partition type. For the analyses of the automorphism effects we refer to the analysis of the effects in a set isomorphic partitions presented above. We show only the 3 invariant measures for both partition comparison measures.

Table 13 Distribution of distances in the set of modularity optimal partitions

Rand distance d_{1-RI}			Variation of information d_{VI}		
d	Frequency	Share	d	Frequency	Share
0.000	60	0.0167	0.000	60	0.0167
0.356	900	0.2500	0.764	420	0.1167
			0.991	480	0.1133
0.533	2640	0.7333	1.282	1200	0.3333
			1.318	1440	0.4000

Table 14 Structural differences of non-optimal and optimal partitions of the same partition type

Five pairs (2, 2, 2, 2, 2)					
Non-optimal partition {{1, 4}{2, 6}{3, 7}{5, 10}{8, 9}}	Optimal partition with any partition of Table 8	d	d_L^*	d_{av}^*	d_U^*
		d_{1-RI}	0.178	0.207	0.222
		d_{VI}	1.109	1.294	1.386
Two rings (5, 5)					
Non-optimal partition {{1, 2, 4, 6, 7}{3, 5, 8, 9, 10}}	Optimal partition with any partition of Table 7	d	d_L^*	d_{av}^*	d_U^*
		d_{1-RI}	0.356	0.504	0.533
		d_{VI}	1.001	1.288	1.346
Modularity optimal (6, 4)					
Non-optimal partition {{1, 3, 5, 7, 9, 10}{2, 4, 6, 8}}	Optimal partition with any partition of Table 9	d	d_L^*	d_{av}^*	d_U^*
		d_{1-RI}	0.356	0.516	0.533
		d_{VI}	0.764	1.263	1.318

6 Summary and Outlook

For graph clustering, the main contribution of this paper is the decomposition of a partition comparison measure in its structural part and in the effect of the automorphism group of the graph. The construction given requires the computation of the automorphism of the graph and an invariant measure on the equivalence classes of partitions isomorphic under the group action of the automorphism group.

We have applied these measures to analyze partitions of the Petersen graph which are the results of three different clustering criteria. The property which makes the analysis of such partitions impossible with standard partition comparison measures is the transitivity of the Petersen graph. A benefit of the Petersen graph is that the Petersen graph has on the one hand an automorphism group rich enough for giving non-trivial applications of measure decomposition and that it is on the other hand still small enough for explicit demonstrations.

The main objection against the methods presented in this contribution is that first symmetries do not occur in large graphs (e.g. based on asymptotic results on random graphs by Erdös & Rényi [9]) and second, even if they occur, they have no impact on the clustering result. However, a large scale empirical study of real world graphs shows that about 70% of 902 simple graphs are symmetric and almost 80% of 797 simplified graphs (Ball & Geyer-Schulz [3]). In a second study of the 1699 graphs of the first study the authors found that for 22% of these graphs, symmetry leads to unstable clustering solutions (Ball & Geyer-Schulz [5]). Combined these two studies provide strong evidence that the analysis of graph clustering results introduced in this contribution also has practical relevance.

References

1. Aumann, R. J., & Shapley, L. S. (1974). *Values of non-atomic games*. Princeton: Princeton University Press.
2. Ball, F., & Geyer-Schulz, A. (2017). *R-package partitionComparison*. Technical Report 1-2017, Information Services and Electronic Markets, Karlsruhe: Institute of Information Systems and Marketing, Karlsruhe Institute of Technology.
3. Ball, F., & Geyer-Schulz, A. (2018a). How symmetric are real-world graphs? A large-scale study. *Symmetry*, *10*(1), 29. (1–17).
4. Ball, F., & Geyer-Schulz, A. (2018b). Invariant graph partition comparison measures. *Symmetry*, *10*(10), 1–24.
5. Ball, F., & Geyer-Schulz, A. (2018c). The impact of graph symmetries on clustering. *Archives of Data Science, Series A, 5*(1), 1–9.
6. Capobianco, M., & Molluzzo, J. C. (1978). *Examples and counterexamples in graph theory*. New York: North Holland.
7. Coxeter, H., & Moser, W. (1965). *Generators and relations for discrete groups* (Vol. 14). *Ergebnisse der Mathematik und ihrer Grenzgebiete*. Berlin: Springer.
8. Darga, P. T., Sakallah, K. A., & Markov, I. L. (2008). Faster symmetry discovery using sparsity of symmetries. In *2008 45th ACM/IEEE Design Automation Conference* (pp. 149 – 154).
9. Erdös, P., & Rényi, A. (1963). Asymmetric graphs. *Acta Mathematica Hungarica*, *14*(3), 295–315.
10. Geyer-Schulz, A., Ovelgönne, M., & Stein, M. (2013). Modified randomized modularity clustering: Adapting the resolution limit. In B. Lausen, D. Van den Poel, & A. Ultsch (Eds.), *Algorithms from and for Nature and Life* (pp. 355–363). Cham: Springer International Publishing.
11. Haar, A. (1933). Der massbegriff in der theorie der kontinuierlichen gruppen. *Annals of Mathematics*, *34*(1), 147–169.
12. Hausdorff, F. (1962). *Set Theory* (2nd ed.). New York: Chelsea Publishing Company.
13. Holton, D. A. and Sheehan, J. (1993). *The Petersen Graph*, volume 7 of *Australian Mathematical Society Lecture Series*. Cambridge University Press.
14. Kemp, R. (1984). *Fundamentals of the average case analysis of particular algorithms*., Wiley-Teubner series in computer science Stuttgart: Teubner.
15. Kempe, A. B. (1886). A memoir on the theory of mathematical form. *Philosophical Transactions of the Royal Society of London*, *177*, 1–70.
16. Lützen, J., Sabidussi, G., & Toft, B. (1992). Julius Petersen 1839–1910 a biography. *Discrete Mathematics*, *100*(1–3), 9–82.
17. Newman, M. E. J., & Girvan, M. (2004). Finding and evaluating community structure in networks. *Phys. Rev. E*, 69(2), 026113. ((3), 1–21).

18. Petersen, J. (1898). Sur le theoreme de tait. *L'Intermediaire des Mathematiciens*, *5*, 225–227.
19. Pisanski, T., & Servatius, B. (2013). *Configurations from a graphical viewpoint. Birkhäuser advanced texts*. Boston: Birkhäuser Boston.
20. von Neumann, J. (1999a). *Construction of haar's invariant measure in groups by approximately equidistributed finite point sets and explicit evaluations of approximations*, chapter 6, (pp. 87–134). In J. von Neumann (Ed.), *Invariant measures*. Providence, Rhode Island: American Mathematical Society.
21. von Neumann, J. (1999b). *Invariant measures*. Providence, Rhode Island: American Mathematical Society.
22. Wielandt, H. (1964). *Finite permutation groups*. New York: Academic Press.
23. Wood, J. (2016). Proof without words: The automorphism group of the Petersen graph is isomorphic to S_5. *Mathematics Magazine*, *86*(4), 267.

Minkowski Distances and Standardisation for Clustering and Classification on High-Dimensional Data

Christian Hennig

Abstract There are many distance-based methods for classification and clustering, and for data with a high number of dimensions and a lower number of observations, processing distances is computationally advantageous compared to the raw data matrix. Euclidean distances are used as a default for continuous multivariate data, but there are alternatives. Here the so-called Minkowski distances, L_1 (city block)-, L_2 (Euclidean)-, L_3, L_4- and maximum distances are combined with different schemes of standardisation of the variables before aggregating them. Boxplot transformation is proposed, a new transformation method for a single variable that standardises the majority of observations but brings outliers closer to the main bulk of the data. Distances are compared in simulations for clustering by partitioning around medoids, complete and average linkage, and classification by nearest neighbours, of data with a low number of observations but high dimensionality. The L_1-distance and the boxplot transformation show good results.

1 Introduction

One thing that I share with Professor Akinori Okada is the affinity for dissimilarities and distances. At the IFCS 2017 in Tokyo, when Professor Okada was President of the International Federation of Classification Societies and I was Secretary, he gave a fascinating presentation on "dissimilarity based on dissimilarity to others", and his work is full of non-standard takes on dissimilarity. In the present paper the dissimilarities of interest will be fairly standard and symmetric distances, but they will still be used in ways that are, in my opinion, under-represented and under-investigated in the literature.

There are many dissimilarity-based methods for clustering and supervised classification, for example, partitioning around medoids (PAM), the classical hierarchical

C. Hennig (✉)
Dipartimento di Scienze Statistiche "Paolo Fortunati", Via delle Belle Arti 41, 40126 Bologna, Italy
e-mail: christian.hennig@unibo.it

T. Imaizumi et al. (eds.), *Advanced Studies in Behaviormetrics and Data Science*, Behaviormetrics: Quantitative Approaches to Human Behavior 5,
https://doi.org/10.1007/978-981-15-2700-5_6

linkage methods (Kaufman & Rousseeuw [9]) and k-nearest neighbours classification (Cover & Hart [3]). Approaches such as multidimensional scaling are also based on dissimilarity data. There is much literature on the construction and choice of dissimilarities (or, mostly equivalently, similarities) for various kinds of non-standard data such as images, melodies, or mixed type data. For standard quantitative data, however, analysis not based on dissimilarities is often preferred (some of which implicitly rely on the Euclidean distance, particularly when based on Gaussian distributions), and where dissimilarity-based methods are used, in most cases the Euclidean distance is employed. In the following, all considered dissimilarities will fulfil the triangle inequality and therefore be distances.

Given a data matrix of n observations in p dimensions $\mathbf{X} = (\mathbf{x}_1, \ldots, \mathbf{x}_n)$ where $\mathbf{x}_i = (x_{i1}, \ldots, x_{ip}) \in I\!R^p,\ i = 1, \ldots, n$, in case that $p > n$, analysis of $n(n-1)/2$ distances $d(\mathbf{x}_i, \mathbf{x}_j)$ is computationally advantageous compared with the analysis of np raw data matrix entries. High dimensionality comes with a number of issues (often referred to as the "curse of dimensionality"; for example, Hall, Marron, & Neeman [5]). This could make distances attractive for high-dimensional data, particularly because the distances do not directly carry information about the dimensionality of the data. But some issues with high dimensions manifest themselves also at the level of distances, for example, some at first sight fairly innocent distributional conditions allow to prove that for fixed n and $p \to \infty$ all Euclidean distances between points converge to a constant (Ahn, Marron, Muller, & Chi [1]). There are however indications that not all reasonable distances are affected in the same way by such problems (Hall, Marron, & Neeman [5]). Murtagh [12] takes a different point of view and argues that the structure of very high-dimensional data can even be advantageous for clustering, because distances tend to be closer to ultrametrics, which are fitted by hierarchical clustering. He also demonstrates that the components of mixtures of separated Gaussian distributions can be well distinguished in high dimensions, despite the general tendency towards a constant. Similarly, for classification, Ahn et al. [1] state that class separation corresponding to the underlying data generation process is still possible.

Here I investigate a number of distances when used for clustering and supervised classification for data with low n and high p, with a focus on two ingredients of distance construction, for which there are various possibilities, namely *standardisation*, i.e., some usually linear transformation based on variation in order to make variables with differing variation comparable, and *aggregation* of a single distance out of the contributions of the individual variables. Particular attention is devoted to the impact of outliers. A new proposal for standardisation is made, the boxplot transformation, which does not only standardise variables unaffected by outliers, but also brings such outliers closer to the main bulk of the data.

In Sect. 2, besides some general discussion of distance construction, various proposals for standardisation and aggregation are made. Section 3 presents a simulation study comparing the different combinations of standardisation and aggregation. Section 4 concludes the paper.

2 Distance Construction

The distances considered here are constructed as follows. First, the variables are standardised in order to make them suitable for aggregation, then they are aggregated according to Minkowski's L_q-principle. These two steps can be found often in the literature, however, their joint impact and performance for high-dimensional classification has hardly been investigated systematically. Before introducing the standardisation and aggregation methods to be compared, the section is opened by a discussion of the differences between clustering and supervised classification problems.

2.1 Clustering Versus Supervised Classification

Superficially, clustering and supervised classification seem very similar. A popular assumption is that for the data there exist true class labels $C_1, \ldots, C_n \in \{1, \ldots, k\}$, and the task is to estimate them. In clustering, all $C_1, \ldots, C_n$ are unknown, whereas in supervised classification they are known, and the task is to construct a classification rule to classify new observations, i.e., to estimate $C_{n+1}, \ldots, C_{n+m} \in \{1, \ldots, k\}$ for given $\mathbf{x}_{n+1}, \ldots, \mathbf{x}_{n+m}$. Obviously the clustering problem is more difficult due to less available information, but underlying model assumptions could be taken to be the same, and approaches could be expected to be related. When comparing distances in Sect. 3, this is in fact the approach that will be taken. I have however argued in Hennig [6] that the clustering situation is somewhat more different in the sense that there could be various legitimate "true" clusterings on the same data set, and that it should depend on background knowledge and the aim of clustering what kind of clustering should be preferred. Particularly, decisions made before the application of a clustering method such as standardisation, variable selection and distance construction, do not only influence the result, but can also be seen as implicitly contributing to the definition of the clusters that will be found. For example, if the data stems from a questionnaire that has general demographic questions as well as detailed questions about a certain issue such as the usage of means of transport, one could be interested in a clustering that aggregates demographic and transport usage information, but one could also be interested in a clustering based primarily on transport usage that may or may not be in some way informed by the demographic information, which may then not be used or downweighted.

An issue regarding standardisation is whether different variations (i.e., scales, or possibly variances where they exist) of variables are seen as informative in the sense that a larger variation means that the variable shows a "signal", whereas a low variation means that mostly noise is observed. This happens in a number of engineering applications, and in this case standardisation that attempts to making the variation equal should be avoided, because this would remove the information in the variations. If class labels are given, as in supervised classification, it is just possible

to compare these alternatives using the estimated misclassification probability from cross-validation and the like. However, in clustering such information is not given. The data therefore cannot decide this issue automatically, and the decision needs to be made from background knowledge. It is even conceivable that for some data both use of or refraining from standardisation can make sense, depending on the aim of clustering. When analysing high-dimensional data such as from genetic microarrays, however, there is often not much background knowledge about the individual variables that would allow making such decisions, so users will often have to rely on knowledge coming from experiments as in Sect. 3 with a single given true clustering.

Finally, in supervised classification class information can be used for standardisation so that it is possible, for example, to pool within-class variances, which are not available in clustering.

2.2 Standardisation

Normally, and for all methods proposed in Sect. 2.4, aggregation of information from different variables in a single distance assumes that "local distances", i.e., differences between observations on the individual variables, can be meaningfully compared. This is obviously not the case if the variables have incompatible measurement units, and fairly generally more variation will give a variable more influence on the aggregated distance, which is often not desirable (but see the discussion in Sect. 2.1). None of the aggregation methods in Sect. 2.4 is scale invariant, i.e., multiplying the values of different variables with different constants (e.g., changes of measurement units) will affect the results of distance-based clustering and supervised classification. Therefore standardisation in order to make local distances on individual variables comparable is an essential step in distance construction.

Normally, standardisation is carried out as

$$x_{ij}^* = \frac{x_{ij} - a_j^*}{s_j^*},\ i = 1, \ldots, n,\ \ j = 1, \ldots, p,$$

where a_j^* is a location statistic and s_j^* is a scale statistic depending on the data. For distances based on differences in individual variables as used here, a_j^* can be ignored here because it does not have an impact on differences between two values.

The most popular standardisation is standardisation to unit variance, for which $(s_j^*)^2 = s_j^2 = \frac{1}{n-1}\sum_{i=1}^n (x_{ij} - a_j)^2$ with a_j being the mean of variable j. The sample variance s_j^2 can be heavily influenced by outliers, though, and therefore in robust statistics often the median absolute deviation from the median (MAD) is used, $s_j^* = \text{MAD}_j = \text{med}\left|\left(x_{ij} - \text{med}_j(\mathbf{X})\right)_{i=1,\ldots,n}\right|$ (by med_j I denote the median of variable j in data set $\mathbf{X}$, analogously later $\min_j$ and $\max_j$). The "outliers" to be negotiated here are outlying values on single variables, and their effect on the aggregated distance involving the observation where they occur; this is not about

full outlying p-dimensional observations (as are often treated in robust statistics). In high-dimensional data often all or almost all observations are affected by outliers in some variables.

If standardisation is used for distance construction, using a robust scale statistic such as the MAD does not necessarily solve the issue of outliers. If the MAD is used, the variation of the different variables is measured in a way unaffected by outliers, but the outliers are still in the data, still outlying, and involved in the distance computation. Unit variance standardisation may undesirably reduce the influence of the non-outliers on a variable with gross outliers, which does not happen with MAD-standardisation, but after MAD-standardisation a gross outlier on a standardised variable can still be a gross outlier and may dominate the influence of the other variables when aggregating them. The results of the simulation in Sect. 3 can be used to compare the impact of these two issues.

The third approach to standardisation is standardisation to a unit range, with $s_j^* = r_j = \max_j(\mathbf{X}) - \min_j(\mathbf{X})$. This is influenced even stronger by extreme observations than the variance. But Milligan and Cooper [11] have observed that range standardisation is often superior for clustering, namely in case that a large variance (or MAD) is caused by large differences between clusters rather than within clusters, which is useful information for clustering and will be weighted down stronger by unit variance or MAD-standardisation than by range standardisation. The same argument holds for supervised classification.

For the same reason, it can be expected that a better standardisation can be achieved for supervised classification if within-class variances or MADs are used instead of involving between-class differences in the computation of the scale functional. As discussed earlier, this is not available for clustering (but see Art, Gnanadesikan, & Kettenring [2], who pool variances within estimated clusters in an iterative fashion). For within-class variances $s_{lj}^2,\ l = 1, \ldots, k,\ j = 1, \ldots, p$, the pooled within-class variance of variable j is defined as $s_j^* = (s_j^{pool})^2 = \frac{1}{\sum_{l=1}^k (n_l - 1)} \sum_{l=1}^k (n_l - 1) s_{lj}^2$, where n_l is the number of observations in class l. Similarly, with within-class MADs and within-class ranges $\text{MAD}_{lj}, r_{lj},\ l = 1, \ldots, k,\ j = 1, \ldots, p$, respectively, the pooled within-class MAD of variable j can be defined as $\text{MAD}_j^{poolw} = \frac{1}{n} \sum_{l=1}^k n_l \text{MAD}_{lj}$, and the pooled range as $r_j^{poolw} = \frac{1}{n} \sum_{l=1}^k n_l r_{lj}$ ("weights-based pooled MAD and range").

There is an alternative way of defining a pooled MAD by first shifting all classes to the same median and then computing the MAD for the resulting sample (which is then equal to the median of the absolute values: "shift-based pooled MAD"). For the variance, this way of pooling is equivalent to computing $(s_j^{pool})^2$, because variances are defined by summing up squared distances of all observations to the class means. For the MAD, however, the result will often differ from weights-based pooling, because different observations may end up in the smaller and larger half of values for computing the involved medians. For variable $j = 1, \ldots, p$: $s_j^* = \text{MAD}_j^{pools} = \text{med}_j(\mathbf{X}^+)$, where $\mathbf{X}^+ = \left(\left|x_{ij}^+\right|\right)_{i=1,\ldots,n,\ j=1,\ldots,p}$, $x_{ij}^+ = x_{ij} - \text{med}\left((x_{hj})_{h:\ C_h = C_i}\right)$. The same idea applied to the range would mean that all data are shifted so that they are within

the same range, which then needs to be the maximum of the ranges of the individual classes r_{lj}, so $s_j^* = r_j^{pools} = \max_l r_{lj}$ ("shift-based pooled range"). Whereas in weights-based pooling the classes contribute with weights according to their sizes, shift-based pooling can be dominated by a single class. The shift-based pooled range is determined by the class with the largest range, and the shift-based pooled MAD can be dominated by the class with the smallest MAD, at least if there are enough shifted observations of the other classes within its range.

2.3 Boxplot Transformation

As discussed above, outliers can have a problematic influence on the distance regardless of whether variance, MAD, or range is used for standardisation, although their influence plays out differently for these choices. The boxplot standardisation introduced here is meant to tame the influence of outliers on any variable. It is inspired by the outlier identification used in boxplots (McGill, Tukey, & Larsen [10]). The boxplot shows lower quartile ($q_{1j}(\mathbf{X})$, where $j = 1, \ldots, p$ once more denotes the number of the variable), median ($\text{med}_j(\mathbf{X})$), and upper quartile ($q_{3j}(\mathbf{X})$) of the data. It defines as outliers observations for which $x_{ij} < q_{1j}(\mathbf{X}) - 1.5\,\text{IQR}_j(\mathbf{X})$ or $x_{ij} > q_{3j}(\mathbf{X}) + 1.5\,\text{IQR}_j(\mathbf{X})$, where $\text{IQR}_j(\mathbf{X}) = q_{3j}(\mathbf{X}) - q_{1j}(\mathbf{X})$ is the interquartile range. An asymmetric outlier identification more suitable for skew distributions can be defined by using the ranges between the median and the upper and lower quartile, respectively, $\text{UQR}_j(\mathbf{X}) = q_{3j}(\mathbf{X}) - \text{med}_j(\mathbf{X})$, $\text{LQR}_j(\mathbf{X}) = \text{med}_j(\mathbf{X}) - q_{1j}(\mathbf{X})$, so that a lower outlier is defined by $x_{ij} < q_{1j}(\mathbf{X}) - 3\,\text{LQR}_j(\mathbf{X})$ and an upper outlier by $x_{ij} > q_{3j}(\mathbf{X}) + 3\,\text{UQR}_j(\mathbf{X})$. The idea of the boxplot transformation is to standardise the lower and upper quantile linearly to $[-0.5, 0.5]$. If there are no outliers smaller than the median according to the above rule, all these observations are standardised in the same way, as are all observations larger than the median if there are no outliers. If there are outliers on the lower side of the median, all observations in $[\min_j(\mathbf{X}), q_{1j}(\mathbf{X})]$ are transformed by a nonlinear transformation that maps the minimum to -2 (which is $-0.5 - 1.5\,\text{IQR}_j$ or $-0.5 - 3\,\text{LQR}_j$ of the transformed data), so that the outliers are brought so close to the main bulk of the data that they are no longer outliers by the boxplot definition. Analogously, observations in $[q_{3j}(\mathbf{X}), \max_j(\mathbf{X})]$ are mapped to $[0.5, 2]$ if there are upper outliers.

The precise computation is as follows.

Step 1 Median centering: $\mathbf{X}^m = \left(x_{ij}^m\right)_{i=1,\ldots,n,\ j=1,\ldots,p}$ where $x_{ij}^m = x_{ij} - \text{med}_j(\mathbf{X})$.

Step 2 For $j \in \{1, \ldots, p\}$ transform lower quantile to -0.5: For $x_{ij}^m < 0$: $x_{ij}^* = \frac{x_{ij}^m}{2\text{LQR}_j(\mathbf{X}^m)}$.

Step 3 For $j \in \{1, \ldots, p\}$ transform upper quantile to 0.5: For $x_{ij}^m > 0$: $x_{ij}^* = \frac{x_{ij}^m}{2\text{UQR}_j(\mathbf{X}^m)}$. $\mathbf{X}^* = \left(x_{ij}^*\right)_{i=1,\ldots,n,\ j=1,\ldots,p}$.

Step 4 If there are lower outliers, i.e., $x_{ij}^* < -2$:

Step 4a Find t_j^l so that $-0.5 - \frac{1}{t_j^l} + \frac{1}{t_j^l\left(-\min_j(\mathbf{X}^*)-0.5+1\right)^{t_j^l}} = -2$.

Step 4b For $x_{ij}^* < -0.5$: $x_{ij}^* = -0.5 - \frac{1}{t_j^l} + \frac{1}{t_j^l\left(-x_{ij}^*-0.5+1\right)^{t_j^l}}$.

Step 5 If there are upper outliers, i.e., $x_{ij}^* > 2$:

Step 5a Find t_j^u so that $0.5 + \frac{1}{t_j^u} - \frac{1}{t_j^u\left(\max_j(\mathbf{X}^*)-0.5+1\right)^{t_j^u}} = 2$.

Step 5b For $x_{ij}^* > 0.5$: $x_{ij}^* = 0.5 + \frac{1}{t_j^u} - \frac{1}{t_j^u\left(x_{ij}^*-0.5+1\right)^{t_j^u}}$.

Step 6 In case of supervised classification of new observations, the boxplot standardisation is computed as above, using the quantiles, t_j^l, t_j^u from the training data $\mathbf{X}$, but values for the new observations are capped to $[-2, 2]$, i.e., everything smaller than -2 is set to -2, and everything larger than 2 is set to 2.

Figure 1 illustrates the boxplot transformation for a given data set. The boxplot transformation is somewhat similar to a classical technique called Winsorisation (Ruppert [14]) in that it also moves outliers closer to the main bulk of the data, but it is smoother and more flexible. Note that for even n the median of the boxplot transformed data may be slightly different from zero, because it is the mean of the two middle observations around zero, which have been standardised by not necessar-

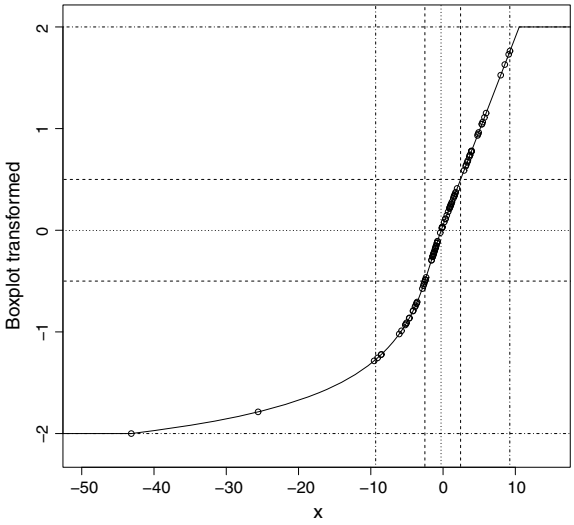

Fig. 1 Illustration of boxplot transformation. Scatterplot of data set $\mathbf{X}$ versus boxplot transformed $\mathbf{X}^*$. Lines orthogonal to the x-axis are, from left to right, lower outlier boundary, first quartile, median, third quartile, upper outlier boundary. Lines orthogonal to the y-axis are, from bottom to top, -2 (lower boundary), -0.5 (first quartile), median, 0.5 (third quartile), 2 (upper boundary). In this example there are only lower outliers, but no upper outliers, so a non-linear part occurs on the lower side but not on the upper side

ily equal $\mathrm{LQR}_j(\mathbf{X}^m)$, $\mathrm{UQR}_j(\mathbf{X}^m)$, respectively. A symmetric version that achieves a median zero would standardise all observations by $1.5\,\mathrm{IQR}_j(\mathbf{X}^m)$, and use this quantity for outlier identification on both sides, but that may be inappropriate for asymmetric distributions.

2.4 Aggregation

Information from the variables is aggregated here by standard Minkowski L_q-distances,

$$d_{Lq}(\mathbf{x}_i, \mathbf{x}_j) = \sqrt[q]{\sum_{l=1}^{p} d_l(x_{il}, x_{jl})^q},$$

where $q = 1$ delivers the so-called city block distance, adding up absolute values of variable-wise differences, $q = 2$ corresponds to the Euclidean distance, and $q \to \infty$ will eventually only use the maximum variable-wise absolute difference, sometimes called L_∞ or maximum distance. See de Amorim and Mirkin [4] for a study on the use of Minkowksi-distances with k-means clustering.

These aggregation schemes treat all variables equally ("impartial aggregation"). Much work on high-dimensional data is based on the paradigm of dimension reduction, i.e., they look for a small set of meaningful dimensions to summarise the information in the data, and on these standard statistical methods can be used, hopefully avoiding the curse of dimensionality. Using impartial aggregation, information from all variables is kept. There is a widespread belief that in many applications in which high-dimensional data arises, the meaningful structure can be found or reproduced in much lower dimensionality. Where this is true, impartial aggregation will keep a lot of high-dimensional noise and is probably inferior to dimension reduction methods. However, there may be cases in which high-dimensional information cannot be reduced so easily, either because the meaningful structure is not low dimensional, or because it may be hidden so well that standard dimension reduction approaches do not find it. My impression is that for both dimension reduction and impartial aggregation, there are situations in which they are preferable, although they are not compared in the present paper.

A side remark here is that another distance of interest would be the Mahalanobis distance. The Mahalanobis distance is invariant against affine linear transformations of the data, which is much stronger than achieving invariance against changing the scales of individual variables by standardisation. It has been argued that affine equi- and invariance are central concepts in multivariate analysis, see, e.g., Serfling [15]. But in high dimensions, things change. Pires and Branco [13] show that for $p \geq n - 1$ all observations have the same Mahalanobis distance to all other observations. Together with the result of Tyler [16] that for $p \geq n - 1$, any affine equivariant scatter statistic must be proportional to the sample covariance matrix as employed

in the Mahalanobis distance; it follows that affine invariance cannot be achieved for high-dimensional data in a non-trivial manner that is informative about the data. This means that some directions in data space necessarily have to be privileged over others, as are the main coordinate axes for the Minkowski distances.

3 Experiments

I ran some simulations in order to compare all combinations of standardisation and aggregation on some clustering and supervised classification problems.

3.1 Setups

The scope of these simulations is somewhat restricted. In all cases, training data was generated with two classes of 50 observations each (i.e., $n = 100$) and $p = 2000$ dimensions. For supervised classification, test data was generated according to the same specifications. All variables were independent. Variables were generated according to either Gaussian or t_2-distributions within classes (the latter in order to generate strong outliers). The mean differences between the two classes were generated randomly according to a uniform distribution, as were the standard deviations in case of a Gaussian distribution; t_2-random variables (for which variance and standard deviation do not exist) were multiplied by the value corresponding to a Gaussian standard deviation to generate the same amount of diversity in variation. Standard deviations were drawn independently for the classes and variables, i.e., they differed between classes. With probability p_t, a variable was chosen to be t_2-distributed, otherwise Gaussian. With probability p_n, a variable was "noise", i.e., there was no distributional difference between the classes. Draws from p_t and p_n were independent, i.e., both noise and informative variables could be Gaussian or t_2-distributed.

There were five different setups:

Simple normal $p_t = p_n = 0$ (all distributions Gaussian and with mean differences), all mean differences 0.1, standard deviations in [0.5, 1.5].

Simple normal (0.99) $p_t = 0$ (all Gaussian) but $p_n = 0.99$, much noise and clearly distinguishable classes only on 1% of the variables. All mean differences 12, standard deviations in [0.5, 2].

Normal, t, and noise (0.1) $p_t = p_n = 0.1$, mean differences in [0, 0.3] (mean difference distributions were varied over setups in order to allow for somewhat similar levels of difficulty to separate the classes in the presence of different proportions of t_2- and noise variables), standard deviations in [0.5, 10]. Weak information on many variables, strongly varying within-class variation, outliers in a few variables.

Normal, t, and noise (0.5) $p_t = p_n = 0.5$, mean differences in [0, 2], standard deviations in [0.5, 10]. Half of the variables with mean information, half of the variables potentially contaminated with outliers, strongly varying within-class variation.

Normal, t, and noise (0.9) $p_t = p_n = 0.9$, mean differences in [0, 10], standard deviations in [0.5, 10]. Only 10% of the variables with mean information, 90% of the variables potentially contaminated with outliers, strongly varying within-class variation.

For clustering, PAM, average and complete linkage were run, all with number of clusters known as 2. Results were compared with the true clustering using the adjusted Rand index (Hubert & Arabie [8]). Results for average linkage are not shown, because it always performed worse than complete linkage, probably mostly due to the fact that cutting the average linkage hierarchy at two clusters would very often produce a one-point cluster (single linkage would be even worse in this respect). For supervised classification, a 3-nearest neighbour classifier was chosen, and the rate of correct classification on the test data was computed. There were 100 replicates for each setup.

3.2 Results

Results are shown in Figs. 2, 3, 4, 5, and 6. These are interaction (line) plots showing the mean results of the different standardisation and aggregation methods. I had a look at boxplots as well; it seems that differences that are hardly visible in the interaction plots are in fact insignificant, taking into account random variation (which cannot be assessed from the interaction plots alone), and things that seem clear are also significant. "pvar" stands for pooled variance, "pm1" and "pr1" stand for weights-based pooled MAD and range, respectively, and "pm2" and "pr2" stand for shift-based pooled MAD and range, respectively.

The clearest finding is that L_1-aggregation is the best in almost all respects, often with a big distance to the others. It is hardly ever beaten; only for PAM and complete linkage with range standardisation clustering in the simple normal (0.99) setup (Fig. 3) and PAM clustering in the simple normal setup (Fig. 2) some others are slightly better. L_1-aggregation delivers a good number of perfect results (i.e., ARI or correct classification rate 1). This is in line with Hinneburg, Aggarwal, and Keim [7], who state that "the L_1-metric is the only metric for which the absolute difference between nearest and farthest neighbour increases with the dimensionality."

Results for L_2 are surprisingly mixed, given its popularity and that it is associated with the Gaussian distribution present in all simulations. It is in the second position in most respects, but performs worse for PAM clustering (normal, t and noise (0.1 and 0.5), simple normal (0.1)), where L_4 holds the second and occasionally even the first position. L_3 and L_4 generally performed better with PAM clustering than with complete linkage and 3-nearest neighbour. The reason for this is that L_3 and L_4 are

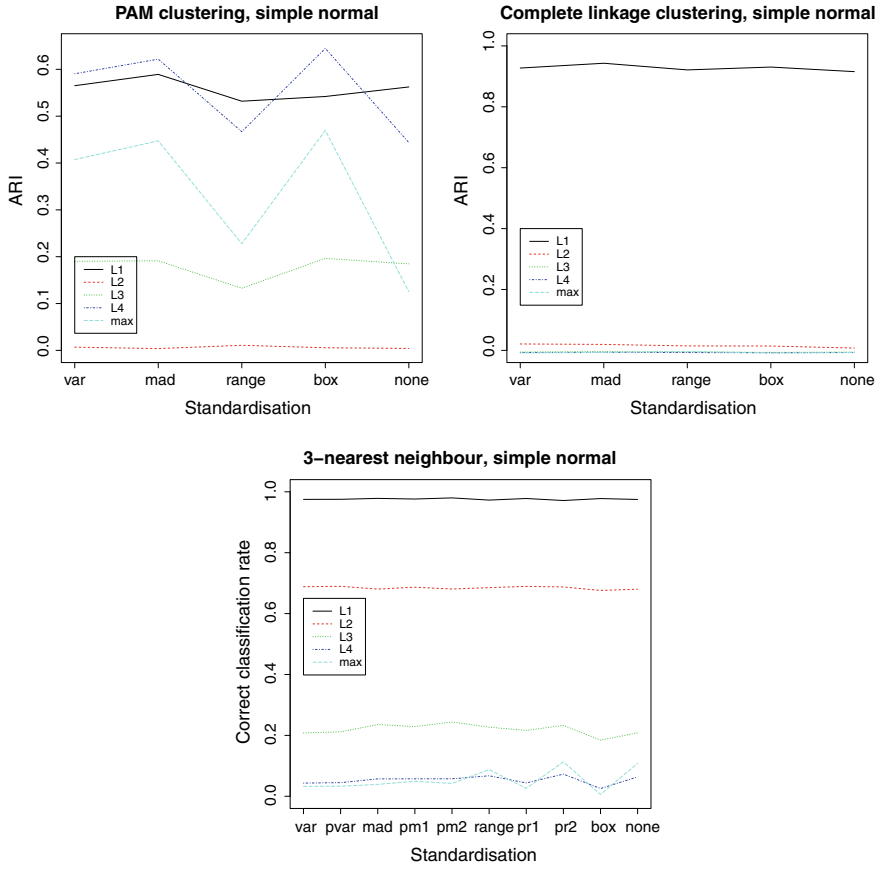

Fig. 2 Results from the simple normal setup, adjusted Rand index (ARI) from PAM and complete linkage, and misclassification rates from 3-nearest neighbours

dominated by the variables on which the largest distances occur. This means that very large within-class distances can occur, which is bad for complete linkage's chance of recovering the true clusters, and also bad for the nearest neighbour classification of most observations. Still PAM can find cluster centroid objects that are only extreme on very few if any variables and will therefore be close to most if not all observations within the same class. On the other hand, almost generally, it seems more favourable to aggregate information from all variables with large distances as L_3 and L_4 do than to only look at the maximum.

Regarding the standardisation methods, results are mixed. The boxplot transformation performs overall very well and often best, but the simple normal (0.99) setup Fig. 3 with a few variables holding strong information and lots of noise shows its weakness. In such a case, for clustering range standardisation works better, and for supervised classification pooling is better. A higher noise percentage is better han-

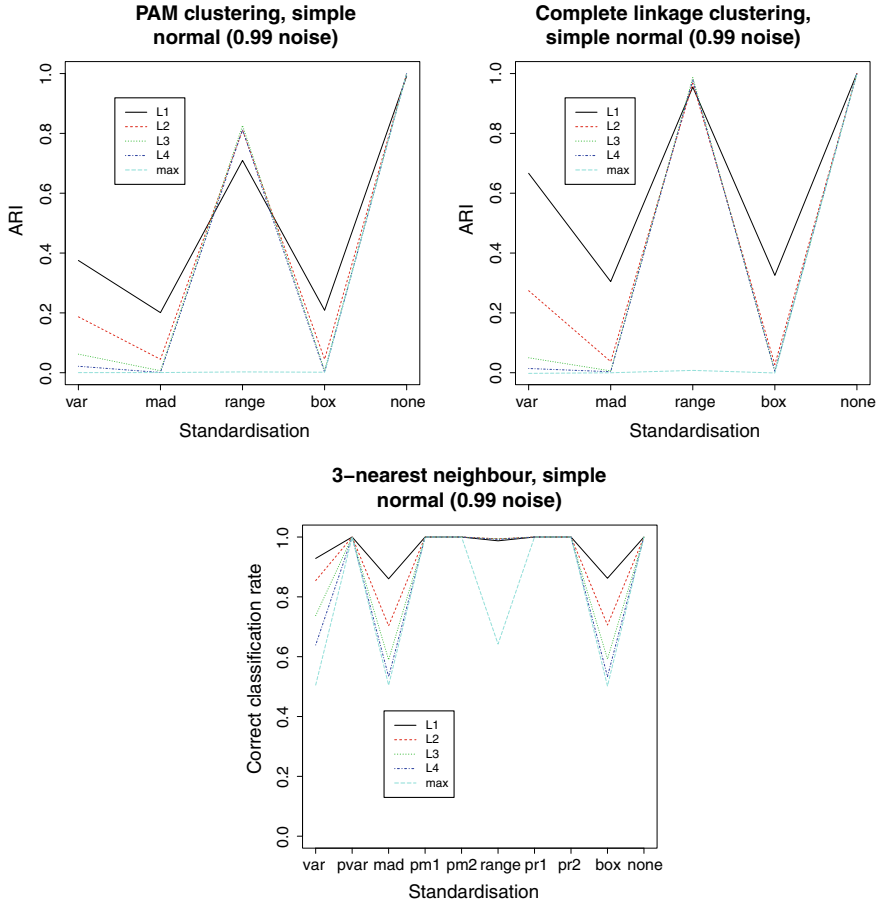

Fig. 3 Results from the simple normal (0.99 noise) setup, adjusted Rand index (ARI) from PAM and complete linkage, and misclassification rates from 3-nearest neighbours

dled by range standardisation, particularly in clustering; the standard deviation, MAD and boxplot transformation can more easily downweight the variables that hold the class-separating information. The simple normal (0.99) setup is also the only one in which good results can be achieved without standardisation, because here the variance is informative about a variable's information content. Otherwise standardisation is clearly favourable (which it will more or less always be for variables that do not have comparable measurement units).

For supervised classification, the advantages of pooling can clearly be seen for the higher noise proportions (although the boxplot transformation does an excellent job for normal, t, and noise (0.9)); for noise probabilities 0.1 and 0.5 the picture is less clear. In the latter case the MAD is not worse than its pooled versions, and the two versions of pooling are quite different. Weight-based pooling is better for the range,

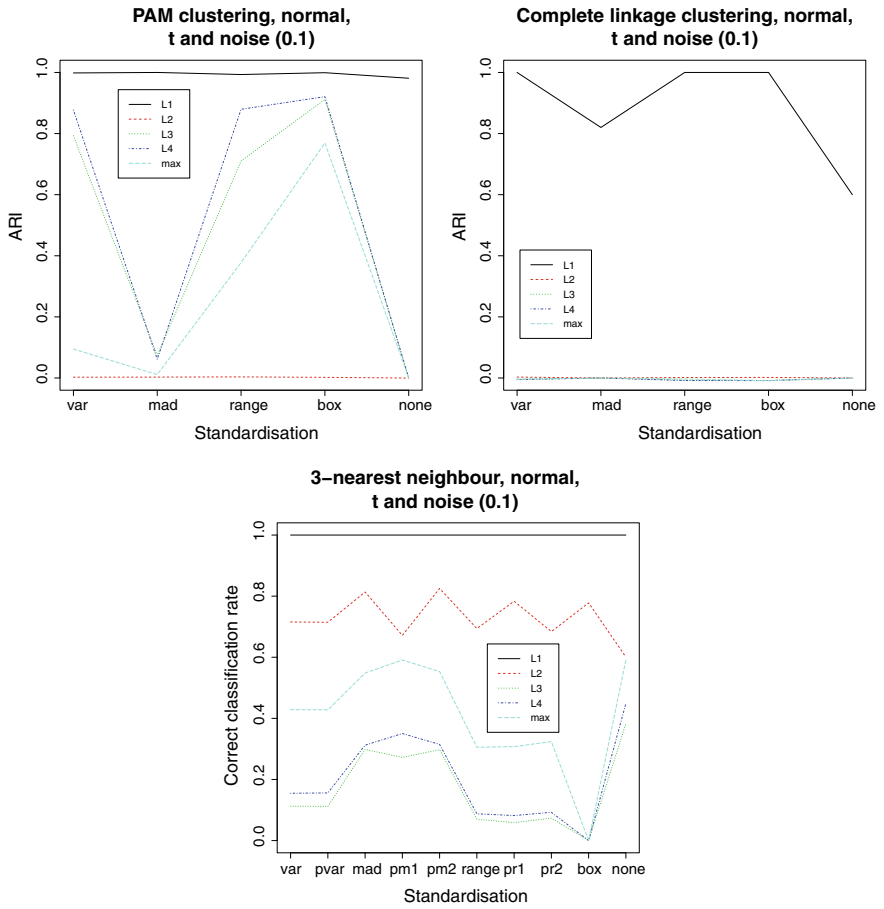

Fig. 4 Results from the normal, t and noise (0.1) setup, adjusted Rand index (ARI) from PAM and complete linkage, and misclassification rates from 3-nearest neighbours

and shift-based pooling is better for the MAD. In these setups the mean differences between the classes are dominated by their variances; pooling is much better only where much of the overall variance, MAD, or range is caused by large between-class differences. On the other hand, with more noise (0.9, 0.99) and larger between-class differences on the informative variables, MAD-standardisation does not do well. Despite its popularity, unit variance and even pooled variance standardisation are hardly ever among the best methods.

A curiosity is that some correct classification percentages, particularly for L_3, L_4, and maximum aggregation, are clearly worse than 50%, meaning that the methods do worse than random guessing, e.g., in the lower graph of Fig. 2. The reason for this is that with strongly varying within-class variances for a given pair of observations

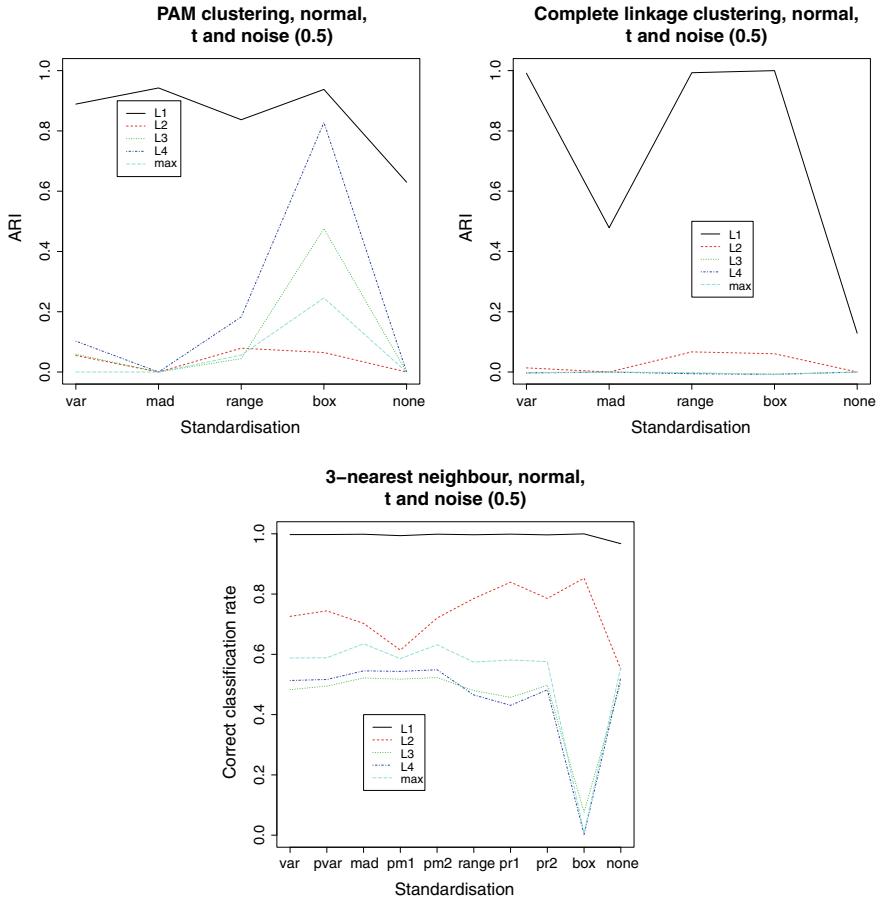

Fig. 5 Results from the normal, t and noise (0.5) setup, adjusted Rand index (ARI) from PAM and complete linkage, and misclassification rates from 3-nearest neighbours

from the same class, the largest distance is likely to stem from a variable with large variance, and the expected distance to an observation of the other class with typically smaller variance will be smaller (although with even more variables it may be more reliably possible to find many variables that have a variance near the maximum simulated one simultaneously in both classes, so that the maximum distance can be dominated by the mean difference between the classes again, among those variables with near-maximum variance in both classes).

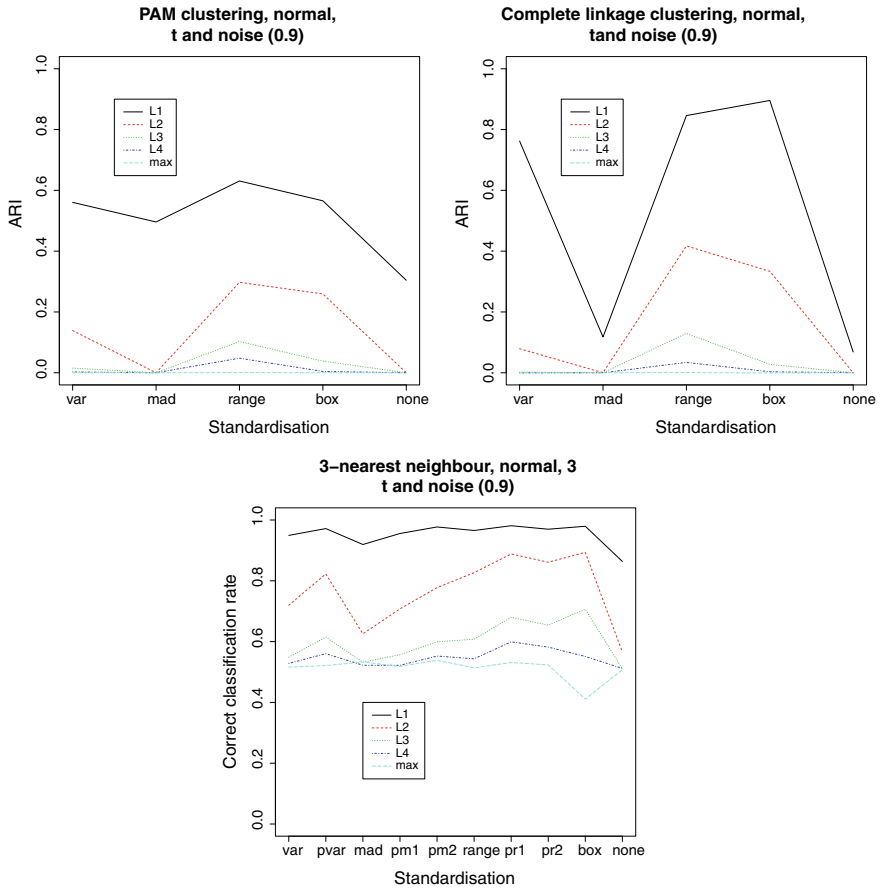

Fig. 6 Results from the normal, t and noise (0.9) setup, adjusted Rand index (ARI) from PAM and complete linkage, and misclassification rates from 3-nearest neighbours

4 Conclusion

Distance-based methods seem to be underused for high-dimensional data with low sample sizes, despite their computational advantage in such settings. This is partly due to undesirable features that some distances, particularly Mahalanobis and Euclidean, are known to have in high dimensions. This work shows that the L_1-distance in particular has a lot of largely unexplored potential for such tasks, and that further improvement can be achieved by using intelligent standardisation. The boxplot transformation proposed here performed very well in the simulations expect where there was a strong contrast between many noise variables and few variables with strongly separated classes. In such situations, dimension reduction techniques will be better than impartially aggregated distances anyway. For supervised classification, it

is often better to pool within-class scale statistics for standardisation, although this does not seem necessary if the difference between class means does not contribute much to the overall variation.

The simulations presented here are of limited scope. Dependence between variables should be explored, as should larger numbers of classes and varying class sizes. Standardisation methods based on the central half of the observations such as MAD and boxplot transformation may suffer in the presence of small classes that are well separated from the rest of the data on individual variables.

References

1. Ahn, J., Marron, J. S., Muller, K. M., & Chi, Y.-Y. (2007). The high dimension, low sample size geometric representation holds under mild conditions. *Biometrika*, *94*, 760–766.
2. Art, D., Gnanadesikan, R., & Kettenring, J. R. (1982). Data-Based Metrics for cluster analysis. *Utilitas Mathematica*, *21A*, 75–99.
3. Cover, T. N., & Hart, P. E. (1967). Nearest neighbor pattern classification. *IEEE Transactions on Information Theory*, *13*, 21–27.
4. de Amorim, R. C., & Mirkin, B. (2012). Minkowski metric, feature weighting and anomalous cluster initializing in K-means clustering. *Pattern Recognition*, *45*, 1061–1075.
5. Hall, P., Marron, J. S., & Neeman, A. (2005). Geometric representation of high dimension low sample size data. *Journal of the Royal Statistical Society: Series B*, *67*, 427–444.
6. Hennig, C. (2015). Clustering strategy and method selection. In C. Hennig, M. Meila, F. Murtagh, & R. Rocci (Eds.), *Handbook of Cluster Analysis* (pp. 703–730). Boca Raton: CRC Press.
7. Hinneburg, A., Aggarwal, C., & Keim, D. (2000). What is the nearest neighbor in high dimensional spaces? *VLDB 2000, Proceedings of 26th International Conference on Very Large Data Bases*, September 10–14 (pp. 506–515). Cairo: Morgan Kaufmann.
8. Hubert, L. J., & Arabie, P. (1985). Comparing partitions. *Journal of Classification*, *2*, 193–218.
9. Kaufman, L., & Rousseeuw, P. J. (1990). *Finding groups in data*. New York: Wiley.
10. McGill, R., Tukey, J. W., & Larsen, W. A. (1978). Variations of box plots. *American Statistician*, *32*, 12–16.
11. Milligan, G. W., & Cooper, M. C. (1988). A study of standardization of variables in cluster analysis. *Journal of Classification*, *5*, 181–204.
12. Murtagh, F. (2009). The remarkable simplicity of very high dimensional data: Application of model-based clustering. *Journal of Classification*, *26*, 249–277.
13. Pires, A.M., & Branco, J.A. (2019). *High dimensionality: The latest challenge to data analysis* (2019). arXiv:1902.04679.
14. Ruppert, D. (2006). Trimming and Winsorization. In S. Kotz, C. B. Read, N. Balakrishnan, B. Vidakovic (Eds.), *Encyclopedia of statistical sciences* (2nd ed. Vol. 14, p. 8765).
15. Serfling, R. (2010). Equivariance and invariance properties of multivariate quantile and related functions, and the role of standardization. *Journal of Nonparametric Statistics*, *22*, 915–936.
16. Tyler, D. E. (2010). A note on multivariate location and scatter statistics for sparse data sets. *Statistics & Probability Letters*, *80*, 1409–1413.

On Detection of the Unique Dimensions of Asymmetry in Proximity Data

Tadashi Imaizumi

Abstract As methods of analyzing the relationship of n objects of proximity matrix, multidimensional scaling (MDS) has been developed and applied to many data sets. However, we take care to apply them to an asymmetric proximity matrix. Okada and Imaizumi have been proposed so-called "circle (or radius–distance) model" by introducing the radius of each object to extract asymmetric parts in data. In this paper, we overview these models for a one-way two-mode asymmetric proximity matrix and propose a method for the detection of asymmetric dimensions by losing the positiveness of asymmetric dimension weights.

1 Introduction

Various kinds of proximities are often collected in many research areas, for example, marketing research, sociology, psychology, and economics. In these research areas, several proximities between objects have been analyzed for understanding the relationship of objects from data and developing some theoretical framework in each area: international trading between nations, brand switching between consumer products, and social mobility among regions. Multidimensional scaling models and methods have been developed and will be the most suitable models and methods for analyzing proximity matrix.

Let s_{jk} be the proximity from object j to object k, such that $s_{jk} \geq 0$, and be two-way proximity matrix of n objects. In many models for analyzing this proximity matrix, we assume a distance model, that is, each object is embedded as a point of t-dimensional space, such as $\mathbf{x}_j = [x_{jt}]$, $t = 1, 2, \ldots, p$ and the distance d_{jk} between two points $\mathbf{x}_j$ and $\mathbf{x}_k$,

$$d_{jk} = \left(\sum_{t=1}^{p} |x_{jt} - x_{kt}|^r\right)^{1/r}, \tag{1}$$

T. Imaizumi (✉)
Tama University, 4-4-1 Hijirigaoka, Tama-shi, Tokyo, Japan
e-mail: imaizumi@tama.ac.jp

T. Imaizumi et al. (eds.), *Advanced Studies in Behaviormetrics and Data Science*,
Behaviormetrics: Quantitative Approaches to Human Behavior 5,
https://doi.org/10.1007/978-981-15-2700-5_7

where $r \geq 1.0$ and d_{jk} are linked with s_{jk} for all (j, k) So, the symmetry of proximities is implicitly assumed,

$$s_{jk} = s_{kj}. \tag{2}$$

However, proximities may be nonsymmetric,$s_{jk} \neq s_{kj}$, for example, international trading. In the case that we treat that the deviates from symmetric values being due to error, then we will symmetrize them for eliminating error, for example, by using the arithmetic mean of the corresponding two elements, $s^*_{jk} = {}^* = (s_{jk} + s_{kj})/2$, or $s_{jk} = \sqrt{s_{jk} \times s_{kj}}$. However, a researcher has some rational hypothesis that nonsymmetric proximities are meaningful; we need to analyze those nonsymmetric proximities by using suitable models and methods.

2 Overview of Models

2.1 Asymmetric Scaling

Models for analyzing an asymmetric proximity matrix may be classified into two types of models: distance-based and non-distance-based models. Borg and Groenen ([2], Chap. 23) reviewed the asymmetric scaling models. Constantine and Gower [5] proposed a decomposition of an asymmetric proximity matrix **S** into a symmetric matrix **M** and skew symmetric matrix **N**

$$\begin{aligned} \mathbf{S} &= \mathbf{M} + \mathbf{N}, \\ \mathbf{M} &= (\mathbf{S} + \mathbf{S}')/2, \\ \mathbf{N} &= (\mathbf{S} - \mathbf{S}')/2. \end{aligned}$$

Chino [4] also proposed the ASYMSCAL model, where he tried to represent **M** and **N** simultaneously.

$$s_{jk} \approx a(x_{j1}x_{k1} + x_{j2}x_{k2}) + b(x_{j1}x_{k2} - x_{j2}x_{k1}) + c.$$

This model represents the similarity from object j to object k by an inner product between two points, j and k $(x_{j1}x_{k1} + x_{j2}x_{k2})$, and by an outer product between these two points $(x_{j1}x_{k2} - x_{j2}x_{k1})$. Harshman [7] proposed the DEDICOM model:

$$\mathbf{S} = \mathbf{YAY}'.$$

Kiers [8] proposed an algorithm to find **A** and **Y** from the observed **S**. These approaches are based on the decomposition of a proximity matrix. The observed proximities are represented as the inner-product or outer-product of the corresponding two vectors.

Another approach is to analyze an asymmetric similarity matrix using a distance-based model such as a variant of the unfolding model. Let δ_{jk} be the dissimilarity from object j to object k. An unfolding model assumes

$$\delta_{jk} \approx \sqrt{\sum_{t=1}^{p}(x_{jt} - y_{kp})^2},$$

where x_j and y_k are two points in p-dimensional Euclidean space, R^p. Young [14] proposed a weighted unfolding model,

$$\delta_{ij} \approx \left(\sum_{t=1}^{p} w_{it}(x_{it} - y_{jt})^2\right)^{1_2},$$

and Zielman and Heiser [15] proposed the slide-vector model:

$$\delta_{jk} \approx \left(\sum_{t=1}^{p}(x_{jt} - x_{kt} + z_t)^2\right)^{1/2},$$

where $\mathbf{z} = [z_t]$ is a so-called slide vector. Krumhansl [9] proposed the distance-density model for analyzing a proxmity matrix:

$$s_{jk} = f^{-1}(\delta_{jk})$$

$$\delta_{jk} \approx \sqrt{\sum_{t=1}^{p}(x_{jt} - x_{kt})^2 + a\iota_j + b\iota_k},$$

where ι_j is the term for the density of object o_j, $\iota_j \geq 0$. Since the distance-based model assumes the relation between δ_{jk} and d_{jk} directly, we can capture the overall relation between objects by configuring the points. The observed proximities are represented by the inter-points distance in these distance-based models. Distance-based models had some advantages over decomposition models and the methods of an asymmetric proximity model when the result was geometrically represented. Therefore, the model discussed in the following sections will be based on these distance-based models.

Bove [3] discussed on the decomposition of skew-symmetric matrix **N**.

2.2 The Circle Model

Okada and Imaizumi [12] proposed the circle model, or the radius–distance model Borg and Groenen [2, Chap. 23] (Fig. 1):

$$m_{jk} = \left(\sum_{t=1}^{p} (x_{jt} - x_{kt})^2 \right)^{1/2} - r_j + r_k. \tag{3}$$

The radii r_j shows the relative dominance of object o_j over the other objects. The larger the dominant object j is, the smaller the radius of the object is. Therefore, object o_j is less dominant than object o_k and

$$s_{jk} \leq s_{kj}.$$

In this circle model (3), each object is represented as a point and a circle (sphere, hypersphere) whose center is at that point in a multidimensional Euclidean space. A generalized version of the circe model will be introduced. Let v_{jk} denote asymmetric

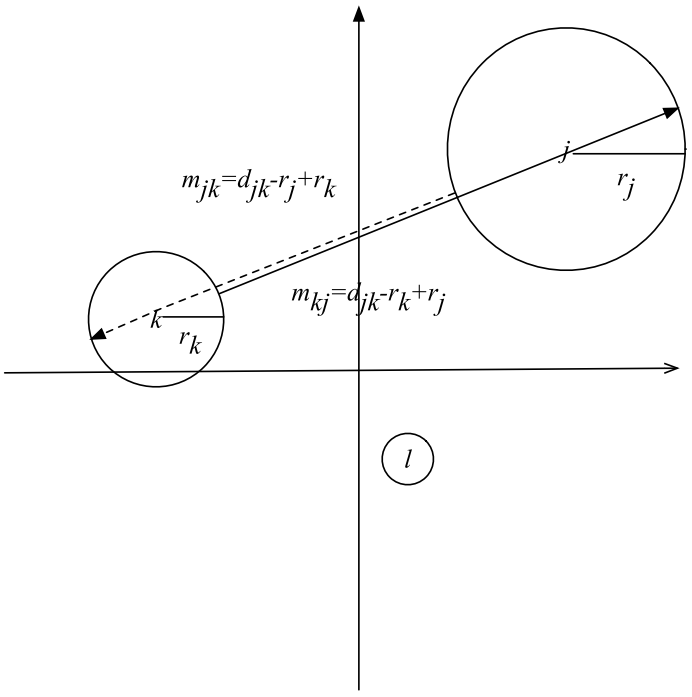

Fig. 1 Circle (radius–distance) model: the radius of each circle represents $r_j - min_k(r_k)$

part from object o_j to the other object o_k, and $-(v_{jk} - v_{kj})$ denote skew-symmetric part between o_j and o_k, then

$$m_{jk} = d_{jk} - (v_{jk} - v_{kj}), \tag{4}$$

$$m_{jj} = 0, \tag{5}$$

$$(m_{jk} + m_{kj})/2 = d_{jk}, \tag{6}$$

$$(m_{jk} - m_{kj})/2 = -(v_{jk} - v_{kj}). \tag{7}$$

We have the cross-product term $\sum_{j=1}^{n}\sum_{k}^{n} d_{jk}(v_{jk} - v_{kj})$ being 0. Let $\bar{m} = \sum_{j=1}^{n}\sum_{k=1}^{n} m_{jk}/n^2$, $\bar{d} = \sum_{j=1}^{n}\sum_{k=1}^{n} m_{jk}/n^2$, and

$$\sum_{j=1}^{n}\sum_{k=1}^{n}(m_{jk} - \bar{m})^2 = \sum_{j=1}^{n}\sum_{k=1}^{n}(d_{jk} - \bar{d})^2 + \sum_{j=1}^{n}\sum_{k=1}^{n}(v_{jk} - v_{kj})^2. \tag{8}$$

A circle model (3) will be the special model such that

$$r_j = \frac{1}{n}\sum_{k=1}^{n} v_{jk}. \tag{9}$$

2.3 Ellipse Model

The circle (radius–distance) model is restricted to asymmetric proximities. Moreover, we could not detect the hidden dimensions, which raises the asymmetric parts of proximities among n objects. Okada [11] proposed the ellipse model instead of the circle model, distance–radius model, and applied car-switching data. This ellipse model is defined by

$$v_{jk} = \left(\sum_{t=1}^{p}(|x_{jt} - x_{kt}|/r_{jt})^2\right)^{-1/2}, r_{jt} > 0 \tag{10}$$

$$m_{jk} = d_{jk} - d_{jk}(v_{jk} - v_{kj}). \tag{11}$$

This ellipse model tries to represent as a point and an ellipse (ellipsoid, hyper-ellipsoid) in a Euclidean space. And each axis of this space will be uniquely determined or accounting for skew-symmetries in s_{jk}.

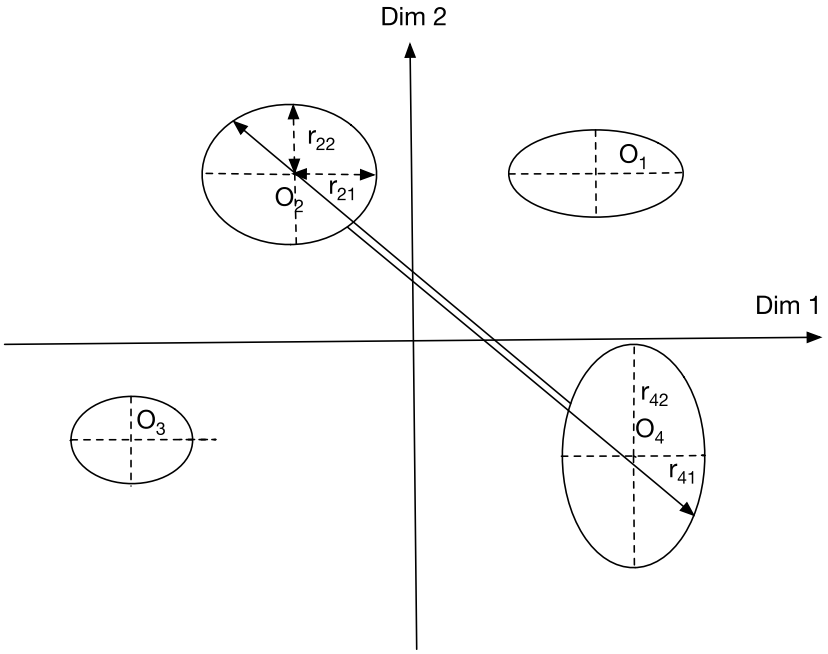

2.4 Other Variants

In the above two models, each object has embedded a point in a Euclidean space and corresponding circle (hypersphere) or ellipsoid (hyper-ellipsoid).

Other models which assume other metric space, for example, the city-block metric space, will be introduced,

$$m_{jk} = \sum_{t=1}^{p} |x_{jt} - x_{kt}| - \sum_{t=1}^{p} |r_{jt} - r_{kt}|.$$

However, the directions of the axes are compounded with symmetric part of s_{jk} and skew-symmetric part of s_{jk}. So it will be difficult to interpret the results and get new knowledge.

One of the other variants will be an intermediate model between the circle model and the ellipse model, that is,

$$v_{jk} = r_j \times d_{jk} / \sqrt{\sum_{t=1}^{p} \left((x_{jt} - x_{kt})/r_t^*\right)^2}, r_t^* > 0. \tag{12}$$

All ellipsoids of objects in this model are different with multiplier r_j only.

3 Algorithm

Okada [11] described the nonmetric algorithm to fit the ellipse model to an asymmetric proximity matrix. We describe it briefly. The algorithm consists of three phases for a given dimensionality p:

a. To construct an initial object configuration and initial values of the semiaxes $\{r_{jt}\}$.

- When p is equal to prespecified maximum dimensionality $pmax$

$$r_{jt} = 1.0;\ j = 1, 2, \ldots, n;\ t = 1, 2, \ldots, pmax$$

- When p is less than $pmax$

As the contribution of each dimension, we define the quantity dim_t,

$$dim_t = \sum_{j=1}^{n} x_{jt}^2 + \sum_{j=1}^{n} v_{jt}^2.$$

We choose the top p contributed dimensions of $dim_t; t = 1, 2, \ldots, p+1$ and this configuration of the top p dimensions will be supplied as the initial configuration.

b. To improve the configuration (object configuration $\mathbf{X} = [x_{jt}]$ and $\mathbf{R} = [r_{jt}]$ using an iterative process.

- Calculate disparities
In general, m_{jk}, which is calculated with the given configuration, is not satisfied with the monotone relationship with s_{jk} in general. Let $M(\mathbf{s})$ denote a nonincreasing function of $\mathbf{s}$, the disparity $\hat{m}_{jk} = M(s_{jk})$ denote a monotone transformed value of $\{s_{jk}\}$. If we could define these disparities well, we can improve configuration by using these disparities. Well-known disparities are the disparities defined by Kruskal's monotonicity principle. Let the quantity S^* be defined by

$$S^* = \sum_{j=1}^{n} \sum_{\substack{k=1 \\ k \neq j}}^{n} (\hat{m}_{jk} - m_{jk})^2. \tag{13}$$

We try to find the disparities $\hat{m}_{jk}$ which minimizes S^* for fixed $\{m_{jk}\}$. So, this problem will be formulated in the framework of the isotonic regression method. The iterative algorithm obtains disparities $\{\hat{m}_{jk}\}$ called the pool adjacent violators algorithm (Barlow, Bartholomew, Bremner, & Brunk [1]; de Leeuw, Hornik, & Mair [6]).

- Improve the configuration
After the disparities were obtained by using the isotonic regression method, the configuration will be improved by using these fixed disparities. As the minimizing function, we adopt the Stress Formula 2 S by Kruskal and Carroll [10],

$$T^* = \sum_{j=1}^{n} \sum_{\substack{k=1 \\ k \neq j}}^{n} (m_{jk} - \bar{m})^2, \tag{14}$$

$$S = \sqrt{S^*}/\sqrt{T^*}. \tag{15}$$

The object configuration $\mathbf{X}$ is improved as to minimize S by using the optimizing function *optim* in R software.
After updating $\mathbf{X}$, asymmetric weights $\mathbf{R}$ will be updated by a similar procedure as updating $\mathbf{X}$. In the model (4), we restricted as r_{jt} being greater than 0, but, m_{jk}, S^*, and T^* will take the same value even if some $r_{jt} < 0$, respectively. So, we do not take care of the positiveness in the optimization process. If the updated r_{jt} was negative, it will be replaced with $|r_{jt}|$.

c. To decide whether further improvement is needed.
The disparities $\{m_{jk}\}$ are updated using the improved $\mathbf{X}$ and $\mathbf{R}$. Furthermore, the value of S is calculated. In the case where S is very small (e.g., $S \leq 0.001$) or the improvement S with respect to previous one (e.g., $|S^{iter} - S^{iter-1}| \leq 0.000001$, this phase b will be terminated. In another case, the phases b and c are repeated.

After obtaining the configuration of the dimensionality p, the initial configuration of the dimensionality $p - 1$ will be set up by the procedure (3).

4 Application

The ellipse model was applied to the Morse code confusion data by Rothkopf [13]. This data is the proximity matrix whose cell is the percentage of "same" responses for all pairs of successively presented aural signals of the international Morse code gathered from 598 respondents (Rothkopf [13]). The configuration was obtained from the dimensionality three, two, and one. The corresponding Stress values were $S_3 = 0.4603$, $S_2 = 0.5077$, and $S_1 = 0.6321$, respectively. The two-dimensional configuration is adopted and is shown in Table 1 and Fig. 2, respectively.

And the corresponding Shepard diagram is also shown in Fig. 3. In Fig. 3, the model fitting looks well. In Fig. 2, dimension one will represent the number of components of Morse code, and dimension two will represent the combination of the dash "-" and the dot ".". And the ellipses of each object indicate

- The combination of the dots and dashes dominates when the number of components is few.
- The number of components dominates when the number of components is increasing.

Table 1 Two-dimensional configuration for the Morse code confusion by Rothkopf [13]

	X		**R**	
	Dim.1($\mathbf{x}_1$)	Dim.2 ($\mathbf{x}_2$)	Dim.1 ($\mathbf{r}_1$)	Dim.2 ($\mathbf{r}_2$)
A .-	−1.1515	−0.9849	0.2796	0.0910
B -...	0.4098	−0.3289	0.0377	0.1325
C -.-.	0.2801	0.1464	0.0589	0.0023
D -..	−0.1462	−0.5645	0.0596	0.1402
E .	−1.8046	0.6132	0.0548	0.0700
F ..-.	0.3504	−0.4785	0.0021	0.0511
G –.	−0.2476	0.4527	0.1552	0.1403
H	0.3293	−1.0187	0.0935	0.2444
I ..	−1.3798	−0.9198	0.1486	0.1308
J .—	0.3726	0.6359	0.0872	0.0216
K -.-	−0.1036	−0.1136	0.0089	0.0666
L .-..	0.2596	−0.2460	0.0329	0.0449
M –	−1.1844	−0.0655	0.2267	0.1635
N -.	−1.3924	−0.5307	0.2550	0.1095
O —	−0.1427	0.8855	0.1502	0.1371
P .–.	0.2954	0.3178	0.0016	0.0373
Q –.-	0.4260	0.5237	0.0023	0.0451
R .-.	−0.4251	−0.4963	0.0065	0.0345
S ...	−0.4634	−1.2597	0.0862	0.0959
T -	−1.7286	0.6980	0.1733	0.1154
U ..-	−0.2703	−0.9285	0.1843	0.1609
V ...-	0.4997	−0.6720	0.0597	0.1341
W .–	−0.2944	−0.1162	0.1687	0.1109
X -..-	0.3412	−0.0012	0.0002	0.0904
Y -.–	0.4331	0.4186	0.0064	0.0004
Z –..	0.4446	0.2823	0.0372	0.0725
1 .—-	0.4351	1.0597	0.0482	0.0515
2 ..—	0.6404	0.5941	0.0542	0.0052
3 ...–	1.0259	0.0778	0.0005	0.0153
4....-	0.7587	−0.5404	0.0839	0.0378
5	0.7339	−0.8619	0.1229	0.1590
6 -....	0.6623	−0.2297	0.0081	0.0012
7 –...	0.6545	0.3121	0.0039	0.0028
8 —..	0.6387	0.7912	0.0316	0.0980
9 —-.	0.3487	1.1863	0.0774	0.1783
0 ——	0.3945	1.3619	0.1643	0.1721

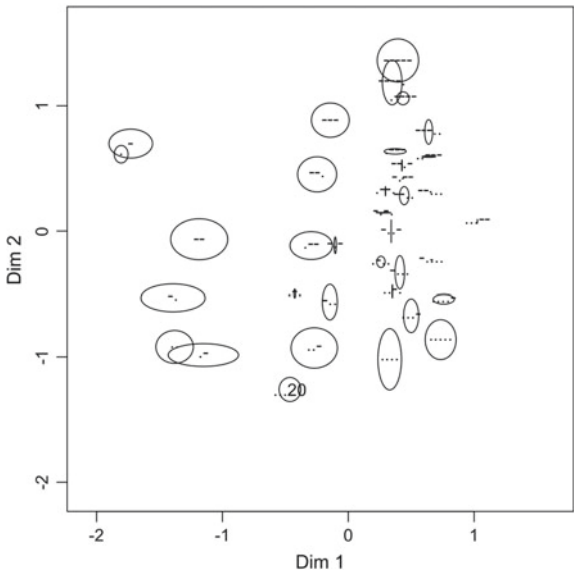

Fig. 2 Two-dimensional configuration

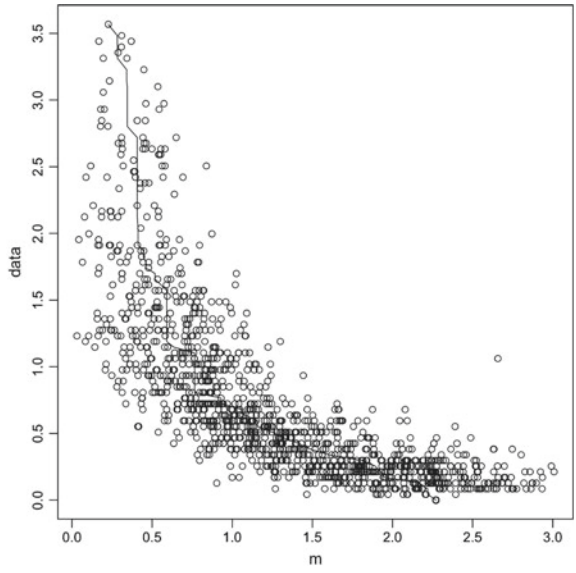

Fig. 3 Shepard diagram

To check the fitness of the ellipse model, we applied the circle model, too, and obtained r_j. We also calculated the row sum of skew-symmetric part of data, correlation coefficients between two items of asymmetric weights $\mathbf{r}_1$, $\mathbf{r}_2$, $\mathbf{r}$, and Sum of Skew Symmetric parts. The correlation between the Row Sum of Skew Symmetric parts indicates that both models were fitted to data. Furthermore, the ellipse model revealed the confusion characteristics of the international Morse code (Table 2).

Table 2 Correlation matrix among radii

	$\mathbf{r}_1$	$\mathbf{r}_2$	$\mathbf{r}$	Row sum of symmetric parts
$\mathbf{r}_1$	1.000	0.555	0.891	0.748
$\mathbf{r}_2$	0.555	1.000	0.839	0.841
$\mathbf{r}$	0.891	0.839	1.000	0.901
Row sum of skew symmetric parts	0.748	0.841	0.901	1.000

5 Conclusion

We briefly surveyed the models for analyzing asymmetric proximities and described on the circle model and the ellipse. In the optimization process to obtain the configuration, the positive constraints on asymmetric weights r_{jt} were relaxed, and it worked well.

When applying the ellipse model, we need to take care of the dimensionality of the configuration. The degree of freedom of data is $n \times (n-1)$ in general. On the other hand, the number of the parameters of the ellipse model is $(n-1) \times p + n \times p$, and that of the circle model is $(n-1) \times p - p \times (p+1)/2 + (n-1)$. So, when n is smaller, or the dimensionality is near to $n/2$, the behavior of the ellipse model may become unstable. In that case, the intermediate model (12) will be useful as a reference model.

When we suspect tat asymmetric proximity matrix is a block diagonal matrix,

$$\mathbf{S} = \begin{pmatrix} \mathbf{S}_{11} & \mathbf{S}_{12} & \cdots & \mathbf{S}_{1G} \\ \mathbf{S}_{21} & \mathbf{S}_{22} & \cdots & \mathbf{S}_{2G} \\ \vdots & \vdots & \ddots & \vdots \\ \mathbf{S}_{G1} & \mathbf{S}_{G2} & \cdots & \mathbf{S}_{GG} \end{pmatrix}, \tag{16}$$

where G is the number of blocks, and the values of the elements of S_{gh} for $g \neq h$ will be relatively smaller than those of S_{gg} or S_{hh}. This case will be found as the number of the object is large, for example, $n > 100$. When we investigate on traveling by air flights, airports will be grouping by regional zone. In this case, the dimensions between blocks may be different. Then we can simplify our problem, which is fit the ellipse model to each block matrix $\mathbf{S}_{gg}$, $g = 1, 2, \ldots, G$. However, we must develop a new model when some dimensions of a block g are shared with those of other blocks $g\prime$.

References

1. Barlow, R. E., Bartholomew, D., Bremner, J. M., & Brunk, H. D. (1972). *Statistical inference under order restrictions; the theory and application of isotonic regression*. New York: Wiley.
2. Borg, I., & Groenen, P. J. F. (2005). *Modern multidimensional scaling*. Springer.
3. Bove, G. (2012). Exploratory approaches to seriation by asymmetric multidimensional scaling. *Behaviormetrika*, *39*, 63–73.
4. Chino, N. (1978). A graphical technique for representing the asymmetric relationships between N objects. *Behaviormetrika*, *5*, 23–40.
5. Constantine, A. G., & Gower, J. C. (1978). Graphic representations of asymmetric matrices. *Applied Statistics*, *27*, 297–304.
6. de Leeuw, J., Hornik, K., & Mair, P. (2009). Isotone optimization in R: Pool-adjacent-violators algorithm (PAVA) and active set methods. *Journal of Statistical Software*, *32*, 1–24.
7. Harshman, R. (1978). Models for analysis of asymmetrical relationships among N objects or stimuli. *Paper presented at the First Joint Meeting of the Psychometric Society and the Mathematical Psychology*. Hamilton, Ontario: McMaster University.
8. Kiers, H. A. L. (1989). An alternating least squares algorithm for fitting the two- and three-way DEDICOM model and the IDIOSCAL model. *Psychometrika*, *54*, 515–521.
9. Krumhansl, C. L. (1978). Concerning the applicability of geometric models to similarity data: The interrelationship between similarity and spatial density. *Psychological Review*, *85*, 445–463.
10. Kruskal, J. B., & Carroll, J. D. (1969). Geometrical models and badness-of-fit functions. In P. R. Krishnaiah (Ed.), *Multivariate analysis* (Vol. 2, pp. 639–671). New York: Academic Press.
11. Okada, A. (1990). *A generalization of asymmetric multidimensional scaling, in knowledge, data and computer-assisted decisions* (pp. 127–138). Heidelberg: Springer.
12. Okada, A., & Imaizumi, T. (1987). Geometric models for asymmetric similarity data. *Behaviormetrika*, *21*, 81–96.
13. Rothkopf, E. Z. (1957). A measure of stimulus similarity and errors in some paired-associate learning tasks. *Journal of Experimental Psychology*, *53*, 94–101.
14. Young, F. W. (1987). Weighted distance models. In F. W. Young & R. M. Hamer (Eds.), *Multidimensional scaling: History, theory, and applications* (pp. 117–158). Hillsdale, NJ: Lawrence Erlbaum.
15. Zielman, B., & Heiser, W. J. (1996). Models for asymmetric proximities. *British Journal of Mathematical and Statistical Psychology*, *49*, 127–147.

Multiple Regression Analysis from Data Science Perspective

Manabu Iwasaki

Abstract Multiple regression analysis is the analytical method that has played a major role in statistical data analysis, and its importance continues in data science. In this paper, we first review the multiple regression analysis from the viewpoint of data science, and explore the future image of it with emphasis on statistical causal inference. In particular, we focus on the variable selection procedure and discuss it in detail with a numerical example.

Keywords Asymmetry multidimensional scaling model · Dimensionality reduction analysis · Topic transition pattern

1 Introduction

In recent years, society's expectations for data science are rapidly increasing. The Japanese government also positions artificial intelligence and data science as an important vehicle of national growth strategy. To meet various demands for educating students with skills and knowledge of data science, some universities recently started brand-new School of Data Science and also established new graduate schools. In addition, new educational programs with a focus on data science are prepared in many universities. Turning our eyes to companies, the shortage of human resources in data science in various business fields has been pointed out, and many data science training programs within and beyond the company are being developed by various organizations.

The question "what is data science?" is difficult to answer, and the answer itself seems to be not unique. There may exist different answers according to each individual or organization. However, the definition that

$$\text{Data science} = (\text{Statistics} + \text{Information Science}) \times \text{Social Applications}$$

M. Iwasaki (✉)
Yokohama City University, Kanazawa-ku, Yokohama 236-0027, Japan
e-mail: iwasakim@yokohama-cu.ac.jp

T. Imaizumi et al. (eds.), *Advanced Studies in Behaviormetrics and Data Science*,
Behaviormetrics: Quantitative Approaches to Human Behavior 5,
https://doi.org/10.1007/978-981-15-2700-5_8

seems not so far from the correct answer. Of course, the weights for each term in the expression above may differ depending on the individual or organization. It can be said, however, that statistics alone nor information science alone cannot provide adequate definition of data science. Social applications based on specific knowledge of the field is essential.

If emphasis is placed on statistics, in addition to the traditional theory and practice of statistics, the development of recent information sciences such as the speed of computers, the increase in storage capacity, and the rapid progress of network work environments in recent years have made and still creating a new paradigm of statistics. On the other hand, if the emphasis is placed on information science, in addition to the research on the traditional field of the efficiency of computer operation or development of fast calculation algorithms, the procedures of effective processing of actual data and acquirement of valuable knowledge from it are becoming a central research area. In summary, it is fair to say that new academic fields are now being created.

One of the recent buzzword is "big data", see, for example, Holms [7]. Dealing with big data cannot be done by statistics alone or information science alone. It is necessary to fuse them with each other, and wisdom is needed to link the knowledge obtained from the individual domain. The research and practice of data science are not limited to big data. So-called small data, which have been handled with traditional statistical procedures, is still involved in data science, but with a little bit different flavor.

The current spread of data science is not limited to the variety of data being handled or the size of the data set themselves. Increasing number and diversity of people who are or will be involved in the data analysis is an important component of data science. Hal Varian, prominent Google's chief economist, once said that "I keep saying the sexy job in the next ten years will be statisticians." He then goes on to say "The ability to take data—be able to understand it, to process it, to extract value from it, to visualize it, to communicate it—that's going to be a hugely important skill in the next decades, not only at the professional level but even at the educational level for elementary school kids, for high school kids, for college kids". It can be said that this part of saying represents the current status and direction of development in the future.

In this paper, mainly from the standpoint of statistics, the focus will be laid on the multiple regression analysis, which has probably played the most important role in statistical data analysis so far. From the viewpoint of data science and statistical causal inference, regression analysis will be critically reviewed, and then from the viewpoint of new data science paradigm some cautious points will be discussed.

In Sect. 2, we will have a comprehensive discussion on the relationship between variables and type of research. In Sect. 3, multiple regression analysis is reviewed from the standpoint of statistical causal reasoning, which includes classification of explanatory variables based on their characteristics. Section 4 discusses the problem of variable selection in multiple regression analysis in detail with a numerical example. A concluding remark will be given in the last Sect. 5.

2 Relationship Between Variables and Type of Study

In data science, and also statistical data analysis so far, we deal with many variables in our analysis of data. We clarify the relationship existing between the variables by using observed data, and then, based on the knowledge obtained, we will proceed to the next stage such as prediction, control, or human intervention. To that end, it is important to understand the relationship among variables at hand.

Ordinary statistical textbooks often describe that the relationship between variables is roughly divided into two categories, that is, causal and correlation, and proceed that correlation does not necessarily mean causality. In this article, we categorize the variables into three types, adding a "regression relationship" to them. The causal relationship is a one-way relationship from cause to effect, which can be used for prediction and control. Correlation is a bidirectional relationship and which cannot be used for prediction or control generally. Textbooks explain that it is important not to confuse the two. The regression relationship added here is in the middle of them and is defined as one-way but not necessarily a causal relationship. Therefore, it can be used for prediction but not necessarily for control.

The relationship between variables is closely related to the type of study. Here, following Rosenbaum [13], three types of research are assumed: experimental research, observational research, and survey. The purpose of both experimental and observational studies are evaluation of the effects of a certain treatment. In experimental studies, research plans such as subject selection and treatment allocation can be conducted by the researcher himself or under his/her supervision. The purpose of the survey is not to consider the treatment effect, but to grasp the current situation or search for the factors behind the data.

The experimental design is said to be the gold standard for establishing causality. It is no doubt so, but there are many types of research that cannot be done as experiments in the practice due to ethical or economic constraints, and it is no exaggeration to say that almost all of the researches in social sciences are non-experimental. Causal inference from such observational studies is one of the major topics in modern statistics. For details, see Imbens and Rubin [8] or Rosenbaum [14]. So-called statistical causal inference does not deal with all causal relationships described in everyday life. It sometimes puts a limitation on the relationship. One particular restriction is manipulability. That is, we restrict ourselves to the relationship between manipulable treatment and the effect caused by it. D. B. Rubin, the advocate of statistical causal reasoning, once stated that

NO CAUSATION WITHOUT MANIPULATION (1)

(Cf. Holland [6]; Rubin [15]). This paper also follows that definition.

3 Formulation and Functions of Multiple Regression Analysis

Multiple regression analysis can be formulated as a statistical analysis based on a linear model between an outcome variable y and explanatory variables $x_1, \cdots, x_p$ written as

$$y = \beta_0 + \beta_1 x_1 + \cdots + \beta_p x_p + \epsilon. \tag{2}$$

Here, the explanatory variables $x_1, \cdots, x_p$ are not only observed variables but also the variables obtained by transformation or combinations of originally observed variables. The term ϵ is a random variable that represents the error, and is usually assumed to be mutually independent with each other and to follow a normal distribution $N(0, \sigma^2)$. Various models that relax such assumptions in the past, such as models that do not assume normality for the error term and also models that have serial correlation between the error terms particularly occurred in economic time series. It is ordinarily assumed that the explanatory variables $x_1, \cdots, x_p$ in (2) are considered constants, which are predetermined values before taking data in experimental studies or observed constants as the outcome of some random variables considered. So, it can be said that the multiple regression model (2) is regarded as a conditional model given the values of the explanatory variables. For details on multiple regression analysis, see statistical textbooks such as Montgomery and Peck [11] and Ryan [16] mentioned a few.

In many statistical textbooks, the model (2) and the error term are assumed in a descending manner, and the results of statistical inferences about unknown parameters under the model will be derived. However, it may be difficult to judge whether the assumed model is valid for real data. One criterion for evaluating the validity of the model is the normality of ϵ. To that end, ϵ is not an assumed error term, but the term we regard as an error which is not included in the main part of the model $\beta_0 + \beta_1 x_1 \cdots + \beta_p x_p$ but may affect the outcome variable y. That is, the term ϵ is regarded as the sum of small effects that affect y just as accidental fluctuation. It should be emphasized that ϵ is not just an error term, but a term that we consider to be an error.

The normal distribution is also called the error distribution. The central limit theorem guarantees that the aggregation of small independent variation follows a normal distribution. Hence, the term is considered as an error as above should follow the normal distribution. From that standpoint, the idea is that if the main part of the fluctuation is extracted, the rest should be normally distributed. So, if ϵ does not follow a normal distribution, it is quite likely that the modeling of the main part is incomplete and some important aspect of the phenomenon considered would be missed. For this reason, it makes sense to make the normality of ϵ as one important criterion of the validity of the model.

It is stated in the above that the explanatory variables in the model (2) are constants. If so, it follows that it is not possible to assume a correlation between the error term ϵ and the explanatory variable. Correlation is defined between random variables, and then the correlation between random variables and constants is zero.

That is, for two random variables X and Y, when their expected values are 0 ($E[X] = E[Y] = 0$), the correlation between them becomes $R[X, Y] = E[XY]$. With this formulation, the correlation between a constant x with a mean of 0 and a random variable Y becomes $R[x, Y] = E[xY] = xE[Y] = 0$. Therefore, ordinary statistical texts will not touch the correlation between explanatory variables and error terms. However, there is no guarantee that the correlation between the explanatory variable and the error term is zero from the standpoint that construction of error tem is responsible to the researcher. Therefore, especially in the case of variable selection described in Sect. 4, it is necessary to pay attention to the presence or absence of a correlation between the explanatory variables and the error term.

Next, we examine the main part $\beta_0 + \beta_1 x_1 + \cdots + \beta_p x_p$ of the model (2). This is a mathematical expression, and because of the abstraction of mathematics, it is very useful in the sense that various models expressed in this form can be handled in a unified manner. However, in actual problems, there are various kinds of explanatory variables, and it would be necessary to change the interpretation of the results according to the nature of those variables.

As described in Sect. 2, the relationship between explanatory variables and outcome variables can be a "regression relationship" for prediction, but the "causal relationship" is required for the relationship between variables in intervention or control. In other words, it is important to identify whether the relationship between variables is causal or regression. In recent years, books that emphasize the statistical causal inference have appeared. For example, Angrist and Pischke [1], Berk [2], Best and Wolf [3], and Gelman and Hill [4].

We will examine variables $x_1, \cdots, x_p$ in the multiple regression model (2) in detail. The variables are collectively called explanatory variables, but their roles played in the model are often different in actual problems. Although mathematical expressions do not reveal the role of variables, recognizing the role of each variable is the key to the success of valid multiple regression analysis.

In recent data science, whether or not it is called big data, it is quite common that the problems we actually deal with have many variables. Also, data are not only newly collected by experiments or planned surveys, but also they have been already collected by other people, or are unintentionally collected without any predetermined purpose. In such cases, it would be difficult to know the characteristics of the data, but it is important to know the characteristics and the role of the data played as much as possible.This role is examined here. It is also important to know the role of variables in variable selection, which will be dealt in Sect. 4.

Although there are several different methods to classify the candidate variables for explanatory variables in the regression model, here we classify them into four types, that is, treatment variables, covariates, confounding variables, and intermediate variables.

The "treatment variable" is the main variable that we want to evaluate the relationship with the outcome variable by multiple regression analysis. It is called the controllable variable that can be manipulated in experimental studies. it is also considered as a variable that plays the role of a causal variable in observational studies. In the context of statistical causal inference, it is regarded as a causal variable that the motto (1) is applied. In the experimental study that evaluates the effect of a treatment,

such a variable will be a dummy variable that takes 1 or 0 according to the presence or absence of the treatment. Of course, not only binary but also continuous quantity maybe considered.

"Covariates" are variables that have some influence on the outcome variable, but not the result variables in the causal relationship from other variables, although they might be correlated with each other. Also, when there exist treatment variables in the multiple regression model, covariates are defined as variables that do not affect the treatment variables, and are called exogenous variables in the context of economics. Variables that can affect both outcome and treatment variables are called "confounding variables". These variables must not be the result of other variables in causal reasoning. The variables, especially those affected by treatment variables, are called "intermediate variables".

It is important to note that confounding variables must always be included in the model, especially when establishing statistical causal relationships with treatment variables. Whether covariates are included in the model depends on how the regression model is used, but in many cases, the accuracy of the estimation of the outcome variable is improved by incorporating it into the model. On the other hand, intermediate variables, which again although depend on how the model is used, should not be included in the model when looking at the relationship between treatment variables and objective variables (cf. Rosenbaum [12]). These points are dealt in detail in the next section with examples.

4 Variable Selection

Variable selection is to identify a set of variables that best explains the outcome variable y from candidate explanatory variables. This topic is commonly dealt in many statistical textbooks, see, for example, Montgomery and Peck [11, Chap. 7] and Ryan [16, Chap. 7]. It should be noted that the selection policy differs depending on the purpose of analysis. In other words, the variables to be selected or not to be selected are determined by the purpose of the analysis. An important viewpoint is that the model selected works well not only for the current data but also for future data.

First, the question must be answered whether or not variable selection is really necessary. The situations that variable selection is unnecessary are as follows: If explanatory variables are determined in advance, the prediction of the outcome variable can be performed from those variables, and hence the variable selection is unnecessary. For example, in the prediction of the score of the university entrance examination from the mock exam of 5 subjects, since we certainly have the scores of the 5 subjects, it is quite natural to use all of them. If the purpose of the analysis is prediction, it is advisable to use as many variables as possible. This is because the risk of not incorporating necessary variables into the model is usually greater than the risk of incorporating unnecessary variables into the model. If an important variable is dropped from the model, the correlation between the explanatory variables and the error term described in Sect. 3 may occur. However, too many variables will not

produce results that may result in overfitting or overtraining of the model. In such a case, the risk of extrapolation can be increased. For the response surface method in the design of experiments, when selecting the optimal value of the outcome variable assuming, for example, a quadratic function, variable selection is not required unless the sample size is very small. There will be no reason to dare to remove the first-order or variable product terms in quadratic functions in the model.

The cases that variable selection is required are as follows: If there are a lot of explanatory variable candidates in the early stage of analysis, and you don't know which of them are needed to explain the outcome variable, for screening purpose we need variable selection. In the survey, when a preliminary survey is conducted before the main survey and the survey items are set using the preliminary results, we need variable selection in order to reduce the cost of the large-scale survey without decreasing the information to be gathered about the population under study. Of course in such cases, you must keep items in the survey which is needed theoretically or practically. When the analytical purpose is control, since it is difficult to control a large number of variables, it is necessary to focus on a limited number of variables which seems to be important, and hence variable selection is required.

To explain the main points of the variable selection of exploratory variables, we will show a simple numerical example. Iwasaki [9] also discussed similar analysis, but we will add a more detailed discussion here. In this simple example, although there are only two explanatory variables, the key points of variable selection will be understood.

Suppose the outcome variable y is the score of the final exam in a statistics class at a certain university. Exploratory variables are the number of class participation (x_1) and the score of assigned homework (x_2). Table 1 shows summary statistics for 40 students.

The single regression and multiple regression equations obtained from Table 1 are as follows. Each number in parentheses is the coefficient of determination of the corresponding model. The purpose of the analysis is what variables should be used to predict the test score y and how to interpret the model.

$$y = 9.70 + 5.18x_1 \quad (R^2 = 0.321) \tag{3}$$

$$y = -3.63 + 0.90x_2 \quad (R^2 = 0.737) \tag{4}$$

$$y = -2.86 - 0.16x_1 + 0.91x_2 \quad (R^2 = 0.739) \tag{5}$$

$$x_2 = 13.60 + 5.88x_1 \quad (R^2 = 0.450) \tag{6}$$

From the correlation coefficients shown in Table 1, we observe positive correlations between each variable, and reflecting this, all regression coefficients in the single regression model between each variable are positive. However, in the multiple regression model (5) using two explanatory variables, the regression coefficient of participation (x_1) is negative. It is no doubt an educational misinterpretation that less participation causes better exam score. The null hypothesis of the partial regression coefficient of x_1 is 0 is not rejected. It is also misinterpretation that student's class participation does not affect the test scores. How should we interpret it? In multiple

Table 1 Scores of exam (y), participation (x_1) and assignments (x_2)

Statistics	Exam (y)	Part (x_1)	Assign (x_2)
Average	75.61	12.73	88.40
SD	15.06	1.65	14.44
Correlation	Exam (y)	Part (x_1)	Assign (x_2)
Exam (y)	1	0.671	0.567
Part (x_1)	0.671	1	0.859
Assign (x_2)	0.567	0.859	1

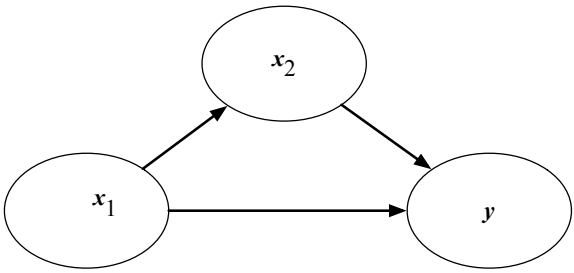

Fig. 1 Arrow diagram among variables

regression analysis in social sciences such as economics, the regression coefficient that should be positive often becomes negative due to the effect of multicollinearity, and this is also the case here.

The relationship among the variables in multiple regression analysis can be clarified by the graphical representation (causal graph) of the variables included. Figure 1 displays the relationship between the variables of our current problem. We will apply the variable taxonomy described in Sect. 3. The purpose of the analysis is to evaluate the impact of class participation on the exam score, the participation (x_1) is the treatment variable, while the outcome variable is the exam score (y). In this case, the assignment (x_2) is an intermediate variable between the causal path from x_1 to y. If you want to see the impact of the assignment on the exam score, the participation (x_2) is the treatment variable and the outcome variable is the exam score (y). In this case, the participation (x_1) affects both x_2 and y, and hence is a confounding variable. Although not included in Table 1, when gender is given as data, gender becomes a covariate. Gender cannot be a treatment variable under the motto (1) because it is usually not artificially controllable.

When the purpose of the analysis is the prediction of y, we have to ask when the prediction is performed. When predicting exam scores when both participation and assignment are observed, both participation (x_1) and assignment (x_2) can be explanatory variables. But, of course, the situation that only participation data is available, assignment (x_2) cannot be an explanatory variable. Interpretation of the results of the regression analysis should take into account the characteristics of the variables as described above.

If the objective of the analysis is to predict y, there is no dominance between the simple regression model (4) and the multiple regression model (5), assuming that

observations of both x_1 and x_2 are available for the prediction. If a simple model is to be preferred under Occam's razor, (4) will be selected. However, since data has already been obtained, there is no harm we select a model (5) because the sample size is not so small. When our purpose of analysis is prediction of outcome variable, we need not interpret the partial regression coefficients of the multiple regression model. Therefore, if the model (5) is selected, there is no problem even if the coefficient of x_1 is negative.

If the purpose of the analysis is to see the impact of participation (x_1) on exam score (y), since assignment (x_2) is an intermediate variable it should not be included in the model. Therefore, the simple regression model (3) is a valid model in this case. If the purpose of the analysis is to see the impact of assignment (x_2) on exam score (y), participation (x_1) is a confounding variable and hence it must be included in the model. In other words, the valid model in this case is the multiple regression model (5), and the coefficient of x_2 in the model is the object of interpretation.

In general, if it is necessary to select explanatory variables and there are many candidates for explanatory variables, it would be necessary to make the selection in a mechanical manner. There are several criteria for selecting explanatory variables, and some of them are commonly installed in ordinary statistical software. Examples of such criteria include the coefficient of determination adjusted for degrees of freedom, Akaike Information Criterion (AIC), Mallows' Cp, and so on. If the sample size is moderate or large, there is no significant difference between the criteria.

Variable selection is sometimes performed by examining the P value of the partial regression coefficient of the explanatory variable. In this case, we have to recognize clearly that the partial regression coefficient shows the conditional effect of the corresponding variable conditional upon the other variables are included in the model, and not the single effect of the variable. It is also important that deleting explanatory variables should be done in one by one manner, and not delete several explanatory variables at once.

In the problem of data science, there may exist many candidates for explanatory variables. In selecting the explanatory variables, the purpose of the analysis is first clarified, as described above, and then the characteristics of each variable are carefully examined. We have to identify the variables that should be incorporated into the model or those that should not be incorporated into the model. Variable selection should be performed after such identification of variables. Never make a mechanical selection without such identification.

5 Concluding Remarks

In data science, machine learning methods are mainly used (cf. James, Witten, Hastie, & Tibshirani [10]; Hastie, Tibshirani, & Friedman [5]). In machine learning, multiple regression analysis is positioned as a supervised learning method. The objective of machine learning is often a prediction of outcome variables or determination of the optimal value of the variable given exploratory variables. There is no doubt that

machine learning techniques represented by deep learning or similar techniques have exhibited considerable power in terms of prediction. However, the prediction scheme obtained there is often a black box. This fact corresponds to the strategy that we do not interpret each regression coefficient in the multiple regression model, described in Sect. 3.

However, in actual problems, prediction alone is not sufficient, and you will often want to know the effect on outcome variables when some kind of artificial intervention is applied to explanatory variables. If the prediction model is a black box, its application to real problems would be hesitant. In that case, it is necessary to classify the explanatory variables as described in Sect. 3, and it is also needed to construct a multiple regression model by the procedure described in Sect. 4.

Even now that actual calculations can be performed instantaneously by computer, the construction of valid and useful prediction models remains a challenge for data scientists. It critically depends upon the ability of each data scientist.

References

1. Angrist, J. D., & Pischke, J. (2009). *Mostly harmless econometrics: An empiricist's companion*. Princeton: Princeton University Press.
2. Berk, R. A. (2004). *Regression analysis. A constructive critique*. California, Thousand Oaks: Sage Publications.
3. Best, H., & Wolf, C. (Eds.). (2015). *The Sage handbook of regression analysis and causal inference*. Los Angeles: Sage Publications.
4. Gelman, A., & Hill, J. (2007). *Data analysis using regression and multilevel/hierarchical models*. New York: Cambridge University Press.
5. Hastie, T., Tibshirani, R., & Friedman, J. (2009). *The elements of statistical learning. Data mining, inference, and prediction* (2nd ed.). New York: Springer.
6. Holland, P. W. (1986). Statistics and causal inference (with discussion). *Journal of the American Statistical Association*, *81*, 945–970.
7. Holms, D. E. (2017). *Big data. A very short introduction*. Oxford: Oxford University Press.
8. Imbens, G. W., & Rubin, D. B. (2015). *Causal inference for statistics, social, and medical sciences: An introduction*. New York: Cambridge University Press.
9. Iwasaki, M. (2017). Perspective of multivariate data analysis and regression analysis. In M. Iwasaki, K. M. Adachi, H. Yadohisa, & M. Haga (2017). *Official study note "statistics III, multivariate data analysis"*.Tokyo: Japan Statistical Association (in Japanese).
10. James, G., Witten, D., Hastie, T., & Tibshirani, R. (2013). *An introduction to statistical learning with applications in R*. New York: Springer.
11. Montgomery, D. C., & Peck, E. A. (1992). *Introduction to linear regression analysis* (2nd ed.). New York: Wiley.
12. Rosenbaum, P. R. (1984). The consequences of adjustment for a concomitant variable that has been affected by the treatment. *Journal of the Royal Statistical Society, Series A*, *147*, 656–666.
13. Rosenbaum, P. R. (2002). *Observational studies* (2nd ed.). New York: Springer.
14. Rosenbaum, P. R. (2017). *Observation & experiment. An introduction to causal inference*. Cambridge: Harvard University Press.
15. Rubin, D. B. (1986). Comment: Which ifs have causal answers. *Journal of the American Statistical Association*, *81*, 961–962.
16. Ryan, T. P. (1997). *Modern regression methods*. New York: Wiley.

Multiway Extensions of the SVD

Pieter M. Kroonenberg

Abstract In this paper, I will provide a pictorial overview of extensions of the two-way singular value decomposition (SVD) to three-way SVD variants; variants because there are several extensions none of which have all the properties of the two-way SVD. Multiway extensions will be mentioned in passing. The level of exposition is primarily at an introductory and conceptual level. This is achieved by presenting concepts in pictures accompanied by the model formula. For the technical aspects, one is referred to the extensive literature.

Keywords Candecomp/Parafac · Canonical polyadic decomposition · HOSVD · Multilinear · Tensor · Three-way data · Tucker models

1 Introduction

Much of the literature on three-way and multiway analysis is couched in heavy mathematical formulations, but for this Festschrift I have chosen to present in this paper[1] a plethora of displays appropriate for a great Fest. Model formulas are given as well plus some properties of the models. Thus, this paper is like a cartoon version of matter which has already been dealt with in earlier mathematically laden papers. It is more in the spirit of an oral presentation than a detailed exposition of the material. This can be found in De Lathauwer et al. (2000), which is the main inspiration for this paper. I will supply a brief selection of publications and references for further study.

[1]This paper is an extended version of a presentation held at Procida Island, Italy, 24–25 September 2015.

P. M. Kroonenberg (✉)
Faculty of Social and Behavioural Sciences, Leiden University, Leiden, The Netherlands
e-mail: kroonenb@fsw.leidenuniv.nl

The Three-Mode Company, Leiden, The Netherlands

T. Imaizumi et al. (eds.), *Advanced Studies in Behaviormetrics and Data Science*,
Behaviormetrics: Quantitative Approaches to Human Behavior 5,
https://doi.org/10.1007/978-981-15-2700-5_9

2 Two and Three-Way Data

Before extending the singular value decomposition from two-way data it is necessary to present three-way data as an extension of two-way.

The kind of two-way data that one comes across in the social and behavioural sciences often consists of subjects (nowadays often referred to as participants; individuals will do as well) by variables. Such variables can have all kinds of "fillings"; they may have the same or different measurement levels, but at present, we will restrict ourselves to numeric, well-behaved, data, even though special three-way SVD generalisations exist and are in use for categorical and binary data; see, e.g. Kroonenberg [3] in connection with three-way correspondence analysis, and Van Mechelen, Ceulemans, and associates in connection with three-way binary data (see e.g. Ceulemans & Van Mechelen [1]). Figure 1 shows the data from seven participants, in particular, their IQ scores and their results on high school English, Arithmetic, and Physical Education. Such measurements are typically not collected once during the high school careers of the students but each year again, leading to three-way data. Obviously, the school administrators want to see the progression over the school years, as well as the changes in the patterns between the school variables, and for this, they will need three-way or three-mode techniques.

Terminology

In statistics the word "way" refers to the size of the data set. One might say "dimension", be it that this word is also used in another technical sense. The word "mode" in this context refers to the different entities that describe the content of the ways (participants, variables, and years). A set of correlation matrices calculated on these school data would be described as three-way two-mode data, as two of the ways both contain the variables (mode 1), the third way is the years (mode 2).

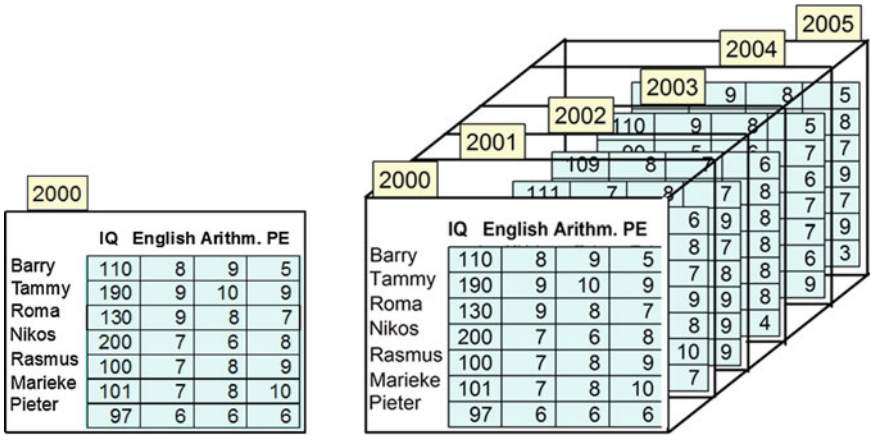

Fig. 1 An example of two-way and three-way data. To the left: scores collected in a single year (two-way data); To the right: scores collected over six consecutive years (three-way data)

Furthermore, two-way data fit into a "matrix" and three-way data fit into an "array".

2.1 A View of Three-Way Data

Let us first introduce a slightly more detailed view of three-way array and its terminology (Fig. 2).

A data array is indicated either with an underlined bold letter **X** or a bold script letter $\mathcal{X}$.

The modes of a three-way array are coded as

- Mode **A** = First way: $i = 1, \ldots, I$. In the displays to follow indicated in red. Example: Individuals
- Mode **B** = Second way: $j = 1, \ldots, J$. In the displays to follow indicated in green. Example: Variables.
- Mode **C** = Third way: $k = 1, \ldots, K$. In the displays to follow indicated in blue.

Multiway arrays are also referred to in mathematics as tensors.

2.2 Some Types of Three-Way Data

Table 1 provides a non-exhaustive list of three-way data that one can come across in social and behavioural sciences, but variants of such tables can be constructed for other disciplines as well. However, in this paper, I will restrict myself to the domain most familiar to me. As indicated above, we will deal in this paper primarily with numeric three-way profile data.

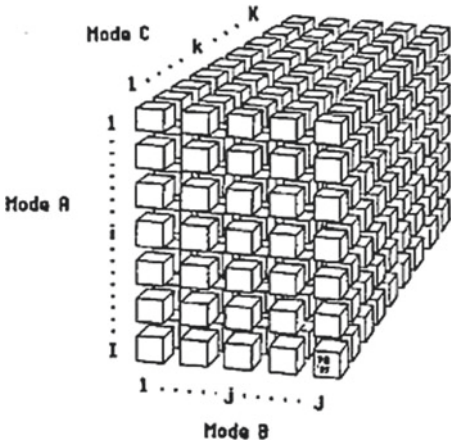

Fig. 2 A three-way data array

Table 1 Three-way data types

Data types	Description
Three-way profile data (continuous, categorical, binary)	Individuals have scores on a number of variables measured under several conditions or on several occasions
Repeated measures data	Participants are measured several times on the same variables
Three-way rating data	Subjects score rating scales in different situations; also stimulus-response data and semantic differential data
Sets of correlation matrices	Correlation matrices of different samples measured on the same variables
Sets of similarity matrices	Similarity matrices of stimuli obtained from different persons
Three-way interactions	Resulting from three-way analysis of variance designs and log linear analyses of three-way contingency tables

3 Four-Way Data

Given we live in a three-dimensional world, it is difficult to picture a four-dimensional array, so the only recourse we have is to display such data via a set of three-data arrays as in Fig. 3.

4 Traditional Ways to Handle Three-Way Data

Before three-way data were common and people had thought about handling them as a particular type of data, they were generally rearranged into some form of two-way data. Figure 4 shows a number of ways in which this was done. Which manner is

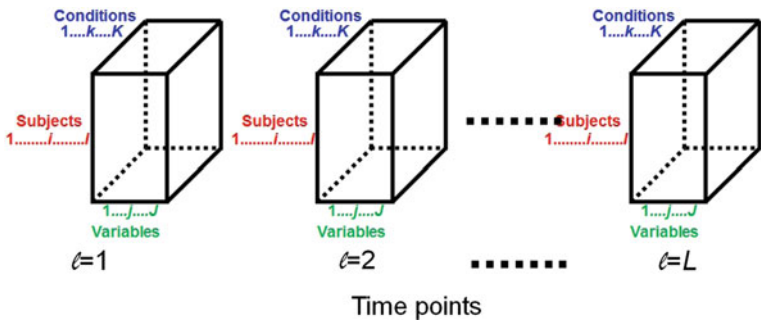

Fig. 3 Four-way profile data

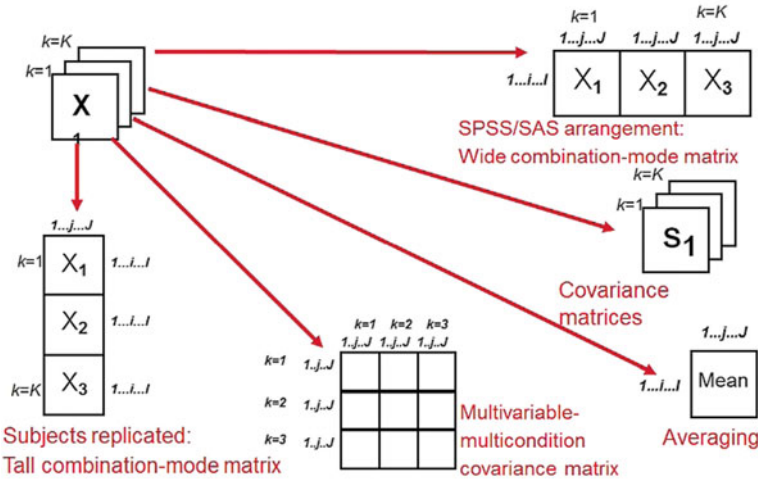

Fig. 4 Traditional ways to handle three-way data

most appropriate in a study obviously depends on the research questions at hand and the assumptions one is prepared to make about the data. Most general (commercial) program suites are geared towards the wide combination-mode arrangement of the data, but programs for structural equation models need multivariable-multicondition covariance matrices, which in particular contexts are referred to as multitrait-multimethod matrices. If one can transform three-way data to two-way data, why bother about three-way or multiway data? A quote from Cichocki et al. ([2], p. 146) explains this

- "*Early multiway data analysis approaches reformatted the data tensor as a matrix and resorted to methods developed for classical two-way analysis. However, such a flattened view of the world and the rigid assumptions inherent in the two-way analysis are not always a good match for multiway data.*
- *It is only through higher-order tensor decomposition that we have the opportunity to develop sophisticated models capturing multiple interactions and couplings instead of pairwise interactions.*"

This echoes the idea that it does not make sense to analyse a three-way analysis of variance design with a two-way analysis of variance. Similarly it does not make sense to neglect in a multivariate repeated measure design the repeatedness of the within-subject factor. In both cases, one neglects an important aspect of the design during the analysis.

5 The Singular Value Decomposition (SVD)

The singular value decomposition is the basic structure of a matrix **X**. To explain what is meant by this, let us assume we only have two correlated variables (x_1 and x_2) and 10 subjects, then we can collect their values in a 10×2 subject×variable matrix. If we plot the 10 subjects as points in a plane defined by the two variables, we get a cloud of points in the plane (Fig. 5a). If for illustration purposes we assume that the two variables have a bivariate zero-mean distribution then this makes for an oval or elliptic cloud of points around the mean. Let us first centre the two variables so that the centered variables (z1 and z2) cross at the origin (see Fig. 5b). A good and standard way to examine the information (variability) in the matrix is to seek a set of perpendicular (i.e. orthogonal) axes (or variables) such that the first new variable lies along the longest axis (PC1) and describes most of the variance and the second variable along the short axis (PC2) what is left of the variance (Fig. 5c). The orthogonality assures that the information described by one axis is independent of that of the other axis. Finally, we rotate the whole picture (both the points and the new variables) so the latter becomes the coordinate axes (Fig. 5d). When there are more variables (or subjects), the process is entirely analogous. Each new axis accounts for as much of the remaining variance as possible.

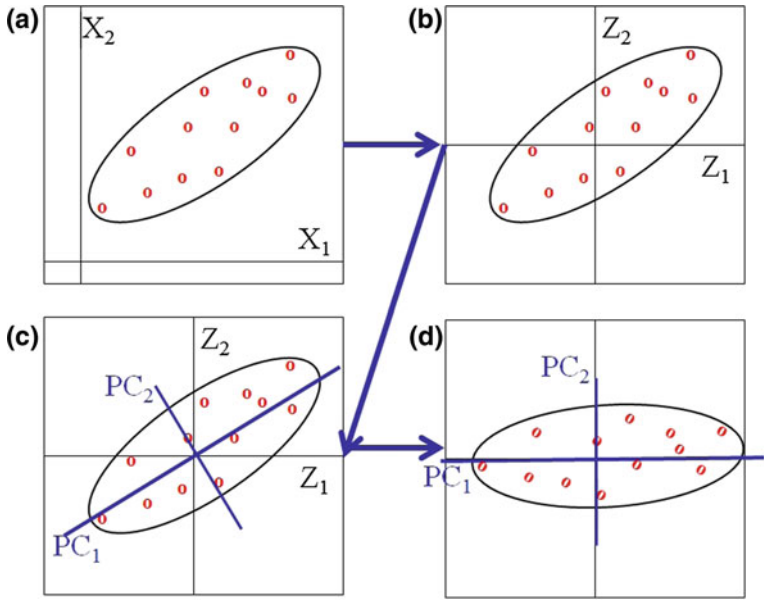

Fig. 5 How the singular value decomposition works

Mathematically this whole process is carried out by the singular value decomposition, which consists of the (10×2) rotation matrix $\mathbf{A}$ for the subjects, a (2×2) rotation matrix $\mathbf{B}$ for the variables, which are scaled such that their columns have lengths 1. This makes $\mathbf{A}$ and $\mathbf{B}$ are orthonormal, orthogonal with length 1 columns. In addition, there is a (2×2) diagonal core matrix $\mathbf{G}$, such that the matrix is decomposed as. $\mathbf{X} = \mathbf{AGB}'$. The matrix $\mathbf{A}$ contains the left singular vectors and the matrix $\mathbf{B}$ the right singular vectors; they are the same as the eigenvectors of $\mathbf{XX}'$ and $\mathbf{X}'\mathbf{X}$, respectively. The diagonal elements of $\mathbf{G}$, the singular values, represent the variability along the coordinate axes. The squared singular values are the eigenvalues and represent the variances of the singular vectors.

Eigen is the German word for own, and refers to the fact that an eigenvector is not rotated when linearly transformed by the matrix $\mathbf{X}$ Thus eigenvalues and eigenvectors are the entities belonging to or "owned" by the matrix $\mathbf{X}$. Another word for eigenvectors is basis vectors again emphasising that they are proprietary to the matrix. This explains why we consider that the singular value decomposition describes the structure of a matrix.

When there are two or three variables, the scores live in a plane or cube. With more variables the scores live in a higher-dimensional hyperspace, but such a hyperspace is more than humans can visualise. However, it is often still possible to examine the structure of the variables and the subject points because we may perform a singular value decomposition which concentrates in the first singular vectors as much as of the systematic variability of the variables as possible. In fact, the first singular vector grabs as much systematic variance as possible. Then the second does the same for what is left of the systematic variance in the data, and so and so forth. It is, therefore, often the case that for the later axes there is only random variability left. Of course, there is no need to look at such axes. If it is such that nearly all systematic variability is concentrated in the first few axes we can again examine what is going on in the dataset by looking at the low-dimensional space. Many people have contributed to the development described in this paper and devoted their efforts to the singular value decomposition in many different ways. The late Gene Golub was such a great contributor to both the theoretical and algorithmic development of the SVD that in December 1992 he was awarded an honorary doctorate by the Katholieke Universiteit Leuven, Belgium.[2] His honorary supervisor Bart De Moor presented him a vanity license plate with 'Prof SVD' for his car.[3]

[2] *Source* http://homes.esat.kuleuven.be/~bioiuser/person.php?persid=15.

[3] Photo taken July 2004 during the Tensor Decompositions Workshop at the American Institute of Mathematics; Palo Alto, CA, USA; photo copyright, Pieter M. Kroonenberg.

In summary the basic structure of a data matrix is defined by two orthonormal matrices **A** and **B**; the orthonormality of the matrices is written technically as $\mathbf{A}'\mathbf{A} = \mathbf{I}$, $\mathbf{B}'\mathbf{B} = \mathbf{I}$, and the diagonal core matrix **G** in which only the diagonal elements $(g_{11}, g_{22}, \ldots, g_{ss})$ are not equal to zero. The first column of **A** is exclusively linked to first column of **B**, and the same for the second and other columns (see Fig. 6).

Figure 6 (middle panel) also gives the algebraic formula for the singular value decomposition (left-hand side) and the tensor formula (right-hand side). The latter expression makes use of the *Kronecker product*. Each $\mathbf{X}_s$ in the bottom panel is a rank-1 matrix. Its elements x_{ij}^s are equal to the product $(a_{is}b_{js}g_{ss})$ of the element-wise summation on the left. There are S of them and the sum up to the original matrix **X**. This same notation will be used later in the three-way SVD.

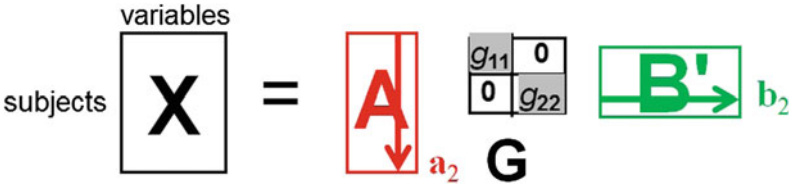

$$x_{ij} = \sum_s (a_{is}b_{js}g_{ss}) \quad \mathbf{X}_s = g_{ss}(\mathbf{a}_s \otimes \mathbf{b}_s), s = 1, \ldots, S$$

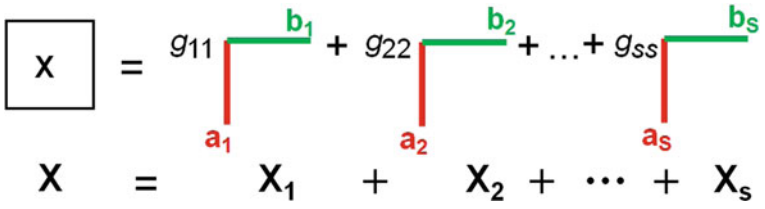

Fig. 6 Graphical view of two-way SVD (top) Formula view (middle); Tensor view using rank-1 terms (bottom)

Two-way SVD: Properties

i. **Orthonormality**. **A** and **B** are orthonormal (orthogonal + unit length);
ii. **Equal number of columns** for all component matrices
iii. **Diagonality core**. $\mathbf{G} = (g_{pq})$, **G** is *square and diagonal*, i.e. $g_{12} = g_{21} = 0$; only $g_{11}\&g_{22}$ are non-zero; singular values g_{ss} are non-negative entries in nonincreasing order; component matrices have equal number of components, $g_{pq} =$ strength of the link between component p and component q; but for the two-way SVD the columns of **A** and **B** come in pairs: $p = q = s$.
iv. **Unique solution**. Any transformation destroys the diagonality of **G**
v. **Complete decomposition**. **X** can always be completely decomposed into its structure $\mathbf{AGB}'$
vi. **Rank revealing**. The decomposition is useful for determining the rank of **X** Rank **X** = number of positive singular values = minimum number of rank-1 matrices $\mathbf{X}_s$ to decompose **X**.
(Rank is a far more difficult concept in multiway analysis)

In the sequel, we will indicate which of the three-way generalisations of the two-way SVD have which of these six properties.

6 Three-Way SVDs

For a matrix called array
there is one additional way:
Looking for its SVD,
we find not one not three,
but many more to our dismay

Different three-way generalisations or models arise when different properties of the two-way SVD are retained. A technical discussion of the reasons why this is the case can be found in De Lathauwer et al., 2000, 2004 (p. 36), and they will not be discussed here. Our main aim is to point out in a more general sense which properties are present and which are lacking in the various proposals for the generalisations. I restrict myself discussing three-way models rather than multiway models. Unfortunately, there is no single three-way SVD with all six indicated properties of the two-way SVD.

Some general characteristics of variants

▷ **Matrix product**. Three-way arrays can always be written as a matrix product of orthonormal matrices and an ordered all orthogonal core array of (three-way) singular values.
Three-way models: The Tucker3 model and the Higher-order SVD (HOSVD).

▷ **Minimal number of rank-1 terms**. *Three-way model*: Canonical decomposition; referred to as Parafac, Candecomp, or Canonical polyadic decomposition.
▷ **Orthonormal transformations**. Such that the singular values are on a "diagonal" core array.
No three-way model. It is not possible to define such a decomposition; only an approximation;
▷ **Deflation/Nesting**. No deflation; complete three-way models are not nested, i.e. the singular vectors of smaller models are different from those of larger models. However, in HOSVD (see below) one could be deflated for each mode separately.

6.1 Replicated SVD

Properties (Fig. 7)

- Replicated SVD is not very exciting. It is not a real three-way model.
- No restrictions on any set of parameters across k.
- Independent solutions for each occasion k.

6.2 Tucker2 Model

Properties (Fig. 8)

i. **Orthonormality** *Yes*. **A** and **B** orthogonal.
ii. **Equal number of columns** for all component matrices, *No*, they may have different numbers of columns.
iii. **Diagonality core** *No* diagonality; full core slices; all components of **A** may have links with all components of **B**.
iv. **Unique solution** *No*. Nonsingular rotations possible without loss of fit.
v. **Complete decomposition** *Yes*.
vi. **Rank revealing** *No*.

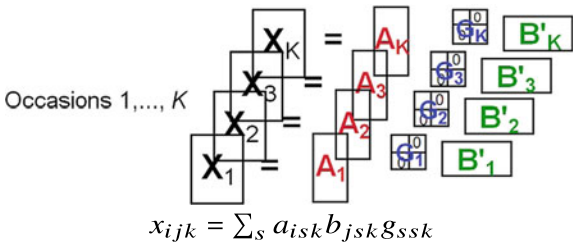

Fig. 7 Replicated Singular Value Decomposition

Fig. 8 Tucker2 model

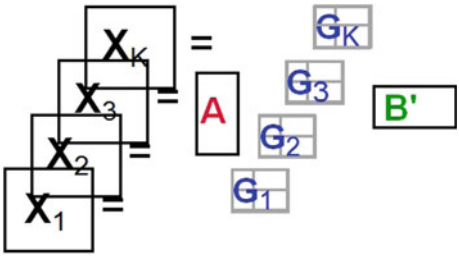

$$x_{ijk} = \sum_p \sum_q a_{ip} b_{jq} g_{pqk}$$

6.3 *Parafac/Candecomp; Canonical Polyadic Decomposition*

Properties (Fig. 9)

i. **Orthonormality**. *No*. Basis solution has correlated components.
ii. **Equal number of columns** for all component matrices. *Yes*.
iii. **Diagonality core**. *Yes*. Is referred to as slice diagonality of extended core array (see also Fig. 15).
iv. **Unique solution**. *Yes*.
v. **Complete decomposition**. *Problematic*.
vi. **Rank revealing**. *Yes*. As in two-way SVD (Fig. 6).

6.4 *Weighted Two-Way SVD*

Properties (Fig. 10)

i. **Orthonormality**. *Yes*.
ii. **Equal number of columns** for all component matrices. *Yes*.
iii. **Diagonality core**. *Yes*. Core array is actually a one-component vector (K elements).

Fig. 9 Parafac, Candecomp, Canonical Polyadic decomposition

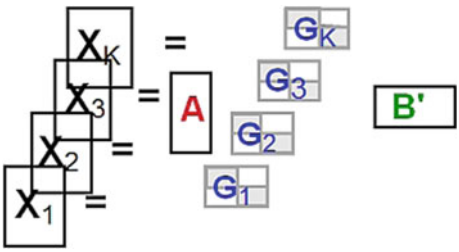

$$x_{ijk} = \sum_s a_{is} b_{js} g_{ssk}$$

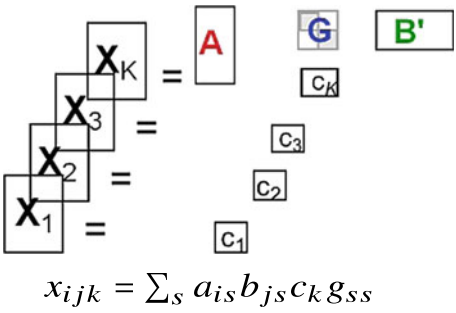

Fig. 10 Weighted two-way SVD

iv. **Unique solution**. *Yes*.
v. **Complete decomposition**. *No*.
vi. **Rank revealing**. *No*.

6.5 Two-Way SVD on Average of $\mathbf{X}_k$

Properties (Fig. 11)

- Not very interesting: no modelling of individual differences.

6.6 Tucker3 Model

Properties (Fig. 12)

i. **Orthonormality**. *Yes*. **A**, **B** and **C** are orthogonal.
ii. **Equal number of columns** for all component matrices. *No*. Component matrices may have different number of components within limits. *Product rule*: Product

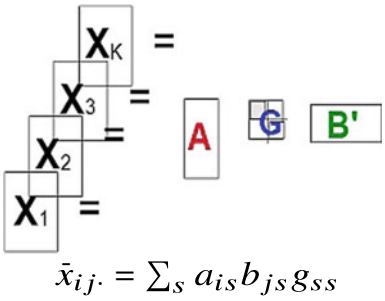

Fig. 11 Two-way SVD on average of the $\mathbf{X}_k$

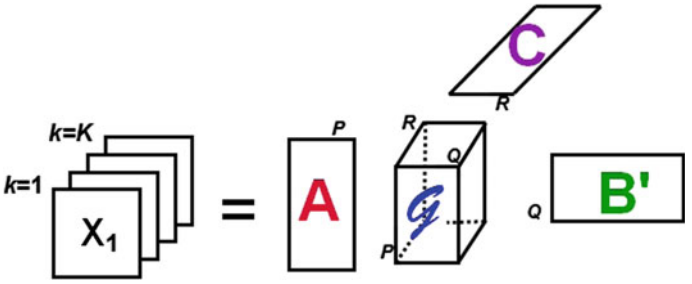

$$x_{ijk} = \sum_p \sum_q \sum_r a_{ip} b_{jq} c_{kr} g_{pqr}$$

Fig. 12 Tucker3 model

of numbers of components of two ways must be larger or equal than that the number of components of the third way, e.g. $P \times Q \geq R$.

iii. **Diagonality core**. *No*. All components of one-way maybe linked to any duo of components of the other two ways.
iv. **Unique solution**. *No*. May be rotated by nonsingular transformations without loss of fit.
v. **Complete decomposition**. *Yes*.
vi. **Rank revealing**. *No*. Rank is problematic; several definitions for the rank of a three-way exist.

6.7 *Higher-Order SVD (HOSVD) [=Tucker (1996) Method I]*

Properties (Fig. 13)

i. **Orthonormality**. *Yes*.
ii. **Equal number of columns** for all component matrices. *No*.

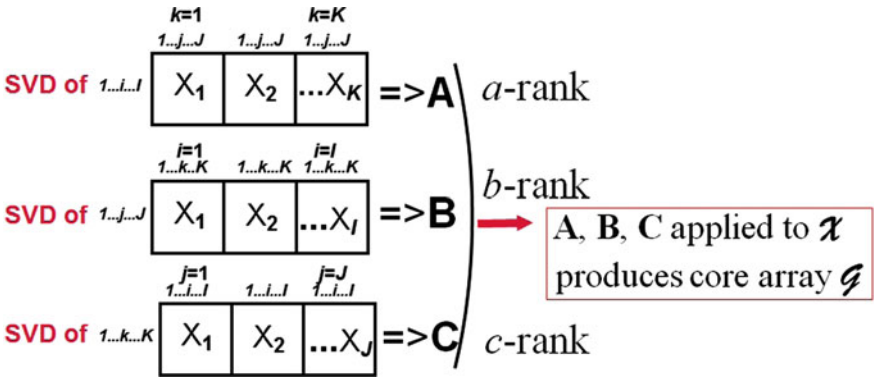

Fig. 13 Higher-order SVD (HOSVD)

iii. **Diagonality core**. *No*.
iv. **Unique solution**. *Yes*. Each of the SVDs is unique, so is the core computed from it, and thus the model is unique given the computational procedure.
v. **Complete decomposition**. *Yes*.
vi. **Rank revealing**. *Yes/No*. n-rank = (a-rank, b-rank, c-rank).

6.8 *Parafac/Candecomp/Canonical Polyadic Model*

Properties (Fig. 14)

i. **Orthonormality**. *No*.; All orthogonal + diagonality not possible. The first, second, and other columns of **A**, **B**, and **C** are exclusively linked to each other as in two-way SVD. Thus the only non-zero core elements present in the model formula are the g_{sss} (see also Fig. 16 for relations between models).
ii. **Equal number of columns** for all component matrices. *Yes*.
iii. **Diagonality core**. *Yes*. $\mathcal{G}$ is superdiagonal
iv. **Unique solution**. *Yes*.
v. **Complete decomposition**. *No?* Model is restricted. Complete decomposition is problematic in practice?
vi. **Rank revealing**. *Yes*. Rank $\mathcal{X}$ is minimum sum of rank-1 matrices.

6.9 *Three-Way SVD: Core Arrays*

See Fig. 15.

(a) Tucker2 model: Extended core array ($R = K$)

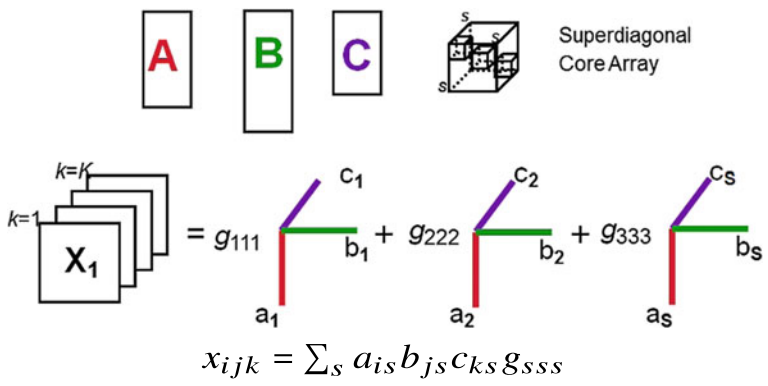

Fig. 14 Parafac, Candecomp, Canonical polyadic decomposition

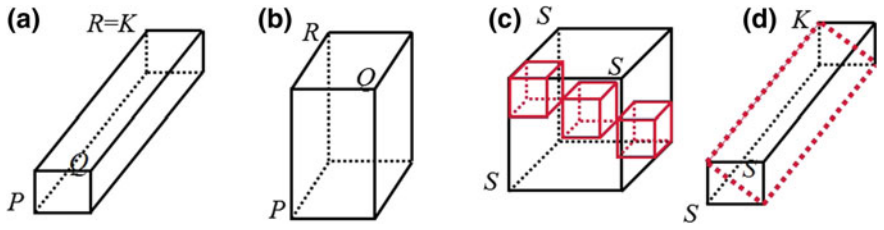

Fig. 15 Three-way SVD: Core arrays

(b) Tucker3 model & HOSVD: Full core array
(c) & (d) Candecomp/Parafac (CP) or Canonical polyadic (CP) model:
(c) Superdiagonal full core array: $S = P = Q = R$
(d) Slice diagonal extended core array: Dashed rectangle = Component matrix **C**.

6.10 Relationships Between Models

See Fig. 16.

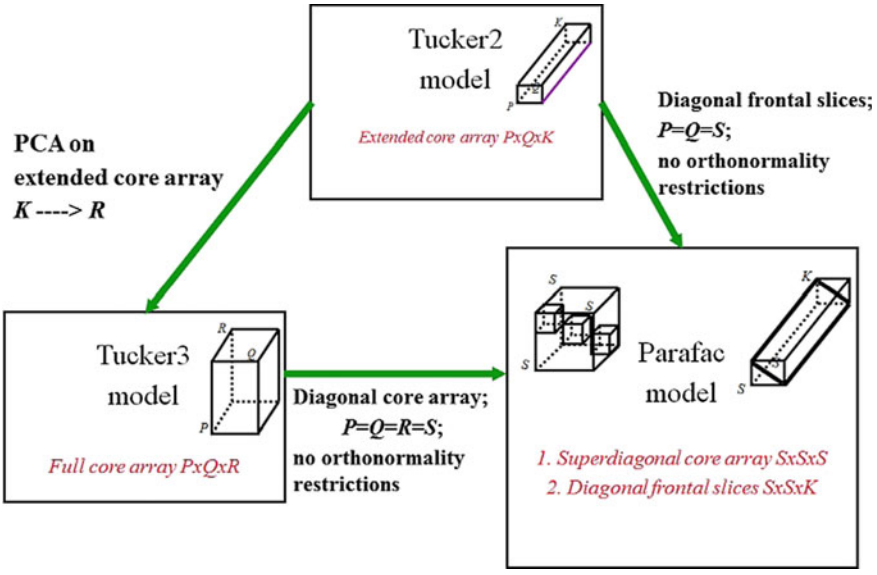

Fig. 16 Relationships between three Three-way SVD models

7 Conclusion

This overview of the multiway extension of the singular value decomposition is an attempt to provide a primarily visual introduction to give the reader an idea of what it is all about. The effect is that the information is relatively scanty and incomplete but below I have listed references to start a serious study of the subject now that I hope to have wetted the appetite for the fascinating extensions of common multivariate analysis, especially variants of principal component analysis. The extensions have been extensively used in various disciplines and references can be found in the mentioned publications. A bibliography was published in Kroonenberg [4], but applications can now be found in nearly every discipline from social and behavioural sciences to the physical sciences and even here and there in the humanities. Again one should consult the publications mentioned below and their references.

8 Treatments of the Multiway Singular Value Decomposition: Some Literature

Compact technical summary of the multiway SVD[4]

De Lathauwer, L. (2009). A survey of tensor methods. In *Proceedings of the 2009 IEEE International Symposium on Circuits and Systems (ISCAS 2009)* (pp. 2773–2776). New York City: Institute of Electrical and Electronics Engineers. (Retrieved September 5, 2019 from ftp://ftp.esat.kuleuven.be/pub/sista/delathauwer/reports/ldl-09-34.pdf).

Extended expositions of the multiway SVD

De Lathauwer, L., De Moor, B., & Vandewalle, J. (2000). A multilinear singular value decomposition. *SIAM Journal of Matrix Analysis and Applications*, *21*, 1253–1278. (Retrieved September 5, 2019 from http://www.sandia.gov/~tgkolda/tdw2004/ldl-94-31.pdf).

Leibovici, D., & Sabatier, R. (1998). A singular value decomposition of a k-way array for a principal component analysis of multiway data, PTA-k. *Linear Algebra and Its Applications, 269*, 307–329.

Leibovici, D. (2010). Spatio-temporal multiway decompositions using principal tensor analysis on k-modes: The R package PTAk. *Journal of Statistical Software, 34*, 1–34.

General books on multiway analysis (non-exhaustive list)

Cichicki, A., Zdunek, R., Phan, A. H., & Amari, S.-I. (2009). *Non-negative matrix and tensor factorizations: Applications to exploratory multiway data analysis and blind source separation*. Chicester, UK: Wiley.

[4]The publications mentioned in this section are not explicitly mentioned in the paper itself.

Coppi, R., and Bolasco, R. (Eds.) (1989). *Multiway data analysis*. Amsterdam, The Netherlands: North Holland.
Kroonenberg, P. M. (1983a). *Three-mode principal component analysis*. Leiden, The Netherlands: DSWO Press.
Kroonenberg, P. M. (2008). *Applied multiway data analysis*. Hoboken, US: Wiley.
Law, H. G., Snyder Jr., C. W., Hattie, J. A., & McDonald, R. P. (Eds.) (1984). *Research methods for multimode data analysis*. New York, NY, USA: Praeger.
Smilde, A. K, Bro, R. & Geladi, P. (2005). *Multiway analysis: Applications in the chemical sciences*. Chicester, UK: Wiley.

Specific papers and reviews on multiway analysis(non-exhaustive list)

Açar, E., & Yener, B. (2009). Unsupervised multiway data analysis: A literature survey. *IEEE Transactions on Knowledge and Data Engineering*, *21*, 6–20.
Bro, R. (1997). PARAFAC. Tutorial and applications. *Chemometrics and Intelligent Laboratory Systems*, *38*, 149–171.
Harshman, R. A., & Lundy, M. E. (1994). PARAFAC: Parallel factor analysis. *Computational Statistics & Data Analysis*, *18*, 39–72.
Kiers, H. A. L., & Van Mechelen, I. (2001). Three-way component analysis: Principles and illustrative application. *Psychological Methods*, *6*, 84–110.
Kolda, T. G., & Bader, B. W. (2009). Tensor decompositions and applications. *SIAM Review*, *51*, 455–500.
Sidiropoulos, N., De Lathauwer, L., Fu, X., Huang, K., Papalexakis, E., & Faloutsos, C. (2017). Tensor decomposition for signal processing and machine learning. *IEEE Transactions on Signal Processing*, *65*, 3551–3582.

References

1. Ceulemans, E., & Van Mechelen, I. (2005). Hierarchical classes models for three-way three-mode binary data.: Interrelations and model selection. *Psychometrika*, *70*, 4461–4480.
2. Cichocki, A., Mandic, D., Phan, A-H., Caiafa, C., Zhou, G., Zhao, Q., & De Lathauwer, L. (2015). Tensor decompositions for signal processing applications. From two-way to multiway component analysis. *IEEE Signal processing magazine*, March 2015, 146–163. (Retrieved September 5, 2019 from https://www.researchgate.net/publication/260911064_Tensor_Decompositions_for_Signal_Processing_Applications_From_Two-way_to_Multiway_Component_Analysis.
3. Kroonenberg, P. M. (1989). Singular value decompositions of interactions in three-way data analysis. In R. Coppi & S. Bolasco (Eds.), *Multiway data analysis* (pp. 169–184). Amsterdam, The Netherlands: Elsevier.
4. Kroonenberg, P. M. (1983). Annotated bibliography of three-mode factor analysis. *British Journal of Mathematical and Statistical Psychology*, *36*, 81–113.
5. Tucker, L. R. (1966). Some mathematical notes on three-mode factor analysis. *Psychometrika*, *31*, 279–311.

Seriation and Matrix Reordering Methods for Asymmetric One-Mode Two-Way Datasets

Innar Liiv and Leo Vohandu

Abstract Analyzing asymmetric datasets and finding novel insights from traces of asymmetries is a non-trivial challenge in data analysis. We propose a novel use of seriation and matrix reordering methods to find insights from asymmetric one-mode two-way datasets. This article addresses the following research questions: How to use seriation and matrix methods with asymmetric one-mode two-way matrices? What insights and patterns can be found from asymmetric structure using such an approach?

1 Introduction

Seriation is an exploratory data analysis technique to reorder objects into a sequence along a one-dimensional continuum so that it best reveals regularity and patterning among the whole series (Liiv [8]). Seriation if often called *matrix reordering*, when applied to two-way datasets. The scope of this paper is limited to asymmetric entity to entity data tables. Using Tucker's terminology (Tucker [22]) and Carroll-Arabie taxonomy (Carroll & Arabie [2]), we focus on one-mode two-way (N × N) data tables.

Definition Seriation can be defined as a combinatorial optimization problem for minimizing a loss function L on a matrix A using permutation matrices Π and Φ for reordering the rows and columns in a way that maximizes the local and global patterns (Liiv [7, p. 51]):

$$\text{argmin}_{\Pi,\Phi} L(\Pi \text{A} \Phi) \tag{1}$$

Seriation methods can be applied to analyze asymmetric one-mode two-way datasets as presented on Fig. 1. Fionn Murtagh has very eloquently called such a data analysis

I. Liiv (✉) · L. Vohandu
Tallinn University of Technology, Tallinn, Estonia
e-mail: innar.liiv@taltech.ee

L. Vohandu
e-mail: leo.vohandu@taltech.ee

T. Imaizumi et al. (eds.), *Advanced Studies in Behaviormetrics and Data Science*,
Behaviormetrics: Quantitative Approaches to Human Behavior 5,
https://doi.org/10.1007/978-981-15-2700-5_10

	O1	O2	O3	O4	O5	O6	O7	O8
O1	1	0	1	0	0	0	1	0
O2	0	1	0	0	0	0	0	1
O3	0	0	1	0	0	0	1	0
O4	1	0	0	1	0	0	1	0
O5	0	1	0	1	1	0	0	1
O6	0	1	0	0	1	1	0	1
O7	0	0	1	0	0	0	1	0
O8	0	1	0	0	0	0	0	1

Original data table

→

	O6	O5	O4	O1	O7	O3	O2	O8
O2	0	0	0	0	0	0	1	1
O8	0	0	0	0	0	0	1	1
O6	1	1	0	0	0	0	1	1
O5	0	1	1	0	0	0	1	1
O4	0	0	1	1	1	0	0	0
O1	0	0	0	1	1	1	0	0
O7	0	0	0	0	1	1	0	0
O3	0	0	0	0	1	1	0	0

After reordering

Fig. 1 An example of two-way seriation: original (left) and reordered data table (right)

approach a "non-destructive data analysis" (Murtagh [15]), emphasizing the essential property of seriation methods that no transformation of the data itself takes place, opposite to a classical transformation in clustering, where a two-mode two-way matrix (or a one-mode two-way asymmetric matrix, as we propose in this article) is converted into a one-mode two-way similarity matrix.

Okada and colleagues have argued in numerous contributions (Okada & Imaizumi [18]; Okada [16]; Okada & Imaizumi [19]; Okada [17]; Okada & Imaizumi [20]; Okada & Tsurumi [21]) that asymmetries in the data should not be regarded as noise, or be eliminated by averaging corresponding elements. Analyzing asymmetric datasets and finding novel insights from traces of asymmetries is a non-trivial challenge in data analysis.

The motivation of this paper is to demonstrate, using the same *cars dataset* as Okada and colleagues (Harshman, Green, Wind, & Lundy [3]; Okada & Imaizumi [18]), how to apply seriation and matrix reordering methods to asymmetric one-mode two-way matrices and to present a discussion on which insights and patterns can be found from asymmetric structure using such an approach.

This section presented the general introduction to seriation and highlighted the main motivations for undertaking the research presented in this paper. The rest of the paper is organized as follows: We will describe datasets used in this paper (in Sect. 2) and explain methods proposed to analyze the data (in Sect. 3). Experimental design and results are presented in Sect. 4, followed by a discussion and conclusions.

2 Data

Harshman et al. [3] presented a car trade-in data (see Table 1, hereafter referred to as *CARS1 dataset*) for a large sample of U.S. buyers of new (1979 model) cars, where recent buyers of news cars were asked to "indicate both the newly purchased model and the old model (if any) disposed of at the time of purchase". Such a dataset is inherently asymmetric since people tend to switch either to similar or better models.

Each cell in Table 1 presents the number of car segments (in rows) traded in, when car segments in columns were purchased. Abbreviations of car segments (i.e. row and column headers in a data table) are presented in Table 2. Okada and Imaizumi [18]

Table 1 *CARS1*. Original car switching data Harshman et al. [3]

	subd	subc	subi	smad	smac	smai	coml	comm	comi	midd	midi	mids	stdl	stdm	luxd	luxi
subd	23272	1487	10501	18944	49	2319	12349	4061	545	12622	481	16329	4253	2370	949	127
subc	3254	1114	3014	2656	23	551	959	894	223	1672	223	2012	926	540	246	37
subi	11344	1214	25986	9803	47	5400	3262	1353	2257	5195	1307	8347	2308	1611	1071	288
smad	11740	1192	11149	38434	69	4880	6047	2335	931	8503	1177	23898	3238	4422	4114	410
smac	47	6	0	117	4	0	0	49	0	110	0	10	0	0	0	0
smai	1772	217	3622	3453	16	5249	1113	313	738	1631	1070	4937	338	901	1310	459
coml	18441	1866	12154	15237	65	1626	27137	6182	835	20909	566	15342	9728	3610	910	170
comm	10359	693	5841	6368	40	610	6223	7469	564	9620	435	9731	3601	5498	764	85
comi	2613	481	6981	1853	10	1023	1305	632	1536	2738	1005	990	454	991	543	127
midd	33012	2323	22029	29623	110	4193	20997	12155	2533	53002	2140	61350	28006	33913	9808	706
midi	1293	114	2844	1242	5	772	1507	452	565	3820	3059	2357	589	1052	871	595
mids	12981	981	8271	18908	97	3444	3693	1748	935	11551	1314	56025	10959	18688	12541	578
stdl	27816	1890	12980	15993	34	1323	18928	5836	1182	28324	938	37380	67964	28881	6585	300
stdm	17293	1291	11243	11457	41	1862	7731	6178	1288	20942	1048	30189	15318	81808	21974	548
luxd	3733	430	4647	5913	6	622	1652	1044	476	3068	829	8571	2964	9187	63509	1585
luxi	105	40	997	603	0	341	75	55	176	151	589	758	158	756	1234	3124

Table 2 Abbreviations of car segments (i.e. row and column headers in datasets)

Abbr	Description
1 SUBD	subcompact/domestic
2 SUBC	subcompact/captive imports
3 SUBI	subcompact/imports
4 SMAD	small specialty/domestic
5 SMAC	small specialty/captive imports
6 SMAI	small specialty/imports
7 COML	low price compact
8 COMM	medium price compact
9 COMI	import compact
10 MIDD	midsize domestic
11 MIDI	midsize imports
12 MIDS	midsize specialty
13 STDL	low price standard
14 STDM	medium price standard
15 LUXD	luxury domestic
16 LUXI	luxury imports

argued that Harshman et al. [3] dataset represents "large differences in the size of frequencies which reflect the large differences in market share", which "should be removed in order to distinctly unveil the factors which control the car switches". A dataset (hereafter referred to as *CARS2 dataset*), where Okada and Imaizumi [18] have adjusted the car switching data by multiplying each row and column by rescaling coefficients, is presented in Table 3. The paper's experimental design retains a neutral stance whether an adjustment is necessary or helps to find insights and, therefore, uses both datasets for experiments.

All necessary data preprocessing steps (e.g. binarization, discretization) to conform with input requirements of specific seriation methods are described in context together with methods and experiments.

3 Methods

We propose to use seriation and matrix reordering methods to find insights from asymmetric one-mode two-way datasets. However, there is no universal loss function to be minimized, let alone for asymmetric datasets, where as far as authors are aware, seriation methods have not been thoroughly studied. Our experiments are based on the idea, that seriation methods can be applied to analyze asymmetric one-mode two-way datasets as if they were two-mode two-way datasets while continuing to keep the information about entities actually belonging to one class.

Table 3 *CARS2*. Adjusted car switching data Okada and Imaizumi [18]

	subd	subc	subi	smad	smac	smai	coml	comm	comi	midd	midi	mids	stdl	stdm	luxd	luxi
subd	10291	4634	5014	7907	5931	4087	7342	4253	1404	3215	1156	5429	2042	1032	903	797
subc	10140	24462	10141	7791	19619	6842	4018	6598	4049	3001	3776	4714	3133	1657	1650	1637
subi	5416	4085	13396	4406	6143	10275	2094	1530	6280	1429	3391	2997	1196	758	1100	1952
smad	4887	3497	5011	15061	7863	8095	3384	2302	2258	2039	2662	7480	1463	1813	3685	2423
smac	5689	5118	0	13332	132540	0	0	14048	0	7669	0	910	0	0	0	0
smai	3123	2695	6892	5728	7718	36861	2637	1306	7578	1655	10245	6542	647	1564	4968	11482
coml	10963	7817	7802	8527	10578	3852	21689	8705	2955	7159	1828	6858	6279	2114	1164	1435
comm	10850	5115	6605	6279	11468	2546	8762	18528	3442	5803	2475	7663	4095	5672	1722	1264
comi	6733	8734	19423	4495	7054	10505	4521	3857	23064	4064	14070	1918	1270	2515	3011	4646
midd	8408	4169	6058	7102	7669	4256	7189	7332	3759	7775	2961	11749	7744	8508	5376	2553
midi	3107	1930	7378	2809	3288	7391	4868	2572	7910	5286	39931	4258	1536	2490	4503	20294
mids	4316	2298	2969	5918	8828	4563	1651	1377	1812	2212	2374	14006	3956	6120	8973	2728
stdl	13355	6394	6729	7201	4468	2531	12217	6636	3307	7832	2447	13494	35429	13658	6804	2045
stdm	7532	3963	5287	4698	4888	3232	4527	6373	3269	5254	2480	9887	7244	35098	20596	3388
luxd	3552	2883	4775	5297	1563	2359	2113	2353	2639	1681	4286	6133	3062	8611	130051	21411
luxi	659	1769	6758	3563	0	8530	633	818	6438	546	20089	3578	1077	4674	16670	278391

Therefore, this paper proposes two sets of experiments to explore different aspects of both versions of car switching data described in Sect. 2: exploratory data analysis and algorithmic experiments. The goal of the exploratory data analysis set of experiments is to compare multiple algorithms producing different permutations for rows and columns using a Visual Matrix Explorer (VME) open source tool (Liiv, Opik, Ubi, & Stasko [9]), which allows us to calculate, visualize and compare 12 different permutations of *CARS1* (see Fig. 2) and *CARS2* datasets (see Fig. 3).

Since most algorithms implemented in that tool assume the input matrix to be in a binary format, we have binarized (discretized into 2 bins) both input datasets. Inspired by Bertin's [1] approach, we set all values having an average or higher value to be "1" and others to be "0". We did try with multiple other approaches to binarization (e.g. median and 75th or 80th percentile), without any significant added value.

Secondly, we propose an algorithm, which is based on Vohandu "minus technique" reordering method (Vohandu [23–25]) and using a monotone systems heuristic (Mullat [12–14]). Our proposal for asymmetric datasets is based on the idea that internal weights will be calculated at every iterative step of the algorithm and the comparison of those weights between rows and columns can give us additional insights about symmetries and asymmetries in the dataset and their extent (e.g. perhaps only some part of the matrix has asymmetries, while the other part is symmetric). The algorithm assumes the input data to be continuous (e.g. frequencies, counts).

Algorithm 1 Seriation method for asymmetric one-mode two-way datasets

1: Discretize object's attributes and re-label them according to their frequency ranking to make them comparable across attributes.
2: Enumeration of the attribute labels for each attribute.
3: Replacement of attribute labels with the actual frequency of that label within that attribute.
4: Conformity weight for objects is calculated using the sum of attribute value frequencies.
5: Print out row with minimal conformity and its weight.
6: Remove a row with minimal conformity weight.
7: Return to Step 2, unless no rows left.
8: Objects are reordered in the order of removals.
9: Enumeration of the attribute labels for each object.
10: Replacement of attribute labels with the actual frequency of that label within that object.
11: Conformity weight for attributes is calculated using the sum of attribute value frequencies.
12: Print out column with minimal conformity and its weight.
13: Remove a column with minimal conformity weight.
14: Return to Step 9, unless no columns left.
15: Columns are reordered in the order of removals.
16: Compare weights at algorithm iterations between rows and columns.

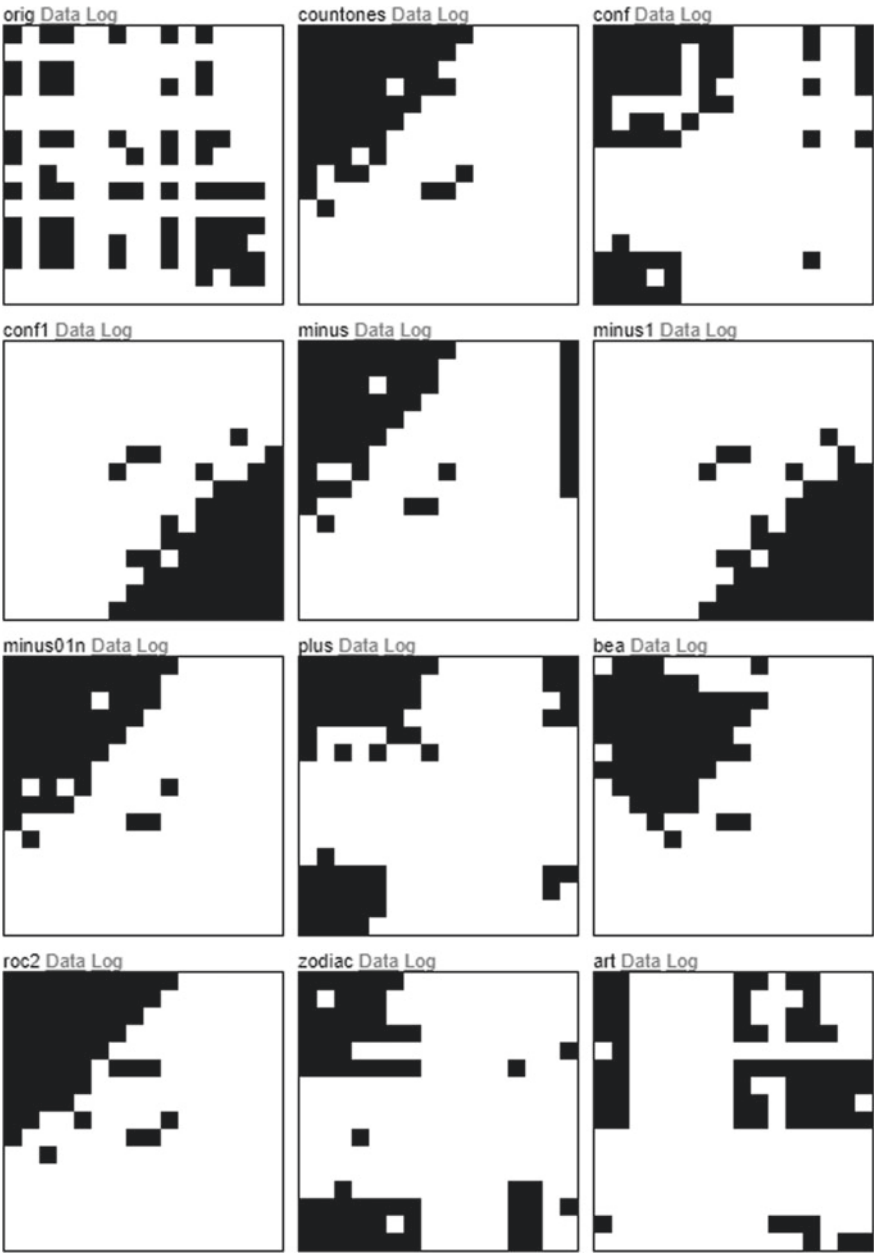

Fig. 2 CARS1 dataset rendered in different permutations using Visual Matrix Explorer

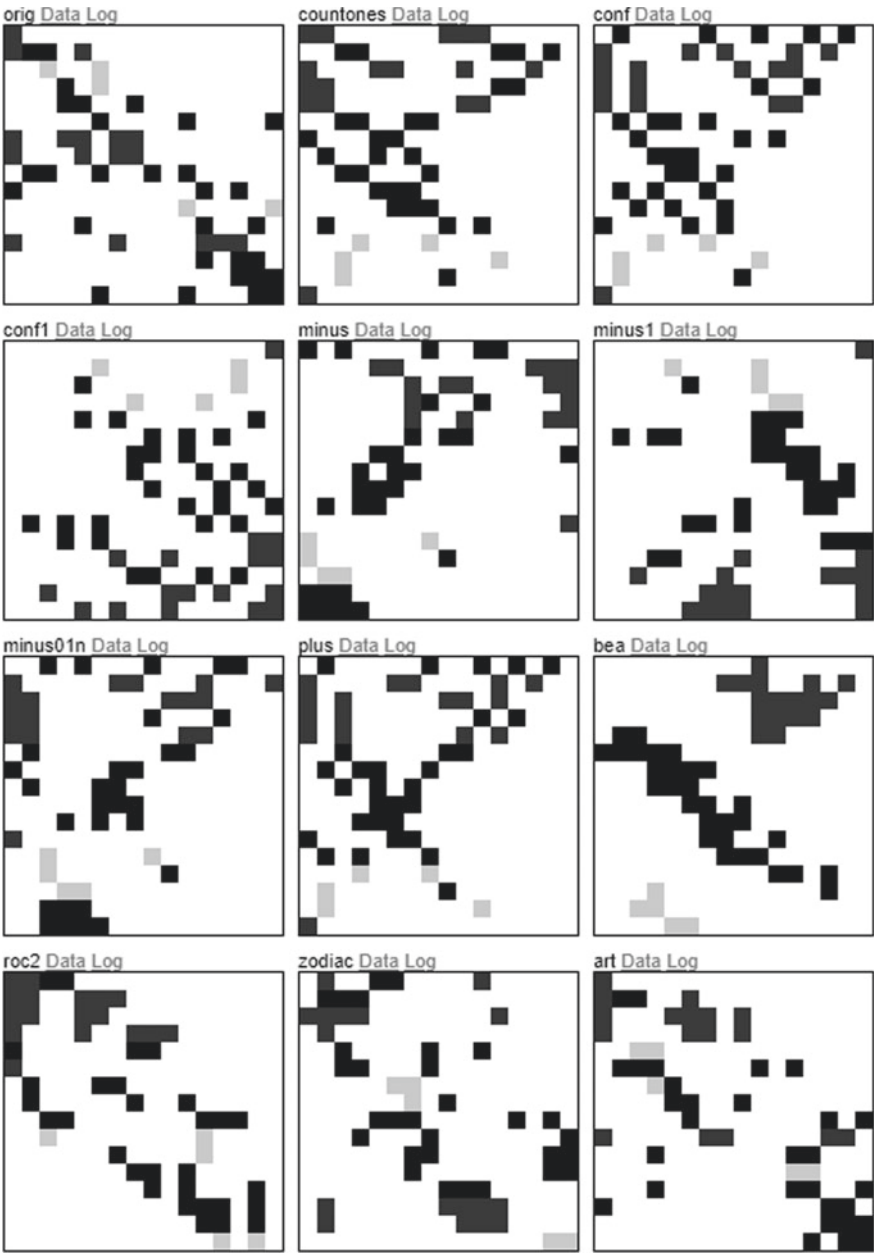

Fig. 3 CARS2 dataset rendered in different permutations using Visual Matrix Explorer

4 Experiments

In our exploratory data analysis phase we used the Visual Matrix Explorer (Liiv et al. [9]) tool to explore the original car switching dataset (Harshman et al. [3]) and adjusted dataset by Okada and Imaizumi [18]. Experiments with the following permutations were presented for both datasets:

- *orig*—binarization (average value equal or greater over all cells) of the dataset;
- *countones*—VME's fast heuristic (Liiv et al. [9]), based on sorting by frequencies of "ones";
- *conf*—sorting by conformity weight; *minus*—minus technique, and *plus*—plus technique (Vohandu [23–25])—algorithms using the monotone systems meta-heuristic by Mullat [12–14];
- *bea*—McCormick's Bond Energy Algorithm (McCormick, Deutsch, Martin, & Schweitzer [10]; McCormick, Schweitzer, & White [11]);
- *roc2*—an enhanced rank order clustering by King and Nakornchai [5]
- *art*—Carpenter-Grossberg neural network based clustering (Kusiak & Chung [6]; Kaparti & Suresh [4]).

The results of exploratory data analysis set of experiments resulting different permutations is presented on Fig. 2 (for *CARS1*) and Fig. 3 (for *CARS2*). The results of the *Bond Energy Algorithm ("bea")* McCormick et al. [11] stand out to be most informative and compact representation of relationship in both datasets. It is evident from the original dataset on Fig. 4, and even more clearly from the adjusted dataset on Fig. 5 that the matrix is not symmetric and it is not possible to find a symmetric permutation.

The reordering result of the adjusted dataset (*CARS2*, Fig. 5) brings out three distinct groups (we have highlighted them as black, dark grey, light grey in the Visual Matrix Explorer tool to highlight same data in different permutations), where two groups away from centre give additional insights about different groups of

	coml	midd	subd	mids	subi	smad	stdl	stdm	luxd	comm	luxi	midi	comi	smai	smac	subc
comm	0	1	1	1	0	0	0	0	0	1	0	0	0	0	0	0
subd	1	1	1	1	1	1	0	0	0	0	0	0	0	0	0	0
midd	1	1	1	1	1	1	1	1	1	1	0	0	0	0	0	0
stdm	1	1	1	1	1	1	1	1	1	0	0	0	0	0	0	0
stdl	1	1	1	1	1	1	1	1	0	0	0	0	0	0	0	0
mids	0	1	1	1	1	1	1	1	1	0	0	0	0	0	0	0
coml	1	1	1	1	1	1	1	0	0	0	0	0	0	0	0	0
smad	0	1	1	1	1	1	0	0	0	0	0	0	0	0	0	0
subi	0	0	1	1	1	1	0	0	0	0	0	0	0	0	0	0
luxd	0	0	0	1	0	0	0	1	1	0	0	0	0	0	0	0
comi	0	0	0	0	1	0	0	0	0	0	0	0	0	0	0	0
luxi	0	0	0	0	0	0	0	0	0	0	0	0	0	0	0	0
midi	0	0	0	0	0	0	0	0	0	0	0	0	0	0	0	0
smai	0	0	0	0	0	0	0	0	0	0	0	0	0	0	0	0
smac	0	0	0	0	0	0	0	0	0	0	0	0	0	0	0	0
subc	0	0	0	0	0	0	0	0	0	0	0	0	0	0	0	0

Fig. 4 Bond energy algorithm result for CARS1 dataset

	comi	subc	subi	smai	midi	luxi	luxd	mids	stdm	subd	smac	comm	coml	smad	stdl	midd
subd	0	0	0	0	0	0	0	0	0	1	0	0	0	0	0	0
stdl	0	0	0	0	0	0	0	1	1	1	0	0	1	0	1	0
coml	0	0	0	0	0	0	0	0	0	1	1	1	1	1	0	0
comm	0	0	0	0	0	0	0	0	0	1	1	1	1	0	0	0
subc	0	1	1	0	0	0	0	0	0	1	1	0	0	0	0	0
comi	1	1	1	1	1	0	0	0	0	0	0	0	0	0	0	0
luxi	0	0	0	1	1	1	1	0	0	0	0	0	0	0	0	0
smai	0	0	0	1	1	1	0	0	0	0	0	0	0	0	0	0
luxd	0	0	0	0	0	1	1	0	1	0	0	0	0	0	0	0
stdm	0	0	0	0	0	0	1	1	1	0	0	0	0	0	0	0
mids	0	0	0	0	0	0	1	1	0	0	1	0	0	0	0	0
midd	0	0	0	0	0	0	0	1	1	1	0	0	0	0	0	0
smac	0	0	0	0	0	0	0	0	0	0	1	1	0	1	0	0
smad	0	0	0	1	0	0	0	0	0	0	0	0	0	1	0	0
subi	0	0	1	1	0	0	0	0	0	0	0	0	0	0	0	0
midi	0	0	0	0	1	1	0	0	0	0	0	0	0	0	0	0

Fig. 5 Bond energy algorithm result for CARS2 dataset

	mids	subi	subd	smad	midd	coml	stdl	stdm	luxd	comm	subc	smac	smai	comi	midi	luxi
midd	1	1	1	1	1	1	1	1	1	1	0	0	0	0	0	0
stdm	1	1	1	1	1	1	1	1	1	0	0	0	0	0	0	0
mids	1	1	1	1	1	0	1	1	1	0	0	0	0	0	0	0
stdl	1	1	1	1	1	1	1	1	0	0	0	0	0	0	0	0
coml	1	1	1	1	1	1	1	0	0	0	0	0	0	0	0	0
subd	1	1	1	1	1	1	0	0	0	0	0	0	0	0	0	0
smad	1	1	1	1	1	0	0	0	0	0	0	0	0	0	0	0
comm	1	0	1	0	1	0	0	0	0	1	0	0	0	0	0	0
subi	1	1	1	1	0	0	0	0	0	0	0	0	0	0	0	0
luxd	1	0	0	0	0	0	0	1	1	0	0	0	0	0	0	0
comi	0	1	0	0	0	0	0	0	0	0	0	0	0	0	0	0
subc	0	0	0	0	0	0	0	0	0	0	0	0	0	0	0	0
smac	0	0	0	0	0	0	0	0	0	0	0	0	0	0	0	0
smai	0	0	0	0	0	0	0	0	0	0	0	0	0	0	0	0
midi	0	0	0	0	0	0	0	0	0	0	0	0	0	0	0	0
luxi	0	0	0	0	0	0	0	0	0	0	0	0	0	0	0	0

Fig. 6 Minus technique result for CARS1 dataset

asymmetries in the dataset (e.g. “SUBI” in the extreme left of the bottom group and “STDL” in the extreme right of the top group).

For comparison with an alternative permutation and for consistency reasons with the second set of experiments, we have also presented the result of a minus technique using the same datasets with the same binarization (see Figs. 6 and 7). Again, it is possible to see from Fig. 6 that the dataset is not symmetric. Additionally, it highlights some structural anomalies (empty cells within otherwise consistent blocks, e.g. COMM-SUBI, COMM-SMAD, and MIDS-COML).

Similarly to bond energy algorithm, the results are much more interesting using the adjusted dataset (see Fig. 7), which finds multiple asymmetric subgroups and identifies “STDL” objects as an outlier in the extreme right position (i.e. the last iteration of the algorithm) within columns, while having a non-outlier position within rows.

	subd	smac	smai	luxi	midi	luxd	mids	stdm	subi	smad	comm	coml	subc	comi	midd	stdl
comi	0	0	1	0	1	0	0	0	1	0	0	0	1	1	0	0
stdl	1	0	0	0	0	0	1	1	0	0	0	1	0	0	0	1
coml	1	1	0	0	0	0	0	0	0	1	1	1	0	0	0	0
subc	1	1	0	0	0	0	0	0	1	0	0	0	1	0	0	0
comm	1	1	0	0	0	0	0	0	0	0	1	1	0	0	0	0
smac	0	1	0	0	0	0	0	0	0	1	1	0	0	0	0	0
midd	1	0	0	0	0	0	1	1	0	0	0	0	0	0	0	0
mids	0	1	0	0	0	1	1	0	0	0	0	0	0	0	0	0
stdm	0	0	0	0	0	1	1	1	0	0	0	0	0	0	0	0
luxd	0	0	0	1	0	1	0	1	0	0	0	0	0	0	0	0
subd	1	0	0	0	0	0	0	0	0	0	0	0	0	0	0	0
subi	0	0	1	0	0	0	0	0	1	0	0	0	0	0	0	0
smad	0	0	1	0	0	0	0	0	0	1	0	0	0	0	0	0
midi	0	0	0	1	1	0	0	0	0	0	0	0	0	0	0	0
smai	0	0	1	1	1	0	0	0	0	0	0	0	0	0	0	0
luxi	0	0	1	1	1	1	0	0	0	0	0	0	0	0	0	0

Fig. 7 Minus technique result for CARS2 dataset

	subc	comi	midi	smac	subi	smai	subd	smad	mids	coml	luxi	comm	midd	luxd	stdl	stdm	
midd	2	3	4	3	3	3	2	3	2	2	2	2	3	0	2	3	38
stdm	0	2	1	1	1	1	3	2	3	1	0	1	1	2	1	2	57
stdl	2	2	1	1	1	1	2	1	4	2	0	1	2	0	3	1	54
subd	4	0	0	2	1	4	4	1	1	4	0	4	1	0	0	0	80
coml	2	0	0	2	1	1	3	2	1	3	0	1	1	0	0	0	70
mids	0	0	2	3	2	3	1	1	2	0	0	0	1	0	0	1	73
smad	0	0	1	4	1	2	1	4	1	1	0	0	0	0	0	0	79
subi	0	3	2	2	3	2	1	2	0	0	0	0	0	0	0	0	78
comm	3	0	0	1	2	0	1	0	0	1	0	3	0	0	0	0	76
comi	3	4	1	0	2	0	0	0	0	0	0	0	0	0	0	0	85
luxd	1	1	1	0	0	0	0	0	0	0	3	0	0	1	0	0	77
subc	0	1	0	1	0	0	0	0	0	0	0	0	0	0	0	0	66
smai	1	0	1	0	0	2	0	0	0	0	0	0	0	0	0	0	55
midi	1	0	3	0	0	0	0	0	0	0	0	0	0	0	0	0	43
luxi	1	1	0	0	0	0	0	0	0	0	1	0	0	0	0	0	31
smac	1	1	0	0	0	0	0	0	0	0	0	0	0	0	0	0	16
	75	88	92	106	102	97	93	85	82	73	67	58	48	40	28	16	

Fig. 8 Seriation of CARS1 dataset, column-oriented discretization

After the exploratory step, in the second set of experiments, we apply the seriation algorithm proposed in Sect. 3 directly to *CARS1* and *CARS2* datasets. A more detailed patterning, together with row and column weights in footer columns and rows is calculated as a result (i.e. Figs. 8, 10, 12, 14).

Since weights printed or stored at algorithm's steps 5 and 12 were assumed to be indicating asymmetries in datasets, we have presented row and column weights as additional line graphs after reordered matrices for detailed analysis (i.e. Figs. 9, 11, 13, 15).

Since step 1 of the proposed algorithm in Sect. 3 did not specify the orientation of discretization (either over rows or columns), we experimented with both, row-oriented and column-oriented discretizations for both datasets.

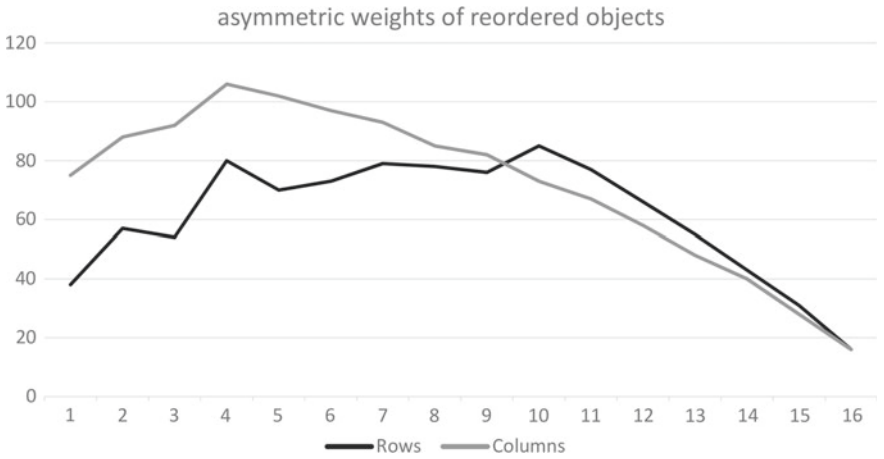

Fig. 9 Asymmetric weights of reordered objects of CARS1 dataset, column-oriented discretization

	midi	subc	smai	coml	comm	midd	luxi	stdl	subi	subd	luxd	smac	comi	smad	stdm	mids	
mids	3	3	2	1	1	2	1	1	1	3	0	0	0	2	1	2	69
subd	0	2	1	2	1	1	0	1	3	2	0	2	1	1	1	1	70
midd	2	4	1	2	1	2	0	1	0	1	0	1	1	1	1	1	62
smad	0	2	3	1	3	1	0	2	1	2	0	1	1	3	0	1	60
subi	3	2	3	1	2	3	1	0	2	1	0	0	2	1	0	0	68
coml	0	1	1	4	2	3	0	2	0	1	0	0	0	0	0	0	94
stdm	0	0	0	0	2	1	1	1	0	0	0	0	0	0	2	1	90
luxd	0	0	1	0	0	0	1	0	0	0	1	0	0	0	1	1	86
stdl	1	1	0	3	4	1	0	3	0	0	0	0	0	0	0	0	88
comm	1	1	0	3	3	0	0	0	0	0	0	2	0	0	0	0	82
smai	0	0	2	0	0	0	0	0	1	0	0	0	0	0	0	0	78
midi	2	0	1	0	0	0	0	0	0	0	0	0	0	0	0	0	69
comi	1	0	0	0	0	0	0	0	0	0	0	0	1	0	0	0	59
luxi	1	0	0	0	0	0	2	0	0	0	0	0	0	0	0	0	45
subc	1	1	0	0	0	0	0	0	0	0	0	0	0	0	0	0	31
smac	1	0	0	0	0	0	0	0	0	0	0	0	0	0	0	0	16
	72	110	118	117	108	102	97	92	84	76	70	60	49	39	29	16	

Fig. 10 Seriation of CARS1 dataset, row-oriented discretization

Reordering results of column-oriented discretized datasets are presented in Fig. 8 (*CARS1*) and Fig. 12 (*CARS2*) and row-oriented in Fig. 10 (*CARS1*) and Fig. 14 (*CARS2*).

Interestingly, differences in weights are more visible with the original dataset, whereas with column-oriented discretization, both datasets indicate non-monotonicity in the second part of the datasets (elements 9–16, Figs. 9 and 15, element order is derived from algorithm's steps 8 and 15).

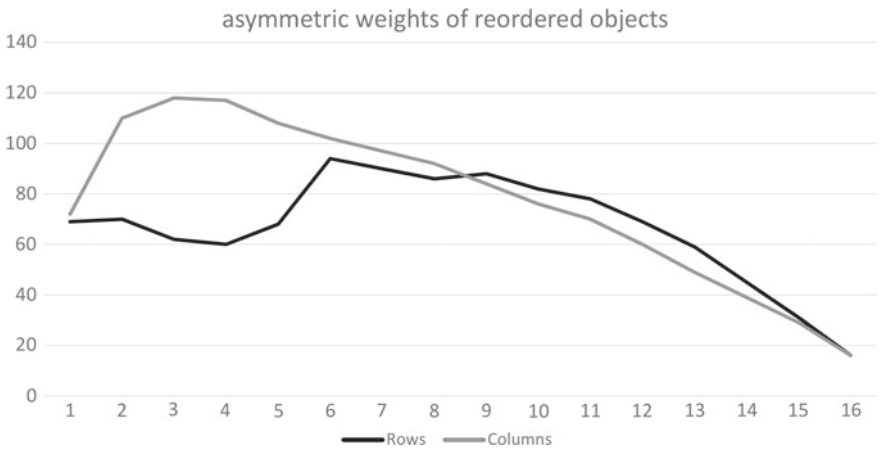

Fig. 11 Asymmetric weights of reordered objects of CARS1 dataset, row-oriented discretization

	mids	midd	subd	smad	coml	comm	subi	smai	comi	midi	subc	stdm	stdl	smac	luxi	luxd	
comi	2	4	4	1	1	0	3	1	2	1	1	0	0	0	0	0	107
stdl	3	1	1	0	2	1	0	0	0	0	1	1	2	0	0	0	113
stdm	4	3	4	1	1	1	0	0	0	0	0	2	1	0	0	0	109
coml	1	1	1	2	3	4	2	0	0	0	1	0	0	0	0	0	103
midd	3	1	3	0	1	1	0	0	0	0	0	1	1	0	0	0	96
smac	2	1	0	3	0	3	1	0	0	0	0	0	0	1	0	0	94
subc	0	0	3	2	0	1	2	0	0	0	2	0	0	0	0	0	88
comm	1	3	1	0	2	2	0	0	0	0	0	0	0	0	0	0	85
luxd	0	2	0	0	0	0	0	0	0	0	0	1	0	0	0	1	80
subd	0	0	3	2	1	0	0	0	0	0	0	0	0	0	0	0	72
mids	3	0	0	0	0	0	1	0	0	0	0	0	0	0	0	0	61
smad	1	0	0	3	0	0	0	1	0	0	0	0	0	0	0	0	55
smai	1	2	2	0	0	0	0	2	1	1	0	0	0	0	0	0	47
subi	2	2	0	1	0	0	4	1	1	0	0	0	0	0	0	0	37
midi	0	3	2	1	1	0	0	1	1	3	0	0	0	0	0	0	28
luxi	0	2	2	1	0	0	0	1	1	2	0	0	0	0	1	0	16
	77	79	74	90	96	89	88	90	83	77	69	64	52	44	30	16	

Fig. 12 Seriation of CARS2 dataset, column-oriented discretization

5 Discussion

The main strength of seriation and matrix reordering methods is that they do not transform, compact or eliminate any part of the dataset, which also means that they do not eliminate asymmetries in the data, if such structural properties happen to exist. Second differentiating strength is the ability to reveal patterns at multiple information levels - from local associations, relations and trends to global. In the case of asymmetric data tables, it enables the researcher to study asymmetry from multiple levels and aspects - local and object level asymmetry, asymmetric subgroups

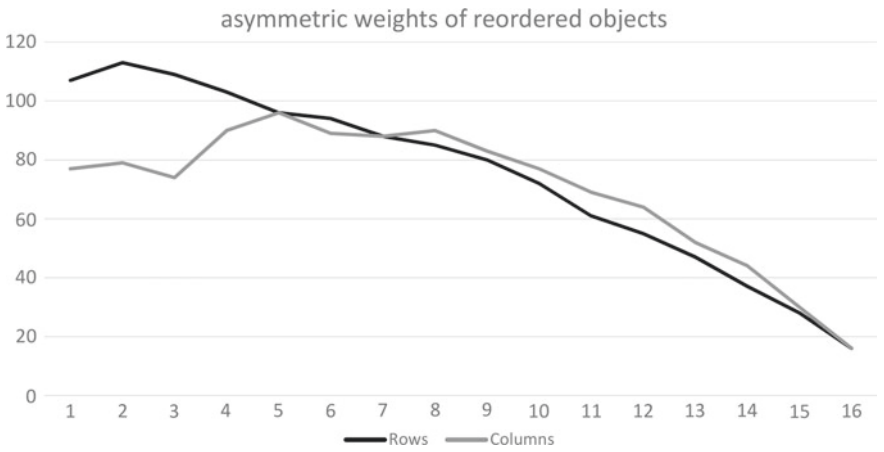

Fig. 13 Asymmetric weights of reordered objects of CARS2 dataset, column-oriented discretization

	subd	comm	midd	coml	mids	subi	subc	comi	smad	stdl	stdm	smai	smac	luxd	midi	luxi	
smac	1	2	0	2	3	2	3	1	1	0	0	0	1	0	0	0	107
subd	4	2	3	2	1	1	1	1	2	1	0	0	0	0	0	0	108
smai	2	0	1	1	1	4	1	2	1	0	0	2	0	0	0	0	107
mids	1	1	4	0	4	0	0	0	1	1	2	0	0	0	0	0	108
subi	1	1	2	0	0	3	1	3	2	0	0	0	0	0	0	0	103
smad	3	1	0	0	1	1	1	0	3	0	0	0	0	0	0	0	99
subc	1	1	1	0	0	1	2	1	0	0	0	0	0	0	0	0	92
midi	0	0	1	1	0	1	0	2	0	0	0	1	0	0	2	0	85
luxi	0	0	1	1	0	0	0	0	0	0	0	1	0	0	1	1	78
luxd	0	0	2	1	2	0	0	0	0	0	1	0	0	1	0	0	71
comi	0	0	1	1	0	2	0	3	0	0	0	0	0	0	0	0	63
stdm	0	1	3	1	1	0	0	0	0	1	3	0	0	0	0	0	55
coml	3	2	0	3	0	0	0	0	0	1	0	0	0	0	0	0	50
stdl	0	0	0	0	1	0	0	0	0	2	0	0	0	0	0	0	39
comm	2	3	0	0	0	0	1	0	0	0	0	0	0	0	0	0	30
midd	2	1	0	0	0	0	0	0	0	0	0	0	0	0	0	0	16
	94	86	96	96	96	90	84	80	77	73	75	68	57	43	31	16	

Fig. 14 Seriation of CARS2 dataset, row-oriented discretization

in the data set and the entire dataset being unbalanced and tilting to some specific direction.

When there are some asymmetries in a data table, we often consider it automatically an entirely asymmetric data table. However, asymmetry can even be partial: some parts of the data table or structure are asymmetric, while others can be symmetric. We have presented row and column weights together with the results of our proposed method. In case of symmetric data, those lines in aforementioned line graphs would either be aligned or at least follow a similar pattern.

This paper proposed two sets of experiments to explore different aspects of both datasets: a preliminary visual exploratory data analysis to understand the context

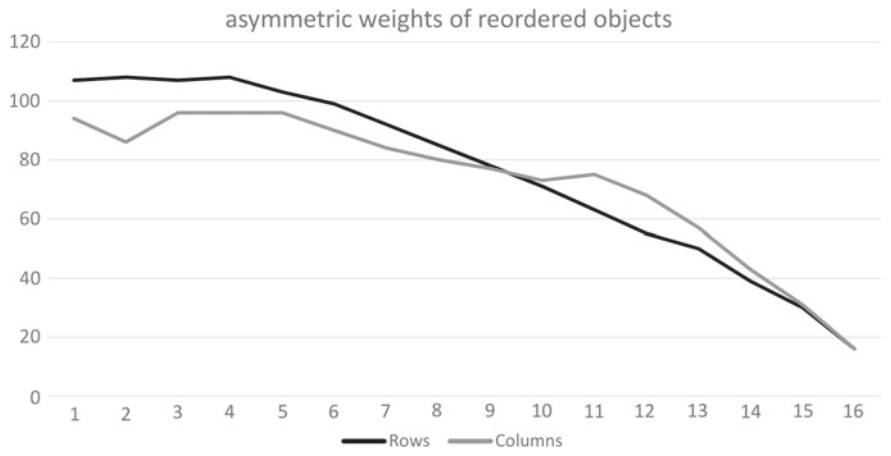

Fig. 15 Asymmetric weights of reordered objects of CARS2 dataset, column-oriented discretization

and general patterning, and secondly, algorithmic experiments for more in-depth analysis of selected asymmetric datasets. The results of the Bond Energy Algorithm McCormick et al. [11] stood out from Figs. 2 and 3 as most informative to present seriation result's ability to identify and visualize asymmetries. We also conducted experiments with a proposed seriation method capable of analyzing *CARS1* and *CARS2* datasets directly. The proposed algorithm had an additional strength compared to other seriation methods: in addition to finding a new permutation of rows and columns, it also extracted weights reflecting datasets' structural properties at every iteration. One application of such weights is to characterize and identify asymmetries in the dataset. Another useful property of presented weights is the ability to identify potential cluster boundaries within seriation results. When we observe weights in the reverse order, all reversals in the direction of weight changes indicate a potential cluster boundary or other structural change in the dataset.

Different seriation algorithms can reveal different structural properties and patterns. For example, the results of the Bond Energy Algorithm of *CARS2* dataset (Fig. 5) demonstrated the asymmetry of the dataset and how relationships are clustered into three distinct groups. A different perspective with minus technique (Fig. 7) allowed us to see even more fine-grained asymmetric subgroups and divide those former three distinct groups into smaller ones. The result in Fig. 7 even indicated multiple "incomplete" clusters, where only few relationships are missing (or are below threshold) from a block cluster, e.g.:

- {STDL, COML, SUBC, COMM} X {SUBD, SMAC};
- {MIDD, MIDS, STDM, LUXD} X {LUXD, MIDS, STDM};
- {SMAI, LUXI} X {SMAI, LUXI, MIDI, LUXD}.

Often, such irregular elements in a larger surrounding subgroup are interesting outliers. Similarly, Fig. 6 highlights several potential structural anomalies (empty cells

within otherwise consistent blocks, e.g. COMM-SUBI, COMM-SMAD and MIDS-COML).

Our experiments also confirmed that data preprocessing has an enormous impact to seriation results. Both sets of experiments highlighted differences between the original dataset (*CARS1*) and adjusted car switching data (*CARS2*). Besides initial transformations and normalizations, further processing (e.g. the choice of the threshold of other strategy for binarization, the choice of orientation for discretization) to match the dataset with required input for algorithms has similarly a strong impact to results.

6 Conclusions

Analyzing asymmetric datasets and finding novel insights from different types and extents of asymmetries is a non-trivial challenge in data analysis. In this paper, we demonstrated how to apply seriation and matrix reordering methods to asymmetric one-mode two-way matrices and presented a discussion on which insights and patterns can be found from asymmetric data using the above-mentioned approach.

We agree with Okada and colleagues (Okada & Imaizumi [18]; Okada [16]; Okada & Imaizumi [19]; Okada [17]; Okada & Imaizumi [20]; Okada & Tsurumi [21]) that asymmetries in the data should not be regarded as noise, or be eliminated by averaging corresponding elements. To put it modestly, out-of-the-box data analytics software and developer frameworks covering mainstream data mining methods do not address the aspect of asymmetries in datasets sufficiently. There is an interesting research avenue to further research asymmetric data analysis at every process step of the knowledge discovery—from data preprocessing choices to similarity measures, to different representations and visualizations.

Acknowledgements The authors would like to thank Tadashi Imaizumi, Atsuho Nakayama and Satoru Yokoyama for their support and patience while preparing this collection.

References

1. Bertin, J. (1967). *Sémiologie graphique: les diagrammes, les résaux, les cartes*. Paris: Mouton.
2. Carroll, J. D., & Arabie, P. (1980). Multidimensional scaling. *Annual Review of Psychology*, *31*, 607–649.
3. Harshman, R. A., Green, P. E., Wind, Y., & Lundy, M. E. (1982). A model for the analysis of asymmetric data in marketing research. *Marketing Science*, *1*(2), 205–242.
4. Kaparthi, S., & Suresh, N. C. (1992). Machine-component cell formation in group technology: A neural network approach. *International Journal of Production Research*, *30*(6), 1353–1367.
5. King, J., & Nakornchai, V. (1982). Machine-component group formation in group technology: Review and extension. *International Journal of Production Research*, *20*(2), 117–133.
6. Kusiak, A., & Chung, Y. K. (1991). GT/ART: Using neural network to form machine cells. *Manufacturing Review*, *4*(4), 293–301.

7. Liiv, I. (2008). *Pattern discovery using seriation and matrix reordering: A unified view, extensions and an application to inventory management*. Tallinn: TUT Press.
8. Liiv, I. (2010). Seriation and matrix reordering methods: An historical overview. *Statistical Analysis and Data Mining: The ASA Data Science Journal*, *3*(2), 70–91.
9. Liiv, I., Opik, R., Ubi, J., & Stasko, J. (2012). Visual matrix explorer for collaborative seriation. *Wiley Interdisciplinary Reviews: Computational Statistics*, *4*(1), 85–97.
10. McCormick, W. T., Deutsch, S. B., Martin, J. J., & Schweitzer, P. J. (1969). *Identification of data structures and relationships by matrix reordering techniques (TR P-512)*. Arlington, Virginia: Institute for Defense Analyses.
11. McCormick, W. T., Schweitzer, P. J., & White, T. W. (1972). Problem decomposition and data reorganization by a clustering technique. *Operations Research*, *20*(5), 993–1009.
12. Mullat, J. E. (1976a). Extremal subsystems of monotonic systems I. *Automation and Remote Control*, *37*, 758–766.
13. Mullat, J. E. (1976b). Extremal subsystems of monotonic systems II. *Automation and Remote Control*, *37*, 1286–1294.
14. Mullat, J. E. (1977). Extremal subsystems of monotonic systems III. *Automation and Remote Control*, *38*, 89–96.
15. Murtagh, F. (1989). Book review. In W. Gaul & M. Schader, (Eds.), *Data, expert knowledge and decisions*. Heidelberg: Springer-Verlag. 1988, pp. viii + 380. *Journal of Classification*, 6, 129–132.
16. Okada, A. (1990). A generalization of asymmetric multidimensional scaling. In *Knowledge, data and computer-assisted decisions* (pp. 127–138). Berlin, Heidelberg: Springer.
17. Okada, A. (2000). An asymmetric cluster analysis study of car switching data. In *Data analysis* (pp. 495–504). Berlin, Heidelberg: Springer.
18. Okada, A., & Imaizumi, T. (1987). Nonmetric multidimensional scaling of asymmetric proximities. *Behaviormetrika*, *14*(21), 81–96.
19. Okada, A., & Imaizumi, T. (1997). Asymmetric multidimensional scaling of two-mode three-way proximities. *Journal of Classification*, *14*(2), 195–224.
20. Okada, A., & Imaizumi, T. (2007). Multidimensional scaling of asymmetric proximities with a dominance point. In *Advances in data analysis* (pp. 307–318). Berlin, Heidelberg: Springer.
21. Okada, A., & Tsurumi, H. (2012). Asymmetric multidimensional scaling of brand switching among margarine brands. *Behaviormetrika*, *39*(1), 111–126.
22. Tucker, L. R. (1964). The extension of factor analysis to three-dimensional matrices. In H. Gulliksen, & N. Frederiksen (Eds.), *Contributions to mathematical psychology* (pp. 110–127). New York: Holt, Rinehart and Winston.
23. Vohandu, L. (1980). Some methods to order objects and variables in data systems (in Russian). *Transactions of Tallinn University of Technology*, *482*, 43–50.
24. Vohandu, L. (1981). Fast methods for data processing (in Russian). In *Computer systems: Computer methods for revealing regularities* (pp. 20–29). Novosibirsk: Institute of Mathematics Press.
25. Vohandu, L. (1989). Fast methods in exploratory data analysis. *Transactions of Tallinn University of Technology*, *705*, 3–13.

Parsimonious Mixtures of Matrix Variate Bilinear Factor Analyzers

Michael P. B. Gallaugher and Paul D. McNicholas

Abstract Over the years, data have become increasingly higher dimensional, which has prompted an increased need for dimension reduction techniques. This is perhaps especially true for clustering (unsupervised classification), as well as semi-supervised and supervised classification. Many methods have been proposed in the literature for two-way (multivariate) data and quite recently methods have been presented for three-way (matrix variate) data. One such method is the mixtures of matrix variate bilinear factor analyzers (MMVBFA) model. Herein, we propose a total of 64 parsimonious MMVBFA models. Simulated and real data are used for illustration.

1 Introduction

One aspect of more complex data collected today is the increasing dimensionality of the data. Therefore, there has been an increased need for parameter reduction and dimension reduction techniques, especially in the area of model-based clustering. Such techniques are abundant in the literature for traditional, multivariate data and include parsimonious models (Celeux & Govaert [7]), mixtures of factor analyzers (Ghahramani & Hinton [17]; McNicholas & Murphy [26]), co-clustering (Hartigan [19]; Nadif & Govaert [32]; Gallaugher, Biernacki, & McNicholas [10]), and penalization methods (Pan & Shen [33]; Zhou, Pan, & Shen [51]; Gallaugher, Tang, & McNicholas [16]). In the case of three-way data, however, there are still considerable gaps in the literature for clustering high dimensional three-way data.

Three-way data can be considered matrices, examples of which include greyscale images and multivariate longitudinal data—the latter consists of multiple variables collected at different time points. In the last few years, many methods have been proposed for analyzing three-way data. One recent example is the mixture of matrix

M. P. B. Gallaugher · P. D. McNicholas (✉)
Department of Mathematics and Statistics, McMaster University, Hamilton L8S 4K1, Canada
e-mail: paulmc@mcmaster.ca

M. P. B. Gallaugher
e-mail: gallump@mcmaster.ca

T. Imaizumi et al. (eds.), *Advanced Studies in Behaviormetrics and Data Science*,
Behaviormetrics: Quantitative Approaches to Human Behavior 5,
https://doi.org/10.1007/978-981-15-2700-5_11

variate bilinear factor analyzers model (Gallaugher & McNicholas [13]), which can be considered as the matrix variate analogue of the mixture of factor analyzers model. Herein, we present a total of 64 parsimonious models in the matrix variate case, which is effectively a matrix variate analogue of the multivariate family presented by McNicholas and Murphy [26]. The remainder of this work is laid out as follows: In Sect. 2, some background on model-based clustering and matrix variate methods is presented. In Sect. 3, the methodology is outlined. Then, simulations and data analyses are presented in Sects. 4 and 5, respectively. We conclude with a discussion and suggestions for future work (Sect. 6).

2 Background

2.1 Model-Based Clustering

Clustering is the process of finding homogenous group structure within heterogeneous data. One of the most established methods in the literature is model-based clustering, which makes use of a finite mixture model. A finite mixture model assumes that a random variable $\mathbf{X}$ comes from a population with G subgroups and its density can be written

$$f(\mathbf{x} \mid \boldsymbol{\vartheta}) = \sum_{g=1}^{G} \pi_g f_g(\mathbf{x} \mid \boldsymbol{\theta}_g),$$

where $\sum_{g=1}^{G} \pi_g = 1$, with $\pi_g > 0$, are the mixing proportions and $f_g(\cdot)$ are the component densities. The mixture of Gaussian distributions has been studied extensively within the literature, with Wolfe [47] being an early example of the use of a mixture of Gaussian distributions for clustering. Other early examples of clustering with a mixture of Gaussians can be found in Baum, Petrie, Soules, and Weiss [4] and Scott and Symons [38].

Because of the flexibility of the mixture modelling framework, many other mixtures have been proposed using more flexible distributions such as those that allow for parameterization of tail weight such as the t distribution (Peel & McLachlan [34]; Andrews & McNicholas [2, 3]; Lin, McNicholas, & Hsiu [23]) and the power exponential distribution (Dang, Browne, & McNicholas [8]), as well as those that allow for the parameterization of skewness and tail weight such as the skew-t distribution (Lin [22]; Vrbik & McNicholas [45, 46]; Lee & McLachlan [21]; Murray, Browne, & McNicholas [29]; Murray, McNicholas, & Browne [31]) and others (Browne & McNicholas [6]; Franczak, Tortora, Browne, & McNicholas [9]; Murray, Browne, & McNicholas [30]; Tang, Browne, & McNicholas [40]; Tortora, Franczak, Browne, & McNicholas [43]).

In addition to the multivariate case, there are recent examples of using matrix variate distributions for clustering three-way data. Such examples include using the

matrix variate normal (Viroli [44]), skewed distributions (Gallaugher & McNicholas [11, 12, 15]), and transformation methods (Melnykov & Zhu [28]). Most recently, Sarkar, Zhu, Melnykov, and Ingrassia [36] present parsimonious models analogous to those used by Celeux and Govaert [7].

2.2 Parsimonious Gaussian Mixture Models

One popular dimension reduction technique for high dimensional multivariate data is the mixture of factor analyzers model. The factor analysis model for p-dimensional $\mathbf{X}_1, \ldots, \mathbf{X}_N$ is given by

$$\mathbf{X}_i = \boldsymbol{\mu} + \boldsymbol{\Lambda}\mathbf{U}_i + \boldsymbol{\varepsilon}_i,$$

where $\boldsymbol{\mu}$ is a location vector, $\boldsymbol{\Lambda}$ is a $p \times q$ matrix of factor loadings with $q < p$, $\mathbf{U}_i \sim \mathcal{N}_q(\mathbf{0}, \mathbf{I})$ denotes the latent factors, $\boldsymbol{\varepsilon}_i \sim \mathcal{N}_q(\mathbf{0}, \boldsymbol{\Psi})$, where $\boldsymbol{\Psi} = \text{diag}(\psi_1, \psi_2, \ldots, \psi_p)$, $\psi_j \in \mathbb{R}^+$, and $\mathbf{U}_i$ and $\boldsymbol{\varepsilon}_i$ are each independently distributed and independent of one another. Under this model, the marginal distribution of $\mathbf{X}_i$ is $\mathcal{N}_p(\boldsymbol{\mu}, \boldsymbol{\Lambda}\boldsymbol{\Lambda}' + \boldsymbol{\Psi})$. Probabilistic principal component analysis (PPCA) arises as a special case with the isotropic constraint $\boldsymbol{\Psi} = \psi\mathbf{I}$, $\psi \in \mathbb{R}^+$ (Tipping & Bishop [42]).

Ghahramani and Hinton [17] develop the mixture of factor analyzers model, where the density takes the form of a Gaussian mixture model with covariance structure $\boldsymbol{\Sigma}_g = \boldsymbol{\Lambda}_g\boldsymbol{\Lambda}_g' + \boldsymbol{\Psi}$. A small extension was presented by McLachlan and Peel [25], who utilize the more general structure $\boldsymbol{\Sigma}_g = \boldsymbol{\Lambda}_g\boldsymbol{\Lambda}_g' + \boldsymbol{\Psi}_g$. Tipping and Bishop [41] introduce the closely related mixture of PPCAs with $\boldsymbol{\Sigma}_g = \boldsymbol{\Lambda}_g\boldsymbol{\Lambda}_g' + \psi_g\mathbf{I}$. McNicholas and Murphy [26] consider all combinations of the constraints $\boldsymbol{\Lambda}_g = \boldsymbol{\Lambda}$, $\boldsymbol{\Psi}_g = \boldsymbol{\Psi}$, and the isotropic constraint to give a family of eight parsimonious Gaussian mixture models (PGMMs). As discussed by McNicholas and Murphy [26], the number of covariance parameters for each PGMM is linear in the data dimension p as compared to the parsimonious models presented by Celeux and Govaert [7], where the majority are quadratic in p and the others assume variable independence. This paper introduces a matrix variate analogue of the PGMM family of McNicholas and Murphy [26].

2.3 Matrix Variate Normal Distribution

In recent years, several methods have been proposed for clustering three-way data. These methods mainly employ matrix variate distributions in finite mixture models. Similar to the univariate and multivariate cases, the most mathematically tractable matrix variate distribution to use is the matrix variate normal distribution. An $n \times p$ random matrix $\mathcal{X}$ follows a matrix variate normal distribution with location parameter $\mathbf{M}$ and scale matrices $\boldsymbol{\Sigma}$ and $\boldsymbol{\Psi}$ of dimensions $n \times n$ and $p \times p$, respectively, denoted by $\mathcal{N}_{n\times p}(\mathbf{M}, \boldsymbol{\Sigma}, \boldsymbol{\Psi})$, if the density of $\mathcal{X}$ can be written

$$f(\mathbf{X} \mid \mathbf{M}, \boldsymbol{\Sigma}, \boldsymbol{\Psi}) = \frac{1}{(2\pi)^{\frac{np}{2}} |\boldsymbol{\Sigma}|^{\frac{p}{2}} |\boldsymbol{\Psi}|^{\frac{n}{2}}} \exp\left\{-\frac{1}{2} \operatorname{tr}\left(\boldsymbol{\Sigma}^{-1}(\mathbf{X}-\mathbf{M})\boldsymbol{\Psi}^{-1}(\mathbf{X}-\mathbf{M})'\right)\right\}. \tag{1}$$

One notable property of the matrix variate normal distribution (Harrar & Gupta [18]) is

$$\mathcal{X} \sim \mathcal{N}_{n\times p}(\mathbf{M}, \boldsymbol{\Sigma}, \boldsymbol{\Psi}) \iff \operatorname{vec}(\mathcal{X}) \sim \mathcal{N}_{np}(\operatorname{vec}(\mathbf{M}), \boldsymbol{\Psi} \otimes \boldsymbol{\Sigma}), \tag{2}$$

where $\mathcal{N}_{np}(\cdot)$ is the np-dimensional multivariate normal density, $\operatorname{vec}(\cdot)$ is the vectorization operator, and $\otimes$ denotes the Kronecker product.

2.4 Mixture of Matrix Variate Bilinear Factor Analyzers

Gallaugher and McNicholas [13] present an extension of the work of Xie, Yan, Kwok, and Huang [48], Yu, Bi, and Ye [49] and Zhao, Philip, and Kwok [50] to derive the MMVBFA model. The MMVBFA model assumes that

$$\mathcal{X}_i = \mathbf{M}_g + \boldsymbol{\Lambda}_g \mathcal{U}_{ig} \boldsymbol{\Delta}_g' + \boldsymbol{\Lambda}_g \mathcal{E}_{ig}^{B} + \mathcal{E}_{ig}^{A} \boldsymbol{\Delta}_g' + \mathcal{E}_{ig} \tag{3}$$

with probability π_g, for $g = 1, 2, \ldots, G$, where $\mathbf{M}_g$ is an $n \times p$ location matrix, $\boldsymbol{\Lambda}_g$ is an $n \times q$ column factor loading matrix, with $q < n$, $\boldsymbol{\Delta}_g$ is a $p \times r$ row factor loading matrix, with $r < p$, and

$$\begin{aligned}
\mathcal{U}_{ig} &\sim \mathcal{N}_{q\times r}(\mathbf{0}, \mathbf{I}_q, \mathbf{I}_r),\\
\mathcal{E}_{ig}^{B} &\sim \mathcal{N}_{q\times p}(\mathbf{0}, \mathbf{I}_q, \boldsymbol{\Psi}_g),\\
\mathcal{E}_{ig}^{A} &\sim \mathcal{N}_{n\times r}(\mathbf{0}, \boldsymbol{\Sigma}_g, \mathbf{I}_r),\\
\mathcal{E}_{ig} &\sim \mathcal{N}_{n\times p}(\mathbf{0}, \boldsymbol{\Sigma}_g, \boldsymbol{\Psi}_g)
\end{aligned}$$

are independent of each other, $\boldsymbol{\Sigma} = \operatorname{diag}\{\sigma_1, \sigma_2, \ldots, \sigma_n\}$, with $\sigma_j \in \mathbb{R}^+$, and $\boldsymbol{\Psi} = \operatorname{diag}\{\psi_1, \psi_2, \ldots, \psi_p\}$, with $\psi_j \in \mathbb{R}^+$. Let $\mathbf{z}_i = (z_{i1}, \ldots, z_{iG})'$ denote the component membership for $\mathbf{X}_i$, where

$$z_{ig} = \begin{cases} 1 & \text{if } \mathbf{X}_i \text{ belongs to component } g,\\ 0 & \text{otherwise,} \end{cases}$$

for $i = 1, \ldots, N$ and $g = 1, \ldots, G$. Using the vectorization of $\mathcal{X}_i$, and property (2), it can be shown that

$$\mathcal{X}_i \mid z_{ig} = 1 \sim \mathcal{N}_{n\times p}(\mathbf{M}_g, \boldsymbol{\Sigma}_g^*, \boldsymbol{\Psi}_g^*),$$

where $\boldsymbol{\Sigma}_g^* = \boldsymbol{\Sigma}_g + \boldsymbol{\Lambda}_g\boldsymbol{\Lambda}_g'$ and $\boldsymbol{\Psi}_g^* = \boldsymbol{\Psi}_g + \boldsymbol{\Delta}_g\boldsymbol{\Delta}_g'$. Therefore, the density of $\mathcal{X}_i$ can be written

$$f(\mathbf{X}_i \mid \boldsymbol{\vartheta}) = \sum_{g=1}^{G} \pi_g \varphi_{n\times p}(\mathbf{X}_i \mid \mathbf{M}_g, \boldsymbol{\Sigma}_g^*, \boldsymbol{\Psi}_g^*),$$

where $\varphi_{n\times p}(\cdot)$ denotes the $n \times p$ matrix variate normal density.

Note that the term "column factors" refers to a reduction in the dimension of the columns, which is equivalent to the number of rows, and not a reduction in the number of columns. Likewise, the term "row factors" refers to the reduction in the dimension of the rows (number of columns). Moreover, as discussed by Zhao et al. [50], we can interpret terms $\mathcal{E}^B$ and $\mathcal{E}^A$ as the row and column noise, respectively, and the final term $\mathcal{E}$ as the common noise.

As discussed by Zhao et al. [50] and Gallaugher and McNicholas [12], by introducing latent variables $\mathcal{Y}_{ig}^B$ and $\mathcal{V}_{ig}^B$, (3) exhibits the two-stage formulation

$$\begin{aligned}
\mathcal{X}_i &= \mathbf{M}_g + \boldsymbol{\Lambda}_g\mathcal{Y}_{ig}^B + \mathcal{V}_{ig}^B,\\
\mathcal{Y}_{ig}^B &= \mathcal{U}_{ig}\boldsymbol{\Delta}_g' + \mathcal{E}_{ig}^B,\\
\mathcal{V}_{ig}^B &= \mathcal{E}_{ig}^A\boldsymbol{\Delta}_g' + \mathcal{E}_{ig}.
\end{aligned}$$

This formulation can be viewed as first projecting $\mathcal{X}_i$ in the column direction onto the latent matrix $\mathcal{Y}_{ig}^B$, and then $\mathcal{Y}_{ig}^B$ and $\mathcal{V}_{ig}^B$ are further projected in the row direction. Likewise, introducing $\mathcal{Y}_{ig}^A$ and $\mathcal{V}_{ig}^A$, (3) can be written

$$\begin{aligned}
\mathcal{X}_i &= \mathbf{M}_g + \mathcal{Y}_{ig}^A\boldsymbol{\Delta}_g' + \mathcal{V}_{ig}^A,\\
\mathcal{Y}_{ig}^A &= \boldsymbol{\Lambda}_g\mathcal{U}_{ig} + \mathcal{E}_{ig}^A,\\
\mathcal{V}_{ig}^A &= \boldsymbol{\Lambda}_g\mathcal{E}_{ig}^B + \mathcal{E}_{ig}.
\end{aligned}$$

The interpretation is the same as before but we now project in the row direction first followed by the column direction.

3 Methodology

3.1 Parsimonious MMVBFA Models

One feature of the MMVBFA model is that each of the resultant scale matrices has the same form as the covariance matrix in the (multivariate) mixture of factor analyzers model. Therefore, MMVBFA lends itself naturally to a matrix variate extension of the PGMM models. Specifically, we apply combinations of the constraints $\boldsymbol{\Lambda}_g = \boldsymbol{\Lambda}$, $\boldsymbol{\Sigma}_g = \boldsymbol{\Sigma}$, $\boldsymbol{\Sigma}_g = \sigma_g\mathbf{I}_n$ with $\sigma_g \in \mathbb{R}^+$, $\boldsymbol{\Delta}_g = \boldsymbol{\Delta}$, $\boldsymbol{\Psi}_g = \boldsymbol{\Psi}$, and $\boldsymbol{\Psi}_g = \psi_g\mathbf{I}_p$ with $\psi_g \in$

Table 1 Row models with the respective number of scale parameters

$\boldsymbol{\Lambda}_g = \boldsymbol{\Lambda}$	$\boldsymbol{\Sigma}_g = \boldsymbol{\Sigma}$	$\boldsymbol{\Sigma}_g = \sigma_g \mathbf{I}_n$	Number of scale parameters
C	C	C	$[nq + n - q(q-1)/2] + 1$
C	C	U	$[nq + n - q(q-1)/2] + n$
C	U	C	$[nq + n - q(q-1)/2] + G$
C	U	U	$[nq + n - q(q-1)/2] + nG$
U	C	C	$G[nq + n - q(q-1)/2] + 1$
U	C	U	$G[nq + n - q(q-1)/2] + n$
U	U	C	$G[nq + n - q(q-1)/2] + G$
U	U	U	$G[nq + n - q(q-1)/2] + nG$

Table 2 Column models with the respective number of scale parameters

$\boldsymbol{\Delta}_g = \boldsymbol{\Delta}$	$\boldsymbol{\Psi}_g = \boldsymbol{\Psi}$	$\boldsymbol{\Psi}_g = \psi_g \mathbf{I}_r$	Number of scale parameters
C	C	C	$[pr + p - r(r-1)/2] + 1$
C	C	U	$[pr + p - r(r-1)/2] + p$
C	U	C	$[pr + p - r(r-1)/2] + G$
C	U	U	$[pr + p - r(r-1)/2] + pG$
U	C	C	$G[pr + p - r(r-1)/2] + 1$
U	C	U	$G[pr + p - r(r-1)/2] + p$
U	U	C	$G[pr + p - r(r-1)/2] + G$
U	U	U	$G[pr + p - r(r-1)/2] + pG$

$\mathbb{R}^+$. This leads to a total of 64 models, which we refer to as the parsimonious mixtures of matrix variate bilinear factor analyzers (PMMVBFA) family. In Tables 1 and 2, the models along with the number of scale parameters are presented for the row and column scale matrices. We will refer to these as the row and column models, respectively.

Maximum likelihood estimation is performed using an alternating expectation maximization (AECM) algorithm in almost an identical fashion to Gallaugher and McNicholas [13]. The only difference is the form of the updates for the scale matrices which is dependent on the model. Below, the general form of the algorithm is presented and the corresponding scale parameter updates are given in the Appendix. We refer the reader to Gallaugher and McNicholas [13] for details regarding the expectations in the E-steps.

AECM Stage 1

In the first stage, the complete-data is taken to be the observed matrices $\mathbf{X}_1, \ldots, \mathbf{X}_N$ and the component memberships $\mathbf{z}_1, \ldots, \mathbf{z}_N$, and the update for $\mathbf{M}_g$ is calculated. The complete-data log-likelihood in the first stage is

$$\ell^{(1)} = C + \sum_{g=1}^{G}\sum_{i=1}^{N} z_{ig}\left\{\log \pi_g - \frac{1}{2}\operatorname{tr}[\boldsymbol{\Sigma}_g^{*^{-1}}(\mathbf{X}_i - \mathbf{M}_g)\boldsymbol{\Psi}_g^{*^{-1}}(\mathbf{X}_i - \mathbf{M}_g)']\right\},$$

where C is a constant with respect to $\mathbf{M}_g$, $\boldsymbol{\Sigma}_g^* := \boldsymbol{\Lambda}_g\boldsymbol{\Lambda}_g' + \boldsymbol{\Sigma}_g$ and $\boldsymbol{\Psi}_g^* := \boldsymbol{\Delta}_g\boldsymbol{\Delta}_g' + \boldsymbol{\Psi}_g$. In the E-Step, the updates for the component memberships z_{ig} are given by the expectations

$$\hat{z}_{ig} = \frac{\pi_g \varphi_{n\times p}(\mathbf{X}_i \mid \hat{\mathbf{M}}_g, \hat{\boldsymbol{\Sigma}}_g^*, \hat{\boldsymbol{\Psi}}_g^*)}{\sum_{h=1}^{G}\pi_h \varphi_{n\times p}(\mathbf{X}_i \mid \hat{\mathbf{M}}_h, \hat{\boldsymbol{\Sigma}}_h^*, \hat{\boldsymbol{\Psi}}_h^*)},$$

where $\varphi_{n\times p}(\cdot)$ denotes the $n \times p$ matrix variate normal density. In the CM-step, the update for $\mathbf{M}_g$ is

$$\hat{\mathbf{M}}_g = \frac{1}{N_g}\sum_{i=1}^{N}\hat{z}_{ig}\mathbf{X}_i,$$

where $N_g = \sum_{i=1}^{N}\hat{z}_{ig}$.

AECM Stage 2

In the second stage, the complete-data is taken to be the observed $\mathbf{X}_1, \ldots, \mathbf{X}_N$, the component memberships $\mathbf{z}_1, \ldots, \mathbf{z}_N$ and the latent factors $\mathcal{Y}_i^B = (\mathcal{Y}_{i1}^B, \mathcal{Y}_{i2}^B, \ldots, \mathcal{Y}_{iG}^B)$. The complete-data log-likelihood is then

$$\begin{aligned}\ell^{(2)} = C - \sum_{g=1}^{G}\frac{N_g p}{2}\log|\boldsymbol{\Sigma}_g| - \frac{1}{2}\sum_{g=1}^{G}\sum_{i=1}^{N} z_{ig}\operatorname{tr}\big[&\boldsymbol{\Sigma}_g^{-1}(\mathbf{X}_i - \mathbf{M}_g)\boldsymbol{\Psi}_g^{*^{-1}}(\mathbf{X}_i - \mathbf{M}_g)' \\ &- \boldsymbol{\Sigma}_g^{-1}\boldsymbol{\Lambda}_g\mathcal{Y}_{ig}^B\boldsymbol{\Psi}_g^{*^{-1}}(\mathbf{X}_i - \mathbf{M}_g)' - \boldsymbol{\Sigma}_g^{-1}(\mathbf{X}_i - \mathbf{M}_g)\boldsymbol{\Psi}_g^{*^{-1}}\mathcal{Y}_{ig}^{B\prime}\boldsymbol{\Lambda}_g' + \boldsymbol{\Sigma}_g^{-1}\boldsymbol{\Lambda}_g\mathcal{Y}_{ig}^B\boldsymbol{\Psi}_g^{*^{-1}}\mathcal{Y}_{ig}^{B\prime}\boldsymbol{\Lambda}_g'\big].\end{aligned} \tag{4}$$

In the E-Step, the following expectations are calculated

$$\begin{aligned} a_{ig}^B &:= \mathbb{E}[\mathcal{Y}_{ig}^B \mid \mathbf{X}_i, z_{ig} = 1, \hat{\boldsymbol{\vartheta}}] = \mathbf{W}_g^{A^{-1}}\hat{\boldsymbol{\Lambda}}_g'\hat{\boldsymbol{\Sigma}}_g^{-1}(\mathbf{X}_i - \hat{\mathbf{M}}_g), \\ b_{ig}^B &:= \mathbb{E}[\mathcal{Y}_{ig}^B\hat{\boldsymbol{\Psi}}^{*^{-1}}\mathcal{Y}_{ig}^{B\prime} \mid \mathbf{X}_i, z_{ig} = 1, \hat{\boldsymbol{\vartheta}}] = p\mathbf{W}_g^{A^{-1}} + a_{ig}^B\hat{\boldsymbol{\Psi}}_g^{*^{-1}}a_{ig}^{B\prime}, \end{aligned} \tag{5}$$

where $\mathbf{W}_g^A = \mathbf{I}_q + \hat{\boldsymbol{\Lambda}}_g'\hat{\boldsymbol{\Sigma}}_g^{-1}\hat{\boldsymbol{\Lambda}}_g$. In the CM-step, $\boldsymbol{\Lambda}_g$ and $\boldsymbol{\Sigma}_g$ are updated (see Appendix).

AECM Stage 3

In the last stage of the AECM algorithm, the complete-data is taken to be the observed $\mathbf{X}_1, \ldots, \mathbf{X}_N$, the component memberships $\mathbf{z}_1, \ldots, \mathbf{z}_N$ and the latent factors $\mathcal{Y}_i^A = (\mathcal{Y}_{i1}^A, \mathcal{Y}_{i2}^A, \ldots, \mathcal{Y}_{iG}^A)$. In this step, the complete-data log-likelihood is

$$\ell^{(3)} = C - \frac{N_g n}{2}\log|\boldsymbol{\Psi}_g| - \frac{1}{2}\sum_{g=1}^{G}\sum_{i=1}^{N} z_{ig}\,\mathrm{tr}\big[\boldsymbol{\Psi}_g^{-1}(\mathbf{X}_i - \mathbf{M}_g)'\boldsymbol{\Sigma}_g^{*^{-1}}(\mathbf{X}_i - \mathbf{M}_g) - \boldsymbol{\Psi}_g^{-1}\boldsymbol{\Delta}_g\mathcal{Y}_{ig}^{A\prime}\boldsymbol{\Sigma}_g^{*^{-1}}(\mathbf{X}_i - \mathbf{M}_g) - \boldsymbol{\Psi}_g^{-1}(\mathbf{X}_i - \mathbf{M}_g)'\boldsymbol{\Sigma}_g^{*^{-1}}\mathcal{Y}_{ig}^{A}\mathbf{B}_g' + \boldsymbol{\Psi}_g^{-1}\boldsymbol{\Delta}_g\mathcal{Y}_{ig}^{A\prime}\boldsymbol{\Sigma}_g^{*^{-1}}\mathcal{Y}_{ig}^{A}\boldsymbol{\Delta}_g'\big].$$

In the E-Step, expectations similar to those at Stage 2 are calculated

$$a_{ig}^{A} := \mathbb{E}[\mathcal{Y}_{ig}^{A} \mid \mathbf{X}_i, z_{ig} = 1, \hat{\boldsymbol{\vartheta}}] = (\mathbf{X}_i - \hat{\mathbf{M}}_g)\hat{\boldsymbol{\Psi}}_g^{-1}\hat{\boldsymbol{\Delta}}_g\mathbf{W}_g^{B^{-1}}$$

and

$$b_{ig}^{A} := \mathbb{E}[\mathcal{Y}_{ig}^{A\prime}\hat{\boldsymbol{\Sigma}}_g^{*^{-1}}\mathcal{Y}_{ig}^{A} \mid \mathbf{X}_i, z_{ig} = 1, \hat{\boldsymbol{\vartheta}}] = n\mathbf{W}_g^{B^{-1}} + a_{ig}^{A\prime}\hat{\boldsymbol{\Sigma}}_g^{*^{-1}}a_{ig}^{A},$$

where $\mathbf{W}_g^B = \mathbf{I}_r + \hat{\boldsymbol{\Delta}}_g'\hat{\boldsymbol{\Psi}}_g^{-1}\hat{\boldsymbol{\Delta}}_g$. In the CM-step, we update $\boldsymbol{\Delta}_g$ and $\boldsymbol{\Psi}_g$ (see Appendix).

3.2 *Model Selection, Convergence, Performance Evaluation Criteria, and Initialization*

In general, the number of components, row factors, column factors, row model, and column model are unknown a priori and, therefore, need to be selected. In our simulations and analyses, the Bayesian information criterion (BIC, Schwarz [37]) is used. The BIC is given by

$$\mathrm{BIC} = 2\ell(\hat{\boldsymbol{\vartheta}}) - \rho\log N,$$

where $\ell(\hat{\boldsymbol{\vartheta}})$ is the maximized log-likelihood and ρ is the number of free parameters.

The simplest convergence criterion is based on the lack of progress in the log-likelihood, where the algorithm is terminated when $l^{(t+1)} - l^{(t)} < \epsilon$, where $\epsilon > 0$ is a small number. Oftentimes, however, the log-likelihood can plateau and then increase again, thus the algorithm would be terminated prematurely using lack of progress, (see McNicholas, Murphy, McDaid, & Frost [27], for examples). Another option, and one that is used for our analyses, is a criterion based on the Aitken acceleration (Aitken [1]). The Aitken acceleration at iteration t is

$$a^{(t)} = \frac{l^{(t+1)} - l^{(t)}}{l^{(t)} - l^{(t-1)}},$$

where $l^{(t)}$ is the (observed) log-likelihood at iteration t. We then have an estimate, at iteration $t+1$, of the log-likelihood after many iterations:

$$l_{\infty}^{(t+1)} = l^{(t)} + \frac{(l^{(t+1)} - l^{(t)})}{1 - a^{(t)}}$$

(Böhning, Dietz, Schaub, Schlattmann, & Lindsay [5]; Lindsay [24]). As suggested by McNicholas et al. [27], the algorithm is terminated when $l_\infty^{(k+1)} - l^{(k)} \in (0, \epsilon)$. It should be noted that we set the value of ϵ based on the magnitude of the log-likelihood in the manner of Gallaugher and McNicholas [14]. Specifically, we set ϵ to a value three orders of magnitude lower than the log-likelihood after five iterations.

To assess classification performance, the adjusted Rand index (ARI, Hubert & Arabie [20]) is used. The ARI is the Rand index (Rand [35]) corrected for chance agreement. The ARI compares two different partitions—in our case, predicted and true classifications—and takes a value of 1 if there is perfect agreement. Under random classification, the expected values of the ARI is 0.

Finally, there is the issue of initialization. In our simulations and data analyses, we used soft (uniform) random initializations for the $\hat{z}_{ig}$. From these initial soft group memberships $\hat{z}_{ig}$, we initialize the location matrices using

$$\hat{\mathbf{M}}_g = \frac{1}{N_g} \sum_{i=1}^{N} \hat{z}_{ig} \mathbf{X}_i,$$

where $N_g = \sum_{i=1}^{N} \hat{z}_{ig}$. The diagonal scale matrices, $\boldsymbol{\Sigma}_g$ and $\boldsymbol{\Psi}_g$ are initialized as follows:

$$\hat{\boldsymbol{\Sigma}}_g = \frac{1}{pN_g} \text{diag} \left\{ \sum_{i=1}^{N} \hat{z}_{ig} (\mathbf{X}_i - \hat{\mathbf{M}}_g)(\mathbf{X}_i - \hat{\mathbf{M}}_g)' \right\}$$

and

$$\hat{\boldsymbol{\Psi}}_g = \frac{1}{nN_g} \text{diag} \left\{ \sum_{i=1}^{N} \hat{z}_{ig} (\mathbf{X}_i - \hat{\mathbf{M}}_g)'(\mathbf{X}_i - \hat{\mathbf{M}}_g) \right\}.$$

The elements of the factor loading matrices are initialized randomly from a uniform distribution on $[-1, 1]$. Note that all initializations are based on the UUU model.

4 Simulations

4.1 Simulation 1

Three simulations were conducted. In the first, we consider $d \times d$ matrices with $d \in \{10, 20\}$, $G = 2$ and $\mathbf{M}_1 = \mathbf{0}, \mathbf{M}_2 = \mathbf{M}_{\text{LT}}^{(\delta)}$, where $\delta \in \{1, 2, 4\}$ and $\mathbf{M}_{\text{LT}}^{(\delta)}$ represents a lower triangular matrix with δ on and below the diagonal. We consider the case where both rows and columns have a CCU model. The parameters for the column factor loading matrices are

$$\boldsymbol{\Lambda}_1 = \boldsymbol{\Lambda}_2 = \begin{bmatrix} \mathbf{1}_5 & \mathbf{0}_5 & \mathbf{0}_5 \\ \mathbf{0}_2 & \mathbf{1}_2 & \mathbf{0}_2 \\ \mathbf{0}_3 & \mathbf{0}_3 & \mathbf{1}_3 \end{bmatrix} (d = 10), \qquad \boldsymbol{\Lambda}_1 = \boldsymbol{\Lambda}_2 = \begin{bmatrix} \mathbf{1}_{10} & \mathbf{0}_{10} & \mathbf{0}_{10} \\ \mathbf{0}_4 & \mathbf{1}_4 & \mathbf{0}_4 \\ \mathbf{0}_6 & \mathbf{0}_6 & \mathbf{1}_6 \end{bmatrix} (d = 20).$$

Table 3 Number of datasets for which the BIC correctly chose the number of groups (G), column factors (q), row factors (r), row model (RM), column model (CM), and the average ARI over 25 datasets (Simulation 1)

δ	N	$d = 10$						$d = 20$					
		G	q	r	RM	CM	$\overline{\text{ARI}}$(sd)	G	q	r	RM	CM	$\overline{\text{ARI}}$(sd)
1	100	0	25	25	25	25	0.000(0.00)	25	24	25	25	25	1.000(0.00)
	200	21	25	25	25	25	0.723(0.33)	25	24	24	25	24	1.000(0.00)
	400	25	25	25	25	25	0.883(0.04)	25	25	25	25	25	1.000(0.002)
2	100	25	25	25	25	25	1.000(0.00)	25	24	25	25	25	1.000(0.00)
	200	25	25	25	25	25	0.999(0.004)	25	25	25	25	25	1.000(0.00)
	400	25	25	25	25	25	1.000(0.002)	25	25	25	25	25	1.000(0.00)
4	100	25	25	25	25	25	1.000(0.00)	25	24	25	25	25	1.000(0.00)
	200	25	25	24	25	25	1.000(0.00)	25	25	25	25	25	1.000(0.00)
	400	25	25	25	25	25	1.000(0.00)	25	25	25	25	25	1.000(0.00)

The row factor loading matrices are

$$\boldsymbol{\Delta}_1 = \boldsymbol{\Delta}_2 = \begin{bmatrix} -\mathbf{1}_{d/2} & \mathbf{0}_{d/2} \\ \mathbf{1}_{d/2} & \mathbf{1}_{d/2} \end{bmatrix},$$

where $\mathbf{1}_c$ and $\mathbf{0}_c$ represent c-dimensional vectors of 1s and 0s, respectively. The error covariance matrices are taken to be

$$\boldsymbol{\Sigma}_1 = \boldsymbol{\Sigma}_2 = \boldsymbol{\Psi}_1 = \boldsymbol{\Psi}_2 = \mathbf{D},$$

where $\mathbf{D}$ is a diagonal matrix with diagonal entries $d_{tt} = t/5$ when $d = 10$ and $d_{tt} = t/10$ when $d = 20$.

Finally, sample sizes of $N \in \{100, 200, 400\}$ are considered with $\pi_1 = \pi_2 = 0.5$. For each of these combinations, 25 datasets are simulated. The model is fit for $G = 1, \ldots, 4$ groups, 1 to 5 row factors and column factors, and all 64 scale models, leading to a total of 6,400 models fit for each dataset.

In Table 3, we display the number of times the correct number of groups, row factors, and column factors are selected by the BIC, as well as the number of times the row and column models were correctly identified. We also include the average ARI over the 25 datasets with associated standard deviations. As expected, as the separation and sample size increase, better classification results are obtained. The correct number of groups, column factors, and row factors are chosen for all 25 datasets in nearly all cases considered. Moreover, the selection of the row and column models is very accurate in all cases considered.

Table 4 Number of datasets for which the BIC correctly chose the number of groups (G), column factors (q), row factors (r), row model (RM), column model (CM), and the average ARI over 25 datasets (Simulation 2)

δ	N	$d = 10$						$d = 20$					
		G	q	r	RM	CM	$\overline{\text{ARI}}$(sd)	G	q	r	RM	CM	$\overline{\text{ARI}}$(sd)
1	100	25	25	25	25	25	0.990(0.02)	25	0	25	25	25	1.000(0.00)
	200	25	25	25	25	1	0.998(0.007)	25	24	25	25	25	1.000(0.00)
	400	25	25	25	25	25	0.997(0.006)	25	25	25	25	25	1.000(0.00)
2	100	25	25	25	25	0	0.998(0.01)	25	0	25	25	25	1.000(0.00)
	200	25	25	25	25	0	1.000(0.00)	25	24	25	25	25	1.000(0.00)
	400	25	25	25	25	25	0.999(0.003)	25	25	25	25	25	1.000(0.00)
4	100	25	25	25	25	0	1.000(0.00)	25	10	25	25	25	1.000(0.00)
	200	25	25	25	25	2	1.000(0.00)	25	23	25	25	25	1.000(0.00)
	400	25	25	24	25	25	1.000(0.00)	25	5	25	25	20	1.000(0.00)

4.2 Simulation 2

In this simulation, similar conditions to Simulation 1 are considered, including using the same mean matrices; however, we place a CUC model on the rows and a UCU model on the columns. The column factor loading matrices are the same as used for Simulation 1, $\mathbf{\Delta}_1$ is the same as in Simulation 1, and the row factor loadings matrix for group 2 is

$$\mathbf{\Delta}_2 = \begin{bmatrix} \mathbf{1}_{d/2} & -\mathbf{1}_{d/2} \\ \mathbf{1}_{d/2} & \mathbf{0}_{d/2} \end{bmatrix}.$$

We take $\mathbf{\Sigma}_1 = \mathbf{I}_d$, $\mathbf{\Sigma}_2 = 2\mathbf{I}_d$ and $\mathbf{\Psi}_1 = \mathbf{\Psi}_2 = \mathbf{D}$, where $\mathbf{D}$ is the same as from Simulation 1.

Results are displayed in Table 4. Overall, we obtain excellent classification results, even when the sample size is small and there is little spatial separation. There is some difficulty in choosing the column model when $d = 10$ but this issue abates for $N = 400$. When $d = 20$, some difficulty is encountered in choosing the correct number of column factors q; however, the classification performance is consistently excellent.

4.3 Simulation 3

In the last simulation, the mean matrices are now diagonal with diagonal entries equal to δ. A CCU model is taken for the rows. In the case of $d = 10$, the parameters are

Table 5 Number of datasets for which the BIC correctly chose the number of groups (G), column factors (q), row factors (r), row model (RM), column model (CM), and the average ARI over 25 datasets (Simulation 3)

δ	N	$d = 10$						$d = 20$					
		G	q	r	RM	CM	$\overline{\text{ARI}}$(sd)	G	q	r	RM	CM	$\overline{\text{ARI}}$(sd)
1	100	0	25	25	25	0	0.000(0.00)	0	25	25	25	0	0.000(0.00)
	200	0	25	25	20	0	0.000(0.00)	0	25	25	25	0	0.000(0.00)
	400	22	12	25	12	16	0.705(0.27)	22	21	24	19	13	0.833(0.32)
2	100	25	24	25	24	17	0.968(0.04)	21	24	25	25	10	0.840(0.37)
	200	25	25	25	25	11	0.984(0.02)	25	25	25	25	11	1.000(0.00)
	400	25	20	25	18	22	0.988(0.01)	25	25	25	25	20	1.000(0.00)
4	100	25	24	25	24	15	1.000(0.00)	25	25	25	25	18	1.000(0.00)
	200	25	25	25	25	10	1.000(0.00)	25	25	25	25	22	1.000(0.00)
	400	25	24	25	20	23	1.000(0.00)	25	25	25	25	17	1.000(0.00)

$$\boldsymbol{\Lambda}_1 = \boldsymbol{\Lambda}_2 = \begin{bmatrix} \mathbf{1}_3 & \mathbf{0}_3 & \mathbf{0}_3 \\ \mathbf{1}_2 & \mathbf{0}_2 & \mathbf{1}_2 \\ -\mathbf{1}_2 & -\mathbf{1}_2 & -\mathbf{1}_2 \\ -\mathbf{1}_3 & -\mathbf{1}_3 & \mathbf{0}_3 \end{bmatrix}, \qquad \boldsymbol{\Sigma}_1 = \boldsymbol{\Sigma}_2 = \mathbf{I}_{d\{\sigma_{2,2}=2,\sigma_{9,9}=4\}}.$$

To clarify this notation, the row scale matrices have 1s on the diagonal except for places 2 and 9 which have values 2 and 4, respectively. The column scale matrices have a UCC model with

$$\boldsymbol{\Delta}_1 = \begin{bmatrix} -\mathbf{1}_5 & \mathbf{0}_5 \\ \mathbf{1}_5 & \mathbf{1}_5 \end{bmatrix}, \qquad \boldsymbol{\Delta}_2 = \begin{bmatrix} -\mathbf{1}_5 & \mathbf{1}_5 \\ \mathbf{1}_5 & \mathbf{0}_5 \end{bmatrix}, \qquad \boldsymbol{\Psi}_1 = \boldsymbol{\Psi}_2 = \mathbf{I}_{10}.$$

In the case of $d = 20$, the parameters are

$$\boldsymbol{\Lambda}_1 = \boldsymbol{\Lambda}_2 = \begin{bmatrix} \mathbf{1}_6 & \mathbf{0}_6 & \mathbf{0}_6 \\ \mathbf{1}_4 & \mathbf{0}_4 & \mathbf{1}_4 \\ -\mathbf{1}_4 & -\mathbf{1}_4 & -\mathbf{1}_4 \\ -\mathbf{1}_6 & -\mathbf{1}_6 & \mathbf{0}_6 \end{bmatrix}, \qquad \boldsymbol{\Sigma}_1 = \boldsymbol{\Sigma}_2 = \mathbf{I}_{30\{\sigma_{2,2}=4,\sigma_{9,9}=2,\sigma_{12,12}=3,\sigma_{19,19}=5\}},$$

and

$$\boldsymbol{\Delta}_1 = \begin{bmatrix} -\mathbf{1}_{10} & \mathbf{0}_{10} \\ \mathbf{1}_{10} & \mathbf{1}_{10} \end{bmatrix}, \qquad \boldsymbol{\Delta}_2 = \begin{bmatrix} -\mathbf{1}_{10} & \mathbf{1}_{10} \\ \mathbf{1}_{10} & \mathbf{0}_{10} \end{bmatrix}, \qquad \boldsymbol{\Psi}_1 = \boldsymbol{\Psi}_2 = \mathbf{I}_{20}.$$

The results are presented in Table 5. In this case, there is more variability in the correct selection of the row and column models, especially the latter. The selection of q and r is generally accurate. The classification performance is generally very good with the exception of the combination of a small sample size N with a low degree of separation δ.

Table 6 Average ARI values and misclassification rates for each level of supervision, with respective standard deviations in parentheses, for datasets consisting of digits 1 and 2 drawn from the MNIST dataset

Supervision (%)	ARI	Misclassification rate
0 (clustering)	0.652(0.05)	0.0962(0.02)
25	0.733(0.059)	0.072(0.02)
50	0.756(0.064)	0.065(0.018)

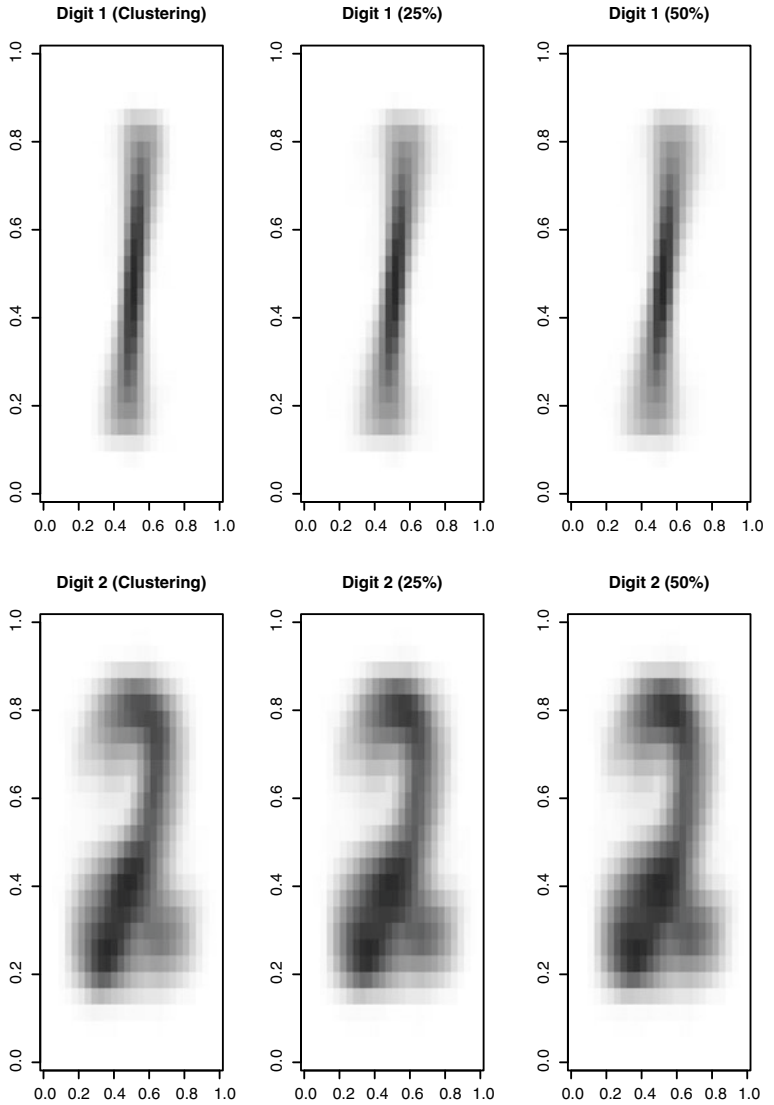

Fig. 1 Heatmaps of the mean matrices, from one of the datasets, for each digit at each level of supervision

5 MNIST Data Analysis

Gallaugher and McNicholas [12, 13] consider the MNIST digits dataset; specifically, digits 1 and 7 because they are quite similar in appearance. Herein, we consider digits 1 and 2. This dataset consists of 60,000 (training) images of Arabic numerals 0–9. We consider different levels of supervision and perform either clustering or semi-supervised classification. Specifically, we look at 0 (clustering), 25, and 50% supervision. For each level of supervision, 25 datasets consisting of 200 images each of digits 1 and 2 are taken. As discussed in Gallaugher and McNicholas [12], because of the lack of variability in the outlying rows and columns of the data matrices, random noise is added to ensure non-singularity of the scale matrices. In Table 6, we present the average ARIs and misclassification rates along with respective standard deviations.

As expected, as the level of supervision is increased, better classification performance is obtained. Specifically, the MCR decreases to around 6.5% with an ARI of 0.756 when the level of supervision is raised to 50%. Moreover, the performance in the completely unsupervised case is fairly good. In Fig. 1, heatmaps for the estimated mean matrices, for one dataset, for each digit and level of supervision are presented. Although barely perceptible, there is a slight increase in clarity as the supervision is raised to 50%. For all levels of supervision, the UUU row model is chosen for all 25 datasets. The chosen model for the columns is the UCU model for 7 of the 25 datasets for 0 and 50% supervision, and 10 datasets for 25% supervision.

6 Discussion

The PMMVBFA family, which comprises a total of 64 models has been introduced and presented. The PMMVBFA family is essentially a matrix variate analogue of the family of multivariate models introduced by McNicholas and Murphy [26]. In all simulations considered, very good classification results were obtained. In some settings, this was true even for small sample sizes and a small amount of spatial separation. Model selection was also generally accurate. In the MNIST analysis, classification accuracy increased with the amount of supervision, as expected, with the MCR decreasing to 6.5% when using a supervision level of 50%.

One very important consideration for future work is the development of a search algorithm as an alternative to fitting all possible models. This would be particularly important for computational feasibility when there is limited parallelization available. These parsimonious models could also be extended to the mixtures of skewed matrix variate bilinear factor analyzers (Gallaugher & McNicholas [14], as well as an extension to multi-way data (e.g., in the fashion of Tait & McNicholas [39]).

7 Appendix

7.1 Updates for Scale Matrices and Factor Loadings

The updates for the scale matrices and the factor loading matrices in the AECM algorithm are dependent on the model. The exact updates for each model are presented here.

Row Model Updates

CCC:

$$\hat{\boldsymbol{\Lambda}} = \left(\sum_{g=1}^{G}\sum_{i=1}^{N}\hat{z}_{ig}(\mathbf{X}_i - \hat{\mathbf{M}}_g)\hat{\boldsymbol{\Psi}}_g^{*^{-1}}a_{ig}^{A\prime}\right)\left(\sum_{g=1}^{G}\sum_{i=1}^{N}\hat{z}_{ig}b_{ig}^{B}\right)^{-1}, \quad \hat{\sigma} = \frac{1}{Npn}\operatorname{tr}\{\mathbf{S}^{(1)}\}.$$

where

$$\mathbf{S}^{(1)} = \sum_{g=1}^{G}\sum_{i=1}^{N}\hat{z}_{ig}\left[(\mathbf{X}_i - \hat{\mathbf{M}}_g)\hat{\boldsymbol{\Psi}}_g^{*^{-1}}(\mathbf{X}_i - \hat{\mathbf{M}}_g)' - \hat{\boldsymbol{\Lambda}}a_{ig}^{B\prime}\hat{\boldsymbol{\Psi}}_g^{*^{-1}}(\mathbf{X}_i - \hat{\mathbf{M}}_g)'\right].$$

CCU:

$$\hat{\boldsymbol{\Lambda}} = \left(\sum_{g=1}^{G}\sum_{i=1}^{N}\hat{z}_{ig}(\mathbf{X}_i - \hat{\mathbf{M}}_g)\hat{\boldsymbol{\Psi}}_g^{*^{-1}}a_{ig}^{B\prime}\right)\left(\sum_{g=1}^{G}\sum_{i=1}^{N}\hat{z}_{ig}b_{ig}^{B}\right)^{-1}, \quad \hat{\boldsymbol{\Sigma}} = \frac{1}{Np}\operatorname{diag}\{\mathbf{S}^{(1)}\},$$

CUU:
For this model, the update for $\boldsymbol{\Lambda}$ needs to be performed row by row. Specifically, the updates are:

$$\hat{\boldsymbol{\Lambda}}_{(j)} = \left(\sum_{i=1}^{N}\hat{z}_{ig}(\mathbf{X}_i - \hat{\mathbf{M}}_g)\hat{\boldsymbol{\Psi}}_g^{*^{-1}}a_{ig}^{B\prime}\right)_{(j)}\left(\sum_{g=1}^{G}\frac{1}{\sigma_{g(jj)}}\sum_{i=1}^{N}\hat{z}_{ig}b_{ig}^{B}\right)^{-1},$$

$$\hat{\boldsymbol{\Sigma}}_g = \frac{1}{N_g p}\operatorname{diag}\{\mathbf{S}_g^{(2)}\},$$

where

$$\mathbf{S}_g^{(2)} = \sum_{i=1}^{N}\hat{z}_{ig}\left[(\mathbf{X}_i - \hat{\mathbf{M}}_g)\hat{\boldsymbol{\Psi}}_g^{*^{-1}}(\mathbf{X}_i - \hat{\mathbf{M}}_g)' - 2\hat{\boldsymbol{\Lambda}}a_{ig}^{B}\hat{\boldsymbol{\Psi}}_g^{*^{-1}}(\mathbf{X}_i - \hat{\mathbf{M}}_g)' + \hat{\boldsymbol{\Lambda}}b_{ig}^{B}\hat{\boldsymbol{\Lambda}}'\right].$$

CUC:

$$\hat{\boldsymbol{\Lambda}} = \left(\sum_{g=1}^{G}\frac{1}{\hat{\sigma}_g}\sum_{i=1}^{N}\hat{z}_{ig}(\mathbf{X}_i-\hat{\mathbf{M}}_g)\hat{\boldsymbol{\Psi}}_g^{*^{-1}}a_{ig}^{B\prime}\right)\left(\sum_{g=1}^{G}\frac{1}{\hat{\sigma}_g}\sum_{i=1}^{N}\hat{z}_{ig}b_{ig}^{B}\right)^{-1},$$
$$\hat{\sigma}_g = \frac{1}{N_g np}\operatorname{tr}\{\mathbf{S}_g^{(2)}\}.$$

UCC:

$$\hat{\boldsymbol{\Lambda}}_g = \left(\sum_{i=1}^{N}\hat{z}_{ig}(\mathbf{X}_i-\hat{\mathbf{M}}_g)\hat{\boldsymbol{\Psi}}_g^{*^{-1}}a_{ig}^{B\prime}\right)\left(\sum_{i=1}^{N}\hat{z}_{ig}b_{ig}^{B}\right)^{-1}, \quad \hat{\sigma} = \frac{1}{Nnp}\operatorname{tr}\{\mathbf{S}^{(3)}\},$$

where

$$\mathbf{S}^{(3)} = \sum_{g=1}^{G}\sum_{i=1}^{N}\hat{z}_{ig}\left[(\mathbf{X}_i-\hat{\mathbf{M}}_g)\hat{\boldsymbol{\Psi}}_g^{*^{-1}}(\mathbf{X}_i-\hat{\mathbf{M}}_g)' - \hat{\boldsymbol{\Lambda}}_g a_{ig}^{B\prime}\hat{\boldsymbol{\Psi}}_g^{*^{-1}}(\mathbf{X}_i-\hat{\mathbf{M}}_g)'\right].$$

UCU:

$$\hat{\boldsymbol{\Lambda}}_g = \left(\sum_{i=1}^{N}\hat{z}_{ig}(\mathbf{X}_i-\hat{\mathbf{M}}_g)\hat{\boldsymbol{\Psi}}_g^{*^{-1}}a_{ig}^{B\prime}\right)\left(\sum_{i=1}^{N}\hat{z}_{ig}b_{ig}^{B}\right)^{-1}, \quad \hat{\boldsymbol{\Sigma}} = \frac{1}{Np}\operatorname{diag}\{\mathbf{S}^{(3)}\}.$$

UUC:

$$\hat{\boldsymbol{\Lambda}}_g = \left(\sum_{i=1}^{N}\hat{z}_{ig}(\mathbf{X}_i-\hat{\mathbf{M}}_g)\hat{\boldsymbol{\Psi}}_g^{*^{-1}}a_{ig}^{B\prime}\right)\left(\sum_{i=1}^{N}\hat{z}_{ig}b_{ig}^{B}\right)^{-1}, \quad \hat{\sigma}_g = \frac{1}{N_g np}\operatorname{tr}\{\mathbf{S}_g^{(4)}\},$$

where

$$\mathbf{S}_g^{(4)} = \sum_{i=1}^{N}\hat{z}_{ig}\left[(\mathbf{X}_i-\hat{\mathbf{M}}_g)\hat{\boldsymbol{\Psi}}_g^{*^{-1}}(\mathbf{X}_i-\hat{\mathbf{M}}_g)' - \hat{\boldsymbol{\Lambda}}_g a_{ig}^{B}\hat{\boldsymbol{\Psi}}_g^{*^{-1}}(\mathbf{X}_i-\hat{\mathbf{M}}_g)'\right].$$

UUU:

$$\hat{\boldsymbol{\Lambda}}_g = \left(\sum_{i=1}^{N}\hat{z}_{ig}(\mathbf{X}_i-\hat{\mathbf{M}}_g)\hat{\boldsymbol{\Psi}}_g^{*^{-1}}a_{ig}^{B\prime}\right)\left(\sum_{i=1}^{N}\hat{z}_{ig}b_{ig}^{B}\right)^{-1}, \quad \hat{\boldsymbol{\Sigma}}_g = \frac{1}{N_g p}\operatorname{diag}\{\mathbf{S}_g^{(4)}\}.$$

Column Model Updates

CCC:

$$\hat{\boldsymbol{\Delta}} = \left(\sum_{g=1}^{G}\sum_{i=1}^{N}\hat{z}_{ig}(\mathbf{X}_i - \hat{\mathbf{M}}_g)'\hat{\boldsymbol{\Sigma}}_g^{*^{-1}}a_{ig}^A\right)\left(\sum_{g=1}^{G}\sum_{i=1}^{N}\hat{z}_{ig}b_{ig}^A\right)^{-1}, \quad \hat{\psi} = \frac{1}{Nnp}\,\mathrm{tr}\{\mathbf{P}^{(1)}\},$$

where

$$\mathbf{P}^{(1)} = \sum_{g=1}^{G}\sum_{i=1}^{N}\hat{z}_{ig}\big[(\mathbf{X}_i - \hat{\mathbf{M}}_g)'\hat{\boldsymbol{\Sigma}}_g^{*^{-1}}(\mathbf{X}_i - \hat{\mathbf{M}}_g) - \hat{\boldsymbol{\Delta}}a_{ig}^{A\prime}\hat{\boldsymbol{\Sigma}}_g^{*^{-1}}(\mathbf{X}_i - \hat{\mathbf{M}}_g)\big].$$

CCU:

$$\hat{\boldsymbol{\Delta}} = \left(\sum_{g=1}^{G}\sum_{i=1}^{N}\hat{z}_{ig}(\mathbf{X}_i - \hat{\mathbf{M}}_g)'\hat{\boldsymbol{\Sigma}}_g^{*^{-1}}a_{ig}^A\right)\left(\sum_{g=1}^{G}\sum_{i=1}^{N}\hat{z}_{ig}b_{ig}^A\right)^{-1}, \quad \hat{\boldsymbol{\Psi}} = \frac{1}{Nn}\,\mathrm{diag}\{\mathbf{P}^{(1)}\}.$$

CUU:
For this model, the update for $\boldsymbol{\Delta}$ needs to be performed row by row. Specifically the updates are:

$$\hat{\boldsymbol{\Delta}}_{(j)} = \left(\sum_{i=1}^{N}\hat{z}_{ig}(\mathbf{X}_i - \hat{\mathbf{M}}_g)'\hat{\boldsymbol{\Sigma}}_g^{*^{-1}}a_{ig}^A\right)_{(j)}\left(\sum_{g=1}^{G}\frac{1}{\psi_{g_{(jj)}}}\sum_{i=1}^{N}\hat{z}_{ig}b_{ig}^A\right)^{-1},$$

$$\hat{\boldsymbol{\Psi}}_g = \frac{1}{N_g n}\,\mathrm{diag}\{\mathbf{P}_g^{(2)}\},$$

where

$$\mathbf{P}_g^{(2)} = \sum_{i=1}^{N}\hat{z}_{ig}\big[(\mathbf{X}_i - \hat{\mathbf{M}}_g)'\hat{\boldsymbol{\Sigma}}_g^{*^{-1}}(\mathbf{X}_i - \hat{\mathbf{M}}_g) - 2\hat{\boldsymbol{\Delta}}a_{ig}^{A\prime}\hat{\boldsymbol{\Sigma}}_g^{*^{-1}}(\mathbf{X}_i - \hat{\mathbf{M}}_g) + \hat{\boldsymbol{\Delta}}b_{ig}^A\hat{\boldsymbol{\Delta}}'\big].$$

CUC:

$$\hat{\boldsymbol{\Delta}} = \left(\sum_{g=1}^{G}\frac{1}{\hat{\psi}_g}\sum_{i=1}^{N}\hat{z}_{ig}(\mathbf{X}_i - \hat{\mathbf{M}}_g)'\hat{\boldsymbol{\Sigma}}_g^{*^{-1}}a_{ig}^A\right)\left(\sum_{g=1}^{G}\frac{1}{\hat{\psi}_g}\sum_{i=1}^{N}\hat{z}_{ig}b_{ig}^A\right)^{-1},$$

$$\hat{\psi}_g = \frac{1}{N_g np}\,\mathrm{tr}\{\mathbf{P}_g^{(2)}\}.$$

UCC:

$$\hat{\boldsymbol{\Delta}}_g = \left(\sum_{i=1}^{N} \hat{z}_{ig}(\mathbf{X}_i - \hat{\mathbf{M}}_g)' \hat{\boldsymbol{\Sigma}}_g^{*^{-1}} a_{ig}^A\right)\left(\sum_{i=1}^{N} \hat{z}_{ig} b_{ig}^A\right)^{-1}, \quad \hat{\psi} = \frac{1}{Nnp}\,\mathrm{tr}\{\mathbf{P}^{(3)}\},$$

where

$$\mathbf{P}^{(3)} = \sum_{g=1}^{G}\sum_{i=1}^{N} \hat{z}_{ig}\left[(\mathbf{X}_i - \hat{\mathbf{M}}_g)' \hat{\boldsymbol{\Sigma}}_g^{*^{-1}} (\mathbf{X}_i - \hat{\mathbf{M}}_g) - \hat{\boldsymbol{\Delta}}_g a_{ig}^{A\prime} \hat{\boldsymbol{\Sigma}}_g^{*^{-1}} (\mathbf{X}_i - \hat{\mathbf{M}}_g)\right].$$

UCU:

$$\hat{\boldsymbol{\Delta}}_g = \left(\sum_{i=1}^{N} \hat{z}_{ig}(\mathbf{X}_i - \hat{\mathbf{M}}_g)' \hat{\boldsymbol{\Sigma}}_g^{*^{-1}} a_{ig}^A\right)\left(\sum_{i=1}^{N} \hat{z}_{ig} b_{ig}^A\right)^{-1}, \quad \hat{\boldsymbol{\Psi}} = \frac{1}{Nn}\,\mathrm{diag}\{\mathbf{P}^{(3)}\}.$$

UUC:

$$\hat{\boldsymbol{\Delta}}_g = \left(\sum_{i=1}^{N} \hat{z}_{ig}(\mathbf{X}_i - \hat{\mathbf{M}}_g)' \hat{\boldsymbol{\Sigma}}_g^{*^{-1}} a_{ig}^A\right)\left(\sum_{i=1}^{N} \hat{z}_{ig} b_{ig}^A\right)^{-1}, \quad \hat{\psi}_g = \frac{1}{N_g np}\,\mathrm{tr}\{\mathbf{P}_g^{(4)}\},$$

where

$$\mathbf{P}_g^{(4)} = \sum_{i=1}^{N} \hat{z}_{ig}\left[(\mathbf{X}_i - \hat{\mathbf{M}}_g)' \hat{\boldsymbol{\Sigma}}_g^{*^{-1}} (\mathbf{X}_i - \hat{\mathbf{M}}_g) - \hat{\boldsymbol{\Delta}}_g a_{ig}^{A\prime} \hat{\boldsymbol{\Sigma}}_g^{*^{-1}} (\mathbf{X}_i - \hat{\mathbf{M}}_g)\right].$$

UUU:

$$\hat{\boldsymbol{\Delta}}_g = \left(\sum_{i=1}^{N} \hat{z}_{ig}(\mathbf{X}_i - \hat{\mathbf{M}}_g)' \hat{\boldsymbol{\Sigma}}_g^{*^{-1}} a_{ig}^A\right)\left(\sum_{i=1}^{N} \hat{z}_{ig} b_{ig}^A\right)^{-1}, \quad \hat{\boldsymbol{\Psi}}_g = \frac{1}{N_g n}\,\mathrm{diag}\{\mathbf{P}_g^{(4)}\}.$$

References

1. Aitken, A. C. (1926). A series formula for the roots of algebraic and transcendental equations. *Proceedings of the Royal Society of Edinburgh*, *45*, 14–22.
2. Andrews, J. L., & McNicholas, P. D. (2011). Extending mixtures of multivariate t-factor analyzers. *Statistics and Computing*, *21*(3), 361–373.
3. Andrews, J. L., & McNicholas, P. D. (2012). Model-based clustering, classification, and discriminant analysis via mixtures of multivariate *t*-distributions: The *t*EIGEN family. *Statistics and Computing*, *22*(5), 1021–1029.
4. Baum, L. E., Petrie, T., Soules, G., & Weiss, N. (1970). A maximization technique occurring in the statistical analysis of probabilistic functions of Markov chains. *Annals of Mathematical Statistics*, *41*, 164–171.

5. Böhning, D., Dietz, E., Schaub, R., Schlattmann, P., & Lindsay, B. (1994). The distribution of the likelihood ratio for mixtures of densities from the one-parameter exponential family. *Annals of the Institute of Statistical Mathematics*, *46*, 373–388.
6. Browne, R. P., & McNicholas, P. D. (2015). A mixture of generalized hyperbolic distributions. *Canadian Journal of Statistics*, *43*(2), 176–198.
7. Celeux, G., & Govaert, G. (1995). Gaussian parsimonious clustering models. *Pattern Recognition*, *28*(5), 781–793.
8. Dang, U. J., Browne, R. P., & McNicholas, P. D. (2015). Mixtures of multivariate power exponential distributions. *Biometrics*, *71*(4), 1081–1089.
9. Franczak, B. C., Tortora, C., Browne, R. P., & McNicholas, P. D. (2015). Unsupervised learning via mixtures of skewed distributions with hypercube contours. *Pattern Recognition Letters*, *58*(1), 69–76.
10. Gallaugher, M. P. B., Biernacki, C., & McNicholas, P. D. (2018). Relaxing the identically distributed assumption in Gaussian co-clustering for high dimensional data. arXiv preprint arXiv:1808.08366.
11. Gallaugher, M. P. B., & McNicholas, P. D. (2017). A matrix variate skew-t distribution. *Stat*, *6*(1), 160–170.
12. Gallaugher, M. P. B., & McNicholas, P. D. (2018a). Finite mixtures of skewed matrix variate distributions. *Pattern Recognition*, *80*, 83–93.
13. Gallaugher, M. P. B. & McNicholas, P. D. (2018b). Mixtures of matrix variate bilinear factor analyzers. In *Proceedings of the Joint Statistical Meetings*, Alexandria, VA. American Statistical Association. Preprint available as arXiv:1712.08664.
14. Gallaugher, M. P. B. & McNicholas, P. D. (2019a). Mixtures of skewed matrix variate bilinear factor analyzers. *Advances in Data Analysis and Classification*. To appear.
15. Gallaugher, M. P. B., & McNicholas, P. D. (2019b). Three skewed matrix variate distributions. *Statistics and Probability Letters*, *145*, 103–109.
16. Gallaugher, M. P. B., Tang, Y., & McNicholas, P. D. (2019). Flexible clustering with a sparse mixture of generalized hyperbolic distributions. arXiv preprint arXiv:1903.05054.
17. Ghahramani, Z., & Hinton, G. E. (1997). The EM algorithm for factor analyzers. Technical Report CRG-TR-96-1, University of Toronto, Toronto, Canada.
18. Harrar, S. W., & Gupta, A. K. (2008). On matrix variate skew-normal distributions. *Statistics*, *42*(2), 179–194.
19. Hartigan, J. A. (1972). Direct clustering of a data matrix. *Journal of the American Statistical Association*, *67*(337), 123–129.
20. Hubert, L., & Arabie, P. (1985). Comparing partitions. *Journal of Classification*, *2*(1), 193–218.
21. Lee, S., & McLachlan, G. J. (2014). Finite mixtures of multivariate skew t-distributions: Some recent and new results. *Statistics and Computing*, *24*, 181–202.
22. Lin, T.-I. (2010). Robust mixture modeling using multivariate skew t distributions. *Statistics and Computing*, *20*(3), 343–356.
23. Lin, T.-I., McNicholas, P. D., & Hsiu, J. H. (2014). Capturing patterns via parsimonious t mixture models. *Statistics and Probability Letters*, *88*, 80–87.
24. Lindsay, B. G. (1995). Mixture models: Theory, geometry and applications. In *NSF-CBMS Regional Conference Series in Probability and Statistics* (vol. 5). California: Institute of Mathematical Statistics: Hayward.
25. McLachlan, G. J. & Peel, D. (2000). Mixtures of factor analyzers. In *Proceedings of the seventh international conference on machine learning* (pp. 599–606). San Francisco. Morgan Kaufmann.
26. McNicholas, P. D., & Murphy, T. B. (2008). Parsimonious Gaussian mixture models. *Statistics and Computing*, *18*(3), 285–296.
27. McNicholas, P. D., Murphy, T. B., McDaid, A. F., & Frost, D. (2010). Serial and parallel implementations of model-based clustering via parsimonious Gaussian mixture models. *Computational Statistics and Data Analysis*, *54*(3), 711–723.
28. Melnykov, V., & Zhu, X. (2018). On model-based clustering of skewed matrix data. *Journal of Multivariate Analysis*, *167*, 181–194.

29. Murray, P. M., Browne, R. B., & McNicholas, P. D. (2014). Mixtures of skew-t factor analyzers. *Computational Statistics and Data Analysis*, *77*, 326–335.
30. Murray, P. M., Browne, R. B., & McNicholas, P. D. (2017). Hidden truncation hyperbolic distributions, finite mixtures thereof, and their application for clustering. *Journal of Multivariate Analysis*, *161*, 141–156.
31. Murray, P. M., McNicholas, P. D., & Browne, R. B. (2014). A mixture of common skew-*t* factor analyzers. *Stat*, *3*(1), 68–82.
32. Nadif, M. & Govaert, G. (2010). Model-based co-clustering for continuous data. In *2010 Ninth international conference on machine learning and applications* (pp. 175–180). IEEE.
33. Pan, W., & Shen, X. (2007). Penalized model-based clustering with application to variable selection. *Journal of Machine Learning Research*, *8*, 1145–1164.
34. Peel, D., & McLachlan, G. J. (2000). Robust mixture modelling using the t distribution. *Statistics and Computing*, *10*(4), 339–348.
35. Rand, W. M. (1971). Objective criteria for the evaluation of clustering methods. *Journal of the American Statistical Association*, *66*(336), 846–850.
36. Sarkar, S., Zhu, X., Melnykov, V., & Ingrassia, S. (2020). On parsimonious models for modeling matrix data. *Computational Statistics & Data Analysis*, *142*, 106822.
37. Schwarz, G. (1978). Estimating the dimension of a model. *The Annals of Statistics*, *6*(2), 461–464.
38. Scott, A. J., & Symons, M. J. (1971). Clustering methods based on likelihood ratio criteria. *Biometrics*, *27*, 387–397.
39. Tait, P. A. & McNicholas, P. D. (2019). Clustering higher order data: Finite mixtures of multidimensional arrays. arXiv preprint arXiv:1907.08566.
40. Tang, Y., Browne, R. P., & McNicholas, P. D. (2018). Flexible clustering of high-dimensional data via mixtures of joint generalized hyperbolic distributions. *Stat*, *7*(1), e177.
41. Tipping, M. E., & Bishop, C. M. (1999a). Mixtures of probabilistic principal component analysers. *Neural Computation*, *11*(2), 443–482.
42. Tipping, M. E., & Bishop, C. M. (1999b). Probabilistic principal component analysers. *Journal of the Royal Statistical Society Series B*, *61*, 611–622.
43. Tortora, C., Franczak, B. C., Browne, R. P., & McNicholas, P. D. (2019). A mixture of coalesced generalized hyperbolic distributions. *Journal of Classification*, *36*(1), 26–57.
44. Viroli, C. (2011). Finite mixtures of matrix normal distributions for classifying three-way data. *Statistics and Computing*, *21*(4), 511–522.
45. Vrbik, I., & McNicholas, P. D. (2012). Analytic calculations for the EM algorithm for multivariate skew-t mixture models. *Statistics and Probability Letters*, *82*(6), 1169–1174.
46. Vrbik, I., & McNicholas, P. D. (2014). Parsimonious skew mixture models for model-based clustering and classification. *Computational Statistics and Data Analysis*, *71*, 196–210.
47. Wolfe, J. H. (1965). A computer program for the maximum likelihood analysis of types. Technical Bulletin 65-15, U.S. Naval Personnel Research Activity.
48. Xie, X., Yan, S., Kwok, J. T., & Huang, T. S. (2008). Matrix-variate factor analysis and its applications. *IEEE Transactions on Neural Networks*, *19*(10), 1821–1826.
49. Yu, S., Bi, J., & Ye, J. (2008). Probabilistic interpretations and extensions for a family of 2D PCA-style algorithms. In *Workshop data mining using matrices and tensors (DMMT '08): Proceedings of a workshop held in conjunction with the 14th ACM SIGKDD international conference on knowledge discovery and data mining (SIGKDD 2008)*.
50. Zhao, J., Philip, L., & Kwok, J. T. (2012). Bilinear probabilistic principal component analysis. *IEEE Transactions on Neural Networks and Learning Systems*, *23*(3), 492–503.
51. Zhou, H., Pan, W., & Shen, X. (2009). Penalized model-based clustering with unconstrained covariance matrices. *Electronic Journal of Statistics*, *3*, 1473.

Interval-Valued Scaling of Successive Categories

Hisao Miyano and Eric J. Beh

Abstract Correspondence analysis represents the row and column categories of a contingency table as points in a low dimensional space, irrespective of whether the categories are successive or not. In this paper, a scaling method is considered for successive categories that are regarded as a series of boxes (intervals) or numbers defined on a line scale. By using this method, each category is represented as a region not as a point under the assumptions that (1) each category is represented by an interval for which the end points lie on the boundary of its adjacent category, and (2) the scale values of the category are uniformly distributed over the interval. It is shown that the proposed method has simple links to correspondence analysis and multiple correspondence analysis. The effectiveness of the method is confirmed by considering some examples.

1 Introduction

As a quantitative method for analysing contingency tables, many researchers have proposed and/or investigated several methods for assigning scores to the rows and columns of a contingency table. For correspondence analysis, one may refer to Benzécri [1], Greenacre [12], Gower and Hand [11], Nenadić and Greenacre [20], and Beh and Lombardo [4]. This issue was also considered for optimal (or dual) scaling (Guttman [13]; Nishisato [22]) quantification method (Hayashi, Higuchi, & Komazawa [14]), and reciprocal averaging (Hill [15]; Mardia, Kent, & Bibby [18]).

H. Miyano (✉)
Chiba University, Chiba, Japan
e-mail: hina_miyan@icloud.com

E. J. Beh
University of Newcastle, Callaghan, NSW, Australia
e-mail: eric.beh@newcastle.edu.au

T. Imaizumi et al. (eds.), *Advanced Studies in Behaviormetrics and Data Science*,
Behaviormetrics: Quantitative Approaches to Human Behavior 5,
https://doi.org/10.1007/978-981-15-2700-5_12

For the analysis of a contingency table with successive categories, correspondence analysis and optimal scaling methods under order constraints have been studied (Schriever [28]; Parsa & Smith [26]; Ritov & Gilula [27]; Beh [2, 3]; Yang & Huh [31]; Lombardo, Beh, & D'Ambra [16]; Nishisato & Arri [24]). Another method is to consider a dual scaling method for successive categories proposed by Nishisato [23] and Nishisato and Sheu [25]. Such a method is a uni-dimensional scaling method which enables one to estimate both the scores of objects and the scale values of category boundaries as the method of successive categories Torgerson [30] does. Nishisato's method is an optimal scaling method which is different from the method of successive categories in the sense that it does not employ any assumption about the distribution of responses Nishisato [21]. Gifi [9] also offered a collection of nonlinear multivariate methods based on optimal scaling which includes an order-constraint uni-dimensional scaling method for successive categories. By extending the Gifi's approach, Mair and de Leeuw [17] proposed a general framework of multivariate analysis with optimal scaling of which the theoretical foundations were given by de Leeuw [8].

When considering these methods, it is commonly assumed that each row and column of a contingency table is represented by a point in a multidimensional space. However, as successive categories are often regarded as a series of intervals defined on a line scale, they are intrinsically consecutive and have more or less ambiguous meanings. In that sense, if the column categories of a contingency table are successive, they might be well represented as successively connected regions or intervals rather than points in the space.

By utilising the idea of Guttman's optimal scaling, this paper presents a new scaling method for successive categories, in which each category is represented as a region but not as a point in a multidimensional space. The scaling method is constructed under the assumptions that (1) each category is represented by a corresponding interval for which the end points are the boundary points of its adjacent categories, and (2) the scores of the object in each category are uniformly distributed over the corresponding interval. The first assumption gives a representation of successive categories by intervals, and the second defines a distribution of object scores within a category.

This paper is structured as follows. First, we shall discuss the scaling problem for a single categorical variable by considering the quantification problem for a contingency table with successive categories. A two-sided eigen equation for interval-valued scaling of successive categories is derived, which has a simple relation to that of correspondence analysis. The interval scaling problem for a contingency table with more than two variables is also addressed, and the two-sided eigen equation corresponding to that for the case of a single categorical variable is provided. Some mathematical discussions are made on the solution of the two-sided eigen equation.

Numerical examples are given to illustrate the effectiveness of the interval-valued scaling method. Discussions are made, in particular, on the scaling method for a general contingency table, which includes both successive and non-successive categorical variables.

2 Scaling of Successive Categories in Contingency Table

In this section, first we give the motivation and the basic idea of our approach to the scaling problem of successive categories, as well as the definitions and the notation used throughout this paper. We then discuss the scaling method for a successive categorical variable.

2.1 Motivation and Basic Idea

As mentioned in the previous section, several methods, including correspondence analysis, optimal scaling, dual scaling, and reciprocal averaging, have been proposed as the quantification method of contingency tables. It is known that these methods are algebraically equivalent to each other (e.g., Greenacre [12]), while having originated in different contexts.

Contingency tables are generally used to describe the association between the row and column variables of the table, where each row and each column in the table represents a category of the corresponding variable. Conventional quantification methods quantify the two variables by assigning scores to the categories, under the assumption that each category is represented by a point in a multidimensional space. However, the assumption of representing categories as points might be not so appropriate if the row or column categories are successive.

As a continuous variable is often categorised by defining the categories in terms of intervals or classes of values it can take, successive categories are typically regarded as a series of boxes (intervals) or numbers defined on a line scale, and verbal descriptions, such as *fairly* and *somewhat*, are often attached to them. Hence, if each successive category is represented as a point in a multidimensional space, then the point is considered to be a representative of the corresponding interval or range represented in the space.

The aim of this paper is to provide a scaling method for successive categories which enables us to evaluate the variations in the scale values of categories. In other words, using the idea of optimal scaling, a new scaling method is developed under the assumption that the scale value assigned to each category has an internal variation. For example, the samples from a certain category of which the scaled interval is $[t_1, t_2]$ are interpreted as selecting values randomly across this interval. As is noted in the symbolic data analysis for interval-valued data, this is not to be confused with uncertainty or the impression when a variable takes a value in that interval with some level of uncertainty (Billard & Diday [6]).

Let $N = (n_{ik})$ be an $r \times c$ matrix where $n_{ik}, i = 1, 2, \ldots, r, k = 1, 2, \ldots, c$, are the frequencies in an $r \times c$ contingency table, r is the number of objects to be observed, and c is the number of categories. Following the conventional notation, we define $R = \mathrm{diag}(n_{i.})$ and $C = \mathrm{diag}(n_{.k})$ to be r-dimensional and c-dimensional diagonal matrices, respectively, where $n_{i.} = \sum_k n_{ik}$, $n_{.k} = \sum_i n_{ik}$, and $n_{..} = \sum_{i,k} n_{ik}$.

Suppose that category k is represented by an interval $[t_k, t_{k+1}]$ or $[t_{k+1}, t_k]$; that is, the categories k and $k+1$ are differentiated at the point t_{k+1}, and the scores at each category are uniformly distributed over the corresponding interval. Then the scores of object i can be considered to be randomly distributed as a mixture of c uniform distributions with mixing proportions $n_{ik}/n_{i.}, k = 1, 2, \ldots, c$; that is, its probability density function $h_i(x)$ is given by

$$h_i(x) = \sum_{k=1}^{c} \frac{n_{ik}}{n_{i.}} u_k(x), \tag{1}$$

where $u_k(x)$ is the probability density function of the uniform distribution corresponding to the k-th interval. Then, the expected score $\bar{x}_i$ and the variance s_i^2 of object i are given by

$$\begin{aligned} \bar{x}_i &= \int x h_i(x) dx \\ &= \sum_{k=1}^{c} \frac{n_{ik}}{n_{i.}} \bar{t}_k, \end{aligned} \tag{2}$$

$$\begin{aligned} s_i^2 &= \int (x - \bar{x}_i)^2 h_i(x) dx \\ &= \sum_{k=1}^{c} \frac{n_{ik}}{n_{i.}} (v_k^2 + (\bar{t}_k - \bar{x}_i)^2) \\ &= \sum_{k=1}^{c} \frac{n_{ik}}{n_{i.}} (v_k^2 + \bar{t}_k^2) - \bar{x}_i^2, \end{aligned} \tag{3}$$

where $\bar{t}_k = (t_k + t_{k+1})/2$, and v_k^2 is the variance of scores within the k-th interval; that is, $v_k^2 = (t_{k+1} - t_k)^2/12$.

Let $\bar{\boldsymbol{x}}$ be a r-dimensional column vector defined by $\bar{\boldsymbol{x}} = (\bar{x}_1, \bar{x}_2, \ldots, \bar{x}_r)'$, $\boldsymbol{t}$ be a $(c+1)$-dimensional vector defined by $\boldsymbol{t} = (t_1, t_2, \ldots, t_{c+1})'$, and O_+ and O_- be $c \times (c+1)$ matrices defined by $O_+ = (\mathbf{0}; I)$ and $O_- = (I; \mathbf{0})$, where I is a $c \times c$ identity matrix, and $\mathbf{0}$ is a c-dimensional vector of zeros. Then, using the matrix $\bar{N}$ defined by $\bar{N} = N(O_+ + O_-)/2$, the mean vector $\bar{\boldsymbol{x}}$ and the variance s_i^2 are represented by

$$\bar{\boldsymbol{x}} = R^{-1} \bar{N} \boldsymbol{t}, \tag{4}$$

$$s_i^2 = \frac{1}{n_{i.}} \boldsymbol{t}' G_i \boldsymbol{t} - \bar{x}_i^2, \tag{5}$$

where, using the matrix given by $D_i = \text{diag}(n_{i1}, n_{i2}, \ldots, n_{ic})$, G_i is defined by

$$G_i = \frac{1}{3}(O_+' D_i O_+ + \frac{1}{2}(O_+' D_i O_- + O_-' D_i O_+) + O_-' D_i O_-). \tag{6}$$

From (1), it is easy to see that our approach is an extension of optimal scaling approach. If μ_k is the score assigned to the k-th category, then, using the delta function $\delta(x)$, $u_k(x)$ is denoted by $u_k(x) = \delta(x - \mu_k)$, and $\bar{x}_i$ becomes the weighted mean of the category scores.

2.2 Scaling Method for Successive Categories

Assuming that $\sum_k n_{.k}\bar{t}_k = 0$, and for notational convenience, defining that $\bar{n}_{.k} = (n_{.k-1} + n_{.k})/2$, $n_{i0} = n_{i(c+1)} = 0$ for any i, the total variance s_t^2 and the between variance s_b^2 are given by

$$\begin{aligned} s_b^2 &= \frac{1}{n_{..}} \sum_{i=1}^{r} n_{i.} \bar{x}_i^2 \\ &= \frac{1}{n_{..}} \boldsymbol{t}' \bar{N}' R^{-1} \bar{N} \boldsymbol{t}, \end{aligned} \tag{7}$$

$$\begin{aligned} s_t^2 &= \sum_{i=1}^{r} \frac{n_{i.}}{n_{..}} s_i^2 + s_b^2 \\ &= \frac{1}{n_{..}} \boldsymbol{t}' G \boldsymbol{t}, \end{aligned} \tag{8}$$

where G is a matrix defined by $G = \sum_i G_i$.

It is easy to show that $\bar{N}' R^{-1} \bar{N}$ is a $(c+1) \times (c+1)$ symmetric matrix of which the (k, k')-element is given by $\sum_i \bar{n}_{ik} \bar{n}_{ik'} / n_{i.}$, $k, k' = 1, 2, \ldots, c+1$, and $(3/2)G$ is a tridiagonal symmetric matrix having $\bar{n}_{.k}$, $k = 1, 2, \ldots, c+1$ as diagonal elements and $n_{.k}/4$, $k = 1, 2, \ldots, c$ as sub-diagonal elements.

Following the traditional optimal scaling approach, the optimal $\boldsymbol{t}$ which maximises the ratio $\eta^2 = s_b^2 / s_t^2$ can be obtained; that is, under the assumption $\boldsymbol{t}' G \boldsymbol{t} = 1$, the optimal $\boldsymbol{t}$ satisfies

$$\bar{N}' R^{-1} \bar{N} \boldsymbol{t} = \lambda G \boldsymbol{t}, \tag{9}$$

where λ is a Lagrange multiplier corresponding to the constraint $\boldsymbol{t}' G \boldsymbol{t} = 1$. Here, $\bar{N}' R^{-1} \bar{N}$ is nonnegative definite, and G is positive definite if $\bar{n}_{.k} > 0$ for any k (Golub & van Loan [10]). Hence assuming that $\bar{n}_{.k} > 0$ for any k, the optimal $\boldsymbol{t}$ is obtained by solving the eigen equation

$$(R^{-\frac{1}{2}} \bar{N} G^{-\frac{1}{2}})' (R^{-\frac{1}{2}} \bar{N} G^{-\frac{1}{2}}) \boldsymbol{z} = \lambda \boldsymbol{z}, \tag{10}$$

where $\boldsymbol{z} = G^{\frac{1}{2}} \boldsymbol{t}$, and $\boldsymbol{z}'\boldsymbol{z} = 1$.

As it is well known in optimal scaling, the above two-sided eigen equation also has a trivial solution which corresponds to $\lambda = 1$, since $\bar{N}' R^{-1} \bar{N} \mathbf{1} = G\mathbf{1} = \bar{\boldsymbol{n}}_C$, where $\bar{\boldsymbol{n}}_C = (\bar{n}_{.1}, \bar{n}_{.2}, \ldots, \bar{n}_{.(c+1)})'$ and $\mathbf{1}$ is a $(c+1)$-dimensional vector of ones. The solu-

tion z_0 corresponding to $\lambda = 1$ is given by $z_0 = G^{1/2}\mathbf{1}/\sqrt{n_{..}}$. Hence, the optimal solution we obtain by removing the trivial solution z_0, from the problem, satisfies the equation

$$(G^{-\frac{1}{2}}\bar{N}'R^{-1}\bar{N}G^{-\frac{1}{2}} - \frac{1}{n_{..}}G^{\frac{1}{2}}\mathbf{1}\mathbf{1}'\mathbf{G}^{\frac{1}{2}})z = \lambda z. \tag{11}$$

This equation means that the optimal solution can be obtained by solving the two-sided eigen equation (9) replacing $\bar{N}'R^{-1}\bar{N}$ with $\bar{N}'R^{-1}\bar{N} - \bar{\boldsymbol{n}}_C\bar{\boldsymbol{n}}_C'/n_{..}$ which is centred at zero.

Another expression of the above two-sided eigen equation can be derived, which leads us to a correspondence analysis method for successive categories. Define $\boldsymbol{n}_R = (n_{1.}, n_{2.}, \ldots, n_{m.})'$, and $\bar{N} = (\bar{n}_{ik})$. Then,

$$\bar{N}'R^{-1}\bar{N} - \bar{\boldsymbol{n}}_C\bar{\boldsymbol{n}}_C'/n_{..} = (\bar{N} - \frac{1}{n_{..}}\boldsymbol{n}_R\bar{\boldsymbol{n}}_C')'R^{-1}(\bar{N} - \frac{1}{n_{..}}\boldsymbol{n}_R\bar{\boldsymbol{n}}_C'). \tag{12}$$

From (11), this equation means that the solution z can be obtained by using a singular value decomposition of the matrix $R^{-1/2}(\bar{N} - \boldsymbol{n}_R\bar{\boldsymbol{n}}_C'/n_{..})G^{-1/2}$, while in traditional correspondence analysis, the singular value decomposition of $R^{-1/2}(N - \boldsymbol{n}_R\boldsymbol{n}_C'/n_{..})C^{-1/2}$ is used, where $\boldsymbol{n}_C = (n_{.1}, n_{.2}, \ldots, n_{.c})'$ and $C = \mathrm{diag}(n_{.1}, n_{.2}, \ldots, n_{.c})$.

3 Numerical Examples

To illustrate the method discussed in the previous section, we will analyse two contingency tables considered in the studies by Beh and Smith [5], and Calimlim, Wardell, Cox, Lasagna, and Sriwatanakul [7]. Since our scaling method provides the end points of the intervals of categories in a representation space, categories are represented as the regions determined by those end points; categories are represented by the rectangles with the vertices defined by the end points in two-dimensional space, and the cuboids in three-dimensional space. However, if we assume that within each category, its scaled values are distributed on the line segment determined by the end points, then categories are represented by the intervals in a multidimensional space.

The contingency tables considered here are such examples mentioned in the literature on correspondence analysis (Beh & Smith [5]; Beh & Lombardo [4]; Parsa & Smith [26]; Greenacre [12]).

3.1 Asbestos Exposure Data

A contingency table analysed by Beh and Smith [5] is considered. The data are based on Selikoff's [29] asbestosis data, which clarify the association between asbestosis grade (severity) diagnosed and occupational years exposed to asbestos. Multiple

Table 1 Obtained Intervals of Asbestosis Grades

	End point t_k		Centre $\bar{t}_k$		CA	
	dim.1	dim.2	dim.1	dim.2	dim.1	dim.2
None	0.0332	−0.0354	0.0231	−0.0114	0.0253	−0.0141
Grade 1	0.0130	0.0126	−0.0094	0.0310	−0.0124	0.0401
Grade 2	−0.0319	0.0494	−0.0507	−0.0090	−0.0538	−0.0263
Grade 3	−0.0695	−0.0675	−0.0692	−0.0730	−0.0647	−0.0648
	−0.0688	−0.0784				

grades of asbestosis are defined as either none or ranging from Grade 1 (the least severe) to Grade 3 (the most severe).

Table 1 represents a two-dimensional solution obtained by our interval scaling method; the first two eigenvalues are 0.4398 (88.0 %) and 0.0539 (11.9 %). For comparison, it also represents the scale values obtained from the conventional or classical CA, of which first two eigenvalues are 0.4892 (84.2 %) and 0.0892 (15.4 %). It is clear that the centres or means of the intervals almost coincide with the scale values of conventional CA, but the variation of scale values in "Grade 3" is extremely small compared with those in other asbestosis grade categories (see Fig. 1).

Figure 1 reveals that (1) a two-dimensional space is needed for asbestosis grades to be represented separately, and (2) "Grade 3" is not separated from "Grade 2" in a uni-dimensional space while the probability of the "Grade 2" scale values taking the interval of "Grade 3" is very small, say about 2%, since the scale values of "Grade 2" are uniformly distributed over the interval [−0.0695, −0.0319] whereas those of "Grade 3" are over the interval [−0.0695, −0.0688]. It also visually confirms Selikoff's "20-year rule" which claims that most workers exposed to asbestos for less than 20 years display normal chest films, but most workers exposed for more than 20 years display abnormal ones. However, since only the centre of "0–9 years" is included in the rectangular of "None", we might assert a "10-year rule"; that is, most workers exposed for more than 10 years display abnormal chest films, but not those for less than 10 years.

3.2 Drugs' Effectiveness Data

A contingency table analysed in Greenacre [12] is considered. The data are from a study by Calimlim et al. [7] and are reproduced in Greenacre [12, p.263, Table 9.5]. A sample of 121 patients is considered and randomly assigned to one of four categories that represent a different analgesic drug (A, B, C, or D). Each patient was asked to rate the effectiveness of the drug on a 5-point scale; poor, fair, good, very good, and excellent.

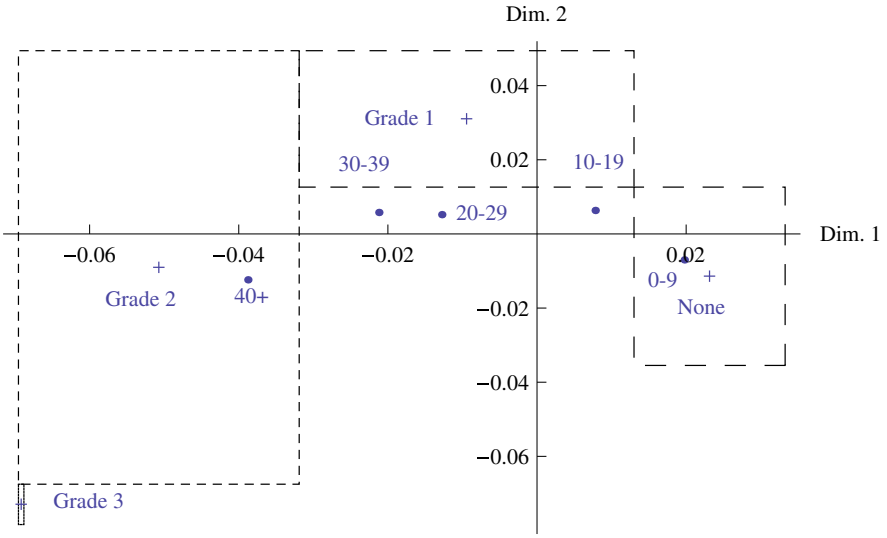

Fig. 1 Two-dimensional display of association between asbestosis grades and occupational exposure to asbestos. The centres of the regions are indicated by "+"

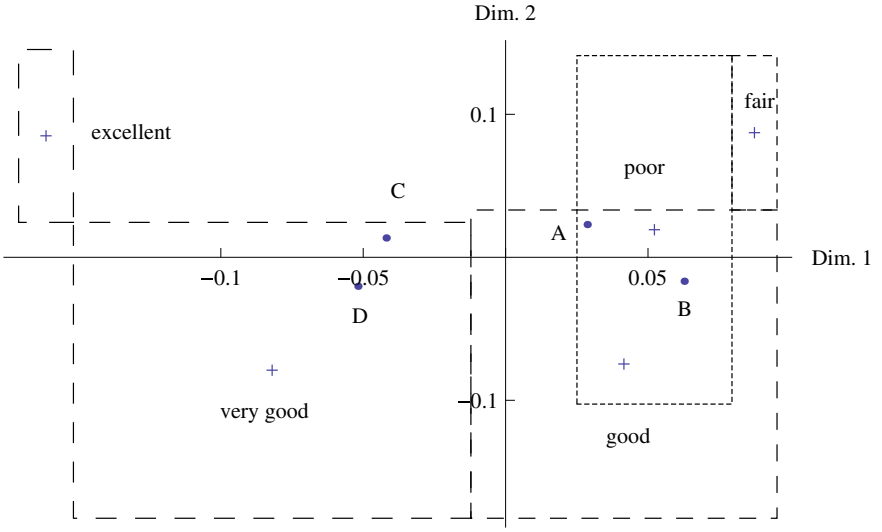

Fig. 2 Two-dimensional display of association between drugs and rating scales; rectangular regions for poor, fair, good, very good, and excellent, of which centres are indicated by "+"

Applying our method to the data, a two-dimensional solution is obtained, following the analysis by Greenacre [12]. The corresponding eigenvalues are 0.279 (85.5%) and 0.042 (12.9%). Figure 2 suggests that the responses "poor", "fair", and

Table 2 Obtained intervals of the effectiveness of four drugs

	End point t_k			Centre $\bar{t}_k$			CA	
	dim.1	dim.2	dim.3	dim.1	dim.2	dim.3	dim.1	dim.2
Poor	−0.0251	0.1027	−0.2788	−0.0523	−0.0192	−0.1442	−0.0406	0.0244
Fair	−0.0795	−0.1410	−0.0096	−0.0874	−0.0871	0.0521	−0.1058	−0.1450
Good	−0.0953	−0.0331	0.1138	−0.0416	0.0747	0.0661	−0.0441	0.0976
Very good	0.0122	0.1825	0.0184	0.0820	0.0790	0.0254	0.0960	0.0512
Excellent	0.1518	−0.0244	0.0325	0.1614	−0.0849	0.0029	0.1557	−0.0902
	0.1710	−0.1453	−0.0266					

"good" cannot be separated, while the responses "very good" and "excellent" can be discriminated. This result coincides with that of Greenacre [12] derived from using a resampling technique, except that the responses "very good" and "excellent" are separated. Also, it might be asserted that the drugs can be separated into two groups: A with B and C with D. This result also coincides with that of Greenacre [12].

A three-dimensional solution is shown in Table 2, from which we can assert that the third dimension is needed to separate all response categories.

4 Scaling of Successive Categories in a Concatenated Contingency Table

The comments made in Sect. 2 can be extended to the interval-valued scaling of successive categories of a concatenated contingency table. Let n_{ijk} be the frequencies $(i = 1, 2, \ldots, r; k = 1, 2, \ldots, c_j)$ in an $r \times c_j$ contingency table defined on the j-th variable X_j, $j = 1, 2, \ldots, p$, where c_j is the number of successive categories X_j takes, and p is the number of variables. Also let $N_j = (n_{ijk})$ be the $r \times c_j$ contingency table for X_j. Then, the concatenated contingency table $N_{(c)}$ is given by $N_{(c)} = (N_1, N_2, \ldots, N_p)$.

Let the interval $[t_{jk}, t_{j(k+1)}]$ be the interval scale value of the k-th category of X_j. Then, under the assumption that the scores within the k-th category of X_j are uniformly distributed, the mean vector $\bar{\boldsymbol{x}}_j$ for X_j is given by

$$\bar{\boldsymbol{x}}_j = R^{-1}\bar{N}_j\boldsymbol{t}_j, \tag{13}$$

where $R = \mathrm{diag}(n_{i\cdot\cdot}/p), \boldsymbol{t}_j = (t_{j1}, t_{j2}, \ldots, t_{j(c_j+1)})'$, and $\bar{N}_j$ is a $r \times (c_j + 1)$ matrix of which (i, k) element $\bar{n}_{ijk}$ is given by $(n_{ij(k-1)} + n_{ijk})/2$.

Suppose that the total score Y is defined by $Y = \sum_{j=1}^{p} X_j$. Then, under the assumption of the uniform distribution, the vector $\bar{\boldsymbol{y}} = (\bar{y}_1, \bar{y}_2, \ldots, \bar{y}_r)'$, where $\bar{y}_i$ is the expected value of Y for object i, is given by

$$\bar{\boldsymbol{y}} = \sum_{j=1}^{p} R^{-1} \bar{N}_j \boldsymbol{t}_j. \tag{14}$$

Suppose that $\sum_{k=1}^{c_j} n_{\cdot jk} \bar{t}_{jk} = 0$ for any j, $j = 1, 2, \ldots, p$; that is, the expected grand mean of scores X_{ij}, $i = 1, 2, \ldots, r$ is 0 for any variable X_j. Then, the total variance s_t^2 of the scores is given by

$$\begin{aligned} s_t^2 &= \frac{1}{n_{\cdots}} \sum_{i=1}^{r} n_{i\cdot\cdot} \sum_{j=1}^{p} E[X_{ij}^2] \\ &= \frac{p}{n_{\cdots}} \sum_{j=1}^{p} \boldsymbol{t}_j' G_j \boldsymbol{t}_j, \end{aligned} \tag{15}$$

where $(3/2)G_j$ is a tridiagonal symmetric matrix with $\bar{n}_{\cdot jk}$, $k = 1, 2, \ldots, c_j + 1$ as diagonal elements and $n_{\cdot jk}/4$, $k = 1, 2, \ldots, c_j$ as sub-diagonal elements.

Also, the between variance s_b^2 is given by

$$\begin{aligned} s_b^2 &= \frac{1}{p n_{\cdots}} \sum_{i=1}^{r} n_{i\cdot\cdot} (E[Y_i])^2 \\ &= \frac{p}{n_{\cdots}} \frac{1}{p} \sum_{j=1}^{p} \sum_{l=1}^{p} \boldsymbol{t}_j' \bar{N}_j' R^{-1} \bar{N}_l \boldsymbol{t}_l. \end{aligned} \tag{16}$$

Hence, the optimal $\boldsymbol{t}_j$, $j = 1, 2, \ldots, p$, which maximises s_b^2 under the constraint s_t^2 being constant, satisfies

$$\sum_{l=1}^{p} \bar{N}_j' R^{-1} \bar{N}_l \boldsymbol{t}_l = \lambda p G_j \boldsymbol{t}_j, \tag{17}$$

where λ is a Lagrange multiplier corresponding to the constraint.

Let G_F be a block diagonal matrix of which diagonal blocks are defined by G_j, $j = 1, 2, \ldots, p$, and $\boldsymbol{t}$ be defined by $\boldsymbol{t} = (\boldsymbol{t}_1', \boldsymbol{t}_2', \ldots, \boldsymbol{t}_p')'$. Then, (17) is rewritten as

$$\bar{N}_{(c)}' R^{-1} \bar{N}_{(c)} \boldsymbol{t} = \lambda p G_F \boldsymbol{t}, \tag{18}$$

where $\bar{N}_{(c)} = (\bar{N}_1, \bar{N}_2, \ldots, \bar{N}_p)$.

For notational convenience, let $F = (F_{jl})$ be a block matrix defined by $F_{jl} = \bar{N}_j' R^{-1} \bar{N}_l$; $F = \bar{N}_{(c)}' R^{-1} \bar{N}_{(c)}$, then the following properties hold for the matrices F and G_F.

1. $F_{jl} = F_{lj}'$, $j, l = 1, 2, \ldots, p$

2. $F_{jl}\mathbf{1}_l = \bar{\boldsymbol{n}}_j$, $j, l = 1, 2, \ldots, p$. where $\mathbf{1}_l$ is a $c_l + 1$-dimensional vector of ones, and $\bar{\boldsymbol{n}}_j$ is a $c_j + 1$-dimensional vector of which elements are $\bar{n}_{\cdot jk}, k = 1, 2, \ldots, c_j + 1$.
3. $F_{jj}\mathbf{1}_j = G_j\mathbf{1}_\mathbf{j}$, $j = 1, 2, \ldots, p$.

From these properties, for a $\sum_{j=1}^{p} c_j + p$-dimensional vector $\mathbf{1}$ of ones, we have $F\mathbf{1} = pG_F\mathbf{1} = p(\bar{\boldsymbol{n}}_1', \bar{\boldsymbol{n}}_2', \ldots, \bar{\boldsymbol{n}}_p')'$. That is, two-sided eigen equation (18) has a solution $\boldsymbol{t} = \mathbf{1}$ corresponding to $\lambda = 1$.

The optimal solution $\boldsymbol{t}$ is obtained by solving the equation

$$(pG_F)^{-\frac{1}{2}} F (pG_F)^{-\frac{1}{2}} \boldsymbol{z} = \lambda \boldsymbol{z}, \tag{19}$$

where $\boldsymbol{z} = (pG_F)^{\frac{1}{2}}\boldsymbol{t}$, and $\boldsymbol{z}'\boldsymbol{z} = 1$.

Equation (19) has a trivial solution $\boldsymbol{z}_0 = G_F^{\frac{1}{2}}\mathbf{1}/\sqrt{n_{\cdots}}$ corresponding to $\lambda = 1$. Hence the optimal solution can be obtained by replacing F with $\tilde{F}$ defined by

$$\begin{aligned} \tilde{F} &= F - \frac{p}{n_{\cdots}} G_F \mathbf{1}\mathbf{1}'\mathbf{G}_\mathbf{F} \\ &= F - \frac{p}{n_{\cdots}} \bar{\boldsymbol{n}}\bar{\boldsymbol{n}}', \end{aligned} \tag{20}$$

where $\bar{\boldsymbol{n}} = (\bar{\boldsymbol{n}}_1', \bar{\boldsymbol{n}}_2', \ldots, \bar{\boldsymbol{n}}_p')'$. This equation equivalently means that the (j, l)-block element $\tilde{F}_{jl}$ is given by

$$\begin{aligned} \tilde{F}_{jl} &= F_{jl} - \frac{p}{n_{\cdots}} \bar{\boldsymbol{n}}_j \bar{\boldsymbol{n}}_l' \\ &= \bar{N}_j' R^{-1} \bar{N}_l - \frac{p}{n_{\cdots}} \bar{\boldsymbol{n}}_j \bar{\boldsymbol{n}}_l' \\ &= (\bar{N}_j - \frac{p}{n_{\cdots}} \boldsymbol{n}_R \bar{\boldsymbol{n}}_j')' R^{-1} (\bar{N}_l - \frac{p}{n_{\cdots}} \boldsymbol{n}_R \bar{\boldsymbol{n}}_l'), \end{aligned} \tag{21}$$

where $\bar{N}_j = (\bar{n}_{ijk})$, $i = 1, 2, \ldots, r, k = 1, 2, \ldots, c_j + 1$, and $\boldsymbol{n}_R = (n_{1\cdot\cdot}, n_{2\cdot\cdot}, \ldots, n_{r\cdot\cdot})'/p$. Therefore, using the notation $\bar{N}_{(c)} = (\bar{N}_1, \bar{N}_2, \ldots, \bar{N}_p)$, $\tilde{F}$ can be rewritten as

$$\tilde{F} = (\bar{N}_{(c)} - \frac{p}{n_{\cdots}} \boldsymbol{n}_R \bar{\boldsymbol{n}}')' R^{-1} (\bar{N}_{(c)} - \frac{p}{n_{\cdots}} \boldsymbol{n}_R \bar{\boldsymbol{n}}'). \tag{22}$$

From this equation, we can assert that the optimal solution can be obtained by using a singular value decomposition of $R^{-1/2}(\bar{N}_{(c)} - (p/n_{\cdots})\boldsymbol{n}_R\bar{\boldsymbol{n}}')(pG_F)^{-1/2}$.

5 Discussions

In this paper, a new scaling method for successive categories has been proposed, which represents the categories as intervals or regions but not points. The advantages of our method are that (1) it clarifies how successive categories are related to each other, (2) variabilities of the scores within categories might be evaluated from the sizes of the corresponding intervals or regions, and (3) it has a simple relation to the classical approaches of two-way correspondence and multiple correspondence analyses.

Generally, multiple correspondence analysis considers a contingency table where more than two categorical variables exist but are not always successive. Hence our method for multi-way contingency table is restricted to the special case where all the categorical variables are successive, but it can be easily extended to accommodate more general cases. For example, if the categories of the first p_1 variables are not successive, then for (18), we only have to define the first p_1 block diagonals of G_F by $G_j = \mathrm{diag}(n_{\cdot j1}, n_{\cdot j2}, \ldots, n_{\cdot jc_j})$, $j = 1, 2, \ldots, p_1$, and the $\bar{N}_{(c)}$ by $\bar{N}_{(c)} = (N_1, N_2, \ldots, N_{p_1}, \bar{N}_{p_1+1}, \ldots, \bar{N}_p)$.

Our scaling method also can be extended to the case where a contingency table consists of successive and non-successive categories. This case will occur when the response category such as "I don't know" is included as a response to a set of successive categories.

In general, the idea of interval-valued scaling of successive categories might be considered in the framework of the scaling method for fuzzy categories. We shall leave this issue for future consideration.

References

1. Benzécri, J.-P. (1973). *L'Analyse des Données*. Vol. 1: *La Taxinomie*. Vol. 2: *L'Analyse des Correspondances*. Paris: Dunod.
2. Beh, E. J. (1997). Simple correspondence analysis of ordinal cross-classifications using orthogonal polynomials. *Biometrical Journal*, *39*, 589–613.
3. Beh, E. J. (1998). A comparative study of scores for correspondence analysis with ordered categories. *Biometrical Journal*, *40*, 413–429.
4. Beh, E. J., & Lombardo, R. (2014). *Correspondence analysis. Theory, practice and new strategies*. Chichester: Wiley.
5. Beh, E. J., & Smith, D. R. (2011). Real world occupational epidemiology. Part 2: A visual interpretation of statistical significance. *Archives of Environmental & Occupational Health*, *66*, 245–248.
6. Billard, L., & Diday, E. (2006). *Symbolic data analysis*. Chichester: Wiley.
7. Calimlim, J. F., Wardell, W. M., Cox, C., Lasagna, L., & Sriwatanakul, K. (1982). Analgesic efficiency of orally Zomipirac sodium. *Clinical Pharmacology and Therapeutics*, *31*, 208.
8. De Leeuw, J. (1988). Multivariate analysis with optimal scaling. In S. Das Gupta & J. K. Ghosh (Eds.), *Proceedings of the International Conference on Advances in Multivariate Statistical Analysis* (pp. 127-160). Calcutta: Indian Statistical Institute.
9. Gifi, A. (1990). *Nonlinear multivariate analysis*. Chichester: Wiley.
10. Golub, G. H., & van Loan, C. F. (1996). *Matrix computation*. Baltimore: Johns Hopkins.

11. Gower, J. C., & Hand, D. J. (1996). *Biplots*. London: Chapman & Hall.
12. Greenacre, M. J. (1984). *Theory and applications of correspondence analysis*. London: Academic Press.
13. Guttman, L. (1941). The quantification of a class of attributes: A theory and method of scale construction. In Horst, P. *et al*. *The Prediction of Personal Adustment*, 319-348. New York: Social Research Council.
14. Hayashi, C., Higuchi, I., & Komazawa, T. (1970). *Joho Syori to Tokei Suri (Information processings and mathematical statistics)*. Tokyo: Sangyo Tosyo. (in Japanese).
15. Hill, M. O. (1974). Correspondence analysis: A neglected multivariate method. *Applied Statistics*, *23*, 340–354.
16. Lombardo, R., Beh, E. J., & D'Ambra, L. (2007). Non-symmetric correspondence analysis with ordinal variables. *Computational Statistics and Data Analysis*, *52*, 566–577.
17. Mair, P., & de Leeuw, J. (2010). A general framework for multivariate analysis with optimal scaling: The R package aspect. *Journal of Statistical Software*, *32*(9), 1–23.
18. Mardia, K. V., Kent, J. T., & Bibby, J. M. (1979). *Multivariate analysis*. London: Academic Press.
19. McNair, D. M., Lorr, M., & Droppleman, L. F. (1971). *Manual for the profiles of mood states*. San Diego, CA: Educational and Industrial Testing Service.
20. Nenadić, O., & Greenacre, M. (2007). Correspondence analysis in R, with two- and three-dimensional graphics: The ca package. *Journal of Statistical Software*, *20*(3), 1–13.
21. Nishisato, S. (1978). Optimal scaling of paired comparisons and rank ordered data: An alternative to Guttman's formulation. *Psychometrika*, *43*, 263–271.
22. Nishisato, S. (1980a). *Analysis of categorical data: Dual scaling and its applications*. Toronto: University of Toronto Press.
23. Nishisato, S. (1980b). Dual scaling of successive categories data. *Japanese Psychological Research*, *22*, 124–143.
24. Nishisato, S., & Arri, P. S. (1975). Nonlinear programming approach to optimal scaling of partially ordered categories. *Psychometrika*, *40*, 525–548.
25. Nishisato, S., & Sheu, W.-J. (1984). A note on dual scaling of successive categories data. *Psychometrika*, *49*, 493–500.
26. Parsa, A. R., & Smith, W. B. (1993). Scoring under ordered constraints in contingency tables. *Communications in Statistics-Theory and Methods*, *22*(12), 3537–3551.
27. Ritov, Y., & Gilula, Z. (1993). Analysis of contingency tables by correspondence models subject to order constraints. *Journal of the American Statistical Association*, *88*, 1380–1387.
28. Schriever, B. F. (1983). Scaling of order dependent categorical variables with correspondence analysis. *International Statistical Review*, *51*, 225–238.
29. Selikoff, I. J. (1981). Household risks with inorganic fibers. *Bulletin of New York Academic Medicine*, *57*, 947–961.
30. Torgerson, W. S. (1958). *Theory and methods of scaling*. New York: Wiley.
31. Yang, K.-S., & Huh, M.-H. (1999). Correspondence analysis of two-way contingency tables with ordered column categories. *Journal of the Korean Statistical Society*, *28*, 347–358.

Orthonormal Principal Component Analysis for Categorical Data as a Transformation of Multiple Correspondence Analysis

Takashi Murakami

Abstract While multiple correspondence analysis (MCA) is a useful tool to visualize the structure in survey data, there exists a difficulty in displaying a solution beyond three dimensions. We devised a procedure for interpreting a multidimensional solution of MCA based on loadings in a similar way as exploratory factor analysis (EFA). It is a simple principal component analysis (PCA) of orthonormal quantified variates derived from categorical variables, which is shown to yield essentially the same solution as standard MCA. In order to facilitate interpretations, bidirectional rotations of the weight matrix approximating simple structure, and orthonormal polynomials for ordered categorical variables are introduced. An illustrative example analyzing survey data of professional baseball spectators is demonstrated.

1 Introduction

Multiple correspondence analysis (MCA) has been commonly used for analyzing survey data (e.g., Greenacre [9]). However, it has two serious shortcomings. First, although it facilitates understandings of data structure through visualization (e.g., Gower, Lubbe, & Le Roux [7]), the graphical representation is usually limited to a two-dimensional surface, and not sufficient to describe the solution consisting of three or more dimensions. This restriction is rather inconvenient in practical situations because survey data often involve a large number of variables with divergent contents, the structure tends to be complex and multidimensional. Second, it is said that MCA often yields some spurious dimensions, which appear in quadratic or higher order functional forms of the dominating dimension (e.g., Bekker & De Leeuw [1]). Particularly, the quadratic relation is sometimes called the *horseshoe phenomenon* (e.g., Greenacre [8]).

We will propose a procedure to cope with the above-mentioned inadequacies. The main strategy is to introduce the loadings of the *locally* quantified variates defined

T. Murakami (✉)
Chukyo University, Nagoya, Japan
e-mail: tandem06@sass.chukyo-u.ac.jp

T. Imaizumi et al. (eds.), *Advanced Studies in Behaviormetrics and Data Science*,
Behaviormetrics: Quantitative Approaches to Human Behavior 5,
https://doi.org/10.1007/978-981-15-2700-5_13

for each categorical variable on quantified variables obtained by standard MCA, and a special rotation method attaining the simple structure. As a result, clues for interpreting output of MCA are shifted to loadings on multiple axes from configurations on a plane. In addition, orthogonal polynomials will be used to quantify categories of ordered categorical variables. This metric quantification together with the rotation may not only make interpretations easier but assist to detach the spurious variations as ignorable axes.

These modifications of the MCA solution are shown not to change its contribution to the total variance, and computed quantified scores. In other words, the method developed here makes it possible to interpret the MCA solution in a similar manner of principal component analysis (PCA), which approximates exploratory factor analysis (EFA).

In the following sections, the process of transformation from MCA to PCA is explained in detail, and an illustrative example using real data is demonstrated.

2 MCA and Transformations of the Solution

2.1 The Basic Formulation and the Algorithm of MCA

Let us consider an n (respondents) by p (categorical variables) data matrix $\boldsymbol{X}$. Let $\boldsymbol{x}_k$ be a k-th column of $\boldsymbol{X}$, and $\boldsymbol{G}_k$ be an $n \times c_k$ indicator matrix for variable k defined as

$$g_{ijk} = \begin{cases} 1 & \text{if} \quad x_{ik} = j \\ 0 & \text{otherwise} \end{cases} \tag{1}$$

where c_k is the number of categories of variable k. We assume that categories are coded by an integer sequence, and there is no empty category. Define

$$c = c_1 + c_2 + \ldots + c_p$$

and assume $n \gg c$. If we define an $n \times c$ indicator matrix as

$$\boldsymbol{G} = \left[\begin{array}{cccc} \boldsymbol{G}_1 & \boldsymbol{G}_2 & \ldots & \boldsymbol{G}_p \end{array} \right] \tag{2}$$

then the basic formula of MCA can be written as

$$\boldsymbol{F} = \boldsymbol{G}\boldsymbol{V}, \tag{3}$$

where[1] $\boldsymbol{V}$ is a $c \times r$ matrix of *quantifications*, $\boldsymbol{F}$ is an $n \times r$ matrix of *quantified variables*, and r is the (in principle) prespecified number of dimensions. We will

[1] In the standard formulation of MCA (e.g., Greenacre [9]), the right-hand side is divided by $\sqrt{p}$, but we omitted it to transform MCA into PCA-form naturally.

employ the maximization of $n^{-1}\text{tr}\ (\boldsymbol{F}'\boldsymbol{F})$ as the criterion to be optimized.[2] A natural formulation of the problem to be solved may be to maximize

$$\phi\,(\boldsymbol{V} \mid \boldsymbol{G}) = n^{-1}\text{tr}\ (\boldsymbol{V}'\boldsymbol{G}'\boldsymbol{G}\boldsymbol{V}) \tag{4}$$

subject to

$$n^{-1}\boldsymbol{V}'\boldsymbol{D}\boldsymbol{V} = \boldsymbol{I}_r \tag{5}$$

where $\boldsymbol{D} = \text{diag}(\boldsymbol{G}'\boldsymbol{G})$ is a $c \times c$ diagonal matrix, elements of which are response frequencies for total categories, and $\boldsymbol{I}_r$ is the $r \times r$ identity matrix. Note that $\mathbf{1}_c'\boldsymbol{D}\mathbf{1}_c = np$, where $\mathbf{1}_c$ is an n-dimensional vector, all elements of which are unity.

While some algorithms obtaining the optimal $\boldsymbol{V}$ are known, we will use the eigenvalue decomposition of a positive semi-definite matrix. Let us define

$$\boldsymbol{B} = \boldsymbol{D}^{-1/2}\boldsymbol{G}'\boldsymbol{G}\boldsymbol{D}^{-1/2} \tag{6}$$

which is called the *normalized Burt matrix* (Gower & Hand [6]).

The rank of $\boldsymbol{B}$ is at most $c - p + 1$ because $\boldsymbol{G}_k'\mathbf{1}_{c_k} = \mathbf{1}_n$ for every k. The eigenvalue decomposition of $\boldsymbol{B}$ may be written as

$$\boldsymbol{B} = \begin{bmatrix} \boldsymbol{k}_0 & \boldsymbol{K} \end{bmatrix} \begin{bmatrix} \lambda_0 & \mathbf{0}' \\ \mathbf{0} & \boldsymbol{\Lambda} \end{bmatrix} \begin{bmatrix} \boldsymbol{k}_0' \\ \boldsymbol{K}' \end{bmatrix} = \lambda_0 \boldsymbol{k}_0 \boldsymbol{k}_0' + \boldsymbol{K}\boldsymbol{\Lambda}\boldsymbol{K}' \tag{7}$$

where λ_0 is the largest eigenvalue of $\boldsymbol{B}$, $\boldsymbol{k}_0$ is the corresponding c-dimensional eigenvector of unit length, $\boldsymbol{\Lambda}$ is the $(c - p) \times (c - p)$ diagonal matrix of remaining eigenvalues, and $\boldsymbol{K}$ is the $c \times (c - p)$ corresponding unit-length eigenvector matrix. The $p - 1$ zero eigenvalues and the corresponding eigenvectors are omitted in (7). If all the elements of $\boldsymbol{\Lambda}$ is arranged in the descending order, we can assume that they are all distinct from each other, $\lambda_1 > \lambda_2 > \ldots > \lambda_{c-p}$. Hence the matrix $\boldsymbol{K}$ is orthonormal, $\boldsymbol{K}'\boldsymbol{K} = \boldsymbol{I}_{c-p}$, and uniquely determined up to signs.

It was shown that $\lambda_0 = p$, and that this is always larger than remaining eigenvalues of $\boldsymbol{B}$ (Gower & Hand [6, p. 55]). The corresponding eigenvector $\boldsymbol{k}_0$ is the c-dimensional vector being proportional to the square roots of response frequencies of all categories,

$$\boldsymbol{k}_0 = (pn)^{-1/2}\boldsymbol{D}^{1/2}\mathbf{1}_c$$

which can be easily confirmed by postmultiplying $\boldsymbol{B}$ by $\boldsymbol{k}_0$. The set of the largest eigenvalue and the corresponding eigenvector is called the *trivial solution,* which conveys no meaningful information, and must be ignored (e.g., Greenacre [8]).

The quantification matrix is defined as

$$\boldsymbol{V} = n^{1/2}\boldsymbol{D}^{-1/2}\boldsymbol{K}_r \tag{8}$$

[2]The formulation of maximization is of course easily shown to be equivalent to least squares (e.g., Ten Berge [16]).

where $\boldsymbol{K}_r$ is the matrix of the eigenvectors corresponding to the r largest eigenvalues, $\boldsymbol{\Lambda}_r$.

Defining $\boldsymbol{v}_0 = n^{1/2}\boldsymbol{D}^{-1/2}\boldsymbol{k}_0$ according to (8), we obtain $\boldsymbol{f}_0 = \boldsymbol{G}\boldsymbol{v}_0 = p\mathbf{1}_n$. This is just the trivial solution, but due to the property, we know that all columns of $\boldsymbol{F}$ are centered, $\boldsymbol{F}'\mathbf{1}_n = \mathbf{0}_r$, because $\boldsymbol{F}'\boldsymbol{f}_0 = \boldsymbol{V}'\boldsymbol{G}'\boldsymbol{G}\boldsymbol{v}_0 = \boldsymbol{K}_r'\boldsymbol{B}\boldsymbol{k}_0 = p\boldsymbol{K}_r'\boldsymbol{k}_0 = \mathbf{0}_r$ using (6) and (7).

Hence, the criterion to be maximized $n^{-1}\mathrm{tr}(\boldsymbol{F}'\boldsymbol{F})$ is interpreted as the sum of variances rather than just the mean sum of squares, and we can evaluate the relative size of contribution of r quantified variables (Greenacre [9]) by

$$(c-p)^{-1}\phi\,(\boldsymbol{V} \mid \boldsymbol{G}) = (c-p)^{-1}\mathrm{tr}\ (\boldsymbol{\Lambda}_r).$$

2.2 The Decomposition of Quantifications

Let us begin by noting a property of MCA solution, which is important for our purpose. If we define the *local quantified variables* as

$$\boldsymbol{F}_k = \boldsymbol{G}_k\boldsymbol{V}_k \tag{9}$$

where $\boldsymbol{V}_k$ is $c_k \times r$ submatrix of $\boldsymbol{V} = \left[\ \boldsymbol{V}_1'\ \boldsymbol{V}_2'\ \ \ldots\ \boldsymbol{V}_p'\ \right]'$, then $\boldsymbol{F}_k$ is just a summand of the quantified variables such as

$$\boldsymbol{F} = \boldsymbol{F}_1 + \boldsymbol{F}_2 + \ldots + \boldsymbol{F}_p$$

Let us call $\boldsymbol{F}$ obtained by (3) the *global quantified variables* to distinct it from the local quantified variables defined in (9).

Then, all the local quantified variables are centered,

$$\boldsymbol{F}_k'\mathbf{1}_n = \mathbf{0}_r \tag{10}$$

as was shown by Gower and Hand [6, p. 60] (also see Appendix of the present chapter). This property has been scarcely mentioned in the literature, but will play the central role in our formulation.

Now, let us decompose $\boldsymbol{V}_k$ into the product of two matrices as

$$\boldsymbol{V}_k = \boldsymbol{U}_k\boldsymbol{W}_k \tag{11}$$

where $\boldsymbol{U}_k$ is a $c_k \times m_k$ matrix of quantifications, $\boldsymbol{W}_k$ is an $m_k \times r$ matrix of weights, $m_k = \min(c_k - 1, r)$, and define $m = m_1 + m_2 + \ldots + m_p$. If we define $\boldsymbol{d}_k = \boldsymbol{G}_k\mathbf{1}_n$, $\boldsymbol{U}_k$ may be necessarily centered owing to (10) because

$$\boldsymbol{W}_k'\boldsymbol{U}_k'\boldsymbol{d}_k = \boldsymbol{V}_k'\boldsymbol{G}_k'\mathbf{1}_n = \boldsymbol{F}_k'\mathbf{1}_n = \mathbf{0}_{m_k}$$

This formula looks only insisting that the m_k-dimensional vector $\boldsymbol{U}_k^{'}\boldsymbol{d}_k$ is orthogonal to all the vectors in $\boldsymbol{W}_k$, but

$$\boldsymbol{U}_k^{'}\boldsymbol{d}_k = \boldsymbol{0}_{m_k} \tag{12}$$

holds almost certainly in real data, where $n \gg c$, because $\boldsymbol{W}_k$ has at least m_k linearly independent (row) vectors, and no non-null vector in m_k-dimensional space can be orthogonal to all of them simultaneously.

In addition, we will constrain $\boldsymbol{U}_k$ to be orthonormal in the sense that

$$n^{-1}\boldsymbol{U}_k^{'}\boldsymbol{D}_k\boldsymbol{U}_k = \boldsymbol{I}_{m_k} \tag{13}$$

where $\boldsymbol{D}_k = \boldsymbol{G}_k^{'}\boldsymbol{G}_k$= diag $\boldsymbol{d}_k$ is a $c_k \times c_k$ diagonal matrix. Note that $\boldsymbol{D} =$ diag $\left(\boldsymbol{D}_1,\ \boldsymbol{D}_2,\ \ldots,\ \boldsymbol{D}_p\right)$. If we define a $c \times m$ block diagonal matrix, $\boldsymbol{U} =$ diag $(\boldsymbol{U}_1,\ \boldsymbol{U}_2,\ \ldots,\ \boldsymbol{U}_p)$, and using (13), we obtain $n^{-1}\boldsymbol{U}^{'}\boldsymbol{D}\boldsymbol{U} = \boldsymbol{I}_m$. Thus, we know that $\boldsymbol{W} = \left[\ \boldsymbol{W}_1^{'}\ \boldsymbol{W}_2^{'}\ \ \ldots\ \boldsymbol{W}_p^{'}\ \right]'$ is orthonormal since

$$\boldsymbol{W}^{'}\boldsymbol{W} = n^{-1}\boldsymbol{W}^{'}\boldsymbol{U}^{'}\boldsymbol{D}\boldsymbol{U}\boldsymbol{W} = n^{-1}\boldsymbol{V}^{'}\boldsymbol{D}\boldsymbol{V} = \boldsymbol{I}_r$$

Now let us define a matrix of scores for each variable,

$$\boldsymbol{Z}_k = \boldsymbol{G}_k\boldsymbol{U}_k \tag{14}$$

Owing to the constraints of (12) and (13), $\boldsymbol{Z}_k$ is also centered and orthonormal,

$$\boldsymbol{Z}_k^{'}\boldsymbol{1}_n = \boldsymbol{0}_{m_k} \ \text{ and } \ n^{-1}\boldsymbol{Z}_k^{'}\boldsymbol{Z}_k = \boldsymbol{I}_{m_k}$$

Next, define $\boldsymbol{Z} = \left[\ \boldsymbol{Z}_1{}'\ \boldsymbol{Z}_2{}'\ \ \ldots\ \boldsymbol{Z}_p{}'\ \right]^{'}$, and compute the following matrix,

$$\boldsymbol{R} = n^{-1}\boldsymbol{Z}^{'}\boldsymbol{Z} = \begin{bmatrix} \boldsymbol{I}_{c_1-1} & \boldsymbol{R}_{12} & \ldots & \boldsymbol{R}_{1p} \\ \boldsymbol{R}_{21} & \boldsymbol{I}_{c_2-1} & \ldots & \boldsymbol{R}_{2p} \\ \vdots & \vdots & \ddots & \vdots \\ \boldsymbol{R}_{p1} & \boldsymbol{R}_{p2} & \ldots & \boldsymbol{I}_{c_p-1} \end{bmatrix} \tag{15}$$

which is an $m \times m$ matrix of correlations, and is also written as $\boldsymbol{R} = n^{-1}\boldsymbol{U}'\boldsymbol{G}'\boldsymbol{G}\boldsymbol{U}$. Therefore,

$$\boldsymbol{W}^{'}\boldsymbol{R}\boldsymbol{W} = n^{-1}\boldsymbol{V}^{'}\boldsymbol{D}^{1/2}\boldsymbol{B}\boldsymbol{D}^{1/2}\boldsymbol{V} = \boldsymbol{K}_r^{'}\boldsymbol{B}\boldsymbol{k}_r = \boldsymbol{\Lambda}_r \tag{16}$$

which means $\boldsymbol{W}$ consists of eigenvectors corresponding to the largest r eigenvalues of $\boldsymbol{R}$. Then, the matrix of (global) quantified variables can be written as

$$\boldsymbol{F} = \boldsymbol{Z}\boldsymbol{W}$$

and the criterion of maximization is to be

$$n^{-1}\text{tr}\,(\boldsymbol{F}'\boldsymbol{F}) = \text{tr}\,(\boldsymbol{W}'\boldsymbol{R}\boldsymbol{W}) \tag{17}$$

subject to $\boldsymbol{W}'\boldsymbol{W} = \boldsymbol{I}_r$, which is PCA of $\boldsymbol{Z}$ (e.g., Ten Berge [16]). In other words, the r largest eigenvalues of $\boldsymbol{R}$ are the same as that of normalized Burt matrix $\boldsymbol{B}$ except for the one corresponding to the trivial solution, and principal component scores, $\boldsymbol{F} = \boldsymbol{Z}\boldsymbol{W} = \boldsymbol{G}\boldsymbol{V}$, agree with (global) quantified variables.

One may consider that the formulation above is practically meaningless because $\boldsymbol{Z}$ is not given without MCA solution $\boldsymbol{V}$. However, by considering an additional indeterminacy of $\boldsymbol{U}_k$ and $\boldsymbol{W}_k$, PCA will be understood as a tool not depending on the MCA solution.

2.3 Indeterminacies in Local Quantifications

Let $\boldsymbol{T}$ be an arbitrary $r \times r$ orthogonal matrix ($\boldsymbol{T}\boldsymbol{T}' = \boldsymbol{I}_r = \boldsymbol{T}'\boldsymbol{T}$), which does not change the maximization criterion because $\text{tr}(\boldsymbol{T}\boldsymbol{V}'\boldsymbol{G}'\boldsymbol{G}\boldsymbol{V}\boldsymbol{T}') = \text{tr}(\boldsymbol{V}'\boldsymbol{G}'\boldsymbol{G}\boldsymbol{V}) = n\text{tr}(\boldsymbol{\Lambda}_r)$. Thus $\boldsymbol{V}_k = \boldsymbol{U}_k\boldsymbol{W}_k$ has indeterminacy of orthogonal rotation from right-hand side.

There exists another indeterminacy in decomposition of (11). By defining $\boldsymbol{S}_k$ as an $m_k \times m_k$ orthogonal matrix, $\boldsymbol{U}_k\boldsymbol{W}_k = \boldsymbol{U}_k\boldsymbol{S}_k\boldsymbol{S}_k'\boldsymbol{W}_k$. This means that $\boldsymbol{W}_k$ has the possibility of bidirectional orthogonal rotations $\boldsymbol{S}_k'\boldsymbol{W}_k\boldsymbol{T}$. This "double indeterminacy" will be able to be used to obtain high simplicity facilitating interpretations as will be discussed in Sect. 3.4.

Moreover, the indeterminacy is extended to a limit. Consider the condition where $r \geq c_k$ for every k. Then (12) insists that $\boldsymbol{U}_k$ exists in the $(c_k - 1)$-dimensional orthogonal complement of $\boldsymbol{d}_k$ because the condition $r \geq c_k$ means that $m_k = c_k - 1$, hence $c_k - 1$ vectors, columns of $\boldsymbol{U}_k\boldsymbol{S}_k$, are entirely arbitrary because any set of vectors satisfying (12) and (13) spans the orthogonal complement of $\boldsymbol{d}_k$, and it reaches any other set of vectors in the space by orthogonal transformation (Murakami [15]).

Then, does any $\boldsymbol{R}$ defined by arbitrary $\boldsymbol{U}_k$ have the same eigenvalues of $\boldsymbol{B}$ conversely, even in cases of $r < c_k$? We will show the answer in the next section.

3 Orthonormal Principal Component Analysis

3.1 Terminologies for Introducing PCA Formulation

Before explaining the derivation of the procedure, we will mention some terminologies to avoid possible confusions. $\boldsymbol{U}_k$ has been called a matrix of quantification without any appropriate alternatives although their sizes and constraints are different

from those of $\boldsymbol{V}_k$. Columns of $\boldsymbol{Z}_k$ in (14) defined by a quantification matrix will be called *variates* to distinct from variables, $\boldsymbol{x}_k$. When quantified by orthonormal polynomials introduced in Sect. 3.5, their columns are referred to as a *linear* variate, a *quadratic* variate, and so on. $\boldsymbol{W}$ and $\boldsymbol{F}$ are called the matrix of (component) *weights* and of (component) *scores*, respectively, according to the tradition of PCA although $\boldsymbol{F}$ is equivalent to (global) quantified variables in MCA. Finally, we will call PCA of $\boldsymbol{R}$ defined in (15) *orthonormal PCA,* or *OPCA* hereafter.

3.2 Arbitrary Quantifications to Categories

Let us begin with a method to obtain a $c_k \times (c_k - 1)$ quantification matrix, $\boldsymbol{U}_k$, satisfying both (12) and (13) simultaneously. We will employ QR factorings as

$$\boldsymbol{D}_k^{1/2} \left[\mathbf{1}_{c_k} \ \boldsymbol{P}_k \right] = \left[\boldsymbol{q}_{0k} \ \boldsymbol{Q}_k \right] \boldsymbol{\Sigma}_k \tag{18}$$

where $\boldsymbol{P}_k$ is a $c_k \times (c_k - 1)$ matrix of random or specified numbers, $\left[\boldsymbol{q}_{0k} \ \boldsymbol{Q}_k \right]$ is the $c_k \times c_k$ orthogonal matrix, $\boldsymbol{q}_{0k} = n^{-1/2} \boldsymbol{D}_k^{1/2} \mathbf{1}_{c_k}$, and $\boldsymbol{\Sigma}_k$ is also the $c_k \times c_k$ upper triangular matrix. Then, the matrix of quantification,

$$\boldsymbol{U}_k = n^{1/2} \boldsymbol{D}_k^{-1/2} \boldsymbol{Q}_k \tag{19}$$

may satisfy the required conditions because $\boldsymbol{U}_k' \boldsymbol{d}_k = n^{1/2} \boldsymbol{Q}_k' \boldsymbol{D}_k^{1/2} \mathbf{1}_{c_k} = n \boldsymbol{Q}_k' \boldsymbol{q}_{0k} = \mathbf{0}_{c_k - 1}$, and $n^{-1} \boldsymbol{U}_k' \boldsymbol{D}_k \boldsymbol{U}_k = \boldsymbol{Q}_k' \boldsymbol{Q}_k = \boldsymbol{I}_{c_k - 1}$. Note that $\mathbf{1}_{c_k}' \boldsymbol{D}_k \mathbf{1}_{c_k} = n$.

While other procedures of orthogonalization also attain the same purpose in cases where random numbers are given to $\boldsymbol{P}_k$, the use of QR factorization (or its equivalence, Gram–Schmidt orthogonalization) may be compulsory for a specified $\boldsymbol{P}_k$, e.g., by polynomials discussed in Sect. 3.5 because the order of orthonormalization is essential. If $\boldsymbol{p}_{1k}$ consists of an arithmetic sequence as in (24), $(j = 1)$, the property must be kept in $\boldsymbol{q}_{1k}$, which is the vector of quantification for a linear variate.

3.3 Equivalence of OPCA to MCA

We will show that PCA of $\boldsymbol{Z} = \boldsymbol{G}\boldsymbol{U}$ yields essentially the same solution as MCA. Let us define a $c \times p$ matrix, $\boldsymbol{J} = \text{diag} \left(\mathbf{1}_{c_1}, \mathbf{1}_{c_2}, \ \ldots \ , \mathbf{1}_{c_p} \right)$, and $\boldsymbol{G} \left[\ \boldsymbol{J} \ \boldsymbol{U} \ \right] = \left[\mathbf{1}_n \mathbf{1}_p' \ \boldsymbol{Z} \right]$. Then, compute the $c \times c$ mean cross product matrix,

$$\boldsymbol{R}^+ = n^{-1} \begin{bmatrix} \mathbf{1}_p \mathbf{1}_n' \\ \boldsymbol{Z}' \end{bmatrix} \left[\mathbf{1}_n \mathbf{1}_p' \ \boldsymbol{Z} \right] = \begin{bmatrix} \mathbf{1}_p \mathbf{1}_p' & \boldsymbol{O}' \\ \boldsymbol{O} & \boldsymbol{R} \end{bmatrix} \tag{20}$$

where $\boldsymbol{O}$ is a $p \times (c-p)$ null matrix. The eigenvalue decomposition of $\boldsymbol{R}^{+}$ may be written as

$$\boldsymbol{R}^{+} = \begin{bmatrix} p^{-1/2}\mathbf{1}_p & \boldsymbol{O} \\ \mathbf{0}_{c-p} & \boldsymbol{L} \end{bmatrix} \begin{bmatrix} p & \mathbf{0}'_{c-p} \\ \mathbf{0}_{c-p} & \boldsymbol{\Delta} \end{bmatrix} \begin{bmatrix} p^{-1/2}\mathbf{1}'_p & \mathbf{0}'_{c-p} \\ \boldsymbol{O}' & \boldsymbol{L}' \end{bmatrix} \tag{21}$$

due to the fact that the only nonzero eigenvalue of $\mathbf{1}_p\mathbf{1}'_p$ is p. We also assumed that $\boldsymbol{R} = \boldsymbol{L}\boldsymbol{\Delta}\boldsymbol{L}'$, where $\boldsymbol{\Delta}$ is the $(c-p) \times (c-p)$ diagonal matrix of eigenvalues and $\boldsymbol{L}$ is an orthogonal matrix of the corresponding eigenvectors.

Now let us define $\boldsymbol{U}^{+} = n^{-1/2}\boldsymbol{D}^{1/2}\begin{bmatrix} \boldsymbol{J} & \boldsymbol{U} \end{bmatrix}$, which is a $c \times c$ orthogonal matrix ($\boldsymbol{U}^{+'}\boldsymbol{U}^{+} = \boldsymbol{I}_c = \boldsymbol{U}^{+}\boldsymbol{U}^{+'}$) owing to $\mathbf{1}'_c\boldsymbol{D}\mathbf{1}_c = n$, and (13). Then,

$$\boldsymbol{R}^{+} = \boldsymbol{U}^{+'}\boldsymbol{D}^{-1/2}\boldsymbol{G}'\boldsymbol{G}\boldsymbol{D}^{-1/2}\boldsymbol{U}^{+} = \boldsymbol{U}^{+'}\boldsymbol{B}\boldsymbol{U}^{+}. \tag{22}$$

Obviously $\boldsymbol{R}^{+}$ has the same eigenvalues as $\boldsymbol{B}$, and the corresponding eigenvectors are in $\boldsymbol{U}^{+\prime}\begin{bmatrix} \boldsymbol{k}_0 & \boldsymbol{K} \end{bmatrix}$.

$$\begin{bmatrix} \boldsymbol{k}_0 & \boldsymbol{K} \end{bmatrix} = \boldsymbol{U}^{+}\begin{bmatrix} p^{-1/2}\mathbf{1}_p & \boldsymbol{O} \\ \mathbf{0}_{c-p} & \boldsymbol{L} \end{bmatrix} = \begin{bmatrix} n^{-1/2}\boldsymbol{D}^{1/2}\mathbf{1}_c & \boldsymbol{U}\boldsymbol{L} \end{bmatrix}$$

Thus, we have shown that $\boldsymbol{\Delta} = \boldsymbol{\Lambda}$ and $\boldsymbol{U}\boldsymbol{L} = \boldsymbol{K}$. Hence, the eigen decomposition of $\boldsymbol{R}$ defined by any arbitrary $\boldsymbol{U}$ results in MCA with the same contribution, and principal component scores, $\boldsymbol{F} = \boldsymbol{Z}\boldsymbol{W}$, agree with the quantified scores of MCA up to orthogonal rotation.

3.4 Rotation Problem

Since the equivalence of the two methods, MCA and OPCA, has been shown even in cases of $r < c_k$, we will concentrate on OPCA hereafter.

By any arbitrary $c_k \times (c_k - 1)$ centered and orthonormal quantification matrix $\boldsymbol{U}_k$, we obtain an $n \times (c_k - 1)$ orthonormal variates $\boldsymbol{Z}_k$ for variable k, compute the $(c-p) \times (c-p)$ correlation matrix $\boldsymbol{R}$, and by eigenvalue decomposition of $\boldsymbol{R}$, we have $\boldsymbol{W}$, the matrix of eigenvectors corresponding to the largest r eigenvalues, $\boldsymbol{\Lambda}_r$.

However, although any random numbers transformed to satisfy (12) and (13) yield essentially the same solutions, the interpretable result may not be obtained without rotations approximating simple structure. In other words, we must determine the solution uniquely through rotations.

The simple structure makes it possible to interpret the solution axis-by-axis separately. Although a similar goal may be pursued by different methods as in the common use of EFA, our rotation procedure has some special characteristics. First, rotated is the matrix of weights rather than of loadings. Second, rotation is done not only from the right-hand side of the matrix by $\boldsymbol{T}$ as usual but also from the left-hand side by $\boldsymbol{S}'_k$ as was mentioned in Sect. 2.3.

The rotation of the orthonormal weights from the right-hand side coincides with the *independent cluster rotation*, a case 2 of "oblique rotation by orthogonal rotation" proposed by Harris and Kaiser [11]. The transformation matrix $\boldsymbol{T}$ itself is orthogonal, but rotated component scores $\boldsymbol{F}$ may be mutually correlated because their variances are not equal to each other.

Independent cluster rotation has three interesting properties. First, the loadings, *standardized partial regression coefficients* of each variate on all components, are column-wisely proportional to component weights such as

$$\boldsymbol{A} = \ddot{\boldsymbol{W}}\left[\text{diag}\ \left(\boldsymbol{T}'\boldsymbol{\Lambda}_r\boldsymbol{T}\right)\right]^{\frac{1}{2}} \tag{23}$$

where $\ddot{\boldsymbol{W}} = \left[\ \boldsymbol{W}_1^{'}\boldsymbol{S}_1\ \boldsymbol{W}_2^{'}\boldsymbol{S}_2\ \ \ldots\ \boldsymbol{W}_p^{'}\boldsymbol{S}_p\ \right]'\boldsymbol{T}$. Second, the column sum of squares coincides with the contribution of the dimension because $\boldsymbol{A}^{'}\boldsymbol{A} = \text{diag}\ (\boldsymbol{T}^{'}\boldsymbol{\Lambda}_r\boldsymbol{T})$, which does not hold in other oblique rotations (Murakami [15]). Third, if we employ following orthomax family (Crawford & Ferguson [3]) as the criterion,

$$\sum_{k=1}^{p}\sum_{j=1}^{c_k}\sum_{l=1}^{r}\ddot{w}_{jkl}^4 - \frac{\gamma}{p}\left(\sum_{k=1}^{p}\sum_{j=1}^{c_k}\sum_{l=1}^{r}\ddot{w}_{jkl}^2\right)^2$$

where γ is a specified positive constant, they are reduced to the simplest *quartimax*, the first term of the above formula, owing to that the second term is constant due to $\ddot{\boldsymbol{W}}^{'}\ddot{\boldsymbol{W}} = \boldsymbol{I}_r$ unless the row-normalization is done (Harris & Kaiser [11]).

Hence rotations from the right-hand side, $\boldsymbol{WT}$, and from the left-hand side, $\boldsymbol{W}_k^{'}\boldsymbol{S}_k\ \ (k = 1, \ldots, p)$, are alternated until convergence. The convergence is guaranteed because the alternating process is apparently monotonic.

3.5 Use of Orthogonal Polynomials for Ordered Categorical Variables

If a set of loadings approximating simple structure is obtained, one may notice that the interpretations are not necessarily easy. Meanings of variables in the usual PCA can easily be understood because analyzed variables are unidimensional quantity. The user of OPCA, on the contrary, may encounter difficulties to recognize the meaning of variates because they are multidimensional, and one cannot know the values given to each category without referring to elements of the matrix of quantification, $\boldsymbol{U}_k\boldsymbol{S}_k$. It must be too laborious to do so for all the variates.

For the remedy of the drawback, we will recommend applying orthogonal polynomials to *ordered* categorical variables. Before applying QR factoring, (18), arithmetic sequence and its powers may be given to columns of $\boldsymbol{P}_k$ as

$$\boldsymbol{p}_{jk} = \left[\ 1^j\ 2^j\ \ \ldots\ c_k^j\ \right]' \qquad j = 1, \ldots, c_k - 1 \tag{24}$$

As a result, the first and second columns of $\boldsymbol{Q}_k$ becomes the centered and normalized linear function of the category numbers, and the quadratic function, centered, normalized and orthogonal with the first, and so on. Columns of $\boldsymbol{U}_k$ defined by (19) are so called weighted orthonormal polynomials (e.g., Kimball [13]). In this case, of course, rotation from left-hand side must not be applied.

For binary variables, $\boldsymbol{U}_k$ is reduced to a vector of two elements, and only simple centering and normalization are sufficient to satisfy (12) and (13).

4 Illustrative Example

4.1 Analyzed Data and MCA Solution

Data set to be analyzed A set of survey data was collected from the spectators of Japanese professional baseball game held in a stadium in the central district of Japan on May 18, 2016. The survey was done as a practice of undergraduate students. While respondents filled the fully structured inventory consisting of 51 questions, only 15 items shown in Table 1 are used for the example.

The number of respondents (n) is equal to 738 (223 cases including missing values were excluded[3]), and the total numbers of categories (c) is 60. Items used here were assembled or written based on the common sense of social survey asking, e.g., demographic attributes, and preferences, habits, and behavior in spectating a professional baseball game. Somewhat special items are three questions (no. 5–7) on identification to a supporting team ("Team identification" in Table 1), which were quoted from an article on the post-disaster social well-being (Inoue, Func, Wann, Yoshida, & Nakazawa [12]) with some modifications (See Footnotes of Table 1). They are Likert-type items which are popular in psychological research.

Solution of MCA We computed eigenvalues of 60×60 normalized Burt matrix defined in (6). The largest 30 eigenvalues except for the trivial solution is shown in Fig. 1. Although 18 eigenvalues are beyond unity, it seems to be too large as interpretable dimensions.

While the decision of the number of components will be discussed in detail later, we will demonstrate the two-dimensional biplot (Gower et al. [7]), a simultaneous representation of both quantifications of categories, and quantified scores of respondents in Fig. 2. To avoid excessive complicatedness caused by concentrations of many category points surrounding the origin in the limited space, only category points of Items 3, 5, 6, 7, and 15 are shown.

A typical "horseshoe" is formed by category points of Likert-type items 5, 6, and 7, and the configuration of quantified scores of respondents. This suggests that three items share overwhelming large amount of common variations because the statements

[3]The unusual numbers of missing values were mainly caused by misunderstandings that only one of three Likert-type items should be responded.

Table 1 Analyzed questionnaire items and response frequencies for each category

	Item	Freq.		Item	Freq.
1	Gender		8	Fan club	
	Male	504		Member	202
	Female	234		Interests	152
2	Age level			No interests	307
	–19 years old	69		Withdrawn	77
	20–29	176	9	Traveling time to Stadium	
	30–39	118		–29 min.	40
	40–49	165		30–59	129
	50–59	104		60	230
	60–	106		61–120	136
3	Interests in professional baseball			121–180	135
	Best of all sports (3–1)[a]	499		181–	68
	Equal to some others (3–2)	184	10	Watching at Stadium so far	
	Less than some others (3–3)	55		First time today	86
4	Supporting team			1–2 times	70
	Home team	389		3–5	148
	Neither/nor	95		6–10	143
	Visitor	254		11–	291
5	Identification 1[a]		11	Accompanying persons	
	Agree (5–1)	367		Alone	63
	Mildly agree (5–2)	243		Family	293
	Neither/nor (5–3)	87		Friend(s)	245
	Mildly disagree (5–4)	15		Partner	46
	Disagree (5–5)	26		Colleague(s)	74
6	Identification 2[b]			Other(s)	17
	Agree (6–1)	290			
	Mildly agree (6–2)	201		Looking forward[e]	
	Neither/nor (6–3)	186	12	Victory of supporting team	506
	Mildly disagree (6–4)	28	13	Seeing favorite players	198
	Disagree (6–5)	33	14	Exciting feelings	381
7	Identification 3[c]				
	Agree (7–1)	235	15	Satisfaction with watching	
	Mildly agree (7–2)	197		Satisfied (15–1)	172
	Neither/nor (7–3)	209		Mildly satisfied (15–2)	391
	Mildly disagree (7–4)	41		Neither/nor (15–3)	128
	Disagree (7–5)	56		(Mildly) unsatisfied[f]	47

[a] Numbers in parentheses are symbols in Fig. 2. Ibid
[b] I consider myself to be a real fan of the team'
[c] 'Being a fan of the team is very important to me'
[d] 'Being a fan of the team is a reason for my life'
[e] 'What do you expect in watching the game today?' (followed by a checklist consisting 11 items)
[f] Two alternatives were merged. The symbol in Fig. 2 is 15–4

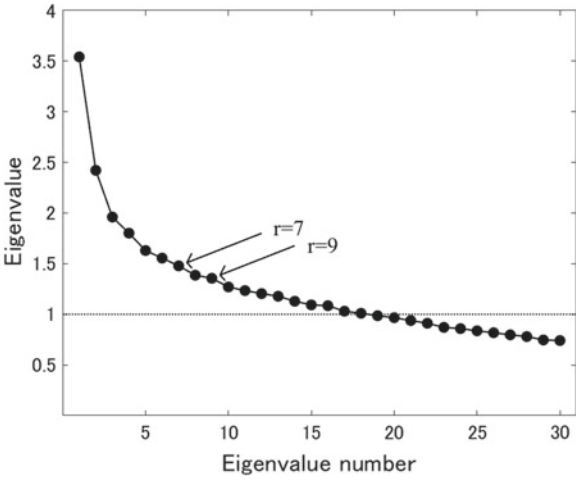

Fig. 1 Scree plot of the normalized Burt matrix. Two arrows directing points before noticeable gaps give clues to decide the number of components of OPCA

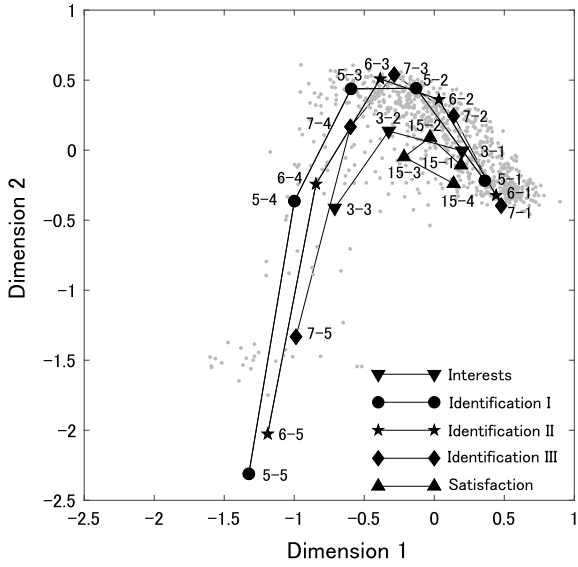

Fig. 2 Biplot demonstrating first two dimensions of MCA. Thin dots denote component scores

are very similar to each other. No one may be able to say that the two-dimensional solution in Fig. 2 represents information included in data fully.

4.2 Solution of OPCA

Coding of categories Integer sequences as in (24) are given to categories of items except for Item 8 and 11, which are treated as unordered categorical variables.

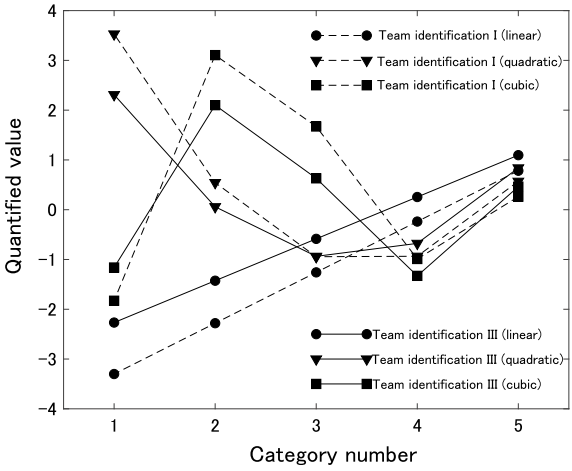

Fig. 3 Orthonormal polynomials, linear, quadratic, and cubic functions, applied to two items, "Team identification I" (dashed lines), and "Team identifications III" (solid lines)

The $c_k - 1$ variates satisfying (12) and (13) were generated for each item. Figure 3 shows linear, quadratic, and cubic variates of Item 5 and 7 as an illustration. Forms of lines of the same degree are slightly different from each other due to the differences in the response rates of categories.

In coding the ordered categories, orders of codes are important. The general rule employed here is that descending sequences are given from categories with the positive meaning to with the negative. For example, code "5" is given to "agree", and "1" to "disagree" in Item 5 and 7 as was seen in Fig. 3, where the larger numbers mean the stronger identification. Similarly, "Best of all sports" in Item 3, "Home team" in Item 6, and "Satisfied" in Item 15 are given the largest integers, respectively. On the other hand, ascending sequences were given to items asking the number of times, and the length of time, Item 2, 9, and 10. For binary items, directions are also important. "Female" in Item 1, and "Checked" in 12–14 were defined as positive. Categories of Item 8 and 11, unordered categorical variables, were given uniformly distributed random numbers in the interval (0,1). Rotated quantification matrices for these two items will be shown in Tables 4 and 5.

Pattern matrix The pattern matrix of 45 variates on 9 components by (23) is shown in Table 2. A notation in row headers, "x.y", denotes number of the item corresponding to Table 1, $1 \leq x \leq 15$, and the orthonormal variate, y, so e.g. 7.3 denotes the cubic variate of Item 7. Components I–IX are arranged according to their contributions. The number of components, 9, was decided by bootstrap sampling explained in the next division. The solution explained about 38.1% of the total variance, 45.0.

All hashed rows and columns in Table 2 will be omitted in interpretations. The second to fourth columns are hashed because salient loadings on the components are all quadratic, cubic, and quantic variates, suggesting that they are spurious. Rows which have no significant loadings will also be ignored in the interpretations. Decision of significance of coefficients was done based on bootstrap sampling.

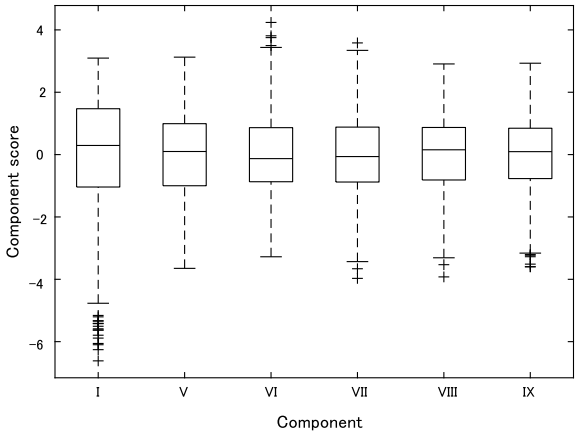

Fig. 4 Box plot of six interpretable components

Bootstrap sampling MCA and PCA in psychological use have been often called *descriptive multivariate analysis*, and inferential statistical tools have been scarcely developed. However, we wish some significance testing to choose loadings referred to in interpretations. In the situation where sampling distributions of estimated coefficients are not easily obtained, the bootstrap method would be useful (Efron & Tibshirani [5]). We employed the Procrustes bootstrap method for PCA developed by Timmerman, Kiers, and Smilde [17].

Two thousand samples are obtained, the mean M and the standard deviation (standard error) s_e was computed for each loading, and $z = M/s_e$ was used for the decision of significance. The decision was done in two stages. In both stages, the absolute value of z is compared with the upper limit of the standard normal distribution $z^{(\alpha/2)}$. In the first stage, multiplicity is considered, hence a was set to be 0.05 divided by the number of loadings, $r(c-p)$ in the manner of Bonferroni. In the second stage, the simple $\alpha = 0.05$ was used. Two criteria are distinguished by different printing types in Table 2. (see footnotes).

Only two solutions, $r = 7$ and $r = 9$ were compared by referring to Fig. 1. While two components with no significant loadings existed in the 7-component solution even in simple 5% level probably due to intrusion of variations from components corresponding to smaller eigenvalues, all components of 9-components solution have at least two significant loadings even considering multiplicity. We will demonstrate and interpret the 9-component solution hereafter.

By omitting hashed rows and columns, 45 variates and 9 components in Table 2 were reduced to 26 and 6 in Table 3, and loadings that are not significant were not displayed. As a result, interpretations of components became rather easy.
Figure 4 is a box plot of interpretable six component scores. Components except for VI are skewed negatively. Especially, skewness of Component I is remarkable.

Table 2 Pattern matrix of total variates and components

Variate	Component									R^2
	I	II	III	IV	V	VI	VII	VIII	IX	
1	*–0.19*	0.07	0.08	–0.06	0.02	0.17	**0.65**	0.07	–0.05	0.48
2.1	0.04	0.00	0.02	–0.04	0.05	0.05	0.02	**0.71**	0.06	0.52
2.2	–0.02	0.00	–0.04	0.00	–0.04	–0.04	0.07	–0.03	**–0.67**	0.47
2.3	–0.04	–0.13	0.12	–0.04	–0.05	–0.13	0.06	–0.23	*0.22*	0.16
2.4	0.13	–0.08	0.18	–0.10	0.02	–0.20	–0.03	0.15	–0.10	0.12
2.5	–0.05	0.03	0.08	–0.08	0.17	0.20	–0.06	–0.21	–0.07	0.13
3.1	**0.50**	0.09	–0.04	–0.02	0.07	0.16	–0.07	–0.12	–0.04	0.35
3.2	0.02	*0.15*	0.01	0.15	0.00	–0.18	0.17	–0.11	0.02	0.12
4.1	**–0.24**	0.03	0.03	0.09	**0.62**	–0.01	–0.09	0.09	–0.13	0.44
4.2	*–0.15*	–0.01	–0.01	0.06	*–0.22*	–0.18	*–0.24*	0.13	0.02	0.22
5.1	**0.87**	*0.09*	*0.07*	*0.01*	0.01	–0.03	–0.05	0.08	0.02	0.77
5.2	*–0.06*	**0.85**	*0.06*	0.03	0.04	0.04	0.01	–0.04	0.03	0.74
5.3	0.02	–0.03	**0.74**	0.04	–0.03	0.01	0.08	–0.05	–0.04	0.56
5.4	0.02	0.01	0.02	**0.71**	–0.04	0.00	–0.05	0.02	–0.06	0.52
6.1	**0.90**	–0.02	0.02	0.03	–0.04	–0.01	–0.02	0.04	0.05	0.80
6.2	*0.03*	**0.90**	0.01	0.00	0.01	–0.02	–0.01	0.01	–0.02	0.81
6.3	0.02	0.00	**0.81**	0.00	0.01	0.00	0.01	–0.05	0.00	0.66
6.4	–0.01	–0.03	0.00	**0.78**	0.04	–0.02	0.07	–0.05	0.03	0.61
7.1	**0.86**	–0.04	0.01	–0.02	–0.05	0.04	–0.07	0.02	–0.02	0.74
7.2	*0.06*	**0.82**	*–0.06*	–0.04	–0.06	–0.04	0.01	0.04	0.04	0.70
7.3	0.03	0.05	**0.73**	–0.01	0.00	–0.02	–0.04	0.08	0.03	0.55
7.4	0.01	0.02	0.01	**0.70**	0.04	0.05	–0.07	0.04	–0.01	0.50
8.1	0.05	–0.03	0.02	–0.04	0.04	**0.68**	*0.15*	0.11	–0.02	0.53
8.2	*–0.28*	0.08	0.07	0.02	**–0.40**	–0.01	0.09	0.12	–0.19	0.34
8.3	*0.25*	0.04	–0.13	0.02	0.02	0.00	*0.22*	*–0.25*	–0.03	0.20
9.1	*0.21*	–0.06	0.04	–0.03	**–0.58**	0.12	–0.10	0.15	–0.05	0.38
9.2	0.03	–0.06	–0.04	0.12	–0.19	*0.34*	–0.02	–0.11	0.22	0.22
9.3	0.03	–0.04	0.14	0.00	–0.01	0.11	–0.01	–0.05	0.15	0.06
9.4	0.03	0.10	0.00	–0.03	0.02	0.12	0.03	0.05	–0.18	0.06
9.5	0.09	–0.04	–0.08	0.03	0.03	–0.15	0.10	0.14	0.19	0.10
10.1	**0.16**	–0.04	–0.01	–0.01	**0.71**	0.05	0.02	0.06	0.06	0.59
10.2	–0.04	0.05	0.05	0.04	0.05	*0.38*	–0.11	–0.11	0.13	0.19
10.3	–0.03	–0.07	0.02	–0.04	0.18	0.02	–0.07	–0.10	–0.22	0.11
10.4	0.08	0.10	–0.11	–0.13	–0.05	0.01	–0.07	–0.14	–0.17	0.10
11.1	0.06	0.00	–0.07	0.04	–0.03	0.02	0.04	**0.69**	–0.07	0.49
11.2	0.05	0.06	–0.08	–0.07	–0.01	–0.06	0.00	–0.05	**0.62**	0.41
11.3	–0.09	–0.03	0.01	–0.01	0.02	–0.01	**0.63**	0.03	0.00	0.40
11.4	0.01	–0.02	–0.08	0.11	–0.08	**0.57**	–0.01	0.01	–0.04	0.34
11.5	–0.02	0.09	0.07	–0.06	0.03	0.00	0.00	0.00	0.00	0.02
12	**0.39**	–0.05	–0.01	–0.09	0.22	*0.16*	*0.21*	–0.02	–0.09	0.37
13	**0.22**	–0.04	–0.06	0.07	–0.13	–0.04	**0.48**	–0.02	–0.09	0.31
14	*0.18*	–0.12	–0.03	0.04	0.04	–0.25	*0.32*	–0.03	0.22	0.23
15.1	**0.27**	0.00	–0.07	0.07	–0.13	–0.27	*0.17*	–0.21	*–0.27*	0.30
15.2	*–0.16*	0.07	0.00	0.04	–0.07	0.00	0.29	0.07	*0.31*	0.23
15.3	–0.13	–0.02	0.02	–0.06	*–0.24*	0.27	–0.02	–0.20	–0.01	0.18
Con.	3.30	2.38	1.92	1.75	1.72	1.58	1.57	1.46	1.46	17.10

* Bold typed figures denote significance at 5% level considering multiplicity. Italicized denotes simple 5% level.

Table 3 Pattern matrix of selected components and variates

Variate		Component					
		I	V	VI	VII	VIII	IX
1. Gender	(+Female)	*−0.19*			**0.65**		
2.1 Age	(Linear)					**0.71**	
2.2	(Quadratic)						**−0.67**
3. Interests in pro. baseball	(Linear)	**0.50**					
4.1 Supporting team	(Linear)	**−0.24**	**0.62**				
4.2	(Quadratic)	*−0.15*	*−0.22*		*−0.24*		
5. Team identification 1	(Linear)	**0.87**					
6. Team identification 2	(Linear)	**0.90**					
7. Team identification 3	(Linear)	**0.86**					
8.1 Fan club	(Strong loyalty)			**0.68**	*0.15*		
8.2	(Floating loyalty)	*−0.28*	**0.40**				
8.3	(Weak loyalty)	*0.25*			*0.22*	*−0.25*	
9.1 Traveling time to Stadium	(Linear)	*0.21*	**−0.58**				
9.2	(Quadratic)			*0.34*			
10.1 Watching in Stadium	(Linear)	**0.16**	**0.71**				
10.2	(Quadratic)			*0.38*			
11.1 Accompanying persons	(Family)					**0.69**	
11.2	(Official)						**0.62**
11.3	(Private)				**0.63**		
11.4	(Alone)		**0.57**				
12. Victory of supporting team		**0.39**		*0.16*	*0.21*		
13. Seeing favorite players		**0.22**			**0.48**		
14. Exciting feelings		*0.18*			*0.32*		
15.1 Satisfaction	(Linear)	**0.27**	*0.17*				*−0.27*
15.2	(Quadratic)	*−0.16*					*0.31*
15.3	(Cubic)	*−0.24*					

Bold typed figures are significant in 5% level considering multiplicity. Italicized are in simple 5%
Item 8 and 11 are unordered categorical variables. Item 1, 12, 13, and 14 are binary variables.

4.3 Interpretations of OPCA Solution

Definitions of variates preserved for interpretations are shown in row headers in Table 3. For example, "Age (quadratic)" means that the variate is an upward concave function of 6 age stages given in Table 1, and "Supporting team (linear)" the variate is an equal-interval descending function of "Home team"—"Neither/nor"—"Visitor." Tables 4 and 5 show rotated quantifications of unordered items, the relationship with "Joining fan club" and "Persons accompanying with", respectively. Names of variates written in row headers were given based on categories with large absolute values.

Table 4 Numbers of categories in variable 8 (Joining fan clubs) for three variates

Variates	Category			
	Member	Interests	No interests	Withdrawn
8.1 Fan club (Strong loyalty)	**1.51**	−0.48	−0.35	**−1.62**
8.2 (Floating loyalty)	**0.60**	−0.35	−0.82	**2.38**
8.3 (Weak loyalty)	−0.03	**1.87**	−0.78	−0.51
Frequency	202	152	307	77

Table 5 Numbers of categories in variable 11 (persons accompanying with) for 4 variates

Variates	Category					
	Alone	Family	Friends	Partner	Colleagues	Other
11.1 Accompanying (Family)	−0.03	**0.94**	−0.66	**−2.79**	0.38	−0.59
11.2 (Official)	1.41	−0.03	**−1.09**	**1.67**	**1.61**	−0.39
11.3 (Private)	−1.34	**0.74**	−0.36	**2.02**	−1.19	−2.88
11.4 (Alone)	**2.53**	0.11	−0.13	−0.10	**−2.10**	0.04
Frequency	63	293	245	46	74	17

Some figures in Tables 4 and 5 are bold typed considering the differences of response rates because rarely responded categories tend to be given extreme values even though the choice is more or less subjective.

Component I is characterized by very high loadings of three "Team identification" items. Interests in professional baseball and expectation for seeing "Victory of the supporting team" also have high loadings. Large negative skewness (−0.96) means that these features are shared by many spectators in Stadium. A low negative loading of "Supporting team" suggests that supporters of Visitor have rather stronger team identification than Home team supporters.

On the contrary, Component V represents the characteristics of Home team supporters. They have often watched games in Stadium, and live in the relatively close districts from Stadium. It is natural that skewness of the score is −0.24 because supporters of Home team are majority of spectators. Relationships between Component I and V are shown in the left panel of Fig. 5. Relative concentration of respondents on the north-east region reflects the skewness of both components.

Respondents whose scores on Component VI are high seem to have a strong loyalty to their supporting teams by judging from large loadings of the first variate on "Fan club". In addition, they tend to watch games alone, and mild loadings of quadratic variates of "Supporting teams", "Traveling time to Stadium", and times of "Watching games in Stadium" suggest that about half of respondents with these properties live in the districts where Visitor locates. The horseshoe-like (but not an artifact) distribution with Component V, shown in the right panel of Fig. 5, also reflects the same tendency. Rather large positive skewness (0.37) suggests that those who have strong loyalty to supporting teams belong to a relatively minor group.

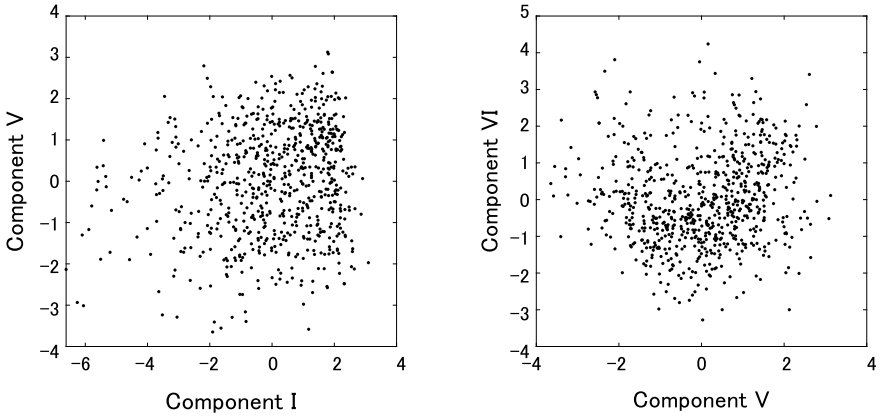

Fig. 5 Left panel: The relationship between Component I (supporters in general) and V (Home team supporters). Both components are skewed negatively, and slightly correlated (0.16). Right panel: The relation between Component V and VI (Strong loyalty). Almost no correlation (−0.09), but horseshoe-like relationship is found. The form of distribution may not be an artifact because there must be supporters with strong loyalty in enthusiastic fans of both Home team and Visitor

Component VII relates to gender differences. Female respondents tend to watch games with familiar persons, family members or the partner. They seem to have stronger interests in some favorite players rather than the result of a game. The distribution of this component is almost symmetric (skewness = −0.07).

Remaining two components are related with the linear function (Component VIII) and the quadratic function (Component IX) of age, respectively. The former shows that the tendency watching games with family members grows with age. The latter means that middle-age spectators tend to visit Stadium with colleagues, and the mild loading of the quadratic variates of Satisfaction suggests the U-shaped relation between age and satisfaction, which is repeatedly confirmed in broad contexts (e.g., Blanchflower & Oswald [2]) and not an artifact again. Since both components skew negatively, (skewnesses are −0.41 and −0.34, respectively), characteristics related to these two components are owned by majority groups.

OPCA has found 6 dimensions, most of which combine attitudes and habits on professional baseball with demographic variables. One may agree with the fact that the dimensions convey more information on individual differences among spectators than the graphical representation obtained by standard MCA (Fig. 2).

Giulianotti [10], for example, classifies football spectators in United Kingdom into four types, Supporters, Followers, Fans, and Flaneurs based on two assumed dimensions, “Traditional–Consumer” and “Hot–Cool”. Our six-dimensional configuration seems to conceptualize more concrete and sound taxonomy of baseball spectators in Japan based on empirical facts.

5 Discussion

We have devised PCA for categorical data, which is essentially equivalent to standard MCA. Although decomposition (11), which is the bridge of MCA and PCA, may be regarded as introducing superfluous complexity to analyses of categorical data, PCA of derived orthonormal variates (OPCA) can be expected to yield an interpretable multidimensional solution by the aid of rotation approximating simple structure and orthonormal polynomials, as was shown in the illustrative example.

The signs of coefficients sometimes cause confusions in interpretations. Although we pointed out the importance of coding orders in Sect. 4.2, routines of QR factoring and of eigenvalue decomposition have usually no rule to determine the signs of columns of $\boldsymbol{Q}_k$ and eigenvectors. In fact, signs of $\boldsymbol{Q}_k$ can be determined uniquely by making all diagonal elements of $\boldsymbol{\Sigma}_k$ positive, but it is difficult to determine the direction of quantifications in unordered categorical variables as long as random numbers are used as initial values. Careful treatment of signs is inevitable.

When the number of categories is so large that $c_k - 1 > r$, the number of variates of variable k can be reduced to r. In our experience, simple quartimax rotation from left-hand side works well to do so by creating a null matrix in $\ddot{\boldsymbol{W}}_k$. But preliminary dimension reduction procedure would be, of course, available.

Another well-known method to treat categorical data in a similar way of EFA is *nonlinear PCA* (NCA; e.g., De Leeuw [4]). It yields a $p \times r$ loading submatrix of the same size as ordinary EFA by imposing "rank-one restriction" (Bekker & De Leeuw [1]) on each variable. However, it seems to be common for categorical variables to have meaningful variations in two or more dimensions as was shown in our example. Although methods giving the different numbers of quantifications for different variables can be developed, it may be too complicated to decide the number for each variable individually. Hence, OPCA proposed here would gain convenience, which gives full-rank quantification to all variables, and the user removes spurious dimensions and variates in the stage of interpretations. Moreover, the method does not require any special algorithm beyond simple decompositions of matrix and a planar rotation routine.

While nonlinear variates of Likert-type items and components on which they load were simply deleted in our example, we do not deny the possibility that a quadratic component, at least, is useful in interpretations as was suggested by Greenacre [8]. The reason why nonlinear components should be discarded in interpretations is explained by Bekker and De Leeuw [1]. They investigated a kind of weighted orthonormal polynomials, Hermite–Chebyshev polynomials, applied to multivariate normally distributed variables. Based on Lancaster [14], they showed if the correlation between two variables is ρ_{kl}, correlations between ν-th degree polynomials becomes $\boldsymbol{\rho}_{kl}^{\nu}$, and correlations between polynomials of the different degrees are zero. Considering eigenvalue decomposition of correlation matrix between all variates defined by several degrees of polynomials, which may be seen as a continuous version of OPCA, the largest eigenvalue for quadratic variates can be larger than the second largest one for linear variates when the variables are highly unidimensional.

This means that the second component is a function of simple square transformations of variables, which is the horseshoe, and brings nothing new.

However, we have found the eigenvalues corresponding to quadratic and higher degree components are far larger than predicted by exponential decreasing of correlations not only in our illustrative example but in other many real data sets (e.g., [15]). These results suggest that higher order variates in real data reflect some empirical facts. This may be a topic in another article.

Appendix: A Proof of Equation (10)

As was mentioned in Sect. 2.2, centrality of global quantified variables, $\boldsymbol{F}^{'}\mathbf{1}_n = \mathbf{0}_r$ is well known, but the same property of local ones, $\boldsymbol{F}_k^{'}\mathbf{1}_n = \mathbf{0}_r$ $(k = 1, \ldots, p)$, seem not to have been taken note so far with some exceptions such as Gower and Hands ([6], pp. 60–61). We will show the essence of their proof in our notation.

From (6), (7), and (8), we know that $\boldsymbol{G}_k^{'}\boldsymbol{G}\boldsymbol{V} = \boldsymbol{D}_k\boldsymbol{V}_k\boldsymbol{\Lambda}_r$, where $\boldsymbol{\Lambda}_r$ is a diagonal matrix of the first r elements of $\boldsymbol{\Lambda}$. Pre-multiplying $\mathbf{1}_{c_k}^{'}$, and using $\mathbf{1}_{c_k}^{'}\boldsymbol{G}_k^{'} = \mathbf{1}_n^{'}$, $\mathbf{1}_n^{'}\boldsymbol{G} = \boldsymbol{d}'$, and $\mathbf{1}_{c_k}^{'}\boldsymbol{D}_k = \boldsymbol{d}_k^{'}$, we obtain $\boldsymbol{d}^{'}\boldsymbol{V} = \boldsymbol{d}_k^{'}\boldsymbol{V}_k\boldsymbol{\Lambda}_r$. The left-hand side is $\mathbf{1}_n^{'}\boldsymbol{F}$, which is $\mathbf{0}_r^{'}$, the centrality of global quantified variables, and the right-hand side is $\mathbf{1}_n^{'}\boldsymbol{F}_k\boldsymbol{\Lambda}_r$. Because $\boldsymbol{\Lambda}_r$ is nonsingular, it means $\boldsymbol{F}_k^{'}\mathbf{1}_n = \mathbf{0}_r$.

References

1. Bekker, P., & De Leeuw, J. (1988). Relations between variants of non-linear principal component analysis. In J. L. A. Van Rijckevorsel & J. De Leeuw (Eds.), *Component and correspondence analysis: Dimension reduction by functional approximation* (pp. 1–31). Chichester: Wiley.
2. Blanchflower, D. G., & Oswald, A. J. (2008). Is well-being U-shaped over the life cycle? *Social Science & Medicine*, *66*, 1733–1749.
3. Crawford, C. B., & Ferguson, G. A. (1970). A general rotation criterion and its use in orthogonal rotation. *Psychometrika*, *35*, 321–332.
4. De Leeuw, J. (2006). Nonlinear principal component analysis. In M. Greenacre. & J. Blasius (Eds.), *Multiple correspondence analysis and related methods* (pp. 107–133). Boca Raton FL: CRC Press.
5. Efron, B., & Tibshirani, R. J. (1993). *An introduction to the Bootstrap*. New York: Chapman & Hall.
6. Gower, J. C., & Hand, D. J. (1996). *Biplots*. London: Chapman & Hall.
7. Gower, J., Lubble, S., & Le Roux, N. (2011). *Understanding biplots*. Chichester: Wiley.
8. Greenacre, M. (1984). *Theory and applications of correspondence analysis*. London: Academic Press.
9. Greenacre, M. (2017). *Correspondence analysis in practice* (3rd ed.). Broken Sound Parkway NW: CRC Press.
10. Giulianotti, R. (2002). Supporters, followers, fans, and flaneurs: A taxonomy of spectator identities in football. *Journal of Sport & Social Issues*, *26*, 25–46.
11. Harris, C. H., & Kaiser, H. F. (1964). Oblique factor analytic solutions by orthogonal transformations. *Psychometrika*, *29*, 347–362.

12. Inoue, Y., Func, D. C., Wann, D. L., Yoshida, M., & Nakazawa, M. (2015). Team identification and postdisaster social well-being: The mediating role of social support. *Group Dynamics: Theory, Research, and Practice*, *19*, 31–44.
13. Kimball, B. F. (1940). Orthogonal polynomials applied to least square fitting of weighted observations. *Annals of Mathematical Statistics*, *11*, 348–352.
14. Lancaster, H. O. (1957). Some properties of the bivariate normal distribution considered in the form of a contingency table. *Biometrika*, *44*, 289–292.
15. Murakami, T. (2016). Orthonormal polynomial principal component analysis as a transformation of multiple correspondence analysis: A new procedure for exploratory analysis of Likert-type items. *Bulletin of Data Analysis of Japanese Classification Society, 5*, 27–47. (in Japanese).
16. Ten Berge, J. M. F. (1993). *Least squares optimization in multivariate analysis*. Leiden: DSWO Press.
17. Timmerman, M., Kiers, H. A. L., & Smilde, A. K. (2007). Estimating confidence intervals for principal component loadings: A comparison between the bootstrap and asymptotic results. *British Journal of Mathematical and Statistical Psychology*, *60*, 295–314.

Identifying Groups With Different Traits Using Fourteen Domains of Social Consciousness: A Multidimensional Latent Class Graded Item Response Theory Model

Miki Nakai and Fulvia Pennoni

Abstract A latent variable model included in the class of finite mixture item response theory models is employed to disentangle some recent sociological aspects of the Japanese society. Data collected via the Stratification and Social Psychology survey project in 2018 are analyzed to examine how people are classified in terms of fourteen different life domains: satisfaction, patriotism, social exclusion, anxiety, fatalism, relationships, system justification, social dominance, opinion on inequality, authoritarianism, gender ideology, political opinion, and religious attitudes. We elucidate how the multidimensional latent variables concerning social and psychological traits that differ with respect to the pattern of response to each attitudinal question measured in an ordinal scale are associated with people's objective socio-economic and socio-demographic characteristics such as gender, age, income, education, and Japanese geographical block. On the basis of the model, we disclose three latent classes, each of which represents distinct attitudinal traits and ideological dimensions.

Keywords Expectation–Maximization algorithm · Maximum posterior probabilities · Social attitudes and values · Subjective well-being

MSC: 62C12 · 62H12 · 62P25 · 62D05 · 91B40

M. Nakai (✉)
Department of Social Sciences, College of Social Sciences, Ritsumeikan University, Kyoto, Japan
e-mail: mnakai@ss.ritsumei.ac.jp

F. Pennoni
Department of Statistics and Quantitative Methods, University of Milano-Bicocca, Milan, Italy
e-mail: fulvia.pennoni@unimib.it

T. Imaizumi et al. (eds.), *Advanced Studies in Behaviormetrics and Data Science*,
Behaviormetrics: Quantitative Approaches to Human Behavior 5,
https://doi.org/10.1007/978-981-15-2700-5_14

1 Introduction

The past three decades have seen increasing social inequality, such as wealth inequality, disparities in educational opportunities and occupational insecurity, which strained the social and welfare systems in many countries (Zucman [56]). It has been said that the increasing gap between the haves and the have-nots undermines trust, empathy for people who are different, and tolerance (Uslaner [54]). At the same time, however, those traits are of particular importance in an era of globalization, where people increasingly interact with others different from oneself. Nevertheless, prejudice, discrimination, and expulsion of ethnic minorities and foreigners are thought to be on the rise worldwide, in public discourse, the media as well as political rhetoric.

Growing inequality may also affect people's subjective well-being (SWB) because comparisons with others may matter. Differences in income and people's perceptions of the quality of their own lives may affect people's happiness. The chronic life stress associated with coping with socio-economic disadvantage may have adverse effects on SWB; on the other hand, the members of advantaged groups may be satisfied with the status quo and report higher self-esteem compared to the disadvantaged.

It is important to assess how diverse types of attitudes about the society exist among people, how socio-economic and socio-demographic positions affect the social attitudes such as opinion towards social systems, and who feels satisfied or dissatisfied in this unequal society. How people's social position in the social stratification system affects the views that people hold about the social world? In the present study, people's responses towards various dimensions of social orientations, opinions on social policies, and political attitudes/ideology are used to answer to the above questions. Firstly, we explore the heterogeneity among the population with regard to social cognition and attitudes by using a latent class graded item response theory model. Secondly, we examine the associations between social status characteristics and latent classes concerning major dimensions of social cognition and attitudes.

We focus on the dimensions of SWB and social orientation/personality traits such as social dominance orientation, system justification, patriotism, status anxiety, authoritarianism, and gender ideology. We choose such emotions as SWB, sense of social exclusion/cohesion, self-esteem, and anxiety, because it has been said that growing inequality in the society increases the interpersonal tensions and strains, which leads to erosion of social cohesion. Moreover, it has been emphasized that rising disparities such as wide income gaps are the threats to the SWB and health in many societies (Wilkinson & Pickett [55]). People in more unequal societies have a greater concern with social status and become more dominated by status competition, which damage individual health through stress reactions. In addition to the above dimensions, we also shed light on the concepts concerning intergroup relationships and social intolerance, ethnocentrism, prejudice, and the social stigmatization of members of minority groups such as racism, and authoritarianism. Xenophobic movements have rapidly grown in the past few years. In Japan, the increasing manifestation of racist hate speech and hate crimes against ethnic minorities has come to the attention of the United Nations (UN). Although Hate Speech Elimination Act

came into force in Japan in June 2016 in response to numerous recommendations from a UN special rapporteur on minority issues to restrict hate speech, the UN Committee on the Elimination of Racial Discrimination urged the Japanese government to enhance its efforts to tackle this problem again in 2018.

In addition to the concepts associated with intergroup conflicts, authoritarianism has attracted attention again for the past several years, since it has been discussed that it is closely related to the recent growth of support for populist political parties, the current appeal of political conservatism, and the emergence of leaders with authoritarian tendencies in many Western societies (MacWilliams [33]; Müller [35]; Norris & Inglehart [36]). The characteristics of populism are antielitism, antipluralism, and mass clientelism, and it has tendencies that may push it towards authoritarianism and/or totalitarianism (Müller [35]).

In the following, we employ a latent variable model included in the class of finite mixture item response theory models to examine how members of contemporary Japanese society are classified in terms of SWB, values, and attitudes. We explore how these traits are associated with the individual's socio-economic features and we provide a comprehensive picture of the contemporary Japanese society. The remainder of this article is organized as follows. In Sect. 2, we describe the data. In Sect. 3, we provide technical details on the proposed model focusing on its formulation based on discrete latent variables. In Sect. 4, we show the results and in Sect. 5, we summarize the main conclusions.

2 Data

Responses to the questionnaire of the Stratification and Social Psychology (SSP) Project in Japan are considered in this study. The project focuses on a web-based survey administered in December 2018. The purpose of the project is to examine relationships among people's socio-economic and socio-demographic position, class identification, personality traits, and cognitive tendencies. Survey requests were sent by email to target individuals, who were both men and women aged between 20 and 64 chosen from an online panel of more than 12 million members, inviting them to participate in the online survey and selected according to demographic quotas such as prefectural census population, age distribution, and gender. Therefore, the respondents represent diversity in terms of gender, Japanese geographical area, and birth cohort. The sample size is made of 2,898 individuals (1,476 men and 1,422 women). We selected 54 items measuring 14 different constructs on social psychological attitudes and personality traits. We specify the complete list of items concerning each dimension in Table 9 (see Appendix). We briefly discuss each dimension by the following points:

– *Satisfaction* is a cognitive evaluation of one's life and a core dimension of SWB. Understanding the factors influencing people's SWB and its correlates is one of the most important issues in the scientific study (OECD [37]). We dispose of four

questions about satisfaction across different domains: life in general, respondent's education, Japanese society, the area respondent lives.

- *Social Dominance Orientation* (SDO) is a general orientation attitude towards anti-egalitarianism, relentless competition between groups, hierarchical relationships between social groups, and group-based dominance. It measures political and economic conservatism, nationalism, cultural elitism, anti-black racism, sexism and the belief in a just world (Pratto, Sidanius, Stallworth, & Malle [41]; Sidanius, Pratto, & Bobo [51]). It follows from this that racism and gender role attitudes are closely related to SDO. In order to measure one's degree of preference for inequality among social groups, nine items are included, see Table 9.
- *System justification* theory emphasizes the human propensity to perceive existing social arrangements, or the status quo, as fair, legitimate, and desirable (Jost & Banaji [23]; Jost, Glaser, Kruglanski, & Sulloway [24]; Kay & Jost [25]). The notion that "*people who are disadvantaged by a social system are especially likely to support it*" is known as the system justification hypothesis, which holds that people who suffer the most from a given state of affairs are paradoxically the least likely to question, challenge, reject, or change it. During this process, complementarity in the social world (the belief that "no one has it all" or "poor but happy") stereotypes makes people feel better about their own position in society and increases the perceived legitimacy of the social system. However, it has been pointed out that system-justifying variables help to explain ingroup ambivalence and the internalization of inferiority among members of disadvantaged groups, help to justify existing inequality and hierarchical relationships among different social groups, therefore, incompatible with ideas of equality. In order to measure beliefs concerning the need for balance and complementarity in the social world, four items are considered which measure this dimension.
- *Authoritarianism* is a psychological disposition defined as a tendency to preserve what is established and hostility to social innovation. The tradition of research on the personality correlates of conservatism began with Adorno's study of authoritarianism and fascist potential in personality, and also, it was central to Mannheim's sociological analysis of conservatism (Adorno, Frenkel-Brunswik, Levinson, & Sanford [1]; Mannheim [31]). Six questions are included for the notion of this ideology. There is a long tradition in sociology and political sciences of arguing the relation between social class and political values. For example, according to Lipset [29], working-class people express more negative attitudes towards ethnic and racial minorities and liberal immigration legislation. In previous empirical research (Carvacho et al. [12]), authoritarianism and SDO were negatively associated with income and education (Celeux & Soromenho [13]).
- *Patriotism and racism*, each of which is one of the forms of group attachment, are closely related to authoritarian personality. Patriotism is a sense of positive identification with and feelings of affective attachment to one's country. However, the concept has two facets: blind attachment and constructive patriotism (Adorno et al. [1]; Schatz, Staub, & Lavine [49]). Also, the concept of racism has two facets: old-fashioned racism and modern racism (McConahay [32]; Taka & Amemiya [53]). The first one is pre-civil-rights-movement racism and it is the familiar stereotype

and support for segregation and for open discrimination. In contrast, the second one is referred to as the post-civil-rights-movement beliefs and its principal tenets are, for example, that people in minority groups are pushing too hard, too fast and into places where they are not wanted, and these tactics and demands are unfair. We use one item as patriotism and four items to measure blind patriotism and racism.

– *Sense of social exclusion* and *status anxiety* are source of stress and can rob people of their self-confidence and happiness (Delhey & Dragolov [16]; Layte & Whelan [27]). Status anxiety is a concern with social status or a worry concerning how others see us. *Fatalism*, which is the sense of being controlled by outside forces, or at the other extreme, it is the sense of personal control and beliefs that one can shape his/her own social outcomes, is also characterized by negative self-evaluations and associated with the above orientations to self and society.
– *Gender ideology* has been investigated by a lot of research to understand if age and education play a role in this system of thinking. Age has been found to be a consistently significant correlate of gender role attitudes: younger people have a more egalitarian gender role attitude than older people (Inglehart & Norris [22]; Kikkawa [26]). It may be because older people were socialized with substantially more traditional gender role norms than younger people. As for the effect of education (Ojima [38]; Suzuki [52]), the highly educated develops egalitarian gender ideology, see, among others, Pennoni and Nakai [40].
– *Social Inequality, Meritocracy, Political Efficacy, Relationships with others, and Religious attitudes* are also included as dimensions in this study and they concern opinions on social and political issues, see Table 9.

All the items in the questionnaire are of multiple choice type, with five categories scored on an ordinal scale ranging from 0 to 5 indicating levels of satisfaction or agreement: (0) satisfied (agree), (1) somewhat satisfied (agree), (2) neither satisfied nor dissatisfied (neither agree nor disagree), (3) somewhat dissatisfied (disagree), (4) dissatisfied (disagree), and (5) don't know.

Table 1 shows the distribution of the item response categories for six (1–4 and 50–51) out of the 54 items measuring the above fourteen dimensions. We notice that 45% of individuals are satisfied or somewhat satisfied with the overall life, 34% neither

Table 1 Distribution of the item response categories for the dimensions concerning satisfaction (items 1, 2, 3, 4) and gender ideology (items 50, 51)

Response category						
	0	1	2	3	4	5
Item 1	0.06	0.39	0.25	0.17	0.13	0.00
Item 2	0.11	0.31	0.32	0.16	0.10	0.00
Item 3	0.01	0.14	0.34	0.29	0.21	0.01
Item 4	0.07	0.35	0.34	0.15	0.10	0.00
Item 50	0.31	0.22	0.34	0.09	0.03	0.01
Item 51	0.17	0.39	0.33	0.07	0.04	0.01

Table 2 Distribution of the available covariates

Variable	Category	Proportion
Gender	Male	0.51
Occupation 1	Regular full-time employee	0.43
Occupation 2	Part-time or temporary worker	0.25
Occupation 3	Self-employed	0.08
Occupation 4	Unemployed	0.24
Marital status 1	Married	0.58
Marital status 2	Never married	0.35
Marital status 3	Divorced and widowed	0.07
Education 1	Lower secondary	0.02
Education 2	Secondary	0.39
Education 3	College or higher	0.59
Housing 1	Own house	0.64
Housing 2	Renting	0.32
Housing 3	Others	0.04
Age 1	[20, 24]	0.06
Age 2	[25, 29]	0.11
Age 3	[30, 39]	0.22
Age 4	[40, 44]	0.13
Age 5	[45, 49]	0.14
Age 6	[50, 54]	0.12
Age 7	[55, 59]	0.11
Age 8	[60, 64]	0.11
Income 1	First quintile	0.23
Income 2	Second quintile	0.26
Income 3	Third quintile	0.20
Income 4	Fourth quintile	0.22
Income 5	Missing	0.09
Family members 1	One-person household	0.19
Family members 2	Two-person household	0.26
Family members 3	Three-person household	0.26
Family members 4	Four-person household	0.20
Family members 5	More than four	0.09
Region 1	Hokkaido	0.04
Region 2	Tohoku	0.07
Region 3	Kanto	0.36
Region 4	Chubu	0.16
Region 5	Kansai	0.17
Region 6	Chugoku	0.06
Region 7	Shikoku	0.03
Region 8	Kyushu	0.11

satisfied nor dissatisfied with the Japanese society; 31% disagree that men should work outside the home and women should maintain the home, and 39% somewhat agree that husbands should do household chores and childcare. Interestingly, 33% are neutral with respect to this question.

The respondents are asked to fill the questionnaire also with a broad range of socio-demographic characteristics. We analyze the polythomously scored items accounting for the effects of these covariates. The observed proportions are reported in Table 2, among which we consider also income classes.[1] We notice that half of the respondents are married, high educational levels are mostly represented in the data and middle age people are mainly resident in the Kanto province of Japan.

3 Latent Class Graded Item Response Theory Model

We apply an item response theory model tailored to cluster individuals according to homogeneous subpopulations sharing similar latent traits and attitudes. The multivariate formulation of the model allows us to account jointly for the answers provided to each item in the questionnaire measured on a five point scale. First introduced by Rasch [43] as a model for dichotomously scored items and later improved by Birnbaum [11] and Lord and Novick [30], the model suggests that the probability to provide a certain answer to an item can be modelled as a function of the person position on a latent trait and the parameters that characterize the item. We consider a finite mixture item response theory model (Bartolucci, Bacci, & Gnaldi [6]; Bartolucci, Pennoni, & Lupparelli [9]) based on a latent class model (Goodman [19]; Lazarsfeld & Henry [28]) . We assume that the same item response model holds for all the individuals in the same latent class and possibly different item response models hold for different latent classes that define homogeneous groups of individuals showing similar traits (Pennoni [39]). We dispose of class-specific item parameters describing the peculiarities of an item when it is answered by individuals belonging to a certain latent class. In particular, by adopting the parameterization proposed by Samejima [46, 47], we are able to account for the ordinal categories. The model for ordered item categories was first proposed by Samejima [48] and named as *Graded Response Model* (GRM). It assumes two item parameters: a difficulty parameter for the threshold of each item and a discrimination parameter. When the categories are ordered, the threshold refers to the comparison between item category y or higher and category $y - 1$ or smaller. The difficulty levels of each item measure the general tendency of responding within a category of a certain item. If it is possible to assume that all the categories within the same item discriminate in the same way, the discriminant parameters are constrained to be constant.

The questionnaire measures similar and related psychological constructs that are unobservable and we need to account for their multidimensional structure (Reckase

[1] The categories of the annual income in yen are the following: (1) less than 750,000, (2) 750,000–2,500,000, (3) 2,500,000–4,500,000, (4) 4,500,000 or more, (5) missing.

[44]). To deal with more than one dimension, Agresti [2] proposed a multidimensional log-linear item response theory model and later on Rijmen and Briggs [45] proposed a multidimensional Rasch model. In the following, we adopt the proposal of Bartolucci [5] based on discrete latent variables (Bartolucci & Pennoni [8]) and we adopt a parameterization with multidimensional latent variables to deal with all the dimensions illustrated in Sect. 2. Therefore, we define the model as a Multidimensional Latent Class Graded Item Response Theory (MLCGIRT) model.

Let Y_{ij} denote the categorical response variable for individual i to item j, $i = 1, \ldots, n$, $j = 1, \ldots, J$, driven from an ordinal polytomous item having the same $r_j = r$ ordinal categories $y = 0, 1, \ldots, r-1$. The vector of responses provided by this individual to the questionnaire is denoted as $\mathbf{Y}_i = (Y_{i1}, \ldots, Y_{ir})'$. The corresponding observed values are denoted in lower case, that is, by y_{ij} and $\mathbf{y}_i$. Let D be the number of different latent traits measured by the J items. We define $\mathbf{U}_i = (U_{1i}, \ldots, U_{Di})'$ the vector of latent variables corresponding to the D latent traits, and $\mathbf{u}_i$ as one of the possible realizations of $\mathbf{U}_i$. We assume that $\boldsymbol{\xi}_{ud}$ represents the vector of values (support points) of $\mathbf{U}_i$ with $u = 1, \ldots, k$ denoting the latent classes and $d = 1, \ldots, D$ denoting the dimensions. The mass probabilities (weights of each latent class) at individual level are defined as $\pi_{i,u,\mathbf{x}} = p(\mathbf{U}_i = \boldsymbol{\xi}_{ud} | \mathbf{x}_i)$ since they depend on the available fixed concomitant variables collected in the column vector $\mathbf{x}_i$ representing the socio-demographic features of the respondent.

The item characteristic curve also known as item response function is

$$p_{jy}(\mathbf{u}_i) = p(Y_{ij} \geq y | \mathbf{u}_i), \quad y = 1, \ldots, r-1,$$

where $\mathbf{u}_i$ denotes the dimensions of the model with elements $u_{id}, d = 1, \ldots, D$, and is assumed as a monotonic non decreasing function of u_i for each $i = 1, \ldots, n$. It is parameterized as

$$\log \frac{p_{jy}(\mathbf{u}_i)}{1 - p_{jy}(\mathbf{u}_i)} = \left(\sum_{d=1}^{D} 1\{j \in I_d\} \xi_{ud} - \beta_{jy} \right), \quad j = 1, \ldots, J, \quad y = 1, \ldots, r-1,$$

where β_{jy} is the difficulty of threshold y of item j and the discrimination parameter for each item is fixed to 1. The assumption of the model is that of *local independence*, according to which the responses in $\mathbf{Y}_i$ are conditionally independent given the latent variables in $\mathbf{U}_i$ and the individual covariates in $\mathbf{x}_i$. This leads to the following

$$p(y_i | \mathbf{u}_i) = \prod_{j=1}^{J} p'_{jy_{ij}}(\mathbf{u}_i), \; i = 1, \ldots, n$$

where $p'_{jy_{ij}} = p(Y_{ij} = y | \mathbf{u}_i)$ is obtained as

$$p_{ij}(\mathbf{u}_i) - p_{ij+1}(\mathbf{u}_i).$$

The concomitant variables at individual level $\mathbf{x}_i$ are supposed to influence the probability of belonging to a certain latent class and they are modelled through reference-category logits of the following type

$$\log \frac{\pi_{i,u,\mathbf{x}}}{\pi_{i,1,\mathbf{x}}} = \gamma_{0u} + \mathbf{x}_i' \boldsymbol{\gamma}_{1u} \quad i = 1, \ldots, n, \quad u = 2, \ldots, k, \tag{1}$$

where γ_{0u} are intercepts specific of each latent class and $\boldsymbol{\gamma}_{1u}$ are vectors of regression parameters with u ranging from 2 to k, see, among others, Dayton and Macready [15] and Formann [18] for further details. The interpretation of the effects of the covariates is straightforward if the ability levels are increasingly ordered.

Given observed data referred to a sample of n subjects, the log-likelihood of the model is

$$\ell(\boldsymbol{\theta}) = \sum_{i=1}^{n} \log p_i(\mathbf{Y}_i = \mathbf{y}_i),$$

where $\boldsymbol{\theta}$ is the vector collecting all the free parameters. Maximum likelihood estimation of the model parameters is performed by maximizing $\ell(\boldsymbol{\theta})$ through the Expectation–Maximization (EM) algorithm (Baum, Petrie, Soules, & Weiss [10]; Dempster, Laird, & Rubin [17]). It relies on the complete data log-likelihood, denoted by $\ell^*(\boldsymbol{\theta})$, which corresponds to the log-likelihood that we would compute if we knew the values of the latent variables. The algorithm alternates two steps (E and M) until convergence. The E-step computes the conditional expected value of $\ell^*(\boldsymbol{\theta})$ given the observed data and the current value of the parameters. This expected value is maximized at the M-step with respect to $\boldsymbol{\theta}$ and the estimate of this parameter vector is updated until convergence. Standard errors are obtained through the square root of the diagonal elements of the inverse of the observed or expected information matrix (Bartolucci, Farcomeni, & Pennoni [7]).

The number of support points of the latent distribution is chosen according to the most popular information criteria: the Bayesian Information Criterion (BIC, Schwarz [50]) and the Akaike Information Criterion (AIC, Akaike [3]). After estimation, an important task consists on the prediction of the latent variables at individual level. In the literature, the *Maximum-A-Posteriori* (MAP) approach is considered as the best rule to allocate each individual in a latent class (Goodman [20, 21]). This rule is employed for finite mixture models in general (McLachlan & Peel [34]) and it consists of selecting the latent class having the highest posterior probability, which corresponds to the conditional distribution of the latent variable given the observed responses and the concomitant variables. This conditional MAP approach is based on the following allocation rule

$$\hat{u}_i = \underset{u=1,\ldots,k}{\operatorname{argmax}} \hat{b}_{i,u}, \quad i = 1, \ldots, n, \tag{2}$$

where $\hat{b}_{i,u}$ is the estimated posterior probability for subject i to be allocated in latent class u given his/her response configuration and covariates.

Table 3 Maximum log-likelihood, number of parameters, values of the Akaike and Bayesian information criteria of the model for a number of latent classes ranging from 1 to 4

k	$\hat{\ell}$	#par	AIC	BIC
1	−22,9631.05	270	459,802.09	461,414.47
2	−22,4922.47	317	450,478.93	452,371.99
3	−22,3160.70	364	447,049.40	449,223.12
4	−22,4044.62	411	448,911.24	451,365.64

Table 4 Estimated support points $\hat{\boldsymbol{\xi}}_{ud}$ (latent traits levels) of the three latent classes for each dimension

Dimension	Latent class 1	Latent class 2	Latent class 3
1 Satisfaction	2.03	3.24	4.81
2 Patriotism	3.97	3.27	1.82
3 Blind patriotism and racism	0.45	1.47	0.46
4 Sense of social exclusion	−1.39	0.47	1.50
5 Status anxiety	−1.19	1.06	1.13
6 Fatalism	2.97	3.49	4.38
7 Relationship with others	1.01	1.96	2.77
8 System justification	2.38	1.86	1.02
9 Social dominance orientation	0.70	1.43	0.81
10 Opinion on inequality or social status	−0.06	0.55	0.25
11 Authoritarian traditionalism	1.93	2.82	1.19
12 Gender ideology	0.37	1.40	0.27
13 Political opinion	3.66	3.22	3.76
14 Religious mind	3.00	3.08	3.79

4 Results

The proposed MLCGIRT model is estimated for a number of support points k of the latent variable ranging from 1 to 4. Table 3 reports on the highest maximum log-likelihood at convergence, the number of free parameters, and the corresponding AIC and BIC values. According to the results, there are three different latent subpopulations. The estimated class weights $\hat{\pi}_{u,\mathbf{x}}$ tell us that the biggest subpopulation is the second with 47% of the Japanese belonging to this class; instead 36% of individuals are in class 1 and the remaining 17% in class 3.

Table 4 shows the estimated support points ($\boldsymbol{\xi}_{ud}$). The latent classes differ in the emphasis they place on some characteristics, especially the extent to which individuals are satisfied with life, feeling self-worth or self-esteem, and have fatalistic life views. These estimates allow us to disentangle the following differences between the three latent subgroups. Individuals grouped in latent class 1 show the pattern of responses of being relatively satisfied with their life, own education, and the area they live, good relationship with others and the community where they live, and sense of

being recognized by others. Moreover, respondents in latent class 1 feel secure in their status and work and have high feeling of self-esteem. At the same time, respondents in latent class 1 tend to choose moderately open-minded and democratic way of thinking. They reject various modes of intergroup inequality, show some disagreement with authoritarianism and traditionalism as well as gendered division of labour.

Latent class 2 groups the respondents that are moderately satisfied with own life but relatively dissatisfied with the Japanese society, and agree to some extent with traditionalism. They show a tendency to choose neutral response options in the middle (neither agree nor disagree) in general. This class may embody average image of the Japanese because some research on cross-cultural differences in response style reported that, compared to North Americans and European people, East-Asian, especially Japanese, exhibit more ambivalent and moderate responding, see, among others, Bagozzi, Wong, and Yi [4] and Chen, Lee, and Stevenson [14]. This means that East-Asian choose the midpoint of the scale more frequently. The result that almost half of Japanese belong to class 2, which shows the highest conditional probability for response category 2 (neither agree nor disagree) all over the items, can be understood in the light of these arguments.

Latent class 3 shows the pattern of responses of those being relatively dissatisfied with own life as well as with Japanese society. They are not only unhappy with their life but also express a sense of being excluded in the community they live, as well as pessimistic and fatalistic views towards life. However, at the same time, they show the most tolerant and open-minded attitudes; they are tolerant towards the ethnic minorities, and take a liberal gender role attitudes to advance gender equality. It is worth noting that the response patterns of latent class 1 are very similar to those of latent class 3 in terms of dimension 3 (blind patriotism and racism), dimension 9 (social dominance orientation), and dimension 12 (gender ideology). Both of them are not racist, reject various modes of intergroup inequality or group-based dominance. Also, both individuals in latent classes 1 and 3 support more equal division of labour between husbands and wives. However, in terms of SWB, the response patterns of latent class 3 are in contrast to those of latent class 1. Respondents in latent class 1 are relatively happy and having high feeling of self-worth, whereas respondents in latent class 3 are not contented with Japanese society, low in perceptions of control or mastery, and low in self-esteem, that is to say that they are more distressed, although latent class 3 concerns people whose psychological traits are the most tolerant and most liberal.

The estimated difficulty levels $\hat{\beta}_{jy}$ for the items measuring satisfaction of each item are reported in Table 5. They represent the point on the latent continuum at which the individual latent traits are located. The difficulty parameter corresponding to the first response category is constrained to zero. The item difficulties are ordered according to the item categories and the probability of positively answering an item decreases as its difficulty increases (the traits being constant) and increases according to the estimated traits (the difficulties being constant). From the results, we notice that the levels of each item are increasing according to a linear trend. Item response category 1 (somewhat satisfied) is more difficult to respond for item two (how satisfied are you with your education). Item response category 2 (neither satisfied nor

Table 5 Estimated difficulties ($\hat{\beta}_{jy}$) for each response category (0 as baseline) of the four items measuring satisfaction

Response categories	1	2	3	4	5
Item 1	0.00	2.80	4.09	5.30	9.25
Item 2	0.68	2.66	4.26	5.52	8.23
Item 3	−1.51	1.11	2.99	4.54	8.27
Item 4	0.08	2.63	4.36	5.61	9.07

Table 6 Estimated conditional response probabilities for the four items measuring satisfaction

	Response category	Item 1	Item 2	Item 3	Item 4
Latent class 1	0	0.12	0.21	0.03	0.13
	1	0.57	0.45	0.26	0.52
	2	0.20	0.25	0.44	0.26
	3	0.08	0.07	0.20	0.06
	4	0.03	0.02	0.07	0.03
	5	0.00	0.00	0.00	0.00
Latent class 2	0	0.04	0.06	0.00	0.04
	1	0.35	0.29	0.10	0.31
	2	0.31	0.38	0.33	0.40
	3	0.19	0.17	0.35	0.16
	4	0.11	0.09	0.21	0.09
	5	0.00	0.01	0.01	0.00
Latent class 3	0	0.01	0.02	0.00	0.01
	1	0.11	0.09	0.02	0.09
	2	0.21	0.26	0.11	0.29
	3	0.29	0.30	0.29	0.30
	4	0.37	0.30	0.54	0.30
	5	0.01	0.03	0.04	0.01

dissatisfied) is more difficult to respond for item one (how satisfied are you with your life overall). Item response category 3 (somewhat dissatisfied) and 4 (dissatisfied) are more difficult to respond for item four (concerning the residential area).

With reference to the estimated conditional probabilities of answering to each response category, Tables 6 and 7 report the estimates referred to items measuring satisfaction and sense of social exclusion, respectively. The interpretation of these estimates is provided in the following as an example.[2] The results in Table 6 concerning satisfaction show that respondents in latent class 1 have high probability (0.57) of answering somewhat satisfied and low probability (0.20) of answering neither satisfied nor dissatisfied, whereas those in latent class 3 have a probability of 0.37 of answering dissatisfied and 0.29 of answering somewhat dissatisfied.

[2]The other results are available from the authors upon request along with the R (R Core Team [42]) code implemented to perform the analyses.

Table 7 Estimated conditional response probabilities for the six items measuring social exclusion

	Response category	Item 1	Item 2	Item 3	Item 4	Item 5	Item 6
Latent class 1	0	0.81	0.61	0.62	0.14	0.26	0.28
	1	0.12	0.19	0.20	0.49	0.54	0.50
	2	0.06	0.15	0.14	0.29	0.15	0.17
	3	0.01	0.04	0.02	0.04	0.03	0.03
	4	0.00	0.01	0.01	0.04	0.02	0.02
	5	0.00	0.00	0.01	0.00	0.00	0.00
Latent class 2	0	0.38	0.19	0.20	0.02	0.05	0.06
	1	0.24	0.18	0.21	0.19	0.33	0.30
	2	0.25	0.36	0.39	0.44	0.36	0.38
	3	0.07	0.18	0.12	0.14	0.12	0.12
	4	0.03	0.06	0.04	0.18	0.13	0.13
	5	0.03	0.03	0.04	0.03	0.01	0.01
Latent class 3	0	0.18	0.08	0.08	0.01	0.02	0.02
	1	0.19	0.10	0.12	0.08	0.16	0.14
	2	0.34	0.31	0.40	0.31	0.33	0.33
	3	0.14	0.29	0.21	0.18	0.18	0.18
	4	0.07	0.14	0.09	0.36	0.29	0.29
	5	0.08	0.08	0.10	0.08	0.02	0.04

Similarly, respondents in latent class 1 have large probabilities of reporting satisfaction on item two (education) and item four (residential area). On the other hand, respondents in latent class 3 have large probabilities of reporting dissatisfaction on items two, three, and four, concerning dissatisfaction with Japanese society above all. Respondents in latent class 2 have a 0.35 probability of answering somewhat satisfied and 0.31 probability of answering neither satisfied nor dissatisfied for item one. Therefore, they are less satisfied with their life overall than those in latent class 1, but they are relatively satisfied with life and neighbourhood.

The results in Table 7 show that respondents in latent class 1 tend to have positive affect because they experience their lives in positive ways; they have 0.80, 0.61, and 0.62 as probabilities of reporting disagreement with the following items "I feel left out of society", "Life has been so complicated today that I almost can't find my way", and "I feel that the value of what I do is not recognized by others", respectively. On the other hand, those in latent class 3 are less likely to have sense of belonging to a community; they give neutral responses to item 1, 2, and 3, but have relatively larger probabilities of reporting disagreement with the following items: "I feel close to people in the area where I live", "I feel emotional attachment to the area where I live", and "I want to keep living in the community where I live".

The interpretation of the regression coefficients in Eq. (1) concerning the effects of the concomitant variables is not straight. Therefore, we show in Table 8 the proportions of Japanese allocated in each latent class according to the posterior probabilities by covariates as in Eq. (2). In this way, we can understand the effects of the socioeconomic features of the respondents on the probability to be allocated in each latent

Table 8 Estimated proportions of Japanese allocated to the latent classes on the basis of the estimated posterior probabilities

Covariates	Latent class 1	Latent class 2	Latent class 3
Male	0.39	0.42	0.19
Female	0.32	0.53	0.15
Occupation 1	0.34	0.54	0.12
Occupation 2	0.36	0.44	0.20
Occupation 3	0.44	0.38	0.18
Occupation 4	0.35	0.43	0.22
Marital status 1	0.42	0.46	0.12
Marital status 2	0.24	0.52	0.24
Marital status 3	0.38	0.41	0.21
Education 1	0.26	0.45	0.29
Education 2	0.30	0.49	0.21
Education 3	0.40	0.46	0.14
Housing 1	0.39	0.46	0.15
Housing 2	0.30	0.49	0.21
Housing 3	0.27	0.57	0.18
Age 1	0.29	0.49	0.22
Age 2	0.26	0.56	0.18
Age 3	0.28	0.53	0.19
Age 4	0.33	0.52	0.15
Age 5	0.33	0.48	0.19
Age 6	0.41	0.43	0.16
Age 7	0.44	0.39	0.17
Age 8	0.58	0.34	0.08
Income 1	0.32	0.44	0.24
Income 2	0.37	0.44	0.19
Income 3	0.31	0.54	0.15
Income 4	0.44	0.47	0.09
Income 5	0.29	0.51	0.19
Family members 1	0.27	0.51	0.22
Family members 2	0.43	0.41	0.16
Family members 3	0.35	0.49	0.16
Family members 4	0.34	0.51	0.15
Family members 5	0.36	0.46	0.18
Region 1	0.44	0.41	0.15
Region 2	0.30	0.50	0.20
Region 3	0.34	0.48	0.18
Region 4	0.36	0.47	0.17
Region 5	0.38	0.49	0.13
Region 6	0.37	0.43	0.20
Region 7	0.39	0.44	0.17
Region 8	0.34	0.48	0.18

subpopulation. Compared to men, less females are allocated in latent class 1. The results suggest that females tend to be less satisfied and more likely than men to perceive existing social arrangement, or the status quo, as unfair. This suggests also that compared to men, women may be more likely to give moderate response styles when answering their opinion towards society.

Concerning the relating socioeconomic position of an individual, such as education, occupational statuses, and respondent's annual income, we make the following observations. Self-employed, married with at least two family members, highly educated, with a relative high income are mainly allocated in latent class 1. This suggests that people of these groups tend to report higher SWB and self-esteem based on their stable personal life such as good health conditions, strong social relationships, and standard of living. These advantaged groups are moderately open-minded, although these members are not as liberal or open-minded as the members in latent class 3. They also tend to bolster and justify aspects of the societal status quo, therefore, express more satisfaction with the status quo. Compared to those who are secure and advantaged, the lowest income quintile group tends to be found in latent class 3, who reports lower SWB and somewhat fatalistic view towards life. Single individuals, unemployed, never married and with just one member in the family, with a basic level of education and a very low income are mainly allocated in latent class 3.

As regards age, the result shows that the younger members of Japanese society tend to belong to latent class 2, whereas relatively older people in their late 50s up to early 60s are more likely to be found in latent class 1. This suggests that Japanese elder members are more contend with Japanese society and their local community, and also, feel secure in their status and work and have a high feeling of self-esteem compared to the younger group.

Residential block does not show clear association, but people living in Hokkaido (island at the north end of Japan) are mainly predicted in latent class 1. On the other hand, Tohoku block (the northernmost region of Japan's main island) has a greater probability of belonging to latent class 3.

5 Conclusions

The MLCGIRT model employed in this study is a suitable analytic tool to disentangle the complex system of SWB, values, and social attitudes and to disclose latent subpopulations associated with the individual social position. People's social environment and their socio-economic positions provide different opportunities and constraints for attaining valued goals in the society. Therefore, whether he or she is likely to belong to a particular latent class, which reflects homogenous subpopulation sharing similar social attitudes, may depend on people's social standings. Those who are relatively advantaged social groups such as wealthy, highly educated, and married people reveal content with the status quo and high SWB. These persons are thought to become unconsciously integrated into an existing social system and therefore conform to the ideas and practices that perpetuate the status quo, which benefit unfairly certain social groups while disadvantaging other groups. People who are

relatively disadvantaged in society, on the other hand, are experiencing a lot of stress and negative impacts on their SWB, lack of a sense of belonging within a network of social support, and therefore they are more likely to manifest critical view with reference to the existing socio-political structure and cultural norms. Further research must be undertaken in these areas to compare and assess the change and stability in SWB and value patterns across different social groups over time by collecting and then utilizing the data of a follow-up study.

Acknowledgements This work is supported by JSPS Grant-in-Aid for Scientific Research (No. 17K04103), and (No. 16H02045) as part of the SSP Project. Nakai thanks the SSP Project for the permission to use the SSP 2018 survey data. Pennoni thanks the financial support from the grant "Finite mixture and latent variable models for causal inference and analysis of socio-economic data" (FIRB—Futuro in ricerca) funded by the Italian Government (RBFR12SHVV).

Appendix

Table 9 Fourteen dimensions of social consciousness of the SSP survey and related items

Satisfaction	
1	How satisfied are you with your life overall
2	How satisfied are you with your education
3	How satisfied are you with Japanese society
4	How satisfied are you with your residential area
Patriotism	
5	I have feeling of pride in being Japanese
Blind patriotism and racism	
6	I would support my country right or wrong[a]
7	It cannot be helped that ethnic minorities experience discrimination even though they acquire Japanese citizenship[a]
8	It is wrong that foreigners and ethnic minorities have equal rights as Japanese in Japanese society[a]
9	Foreigners and ethnic minorities are getting too demanding in their push for equal rights[a]
Sense of social exclusion	
10	I feel left out of society[a]
11	Life has been so complicated today that I almost can't find my way[a]
12	I feel that the value of what I do is not recognized by others[a]
13	I feel close to people in the area where I live
14	I feel emotional attachment to the area where I live
15	I want to keep living in the community where I live

(continued)

Table 9 (continued)

Status anxiety	
16	Some people look down on me because of my job situation or income[a]
17	I worry that while I am dawdling, everyone will get ahead of me[a]
18	I worry that while I am not paying attention, I might lose everything I have gained so far[a]
Fatalism	
19	I'm always optimistic about my future
20	I put importance on enjoying today's life rather than saving money or making efforts for the future
21	I want to live my life making plans and carry them out within a certain year
22	I want to realize my dream no matter how it is difficult
23	The natural abilities and qualities of a person decide his/her success[a]
24	By hard work, we can achieve anything
25	People's life is predetermined by fate[a]
Relationship with others	
26	I have trouble getting along with friends frequently[a]
27	I want to enjoy leisure time with friends
System justification	
28	All in all, the world is a 'balanced' place[a]
29	A person who has recently experienced a string of bad breaks probably has something good coming to him or her[a]
30	Some people have everything, while others have nothing
31	Everything has its advantages and disadvantages[a]
Social dominance orientation	
32	No one group should dominate in society
33	In getting what your group wants, it is sometimes necessary to use force against other groups[a]
34	To get ahead in life, it is sometimes necessary to step on other groups[a]
35	It's ok if some groups have more of a chance in life than others[a]
36	We should do what we can to equalize conditions for different groups
37	Sometimes other groups must be kept in their place[a]
38	It's probably a good thing that certain groups are at the top and other groups are at the bottom[a]
39	All groups should be given an equal chance in life
40	We would have fewer problems if we treated people more equally
Opinion on inequality or social status	
41	I see no problem even if the economic gap widens in the future in Japan[a]
42	Parents should give their children best education possible
43	Educational levels reflect people's ability

(continued)

Table 9 (continued)

Authoritarian traditionalism	
44	One should always respect our elders[a]
45	Children should obey to their parents' intension[a]
46	One should always show respect to those in authority[a]
47	It generally works out best to keep on doing things the way they have been done before[a]
48	People who question the old and accepted ways of doing things usually just end up causing trouble[a]
49	In this complecated world, the only way to know what to do is to rely on leaders and experts[a]
Gender ideology	
50	Men should work outside the home and women should maintain the home[a]
51	Husbands should do household chores and childcare
Political opinion	
52	Politics should be left to the people who want to do it
53	Nuclear power plants should be shut down hereafter
Religious mind	
54	It is important to have a religious mind

[a]For items whose ordered categories from 1 to 5 are taken in reverse order

References

1. Adorno, T. W., Frenkel-Brunswik, E., Levinson, D. J., & Sanford, R. N. (1950). *The authoritarian personality*. New York: Harper.
2. Agresti, A. (1993). Computing conditional maximum likelihood estimates for generalized Rasch models using simple loglinear models with diagonal parameters. *Scandinavian Journal of Statistics*, *20*, 63–71.
3. Akaike, H. (1973). Information theory as an extension of the maximum likelihood principle. In B. N. Petrov, & F. Csaki (Eds.), *Second International Symposium on Information Theory* (pp. 267–281). Budapest: Akademiai Kiado.
4. Bagozzi, R. P., Wong, N., & Yi, Y. (1999). The role of culture and gender in the relationship between positive and negative affect. *Cognition and Emotion*, *13*, 641–672.
5. Bartolucci, F. (2007). A class of multidimensional IRT models for testing unidimensionality and clustering items. *Psychometrika*, *72*, 141–157.
6. Bartolucci, F., Bacci, S., & Gnaldi, M. (2015). *Statistical analysis of questionnaires: A unified approach based on R and stata*. Boca Raton: Chapman and Hall/CRC Press.
7. Bartolucci, F., Farcomeni, A., & Pennoni, F. (2013). *Latent Markov models for longitudinal data*. Boca Raton: Chapman and Hall/CRC Press.
8. Bartolucci, F., & Pennoni, F. (2007). On the approximation of the quadratic exponential distribution in a latent variable context. *Biometrika*, *94*, 745–754.
9. Bartolucci, F., Pennoni, F., & Lupparelli, M. (2008). Likelihood inference for the Latent Markov Rasch model, In: N. Huber, M. Limnios, M. Mesbah & M. Nikulin (Eds.), *Mathematical Methods for survival analysis, reliability and quality of life* (pp. 243–257). Wiley.

10. Baum, L. E., Petrie, T., Soules, G., & Weiss, N. (1970). A maximization technique occurring in the statistical analysis of probabilistic functions of Markov chains. *Annals of Mathematical Statistics*, *41*, 164–171.
11. Birnbaum, A. (1968). Some latent trait models and their use in inferring an examinee's ability. In F. M. Lord & M. R. Novick (Eds.), *Statistical theories of mental test scores* (pp. 395–479). Reading, MA: Addison-Wesley.
12. Carvacho, H., Zick, A., Haye, A., Gonzalez, R., Manzi, J., Kocik, C., & Bertl, M. (2013). On the relation between social class and prejudice: The roles of education, income, and ideological attitudes. *European Journal of Social Psychology*, *43*, 272–285.
13. Celeux, G., & Soromenho, G. (1996). An entropy criterion for assessing the number of clusters in a mixture model. *Journal of Classification*, *13*, 195–212.
14. Chen, C., Lee, S. Y., & Stevenson, H. W. (1995). Response style and cross-cultural comparisons of rating scales among East Asian and North American students. *Psychological Science*, *6*, 170–175.
15. Dayton, C. M., & Macready, G. B. (1988). Concomitant-variable latent-class models. *Journal of the American Statistical Association*, *83*, 173–178.
16. Delhey, J., & Dragolov, G. (2014). Why inequality makes europeans less happy: The role of distrust, status anxiety, and perceived conflict. *European Sociological Review*, *30*, 151–165.
17. Dempster, A. P., Laird, N. M., & Rubin, D. B. (1977). Maximum likelihood from incomplete data via the EM algorithm (with discussion). *Journal of the Royal Statistical Society, Series B*, *39*, 1–38.
18. Formann, A. K. (2007). Mixture analysis of multivariate categorical data with covariates and missing entries. *Computational Statistics & Data Analysis*, *51*, 5236–5246.
19. Goodman, L. A. (1974). Exploratory latent structure analysis using both identifiable and unidentifiable models. *Biometrika*, *61*, 215–231.
20. Goodman, L. A. (1974). The analysis of systems of qualitative variables when some of the variables are unobservable. *American Journal of Sociology*, *79*, 1179–1259.
21. Goodman, L. A. (2007). On the assignment of individuals to latent classes. *Sociological Methodology*, *37*, 1–22.
22. Inglehart, R., & Norris, P. (2003). *Rising tide*. Cambridge: Cambridge University Press.
23. Jost, J. T., & Banaji, M. R. (1994). The role of stereotyping in system justification and the production of false consciousness. *British Journal of Social Psychology*, *33*, 1–27.
24. Jost, J. T., Glaser, J., Kruglanski, A. W., & Sulloway, F. J. (2003). Political conservatism as motivated social cognition. *Psychological Bulletin*, *129*, 339–375.
25. Kay, A. C., & Jost, J. T. (2003). Complementary justice: Effects of 'poor but happy' and 'poor but honest' stereotype exemplars on system justification and implicit activation of the justice motive. *Journal of Personality and Social Psychology*, *85*, 823–837.
26. Kikkawa, T. (1998). Social determinants of gender role attitudes. In F. Ojima (Ed.), *Sociological functionning of gender and stratification* (pp. 49–70). The 1995 SSM Research Committee, Tokyo.
27. Layte, R., & Whelan, C. T. (2014). Who feels inferior? A test of the status anxiety hypothesis of social inequalities in health. *European Sociological Review*, *30*, 525–535.
28. Lazarsfeld, P. F., & Henry, N. W. (1968). *Latent structure analysis*. Boston: Houghton Mifflin.
29. Lipset, S. M. (1959). Democracy and working-class authoritarianism. *American Sociological Review*, *24*, 482–501.
30. Lord, F. M., & Novick, M. R. (1968). *Statistical theories of mental test scores*. Reading, MA: Addison- Wesley Publishing Company Inc.
31. Mannheim, K. ([1927] 1986). In D. Kettler, V. Meja & N. Stehr (Eds.), *Conservatism: A contribution to the sociology of knowledge*. New York: Routledge and Kegan Paul.
32. McConahay, J. B. (1986). Modern racism, ambivalence, and the modern racism scale. In J. F. Dovidio & S. L. Gaertner (Eds.), *Prejudice, discrimination, and racism* (pp. 91–125). Orlando: Academic Press.
33. MacWilliams, M. C. (2016). *The rise of Trump: America's Authoritarian Spring*. Amherst, MA: Amherst College Press.

34. McLachlan, G. J., & Peel, D. (2000). *Finite mixture models*. New York: Wiley.
35. Müller, J.-W. (2016). *What is populism?* Philadelphia: University of Pennsylvania Press.
36. Norris, P., & Inglehart, R. (2019). *Cultural backlash: Trump, Brexit and Authoritarian Populism*. New York: Cambridge University Press.
37. OECD. (2013). *OECD guidelines on measuring subjective well-being*. OECD Publishing. Retrieved from http://dx.doi.org/10.1787/9789264191655-en.
38. Ojima, F. (1998). Changes in gender-role attitudes of Japanese women, 1985–1995. In: F. Ojima (Ed.), *Sociological functionning of gender and stratification* (pp. 1–22). The 1995 SSM Research Committee, Tokyo.
39. Pennoni, F. (2014). *Issues on the estimation of latent variable and latent class models*. Saarbücken: Scholars'Press.
40. Pennoni, F., & Nakai, M. (2019). A latent class analysis towards stability and changes in breadwinning patterns among coupled households. *Dependence Modeling*, *7*, 234–246.
41. Pratto, F., Sidanius, J., Stallworth, L., & Malle, B. F. (1994). Social dominance orientation: A personality variable predicting social and political attitudes. *Journal of Personality and Social Psychology*, *67*, 741–763.
42. R Core Team. (2019). R: A language and environment for statistical computing. In *R Foundation for Statistical Computing*. Vienna, Austria. http://www.R-project.org/.
43. Rasch, G. (1960). *Probabilistic models for some intelligence and attainment tests*. Copenhagen, Denmark: Danish Institute for Educational Research.
44. Reckase, M. D. (2009). *Multidimensional item response theory*. New York: Springer.
45. Rijmen, F., & Briggs, D. (2004). Multiple person dimensions and latent item predictors. In M. Wilson & P. De Boeck (Eds.), *Explanatory item response models: A generalized linear and nonlinear approach* (pp. 247–265). New York: Springer.
46. Samejima, F. (1969). *Estimation of ability using a response pattern of graded scores*. Psychometrika Monograph, 17. Psychometric Society, Richmond, VA.
47. Samejima, F. (1972). *A general model for free-response data*. Psychometrika Monograph, 18. Psychometric Society, Richmond, VA.
48. Samejima, F. (2007). Profiles in research. *Journal of Educational and Behavioural Statistics*, *32*, 206–222.
49. Schatz, R. T., Staub, E., & Lavine, H. (1999). On the varieties of national attachment: Blind versus constructive patriotism. *Political Psychology*, *20*, 151–174.
50. Schwarz, G. (1978). Estimating the dimension of a model. *Annals of Statistics*, *6*, 461–464.
51. Sidanius, J., Pratto, F., & Bobo, L. (1994). Social dominance orientation and the political psychology of gender: A case of invariance? *Journal of Personality and Social Psychology*, *67*, 998–1011.
52. Suzuki, A. (1991). Predictors of women's sex role attitudes across two cultures: United States and Japan. *Japanese Psychological Research*, *33*, 126–133.
53. Taka, F., & Amemiya, Y. (2013). A basic investigation of old-fashioned and modern racisms against Zainichi Koreans. *Japanese Journal of Social Psychology*, *28*, 67–76.
54. Uslaner, E. M. (2004). Divided citizens: How inequality undermines trust in America. *working paper*, New York: Demos. Retrieved from https://www.demos.org/sites/default/files/publications/DividedCitizens,6.3.04.pdf.
55. Wilkinson, R., & Pickett, K. (2010). *The spirit level: Why equality is better for everyone*. London: Penguin Books.
56. Zucman, G. (2019). Global wealth inequality. *Annual Review of Economics*, *11*, 109–138.

Quantification Theory: Categories, Variables and Modal Analysis

Shizuhiko Nishisato

Abstract Quantification theory (QT) is known by many names such as dual scaling, Hayashi's quantification theory, optimal scaling, homogeneity analysis and correspondence analysis. It is in essence singular value decomposition of categorical data. As Torgerson [29] called QT as principal component analysis (PCA) of categorical data, one may get some ideas about what QT is. The fact that there are so many aliases is interesting and suggests its versatility. Some names reflect certain mathematical aspects and the others quite different characteristics. No matter what aliases one may adopt, it is certain that QT has many hidden characteristics. As we glance at its general developments, we cannot help but wonder why there are still so many problems associated with QT unsolved. The current paper is an essay with its focus on QT's very basic foundation problems, which have somehow escaped enough attention of researchers. Following Torgerson's naming of QT as PCA of categorical data, we first look at the most fundamental difference between PCA and QT, and then move on to look at some aspects peculiar to QT. We will conclude the paper with some warnings on the characteristics of input data for QT, to avoid the situation of garbage in garbage out.

1 Principal Component Analysis and Graphs

Pearson [28] and Hotelling [11] have laid the foundation of principal component analysis (PCA). Given a set of n standardized continuous variables, PCA is a technique to derive a liner combination of the n variables in such a way that the variance of the linear combination be a maximum, under the condition that the sum of squares of weights for the variables is equal to 1.

Such a linear combination is called the first principal component, and the set of weights, adjusted by the singular values, are called principal coordinates of the n variables. After eliminating the first principal component scores from the original

S. Nishisato (✉)
University of Toronto, Toronto, Canada
e-mail: shizuhiko.nishisato@utoronto.ca

T. Imaizumi et al. (eds.), *Advanced Studies in Behaviormetrics and Data Science*,
Behaviormetrics: Quantitative Approaches to Human Behavior 5,
https://doi.org/10.1007/978-981-15-2700-5_15

data, the residuals are then subjected to the variance-maximization process to arrive at the principal coordinates of the second component, which is orthogonal to the first component. In this way, we continue to extract as many components as the data allow, and we will eventually arrive at Euclidean orthogonal coordinates of n variables. What PCA accomplishes is to start with correlated variables and produces a set of orthogonal components, of which elements are Euclidean coordinates.

Although we know that PCA and QT deal with continuous variables and categorical variables, respectively, there exists another important difference between them. Historically PCA has been used for *uni-modal analysis*. For example, consider a variety of barleys planted at randomly sampled farms, and the crop data were collected and analyzed by PCA. The sole interest of the researchers lies in identifying relations between the variety of barleys (e.g., which variety of barleys grow better than the others, or are there any clusters of barleys which seem to flock together in different components?). In other words, although the data are summarized in a two-way table of a variety of barleys-by-farms, the researcher's interest is focused only on the relations between barleys, and not on the farms. This is a typical example of uni-modal analysis. PCA is likely to provide principal coordinates of barleys in several dimensions, and using those coordinates, the investigators can present the results in multidimensional graphs.

2 Quantification Theory and Graphs

Since uni-modal analysis is mentioned above, let us introduce QT (quantification theory) as typically used for *bi-modal analysis*. Suppose that 10,000 seeds of six varieties of barleys are planted at 10 farms in different provinces, and at the harvest, randomly chosen 2,000 seeds from each farm are classified into the 6 (barleys)$\times$10 (provinces) contingency table. Then. our main interest lies in the interactions between barleys and provinces, that is, how different provinces affect the growth of different kinds of barleys. This is a typical example of data analysis that QT deals with, that is, bi-modal analysis.

QT has been developed since the early years of the last century. Perhaps the best source for its historical developments is an excellent compendium by Beh and Lombardo [1], which covers contemporary developments of relevant topics. Excellent sources of traditional QT can be found in Gifi [9] and Nishisato [19].

The basic type of QT is often characterized by the following bilinear expansion of the contingency table with typical element f_{ij}:

$$f_{ij} = \frac{f_{i.} f_{.j}}{f_t}(1 + \rho_1 y_{1i} x_{1j} + \rho_2 y_{2i} x_{2j} + \rho_3 y_{3i} x_{3j} \cdots + \rho_K y_{Ki} x_{Kj}) \qquad (1)$$

.

where $f_{i.}$, $f_{.j}$ are marginals of row i and column j, respectively, f_t is the total frequency, ρ_k is the k-the singular value, y_{ki}, x_{kj} are, respectively, i-th and j-th

elements of singular vectors $\mathbf{y_k}$ and $\mathbf{x_k}$. One may note that this is nothing but singular value decomposition of a two-way table, known for many years (e.g., Beltrami [2]; Jordan [12]; Eckart & Young [7]).

As may be inferred from this formula, QT is typically concerned with bi-modal analysis, that is, rows and columns are equally treated for analysis, an aspect which is of particular importance. This aspect is related to the expression "joint graphical display". In other words, the researchers are typically interested in plotting both row variables and column variable in common space (note the word "joint"). An inevitable question then is "What multidimensional coordinates can we use to plot both row variables and column variables in common space?"

It is well known that the rows and the columns of the contingency table are generally correlated, but not perfectly, thus the space for rows and the space for columns are different. The ignoring of this space discrepancy sounds like outrageous, but the undeniable fact is that most researchers in QT have ignored this discrepancy!

The currently most popular joint graphical method is called "symmetric scaling" or French plot, developed and extensively used in France. In spite of the fact that it ignores the space discrepancy, it has been routinely used by most QT researchers! Symmetric scaling is correct only when the rows and the columns are perfectly correlated, a case which would not interest any researchers.

An alternative method is called non-symmetric scaling, which is based on the idea of projecting rows, for example, onto the space for columns, or vice versa. Some researchers call this graphical method logical, but it is not the case at all because the projection of standard coordinates of rows onto the standard coordinates of columns, as is done in non-symmetric scaling, is *utterly meaningless*: data structure is depicted by principal coordinates and not by standard coordinates. Thus, if one wants to be logical, then the principal coordinates of rows should be projected onto principal coordinates of columns—the only problem is that the norms of rows and columns in the graph are different, and this is against our attempt to compare the rows and the columns in a justifiable way, namely on the equal footing.

The history shows that Carroll, Green, and Schaffer [4–6] proposed the so-called CGS scaling for accommodating both rows and columns in common space, but the CGS scaling was severely criticized by Greenacre [10] and did not survive the criticism.

However, the justification for the CGS scaling was described six years before the proposal of the CGS scaling by Nishisato [13]: he described that the contingency table could be reformatted into the response-pattern table, and stated that the latter, which contains both rows and columns of the contingency table in common space, requires at least doubled multidimensional space. In other words, if one wants to represent rows and columns in common space, the dimensionality of space must be at least doubled. This discovery, coupled with the Young–Householder theorem (Young & Householder [30]), offers a solution to the CGS scaling. Recently, Nishisato [20] and Nishisato, Beh, Lombardo, and Clavel [22] promoted his solution to the perennial problem of joint graphical display, that is, mapping rows and columns of the contingency table in common space.

According to Nishisato, the quantification space can be partitioned into several types of space, namely, contingency space which is used by the current practice of contingency table analysis, dual space, which accommodates both rows and columns of the contingency table and residual space. Furthermore, dual space can be partitioned into subspaces which can be used to show how inaccurate or accurate the currently most popular symmetric scaling is. Since the matter has been thoroughly discussed and illustrated in the aforementioned papers, we will simply borrow the same example and present the partitioned multidimensional space used by QT.

3 Decompostion of Quantification Space

Nishisato [20] and Nishisato et al. [22] illustrated how quantification space can be partitioned and how to identify exact Euclidean coordinates for both rows and columns in common space (this is the solution to the perennial problem of joint graphical display). We will use the same numerical example and look at the partitioned quantification space. The data used here is a subset of the original data reported by Garmize and Rychlak [8], in which it was assumed that subjects' perceptions of Rorschach inkblots are influenced by the moods of the subjects. The researchers collected the data obtained under experimentally induced moods. The subset of the data consists of frequencies of observations of three different Rorschach inkblots under six moods, as shown in Table 1 (Contingency Table).

Nishisato [13] discussed the condensed response-pattern table, corresponding to the contingency table, as shown in Table 2, as equivalent to the incidence table, consisting of 1s and 0s. The equivalence of the condensed response-pattern table and the (1, 0) incidence table can be demonstrated by Benzécri's principle of distributional equivalence (Benzécri [3]) and Nishisato's principle of equivalent partitioning of forced classification (Nishisato [14]).

Chapter 4 of his 1980 book contains a description of a number of mathematical relations between the contingency table and the response-pattern table formats. The most relevant to our discussion is that the condensed response-pattern table contains both rows and columns of the contingency table in columns. From the graphical point of view, this means that quantification of the response-pattern table yields coordinates for both rows and columns of the contingency table in common space (see Young &

Table 1 Contingency table

Rorschach response	Induced moods					
	Fear	Anger	Depression	Ambition	Security	Love
Bat	33	10	18	1	2	6
Butterfly	0	2	1	26	5	18
Mountains	2	1	4	1	18	2

Table 2 Response-pattern table

Rorschach responses			Moods					
Bat	Butterfly	Mountains	Fear	Anger	Depression	Ambition	Security	Love
33	0	0	33	0	0	0	0	0
10	0	0	0	10	0	0	0	0
18	0	0	0	0	18	0	0	0
1	0	0	0	0	0	1	0	0
2	0	0	0	0	0	0	2	0
6	0	0	0	0	0	0	0	6
0	2	0	0	2	0	0	0	0
0	1	0	0	0	1	0	0	0
0	26	0	0	0	0	26	0	0
0	5	0	0	0	0	0	5	0
0	18	0	0	0	0	0	0	18
0	0	2	2	0	0	0	0	0
0	0	1	0	1	0	0	0	0
0	0	4	0	0	4	0	0	0
0	0	1	0	0	0	1	0	0
0	0	18	0	0	0	0	18	0
0	0	2	0	0	0	0	0	2

Householder [30]). Since our interest lies in finding coordinates of these variables in common space, we now look at only the quantification outcome of the response-pattern table. For detailed comparisons of the two response formats, please refer to Nishisato [20] and Nishisato et al. [22].

First, let us note that multidimensional data structure of rows and columns of the contingency table can be represented by principal coordinates, obtained from the response-pattern representation of the contingency table. Second, notice that those principal coordinates must be identified from a set of components in terms of some mathematical constraints associated with multidimensional decomposition. Table 3 (Principal Coordinates in Different Types of Space) shows the decompositions of the response-pattern structure of the contingency table, as reported in Nishisato [20] and Nishisato et al. [22].

In this example, the contingency table yields two components, of which principal coordinates are listed under the contingency space (C-space). Although this is a two-dimensional decomposition, we know that for each component, the row space and the column space are not identical, but discrepant by the angle θ where

$$\theta_k = \cos^{-1} \rho_k$$

Table 3 Principal coordinates in different types of space

Space	C-space		C-space				
	D-space DSub-1	D-space DSub-1	D-Space DSub-2	D-space DSub-2			
					R-space	R-space	R-space
	T-space	T-space	T-space	T-space	T-space	T-space	T-space
Component	1	7	2	6	3	4	5
Bat	−092	−0.31	−0.39	−0.19	0.00	0.00	0.00
Butterfly	1.19	0.41	−0.49	−0.23	0.00	0.00	0.00
Mountain	0.09	0.03	1.88	0.91	0.00	0.00	0.00
Fear	−1.10	0.38	−0.42	0.20	−0.01	−1.25	0.29
Anger	−0.66	0.23	−0.37	0.18	2.74	1.23	0.78
Depression	−0.83	0.28	0.00	0.00	−1.48	1.75	−0.42
Ambition	1.37	−0.47	−0.63	−0.31	−0.09	0.11	1.23
Security	0.29	−0.10	1.97	−0.95	0.20	−0.29	0.16
Love	0.78	−0.27	−0.45	0.22	−0.14	−0.31	−1.88
Eigenvalue ρ^2	0.895	0.105	0.811	0.189	0.500	0.500	0.500

for component k (Nishisato & Clavel [23]) . In our example, the contingency table yields two eigenvalues $\rho_1^2 = 0.62$ and $\rho_2^2 = 0.39$ so that the angles between row spaces and column spaces are 42° and 57° for components 1 and 2, respectively. This means that we need four-dimensional space to accommodate both rows and columns of this contingency table, which is called dual space. Which four components, out of 7, will constitute dual space? The mathematical constraint on dual space is that the average eigenvalue is 0.5. Since we already have two components from the contingency table analysis (note that the distributions of eigenvalues are different between the contingency table and the response-pattern table as fully discussed in Nishisato [13], and these two components are in fact those from the response-pattern table which correspond to those in the contingency table), it is easy to find two more components that will make the average eigenvalue of the four components as 0.5. Dual space then consists of components 1, 7, 2 and 6 as seen in Table 3. The four components in dual space are further grouped into two sets of two components each under the restriction that the average of the two components is 0.5. The two sets are listed under Subspace 1 and 2.

As Nishisato [20] and Nishisato et al. [22] has shown, it is remarkable that if we plot two components in Subspace 1 or 2, the two-dimensional graph shows the distribution of rows and columns of the contingency table variables in such a way that all row variables are aligned to one line and all column variables are lined on another, and that the angle between the two lines is exactly equal to the discrepancy angle, calculated by the above formula. In other words, the two-dimensional graph of each subspace demonstrates how good or bad symmetric scaling's unidimensional graph is!

The remaining three-dimensional space is residual space, in which three Rorschach inkblots have no more contributions. In other words, the total association between the rows and the columns of the contingency table is completely accounted for by dual space. This strongly suggests that QT of the contingency table should be restricted only to dual space, a good way to justify the name "dual scaling." Another point to note here is that the eigenvalue of each component in residual space is equal to 0.5.

4 Distribution of Information

The previous section has revealed a number of important aspects of quantification theory. If we are to ignore residual space, the only strategy is to use the equal numbers of rows and columns so that residual space is null and dual space is identical to total space.

In expanding the scope of dual scaling, Nishisato [13] treated the contingency table as two multiple-choice data, to handle the extension of quantification from two variables to many variables, which is dual scaling of multiple-choice data or multiple correspondence analysis.

When we have three categorical variables, we can consider two ways of representing the data as Nishisato [13] did for two-variable case, namely the three-dimensional contingency table and the three-item response-pattern table. The tri-variate expansion of the data with the typical element f_{ijk} can be expressed as

$$f_{ijk} = \frac{f_{i..} f_{.j.} f_{..k}}{f_t}(1 + \rho_1 y_{1i} x_{1j} z_{1k} + \rho_2 y_{2i} x_{2j} z_{2k} + \rho_3 y_{3i} x_{3j} z_{3k} \cdots + \rho_K y_{Qi} x_{Qj} z_{Qk}) \tag{2}$$

The corresponding response-pattern table is nothing but the joined table of three response-pattern matrices, which we can express as

$$F = [F_1, F_2, F_3]$$

When we consider all possible relations between two variables, it was relatively clear as we saw in the previous section. But, the relations involving more than two sets of variables are more complex than the previous case. In order to look into a complex case, there is a general framework for capturing data structure, proposed by Nishisato and Lawrence [26], which describes the multiple-response-pattern table as

$$F = (\Sigma_i P_i) F (\Sigma_j P_j),$$

where P_i and P_j are projection operators such that

$$\Sigma_i P_i = I_m,$$

$$\Sigma_j P_j = I_n.$$

In our case, the rows are distinct response combinations of n categorical variables and we are not interested in the structure of the rows. Therefore, we will not consider the decomposed structure of the rows, that is, we treat the left-hand side as the identity matrix, and consider only the structure of columns.

To advance our discussion, let us again use the case of two categorical variables, that is, $F = [F_1, F_2]$. In our example, the number of columns of F_1 was smaller than that of F_2. Therefore, if we form the projection operator of the columns of F_1 by

$$P_1 = F_1(F_1'F_1)^{-1}F_1'$$

and subject the matrix FP_1 to quantification, we obtain the principal coordinates of dual space. If we subject $F(I - P_1)$ to quantification, we will obtain the principal coordinates of residual space.

With more than three categorical variables, the situation becomes complicated, the quantification of the response-pattern matrix will no longer yield distinct separation of different types of space. The question then is which one of the following matrices we should subject to quantification process:

- Data FP_j to obtain the coordinates which totally account for the categorical variable j
- Data $F(I - P_j)$ to obtain the coordinates of the components which are free from the influence of variable j
- Data FP_jP_k to look at the data structure associated fully with the two variables j and k
- Data $FP_1P_2P_3(I - P_4)$ to extract components, associated with variables 1, 2 and 3, but free from the influence of variable 4
- and so on.

These are the topics of forced classification analysis in QT (see Nishisato [14–17, 19]; Nishisato & Hilsdale [25]; Nishisato & Lawrence [26]; Nishisato & Gaul [24]; Nishisato & Baba [21]). Please see these relevant papers about applications of forced classification.

The task of identifying different kinds of spaces, subspaces will become very complicated when we have more than three categorical variables, and it is certain that we must introduce definitions of a larger variety of spaces and subspaces than what we saw for the two-variable case. This is too large a problem to deal with in the current paper and this expansion will, therefore, be left for future work.

5 Categories, Variables and Standardization

We often spend most of our time for developing methods of data analysis and forget the strategy of data collection methods. But, we should remember that the quality of data should be the first concern and thus be treated here as a topic of top priority.

This is a problem peculiar to categorical data analysis because it is often up to the researchers to decide how to collect data for analysis (e.g., the determination of the number of categories is up to the researchers), and remember that QT determines the decomposition of data through "optimization." For example, the correlation between two categorical variables would increase as the number of categories of each variable increases, because of the increased freedom to manipulate, the aspect which does not exist with continuous variables, where the only possibility we have is to determine the weight for the variable and not individual values. More concretely, consider finding the relation between the body strength and the age. Suppose that one investigator used three rating scale of [weak, average, strong] for body strength and two age groups [under 50, over 50] for the variable "age." Suppose further that the other researcher used 10 rating scales from very weak to extremely strong for body strength and 10 groups [younger than 10, 11–20, 21–30, ..., 91–100] for age. It may not be obvious but the second researcher will find a higher value of the correlation between the two categorical variables, simply because the second researcher has greater freedom to determine the values of the categories. This aspect of manipulation in QT is an essential difference between quantification analysis and analysis of continuous data. Note that we do not manipulate the values of continuous data, the only allowance there being to manipulate the weights for variables. In the above example, it is likely that the second researcher will find a nonlinear relation between the age and the body strength through nonlinear assignments of weights to the categories.

This problem is discussed in Nishisato [25], but because of its importance, we will look at some problems here. The source of our main concern is that quantification theory is based on "optimization" and that the outcome of optimization is often in the hands of the investigator.

When we analyze multiple-choice data $[F_1, F_2, ..., F_n]$ by QT, it is well known (for example, see Nishisato [25]) that

- The smaller the frequency of category p of variable j, the greater the influence of the category over quantification because the sum of squares of category p of variable j, SS_{jp}, is given by

$$SS_{jp} = \frac{N - f_{jp}}{nN}$$

  where N is the total number of rows of the response-pattern table, f_{jp} is the frequency of category p of variable j and n is the number of categorical variables. Note the relation: the smaller the frequency of the category, the greater the contribution of the category to SS_{jp}. This sounds like just the opposite of what we might expect.

- The larger the number of categories of variable j, m_j, the greater the contribution of the variable to the total variance, SS_j, because

$$SS_j = \Sigma_p SS_{jp} = \frac{(m_j - 1)}{n}$$

where n is the number of variables. This means that the variable with many more categories than others will exert greater influence on the outcome of quantification.
- The larger the average number of categories in the data set, the greater the contribution of the data set, SS_t, for

$$SS_t = \Sigma_j \frac{m_j - 1}{n}$$

This means that the outcome of quantification is heavily influenced by the average number of categories used in the data set. This information becomes relevant when one wants to compare the results between data sets.

The above discussion inevitably leads to the question of standardization for QT. Without standardization, how can we compare the results of different studies where, for example, different numbers of categories are used in multiple-choice questions?

Interested readers may refer to Nishisato [18], in which he proposed standardized dual scaling and demonstrated what effects would be shown on the results (1) if the effects of the number of categories are partialled out and (2) if the category frequency effects are partialled out. He demonstrated, for example, that the standardization of category frequencies have the effects of eliminating the so-called "outlier" effects—it is known in QT that a category with only one response, for example, will have decisive effects on the outcome in such a way that the first component may be determined by the outlier (the category with only one response). It is usual in QT practice that researchers will adopt only the first few major components for interpretation, but what if the most major component is a reflection of one category of one variable?

Standardized dual scaling has not been further pursued, but it may be worth investigating, considering that how categories are introduced in research is in the hands of researchers, and that some researchers may want to compare the results of QT from different studies. How can we make sure that one can compare two studies on the same topic appropriately?

We have a lesson on this topic, however, from the well established PCA, where investigators sometimes use the decomposition of the variance–covariance matrix V and sometimes the correlation matrix R of the same data set. It is known (see Nishisato & Yamauchi [27]) that the principal components from V are totally different from principal components from R. In other words, in PCA, the standardization changes the structure of data substantially. The same may be the case with QT. To the best of the current author's knowledge, this problem of standardization versus non-standardization for PCA has not been solved, and it is likely that the same problem may exist for QT.

6 Concluding Remarks

This is an essay on quantification problems based on half a century work of the author. The idea of quantification arises from the need for quantitative description of categorical, qualitative or subjective data. In spite of many studies in QT and remarkable advancement of theory, there are still a number of problems to investigate, or rather it seems to the current author that the more we know, the less we are certain about what we can do with our knowledge to understand analysis of categorical data. It is hoped that the current essay may nurture some thought for further development of quantification theory in a more convincing way than now.

The current discussion of QT also has implications for the traditional uni-modal analysis when it is extended to bi-modal analysis. For example, consider factor analysis. When we derive factor loadings of variables, the researchers may also wish to estimate factor scores for the subjects. The current practice is to estimate such factor scores for the subjects from factor loadings of variables. This can be interpreted as projecting factor scores of subjects onto the space of factor loadings of variables. But, would it not be better if we can find the coordinates of both variables and subjects in common space? In this case, the problem is the same as that of joint graphical display of QT. We must double multidimensional space to arrive at principal coordinates of both variables and subjects.

References

1. Beh, E. J., & Lombardo, R. (2014). *Correspondence analysis: Theory, practive and new strategies*. Wiley.
2. Beltrami, E. (1873). Sulle funzioni bilineari (On the bilinear functions). In G. Battagline, & E. Fergola (Eds.), *Giornale di Mathematiche* (Vol. 11, pp.98–106).
3. Benzécri, J. P., et al. (1973). *L'analyse des données: II. L'analyse des correspondances*. Paris: Dunod.
4. Carroll, J. D., Green, P. E., & Schaffer, C. M. (1986). Interpoint distance comparisons in correspondence analysis. *Journal of Marketing Research*, *23*, 271–280.
5. Carroll, J. D., Green, P. E., & Schaffer, C. M. (1987). Comparing interpoint distances in correspondence analysis: A clarification. *Journal of Marketing Research*, *24*, 445–450.
6. Carroll, J. D., Green, P. E., & Schaffer, C. M. (1989). Reply to Greenacre's commentary on the carroll-green-schaffer scaling of two-way correspondence analysis solutions. *Journal of Marketing Research*, *26*, 366–368.
7. Eckart, C., & Young, G. (1936). The approximation of one matrix by another of lower rank. *Psychometrika*, *1*, 211–218.
8. Garmize, L. M., & Rychlak, J. F. (1964). Role-play validation of a socio-cultural theory of symbolism. *Journal of Consulting Psychology*, *28*, 107–116.
9. Gifi, A. (1990). *Nonlinear multivariate analysis*. Wley.
10. Greenacre, M. J. (1989). The Carroll-Green-Schaffer scaling in correspondence analysis: A theoretical and empirical appraisal. *Journal of Marketing Research*, *26*, 358–365.
11. Hotelling, H. (1933). Analysis of complex of statistical variables into principal components. *Journal of Educational Psychology, 24*, 417–441, and 498–520.
12. Jordan, C. (1874). Mémoire sur les formes bilinieres (Note on bilinear forms). *Journal de Mathématiques Pures et Appliquées, deuxiéme Série*, *19*, 35–54.

13. Nishisato, S. (1980). *Analysis of categorical data: Dual scaling and its applications*. Toronto: University of Toronto Press.
14. Nishisato, S. (1984). Forced classification: A simple application of a quantification technique. *Psychometrika*, *49*, 25–36.
15. Nishisato, S. (1986). Generalized forced classification for quantifying categorical data. In E. Deday, et al. (Eds.), *Data analysis and informatics* (pp. 351–362). Amsterdam: North-Holland.
16. Nishisato, S. (1988a). Forced classificaiton procedure of dual scaling: its mathematical properties. In H. H. Bock (Ed.), *Classificaiton and related methods* (pp. 523–532). Amsterdam: North-Holland.
17. Nishisato, S. (1988b). Market segmentation by dual scaling through generalized forced classification. In W. Gaul & M. Schader (Eds.), *Data, expert knowledge and decisions* (pp. 268–278). Berlin: Springer-Verlag.
18. Nishisato, S. (1991). Standardizing multidimensional space for dual scaling. In *Proceedings of the 20th Annual Meeting of the German Operations Research Soceity* (pp. 584–591). Hohenheim University.
19. Nishisato, S. (2007). *Multidimensional nonlinear descriptive analysis*. London: Chapman and Hall/CRC.
20. Nishisato, S. (2019). Reflection: Quantification theory and graphs. *Theory and Applications of Data Analysis, 8*(1), 47–57. (in Japanese).
21. Nishisato, S., & Baba, Y. (1999). On contingency, projection and forced classification of dual scaling. *Behaviormetrika*, *26*, 207–219.
22. Nishisato, S., Beh, E., Lombardo, R., & Clavel, J.G. (2020, in press). *Modern Quantifiation Theory: Joint Grapphical Display, Biplots and Alternatives*. Springer: Singapore.
23. Nishisato, S., & Clavel, J. G. (2002). A note on between-set distances in dual scaling and correspondence analaysis. *Bahaviormetrika*, *30*, 207–219.
24. Nishisato, S., & Gaul, W. (1990). An approach to marketing data analysis. *Journal of Marketing Research*, *27*, 354–360.
25. Nishisato, S. & Hilsdale, N. J. (1994). *Elements of dual scaling: An introduction to practical data analysis*. Lawrence Erlbaum Associates.
26. Nishisato, S., & Lawrence, D. R. (1989). Dual scaling of multiway data matrices: Several variants. In R. Coppi & S. Bolasco (Eds.), *Multiway data analysis* (pp. 317–326). Amsterdam: Elsevier Science Publishers.
27. Nishisato, S., & Yamauchi, H. (1974). Principal components of deviation scores and standard scores. *Japanese Psychological Research*, *16*, 162–170.
28. Pearson, K. (1901). On lines and planes of closest fit to systems of points in space. *Philosophical Magazines and Journal of Science, Series*, *6*(2), 559–572.
29. Torgerson, W. S. (1958). *Theory and methods of scaling*. New York: Wiley.
30. Young, G., & Householder, A. S. (1938). Discussion of a set of points in terms of their mutual distances. *Psychometrika*, *3*, 19–22.

Clustering via Ant Colonies: Parameter Analysis and Improvement of the Algorithm

Jeffry Chavarría-Molina, Juan José Fallas-Monge and Javier Trejos-Zelaya

Abstract An ant colony optimization approach for partitioning a set of objects is proposed. In order to minimize the intra-variance, or within sum-of-squares, of the partitioned classes, we construct ant-like solutions by a constructive approach that selects objects to be put in a class with a probability that depends on the distance between the object and the centroid of the class (visibility) and the pheromone trail; the latter depends on the class memberships that have been defined along the iterations. The procedure is improved with the application of K-means algorithm in some iterations of the ant colony method. We performed a simulation study in order to evaluate the method with a Monte Carlo experiment that controls some sensitive parameters of the clustering problem. After some tuning of the parameters, the method has also been applied to some benchmark real-data sets. Encouraging results were obtained in nearly all cases.

1 Introduction

Cluster analysis, or clustering, is one of the main tools in Data Analysis and Machine Learning, since it intends to discover groups or classes in large data sets of objects described by observed variables, simplifying this way the set with a small number of clusters. Most clustering methods are based on dissimilarities, graphs, models, or densities. In our case, we will deal with dissimilarities or distances for numerical data sets. There are two main families in this case: partitioning methods and hierarchical ones, being K-means and agglomerative hierarchical methods, respectively,

J. Chavarría-Molina · J. J. Fallas-Monge
School of Mathematics, Costa Rica Institute of Technology, Cartago, Costa Rica
e-mail: jchavarria@itcr.ac.cr

J. J. Fallas-Monge
e-mail: jfallas@itcr.ac.cr

J. Trejos-Zelaya (✉)
CIMPA–School of Mathematics, University of Costa Rica, San José, Costa Rica
e-mail: javier.trejos@ucr.ac.cr

T. Imaizumi et al. (eds.), *Advanced Studies in Behaviormetrics and Data Science*,
Behaviormetrics: Quantitative Approaches to Human Behavior 5,
https://doi.org/10.1007/978-981-15-2700-5_16

the most widely used in practice. Both have local optimality problems: local minima that depend on initialization for K-means, greedy procedure for agglomerative hierarchical clustering.

Several combinatorial optimization metaheuristics have been used for cluster partitioning (Handl & Knowles [14]; Ng & Wong [21]; Sarkar, Yegnanarayana, & Khemani [23]; Trejos, Murillo, & Piza [27]). In this article, we deal with partitioning for numerical data sets, using an ant colony optimization (ACO) approach in order to overcome the local optima problem.

According to Handl and Knowles [14], published in 2006, "a few implementations of ACO have been proposed for data clustering, with the construction graph typically employed to directly represent cluster assignments (Handl & Meyer [15]; Runkler [22])".

In 2004, we published a first paper on clustering using an ant colony optimization approach (Trejos, Murillo, & Piza [28]) for the minimization of the within sum-of-squares criterion. In that method, ants were associated with partitions that were modified during the iterations, according to a probability of selection that depends on the visibility (proportional to the distance between the objects) and the pheromone trail (which depends on the fact that the objects have been classified together in the partitions). The pheromone matrix measured relation intensity between pairs of objects.

By that time, Shelokar, Jayaraman, and Kulkarni [24] published another clustering method based on ACO for minimizing the same criterion as in Trejos, Murillo, and Piza [28], with a pheromone trail but no local heuristic. The pheromone matrix relates objects and clusters, and it is defined by the inverse of the objective function. The matrix is used as a kind of adaptive memory that contains information provided by the previously found superior solutions, and is updated at the end of each iteration (Shelokar et al. [24]). This information is considered by the other ants to continue the clustering process. However, it is not clear how the authors selected the parameters to execute the ACO algorithm. They indicate that several simulations were performed to find the algorithm parameters (Shelokar et al. [24]), but they do not present details about the process. They also present a comparison among their ants algorithm and other heuristic methods such as genetic algorithm, simulated annealing, and tabu search.

Later on, Kao and Cheng in a short paper [17] improved Shelokar's algorithm introducing a local heuristic or visibility based on the inverse of the distance between objects and class centers. The pheromone trail is also defined by the inverse of the criterion and the algorithm follows almost the same steps as Shelokar algorithm (Shelokar et al. [24]), with the difference that visibility is introduced.

Neither Shelokar et al. [24] nor Kao and Cheng [17] give a detailed analysis on the choice of parameters for their methods.

In the present article, we use ACO with ants constructing partitions. The strategy is based on the traveling salesman problem (TSP) in a similar way as it was tackled in Bonabeau, Dorigo, and Theraulaz [4] with ACO, in our case for the clustering problem. It is a constructive method, in which each ant builds a partition. This part of the process is similar to the ideas presented in Kao and Cheng [17] and Shelokar et al. [24], which were previously presented; but this paper deals with three different

aims: first, developing a fitting parameters analysis studying the algorithm behavior in the clustering problem according to its parameters. Second, we introduce a local search procedure based on the K-means algorithm, to improve the basic ACO (BACO) algorithm performance. And finally, to develop a performance comparison among the K-means algorithm (KM), the BACO algorithm and the BACOK (BACO improved with the local search procedure) algorithm.

The article is organized as follows. Section 2 contains the mains concepts of clustering we use in the article, introducing the main notation we need. In Sect. 3 the artificial ant concept is explained and the ACO classical algorithm is presented. In Sect. 4 we introduce the proposed ACO algorithm. Section 5 describes the experiment performed. Sections 6 and 7 present the results and some remarks.

2 Clustering

Cluster analysis, or clustering, deals with finding homogeneous groups of objects such that similar objects belong to the same class and it is possible to distinguish between objects in different classes. Cluster analysis can be defined as an optimization problem in which a given function consisting of *within cluster similitary* and *among clusters dissimilarities* need to be optimized (Jafar & Sivakumar [16]; Xavier & Xavier [30]). In the numerical case, there is a set of objects $\Omega = \{\mathbf{x}_1, \mathbf{x}_2, \ldots, \mathbf{x}_n\}$ such that $\mathbf{x}_i \in \mathbb{R}^p$, for all i, that is, the objects are described by p numerical or quantitative variables. The most widely used criterion (Everitt, Landau, Leese, & Stahl [9]) is the minimization of the within sum-of-squares, also known as within inertia or variance:

$$W = \frac{1}{n} \sum_{k=1}^{K} \sum_{\mathbf{x}_i \in C_k} \|\mathbf{x}_i - \mathbf{g}_k\|^2, \tag{1}$$

where K is the number of classes or clusters (number fixed a priori), $P = (C_1, C_2, \ldots, C_K)$ is a partition of Ω, and $\mathbf{g}_k$ is the barycenter or mean vector of C_k. Minimizing $W(P)$ is equivalent to maximizing the between sum-of-squares (between inertia and variance):

$$B = \sum_{k=1}^{K} \frac{|C_k|}{n} \|\mathbf{g}_k - \mathbf{g}\|^2,$$

where $\mathbf{g}$ is the overall barycenter and $|C_k|$ is the cardinality of class C_k, since the sum $I = W(P) + B(P)$ is a constant (the total inertia) (Everitt, Landau, Leese, & Stahl [9]).

The $W(P)$ function is not a convex function, thus $W(P)$ could have several local minima (Ng & Wong [21]; Sarkar et al. [23]). This feature causes the traditional clustering algorithms based on local search, such as K-means, to find mostly local minima (Trejos et al. [27]). Furthermore, the global optimization algorithms (such as linear programming, interval methods, branch, and bound methods) present a high sensitivity to relatively high-dimensional data tables, in which the algorithms'

probability for finding the optimal partition is very low. In those cases, algorithms report solutions that differ significantly from the optimum clustering (Bagirov [2]). Those features represent a challenge to try to find alternative optimization strategies, and combinatorial optimization heuristics are a viable option.

In recent years heuristic algorithms have been used to solve complex optimization problems, since their random nature is useful to efficiently avoid the convergence to local minima (Babu & Mutry [1]; Klein & Dubes [19]; Trejos et al. [27]). As particular examples of optimization heuristics used in clustering it is possible to cite simulated annealing, tabu search, genetic algorithms, particle swarm optimization, and ant colony optimization.

In the particular case of ant colony optimization, there are several contributions, as the already mentioned (Kao & Cheng [17]; Shelokar et al. [24]; Trejos et al. [28]), and some other more recent (Handl & Meyer [15]; Handl & Knowles [14]; Runkler [22]; Zhe et al. [31]).

3 Artificial Ant Colonies

The optimization approach based on ant colonies (ACO) is part of a large group based on swarm intelligence. It was proposed by Marco Dorigo in 1992, to solve several discrete optimization problems (Dorigo, DiCaro, & Gambardella [6]; Jafar & Sivakumar [16]), and since then it has been applied to several combinatorial optimization problems. This method, like every metaheuristic, depends on parameters which control several decisions taken in the process. There are several papers which develop parameters analysis for the ACO algorithm. In Gaertner and Clark [13] an empirical analysis of the sensitivity of the ACO algorithm to variations of some parameters for different instances of the TSP (traveling salesman problem) is presented. Similarly, in Wei [29] an experiment with parameter combinations is shown, in order to improve the speed of convergence of the ACO algorithm in the TSP. Also, this author indicates that at present the parameter settings and properties research of basic ant colony algorithm are mostly still in the experimental stage (Wei [29]) Meanwhile, Stützle et al. [25] provides an extensive review of available research results on parameter adaptation in ACO algorithms. They mention that ACO algorithms involve a number of parameters that need to be set appropriately, in particular α, β (both used to weigh the relative influence of the pheromone) and ρ (evaporation rate parameter, $0 \leq \rho \leq 1$). A parameter selection in the TSP context is developed in Dorigo, Maniezzo, and Colorni [8], in three different experiments. They tested the ranges: $\alpha \in \{0, 0.5, 1, 2, 5\}$, $\beta \in \{0, 1, 2, 5\}$, $\rho \in \{0.3, 0.5, 0.7, 0.99, 0.999\}$ and $Q \in \{1, 100, 10000\}$. The numbers $\alpha = 1$ and $\beta = 5$, were selected as the best values for these parameters. Parameter ρ was fixed, depending on the experiment, in 0.99, 0.99 or $\rho = 0.5$. And finally, parameter Q was found to be negligible.

In nature, the optimization developed by ants while they look for food consists basically of minimizing the distance between the nest and food. For this reason, the first application of ACO was to the TSP (Bonabeau et al. [4]). In that problem the agent should visit n cities, all interconnected, visiting all cities just one time and then returning to the departure city, minimizing the distance.

In this paper, the TSP idea is used to study the clustering optimization problem. Thus, it is necessary to introduce artificial ants; that is, agents in charge of finding a feasible solution in the search space. During this process the ant will drop artificial pheromones so that other ants can rebuild the same solution. Pheromones should be volatile (disappear in time on the trails that have not been intensified) and have to increase on the shortest trails while the number of iterations increases (Dorigo et al. [6]).

The pheromone update formula applied in the TSP is given by $\tau_{uv} = (1-\rho)\tau_{uv} + \rho\Delta\tau_{uv}$ (Barcos, Rodríguez, Álvarez, & Robusté [3]; Dorigo, Birattari, & Stützle [5]; Dorigo & Gambardella [7]), where τ_{uv} is the pheromone present on the trail from u to v, ρ is the evaporation rate, and

$$\Delta\tau_{uv} = \sum_{m=1}^{M} \Delta\tau_{uv}^{m},$$

where M is the number of ants, and $\Delta\tau_{uv}^{m}$ is the pheromone dropped by the m-th ant on the trail (u, v), normally given by

$$\Delta\tau_{uv}^{m} = \begin{cases} Q/d_m & \text{if ant } m \text{ walks across } (u, v) \\ 0 & \text{otherwise;} \end{cases}$$

where Q is a parameter to be fitted and d_m represents the total distance walked by ant m.

An alternative way to deal with pheromones is to make local updatings, that is, every time an ant goes from node u to node v, a local pheromone update is applied on the trail (u, v) (Dorigo & Gambardella [7]). A possible local update formula is $\tau_{uv} = \tau_{uv} + \dfrac{Q}{d_{uv}}$, where Q is a parameter to be fitted and d_{uv} is the distance between u and v. When all ants finish their trips, the pheromone is updated by applying the evaporation rate.

On the other hand, each ant has to decide to which node it goes from the current node. In that choice three factors are fundamental: visibility, pheromone trail, and a probabilistic factor. Thus, if T_m represents the route built by the ant m while it is on the node u, then the probability of going to the node v is given by

$$p_{uv}^{m} = \begin{cases} \dfrac{[\tau_{uv}]^{\alpha} \cdot [\eta_{uv}]^{\beta}}{\sum\limits_{s \notin T_m} [\tau_{us}]^{\alpha} [\eta_{us}]^{\beta}} & \text{if } v \notin T_m \\ 0 & \text{if } v \in T_m; \end{cases}$$

where η_{uv} is the visibility, defined by $\eta_{uv} = 1/d_{uv}$, with d_{uv} the distance from the node u to node v; τ_{uv} is the pheromone on the trail (u, v), and α and β are parameters to be fitted (Barcos et al. [3]; Dorigo et al. [6]; Kennedy & Eberhart [18]).

To stop the algorithm, Bonabeau et al. [4] proposed using a maximum iteration number. The disadvantage of this procedure is that it could stop the algorithm while

it is still improving the solutions. Also, Dorigo et al. [8] considered investigating a stagnation behavior of all ants traveling the same path. A stagnation process is present if a percentage of the ants has the same distance in their paths. Thus, it is almost certain that those ants are traveling the same path, or at least, that they are traveling paths with the same cost value.

In Algorithm 1, the classical ACO algorithm is shown.

Algorithm 1 ACO algorithm

```
Require: Initial parameters.
Set parameters and initialize pheromone trails.
while stop criterion is not satisfied do
  for t ← 1 to total of nodes do
    for m ← 1 to M do
      Move ant m to a new position.
      Update T_m.
      Update the local pheromones (optional).
    end for
  end for
  Update the global pheromones.
  Keep the best solution in this iteration if it improves the best in memory.
end while
return The best solution built.
```

4 Description of the Proposed ACO Algorithm

The method starts by defining a list of M artificial ants $\mathbf{h}_1, \mathbf{h}_2, \ldots, \mathbf{h}_M$, that will build a data clustering in K classes (or clusters). At the beginning, it is possible to define the best ant in the colony, denoted by $\mathbf{h}^*$, equal to $\mathbf{h}_m$ for some $m = 1, 2, \ldots, M$, because in that moment there is no comparison parameter among them; thus the assignment could be random.

For ant $\mathbf{h}_m$, with $m = 1, 2, \ldots, M$, K random points in the space of individuals (a hyperrectangle that contains all individuals) are considered, denoted by $\mathbf{g}_1^m, \mathbf{g}_2^m, \ldots, \mathbf{g}_K^m$. These points are interpreted as the initial centroids. C_k^m denotes the class k, with centroid $\mathbf{g}_k^m$, which has been built by ant m. Also, $\mathbf{h}_m$ has a tabu list L_m, which is a short term memory that contains the objects classified by $\mathbf{h}_m$. In each iteration, in order to complete the tour, ant m has to classify the objects not in L_m. When the iteration is done, all objects should be in L_m, this guarantees that the clustering process is complete.

During the clustering process, each ant randomly chooses an object that is not in its tabu list. Then, the ant should randomly select a class in which to classify the object. If ant m selects object i, then the process to choose the class uses a probabilistic roulette (see Talbi [26]). The probability that $\mathbf{h}_m$ assigns object i to class C_k^m is denoted by p_{ik}^m. To calculate this probability it is necessary to consider the following factors:

- **Visibility**: This factor is denoted by η_{ik}^m, and it consists of the visibility of $\mathbf{h}_m$, located on object $\mathbf{x}_i$, to "see" class C_k^m. The visibility is defined as the reciprocal of the distance from object $\mathbf{x}_i$ to $\mathbf{g}_k^m$, the centroid of class C_k^m. Thus, $\eta_{ik}^m := \frac{1}{d_{ik}^m}$, where $d_{ik}^m = d^2(\mathbf{x}_i, \mathbf{g}_k^m) = \left\|\mathbf{x}_i - \mathbf{g}_k^m\right\|^2$. If the visibility which $\mathbf{h}_m$ has of class C_k^m is large, then the probability of classifying $\mathbf{x}_i$ in class k is also large.
- **The pheromone trail**: The pheromone trail perceived by $\mathbf{h}_m$ on the arc from $\mathbf{x}_i$ to $\mathbf{g}_k^m$ is denoted by τ_{ik}. It quantifies pheromones that have been dropped by all ants which have classified the same object $\mathbf{x}_i$ in its respective class k. If τ_{ik} is large, then the probability of assigning class k to cluster $\mathbf{x}_i$ is going to increase.

Equation (2) shows the formula used to calculate p_{ik}^m, considering visibility and the pheromone trail, inspired by the corresponding formula used by the agent in the TSP:

$$p_{ik}^m := \frac{[\tau_{ik}]^\alpha \cdot [\eta_{ik}^m]^\beta}{\sum_{r=1}^{K} [\tau_{ir}]^\alpha \cdot [\eta_{ir}^m]^\beta}, \tag{2}$$

where α and β are parameters to be fitted.

On the other hand, when $\mathbf{h}_m$ chooses class C_k^m for object $\mathbf{x}_i$, the ant will register index i in the respective tabu list L_m. Futhermore, $\mathbf{h}_m$ should do the following processes related to the assignment.

- **Local pheromone update**: Ant $\mathbf{h}_m$ should drop a pheromone trail between object $\mathbf{x}_i$ and class C_k^m. To do this, an auxiliary pheromone matrix was defined, denoted by Γ_{aux} with size $n \times K$, such that entry ik of Γ_{aux} contains pheromones between x_i and class k. This matrix has the format presented in Table 1.

  Ant $\mathbf{h}_m$ will drop $\Delta\tau_{ik}^m$ pheromones. This quantity is defined by $\Delta\tau_{ik}^m := \frac{Q}{d_{ik}^m}$, where Q is a parameter to be fitted. Finally, the local pheromone update is done by adding $\Delta\tau_{ik}^m$ with the current entry ik of Γ_{aux}.
- **Centroid update**: The final step in this process is to update the centroid $\mathbf{g}_k^m$ of class C_k^m. One possibility is using its definition $\mathbf{g}_k^m := \frac{1}{|C_k^m|} \sum_{\mathbf{x} \in C_k^m} \mathbf{x}$. This option is not advisable because there are several unnecessary calculations. If fact, it is possible to update $\mathbf{g}_k^m$ recursively using its value in the previous iteration in case object $\mathbf{x}_i$

Table 1 Auxiliary pheromone matrix Γ_{aux}

	C_1	C_2	C_3	$\cdots$	C_K
$\mathbf{x}_1$					
$\mathbf{x}_2$					
$\mathbf{x}_3$					
$\vdots$					
$\mathbf{x}_n$					

is transferred to class C_k^m. In Trejos et al. [27] the following formula is proven and is used to update the centroids more efficiently: $\mathbf{g}_k^m := \frac{1}{|C_k^m|}\left[\left(|C_k^m| - 1\right)\mathbf{g}_k^m + \mathbf{x}_i\right]$.

After each ant has clustered one object, it should randomly select a new object that is not in its tabu list. Next, the ant should follow the process previously described. This process is done n times, clustering all objects by all ants.

When the process ends, each ant has a complete clustering of objects with the respective barycenters. Also, matrix Γ_{aux} contains pheromones that were dropped by ants. Entry ik of Γ_{aux} contains pheromone $\Delta\tau_{ik}$, which has been dropped by all ants that classified object i in its respective class k. This quantity is represented by

$$\Delta\tau_{ik} = \sum_{m=1}^{M} \Delta\tau_{ik}^m.$$

The next step is to calculate, for each ant, the within inertia. To do this, the classification done by each ant, and the respective barycenters, should be considered. Also, if one of the ants has a within inertia less than $W(\mathbf{h}^*)$ (the best inertia so far in memory), then $\mathbf{h}^*$ (the best ant in memory) is required to be updated.

Global pheromones are stored in a matrix Γ with the same structure as Γ_{aux}. At the beginning, this matrix is initialized with values close to zero (indicating pheromone absence). When the travels of all ants finish, Γ is updated in entry ik by $\Gamma_{ik} := (1-\rho)\Gamma_{ik} + \rho\Delta\tau_{ik}$, where ρ is the pheromone evaporation rate.

When the pheromone updating process is done, matrix Γ_{aux} is initialized, to be used in the next iteration. Also, tabu lists (one per ant) are initialized, to start a new classification process.

As the final step to conclude the current iteration, an intensification process done by the best ant (the ant with lowest within inertia, denoted by $\mathbf{h}^*$) is developed. $\mathbf{h}^*$ repeats her path dropping extra pheromones in arcs it visited. The intensification follows the following rule:

$$\Gamma_{ik} := \begin{cases} \Gamma_{ik} + \frac{Q}{W(\mathbf{h}^*)} & \text{if the object } i \text{ is in the class } k \text{ of } \mathbf{h}^*, \\ \Gamma_{ik} & \text{otherwise;} \end{cases}$$

where $W(\mathbf{h}^*)$ denotes the within inertia of the classification done by $\mathbf{h}^*$. This ends the current iteration and a new clustering process is started, considering the following information: the global pheromone matrix Γ, the barycenters of ants, which will be used as the initial centroids for the new classes, and the best ant $\mathbf{h}^*$.

Algorithm 2 presents a detailed pseudocode of the BACOK. The K-means algorithm was applied (see line 19 in Algorithm 2) to each ant. The method is applied after all ants have built their respective classifications, and until the absolute difference between current inertia and previous inertia is less than 0.0001. Algorithm 3 shows how the local search strategy based on K-means works. If lines from 19 to 22 are eliminated from Algorithm 2, then BACO algorithm pseudocode is obtained. Finally, in the event that there has been no improvement, Algorithm 2 uses an iteration number (10 iterations) as stopping criterion (see line 4). Consider that, Counter

is increments in line 5, but its value must be returned to zero every time a better solution (comparing with the best in memory) is found. This stopping criterion is based on the stagnation behavior concept presented in Dorigo et al. [8].

Algorithm 2 BACOK algorithm.

Require: n (number of individuals), p (number of variables), K (number of clusters), M (number of ants), and the parameters α, β, Q and ρ.

1: Build the initial colony with m ants: $\mathbf{h}_1, \mathbf{h}_2, \ldots, \mathbf{h}_M$.
2: For each $m = 1, 2, \ldots, M$ define $L_m = \varnothing$, and randomly choose $\mathbf{g}_1^m, \ldots, \mathbf{g}_K^m$.
3: Counter $\leftarrow 0$
4: **while** Counter ≤ 10 **do**
5: Counter $\leftarrow$ Counter $+ 1$
6: **for** $I := 1$ **to** n **do**
7: **for** $m := 1$ **to** M **do**
8: Ant $\mathbf{h}_m$ chooses a random individual $\mathbf{x}_i$, such that $i \notin L_m$.
9: Ant $\mathbf{h}_m$ chooses $k :=$ Roulette(p_{ik}^m), where $p_{ik}^m := \frac{[\tau_{ik}]^\alpha \cdot [\eta_{ik}^m]^\beta}{\sum_{r=1}^{K} [\tau_{ir}]^\alpha \cdot [\eta_{ir}^m]^\beta}$.
10: Individual $\mathbf{x}_i$ and index i are assigned to C_k^m and L_m, respectively.
11: Let $\langle \Gamma_{aux} \rangle_{ik} := \langle \Gamma_{aux} \rangle_{ik} + \Delta\tau_{ik}^m$, where $\Delta\tau_{ik}^m = \frac{Q}{d_{ik}^m}$.
12: Let $\mathbf{g}_k^m := \frac{1}{|C_k^m|} \left[\left(|C_k^m| - 1 \right) \mathbf{g}_k^m + \mathbf{x}_i \right]$.
13: **end for**
14: **end for**
15: Let $\mathbf{h}^* :=$ BestAnt$(\mathbf{h}_1, \ldots, \mathbf{h}_M, \mathbf{h}^*)$.
16: For $i = 1, \ldots, n$ and $k = 1, \ldots, K$ let $\langle \Gamma \rangle_{ik} := \tau_{ik}$, where $\tau_{ik} := (1 - \rho) \ \langle \Gamma \rangle_{ik} + \rho \ \langle \Gamma_{aux} \rangle_{ik}$.
17: Intensify the best trail. For all $i (i = 1, \ldots, n)$, if individual i in $\mathbf{h}^*$ was classified in cluster k do $\langle \Gamma \rangle_{ik} = \langle \Gamma \rangle_{ik} + Q/W(\mathbf{h}^*)$
18: If the inertia of $\mathbf{h}^*$ improves the best inertia keeped in memory, reset Counter.
19: **for** $m := 1$ **to** M **do**
20: Apply K-means to $\mathbf{h}_m$.
21: Update $\mathbf{h}^*$ if there was an improvement from the K-means application.
22: **end for**
23: **end while**
24: **return** $\mathbf{h}^*$

5 Parameter Analysis

To develop the parameter analysis three data tables (T105, T525, and T2100) were built, with randomly generated normal variables. The data sets T105 ($n = 105$ and $p = 6$) and T525 ($n = 525$ and $p = 6$) consists of 105 and 525 objects, respectively. Both sets have seven clusters ($K = 7$), such that six classes have variance equal to $\sigma^2 = 1$, and the seventh class has $\sigma^2 = 3$. The data set T105 has a "big" class with 51 objects, and the remaining six groups with 9 objects. Meanwhile, T525 has a class with 265 objects, and the remaining objects are equitably distributed in the other groups. The $W(P)$ reference values for T105 and T525 were calculated using the Eq. (1), thereby 7.62467183 and 7.45610263 were obtained for these tables,

Algorithm 3 Local search strategy based on K-means applied in BACO.

Require: One ant $\mathbf{h}$.
1: PreviousInertia$\leftarrow -1$.
2: **while** $|\text{PreviousInertia} - W(\mathbf{h}_m)| > 0.001$ **do**
3: PreviousInertia$\leftarrow W(\mathbf{h}_m)$
4: For $\mathbf{h}$, build clusters $C_1, C_2, \ldots, C_K$, using barycenters $\mathbf{g}_1, \ldots, \mathbf{g}_K$. To do that, assign each individual $\mathbf{x}_i$ to the class with its barycenter closest to $\mathbf{x}_i$.
5: Recalculate the barycenters $\mathbf{g}_1, \mathbf{g}_2, \ldots, \mathbf{g}_K$ with:
$$\mathbf{g}_k = \frac{1}{|C_k|} \sum_{\mathbf{x}_i \in C_k} \mathbf{x}_i, \text{ for all } k = 1, 2, \ldots, K.$$
6: **end while**
7: **return** A new ant $\widehat{\mathbf{h}}$.

respectively. Table T2100 has 2100 objects, seven clusters with the same cardinality and all classes have different variances. The $W(P)$ reference value for this set is 22.56959210.

The Algorithm 2 has four parameters that should be fitted, with the aim of achieving good performance. Parameters α and β control the relative weights assigned to pheromone concentration and ant visibility, respectively. Meanwhile, ρ represents the pheromone evaporation rate, used to update the pheromone matrix. Finally, parameter Q is a *pheromone amplification constant*.

To develop the parameter analysis tables T105 and T525 were used, and for each table, and for each parameter combination, 200 multistart runs were done. Based on the ranges presented in Dorigo et al. [8], in the current experiment a further analysis was developed, using $\rho \in \{0.1, 0.2, \ldots, 0.9\}, \alpha, \beta \in \{0, 0.5, 1, 1.5, \ldots, 6\}$, and $Q \in \{50, 100, 150, \ldots, 500\}$. In total $9 \times 13 \times 13 \times 10 = 15210$ combinations were run for each table. This analysis used $M = 10$ (the number of ants).

The pictures in Fig. 1 show some examples of the 90 contour maps built with the performance percentages (each percentage represents how many times the algorithm scores the $W(P)$ reference value, in the 200 runs) obtained with table T105, for the different parameter combinations. For example, Fig. 1a shows the contour map for $\rho = 0.1$, $Q = 50$ and $\alpha, \beta \in \{0, 0.5, 1, 1.5, \ldots, 6\}$. This analysis showed that $\rho = 0.5$ was the best option, because the best performance zone for $\rho = 0.5$ (the darker red zone in Fig. 1b) is better (largest area) than those of the remaining ρ values.

On the other hand, very similar contour maps were obtained when ρ was fixed, and Q varied from 50 to 500 (10 contour maps per each ρ value). This showed evidence that Q was not an important parameter in this experiment. And this coincides with the observation presented in Dorigo et al. [8], which indicates that Q has a negligible influence in the algorithm. Therefore, the parameter Q was fixed at 250 (the range middle value), but also could be fixed at 100, as they did.

Next, an analysis for α and β was developed with tables T105 and T525, using $\rho = 0.5$, $Q = 250$, and $\alpha, \beta \in \{0, 0.25, 0.5, 0.75, \ldots, 6\}$. Figure 2 shows the contour maps obtained in this process. This analysis was not enough to determine optimum values for α and β. Figure 2a and b only suggest that the best performance is probably obtained when $1.5 \leq \beta \leq 5$ and $0 < \alpha \leq 2.5$. For this reason, an extra analysis was

Fig. 1 Some examples of contour maps created with the performance percentages, for $Q = 50$, $\rho = 0.1, 0.5, 0.9$, and variants values for α and β. Analysis done with table T105

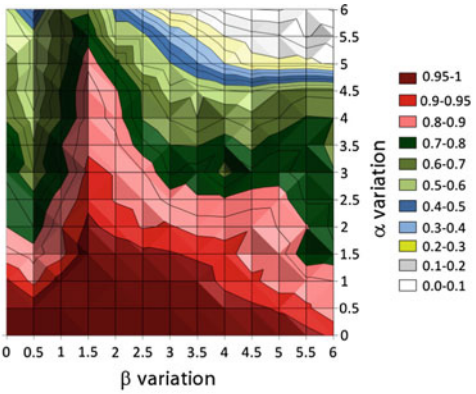

(a) Contour map for $\rho = 0.1$ and $Q = 50$

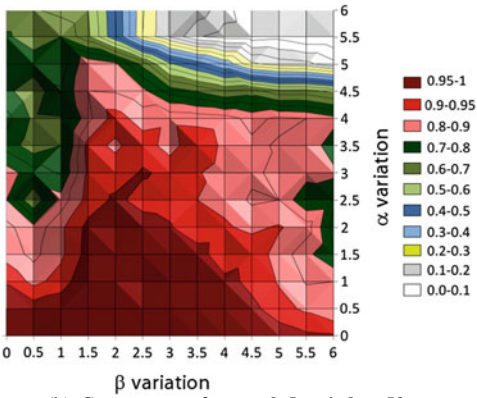

(b) Contour map for $\rho = 0.5$ and $Q = 50$

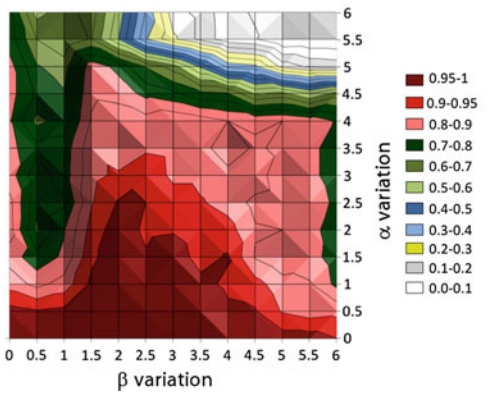

(c) Contour map for $\rho = 0.9$ and $Q = 50$

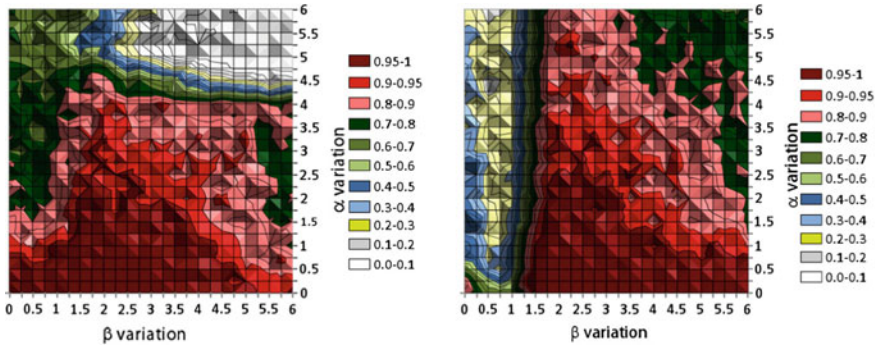

(a) Results obtained with table T105 (b) Results obtained with table T525

Fig. 2 Contour maps created with the performance percentages, with the fixed values $\rho = 0.5$ and $Q = 250$

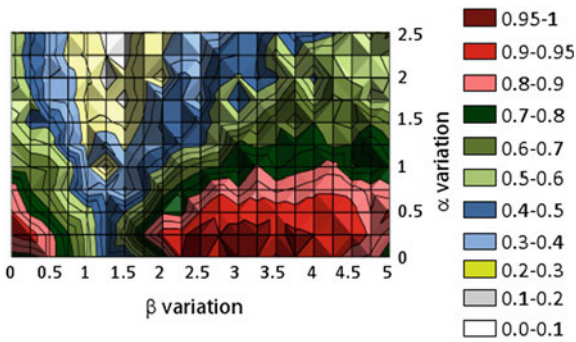

Fig. 3 Contour maps created with the performance percentages, with the fixed values $\rho = 0.5$ and $Q = 250$, in table T2100

developed with table T2100. Figure 3 shows that any combination for α and β in the dark red region could be taken. Therefore, for this experiment the combination $\beta = 2.5$ and $\alpha = 0.25$ was selected. Summarizing, the parameters were chosen as $\alpha = 0.25$, $\beta = 2.5$, $\rho = 0.5$, and $Q = 250$.

6 Extra Data Sets, Results, and Discussion

A personal computer with 8 GB of RAM memory and an Intel Core i7-4712MQ CPU@2.30 GHz processor, was used in this experiment. In order to develop a comparison among the algorithms BACO, BACOK and KM, five real-life data sets were downloaded from the website of UCI repository of machine learning databases (UCI [20]): iris ($n = 150$, $K = 3$ and $p = 4$), wine ($n = 178$, $K = 3$ and $p = 13$), glass identification ($n = 214$, $K = 6$, $p = 9$), red wine quality ($n = 1599$, $K = 3$, $p = 11$) and white wine quality ($n = 4898$, $K = 3$, $p = 11$) data sets. In *glass* data set the first attribute was not considered as a variable, because it is an identification number (for this reason $p = 9$). Furthermore, K was fixed at 6 because the type of glass number 4

is not present in this data set (in total, there are 7 types of glass). In *wine quality* (both tables), the attribute number 12 was not considered because it is an output variable. Additionally, two groups (A and S) of bidimensional synthetic data sets were considered (downloaded from Fränti & Sieranoja [12]), which are described on Fränti and Sieranoja [11]. Group A (3 sets) varies the number of clusters, and the group S varies the overlapping among the clusters (4 sets). All cases use $p = 2$. Table 2 summarizes the main features of these sets and Fig. 4 shows a bidimensional representation for each set. Also, the *ground truth* centroids for these data sets are available on Fränti and Sieranoja [12]; hence, it was possible to analyze if the proposed BACOK algorithm was generating a reasonable clustering for the data. The *centroid index* (CI) presented in Fränti, Rezaei, and Zhao [10] is a cluste- level similarity measure, based on the cluster centroids, which can be used to compare one clustering against other solution or the ground truth, if is available. The algorithm BACOK was executed 100 times on sets A1, A2, A3, S1, S2, S3, and S4, and the best solution found, in each case, was compared with the ground truth solution, using the CI value. In all cases, the CI value was equal to zero, therefore according to Fränti and Sieranoja [11], our algorithm is properly clustering those datasets. This experiment was made with 20 ants ($M = 20$) and the parameters $\alpha = 0.25$, $\beta = 2.5$, $\rho = 0.5$, and $Q = 250$. Finally, using for each set the centroids of the best solution and the definition of $W(P)$ (see Eq. 1), the best within inertia for each set (W_{best}) was calculated (see column number 4 on Table 2).

Table 3 summarizes the results obtained with the three algorithms. The performance of each algorithm is represented by a percentage, and this corresponds to the number of times in which the algorithm scored the W_{best} value in 100 multistart runs. The algorithm BACO also used $M = 20, \alpha = 0.25, \beta = 2.5, \rho = 0.5$, and $Q = 250$. Meanwhile, the KM algorithm iterates until the difference between two consecutive within inertias is less than 0.001. The symbol "-" used in Table 3 means the algorithm did not attend the W_{best} reference value in any of the 100 runs. Also, the standard deviation of inertia, the average time and the standard deviation of time, in those 100 executions, are presented in Table 3.

Table 3 shows how the algorithm BACOK performed very good on the available data sets. This final comparison is valuable because it reinforces one of the princi-

Table 2 Main features for sets on group A ans S

Data set	n	K	$W(P)$ reference value
A1	3000	20	4048752.50
A2	5250	35	3864140.31
A3	7500	50	3858322.01
S1	5000	15	1783523123.37
S2	5000	15	2655821898.14
S3	5000	15	337791436.87
S4	5000	15	3140628447.25

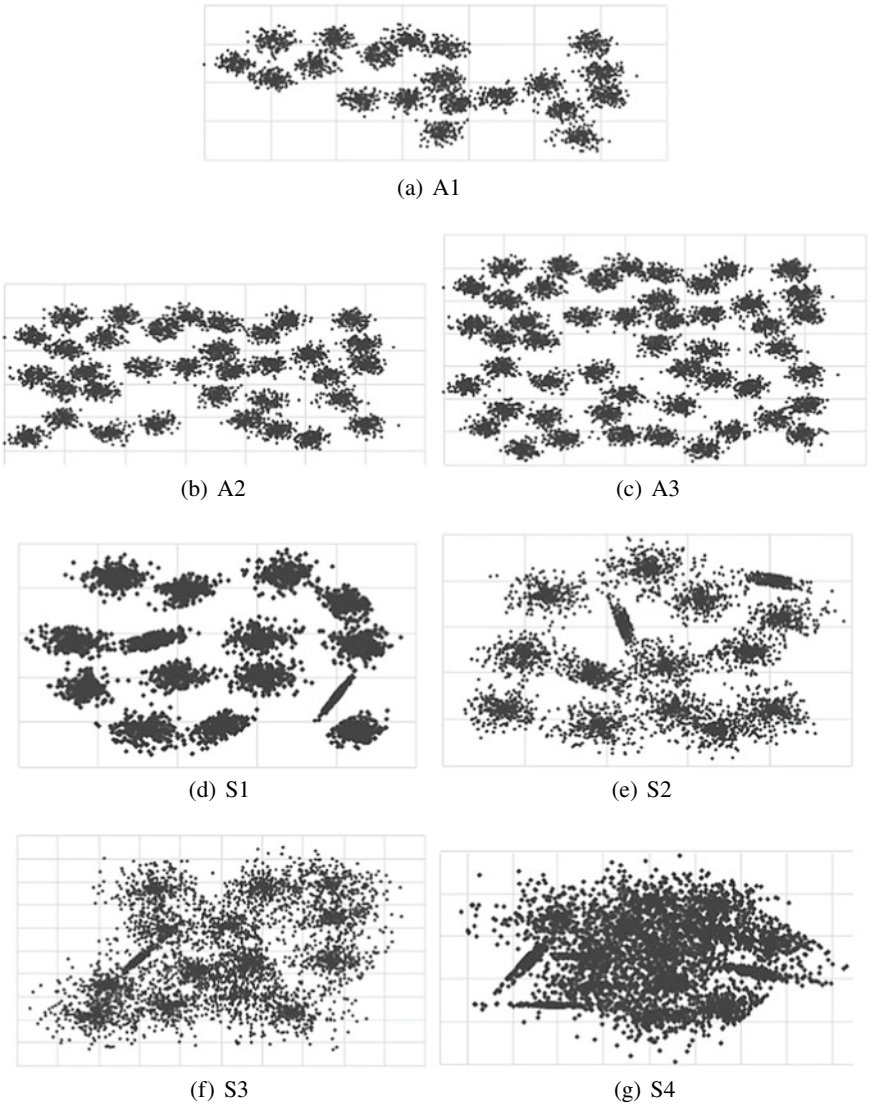

(a) A1

(b) A2

(c) A3

(d) S1

(e) S2

(f) S3

(g) S4

Fig. 4 Two-dimensional representation for the datasets on groups A and B

Table 3 Performance comparison among BACO, BACOK, and KM

Data set	W_{best}	Performance-Standard deviation of inertia			Average time-Standard deviation of time (s)		
		BACO	KM	BACOK	BACO	KM	BACOK
Iris	0.52136	34% – 0.00104	5% - 0.19743	100% - 0	0.16467 - 0.05200	0.00027 - 0.00008	0.13550 - 0.02911
Wine	13318.48	8% - 41.3007	100% - 0	100% - 0	0.25580 - 0.08328	0.00048 - 0.00004	0.31380 - 0.04476
Glass	1.570377	-	-	93% - 0.0001	-	-	0.64427 - 0.17442
Red wine Q	247.2075	-	1% - 0.00717	100% - 0	-	0.00794 - 0.00072	3.28075 - 0.25986
White wine Q	560.4186	-	83% - 0.00022	100% - 0	-	0.03349 - 0.00778	16.59486 - 2.48081
A1	4048752.50	-	-	80% - 244433.51	-	-	14.84363 - 4.49093
A2	3864140.31	-	-	90% - 70488.07	-	-	62.97577 - 15.71993
A3	3858322.01	-	-	50% - 139284.45	-	-	164.00306 - 54.02449
S1	1783523123.37	-	-	100% - 0	-	-	11.94175 - 3.86356
S2	2655821898.14	-	-	100% - 0	-	-	12.65522 - 0.93671
S3	3377914369.87	-	-	87% - 1390.99	-	-	22.69879 - 5.31946
S4	3140628447.25	-	-	10% - 7221.77	-	-	30.60434 - 8.88218

pal contributions of this paper: the BACO and KM algorithms did not show good results in most all data sets, but our algorithm uses the potential of K-means to improve the algorithm BACO, and then significantly better results were obtained. That hybridization process presented in algorithm BACOK reveals how the K-means algorithm itself could not work well, but it can be used to improve other heuristic algorithms. Finally, the lowest performance reported by algorithm BACOK was in the set S4, which has the highest level of overlap (see Fig. 4).

7 Conclusions

We have presented a hybrid clustering method based on the ant colony optimization metaheuristic and the K-means algorithm. The method is based on some features developed for ACO in the traveling salesman problem and it is improved by the K-means algorithm in each iteration. The adaptation to the clustering problem takes into account the representation of clusters by barycenters, and therefore the distance between objects and barycenters is used for defining visibility and the pheromone trail.

After an extensive parameter fitting, an experimentation was implemented in order to evaluate the method. It performed very well, attaining the reference value for the inertia in each data table, in reasonable time. Furthermore, the method showed very good results when it was applied to other benchmark data sets, where the ground truth for each set was available.

Finally, the experiment revealed the parameter Q does not have a relevant role in the ACO algorithm, but the algorithm is very sensitive to the values assigned to the parameters α, β and ρ. The parameter fitting process was necessary to improve the algorithm performance and it gave the combination $\alpha = 0.25$, $\beta = 2.5$ and $\rho = 0.5$.

Acknowledgements J. Chavarría and J.J. Fallas were supported with project 5402-1440-3901 of the Research Vice-Rectory, Costa Rica Institute of Technology. J. Trejos was supported with project 821-B1-122 of the Research Vice-Rectory, University of Costa Rica.

References

1. Babu, G. P., & Murty, M. N. (1994). Clustering with evolution strategies. *Pattern Recognition*, *27*(2), 321–329. https://doi.org/10.1016/0031-3203(94)90063-9.
2. Bagirov, A. M. (2008). Modified global k-means algorithm for minimum sum-of-squares clustering problems. *Pattern Recognition*, *41*(10), 3192–3199. https://doi.org/10.1016/j.patcog.2008.04.004.
3. Barcos, L., Rodríguez, V. M., Álvarez, M. J., & Robusté, F. (2004). Routing design for less-than-truckload motor carriers using ant colony techniques. *Business Economics Series*, *14*, 4–38. https://doi.org/10.1016/j.tre.2009.11.006.
4. Bonabeau, E., Dorigo, M., & Theraluz, G. (1999). *Swarm Intelligence. From Natural to Artificial Systems*. New York: Oxford University Press. ISBN-13: 978-0195131598.

5. Dorigo, M., Birattari, M., & Stützle, T. (2006). Ant colony optimization: Artificial ants as a computational intelligence technique. *IEEE Computational Intelligence Magazine*, *1*(4), 28–39. https://doi.org/10.1109/CI-M.2006.248054.
6. Dorigo, M., Di Caro, G., & Gambardella, L. M. (1994). Ant algorithms for discrete optimization. *Artificial Life*, *5*(2), 137–172. https://doi.org/10.1162/106454699568728.
7. Dorigo, M. & Gambardella, L. C. (1997). Ant colony system: A cooperative learning approach to the traveling salesman problem. *IEEE Trans. on Evolutionary Computation*, *1*(1), 53–66. https://doi.org/10.1109/4235.585892.
8. Dorigo, M., Maniezzo, V. & Colorni A. (1996). Ant system: Optimization by a colony of cooperating agents. *IEEE Transactions on Systems, Man, and Cybernetics-Part B*, *26*(1), 1–13. https://doi.org/10.1109/3477.484436.
9. Everitt, B. S., Landau, S., Leese, M., & Stahl, D. (2011). *Cluster analysis* (5th ed.). Chichester: Wiley. https://doi.org/10.1002/9780470977811.
10. Fränti, P., Rezaei, M., & Zhao, Q. (2018). Centroid index: Cluster level similarity measure. *Pattern Recognition*, *47*(9), 3034–3045. https://doi.org/10.1016/j.patcog.2014.03.017.
11. Fränti, P., & Sieranoja, S. (2018a). K-means properties on six clustering benchmark datasets. *Applied Intelligence*, *48*(12), 4743–4759. https://doi.org/10.1007/s10489-018-1238-7.
12. Fränti, P., & Sieranoja, S. (2018b). *Machine Learning Repository*. Joensuu, Finland: University of Eastern Finland, School of Computing. http://cs.joensuu.fi/sipu/datasets/.
13. Gaertner, D., & Clark, K. (2005). On optimal parameters for ant colony optimization algorithms. In *Proceedings of the 2005 International Conference on Artificial Intelligence, 27–30 june 2005* (pp. 83–89) Las Vegas NV, USA. DBLP:conf/icai/GaertnerC05.
14. Handl, J., & Knowles, J. (2015). Nature-inspired clustering approaches. In C. Hennig (Ed.), *Handbook of Cluster Analysis* (pp. 419–439). London, UK: Chapman & Hall.
15. Handl, J., & Meyer, B. (2007). Ant-based and swarm-based clustering. *Swarm Intelligence*, *1*: 95–113. https://doi.org/10.1007/s11721-007-0008-7.
16. Jafar, O. M., & Sivakumar, R. (2010). Ant-based clustering algorithms: A brief survey. *International Journal of Computer Theory and Engineering*, *2*(5), 787–796. https://doi.org/10.7763/IJCTE.2010.V2.242.
17. Kao, Y., & Cheng, K. (2006). An ACO-based clustering algorithm. In M. Dorigo et al. (Eds.), *Ant colony optimization and swarm intelligence, Lecture Notes in Computer Science 4150* (pp. 340–347). Berlin, Germany: Springer. https://doi.org/10.1007/11839088_31.
18. Kennedy, J., & Eberhart, R. C. (2001). *Swarm intelligence*. San Francisco CA, USA: Morgan Kaufmann. ISBN 9781558605954.
19. Klein, R. W. & Dubes, R. C. (1989) Experiments in projection and clustering by simulated annealing. *Pattern Recognition* 22(2), 213–220. https://doi.org/10.1016/0031-3203(89)90067-8.
20. UCI (1998). UCI Machine Learning Repository. Irvine CA, USA: University of California, School of Information and Computer Science. Retrieved September 13, 2019, from http://archive.ics.uci.edu/ml.
21. Ng, M. K., & Wong, J. C. (2002). Clustering categorical data sets using tabu search techniques. *Pattern Recognition*, *35*(12), 2783–2790. https://doi.org/10.1016/S0031-3203(02)00021-3.
22. Runkler, T. A. (2005). Ant colony optimization of clustering models. *International Journal of Intelligent Systems*, *20*(12), 1233–1251. https://doi.org/10.1002/int.20111.
23. Sarkar, M., Yegnanarayana, B. & Khemani, D. (1997). A clustering algorithm using an evolutionary programming-based approach. *Pattern Recognition Letters 18*(10), 975–986. https://doi.org/10.1016/S0167-8655(97)00122-0.
24. Shelokar, P. S., Jayaraman, V. K., & Kulkarni, B. D. (2004). An ant colony approach for clustering. *Analytica Chimica Acta*, *509*(2), 187–195. https://doi.org/10.1016/j.aca.2003.12.032.
25. Stützle, T., López-Ibáñez, M., Pellegrini, P., Maur, M., Montes de Oca, M., Birattari, M., & Dorigo, M. (2012). Parameter Adaptation in Ant Colony Optimization. In Y. Hamadi, E.Monfroy & F. Saubion (Eds.), *Autonomous Search* (pp. 191–215). Berlin, Germany: Springer. https://doi.org/10.1007/978-3-642-21434-9_8.

26. Talbi, E. G. (2009). *Metaheuristics: From design to implementation*. Hoboken NJ, USA: Wiley.
27. Trejos, J., Murillo, A., & Piza, E. (1998). Global stochastic optimization techniques applied to partitioning. In A. Rizzi, M. Vichi & Bock, H. H. (Eds.), *Advances in data science and classification* (pp. 185–190). Berlin, Germany: Springer. https://doi.org/10.1007/978-3-642-72253-0_25.
28. Trejos, J., Murillo, A., & Piza, E. (2004). Clustering by ant colony optimization. In D. Banks, L. House, F. R. McMorris, P. Arabie & W. Gaul (Eds.), *Classification, clustering, and data mining applications* (pp. 25–32). Berlin, Germany: Springer. https://doi.org/10.1007/978-3-642-17103-1_3.
29. Wei, X. (2014). Parameters analysis for basic ant colony optimization algorithm in TSP. *International Journal of u-and e-Service, Science and Technology*, *7*(14), 159–170. https://doi.org/10.14257/ijunesst.2014.7.4.16.
30. Xavier, A. E., & Xavier, V. L. (2011). Solving the minimum sum-of-squares clustering problem by hyperbolic smoothing and partition into boundary and gravitational regions. *Pattern Recognition*, *44*, 70–77. https://doi.org/10.1016/j.patcog.2010.07.004.
31. Zhe, G., Dan, L., Baoyu, A., Yangxi, O., Xinxin, N., & Yang, X. (2011) An analysis of ant colony clustering methods: Models, algorithms and applications. *International Journal of Advancement in Computing Technology*, *3*(11), 112–121. https://doi.org/10.4156/ijact.vol3.issue11.15.

PowerCA: A Fast Iterative Implementation of Correspondence Analysis

Alfonso Iodice D'Enza, P. J. F. Groenen and M. Van de Velden

Abstract The visual exploration of big data requires interactivity as well as the possibility to update an existing solution as new data becomes available in real time. Enhanced exploratory data visualization is provided by dimension reduction methods. Eigenvalue and singular value decompositions are the core of most of the dimension reduction techniques, such as principal component analysis (PCA) and multiple correspondence analysis (MCA). An efficient implementation of MCA, called PowerCA, is proposed that exploits enhanced computations of the sparse matrix transformations and fast iterative methods provided by intelligent initializations in case of repeated analyses. The aim is to extend the applicability of MCA to computational demanding application such as streaming text and web-log data visualization as well as bootstrap-based sensitivity analysis.

1 Introduction

Big data is one of the research priorities set by Marketing Science for 2012–2014. In particular, it is stated that

> (...) the explosive growth in the sources and quantity of data available to firms is leading them to employ new methods of analysis and reporting, such as machine learning and data visualization (...)

A. Iodice D'Enza
Department of Political Sciences, Università degli Studi di Napoli Federico II, Naples, Italy
e-mail: iodicede@unina.it

P. J. F. Groenen
Econometric Institute, Erasmus University, Rotterdam, The Netherlands
e-mail: groenen@ese.eur.nl

M. Van de Velden (✉)
Econometric Institute, Erasmus University, Rotterdam, The Netherlands
e-mail: vandevelden@ese.eur.nl

T. Imaizumi et al. (eds.), *Advanced Studies in Behaviormetrics and Data Science*,
Behaviormetrics: Quantitative Approaches to Human Behavior 5,
https://doi.org/10.1007/978-981-15-2700-5_17

The visual exploration of big data requires interactivity as well as the possibility to update an existing solution as new data becomes available in real time. Enhanced exploratory data visualization is provided by dimension reduction methods. The eigenvalue decomposition (EVD) and the related singular value decomposition (SVD) are the core steps of several dimension reduction methods, such as principal components analysis (PCA). In fact, PCA consists of an eigendecomposition of the correlation matrix resulting from a set of p quantitative variables observed on n units, and it leads to a low-dimensional representation of the relation structure underlying the data set in question (see, e.g., Jolliffe [9], for an in-depth exposition of PCA). Applications in which dimension reduction can be particularly useful are in text mining, web-log analysis and market basket analysis: in all of these applications, the information can be collected in a binary data matrix, where the rows record the presence/absence of the set of considered attributes. As an example, in the context of text mining, data can be arranged in a document-by-word matrix, whose general element (i, j) $(i = 1, \ldots, n, j = 1, \ldots, p)$ is "1" if the jth word is present in the ith document.

The qualitative data counterpart of PCA is multiple correspondence analysis (MCA, Greenacre [6]), that aims to describe in a low-dimensional space the multiple association structure characterizing p categorical or binary variables. As PCA, MCA is also characterized by the EVD or SVD of a properly transformed data matrix.

In the context of large data sets, the application of standard implementations of both EVD and SVD becomes unfeasible due to their high computational cost. The EVD is traditionally computed by a batch time algorithm with computational complexity $O(p^3)$, whereas the SVD has a computational complexity of $O(n^2 p)$ assuming $n \geq p$ (Golub & van Loan [4]). Thus, both methods become computationally infeasible for large datasets. Several methods in the literature can be used to efficiently compute the EVD and SVD. In particular, iterative EVD methods, such as the LR transformation and the QR transformation (Golub & van Loan [4], are widely used; on the SVD side, Lanczos' bilinear diagonalization methods reduce the computational complexity of the procedure (Baglama & Reichel [1]) considerably. These methods are referred to as batch methods because they require that all the data is available to perform the decomposition. When the full dataset is not completely available from the beginning, or when data changes (e.g., when values get updated over time or when some type of resampling is employed), two approaches can be considered: complete new decompositions are considered each time data changes, or the EVD or SVD is updated using the previous solution and the new data (see Baker, Gallivan & Van Dooren [3], for an overview).

We can distinguish three types of applications requiring repeated fast-paced analyses using dimension reduction can be thought of. First, when data flows change over time, fast updated dimension reduction solutions may be needed to visualize the changes. Second, in the context of interactive visualization of dimension reduction methods, the interface may need to react instantly to user interaction (e.g., such as the selection of different variables or the elimination of one or more categories). In such a scenario, the analysis has to be repeated on-the-fly to reproduce on screen the changes to the solution. Third, the use of bootstrap techniques and permutation

tests to assess stability and the significance of PCA and MCA solutions, requires the analyses to be repeated many times. Here, in order to obtain the results in reasonable time, fast procedures are needed. All these situations illustrate the need for fast and efficient computations for the dimension reduction solution.

The majority of the matrix decomposition procedures focus on the analysis of quantitative variables only. However, when dealing with categorical data, in particular with binary variables, a further peculiarity arises that needs to be taken into account: the sparsity of the matrix being analyzed.

In the present paper, an efficient implementation of MCA is proposed that addresses the issues presented above. In particular, the aim is to extend the suitability of the MCA to computational demanding applications such as dynamic visualization of data streams of texts and web-log analysis. Furthermore, the proposed procedure aims to increase the feasibility of interactive visualizations and stability analysis when large amounts of data are repeatedly analyzed. The fast MCA algorithm we propose here, powerCA, exploits enhanced computations of the sparse matrix transformations together with fast iterative eigendecomposition methods that exploit "warm starts" (i.e., algorithm initializations that are potentially "close" to the solutions) in case of repeated analyses.

The paper is structured as follows. In Sect. 2, data structures and basic computations of MCA are introduced. Section 3 discusses and evaluates a method to exploit sparse matrix multiplication in the context of MCA. A fast iterative procedure to compute the dominant eigenvalues of a matrix is described in the Sect. 4. Following that, Sect. 4.1 presents a simulation study to evaluate the computational performance and accuracy of the iterative procedure compared to the standard EVD implementation available in CRAN-R environment. In Sect. 5, an application of the proposed procedure to construct bootstrap confidence ellipses is presented and compared with a standard MCA implementation. The last section is for conclusions.

2 Correspondence Analysis

Correspondence analysis (CA) is a well-known exploratory method to describe and visualize the association structure of a cross tabulation table involving two categorical variables (Greenacre [6]). The generalization of CA to the case of p categorical variables is multiple correspondence analysis (MCA). Let $\mathbf{N}$ be the cross tabulation table of two categorical variables with r and c levels, respectively. The so-called *correspondence matrix* is $\mathbf{P} = n_{++}^{-1}\mathbf{N}$, where n_{++} is the grand total of $\mathbf{N}$. Let $\mathbf{r} = \mathbf{P}\mathbf{1}_c$ and $\mathbf{c} = \mathbf{P}^\top \mathbf{1}_r$ be the row and column margins of $\mathbf{P}$, respectively; $\mathbf{1}_r$ and $\mathbf{1}_c$ are vectors with r and c elements all equal to "1". Define the diagonal matrices of row and column margins, respectively, $\mathbf{D_r}$ and $\mathbf{D_c}$.

Let the standardized residuals matrix $\mathbf{S}$ be

$$\mathbf{S} = \mathbf{D_r}^{-1/2}\left(\mathbf{P} - \mathbf{r}\mathbf{c}^\top\right)\mathbf{D_c}^{-1/2} \tag{1}$$

with general element $s_{ij} = (p_{ij} - r_i c_j)(r_i c_j)^{-1/2}$, with $i = 1, \ldots, r$ and $j = 1, \ldots, c$. The core step of CA is based on the decomposition of the $\mathbf{S}$ matrix, via the singular value decomposition (SVD)

$$\mathbf{S} = \mathbf{U}\boldsymbol{\Sigma}\mathbf{V}^\top \quad \text{with} \quad \mathbf{U}^\top\mathbf{U} = \mathbf{V}^\top\mathbf{V} = \mathbf{I}, \tag{2}$$

where $\mathbf{U}$ and $\mathbf{V}$ are the left and right singular vectors, and $\boldsymbol{\Sigma}$ is the diagonal matrix of the singular values. The solution can also be obtained by means of the eigenvalue decomposition (EVD)

$$\mathbf{S}\mathbf{S}^\top = \mathbf{U}\boldsymbol{\Lambda}\mathbf{U}^\top \quad \text{and} \tag{3}$$

$$\mathbf{S}^\top\mathbf{S} = \mathbf{V}\boldsymbol{\Lambda}\mathbf{V}^\top \tag{4}$$

to obtain the orthonormal matrices $\mathbf{U}$ and $\mathbf{V}$, with $\boldsymbol{\Lambda} = \boldsymbol{\Sigma}^2$ being the diagonal matrix of eigenvalues. Often the row and columns are visualized as points on a low-dimensional factorial map using the column principal standardization in CA with row coordinates $\mathbf{F} = {\mathbf{D_r}}^{-1/2}\mathbf{U}$ and column coordinates $\mathbf{G} = {\mathbf{D_c}}^{-1/2}\mathbf{V}\boldsymbol{\Sigma}$.

One way to compute the MCA solution uses the so-called super indicator matrix $\mathbf{Z}$ consisting of one dummy variable for each category of each variable with a 1 if the category is observed and 0 else. If variable j has p_j categories, then $\mathbf{Z}$ is $n \times s$ with $s = \sum_{j=1}^{p} p_j$. MCA can be computed as CA with $\mathbf{N} = \mathbf{Z}$. Hence, going through the standard computations of (1), the MCA solution is computed by means of the SVD in (2) on the transformed version of $\mathbf{Z}$. However, when $n \gg s$, it is more efficient to use (4) with $\mathbf{S}^\top\mathbf{S} = \mathbf{Z}^\top\mathbf{Z} = \mathbf{B}$ which is $s \times s$. In MCA, the matrix $\mathbf{B}$ is called the Burt matrix: a partitioned block matrix with as off-diagonal blocks the contingency tables of variables j and j' and as diagonal blocks the diagonal matrices with marginal frequencies for the categories of variable j. The correspondence matrix is $\mathbf{C} = (ns^2)^{-1}\mathbf{B}$, and since $\mathbf{C}$ is square and symmetric by definition, its standardized residual matrix is

$$\mathbf{S}_B = {\mathbf{D_c}}^{-1/2}\left(\mathbf{C} - \mathbf{c}\mathbf{c}^\top\right){\mathbf{D_c}}^{-1/2}. \tag{5}$$

The EVD of $\mathbf{S}_B = \mathbf{V}\boldsymbol{\Lambda}\mathbf{V}^\top$ leads to principal coordinates $\mathbf{F} = \mathbf{G} = {\mathbf{D_c}}^{-1/2}\mathbf{V}\boldsymbol{\Lambda}^{1/2}$. Although the Burt matrix-based computations only yield the attribute coordinates directly, one can calculate the coordinates for the observations as well by using so-called transition formulas (see e.g., Greenacre [6]).

3 Efficient Computation of the Burt Matrix

MCA based on the Burt matrix involves a decomposition of an $s \times s$ matrix, irrespective of the number of rows n. When n is very large, however, direct computation of the Burt matrix as the matrix product $\mathbf{Z}^\top\mathbf{Z}$ becomes problematic. However, the computational cost of this matrix multiplication can be dramatically improved

using sparse matrix algebra packages. In fact, the indicator matrix is partitioned as $\mathbf{Z} = [\mathbf{Z}_1, \ldots, \mathbf{Z}_p]$, where each $n \times p_j$ block has just one nonzero element per row. This means that there are $n \times p$ nonzero entries out of $n \times s$. In other words, the larger the number of categories per variable, the higher the sparsity of $\mathbf{Z}$. The advantage of sparse matrix multiplication is proportional to the sparsity of the matrices involved.

In several applications, such as text mining, web-log analysis, and market basket analysis, each attribute is binary. Binary data represents a particular case in the context of MCA. In the binary data case, $\mathbf{Z}$ is characterized by a constant sparsity: in particular, the ratio between the nonzero entries and the total entries in the table is 0.5, since $s = 2p$ by definition. The computation of the Burt matrix is then only slightly improved using sparse matrix multiplication.

We propose an alternative way of computing the Burt matrix that allows to exploit sparse matrix multiplication in case of binary data. Recall that the Burt matrix is a block square matrix: diagonal blocks are diagonal matrices containing the column margins of $\mathbf{Z}_j$, $j = 1, \ldots, p$ (the indicator matrix with dummy coding for all categories for variable j); the (ij)th off-diagonal block is a cross tabulation matrix, given by $\mathbf{Z}_i^\top \mathbf{Z}_j$. In the special case of binary variables, all the blocks are two-by-two matrices: given two attributes i and j, the corresponding block is

$$\mathbf{Z}_i^\top \mathbf{Z}_j = \begin{array}{c} \left[\begin{array}{cc} a & b \\ c & d \end{array}\right] \begin{array}{c} c_i \\ n - c_i \end{array} \\ \begin{array}{cc} c_j & n - c_j \end{array} \quad n \end{array}, \tag{6}$$

where a indicates the number of copresences of the attributes, d the number of co-absences, b and c are the mismatches; element c_i of the p vector $\mathbf{c}$ contains the marginal frequency of presences of attribute i. By knowing the margins and the copresences a, it is possible to compute b, c and d. Let $\mathbf{B}_a = \tilde{\mathbf{Z}}^\top \tilde{\mathbf{Z}}$ be the $p \times p$ matrix containing the copresences only; $\tilde{\mathbf{Z}}$ is the $n \times p$ starting binary data matrix, with $\tilde{z}_{ij} = 1$ if the ith observation is characterized by the jth attribute and $\tilde{z}_{ij} = 0$ otherwise. In many applications, $\tilde{\mathbf{Z}}$ has very few nonzero entries, so that the sparse matrix multiplication $\tilde{\mathbf{Z}}^\top \tilde{\mathbf{Z}}$ is computationally very efficient to obtain $\mathbf{B}_a$. The co-absence matrix $\mathbf{B}_d$ and the mismatch matrices $\mathbf{B}_b$ and $\mathbf{B}_c$ can be computed as a function of $\mathbf{B}_a$, that is,

$$\mathbf{B}_b = \mathbf{1}_c \mathbf{c}^\top - \mathbf{B}_a^\top, \quad \mathbf{B}_c = \mathbf{c}\mathbf{1}_c^\top - \mathbf{B}_a^\top, \quad \mathbf{B}_d = n\mathbf{1}\mathbf{1}^\top - (\mathbf{B}_a + \mathbf{B}_b + \mathbf{B}_c). \tag{7}$$

Then, each two-by-two block of the complete Burt matrix $\mathbf{B}$ is filled up taking values from $\mathbf{B}_a$, $\mathbf{B}_b$, $\mathbf{B}_c$ and $\mathbf{B}_d$, respectively, in the top left, top right, bottom left, and bottom right positions.

To study the gain in efficiency of our Burt matrix computation for binary data, with respect to using regular sparse matrix computations, a simulation study was performed. Three factors were varied: the number of rows (i.e., observations) of $\mathbf{Z}$, $n \in \{500; 1{,}000; 5{,}000; 10{,}000\}$, the number of columns (i.e., attributes),

Table 1 Ratio of computational time for computing the Burt matrix through regular sparse matrix computations and our efficient computation in (7) for different numbers of observations n and attributes p, and degree of sparsity π

π	n	p			
		50	100	250	500
0.4	500	1.40	2.67	3.06	2.87
	1,000	2.17	3.38	3.93	4.45
	5,000	4.06	6.31	5.06	5.00
	10,000	6.06	4.93	4.70	5.00
0.3	500	1.75	3.28	3.75	3.57
	1,000	3.25	4.09	5.25	5.93
	5,000	5.75	8.97	8.14	7.90
	10,000	8.27	8.50	7.32	7.74
0.2	500	1.50	3.83	4.31	4.03
	1,000	4.00	5.62	6.86	7.85
	5,000	7.33	13.95	15.60	14.31
	10,000	13.28	17.16	14.08	14.09
0.1	500	2.00	4.80	4.84	4.60
	1,000	4.00	9.00	8.82	9.34
	5,000	10.83	26.00	30.90	29.32
	10,000	21.57	31.28	39.18	35.60

$p \in \{50; 100; 250; 500\}$, and the sparsity $\pi \in \{0.1; 0.2; 0.3; 0.4\}$, with π being the probability of getting a "1" for each of the p considered attributes. For each combination of the factors, a data set $\mathbf{Z}$ was generated and the ratio of CPU time for computing the Burt matrix through both methods is reported in Table 1. The proposed efficient computation always outperforms the regular sparse computation of the Burt matrix. The computational speed gain due to the smart computation increases with increasing sparseness and increasing n, whereas the effect of p is less pronounced.

4 The Power Method

The power method represents one of the oldest techniques to solve eigenvalue problems. In particular, the power method aims at identifying the largest eigenvalue and corresponding eigenvector of a symmetric $(p \times p)$ matrix $\mathbf{A}$. The rationale of the method is based on the fact that, if a p-dimensional vector $\mathbf{q}_0$ is multiplied by the matrix $\mathbf{A}$, the contribution of the eigenvector corresponding to the largest eigenvalue increases more than the contribution of the other eigenvectors. Upon repeating several times the product of the vector $\mathbf{q}_0$ by the matrix $\mathbf{A}$, the contribution of the eigenvector dominates, and the iteration vector converges to the eigenvector in question

(Vuik & Lahaye [16]). In other words, the method consists of generating a sequence $\mathbf{A}^k\mathbf{q}_0$ which, with a proper normalization, converges to the dominant eigenvector. The pseudocode for the implementation of the power method is in Algorithm 1.

Algorithm 1 The power method

Require: $\mathbf{A}$ {square symmetric matrix}
$k := 1$ {initialization of the counter}
choose $\mathbf{q}^{(k)}$ {random initialization of the eigenvector }
$\mathbf{q}^{(k)} := \mathbf{q}^{(k)} \left(\mathbf{q}^{(k)\mathsf{T}}\mathbf{q}^{(k)}\right)^{-1/2}$ {set the norm of $\mathbf{q}^{(k)}$ equal to one}
$\mathbf{y}^{(k)} := \mathbf{A}\mathbf{q}^{(k)}$
$\lambda^{(k)} := \mathbf{q}^{(k)^{\mathsf{T}}}\mathbf{y}^{(k)}$ {computation of the eigenvalue }
$\lambda^{(k-1)} := \lambda^{(k)} - 2\epsilon$
while $((\lambda^{(k)} - \lambda^{(k-1)})/\lambda^{(k)} > \epsilon)$ **do**
  $k := k + 1$
  $\mathbf{q}^{(k)} := \mathbf{y}^{(k-1)} \left(\mathbf{y}^{(k-1)\mathsf{T}}\mathbf{y}^{(k-1)}\right)^{-1/2}$ {set the norm of $\mathbf{q}^{(k)}$ equal to one}
  $\mathbf{y}^{(k)} := \mathbf{A}\mathbf{q}^{(k)}$
  $\lambda^{(k)} := \mathbf{q}^{(k)\mathsf{T}}\mathbf{y}^{(k)}$ {computation of the eigenvalue }
end while
Ensure: $\mathbf{q}^{(k)}, \lambda^{(k)}$

The generalization of the power method to the multiple eigenvalue/eigenvector identification case may be referred to as simple subspace iteration (Saad [15]), and is based on the relation

$$\mathbf{Q}^{(k)} = \mathbf{A}^k\mathbf{Q}_0. \tag{8}$$

The orthonormalization, however, involves a singular value decomposition of $\mathbf{Q}^{(k)}$ at each iteration, and it might have a high computational cost.

An alternative way is to apply the standard power method to obtain the dominant eigen-pair λ_1 and $\mathbf{q}_1$, that is, the largest eigenvalue and the corresponding eigenvector, and then re-apply the procedure to $\mathbf{A} - \lambda_1\mathbf{q}_1\mathbf{q}_1^{\mathsf{T}}$ to obtain λ_2 and $\mathbf{q}_2$ (see, e.g., Husson, Josse, Narasimhan, & Robin [10]). More generally, the dth eigen-pair $(\lambda_d, \mathbf{q}_d)$ is obtained by decomposing the input matrix $\mathbf{A}$ minus its rank-$(d-1)$ approximation, formally

$$\mathbf{A} - \sum_{j=1}^{d-1} \lambda_j \mathbf{q}_j \mathbf{q}_j^{\mathsf{T}}.$$

This approach can also use a warm start for repeated decompositions. Suppose a new data matrix $\mathbf{A}^+$ is available that updates the matrix $\mathbf{A}$, that is $\mathbf{A}^\star \leftarrow \mathbf{A} + \mathbf{A}^+$. If the rank-$d$ approximation of $\mathbf{A}$ is available, $\mathbf{A} \approx \mathbf{Q}^{(k)}\mathbf{\Lambda}^{(k)}\mathbf{Q}^{(k)\mathsf{T}}$, the idea is to use the power method to obtain the rank-d decomposition of $\mathbf{A}^\star$ by using $\mathbf{Q}^{(k)} = \left[\mathbf{q}_1, \mathbf{q}_2, \ldots, \mathbf{q}_d\right]$, eigenvectors of $\mathbf{A}$, as a warm initialization of the algorithm. The procedure is detailed in Algorithm 2. For the simple power method, we used the function `powerMethod` from the `matlib` package (Friendly, Fox, & Chalmers [5]).

Algorithm 2 Multiple power method with warm start

Require: $\mathbf{A}, \mathbf{q}_1, \mathbf{q}_2, \ldots, \mathbf{q}_d, \epsilon$ {square symmetric matrix, starting eigenvectors, tolerance}
1: **for** j in $1, 2, \ldots, d$ **do**
2: $k := 1$ {initialization of the counter}
3: $\mathbf{q}_j^{(k)} := \mathbf{q}_j$ {warm initialization of the eigenvector}
4: $\mathbf{y}^{(k)} := \mathbf{A}\mathbf{q}_j^{(k)}$
5: $\lambda_j^{(k)} := \mathbf{q}_j^{k\mathsf{T}}\mathbf{y}_j^{(k)}$ {computation of the eigenvalue}
6: $\lambda_j^{(k-1)} := \lambda_j^{(k)} - 2\epsilon$
7: **while** $((\lambda_j^{(k)} - \lambda_j^{(k-1)})/\lambda_j^{(k)} > \epsilon)$ **do**
8: $k := k + 1$
9: $\mathbf{q}_j^{(k)} := \mathbf{y}_j^{(k-1)} \left(\mathbf{y}_j^{(k-1)\mathsf{T}}\mathbf{y}_j^{(k-1)}\right)^{-1/2}$ {set the norm of $\mathbf{q}_j^{(k)}$ equal to one}
10: $\mathbf{y}_j^{(k)} := \mathbf{A}\mathbf{q}_j^{(k)}$
11: $\lambda_j^{(k)} := \mathbf{q}_j^{(k)\mathsf{T}}\mathbf{y}_j^{(k)}$ {computation of the eigenvalue}
12: **end while**
13: $\mathbf{A} := \mathbf{A} - \mathbf{q}_j^{(k)}\lambda_j^{(k)}\mathbf{q}_j^{(k)\mathsf{T}}$ {update $\mathbf{A}$ by removing the rank-1 approximation}
14: **end for**
Ensure: $\mathbf{q}_1^{(k)}, \ldots, \mathbf{q}_d^{(k)}; \lambda_1^{(k)}, \ldots, \lambda_d^{(k)}$

4.1 Comparison with Standard EVD Implementation

We assess the performance of the multiple power method compared to the standard `eigen()` function for eigendecomposition in CRAN-R. Consider a moving-window scenario. Let $\mathbf{Z}$ be the $n \times p$ starting random binary matrix and let $\mathbf{B}$ be the corresponding Burt matrix. The EVD is applied to the standardized residual version of $\mathbf{B}$, see (5). Each update of the Burt matrix is obtained as follows: let $\mathbf{Z}^+$ be a new $n_{up} \times p$ matrix of *new* observations and let $\mathbf{B}^+$ the corresponding Burt matrix. Similarly, let $\mathbf{Z}^-$ be the n_{up} rows of $\mathbf{Z}$ to be discarded, as they fall outside the active window, and let $\mathbf{B}^-$ be the corresponding Burt matrix. Then the current Burt matrix becomes

$$\mathbf{B} = \mathbf{B} + \mathbf{B}^+ - \mathbf{B}^-$$

and the resulting standardized residuals matrix is decomposed.

To compare the computational efficiency for moving windows, we use the following settings in a simulation:

- the number of observations $n = 5000$,
- the number of observations that is being updated $n_{up} = 2000$,
- the number of updates 5,
- the number of binary attributes $p \in \{500, 1000, 1500\}$, and
- the level of tolerance $\epsilon \in \{10^{-10}, 10^{-12}\}$.

All binary attributes are randomly generated with probability for presence $\pi = 0.25$. We only consider two dimensional solutions.

The efficiency is compared on two aspects: (a) the computational speed in CPU seconds as measured by the mean over 10 replicates of each decomposition, and (b) the accuracy for each update by the median of the relative absolute differences,

$$\text{median}\left(\left|\frac{q_{1j}^{(pm)}-q_{1j}^{(evd)}}{q_{1j}^{(evd)}}\right|,\left|\frac{q_{2j}^{(pm)}-q_{2j}^{(evd)}}{q_{2j}^{(evd)}}\right|,\ldots,\left|\frac{q_{dj}^{(pm)}-q_{dj}^{(evd)}}{q_{dj}^{(evd)}}\right|\right),$$

averaged over the dimensions and replicates, where $\mathbf{q}_j$ stands for eigenvector j and the superscripts pm refers to the power method and evd to standard `eigen()` function for EVD.

The results of the computational speed assessment are reported in Fig. 1. We see that, irrespective to the tolerance level, the `eigen()` computational time grows with the number of attributes, whereas the multiple power method is considerably less affected by the size of the matrix. As a result, the advantage in terms of speed of multiple power method over the standard implementation becomes considerable for larger matrices. This is due to the fact that (i) the power method only computes the dominant eigen-pairs (ii) and uses warm starts. In the first update, the eigenvectors of the initial matrix are used as a warm start. Subsequently, in each of the following updates, the eigenvectors obtained in the last update are used as warm starts.

The accuracy measures are reported in Table 2. The power method computes approximated eigen-pairs and it is known to have convergence and accuracy issues when eigenvalues do not differ much. That is, when the ratio of the computed eigenvalues is such that $|\lambda_2|/|\lambda_1| \to 1$. This is the case with the random matrices being

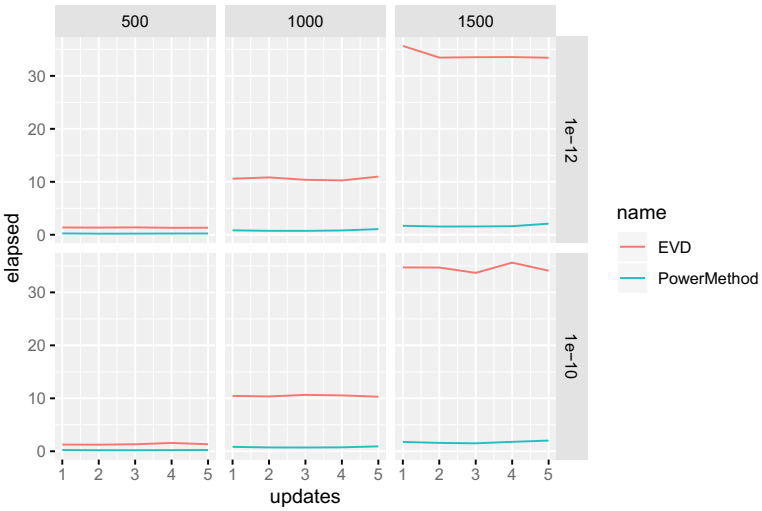

Fig. 1 Average elapsed time in seconds for eigendecompositions of matrices of different number of attributes ($p = \{500, 1500, 2000\}$) and tolerance levels ($\epsilon \in \{10^{-10}, 10^{-12}\}$)

Table 2 Average median relative absolute differences of the power method-based solution and standard EVD

p	ϵ	B_1	B_2	B_3	B_4	B_5
500	1e-10	0.148	0.339	0.339	0.162	0.323
	1e-12	0.364	0.351	0.293	0.056	0.336
1000	1e-10	0.123	0.183	0.252	0.236	0.245
	1e-12	0.081	0.357	0.259	0.124	0.362
1500	1e-10	0.372	0.336	0.331	0.342	0.375
	1e-12	0.170	0.097	0.168	0.361	0.356

decomposed in this simulation study. However, when an underlying association structure exists, consecutive eigenvalues are likely to differ from each other and these issues are mitigated, as reported in Sect. 5.

5 PowerCA and the Bootstrap

A common application involving repeated MCA analyses is the construction of bootstrap ellipses to assess the stability of the solution. A procedure for constructing balanced bootstrap ellipses is the one proposed by Linting, Meulman, Groenen, and van der Kooij [12]. Such a procedure can be seen as a sensitivity analysis (Ringrose [14]). We apply this procedure using both powerCA and ordinary MCA, and assess the computational gain and accuracy of the powerCA with respect to ordinary MCA using the `ca` package (Greenacre & Nenadic [7]). The dependent variables in our experimental setup are the CPU time and the accuracy of the solution. With respect to the accuracy, both the attribute coordinates and the constructed ellipses are compared. In particular, for the attribute coordinates, the Procrustean index R between `mjca` and powerCA solutions is computed. The procrustean index R is defined as $R = \sqrt{1 - m^2}$ with m^2 is the symmetric orthogonal Procrustes statistic (Jackson [8]) that is a measure of concordance, or similarity, between the two attribute configurations in question (PowerCA and MCA). The index ranges from 0 to 1 and can be interpreted as a correlation coefficient. It was calculated using the function `protest` of the R package `vegan` (Oksanen et al. [13]). To measure the constructed ellipses we refer to the *relative mean squared error* (Van de Velden, De Beuckelaer, Groenen, & Busing, [17]),

$$\text{RMSE} = \frac{\sum_{j=1}^{J}\sum_{b=1}^{B}\left(\mathbf{f}_{jb} - \hat{\mathbf{f}}_j\right)^{\mathsf{T}}\left(\mathbf{f}_{jb} - \hat{\mathbf{f}}_j\right)}{B\sum_{j=1}^{J}\hat{\mathbf{f}}_j^{\mathsf{T}}\hat{\mathbf{f}}_j},$$

where $\mathbf{f}_{jb}$ contains the coordinates of the jth attribute in the bth bootstrap replicate and $\hat{\mathbf{f}}_j$ is the coordinate of attribute j in the original (full data) solution. The accuracy of the ellipses constructed via powerCA and via ordinary MCA is measured in terms of the absolute value of the relative discrepancy between RMSEs:

$$\text{accuracy} = \left| \frac{\text{RMSE}_{\text{powCA}} - \text{RMSE}_{\text{mca}}}{\text{RMSE}_{\text{mca}}} \right|. \tag{9}$$

The dependent variables accuracy and CPU time are measured while varying tolerance levels and the amount of imposed structure in the generated data set.

For our comparisons, we consider the following settings:

- the size of the data $n = 2{,}500$ and $p = 250$,
- the number of bootstrap replicates $B = 250$,
- the tolerance level $\epsilon \in \left\{10^{-2}, 10^{-4}, 10^{-6}, 10^{-8}, 10^{-10}, 10^{-12}\right\}$
- the strength of association structure by varying combinations of low and high probabilities $(p_{\text{low}}, p_{\text{high}})$ of an occurrence in a cell in three levels: no, medium, and high structure, that is, $(p_{\text{low}}, p_{\text{high}}) \in \{(0.4, 0.4), (0.3, 0.5), (0.2, 0.7)\}$. Figure 2 shows these three levels of association structure considered, in increasing order, from left to right.

The first interest here is to see how the computational times of MCA and powerCA vary depending on the tolerance levels (only for powerCA) and the amount of structure in the data. Figure 3 shows these results. If there is no structure in the data, powerCA is approximately 20 to 5 times faster than MCA for low levels of tolerance. The computational time increases as the level of tolerance decreases. For medium and highly structured data, the computational time of powerCA is steady with respect to the tolerance level. For those scenarios, powerCA is around 50 times faster than ordinary MCA.

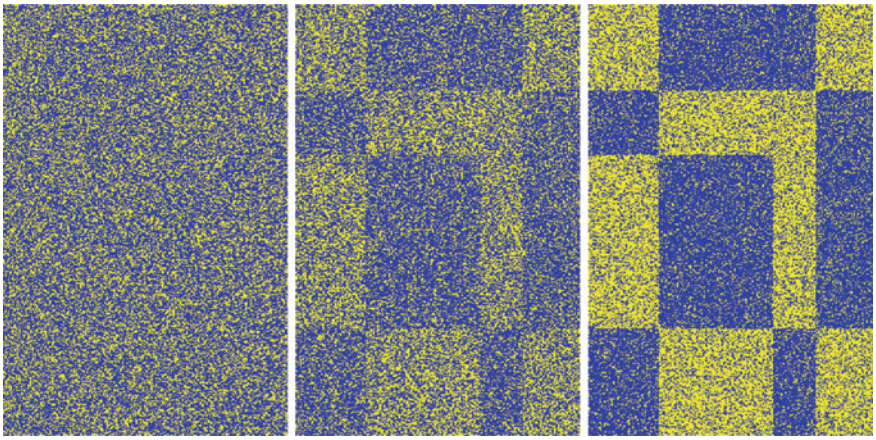

Fig. 2 Three matrices with increasing association structure: the left panel has no structure $(p_{\text{low}}, p_{\text{high}}) = (0.4, 0.4)$, the middle panel medium structure $(p_{\text{low}}, p_{\text{high}}) = (0.3, 0.5)$, and the right panel high structure $(p_{\text{low}}, p_{\text{high}}) = (0.2, 0.7)$

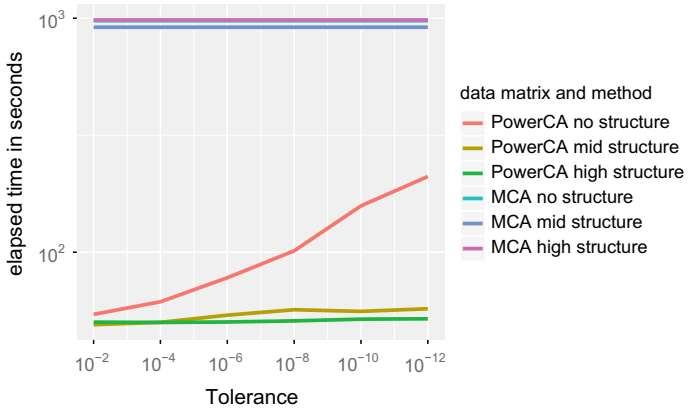

Fig. 3 Computational time results over different tolerance values and association strength. Each line represents a combination of method and association strength

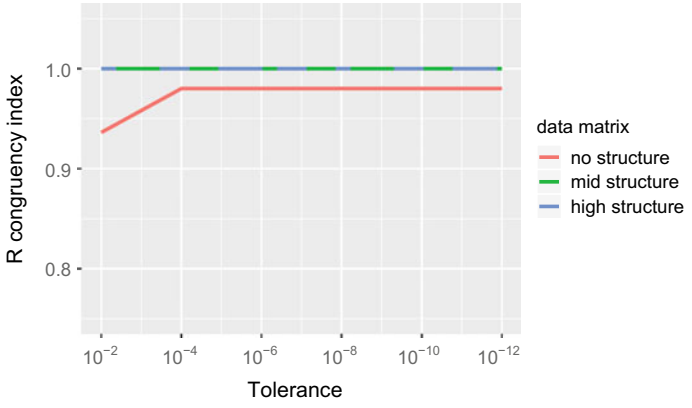

Fig. 4 Congruency R index of the MCA and powerCA solutions for different association structures and tolerance levels

To identify the level needed to provide accurate results, we compute the Procrustes congruency index R as a measure of similarity between the powerCA and MCA solutions. Figure 4 shows the results. In case of data with no structure, the powerCA only approximates the MCA solutions and lowering the tolerance does not help. This result is no surprise as it depends on the power method's convergence and accuracy issues (see Sect. 4.1). For medium and highly structured data, however, even a tolerance of 10^{-2} suffices to reproduce the MCA solution.

With respect to the accuracy of the bootstrap ellipses, we report in Fig. 5, the log of the values of accuracy index defined in Formula 9, for all scenarios. We see that the powerCA-based bootstrap solution has low accuracy when the data has

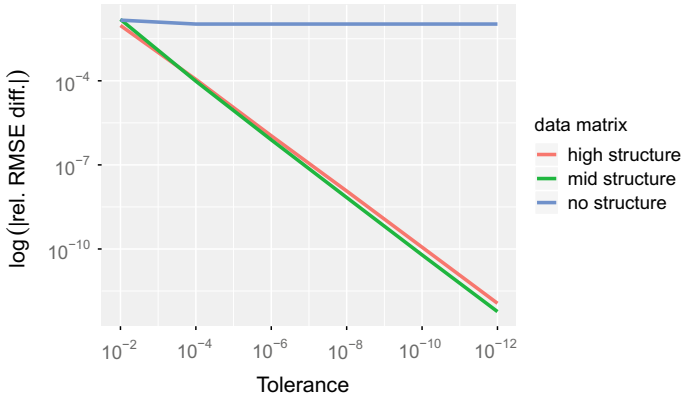

Fig. 5 RMSE-based accuracy of the bootstrap ellipses for different tolerance levels and association structures

no association structure, but for the scenarios with medium and high structure, it becomes increasingly accurate as the tolerance level decreases.

6 Conclusion

The proposed method, called powerCA, can be a useful tool when repeated exploratory analyses of large and sparse binary data tables are needed. We showed that in a setting requiring many repeated eigendecompositions of only partially changed binary data tables the powerCA provides fast and accurate solutions. The powerCA procedure exploits the power method-based eigen-decomposition which is most effective when warm starts are provided. The experiments pointed out the limitations of the power method, that is, when there is no (or, weak) association structure in the binary data table, it may have convergence and accuracy issues. Such issues, however, can be considered a mild concern: in fact, if there is no association structure characterizing the data, the application of PowerCA, or of MCA, is pointless in the first place. It should be noted that the power method is at the base of several modern procedures such as the augmented implicitly restarted Lanczos bi-diagonalization algorithm (Baglama & Reichel [1]), and the "thick-restart" Lanczos method (Wu & Simon [18] (available in R packages in `irlba` (Baglama & Reichel [2]) and `svd` (Korobeynikov [11])): such modern procedures can be considered as evolutions of the power method. It would be interesting to also consider the performance of such methods in the MCA setting considered in this paper.

References

1. Baglama, J., & Reichel, L. (2007). Augmented implicitly restarted Lanczos bidiagonalization methods. *SIAM Journal on Scientific Computing*, *27*, 19–42.
2. Baglama, J., & Reichel, L. (2012). irlba: Fast partial SVD by implicitly-restarted Lanczos bidiagonalization. http://CRAN.R-project.org/package=irlba.
3. Baker, C., Gallivan, K., & Van Dooren, P. (2012). Low-rank incremental methods for computing dominant singular subspaces. *Linear Algebra and its Applications*, *436*(8), 2866–2888.
4. Golub, G., & van Loan, A. (1996). *Matrix computations*. John Hopkins University Press.
5. Friendly, M., Fox, J., & Chalmers, P. (2019). matlib: Matrix functions for teaching and learning linear algebra and multivariate statistics. R package version 0.9.2. https://CRAN.R-project.org/package=matlib.
6. Greenacre, M. J. (2007). *Correspondence analysis in practice* (2nd ed.). Hapman and Hall/CRC.
7. Greenacre, M. J., & Nenadic, O. (2007). Correspondence Analysis in R, with two- and three-dimensional graphics: The ca package. *Journal of Statistical Software*, *20*(3), 1–13.
8. Jackson, D. A. (1995). PROTEST: A Procrustean randomization test of community environment concordance. *Ecoscience*, *2*, 297–303.
9. Jolliffe, I. T. (2002). *Principal component analysis* (2nd ed.). Springer.
10. Husson, F., Josse, J., Narasimhan, B., & Robin, G. (2019). Imputation of mixed data with multilevel singular value decomposition. *Journal of Computational and Graphical Statistics*, *28*(3), 552–566.
11. Korobeynikov, A. (2011). svd: Interfaces to various state-of-art SVD and eigensolvers. http://CRAN.R-project.org/package=svd.
12. Linting, M., Meulman, J. J., Groenen, P. J. F., & van der Kooij, A. J. (2007). Stability of nonlinear principal components analysis: an empirical study using the balanced bootstrap. *Psychological Methods*, *12*(3), 359–379.
13. Oksanen, J., Kindt, R., Legendre, P., O'Hara, B., Simpson, G. L., Solymos, P., et al. (2008). *Vegan: Community ecology package*.
14. Ringrose, T. J. (2012). Bootstrap confidence regions for correspondence analysis. *Journal of Statistical Computation and Simulation.*, *82*(10), 1397–1413.
15. Saad, Y. (2011). *Numerical methods for large eigenvalue problems* (Revised ed.). Society for industrial and applied mathematics.
16. Vuik, C., & Lahaye, D. J. P. (2011). *Scientific computing*. Delft institute of applied mathematics.
17. Van de Velden, M., De Beuckelaer, A., Groenen, P. J. F., & Busing, F. M. T. A. (2013). Solving degeneracy and stability in nonmetric unfolding. *Food Quality and Preference*, *27*(1), 85–95.
18. Wu, K., & Simon, H. (2000). Thick-restart Lanczos method for large symmetric eigenvalue problems. *SIAM Journal on Matrix Analysis and Applications*, *22*(2), 602–616.

Modeling Asymmetric Exchanges Between Clusters

Donatella Vicari

Abstract A nonhierarchical clustering model is proposed here which jointly fits the symmetric and skew-symmetric components of an asymmetric pairwise dissimilarity matrix. Two similar clustering structures are defined depending on two (generally different) partitions of the objects: a "complete" partition fitting the symmetries (where all objects belong to some cluster) and an "incomplete" partition fitting the skew-symmetries, where only a subset of objects is assigned to some cluster, while the remaining ones may remain non-assigned. The exchanges between clusters are accounted for by the model which is formalized in a least squares framework and an appropriate Alternating Least Squares algorithm is provided to fit the model to illustrative real data.

1 Introduction and Background

Asymmetric proximity data arise in many domains where the exchanges between (generally speaking) objects are under investigation. In fact, the analysis of asymmetric relationships can profitably shed light on relevant aspects of the directions of the exchanges or flows and not only on their average amounts. Examples of such data are brand-switching, migration flows, import–export data, socio-matrices, preferences, confusion data, which may be either directly observed or derived by indirect measurements.

Since such kinds of data are often intrinsically asymmetric, appropriate methodologies need to be used to exploit all the information from the data in terms of both amounts exchanged and directions, and also the visualization of the results plays a key role in their interpretation.

Many methodologies have been proposed in the literature for the analysis of the asymmetric pairwise proximities and systematic reviews may be referred to in order to get an overview of the many contributions: Chap. 23 in Borg and Groenen [1] is

D. Vicari (✉)
Dipartimento di Scienze Statistiche, Sapienza Università di Roma, Rome, Italy
e-mail: donatella.vicari@uniroma1.it

T. Imaizumi et al. (eds.), *Advanced Studies in Behaviormetrics and Data Science*,
Behaviormetrics: Quantitative Approaches to Human Behavior 5,
https://doi.org/10.1007/978-981-15-2700-5_18

specifically devoted to asymmetry; the book by Saito and Yadohisa [20] contains a comprehensive review of the many models presented in the literature; Bove and Okada [2], in their paper included in the Special Issue on Analysis of Asymmetric Relationships of the journal Data Analysis and Classification, provide an up-to-date review of the most recent models and methods on multidimensional scaling and cluster analysis for dealing with asymmetric proximity data.

Specifically, in the view of a visualization of the data, many methodologies aim at embedding the data in low-dimensional spaces based on generalizations of the MDS methods and to a lesser extent on cluster analysis. In many cases, they rely on the decomposition of the asymmetry into symmetric and skew-symmetric effects, which allows to deal independently with the average amounts (symmetric component) and the imbalances (skew-symmetric component) due to their orthogonality. While the symmetric part may be represented and modeled by the usual methods for symmetric data, appropriate models have been proposed to fit the skew-symmetries. An interesting decomposition of a skew-symmetric matrix has been given by Gower [8] and Constantine and Gower [4, 5] where a graph of the objects is obtained in a plane where the angles subtended by the vectors have a fixed meaning: the skew-symmetries are embedded into the MDS representation of the symmetrized data by drawing arrows (drift vectors) from any point in the configuration so that these vectors correspond in length and direction to the values in the rows of the skew-symmetric matrix.

Differently, models for fitting asymmetry directly are based on a representation of the objects by circles with different radii Okada and Imaizumi [12] or by ellipsoids (Okada [11]).

In the same multidimensional scaling framework, several models have been proposed to represent the symmetry and the skew-symmetry of the data in low-dimensional spaces, (for example, Escoufier & Grorud [6]; Zielman & Heiser [24]; Rocci & Bove [19]; see also Borg & Groenen [1]).

Clustering methodologies for asymmetric data have been proposed under two major approaches where the asymmetric proximities are regarded either as a special case of two-mode two-way data (the rows and the columns are considered two different modes) or, in accordance with the original form of the data, as one-mode two-way data (for extensive reviews, see Chap. 5 of the book by Saito and Yadohisa [20] and Bove and Okada [2]). Most of the proposals are actually extensions of the classical hierarchical algorithms for symmetric data (Hubert [10]; Okada & Iwamoto [14]; Takeuchi, Saito, & Yadohisa [21]), while Brossier [3] proposes to embed a one-dimensional solution from the skew-symmetries into the dendrogram of the standard average linkage fitted to the symmetric part.

On the other hand, less attention has been paid to nonhierarchical methods for asymmetric data.

The clustering model for asymmetric data by Vicari [22] is framed in the one-mode approach and relies on the decomposition of the asymmetric dissimilarity matrix into *symmetric* and *skew-symmetric* effects both decomposed in *within* and *between* cluster effects. Two different clustering structures depending on two (generally different) partitions of the objects are fitted to the symmetries and skew-symmetries, separately. Specifically, objects belonging to the same clusters from the skew-symmetric com-

ponent: (1) share the same behaviors in terms of exchanges directed to the other clusters and identify,"origin" and "destination" clusters, (2) form closed systems of internal exchanges. When a unique partition is assumed to exist, a parsimonious model allows for a simpler and more interpretable solution which can be graphically displayed and clusters can be jointly interpreted in terms of similar average amounts and imbalances exchanged.

An extension of the model termed CLUSKEXT (Vicari [23]) introduces the possibility to incorporate external variables into the model in order to explain imbalances between objects.

Other nonhierarchical clustering methods are extensions of the k-means clustering dealing with different asymmetric proximities or using asymmetric coefficients Olszewski [16, 17]; Olszewski & Ster [18]), while Okada and Yokoyama [15] propose a clustering algorithm which uses the dominant object (Okada & Imaizumi [13]).

Following the same line of Vicari [22, 23], a nonhierarchical clustering model is proposed here which jointly fits the symmetric and skew-symmetric components of the asymmetric pairwise dissimilarities by two similar clustering structures depending on two partitions of the objects: a "complete" partition fitting the symmetries (where all objects belong to some cluster) and an "incomplete" partition fitting the skew-symmetries, where only a subset of objects are assigned to some cluster, while the remaining ones may remain non-assigned.

The paper is structured as follows. In order to motivate and present the methodology, an illustrative real example is introduced in Sect. 2. After providing the essential notation, the joint clustering model for asymmetric dissimilarity data is formalized in Sect. 3 and an appropriate Alternating Least Squares algorithm is presented in Sect. 4. Some considerations on the estimates and their interpretations are discussed in Sect. 5, while in Sect. 6 the model is applied on the real data introduced in Sect. 2. Finally, some concluding remarks are reported in Sect. 7.

2 Illustrative Example: Language Data

In order to give a flavor of the motivation for the methodology which will be fully formalized in Sect. 3, the Language Data shown in Everitt and Rabe-Hesketh [7], adapted from Hartigan [9], have been analyzed as an illustrative example. The data report the percentage of people in various European countries who claim to speak the other European languages enough to make themselves understood. Dissimilarities have been derived by subtracting the original percentages from 100, so that they indicate the percentages of people in each country who *do not speak* a given language (Table 1).

As expected the percentages reveal different profiles and their asymmetry, even if small (0.62%), cannot be assumed to be due to noise. The maps of the languages in terms of average amounts of the symmetrized percentages and imbalances between percentages are graphically represented in Fig. 1 and Fig. 2, respectively.

Table 1 Language Data: % of persons who do not speak a language "enough to make yourself understood"

Country	Languages										
	German (Ger)	Italian (Ital)	French (Fr)	Dutch (Dch)	English (Eng)	Portuguese (Port)	Swedish (Swed)	Danish (Dan)	Norwegian (Nor)	Finnish (Finn)	Spanish (Spn)
Germany	0	98	90	98	79	100	100	100	100	100	99
Italy	97	0	89	100	95	100	100	100	100	100	99
France	93	88	0	99	90	99	98	97	100	100	93
Netherlands	53	98	84	0	59	100	100	100	100	100	93
Great Britain	93	97	85	100	0	100	100	100	100	100	98
Portugal	100	99	90	100	91	0	100	100	100	100	98
Sweden	75	99	94	100	57	100	0	90	89	95	99
Denmark	64	97	90	99	62	100	78	0	80	100	99
Norway	81	99	96	100	66	99	75	81	0	100	100
Finland	89	99	98	100	88	100	77	100	100	0	100
Spain	99	98	89	100	95	100	100	100	100	100	0

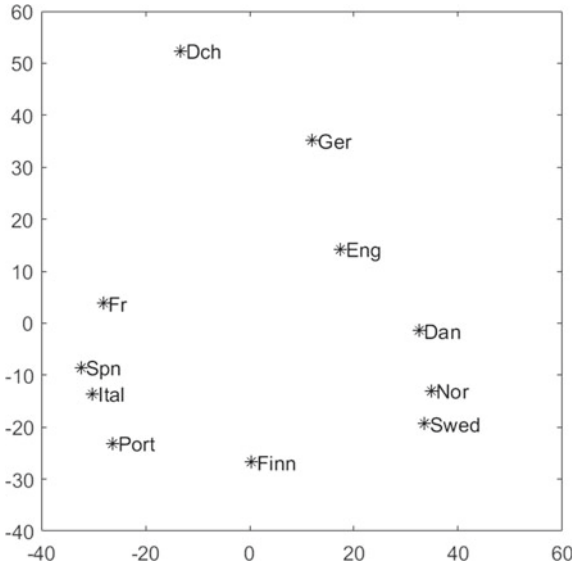

Fig. 1 Language Data: classical MDS map from the symmetrized percentages of non-spoken languages

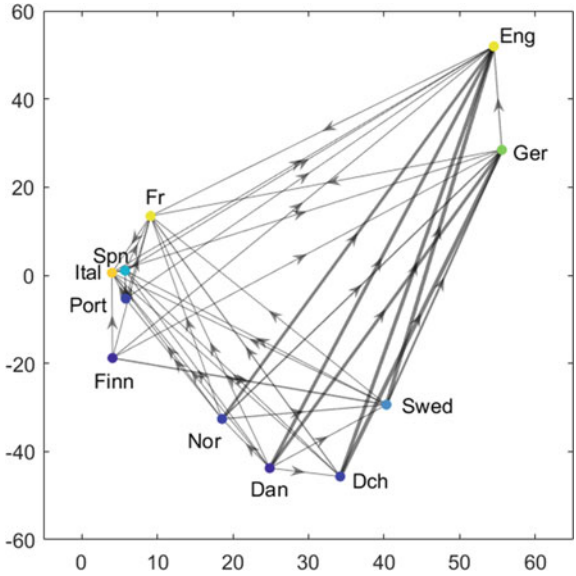

Fig. 2 Language Data: Canonical decomposition (arrowed lines display the directions of the skew-symmetries)

Specifically, Fig. 2 displays the two-dimensional classical MDS configuration from the symmetric part of the dissimilarity data matrix, while Fig. 2 shows the map of the languages in the first bimension from the canonical decomposition of the skew-symmetries (Gower [8]; Constantine & Gower [4, 5]) with arrowed lines indicating the directions of the exchanges.

In Fig. 2, nodes identifying languages are colored according to their different in-degree which is equal to the number of arcs with that node as the target: the lighter the color, the larger the number of arcs directed to that node, i.e., the English node is light yellow because the percentage of people speaking English also as a second language is very large (we may say English is a "destination" or "target" language); conversely, the Finnish node is colored dark blue, because only Swedish people claim to speak Finnish. Moreover, the larger the imbalance, the thicker the arrowed line.

From Fig. 2, it emerges that the first MDS dimension from the symmetrized percentages of non-spoken languages separates the Romance Languages (originating from Latin) from the German ones with the Finnish (Ural language) just in between, while the second dimension retrieves the extent at which people do not speak other languages in addition to their native ones.

The information from the substantial asymmetry come from the analysis of the "directions" of the percentages ("who speaks what") which is evident especially for some countries: for example, the percentage of people who do not speak German in Netherlands is just 53%, while the percentage of Germans who do not speak Dutch is much larger (98%). As known, in Fig. 2 the positions of the languages are derived so that the area of each triangle, formed by connecting the points for languages i and j to each other and to the origin, is (approximately) proportional to the corresponding skew-symmetry between languages i and j themselves. Thus, it can be noted that some (groups of) languages lack of reciprocity in speaking, regardless of the average percentages. For example, Italian, Spanish, Portuguese, and Finnish are close to a straight line from the origin giving triangles with small areas (the submatrix formed by such languages are almost symmetrical), while the triangle formed by each of such languages and English is quite larger: more people from Italy, Spain, Portugal, or Finland speak English than the reverse.

Starting from the observed asymmetries in speaking foreign languages, the interest here is in clustering the languages by taking into account not only their average percentages (symmetries) but also their "directions" (skew-symmetries) so that groups of languages can be identified sharing similar patterns between groups. Generally speaking, this is even more important when the number of objects (languages here) to be clustered is large, because the graphical analysis may be difficult or misleading.

The results of the methodology formalized in Sect. 3 and applied to the Language Data are reported in Sect. 6.

3 The Model

Let $\mathbf{A} = [a_{ij}]$ be an $(N \times N)$ two-way one-mode matrix of dissimilarities measured on N objects, where a_{ij} is generally different from a_{ji}.

Let us recall that any square matrix $\mathbf{A}$ can be uniquely decomposed into a sum of a symmetric matrix $\mathbf{S}$ and a skew-symmetric matrix $\mathbf{K}$

$$\mathbf{A} = \mathbf{S} + \mathbf{K} = \frac{1}{2}\left(\mathbf{A} + \mathbf{A}^{'}\right) + \frac{1}{2}\left(\mathbf{A} - \mathbf{A}^{'}\right) \tag{1}$$

where $\mathbf{S}$ and $\mathbf{K}$ are orthogonal to each other, i.e., $trace(\mathbf{SK}) = 0$.

The entry s_{ij} of $\mathbf{S}$ represents the average amount of the exchange between objects i and j, while the entry k_{ij} of $\mathbf{K}$ represents the imbalance between i and j, i.e., the amount by which k_{ij} differs from the mean s_{ij}.

The model proposed here aims at clustering the N objects with respect to both rows and columns of matrix $\mathbf{A}$, by decomposing the asymmetries into *symmetric* and *skew-symmetric* effects, modeled as functions of two partitions of the objects which subsume the clustering structures of the dissimilarity data.

Specifically, we consider here a partition of the N objects into J disjoint clusters uniquely identified by an $(N \times J)$ binary membership matrix $\mathbf{U} = [u_{ij}]$ specifying for each object i whether it belongs to cluster j, $(j = 1, \ldots, J)$ or not, i.e., $u_{ij} = 1$ if i belongs to cluster j, $u_{ij} = 0$ otherwise, and $\sum_{j=1}^{J} u_{ij} = 1, \quad (i = 1, \ldots, N)$. Here, such a partition is referred to as *complete partition* because any object is required to be assigned to some cluster.

Furthermore, an *incomplete partition* of the N objects, identified by an *incomplete* membership matrix $\mathbf{V}$, is defined here as a set of J clusters where a number N_0 out of the N objects are allowed to remain non-assigned to any cluster, i.e., let $\mathbf{V} = \left[v_{ij}\right]$ be an *incomplete* $(N \times J)$ binary membership matrix where $v_{ij} = 1$ if i belongs to cluster j, $v_{ij} = 0$ otherwise. Note that matrix $\mathbf{V}$ actually identifies uniquely a complete partition of the subset of the N objects corresponding to the $(N–N_0)$ nonzero row profiles in $\mathbf{V}$.

The idea here is to account for the *between* clustering effects by approximating the symmetric and skew-symmetric components of the dissimilarities by two clustering structures depending on matrices $\mathbf{U}$ and $\mathbf{V}$, respectively.

Specifically, the skew-symmetries in $\mathbf{K}$ are modeled by the clustering structure introduced in Vicari [22, 23], based on the canonical approximation of any skew-symmetric matrix as a sum of a number of skew-symmetric matrices of rank 2

$$\mathbf{K} = \mathbf{VD}(\mathbf{1}_{NJ} - \mathbf{V})^{'} - (\mathbf{1}_{NJ} - \mathbf{V})\,\mathbf{DV}^{'} + \mathbf{E_K} \tag{2}$$

where $\mathbf{D}$ is a diagonal weight matrix of size J, $\mathbf{1}_{XY}$ generally denotes the matrix of size $(X \times Y)$ of all ones, and the error term $\mathbf{E_K}$ represents the part of $\mathbf{K}$ not accounted for by the model. For identifiability reasons, matrix $\mathbf{VD}$ is constrained to sum to zero: $\mathbf{1}_N^{'}(\mathbf{VD})\,\mathbf{1}_J = 0$.

Differently from Vicari [22, 23], the membership matrix $\mathbf{V}$ here can be possibly incomplete with a number N_0 of zero row profiles because of the objects non-assigned to any group and $\mathbf{K}$ is actually modeled only by a subset of $(N–N_0)$ objects.

Similarly, the symmetric component $\mathbf{S}$ is modeled by defining a clustering structure again as a sum of J terms, depending on the (complete) membership matrix $\mathbf{U}$

$$\mathbf{S} = \mathbf{UC}(\mathbf{1}_{NJ} - \mathbf{U})^{'} + (\mathbf{1}_{NJ} - \mathbf{U})\,\mathbf{CU}^{'} + \mathbf{E_S} \tag{3}$$

where $\mathbf{C}$ is a diagonal weight matrix of size J, and the error term $\mathbf{E_S}$ represents the part of $\mathbf{S}$ not accounted for by the model.

Models (2) and (3) can be combined to specify the model accounting for the asymmetric dissimilarities *between* clusters

$$\mathbf{A} = \mathbf{S} + \mathbf{K} = \left[\mathbf{UC}(\mathbf{1}_{NJ} - \mathbf{U})' + (\mathbf{1}_{NJ} - \mathbf{U})\,\mathbf{CU}'\right] + \left[\mathbf{VD}(\mathbf{1}_{NJ} - \mathbf{V})' - (\mathbf{1}_{NJ} - \mathbf{V})\,\mathbf{DV}'\right] + b\,(\mathbf{1}_{NN} - \mathbf{I}_N) + \mathbf{E} \quad (4)$$

subject to

$$u_{ij} \in \{0, 1\}, (j = 1, \ldots, J); \sum_{j=1}^{J} u_{ij} = 1, \quad (i = 1, \ldots, N) \qquad (4a)$$

$$v_{ij} \in \{0, 1\}, (j = 1, \ldots, J); \sum_{j=1}^{J} v_{ij} \leq 1, \quad (i = 1, \ldots, N) \qquad (4b)$$

$$\mathbf{1}_N'\,(\mathbf{VD})\,\mathbf{1}_J = 0 \qquad (4c)$$

where $\mathbf{I}_N$ denotes the identity matrix of size N, b is the additive constant term and the general error term $\mathbf{E}$ represents the part of $\mathbf{A}$ not accounted for by the model.

The first two sets of constraints (4*a*) and (4*b*) define the complete membership matrix $\mathbf{U}$ and the incomplete membership matrix $\mathbf{V}$, respectively, while constraints (4*c*) assure that the entries of $\mathbf{VD}$ sum to zero.

Model (4) is fitted in the Least Squares sense by minimizing

$$\begin{aligned} F(\mathbf{U}, \mathbf{V}, \mathbf{C}, \mathbf{D}, b) &= \left\| \mathbf{A} - \left[\mathbf{UC}(\mathbf{1}_{NJ} - \mathbf{U})' + (\mathbf{1}_{NJ} - \mathbf{U})\,\mathbf{CU}'\right] \right. \\ &\quad \left. - \left[\mathbf{VD}(\mathbf{1}_{NJ} - \mathbf{V})' - (\mathbf{1}_{NJ} - \mathbf{V})\,\mathbf{DV}'\right] - b\,(\mathbf{1}_{NN} - \mathbf{I}_N) \right\|^2 \\ &= \left\| \mathbf{S} - \left[\mathbf{UC}(\mathbf{1}_{NJ} - \mathbf{U})' + (\mathbf{1}_{NJ} - \mathbf{U})\,\mathbf{CU}'\right] - b\,(\mathbf{1}_{NN} - \mathbf{I}_N) \right\|^2 \\ &\quad + \left\| \mathbf{K} - \left[\mathbf{VD}(\mathbf{1}_{NJ} - \mathbf{V})' - (\mathbf{1}_{NJ} - \mathbf{V})\,\mathbf{DV}'\right] \right\|^2 \end{aligned} \qquad (5)$$

subject to the sets of constraints (4*a*), (4*b*), and (4*c*) and where the last expression is due to the orthogonality of $\mathbf{S}$ and $\mathbf{K}$.

In order to minimize the loss function (5), an Alternating Least Squares (ALS) algorithm is described in Sect. 4.

3.1 A Constrained Model

A parsimonious model may be specified by assuming ($\mathbf{V} \subseteq \mathbf{U}$), i.e., the incomplete partition into J clusters $\{G_1, \ldots, G_j, \cdots, G_J\}$ given by matrix $\mathbf{V}$, is constrained to be included into the complete partition $\{M_1, \ldots, M_j, \ldots, M_J\}$identified by matrix $\mathbf{U}$. This is equivalent to say that the two partitions are linked to each other being $G_j \subseteq M_j$ ($j = 1, \ldots, J$), i.e., any cluster $G_j$of the incomplete partition is formed either by a subset of the corresponding cluster M_j of the complete partition or by M_j itself. Note that objects possibly non-assigned to cluster G_j denote objects with small asymmetries in the data.

In order to fit the parsimonious model, constraints (4b) on the entries of matrix $\mathbf{V}$ need to be modified as follows

$$v_{ij} \in \{0, 1\}, v_{ij} \leq u_{ij} \ (i = 1, \ldots, N; \ j = 1, \ldots, J) \qquad (4b_1)$$

to specify that any object i belonging to cluster M_j of the complete partition can be either belong to cluster G_j (within M_j) of the incomplete partition or remain non-assigned.

4 ALS Algorithm

The constrained problem of minimizing (5) subject to (4a), (4b), and (4c) can be solved by using an Alternating Least Squares (ALS) algorithm, which alternates between two main allocation/regression steps: updating ($\mathbf{U}$, $\mathbf{C}$) and updating ($\mathbf{V}$, $\mathbf{D}$) steps.

Initialization. (*Starting partitions* $\mathbf{U}$ and $\mathbf{V}$)
Starting feasible partitions $\widehat{\mathbf{U}}$ and $\widehat{\mathbf{V}}$ are chosen randomly or in a rational way and a number $N_0 = N/2$ of rows of $\widehat{\mathbf{V}}$ are randomly set to zero. A random starting value $\hat{b}$ for the constant is also chosen.

STEP 1 Updating membership matrix $\mathbf{U}$ and weight matrix $\mathbf{C}$
Let $\widetilde{\mathbf{R}} = \mathbf{A} - \left[\widehat{\mathbf{V}}\widehat{\mathbf{D}}\left(\mathbf{1}_{NJ} - \widehat{\mathbf{V}}\right)' - \left(\mathbf{1}_{NJ} - \widehat{\mathbf{V}}\right)\widehat{\mathbf{D}}\widehat{\mathbf{V}}'\right] - \hat{b}\,(\mathbf{1}_{NN} - \mathbf{I}_N)$ denote the residual of the data matrix $\mathbf{A}$ not depending on $\mathbf{C}$ and $\mathbf{U}$.

Step 1.1 Updating $\mathbf{U}$ (*Allocation substep*)
The membership matrix $\mathbf{U}$ is updated, given the current estimates of $\widehat{\mathbf{V}}$, $\widehat{\mathbf{C}}$, $\widehat{\mathbf{D}}$ and $\hat{b}$ by solving N assignment problems minimizing

$$F'\left(\mathbf{U}; \widetilde{\mathbf{R}}, \widehat{\mathbf{C}}\right) = \left\|\widetilde{\mathbf{R}} - \left[\mathbf{U}\widehat{\mathbf{C}}(\mathbf{1}_{NJ} - \mathbf{U})' + (\mathbf{1}_{NJ} - \mathbf{U})\,\widehat{\mathbf{C}}\mathbf{U}'\right]\right\|^2 + g \qquad (6)$$

over $\mathbf{U}$, subject to constraints (4a) and where g is the part of the loss function not depending on $\mathbf{U}$.

This problem is sequentially solved for the different rows of $\mathbf{U}$ by taking $\hat{u}_{ij} = 1$, if column j attains $F^{'}\left(\left[u_{ij} = 1\right]; \circ\right) = min\left\{F^{'}\left(\left[u_{ip} = 1\right]; \circ\right) : p = 1, \ldots, J\right\}$ and $\hat{u}_{ij} = 0$, otherwise. Given row i, for any possible choice $u_{ip} = 1$ $(p = 1, \ldots, J)$, matrix $\widehat{\mathbf{C}}$ is also updated (see Step 1.2) for computing the loss value (6).

Step 1.2 Updating $\mathbf{C}$ (*Regression substep*)
The substep updating $\mathbf{C}$ is nested into step 1.1, being $\widehat{\mathbf{C}}$ computed for any possible choice of the different rows of $\mathbf{U}$ (see Step 1.1).

The weight matrix $\mathbf{C}$ is updated, given the current $\widehat{\mathbf{U}}$, $\widehat{\mathbf{V}}$, $\widehat{\mathbf{D}}$ and $\hat{b}$ by minimizing

$$F^{''}\left(\mathbf{C}; \widetilde{\mathbf{R}}, \widehat{\mathbf{U}}\right) = \left\| \widetilde{\mathbf{R}} - \left[\widehat{\mathbf{U}}\mathbf{C}\left(\mathbf{1}_{NJ} - \widehat{\mathbf{U}}\right)^{'} + \left(\mathbf{1}_{NJ} - \widehat{\mathbf{U}}\right)\mathbf{C}\widehat{\mathbf{U}}^{'}\right]\right\|^2 + g \tag{7}$$

over $\mathbf{C}$. Actually, by denoting with $\mathbf{c}$, the J-vector of the main diagonal of $\mathbf{C}$, which contains the very unknown weights to be estimated, model (4) can be also rewritten as

$$vec\left(\widetilde{\mathbf{R}}\right) = \left[\widehat{\mathbf{U}} * \left(\mathbf{1}_{NJ} - \widehat{\mathbf{U}}\right) + \left(\mathbf{1}_{NJ} - \widehat{\mathbf{U}}\right) * \widehat{\mathbf{U}}\right]\mathbf{c} + \mathbf{e_c} \tag{8}$$

where $*$ and *vec* denote the Khatri-Rao product and the vec operator, respectively, and $\mathbf{e_c}$ is the vectorized error term. The minimum of (7) is attained for vector $\widehat{\mathbf{c}}$ which solves the equivalent regression problem (8), i.e., by denoting $\mathbf{Q}_{\widehat{\mathbf{U}}} = \left[\widehat{\mathbf{U}} * \left(\mathbf{1}_{NJ} - \widehat{\mathbf{U}}\right) + \left(\mathbf{1}_{NJ} - \widehat{\mathbf{U}}\right) * \widehat{\mathbf{U}}\right]$, the optimal $\widehat{\mathbf{c}} = \left(\mathbf{Q}'_{\widehat{\mathbf{U}}}\mathbf{Q}_{\widehat{\mathbf{U}}}\right)\mathbf{Q}'_{\widehat{\mathbf{U}}} vec\left(\widetilde{\mathbf{R}}\right)$ is obtained. Updating $\widehat{\mathbf{C}}$ follows, straightforwardly by setting $\widehat{\mathbf{C}} = diag(\widehat{\mathbf{c}})$.

STEP 2 Updating membership matrix $\mathbf{V}$ and weight matrix $\mathbf{D}$

Step 2.1 Updating $\mathbf{V}$ (*Allocation step*)
The incomplete membership matrix $\mathbf{V}$ is updated, given the current estimates of $\widehat{\mathbf{U}}$, $\widehat{\mathbf{C}}$, $\widehat{\mathbf{D}}$ and $\hat{b}$ by minimizing

$$F^{'''}\left(\mathbf{V}; \widehat{\mathbf{D}}\right) = \left\| \mathbf{K} - \left[\mathbf{V}\widehat{\mathbf{D}}(\mathbf{1}_{NJ} - \mathbf{V})^{'} - (\mathbf{1}_{NJ} - \mathbf{V})\widehat{\mathbf{D}}\mathbf{V}^{'}\right]\right\|^2 + h \tag{9}$$

over $\mathbf{V}$, subject to constraints (4b) and where h is the part of the loss function not depending on $\mathbf{V}$.

This problem is sequentially solved for the different rows of $\mathbf{V}$ by considering that, given row i, (J+1) possible choices are available: $\hat{v}_{ij}$ can be either 0 or 1 ($j = 1, \ldots, J$), with the constraint that the row sum is not greater than 1, i.e., for row i a zero profile is allowed and object i can be either allocated to only one cluster or remain non-assigned.

Thus, given row i, the updating of v_{ij} is achieved by taking $\hat{v}_{ij} = 1$, if column j attains $F^{'''}\left(\left[v_{ij} = 1\right]; \circ\right) = min\left\{\left(F^{'''}\left(\left[v_{ip} = 1\right]; \circ\right) : p = 1, \ldots, J\right); F^{'''}\left(\left[v_{ij} = 0\right]; \circ\right)\right\}$ and $\hat{v}_{ij} = 0$, otherwise. Given row i, for any possible choice for either $\hat{v}_{ij} = 1$ or $\hat{v}_{ij} = 0$ $(j = 1, \ldots, J)$, matrix $\widehat{\mathbf{D}}$ is also updated (see Step 2.2) and the loss value (9) computed.

The number $\hat{N}_0$ of the non-assigned objects in the current optimal solution follows straightforwardly.

Step 2.2 Updating **D** (*Regression step*)
The weight matrix **D** is updated, given $\widehat{\mathbf{U}}$, $\widehat{\mathbf{V}}$, $\widehat{\mathbf{C}}$ and $\hat{b}$ by minimizing

$$F^{'v}\left(\mathbf{D};\widehat{\mathbf{V}}\right)=\left\|\mathbf{K}-\left[\widehat{\mathbf{V}}\mathbf{D}\left(\mathbf{1}_{NJ}-\widehat{\mathbf{V}}\right)^{'}-\left(\mathbf{1}_{NJ}-\widehat{\mathbf{V}}\right)\mathbf{D}\widehat{\mathbf{V}}^{'}\right]\right\|^{2}+h \tag{10}$$

over **D**, subject to constraints (4*c*). By denoting with **d** the J-vector of the main diagonal of **D** and similarly to Step 1.2, model (4) can be also rewritten as

$$vec\left(\mathbf{K}\right)=\left[\left(\mathbf{1}_{NJ}-\widehat{\mathbf{V}}\right)*\widehat{\mathbf{V}}-\widehat{\mathbf{V}}*\left(\mathbf{1}_{NJ}-\widehat{\mathbf{V}}\right)\right]\mathbf{d}+\mathbf{e_d}=\mathbf{Q}_{\widehat{\mathbf{V}}}\,\mathbf{d}+\mathbf{e_d} \tag{11}$$

where $\mathbf{e_d}$ is the vectorized error term. The Least Squares estimate of **d** is given by $\widehat{\mathbf{d}}=\left(\mathbf{Q}'_{\widehat{\mathbf{V}}}\mathbf{Q}_{\widehat{\mathbf{V}}}\right)\mathbf{Q}'_{\widehat{\mathbf{V}}}vec\left(\mathbf{K}\right)$ and, in order to fulfill constraint (4*c*), the optimal weights in $\widehat{\mathbf{d}}$ are transformed so that the $\hat{N}_0$ entries of vector $\widehat{\mathbf{V}}\widehat{\mathbf{d}}$ sum to zero

$$\widehat{\mathbf{d}}^{*}=\widehat{\mathbf{V}}^{+}\left(\widehat{\mathbf{V}}\widehat{\mathbf{d}}-\frac{\mathbf{1}'_{N}\widehat{\mathbf{V}}\widehat{\mathbf{d}}}{(N-\hat{N}_0)}\widehat{\mathbf{V}}\mathbf{1}_{J}\right)$$

where $\mathbf{1}_N$ denotes the N-vector of ones and $\widehat{\mathbf{V}}^{+}$is the Moore–Penrose inverse of $\widehat{\mathbf{V}}$.

Updating $\widehat{\mathbf{D}}=diag\left(\widehat{\mathbf{d}}^{*}\right)$follows.

STEP 3 Updating constant b
Since the constant term in (4) is added to all off-diagonal terms of the fitted matrix, its estimation actually involves only the symmetric component **S**. Hence, given the current estimates $\widehat{\mathbf{U}}$, $\widehat{\mathbf{V}}$, $\widehat{\mathbf{C}}$ and $\widehat{\mathbf{D}}$, the estimation of the constant b is achieved by successive residualizations and it is given by

$$\hat{b}=\left[\mathbf{S}-\left(\widehat{\mathbf{U}}\widehat{\mathbf{C}}\left(\mathbf{1}_{NJ}-\widehat{\mathbf{U}}\right)^{'}+\left(\mathbf{1}_{NJ}-\widehat{\mathbf{U}}\right)\widehat{\mathbf{C}}\widehat{\mathbf{U}}^{'}\right)\right]/(N(N-1)).$$

Stopping rule
The loss value $F\left(\widehat{\mathbf{U}},\widehat{\mathbf{V}},\widehat{\mathbf{C}},\widehat{\mathbf{D}},\hat{b}\right)$ is computed for the current estimates. When such updated values have decreased considerably (more than an arbitrary small convergence tolerance) the function value, then $\widehat{\mathbf{U}}$, $\widehat{\mathbf{V}}$, $\widehat{\mathbf{C}}$, $\widehat{\mathbf{D}}$, $\hat{b}$ are updated once more according to Steps 1 through 3. Otherwise, the process is considered to have converged.

The algorithm monotonically does not increase the loss function and, since function $F$is bounded from below, it converges to a point which can be expected to be at least a local minimum. To increase the chance of finding the global minimum, the algorithm should be run several times, with different initial estimates of **U** and **V** and retaining the best solution in terms of loss function value.

4.1 Algorithm for the Constrained Model

When the constrained model (Sect. 3.1) is fitted, the two main steps of the algorithm cannot be run sequentially. In fact, because of constraints ($4b_1$) on $\mathbf{V}$, given row i, only two possible choices are available: $\hat{v}_{ij} = 0$ or $\hat{v}_{ij} = \hat{u}_{ij}$ ($j = 1, \ldots, J$), i.e., for row i a zero profile is allowed and object i can be either allocated to the same cluster of $\mathbf{U}$ or remain non-assigned.

Thus, in order to assure the loss function is nondecreasing, matrices $\mathbf{U}$ and $\mathbf{V}$ are jointly updated and Step 2 needs to be nested within Step 1 as described in the following pseudocode.

A. Main loop. For $i = 1, \ldots, N$
  B. For $j = 1, \cdots, J$
    $\boldsymbol{B}_1$) Set $u_{ij} = 1$ (*Step* 1.1)
    $\boldsymbol{B}_2$) Update $\mathbf{C}$ (*Step* 1.2)
    $\boldsymbol{B}_3$) Set $v_{ij} = 1$ or $v_{ij} = 0$ (*Step* 2.1)
    $\boldsymbol{B}_4$) Update $\mathbf{D}$ (*Step* 2.2)
  End B
  C. Update b (*Step* 3)
End *A*

---

5 On the Estimates

5.1 Weight Matrix D

In order to evaluate the meaning of the estimated weights, let us consider the incomplete matrix $\mathbf{V} = \left[\mathbf{v}_1, \ldots, \mathbf{v}_j, \ldots, \mathbf{v}_J\right]$ and the corresponding incomplete partition into J clusters $\left\{G_1, \ldots, G_j, \cdots, G_J\right\}$.

Thus, any entry d_j $(j, \ldots, J)$ of the diagonal weight matrix $\mathbf{D}$ is the weighted average imbalance originating from all objects i in cluster G_j ($i \in G_j$) directed to all objects h in clusters different from G_j ($h \notin G_j$), corrected for the average imbalance directed to cluster G_j.

Moreover, let $\widetilde{\mathbf{d}}$ denote the vector of size $(N - N_0)$ having (non-null) weights corresponding to the $(N - N_0)$ objects assigned to clusters $\left\{G_1, \ldots, G_j, \cdots, G_J\right\}$. Note that objects belonging to the same clusters have the same weights $\tilde{d}_i$ and such weights sum to zero (constraints ($4c$)), which means that the total imbalance between clusters is null on average and a "closed" system of reciprocal exchanges between clusters is defined.

Thus, for any object i belonging to cluster G_j, weight $\tilde{d}_i$ is

$$\tilde{d}_i = \tilde{\mathbf{v}}_j \tilde{\mathbf{K}} \left(1 - \tilde{\mathbf{v}}_j\right) / \left((N - N_0) N_j\right), \text{ if } i \in G_j, (j = 1, \ldots, J)$$

where $\tilde{\mathbf{v}}_j$ and $\tilde{\mathbf{K}}$ denote the subvector of $\mathbf{v}_j$ and the submatrix of $\mathbf{K}$, respectively, corresponding to the N-N_0 objects assigned to the J clusters in $\mathbf{V}$.

Hence, any object i with positive (negative) weight $\tilde{d}_i$ is mainly a "destination" ("origin") of the exchanges and any cluster G_j actually includes objects having on average similar behaviors in terms of exchanges directed toward the other clusters.

Note that the N_0 ($N_0 \leq N$) objects possibly non-assigned to any cluster are actually objects which generate (almost) null imbalances or equivalently their corresponding exchanges in the data matrix $\mathbf{A}$ are (almost) symmetric.

5.2 *Weight Matrix* C and Constant *b*

Following the same lines of Sect. 5.1, let us consider the partition into J clusters $\{M_1, \ldots, M_j, \ldots, M_J\}$ identified by the (complete) membership matrix $\mathbf{U}$. Then, any entry c_j ($j = 1, \ldots, J$) of the diagonal weight matrix $\mathbf{C}$ represents the average amount between clusters M_j and M_h ($h \neq j$), corrected for the mean of the average amounts between all clusters different from M_j.

Thus, large (small) values for c_j denote clusters with large (small) amounts of exchanges on average.

Note that when $J = 2$, the estimation of weights c_j ($j = 1, 2$) actually results to be always the mean of the average amounts between the two clusters and $\hat{c}_1 = \hat{c}_2$ follows.

Moreover, the constant term b represents the *baseline* average amount of the flows regardless of any clustering and, since it is supposed to be added to all exchanges between objects, it affects only the average amounts of the exchanges (the symmetric component $\mathbf{S}$) and not their directions.

6 Application: Language Data

Both clustering model (4) and its parsimonious version (Sect. 3.1) have been applied to the Language Data presented in Sect. 2 by running the algorithm for any choice of the number of clusters from 2 to 5 and by retaining the best partition in 100 runs from different random initial starts. The choice of the number of clusters has been done by analyzing the scree plots of the loss function values as J increases and in both cases, the partitions into three clusters have been chosen.

Since the relative loss values of the two solutions are very close (0.00552 vs. 0.00548, respectively), the constrained model has been preferred to be analyzed in detail as usual in a confirmative perspective.

Table 2 Language data: estimated symmetric and skew-symmetric percentages of non-spoken languages

$\hat{S}_B$	Ital, *Fr*, Port, Finn, Spn	Ger, Eng	Dch, *Swed*, Dan, Nor	$\hat{K}_B$	Ital, Port, Finn, Spn	Ger, Eng	Dch, Dan, Nor
Ital, *Fr*, Port, Finn, Spn	0	95.20	97.82	Ital, Port, Finn, Spn	0	−7.29	3.90
Ger, Eng	95.20	0	82.19	Ger, Eng	7.29	0	11.19
Dch, *Swed*, Dan, Nor	97.82	82.19	0	Dch, Dan, Nor	−3.90	−11.19	0

From the average percentages the following three clusters of languages result (matrix **U**):

Cl_1: (Italian, *French*, Portuguese, Finnish, Spanish)
Cl_2: (German, English)
Cl_3: (Dutch, *Swedish*, Danish, Norwegian)

which coincide with the three clusters from the skew-symmetric component (matrix **V**) up to two languages which remain non-assigned: French and Swedish (in italic).

The *baseline* average percentage of the people nonspeaking foreign languages ($\hat{b} = 94.21$) is quite large and, in order to estimate the symmetric component of the data, it needs to be added to the estimated symmetric dissimilarities computed by using the weights $\widehat{\mathbf{c}} = (8.31; -7.32; -4.70)$. The estimated weights of the imbalances between clusters result $\widehat{\mathbf{d}} = (-0.32; 6.97; -4.22)$, where the positive weight of Cl_2 qualifies English and German as "target" languages, in the sense that many people speak them, but the reverse is less frequent. Conversely, the large negative weight of Cl_3 reveals that Dutch, Danish, and Norwegian are the least spoken languages by the others. Note that the two sets of weights provide a ranking of the clusters from two different perspectives: (a) from $\widehat{\mathbf{c}}$, the ranking of the clusters (Cl_1, Cl_3, Cl_2) in terms of decreasing average % of non-spoken languages, regardless the directions, is derived; (b) from $\widehat{\mathbf{d}}$, the ranking of the clusters (Cl_2, Cl_1, Cl_3) indicates the directions of the spoken language, i.e., Cl_2 is the "target" language cluster.

Table 2 reports both the estimated symmetrized percentages of non-spoken languages between clusters ($\widehat{\mathbf{S}}_B$) from the *complete* partition ($\widehat{\mathbf{U}}$) and the estimated imbalances between clusters ($\widehat{\mathbf{K}}_B$) from the *incomplete* partition ($\widehat{\mathbf{V}}$). Moreover, the same solutions have been graphically displayed in Fig. 3 by representing languages as nodes and the estimated symmetric and skew-symmetric percentages, respectively, as arcs.

By analyzing the percentages in Table 2, it can be observed that the solution actually represents a compromise between what already seen in Figs. 1 and 2:

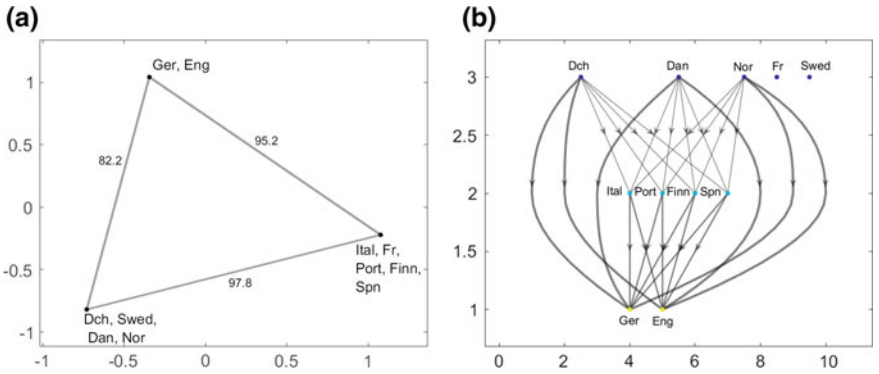

Fig. 3 Language Data: Estimated symmetries (**a**) and skew-symmetries (**b**) between clusters

Cl_1: (Romance + Ural) languages
Cl_2: German languages
Cl_3: Scandinavian languages + Dutch

where the largest average percentage of non-spoken languages (97.82%) is found between Romance and Scandinavian languages. Moreover, the positive imbalance (3.90%) between such two clusters specifies that people in (Italy, France, Portugal, Spain, and Finland) speak neither the Scandinavian languages nor Dutch. Conversely, the lowest average percentage (82.19%) of non-spoken languages results between German and Scandinavian languages with a large positive imbalance (11.19%) in favor of Cl_2: as known, English and German are spoken by almost everyone and, especially, by Scandinavian and Dutch people at a larger extent than Romance language speaking people, but the reverse is much less frequent. This reflects what observed in Fig. 2 where English and German form a group far apart due to few British and Germans speaking other languages.

Interestingly, Fig. 3b visualizes the ranking of the clusters with the "target" languages below and since French and Swedish remain non-assigned to any cluster, they actually do not contribute to estimate the imbalances. In fact, French is generally little spoken and few French speak other languages, while Swedish, which is actually less similar to the other two Scandinavian languages, has an almost symmetrical profile in the original data (with the exception of Swedish speaking German and English).

7 Concluding Remarks

In the view of analyzing asymmetric exchanges, a model for clustering asymmetric dissimilarities between pairs of objects has been proposed. The model relies on the decomposition of the observed asymmetric matrix into symmetric and skew-symmetric components which are modeled to identify clusters of objects which

best account for the between cluster exchanges. Two similar nonhierarchical clustering structures have been presented for jointly fitting the symmetries and skew-symmetries, by assuming that a "complete" partition of the objects (where any object belongs to some cluster) fits the symmetries, while an "incomplete" partition (where only a subset of objects belong to clusters, while the remaining ones may possibly be non-assigned) may fit the skew-symmetries. A parsimonious model has been also proposed where the two clustering structures for the between cluster exchanges depend on the same partition up to a number of possible non-assigned objects.

The model has been formalized in a least squares framework and an efficient ALS algorithm has been provided. By using graphical representations of the results, it is possible to simply visualize how objects interact in terms of exchanges between clusters, because origins and destinations of the exchanges identify objects with similar behaviors in terms of both average amounts and directions of the exchanges.

Further developments may regard, on one hand, different specifications of the clustering structures and, on the other hand, a deeper investigation of the performance of the model in fitting different kinds of data.

References

1. Borg, I., & Groenen, P. (2005). *Modern multidimensional scaling. Theory and applications* (2nd ed.). Berlin: Springer.
2. Bove, G., & Okada, A. (2018). Methods for the analysis of asymmetric pairwise relationships. *Advanced Data Analysis and Classification*, *12*(1), 5–31.
3. Brossier, G. (1982). Classification hiérarchique a partir de matrices carrées non symétriques. *Statistiques et Analyse des Données*, *7*, 22–40.
4. Constantine, A. G., & Gower, J. C. (1978). Graphic representations of asymmetric matrices. *Applied Statistics*, *27*, 297–304.
5. Constantine, A. G., & Gower, J. C. (1982). Models for the analysis of interregional migration. *Environment and Planning A*, *14*, 477–497.
6. Escoufier, Y., & Grorud, A. (1980). Analyse factorielle des matrices carrées non-symetriques. In E. Diday, et al. (Eds.), *Data analysis and informatics* (pp. 263–276). Amsterdam: North Holland.
7. Everitt, B. S., & Rabe-Hesketh, S. (1997). *The analysis of proximity data*. London: Arnold.
8. Gower, J. C. (1977). The analysis of asymmetry and orthogonality. In J. R. Barra, F. Brodeau, G. Romier, & B. Van Cutsem (Eds.), *Recent Developments in Statistics* (pp. 109–123). Amsterdam: North Holland.
9. Hartigan, J. A. (1975). *Clustering algorithms*. New York: Wiley.
10. Hubert, L. (1973). Min and max hierarchical clustering using asymmetric similarity measures. *Psychometrika*, *38*, 63–72.
11. Okada, A. (1990). A generalization of asymmetric multidimensional scaling. In M. Schader & W. Gaul (Eds.), *Knowledge, data and computer-assisted decisions* (pp. 127–138). Berlin: Springer.
12. Okada, A., & Imaizumi, T. (1987). Geometric models for asymmetric similarity data. *Behaviormetrika*, *21*, 81–96.
13. Okada, A., & Imaizumi, T. (2007). Multidimensional scaling of asymmetric proximities with a dominance point. In D. Baier, R. Decker, & H. J. Lenz (Eds.), *Advances in data analysis* (pp. 307–318). Berlin: Springer.

14. Okada, A., & Iwamoto, T. (1996). University enrollment flow among the Japanese prefectures: A comparison before and after the joint first stage achievement test by asymmetric cluster analysis. *Behaviormetrika*, *23*, 169–185.
15. Okada, A., & Yokoyama, S. (2015). Asymmetric CLUster analysis based on SKEW-Symmetry: ACLUSSKEW. In I. Morlini, T. Minerva, & M. Vichi (Eds.), *Advances in statistical models for data analysis* (pp. 191–199). Heidelberg: Springer.
16. Olszewski, D. (2011) Asymmetric k-means algorithm. In: A. Dovnikar, U. Lotric, & B. Ster, (Eds.) *International Conference on Adaptive and Natural Computing Algorithm (ICANNGA 2011) Part II* (Vol. 6594, pp. 1–10). Lecture notes in computer science. Heidelberg: Springer.
17. Olszewski, D. (2012). K-means clustering of asymmetric data. In E. Corchado, et al. (Eds.), *Hybrid artificial intelligent systems 2012, part I* (Vol. 7208, pp. 243–254). Lecture notes in computer science Berlin: Springer.
18. Olszewski, D., & Ster, B. (2014). Asymmetric clustering using the alpha-beta divergence. *Pattern Recognition*, *47*, 2031–2041.
19. Rocci, R., & Bove, G. (2002). Rotation techniques in asymmetric multidimensional scaling. *Journal of Computational and Graphical Statistics*, *11*, 405–419.
20. Saito, T., & Yadohisa, H. (2005). *Data analysis of asymmetric structures*. Advanced approaches in computational statistics. New York: Marcel Dekker.
21. Takeuchi, A., Saito, T., & Yadohisa, H. (2007). Asymmetric agglomerative hierarchical clustering algorithms and their evaluations. *Journal of Classification*, *24*, 123–143.
22. Vicari, D. (2014). Classification of asymmetric proximity data. *Journal of Classification*, *31*(3), 386–420.
23. Vicari, D. (2018). CLUXEXT: CLUstering model for Skew-symmetric data including EXTernal information. *Advanced Data Analysis and Classification*, *12*, 43–64.
24. Zielman, B., & Heiser, W. J. (1996). Models for asymmetric proximities. *British Journal of Mathematical and Statistical Psychology*, *49*, 127–146.

Exploring Hierarchical Concepts: Theoretical and Application Comparisons

Carlo Cavicchia, Maurizio Vichi and Giorgia Zaccaria

Abstract Phenomena are usually multidimensional and their complexity cannot be directly explored via observable variables. For this reason, a hierarchical structure of nested latent concepts representing different levels of abstraction of the phenomenon under study may be considered. In this paper, we provide a comparison between a procedure based on hierarchical clustering methods and a novelty model recently proposed, called Ultrametric Correlation Matrix (UCM) model. The latter aims at reconstructing the data correlation matrix via an ultrametric correlation matrix and supplies a parsimonious representation of multidimensional phenomena through a partition of the observable variables defining a reduced number of latent concepts. Moreover, the UCM model highlights two main features related to concepts: the correlation among concepts and the internal consistency of a concept. The performances of the UCM model and the procedure based on hierarchical clustering methods are illustrated by an application to the Holzinger data set which represents a real demonstration of a hierarchical factorial structure. The evaluation of the different methodological approaches—the UCM model and the procedure based on hierarchical clustering methods—is provided in terms of classification of variables and goodness of fit, other than of their suitability to analyse bottom-up latent structures of variables.

1 Introduction

In many areas of study, the real problems pertain multidimensional and complex phenomena that cannot be directly observed. These phenomena may be hypothesised to have a nested latent structure representing different levels of abstraction, thus forming

C. Cavicchia · M. Vichi (✉) · G. Zaccaria
University of Rome La Sapienza, Piazzale Aldo Moro 5, 00185 Rome, Italy
e-mail: maurizio.vichi@uniroma1.it

C. Cavicchia
e-mail: carlo.cavicchia@uniroma1.it

G. Zaccaria
e-mail: giorgia.zaccaria@uniroma1.it

T. Imaizumi et al. (eds.), *Advanced Studies in Behaviormetrics and Data Science*,
Behaviormetrics: Quantitative Approaches to Human Behavior 5,
https://doi.org/10.1007/978-981-15-2700-5_19

a tree-shape structure which involves "ranked" relationships between concepts and detects the logic hierarchy related to the dimensions of the phenomenon under study. The root of the tree represents the highest level of abstraction, i.e., the multidimensional (general) concept not directly observable, whereas the leaves of the tree define the evidence, i.e., the observable variables. Each node represents a nested cluster of variables defining a hierarchy that generally has a parsimonious form.

The investigation of the relationships between latent concepts defining a multidimensional phenomenon is the aim of the model proposed by Cavicchia, Vichi, and Zaccaria [2], in which the parsimonious hierarchy of nested partitions of the variable space is formally defined through an ultrametric matrix. It is worthy to notice that an ultrametric distance matrix does not correspond to an ultrametric matrix, as stressed in Cavicchia et al. [2], even if there exists a relationship between the two. However, the researchers could think to use a procedure based on a classical hierarchical clustering algorithm, to build the whole hierarchy from J observed variables to the most general latent concept and to cut the tree identifying Q main latent concepts and maintaining the corresponding hierarchy. This sequential strategy does not guarantee an optimal solution since the classification errors made in the first steps can never be corrected. It is worthy to remember that in this case the aim of the analysis is to detect Q reliable latent concepts together with the corresponding hierarchy.

In this paper we compare the above described procedure based on traditional agglomerative clustering methods—in particular, single linkage (Florek, Łukaszewicz, Perkal, Steinhaus, & Zubrzycki [8]), complete linkage (McQuitty [22]), Ward's method (Ward [26]), and average linkage (Sokal & Michener [24])—with the model proposed by Cavicchia et al. [2]. Their application to a benchmark data set made up of groups of variables identifying latent concepts highlights the potential of the latter with respect to the formers. Furthermore, the aforementioned proposal is based upon a parsimonious representation of the relationships among variables, which allows to reduce the time complexity of the bottom-up algorithms and the possibility that misclassifications at the bottom of the hierarchy affect its upper levels.

The paper is organised as follows. In Sect. 2, a brief review of the four aforementioned agglomerative clustering methods is depicted. The new methodology proposed by Cavicchia et al. [2] is illustrated in Sect. 3. Section 4 provides a deep comparison among methods described in the paper herein via a benchmark data set, in order to highlight their advantages and weaknesses in searching for hierarchical relationships among variables—not only with the clustering objective—associated with a latent concept structure. A final discussion completes the paper in Sect. 5.

2 Hierarchical Classification of Variables

Hierarchical classification defines a set of methods that have been proposed to pinpoint hierarchically nested classes of units, even variables,[1] defining a set of partitions

[1] In this paper we use the term *objects* as a synonym of both units and variables.

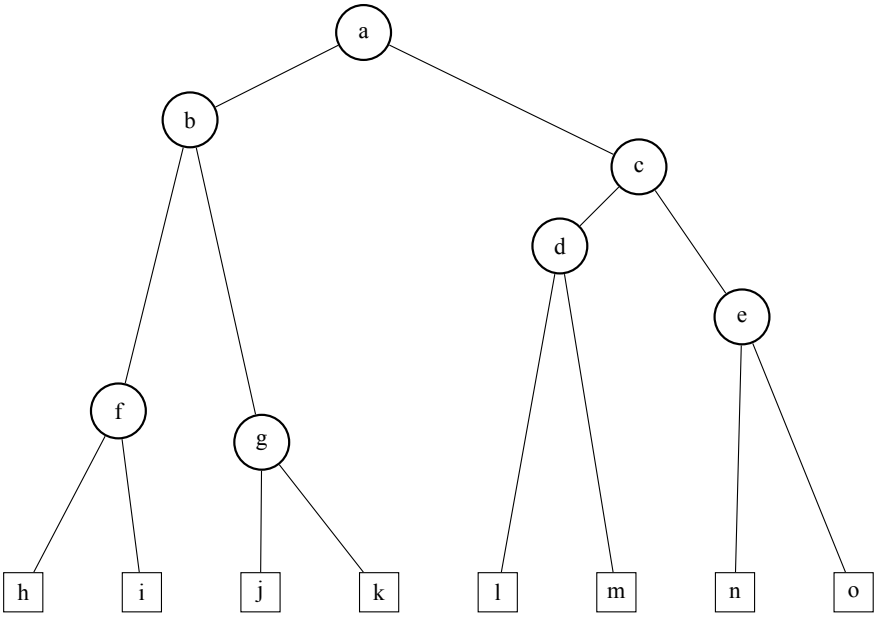

Fig. 1 N-tree representation: root node (a), internal nodes (b, c, d, e, f, g), terminal nodes (h, i, j, k, l, m, n, o)

represented by tree-shape structures. For completeness, we firstly define an *n-tree* (Bobisud & Bobisud [1]; McMorris, Meronk, & Neumann [21]) as follows.

Definition 1 An n-tree on a set of objects $O = \{1, 2, ..., J\}$ is a set T of subsets of O satisfying the following conditions: $O \in T, \emptyset \notin T, \{j\} \in T\ \forall j \in O$ and $A \cap B \in \{\emptyset, A, B\}\ \forall A, B \in T$.

An n-tree is composed of a root node, which represents the whole set of objects, some internal nodes, which define the nested classes of objects, and the terminal nodes (leaves), which are the observable objects, all connected by branches as represented in Fig. 1, with at most n-2 internal nodes corresponding to a binary tree.

A particular n-tree, called *dendrogram*—the main graphical representation used in the paper herein (see Sect. 4)—is defined in Definition 2.

Definition 2 A dendrogram is a valued n-tree where given a mapping b on $\mathbb{R}^+$, any two internal nodes A and B of T, such that $A \cap B \neq \emptyset$, then $b(A) \leq b(B) \Leftrightarrow A \subset B$.

The hierarchical classification methods usually produce a complete dendrogram. Nevertheless, especially for large data sets, a complete hierarchy of nested partitions frequently has low interest and the construction of a *parsimonious* tree, which contains a limited number of internal nodes, is preferred and turns out to be clearer albeit the loss of information related to the dimensionality reduction (Gordon [10]).

The hierarchical clustering algorithms we take into account are the *agglomerative* ones, whose criterion for the construction of the dendrogram starts from J singleton

sets of objects and recursively merges two of them—from the bottom upwards—to obtain the whole hierarchy. All these methods are computed on a distance matrix, as a measure of dissimilarity, and they differ in the way of defining distance between two groups of objects (or between a group of objects and a singleton). It is worthy of remark that the distance matrices have diagonal elements equal to zero, nonnegative off-diagonal elements and they must be symmetric.

For variables, it is often suggested to use the correlation coefficient to quantify the similarity among variables (e.g., Cliff, Haggett, Smallman-Raynor, Stroup, & Williamson [4]; Gordon [10]; Strauss, Bartko, & Carpenter [25]). Therefore, even if the classical hierarchical clustering methods are defined for clustering units, they can be employed for classifying variables. Indeed, it is possible to transform a measure of similarity—the correlation coefficient in this case—into a dissimilarity between objects, as follows

$$d_{jh} = 1 - r_{jh} \quad \rightarrow \quad d_{jh} \in [0, 1] \text{ when } r_{jh} \text{ is assumed to be nonnegative,} \tag{1}$$

where d_{jh} is the distance between the object $\{j\}$ and the object $\{h\}$ of O. Moreover, if a similarity matrix is positive semidefinite—as the correlation matrix is—then the distance matrix defined by

$$d_{jh} = \sqrt{1 - r_{jh}} \tag{2}$$

is Euclidean (Gower [11]).

The four hierarchical clustering methods we consider herein—single linkage, complete linkage, average linkage, Ward's method—can be obtained as special cases of the following equation proposed by Lance and Williams [18, 19], and generalised by Jambu [15],

$$\begin{aligned} d(C_i \cup C_h, C_k) = {} & \alpha_i \, d(C_i, C_k) + \alpha_h \, d(C_h, C_k) + \beta \, d(C_i, C_h) \\ & + \gamma \, |d(C_i, C_k) - d(C_h, C_k)|, \end{aligned} \tag{3}$$

where C_i, C_h, C_k are clusters of objects of O with $1 \leq |C_i| \leq J - 2$, $(\forall C_i \in O)$. The parameters $\alpha_i, \alpha_h, \beta, \gamma$ in Eq. (3) define different clustering techniques, as shown among others in Everitt, Landau, Leese, and Stahl [7] and Lance and Williams [19].

All these methods are agglomerative techniques which do not produce *reversals* in the dendrogram representation, i.e., the following conditions for Lance and William's Eq. (3) hold:

$$\begin{aligned} & \gamma \geq -\min\{\alpha_i, \alpha_h\} \\ & \alpha_i + \alpha_h \geq 0 \\ & \alpha_i + \alpha_h + \beta \geq 1. \end{aligned}$$

Moreover, these methods—as the Definition 2 in turn—satisfy a fundamental condition: the ultrametric property (e.g., Hartigan [12]). This property may be expressed

in two different ways, with respect to distances and to the components of a dendrogram, respectively as follows:

$$d(C_i, C_h) \leq \max\{d(C_i, C_k), d(C_h, C_k)\} \quad C_i, C_h, C_k \in O \tag{4}$$

$$b(A, B) \leq \max\{b(A, C), b(B, C)\} \quad A, B, C \in T. \tag{5}$$

Starting from a distance matrix, the hierarchical clustering algorithms produce a complete dendrogram. In this framework, the optimal number of clusters is chosen by cutting the n-tree at a specific level. For a deeper review of the hierarchical classification algorithms see Gordon [9].

The procedure based on the above-described hierarchical clustering algorithms for the classification of variables works as follows:

Step 1 (*Transformation of correlations into distances*) Given a data correlation matrix $\mathbf{R}$, the corresponding distance matrix is obtained by applying Eq. (1) with respect to the elements of $\mathbf{R}$.

Step 2 (*Hierarchical clustering algorithm*) According to Eq. (3), a hierarchical clustering algorithm is chosen and computed on the distance matrix defined in Step 1. A complete dendrogram and the corresponding estimated ultrametric distance matrix are obtained.

Step 3 (*Parsimonious hierarchy*) To define a parsimonious hierarchy in Q groups of variables—for a given Q—the dendrogram obtained in Step 2 is cut at the Qth level, i.e., pinpointing Q groups of variables which may correspond to Q latent concepts. The bottom-up aggregations from the aforementioned level upwards identify the parsimonious hierarchy.

Step 4 (*Model fit*) To evaluate the solution obtained in Step 3, the estimated ultrametric distance matrix has to be transformed into the ultrametric correlation matrix through the inverse relationship to that of Eq. (1). The least squares difference between the data correlation matrix $\mathbf{R}$ and the estimated—according the hierarchical clustering method chosen in Step 2—correlation matrix is computed with respect to the total correlation of the data.

3 The Ultrametric Correlation Model

Considering a *nonnegative* correlation matrix $\mathbf{R}$ of order J, the Ultrametric Correlation Matrix (UCM) model proposed by Cavicchia et al. [2] is defined by the following equation

$$\mathbf{R} = \mathbf{R_u} + \mathbf{E}, \tag{6}$$

where $\mathbf{R_u}$ is the $(J \times J)$ matrix representing the hierarchical structure of the latent concepts and $\mathbf{E}$ is the $(J \times J)$ random error matrix, i.e., the residual matrix. The

authors have put a non-negativity assumption on $\mathbf{R}$ and, consequently, on $\mathbf{R_u}$ to avoid a compensatory effect into the hierarchy. Nevertheless, in the paper herein this assumption allows to compare the hierarchical clustering methods recalled in Sect. 2 with the model (6), since both distances and correlations turn out to be nonnegative. Moreover, they belong to the interval [0, 1] according to Eq. (1).

$\mathbf{R_u}$ is an ultrametric correlation matrix, where the ultrametric property of the matrix (Dellacherie, Martinez, & San Martin [6, pp. 58–59]) formalises the mathematical counterpart of the latent concepts hierarchy. It is formally specified as follows:

$$\mathbf{R_u} = \mathbf{V}(\mathbf{R_B} - \mathbf{I_Q})\mathbf{V}' + \mathbf{V}\mathbf{R_W}\mathbf{V}' - diag\big(dg(\mathbf{V}\mathbf{R_W}\mathbf{V}')\big) + \mathbf{I_J}, \tag{7}$$

subject to constraints

$$\mathbf{V} = [v_{jq} \in \{0, 1\} : j = 1, ..., J, q = 1, ..., Q]; \tag{8}$$

$$\mathbf{V1_Q} = \mathbf{1_J} \quad \text{i.e.,} \quad \sum_{q=1}^{Q} v_{jq} = 1 \quad j = 1, ..., J; \tag{9}$$

$$\mathbf{R_B} \text{ is an ultrametric correlation matrix (Definition 2 in [2]);} \tag{10}$$

$$\min\{_W r_{qq} : q = 1, ..., Q\} \geq \max\{_B r_{qh} : q, h = 1, ..., Q, h \neq q\}. \tag{11}$$

In Eq. (7), $\mathbf{V}$ is the $(J \times Q)$ membership matrix, which defines a partition of the variable space thanks to constraint (9), i.e., it identifies $Q < J$ nonoverlapping groups of variables $(C_1, ..., C_Q)$; $\mathbf{R_B}$ is the $(Q \times Q)$ between-concept correlation matrix, whose elements $_B r_{qh}$ $(q, h = 1, ..., Q, h \neq q)$ denote the correlation between two latent concepts, each one associated with a group of variables (C_q and C_h) and $\mathbf{R_W}$ is the $(Q \times Q)$ diagonal within-concept consistency matrix, whose elements on the main diagonal, i.e., $_W r_{qq}$ $(q = 1, ..., Q)$, represent the consistency within each group of variables and the off-diagonal elements are equal to zero. The two latter matrices $\mathbf{R_B}$ and $\mathbf{R_W}$ embody two different features related to the variable groups: the correlation between concepts and the internal consistency of a concept, respectively (Cavicchia, Vichi & Zaccaria [3]).

The model (6) is estimated by Cavicchia et al. [2] in a least-squares framework, minimising the squared norm of the difference between the data correlation matrix $\mathbf{R}$ and the reconstructed ultrametric correlation matrix $\mathbf{R_u}$.

In the next section, a comparison between the models described herein is carried out by stressing the strong potential of the Cavicchia et al. [2] proposal in investigating the hierarchical relationships between latent concepts, whenever they exist and even if not known a priori, with respect to the traditional agglomerative clustering algorithms.

4 A Comparison Between the Ultrametric Correlation Model and the Agglomerative Clustering Algorithms

The Holzinger data set[2] (Holzinger & Swineford [13]) is a benchmark example very useful to inspect the hierarchical factorial structure of a multidimensional phenomenon—represented in this case by the general ability of an individual—composed of different latent dimensions (concepts). It is defined as a (14×14) correlation matrix ($J = 14$), with $Q = 4$ latent concepts (*Spatial*, *Mental Speed*, *Motor Speed* and *Verbal*) corresponding to the abilities tested for 355 individuals and described in Table 1. The optimal number of latent concepts may be assessed by means of the classical criteria to choose the number of factors or principal components (e.g., Kaiser's method [16]).

It is worthy to highlight that we aim at defining reliable concepts and, in addition, at identifying the hierarchical structure over these concepts which pinpoints the hierarchical relationships between them. To achieve this goal we assess the potential of the model described in Sect. 3 with respect to the traditional clustering methods cited in Sect. 2, when there exists a particular hierarchical latent structure underlying the data.

Firstly, we compute the UCM model to the Holzinger correlation matrix to obtain the parsimonious bottom-up structure of the four latent concepts. It is worthy to notice that to apply the model (6) the non-negativity condition on the correlation matrix must hold. The original one has three negative correlation coefficients close to zero which turn out to be statistically nonsignificant (Holzinger & Swineford [13]), as the other values in the Holzinger correlation matrix whose magnitude is lower than 0.1; thus, we can set these three negative values to zero. The resulting nonnegative correlation matrix shown in Fig. 2 points out the existence of the four theoretical groups—corresponding to the latent concepts of the *Spatial*, *Mental Speed*, *Motor Speed* and *Verbal* ability—3 out of 4 internally highly correlated, whereas the variables representing the *Motor Speed* ability have lower correlations within the group. As a result, this weak relationship between the objects in C_3^{th} could entail their misclassification, as we will see thereafter.

Unlike the traditional hierarchical clustering algorithms which produce complete dendrograms, i.e., they define a complete hierarchy over the J variables, the UCM model starts from the classification of variables in $Q < J$ groups before searching for their optimal bottom-up aggregations. As shown in Table 2 and Fig. 3, all the abilities are well-classified except for the variable T36a which is assigned to C_2^{UCM} rather than to C_3^{UCM}. Indeed, it can be noticed that this variable has a low correlation with those in C_3^{th} and a higher correlation with the others (see Fig. 2).

The estimates of the between-concept correlation matrix and the within-concept consistency matrix of Eq. (7) are the following:

[2] It is available on `psych` package in R.

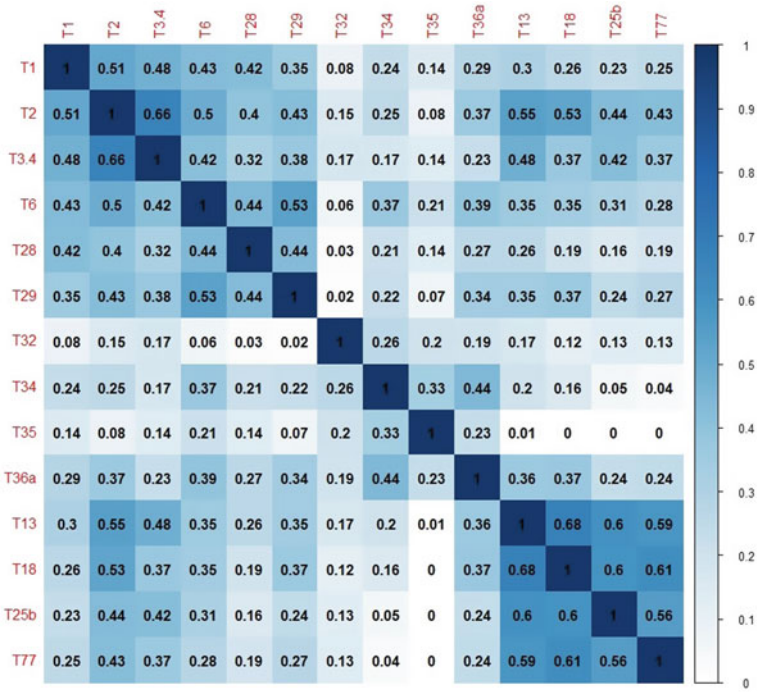

Fig. 2 Heatmap of the Holzinger (14×14) correlation matrix of ability tests

Table 1 Holzinger data set: variables and latent dimensions (ability) description

C_q^{th}	Latent concept (ability)	Variables
C_1^{th}	Spatial tests	T1, T2, T3.4
C_2^{th}	Mental speed tests	T6, T28, T29
C_3^{th}	Motor speed tests	T32, T34, T35, T36a
C_4^{th}	Verbal tests	T13, T18, T25b, T77

$$\mathbf{R_B} = \begin{bmatrix} 1 & 0.330 & 0.144 & 0.386 \\ 0.330 & 1 & 0.144 & 0.330 \\ 0.144 & 0.144 & 1 & 0.144 \\ 0.386 & 0.330 & 0.144 & 1 \end{bmatrix} \quad \mathbf{R_W} = \begin{bmatrix} 0.551 & 0 & 0 & 0 \\ 0 & 0.402 & 0 & 0 \\ 0 & 0 & 0.386 & 0 \\ 0 & 0 & 0 & 0.606 \end{bmatrix}.$$

It has to be highlighted that the UCM algorithm involves an UPGMA step to obtain an ultrametric matrix $\mathbf{R_B}$, using the inverse relationship to that between distances

Table 2 Variable groups of the UCM model with $Q = 4$

C_q^{UCM}	Variables
C_1^{UCM}	T1, T2, T3.4
C_2^{UCM}	T6, T28, T29, T36a
C_3^{UCM}	T32, T34, T35
C_4^{UCM}	T13, T18, T25b, T77

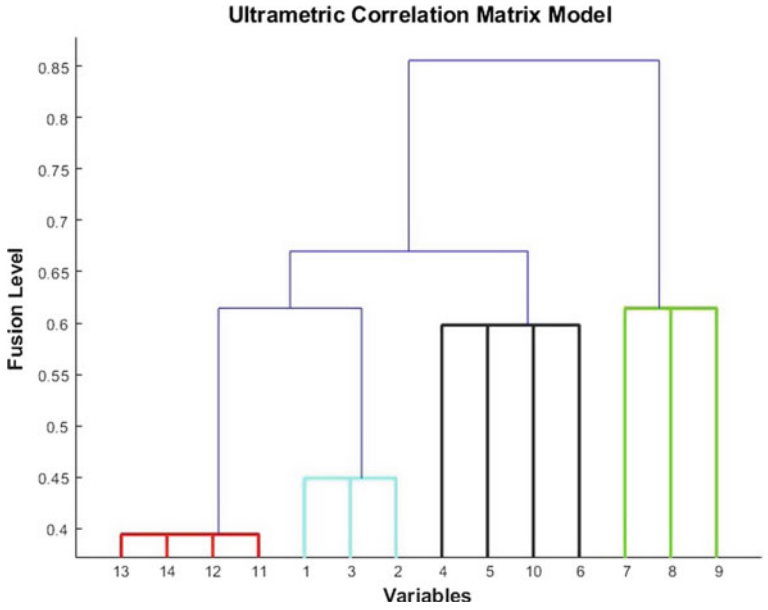

Fig. 3 Dendrogram of the ultrametric distance matrix obtained by computing the Ultrametric Correlation Matrix model on the Holzinger (14×14) correlation matrix of ability tests and applying Eq. (1) on the result

and correlations in Eq. (1). Since the data correlation coefficients are nonnegative by hypothesis, all the distances belong to the interval [0, 1] and vice versa.

Looking at Fig. 3, the hierarchy of the four latent concepts is built by merging the *Spatial* and *Verbal* abilities first, then the latter with the *Mental* ability; all of these are engendered by the brain. The last aggregation lumps together the broad group of C_1^{UCM}, C_2^{UCM}, C_4^{UCM} and C_3^{UCM}, whose corresponding latent concept is related to the movement ability. It is worthy of remark that Holzinger and Swineford data set has been analysed by many authors; in particular, Loehlin and Beaujean [20, pp. 235-239] have conducted a higher-order exploratory analysis (Schmid & Leiman [23]) on their correlation matrix pinpointing a strong correlation between the *Spatial* and

Table 3 Variable clusters at $Q = 4$ level of the clustering methods hierarchy

C_q^m	Single link and average link	Complete link and Ward's method
C_1^m	T1, T2, T3.4, T6, T28, T29, T13, T18, T25b, T77	T1, T2, T3.4, T6, T28, T29
C_2^m	T34, T36a	T32
C_3^m	T32	T13, T18, T25b, T77
C_4^m	T35	T34, T35, T36a

Verbal tests—corresponding to the first aggregation w.r.t. the UCM model—and a low correlation between the *Motor speed*—which partially overlaps the *Mental speed* ability - and the other abilities. The latter bears the UCM model out, since the C_3^{UCM} is lumped together with the other groups in the last aggregation as an additional ability.

To make a comparison between the hierarchical classification methods, we apply the Single, Complete, Average Linkage, and Ward's Method to the distance matrix obtained by transforming the Holzinger correlation matrix by means of Eq. (1) and complying the procedure described in Sect. 2. The results are shown in Fig. 4, where the groups corresponding to the 4th level of the hierarchy ($Q = 4$) are coloured. It is worthy to remark that to identify the aforementioned level of the hierarchy, and the corresponding partition of variables, a complete dendrogram must be computed. Indeed, the hierarchical clustering algorithms taken into account in the paper herein do not allow to choose the optimal number of clusters a priori, as the UCM model does. The four groups, i.e., the 4th level of the hierarchy from the top downwards, of each hierarchical clustering method are illustrated in Table 3. The different composition of these groups with respect to the theoretical and the UCM ones immediately stands out. In fact, even if on one hand the variable T36a is always merged with the other variables in C_3^{th}—conversely to the UCM model—on the other hand C_1^{th} and C_2^{th} are never pinpointed separately at the 4th hierarchical level. The aforementioned difference between those methods and the model illustrated in Sect. 3 affects also the Adjusted Rand Index (ARI, Hubert & Arabie [14]), which compares the estimated partitions of the 14 variables in 4 groups for each algorithm with the theoretical one. Looking at Table 4, it can be noticed that the highest ARI is achieved by the UCM model, since its partition in four groups of variables is the most similar (equal except for T36a) to the one hypothesised by Holzinger and Swineford. Moreover, an additional examination of the Cronbach's α (Cronbach [5]) has been carried out, revealing the existence of a general latent factor associated with all the variables; thus, the Cronbach's αs are suitable for both the procedure based on the hierarchical clustering methods and the UCM model.

The parsimony of the model (6) allows both to compute a dimensionality reduction of the problem under study, loosing as less information as possible, and to obtain the most similar partition of the variables to the theoretical one. This highlights the potential of the UCM model with respect to the traditional ones, which "suffer from

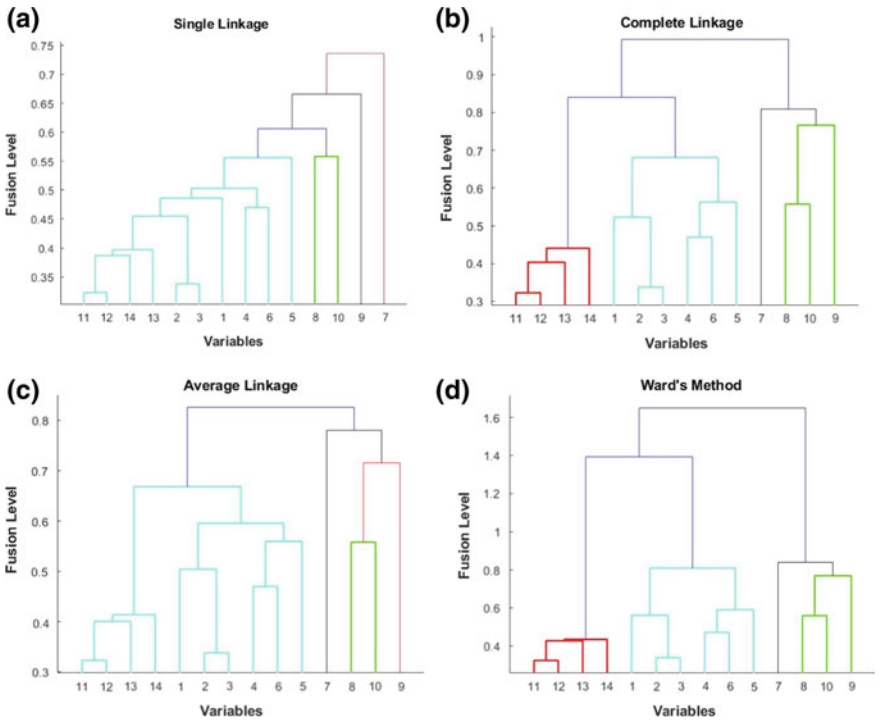

Fig. 4 Dedrogram of **a** Single Linkage, **b** Complete Linkage, **c** Average Linkage, **d** Ward's Method on the distance matrix obtained by transforming the Holzinger (14×14) correlation matrix of ability tests according to Eq. (1)

Table 4 Adjusted Rand Index between the theoretical membership matrix defined in Holzinger and Swineford [13] and the membership matrices referred to the traditional hierarchical clustering methods at level $Q = 4$ and the Ultrametric Correlation Matrix model; fit of each methods/model taken into account

Method/Model	ARI	Fit
UCM model	**0.7922**	**0.0437**
Single link	0.1703	0.1440
Complete link	0.6308	0.1536
Average link	0.1703	0.0449
Ward's method	0.6308	0.1354

the defect that they can never repair what was done in the previous steps" (Kaufman & Rousseeuw [17]).

To have a deeper comparison between the hierarchical clustering methods and the UCM model, we compute their fit by taking into account the least-squares difference between the data correlation matrix and the estimated ones that we want to minimise.

The results are shown in Table 4. The fit of the UCM model turns out to be the best with respect to the other methods. Indeed, only the Average Linkage has a similar fit, whereas the Single, Complete Linkage, and Ward's method have a three times higher fit.

The results shown in this section illustrate the difference between the procedure based on the traditional classification methods (see Sect. 2) and the Ultrametric Correlaton Matrix model described in Sect. 3. Starting from J manifest variables and building a complete hierarchy over them turns out to be not sufficient, as shown in this section, when there exists a hierarchical latent structure in the data. Furthermore, if the number of the original variables is too large a dimensionality reduction of the problem, means a parsimonious representation, is needed. From a theoretical point of view, the UCM model provides a parsimonious representation of the relationships among variables, starting from Q groups each one associated with (forming) a latent concept. It is worthy to highlight once again that the hierarchical clustering methods are not able to repair the errors done in the initial levels of the complete hierarchy, whenever they occur. Conversely, thanks to its features, the model (6) does not suffer from the errors underneath the Qth level of the hierarchy, given that the Q variable groups are directly pinpointed in a dimensionality reduction approach without going through binary aggregations of variables from J to Q. Moreover, since the UCM model works on a correlation matrix, the latent concepts of a phenomenon might also be quantified.

5 Conclusions

In this paper, a comparison between a procedure based on the well-known hierarchical clustering methods and the novelty model proposed by Cavicchia et al. [2] is provided. The latter allows to pinpoint a parsimonious representation of multidimensional phenomena through the partition of the observable variables into a reduced number of concepts—each one associated with a latent dimension—and to study the relationships among the latent concepts which belong to a broader general concept. The difference between the procedure based on traditional clustering algorithms and the methodology illustrated in Sect. 3 is appreciated thanks to their application to a benchmark data set, which represents a real hierarchical factorial structure.

As well as the construction of a hierarchy of latent concepts, the UCM model illustrated herein entails a dimensionality reduction of the problem under study, starting from a parsimonious representation of variables in groups. The number of groups is chosen a priori by means of the traditional criteria for selecting the optimal number of factors/components, instead of cutting the n-tree as usually done for the hierarchical clustering methods. Differently from those aforementioned algorithms, the model described in Sect. 3 does not suffer from the errors that could turn up in the lower levels of the dendrogram, since it starts from a parsimonious partition in $Q < J$ variable groups.

References

1. Bobisud, H. M., & Bobisud, L. E. (1972). A metric for classifications. *Taxon*, *21*(5/6), 607–613.
2. Cavicchia, C., Vichi, M., & Zaccaria, G. (2019). The ultrametric correlation matrix for modelling hierarchical latent concepts. Submitted.
3. Cavicchia, C., Vichi, M., & Zaccaria, G. (2019). Dimensionality reduction via hierarchical factorial structure. In G. C. Porzio, F. Greselin, & S. Balzano (Eds.), *CLADAG 2019, 11–13 September 2019, Cassino: Book of Short Papers* (pp. 116–119), Cassino: Centro Editoriale di Ateneo Università di Cassino e del Lazio Meridionale. Retrieved from http://cea.unicas.it/e_book/Porzio.pdf.
4. Cliff, A. D., Haggett, P., Smallman-Raynor, M. R., Stroup, D. F., & Williamson, G. D. (1995). The application of multidimensional scaling methods to epidemiological data. *Statistical Methods in Medical Research*, *4*(2), 102–123.
5. Cronbach, L. J. (1951). Coefficient alpha and the internal structure of tests. *Psychometrika*, *16*(3), 297–334.
6. Dellacherie, C., Martinez, S., & San Martin, J. (2014). *Inverse M-matrix and ultrametric matrices*. Lecture Notes in Mathematics. Springer International Publishing.
7. Everitt, B. S., Landau, S., Leese, M., & Stahl, D. (2011). *Cluster analysis* (5th ed.). Wiley Series in Probability and Statistics.
8. Florek, K., Łukaszewicz, J., Perkal, J., Steinhaus, H., & Zubrzycki, S. (1951). Sur la liaison et la division des points d'un ensemble fini. In *Colloquium Mathematicum* (Vol. 2, No. 3/4, pp. 282–285).
9. Gordon, A. D. (1987). A review of hierarchical classification. *Journal of the Royal Statistical Society: Series A-G*, *150*(2), 119–137.
10. Gordon, A. D. (1999). *Classification* (2nd ed.). Monographs on statistics & applied probability. Chapman & Hall/CRC.
11. Gower, J. C. (1966). Some distance properties of latent root and vector methods used in multivariate analysis. *Biometrika*, *53*(3/4), 325–338.
12. Hartigan, J. A. (1967). Representation of similarity matrices by trees. *Journal of the American Statistical Association*, *62*(320), 1140–1158.
13. Holzinger, K. J., & Swineford, F. (1937). The bi-factor method. *Psychometrika*, *2*(1), 41–54.
14. Hubert, L., & Arabie, P. (1985). Comparing partitions. *Journal of Classification*, *2*(1), 193–218.
15. Jambu, M. (1978). *Classification authomatique pour l'analyse des donnés, tome 1*. Paris: Dunod.
16. Kaiser, H. F. (1960). The application of electronic computers to factor analysis. *Educational and Psychological Measurement*, *20*(1), 141–151.
17. Kaufman, L., & Rousseeuw, P. J. (1990). *Finding groups in data. An introduction to cluster analysis*. New York: Wiley.
18. Lance, G. N., & Williams, W. T. (1966). A generalized sorting strategy for computer classifications. *Nature*, *212*, 218.
19. Lance, G. N., & Williams, W. T. (1967). A general theory of classificatory sorting strategy I. Hierarchical systems. *The Computer Journal*, *9*(4), 373–380.
20. Loehlin, J. C., & Beaujean, A. A. (2017). *Latent variable models: an introduction to factor, path, and structural equation analysis* (5th ed.). New York: Routledge.
21. McMorris, F. R., Meronk, D. B., & Neumann, D. A. (1983). A view of some consensus methods for tree. In J. Felsenstein (Ed.), *Numerical taxonomy* (pp. 122–126). Berlin: Springer.
22. McQuitty, L. L. (1960). Hierarchical linkage analysis for the isolation of types. *Educational and Psychological Measurement*, *20*(1), 55–67.
23. Schmid, J., & Leiman, J. (1957). The development of hierarchical factor solutions. *Psychometrika*, 22(1), 53–61.
24. Sokal, R. R., & Michener, C. D. (1958). A statistical method for evaluating systematic relationships. *University of Kansas Science Bulletin*, *38*, 1409–1438.

25. Strauss, J. S., Bartko, J. J., & Carpenter, W. T. (1973). The use of clustering techniques for the classification of psychiatric patients. *The British Journal of Psychiatry*, *122*(570), 531–540.
26. Ward, J. H. (1963). Hierarchical grouping to optimize and objective function. *Journal of the American Statistical Association*, *58*(301), 236–244.

Improving Algorithm for Overlapping Cluster Analysis

Satoru Yokoyama

Abstract Several overlapping cluster analysis models have been suggested, and various kinds of data have been analyzed by these models. ADCLUS suggested by Shepard and Arabie [9] can be adapted to one-mode two-way proximity data. INDCLUS (Carroll and Arabie [4]) is for two-mode three-way data, and GENNCLUS (DeSarbo [6]) is the generalized model for two-way data. In addition, Yokoyama et al. [10] suggested a model for one-mode three-way similarities. The algorithm of these models is based on MAPCLUS (Arabie and Carroll [1]) , which is the most general algorithm for overlapping cluster analysis. This algorithm consists of an alternating least squares approach and a combinatorial optimization procedure. Therefore, it takes a long time to obtain the result and it is likely to obtain local results when data consisting of a large number of objects are analyzed. In the present paper, the author tries to improve the algorithm in several ways.

1 Introduction

From the late 1970s, several overlapping cluster analysis models have been suggested by researchers. Shepard and Arabie [9] introduced a model for one-mode two-way similarity data; this model is called the ADditive CLUStering (ADCLUS) model. INdividual Differences CLUStering (INDCLUS, Carroll and Arabie [4]) applies to two-mode three-way similarities. In addition, Yokoyama, Nakayama, and Okada [10] suggested a model for one-mode three-way similarities. These models are based on Arabie and Carroll [1] algorithm. Arabie and Carroll [1] suggested an alternative algorithm for fitting the ADCLUS model called MAthematical Programming CLUStering (MAPCLUS). Furthermore, DeSarbo [6] suggested an algorithm called GENNCLUS, which extended it for rectangular data.

However, in these algorithms, when the number of subjects increases, the result tends to be local solutions or an increase in the computation time. The problem is

S. Yokoyama (✉)
Department of Marketing, School of Business, Aoyama Gakuin University,Tokyo, Japan
e-mail: yokoyama@busi.aoyama.ac.jp

T. Imaizumi et al. (eds.), *Advanced Studies in Behaviormetrics and Data Science*,
Behaviormetrics: Quantitative Approaches to Human Behavior 5,
https://doi.org/10.1007/978-981-15-2700-5_20

expressed as "NP-hard" or "complex" in various papers. Several algorithms have been suggested, such as SINDCLUS (Chaturvedi & Carroll [5]), SYMPRES (Kiers [8]), and France, Chen, and Deng [7], but it seems that each algorithm has the same problem.

In the present study, the author tries to improve the algorithm to improve the stability of results and reduce computation time.

First, the computation time and the result of VAF (variance accounted for) are compared between data with a small number of objects and data with a large number. In particular, the author examines the difference in computation time and VAF depending on whether the alternating least squares (ALS) approach or the combinatorial optimization procedure is done. Furthermore, the results vary depending on the initial clusters. The author examines the change in results when the method of generating initial clusters is changed.

2 Overlapping Cluster Analysis

2.1 ADCLUS Model

Shepard and Arabie [9] introduced overlapping cluster analysis model for one-mode two-way data. This model represents similarities as the sum of discrete overlapping properties. It represents the similarity, s_{ij} ($i, j = 1, \ldots, n$, where n is the number of objects) as

$$s_{ij} \cong \sum_{r=1}^{R} w_r p_{ir} p_{jr} + c \tag{1}$$

where $w_r (r = 1, \ldots, R)$ is the nonnegative weight (assumed to be nonnegative) of the rth cluster, the p_{ir} is binary; if the object $i\Gamma (i = 1, \ldots, n)$ belongs to cluster r is 1, otherwise it is 0. The c is the additive constant, it can be represented as the weight of the $(R + 1)$-th cluster, so that Eq. (1) can be rewritten as

$$s_{ij} \cong \sum_{r=1}^{R+1} w_r p_{ir} p_{jr}. \tag{2}$$

2.2 MAPCLUS Algorithm

The MAPCLUS algorithm uses a gradient approach to minimizing a loss function to maximize the variance accounted for (VAF), and a combinatorial optimization procedure. Equation (3) is the loss function which was shown in Arabie and Carroll

[1, p. 214] and Arabie, Carroll, DeSarbo, and Wind [2, pp. 313–314]. This loss function is the weighted sum of two terms: one is a normalized measure of the sum of the squared errors and the other consists of a penalty function in the form of a polynomial over all pairwise products $p_{ir}p_{jr}$ toward 0 or 1.

$$L_k(\alpha_k, \beta_k, \Delta, \boldsymbol{P}) = \alpha_k \frac{a_k}{d_k} + \beta_k \frac{u_k}{v_k} \tag{3}$$

here

$$a_k = \sum_{i<j}^{n} \sum^{n-1} (\delta_{ij}^{(k)} - w_k p_{ik} p_{jk})^2,$$

$$d_k = 4 \sum_{i<j}^{n} \sum^{n-1} \delta_{ij}^{(k)2} / M,$$

$$u_k = \frac{1}{2} \sum_{i}^{n} \sum_{j}^{n} [(p_{ik} p_{jk} - 1) p_{ik} p_{jk}]^2,$$

$$v_k = \sum_{i<j}^{n} \sum^{n-1} (p_{ik} p_{jk} - T_k)^2,$$

$$\delta_{ij}^{(k)} = s_{ij} - \sum_{i \neq k} w_r p_{ir} p_{jr},$$

$$T_k = \frac{1}{M} \sum_{i<j}^{n} \sum^{n-1} p_{ik} p_{jk},$$

$$M = \frac{n(n-1)}{2},$$

$$\alpha_k + \beta_k = 1.$$

The p_{ir} and weight w_r are computed in two steps. First, given the first subset $p_{i1} = [p_{11}, \ldots, p_{n1}]$, p_{i1} are iteratively improved, and w_1 estimate to use linear regression. Then the values of second cluster (p_{i2} and w_2) are calculated using an alternating least squares (ALS) approach, and so on. These procedures (main loop) are repeated while gradually decreasing the value of the loss function. When no further improvement in VAF is forthcoming or the predetermined number of iterations is reached, while p_{ir} are made binary, the p_{ir} and weight w_r are computed as ALS approach (polish loop).

Then, the combinatorial optimization step begins when the improvement in VAF becomes negligible. The combinatorial optimization consists of doubleton and singleton strategies. These strategies repeat the round robin loop until there are no further improvement in VAF. After that, the p_{ir} and w_r are determined to be the final solution.

3 Improvement of Algorithm

As an improvement of the algorithm, the number of iterations of the ALS approach and the combinatorial optimization procedure is examined in this section.

In general, when the number of objects increases, the estimation of the clusters and weights by the ALS approach tends toward solutions, and combinatorial optimization takes a long time. Here, a dataset with a relatively small amount of data and slightly larger dataset is used, The author verified how the results and computation times change by changing the number of iterations of the ALS approach and the combinatorial optimization. The relatively small dataset is POS data, which is used in Yokoyama et al. [10]. This data is simultaneous purchase data for categories of liquor at convenience stores. The slightly larger dataset is the survey data, which is the purchasing experience of 64 types of foods in a certain period, where a purchase experience is defined as a simultaneous purchase.

In the present paper, the following five patterns of algorithms were used:

(A) use ALS approach (maximum number of iterations of the main loop is 1, of the polish loop is 5), use combinatorial optimization,
(B) use ALS approach (maximum number of iterations of the main loop is 1, of the polish loop is 5), use combinatorial optimization,
(C) use ALS approach (maximum number of iterations of the main loop is 10, of the polish loop is 10), no combinatorial optimization,
(D) use ALS approach (maximum number of iterations of the main loop is 10, of the polish loop is 10), no combinatorial optimization,
(E) combinatorial optimization only.

The number of clusters varied from 7 to 3, and the initial clusters were changed 100 times at random in each analysis.

For the analysis, a program written in C was used on a computer running Windows 7 with an Intel Core i7-4790 3.60 GHz CPU and 32 GB of memory.

The results are shown in Tables 1, 2, and 3. Table 1 shows the maximum VAF for each number of clusters. Table 2 shows the ratio of acceptable results, which means 90% of the maximum VAF for each cluster. Table 3 shows the index of the average computation time for each analysis when pattern A is 100%.

For the POS data, the maximum VAF was almost the same for each cluster with all five methods, but the acceptable VAF ratio was low for methods (C), (D), and (E), which all used either the ALS approach or combinatorial optimization, but not both. The computation times of these three methods are short. On the other hand, for the survey data, the maximum VAF was almost the same in the three methods (A), (B), and (E), which all used combinatorial optimization. However, that of methods (C) and (D) were smaller than the others; the acceptable VAF ratios of these two methods were close to zero. We conclude that combinatorial optimization is necessary in the analysis. In addition, the acceptable VAF ratio for method (E) was low, ALS approach is also necessary. Methods (C) and (D) showed a tendency for the computation times to increase compared to method (A). When the number of objects is large, it is thought that a combination of the ALS approach and combinatorial optimization is required.

Table 1 Maximum VAF of each algorithm of real data analysis

	POS					Survey				
	7	6	5	4	3	7	6	5	4	3
(A)	0.979	0.972	0.961	0.942	0.900	0.862	0.844	0.819	0.783	0.731
(B)	0.979	0.972	0.961	0.942	0.900	0.862	0.845	0.822	0.783	0.731
(C)	0.969	0.954	0.912	0.926	0.896	0.709	0.693	0.666	0.656	0.658
(D)	0.959	0.951	0.951	0.940	0.896	0.760	0.760	0.742	0.706	0.666
(E)	0.979	0.972	0.961	0.942	0.900	0.858	0.840	0.813	0.779	0.728

Table 2 Acceptable VAF ratio of each algorithm of real data analysis

	POS					Survey				
	7	6	5	4	3	7	6	5	4	3
(A) (%)	60.0	68.2	80.7	87.9	96.4	79.7	84.2	86.8	90.3	96.3
(B) (%)	69.3	80.3	87.4	93.5	98.3	86.8	88.2	92.5	94.8	97.1
(C) (%)	3.0	2.7	4.0	4.8	4.9	0.0	0.0	0.0	0.0	0.0
(D) (%)	11.5	10.9	13.6	14.8	11.9	0.0	0.0	0.1	0.1	0.3
(E) (%)	14.6	17.4	20.4	29.2	40.4	8.1	10.0	14.8	20.8	29.4

Table 3 Computation time of each algorithm of real data analysis

	POS					Survey				
	7	6	5	4	3	7	6	5	4	3
(A) (%)	100	100	100	100	100	100	100	100	100	100
(B) (%)	106.2	106.1	114.9	114.1	128.8	93.4	93.8	91.7	94.1	95.2
(C) (%)	50.7	55.6	58.9	61.7	70.3	3.7	3.9	4.2	4.2	4.3
(D) (%)	63.4	70.4	71.4	78.9	94.6	4.4	4.6	4.8	5.0	5.0
(E) (%)	69.2	63.3	63.2	61.9	59.0	127.1	135.1	139.6	151.2	156.1

A more detailed analysis was performed with artificial data. The artificial data were created under the following conditions: the number of clusters was 6, weights were fixed at 4.00, 2.75, 1.75, 1.00, 0.50, and 0.25; number of objects were 10, 25, 50, and 100; the cluster structures were patterned and random. Similarity data were calculated from these cluster structures using the ADCLUS model formula Eq. (1). Then these similarity data were analyzed using the five methods.

The results are shown in Tables 4, 5, and 6. In Table 4, the maximum VAF of methods (A), (B), (D), and (E) was almost close to 1; the original cluster structure can be reproduced. But with method (D), it cannot be reproduced when the number of objects increases. Table 5 shows that methods (A) and (B) had a high ratio of acceptable VAF and can reproduce the original cluster structure for many initial clusters, but the ratio of methods (D) and (E) was low, showing that these methods depend on the initial clusters. It is also characteristic that the ratio depends on the method,

Table 4 Maximum VAF of each algorithm of artificial data analysis

	Artificial data 1 (patterned)				Artificial data 2 (random)			
	n = 10	n = 25	n = 50	n = 100	n = 10	n = 25	n = 50	n = 100
(A)	1.000	1.000	1.000	1.000	1.000	1.000	1.000	1.000
(B)	1.000	1.000	1.000	1.000	1.000	1.000	1.000	1.000
(C)	0.992	0.757	0.712	0.863	0.998	0.902	0.771	0.763
(D)	0.998	0.967	0.996	1.000	1.000	0.995	0.993	0.992
(E)	1.000	1.000	1.000	1.000	1.000	1.000	1.000	1.000

Table 5 Acceptable VAF ratio of each algorithm of artificial data analysis

	Artificial data 1 (patterned)				Artificial data 2 (random)			
	n = 10	n = 25	n = 50	n = 100	n = 10	n = 25	n = 50	n = 100
(A) (%)	80.0	87.0	92.0	91.0	94.0	91.0	94.0	97.0
(B) (%)	82.0	87.0	88.0	91.0	94.0	95.0	93.0	95.0
(C) (%)	13.0	0.0	0.0	0.0	19.0	1.0	0.0	0.0
(D) (%)	18.0	2.0	6.0	5.0	12.0	4.0	2.0	3.0
(E) (%)	41.0	45.0	41.0	45.0	55.0	45.0	38.0	30.0

Table 6 Computation time of each algorithm of artificial data analysis

	Artificial data 1 (patterned)				Artificial data 2 (random)			
	n = 10	n = 25	n = 50	n = 100	n = 10	n = 25	n = 50	n = 100
(A) (%)	100	100	100	100	100	100	100	100
(B) (%)	85.1	101.7	98.0	93.4	85.5	103.0	92.9	90.9
(C) (%)	68.5	26.5	7.0	1.5	70.4	29.3	6.6	1.2
(D) (%)	55.9	36.7	9.8	2.2	108.9	30.8	9.1	1.9
(E) (%)	44.4	98.9	151.5	191.2	62.1	100.4	140.5	149.6

regardless of the number of subjects. Regarding computation time, Table 6 shows that method (B) was almost the same as method (A), while method (E) increases as the number of objects increases. Methods (C) and (D) were short in time because the cluster structure cannot be reproduced.

From the above research, it can be seen that when the number of objects is large, the method using only combinatorial optimization reduces the ratio of acceptable VAF and increases the computation time compared to the methods that used both the ALS approach and combinatorial optimization. Therefore, the ALS approach is necessary. In addition, the ratio of acceptable VAF is significantly reduced when using only the method of ALS approach, combinatorial optimization is also necessary. It was also found that increasing the number of iterations in the ALS approach does not improve the results.

4 Improvement Byinitial Cluster

From the analysis in the previous section, it was found that the MAPCLUS algorithm may depend heavily on the method and the initial cluster.

The problem of dependency on the initial cluster is the same as k-means clustering. K-means++ was suggested by Arthur and Vassilvitskii [3]. The k-means model gives cluster centers randomly, but k-means++ gives the first center randomly, and then uses a weighted probability, where objects close to the centers are less likely to be chosen as the next center. The results and calculation speeds are improved dramatically.

In the original method of MAPCLUS algorithm, the initial cluster uses the result of the singular value decomposition (SVD) of similarity data or random data. The analysis in the previous section used random data for the initial cluster. In this section, we will improve the result by changing the method of generating initial clusters.

The proposed method is as follows:

1. A cluster is randomly generated.
2. The weight and VAF are calculated.
3. The VAF is positive, the cluster is taken as a candidate for an initial cluster.
4. Repeat steps 1 to 3 until there is a sufficient number of candidates above the number of clusters required for the analysis.
5. The initial cluster consists of a combination of clusters, each of which has a large VAF compared to other candidates.

In the present analysis, each dataset was analyzed with 20 initial clusters, which were created by changing the combination. For the analysis, a program created in R was used on a computer running CentOS 7 with an Intel Core i7-4790 3.60 GHz CPU and 32 GB of memory.

The loss function of this program is

$$L = \sum_{k=1}^{R+1} \sum_{\substack{i \\ i<j}}^{n} \sum_{j}^{n-1} (s_{ij} - w_k p_{ik} p_{jk})^2,$$

the `optim` function of R was used for optimization.

First, the proposed procedure was applied to the two artificial datasets used in Sect. 3. For this analysis, data in which the number of objects was 10, 25, and 50 were used. In the original method, 20 initial values were randomly created.

Tables 7 and 8 show the results, such as the maximum VAF, the average VAF, the number of iterations of both the main loop and the polish loop, combinatorial optimization, and computation time.

Using patterned artificial data, there is no difference in the values between the proposed method and the original method. Computational time was reduced by 35. Using random artificial data, when the number of objects was small, the proposed method had a higher number of iterations and computation time. But as the number of subjects increased, the results were almost the same between the two methods,

Table 7 The result of artificial data 1

	Artificial data 1 (patterned)					
Number of objects	10		25		50	
Method	Original	Proposed	Original	Proposed	Original	Proposed
Number of generated initial clusters (Max. 20)	20	7	20	20	20	20
Maximum VAF	100%	99.9%	99.2%	99.1%	91.9%	91.9%
Average VAF	99.9%	99.9%	95.3%	96.7%	91.1%	90.3%
Average of main loop (Max. 20)	19.45	20	18.8	15.4	18.95	20
Average of polish loop (Max. 10)	4.3	9.71	6.65	10	9.8	10
Average of combinatorial optimization (Max. 10)	8.6	9.43	9.25	10	10	10
Average of computation time	4.24	2.77	32.15	19.71	269.96	165.76

Table 8 The result of articial data 2

	Artificial data 2 (random)					
Number of objects	10		25		50	
Method	Original	Proposed	Original	Proposed	Original	Proposed
Number of generated initial clusters (Max. 20)	20	20	20	20	20	20
Maximum VAF	1	1	0.998	0.997	0.989	0.989
Average VAF	1	1	0.954	0.967	0.911	0.904
Average of main loop (Max. 20)	19.7	20	18.8	15.4	18.95	20
Average of polish loop (Max. 10)	6.95	10	6.65	10	9.8	10
Average of combinatorial optimization (Max. 10)	7.45	10	9.25	10	10	10
Average of computation time (sec.)	3.56	7.70	33.32	19.80	202.32	134.32

and the computation time was lower by 30–40% in the proposed method. Since the number of initial clusters is 20, the maximum VAF is slightly smaller than in Table 4.

In addition, this procedure was applied to the POS data and survey data. In these analyses, the number of clusters was set to 5 for both datasets. The results are shown in Table 9.

For the POS data, the average VAF was slightly smaller, the maximum VAF was larger, and the computation time was about half. Both methods were analyzed with only 20 initial clusters, so although the maximum VAF in Table 1 is less than 0.961,

Table 9 The result of POS and survey data

	POS		Survey	
Number of objects	15		64	
Method	Original	Proposed	Original	Proposed
Number of generated initial clusters (Max. 20)	20	20	20	20
Maximum VAF	0.949	0.955	0.447	0.736
Average VAF	0.943	0.930	0.432	0.720
Average of main loop (Max. 20)	19.2	20	16.2	20
Average of polish loop (Max. 10)	9.6	9.9	10	7.3
Average of combinatorial optimization (Max. 10)	10	8.25	10	8.85
Average of computation time (sec.)	8.36	3.94	387.47	292.63

acceptable solutions were obtained. For the survey data, the maximum VAF was 0.447 for the original and 0.736 for the proposed method. That value in Table 1 was 0.822, so the result of the proposed method is not good, but the computation time was improved by about 24.5%. The proposed method is considered to be sufficiently effective.

5 Conclusion

In the present study, the author focused on the stability of the result and the computation time of overlapping cluster analysis. Section 3 clarified the problem of the relationship between the ALS approach, combinatorial optimization, and the number of objects in the MAPCLUS algorithm, using both real and artificial data. For the stability of results, it was confirmed that combinatorial optimization is a necessary procedure, but combining it with the ALS approach is indispensable. In addition, it was also found that increasing the number of iterations of the ALS approach does not improve the results.

Next, in Sect. 4, the author examined whether the results could be improved by generating the initial clusters. The proposed method obtained better results than the original method.

There are several ways to improve the algorithm of MAPCLUS. It is possible to improve the loss function, and the content of the combinatorial optimization process can be changed. The present study proposed a method to generate initial clusters based on the k-means++ concept. The idea is to obtain good results by collecting good initial clusters with a good VAF for each cluster. Considering that the proposed method achieved better results than the original method, it is necessary to examine further the best way to generate the initial clusters. In the future, the proposed method should be verified with the INDCLUS model and the one-mode three-way model.

References

1. Arabie, P., & Carroll, J. D. (1980). MAPCLUS: A mathematical programming approach to fitting the ADCLUS model. *Psychometrika*, *45*, 211–235.
2. Arabie, P., Carroll, J. D., DeSarbo, W. S., & Wind, J. (1981). Overlapping clustering: A new method for product positioning. *Journal of Marketing Research*, *18*, 310–317.
3. Arthur, D., & Vassilvitskii, S. (2007). k-means++: The advantages of careful seeding. In *Proceedings of the eighteenth annual ACM-SIAM symposium on discrete algorithms* (pp. 1027–1035). Society for Industrial and Applied Mathematics Philadelphia, PA, USA.
4. Carroll, J. D., & Arabie, P. (1983). INDCLUS: An individual differences generalization of the ADCLUS model and the MAPCLUS algorithm. *Psychometrika*, *48*, 157–169.
5. Chaturvedi, A., & Carroll, J. D. (1994). An alternating combinatorial optimization approach to fitting the INDCLUS and generalized INDCLUS models. *Journal of Classification*, *11*, 155–170.
6. DeSarbo, W. S. (1982). GENNCLUS: New models for general nonhierarchical clustering analysis. *Psychometrika*, *47*, 449–475.
7. France, S. L., Chen, W., & Deng, Y. (2017). ADCLUS and INDCLUS: Analysis, experimentation, and meta-heuristic algorithm extensions. *Advances in Data Analysis and Classification*, *11*, 371–393.
8. Kiers, H. A. L. (1997). A modification of the SINDCLUS algorithm for fitting the ADCLUS and INDCLUS models. *Journal of Classification*, *14*, 297–310.
9. Shepard, R. N., & Arabie, P. (1979). Additive clustering: Representation of similarities as combinations of discrete overlapping properties. *Psychological Review*, *86*, 87–123.
10. Yokoyama, S., Nakayama, A., & Okada, A. (2009). One-mode three-way overlapping cluster analysis. *Computational Statistics*, *24*, 165–179.

Part II
Application-Oriented

Increasing Conversion Rates Through Eye Tracking, TAM, A/B Tests: A Case Study

Daniel Baier and Alexandra Rese

Abstract Online retailers are permanently confronted with the question how to increase conversion rates of their shops (e.g., the percentage of visits that end with a purchase). Successful seem to be shops where landing pages arouse attention and interest as well as quickly to interesting offers. However, whereas many layout and navigation improvements sound reasonable in general, only few of them result in increased conversions when going online. In this paper, we discuss how eye tracking, technology acceptance modeling (TAM), and A/B tests can help to tune them before going online. The improvement of the navigation menu position on landing pages at a major European online fashion shop is used for demonstration. The complete process from idea generation to integration is discussed.

1 Introduction

Using the information how visitors navigate and search for products in an online shop has long been recognized as an online retailer's road to success (Kim, Albuquerque, & Bronnenberg [9]; Ringel & Skiera [15]). So, e.g., Kim et al. [9] discuss how a major online retailer (amazon.com) collects and analyzes customer search data (clickstreams) and successfully uses this information to modify the navigation and quickly lead visitors to interesting products. Moreover, the authors develop a visualization tool based on Okada and Imaizumi [11]'s asymmetric MDS to support this. Ringel and Skiera [15] extend this tool to larger amounts of search data with respect to thousands of products offered in the shop. Other authors (e.g. Baier, Rese, Nonenmacher, Treybig, & Bressem [2]; Baier, Rese, & Röglinger [3]) demonstrate that interactive tools like attended shopping, curated shopping, messaging services,

D. Baier (✉) · A. Rese
Chair of Marketing and Innovation, Universitaetsstrasse 30, University of Bayreuth, 95447 Bayreuth, Germany
e-mail: daniel.baier@uni-bayreuth.de

A. Rese
e-mail: alexandra.rese@uni-bayreuth.de

T. Imaizumi et al. (eds.), *Advanced Studies in Behaviormetrics and Data Science*,
Behaviormetrics: Quantitative Approaches to Human Behavior 5,
https://doi.org/10.1007/978-981-15-2700-5_21

scanned shopping, or voice assistants support the navigation and the finding of interesting products. They were categorized as attractive by customers of a major online fashion shop (baur.de).

All these improvements have one thing in common: Their effect on conversion rates is unclear before integration into the online shop, but this implementation is costly. Consequently, many online retailers have installed a filtering and tuning process that allows to develop "best" improvements in a money-saving stage-by-stage manner (see for overviews Baier et al. [2]; Baier et al. [3]): In early stages, technological, market scouting as well as expert knowledge is used to generate large numbers of promising improvement ideas at low costs. Then, internal workshops and customer surveys help to select few promising alternatives, which then are testwise implemented and made available to small customer samples in user-labs. Finally, "best" alternatives have to demonstrate their effects on conversion rates across large customer samples when implemented and integrated in the online shop.

In this paper, we show how the authors generated, tuned, and tested one improvement idea—a modified navigation menu position on landing pages—at a major European online fashion retailer (zalando.de). In Sect. 2, the underlying landing page improvement problem is discussed. In Sect. 3, we describe how eye tracking, technology acceptance modeling (TAM), and A/B testing can be used to select and tune improvements. Sections 4 and 5 discuss the empirical application from idea generation to testing, tuning, implementation, and integration. The paper closes with conclusions and outlook.

2 Increasing Conversions via Improved Landing Pages

Landing pages are first pages a consumer is confronted with when visiting an online shop (Ash, Ginty, & Page [1]). These first pages may depend on how the visitor accessed the site: It could be the homepage of the online shop if accessed directly or a more specific page, say, e.g., a category page, a brand page, or a product page if accessed via a search engine, a banner, a newsletter, or another advertisement with a specific focus. In most of these cases, the landing pages have a similar navigation and page layout as all pages of the shop. However, many websites also have specific landing pages, e.g., microsites (a subselection of pages of the site) or stand-alone pages, where visitors are guided to as the result of a marketing campaign. These landing pages may have a far more pronounced call-to-action and a modified page layout (Ash et al. [1]).

Across all types, landing pages are important for the success of their websites. Since they are the first pages visitors are confronted with and maybe the last ones if they immediately quit, goal achievements (e.g., downloads, comments, ratings, registrations, subscriptions, purchases) are only possible when the visitors' attention and interest are aroused there, expectations are fulfilled, and trust, orientation, as well as call-to-action are present (Gofman, Moskowitz, & Mets [8]; Ash et al. [1]). Consequently, their navigation and page layout as well as their permanent improvement are big challenges for online retailers.

So, for making them successful, among others, the following navigation and layout elements have to be carefully selected (see Ash et al. [1]): Size and contents of page header, size and contents of page footer, size and location of page navigation, placement of trust symbols and credibility logos, separation of page shell and navigation from page content, size and location of forms or other calls-to-action, mirror images (swapping) of key page sections (e.g., a form located to the left of the text or to the right), vertical stacking versus horizontal arrays of page sections, and single versus multiple columns. Additionally, decisions on presentation formats are needed: Degree of detail (e.g., full text, or links to supporting information), writing format, choice of input elements (e.g., radio buttons or pulldown lists), action format (e.g., buttons, text links, or both), editorial tone, use of alternative formats and modalities (e.g., charts, figures, audio clips, videos, presentations, demos).

For reducing the large number of improvement options to a few, customer surveys based on conjoint analysis have been proposed as useful and applied (see, e.g. Gofman et al. [8]; Schreiber & Baier [16]). So, Schreiber and Baier [16] collected preference data from the customers of a major German Internet pharmacy. Using choice-based conjoint analysis, a sample of 2,489 respondents was confronted with 15 choice tasks among four landing page alternatives. The alternatives resembled the actual pharmacy's home page, but varied w.r.t. the following elements and formats: navigation menu (at the top, at the left, in the middle), search and shopping basket area (static, flexible), button size (small, large), font size (small = 12pt, large = 14pt), and advertising banner (big size banner, junior page, full banner, skyscraper banner, button). The respondents had to select in each task a preferred landing page. After analyzing the collected preferences it could be demonstrated that the font size and the navigation menu had the strongest influence on the customers' preference and that the landing page, with navigation menu (at the left), search and shopping basket area (flexible), button size (large), font size (large = 14pt), and advertising banner (button), was the favorite. Gofman et al. [8] conducted a similar survey to improve the landing pages of an online grocery store. Using traditional conjoint analysis, a target segment sample of 172 consumers was asked to rate 27 landing page alternatives concerning their interest to purchase groceries from this online shop on a 9-point Likert scale. The landing page alternatives varied w.r.t. shipment options, promotions, featured items, and main pictures. The traditional conjoint analysis results were used to develop two different landing pages, one for value-oriented consumers (with a focus on cost saving) and one for impulsive consumers (with a focus on mouth-watering images).

Whereas the up-to-now discussed preference data collection approach is suited to select promising improvements among a large number of alternatives in early stages of the filtering and tuning process at low costs, in the following, more in-depth testing and tuning methods are discussed which can be applied—in contrast to the above-described approach—only to few alternatives at reasonable costs.

3 Tuning Through Eye Tracking, TAM, and A/B Tests

When preceding stages have reduced the number of improvement alternatives to a few promising ones, these can be testwise implemented and more advanced—and more costly—approaches can be used to measure their acceptance by the customers and their ability to increase conversion rates.

From a more practical point of view, a so-called A/B test is the ultimate proof that an improvement increases the conversion rate (Ash et al. [1]; Gofman et al. [8]). The original version of the landing page and one (or more than one) variants are made available for large target segment samples. A splitting technique is used to guide comparable subsamples to different landing page versions, using, e.g., time slots where versions are online (sequential testing) or alternating links (parallel testing). For each visit, the adherence to a subsample/landing page version and the goal achievement (e.g., download, comment, rating, registration, subscription, purchase: yes or no) is stored and used to calculate the conversion rate of each version (number of goal achievements per visits) as a basis for the final decision. The necessary duration of such an A/B test depends on the expected number of conversions per day, the number of versions to be compared, the expected increase of the conversion rate, and the necessary confidence in the results (see Ash et al. [1]). However, in practical settings, a duration of at least 2–3 weeks with comparable and stable environments for all versions is needed which makes it clear that the A/B test should be reserved to final decisions.

Consequently, before starting an A/B test, testing and tuning with smaller target segment samples is needed. Ash et al. [1] propose for this purpose usability testing, eye tracking, focus groups, customer surveys, customer service representatives interviewing, usability reviews, forums, and blogs.

Usability testing means that few customers (say, e.g., three to six) are invited into a laboratory (user-lab) and confronted there with a testwise implementation of the improvement. They are asked to complete a specific task (use case scenario). The developers quietly observe the process and use the information for tuning the testwise implemented improvement afterward. Often, usability tests are combined with so-called eye tracking, a special form of observation where technology is used to show what the customers are looking at, in what order, and how long (Ash et al. [1]; Meißne, Musalem, & Huber [10]). The widespread technology for this purpose is to track positions and movements of the eye via reflections of an infrared light beam into the eye. The position and movement of the eye then are used to calculate points where the customer is looking at on a screen or a video recording. Usually, fixations (points where the eye rests at least a minimum duration, e.g., 0.15–0.3 s) and saccades (points where the eye is on the move to another point) are distinguished, since it is assumed that humans need a minimum fixation duration to understand the looked at content. Across a sample of tracked customers, the distribution of the fixation durations can be summarized by so-called heat maps. Here, zones with high (sums of) fixation durations across the sample are colored in red and zones with lower fixation durations are colored in yellow or green. Heat maps are assumed to

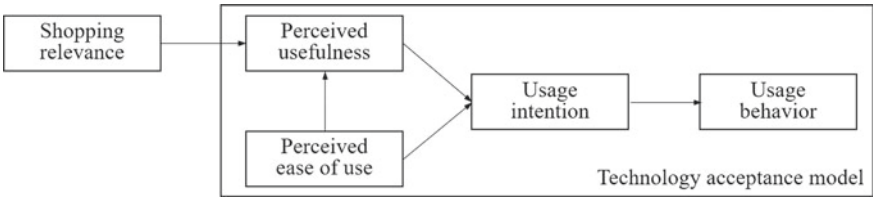

Fig. 1 TAM assumptions following Davis [5], Venkatesh and Davis [18]

be the best-known visualization technique for eye-tracking results since they allow to draw simple conclusions whether screen (or video recording) elements have been looked at or not.

Usually, usability testing and eye tracking are accompanied by a customer survey or focus groups where likes and dislikes of the testwise implementation are collected. In this paper, we propose to use surveys based on the well-known technology acceptance model (TAM) for this purpose. TAM is an information systems theory with roots in the behavioral sciences (e.g. Fishbein & Ajzen [7]) that was developed by Davis [5] for measuring the acceptance of information systems in a work environment. It models how users come to accept and use a technology at the working place. The model suggests that when users are presented with a new technology, a number of factors influence their usage intention and usage behavior, especially their so-called perceived usefulness and their perceived ease of use are assumed to be decisive. Figure 1 reflects these main modeling assumptions.

Numerous applications of TAM also outside the work environment—for example, w.r.t. new technologies in offline and online shopping, see Pavlou [12], Baier and Stüber [4], Rese, Baier, Geyer-Schulz, and Schreiber [13], and Rese, Schreiver, and Baier [14]—have shown that the model is well suited to explain and predict usage behavior. Users are confronted with a new technology and have to answer standardized questionnaires. An analysis of the collected data using variance- or covariance-based estimation methods for structural equation models allows to explain and predict the acceptance by the target segment. Over the years, TAM was extended by Venkatesh and Davis [18] as TAM2, by Pavlou [12], by Venkatesh, Morris, Davis, and Davis [19] as UTAUT (unified theory of acceptance and use), and by Venkatesh, Thong, and Xu [20] as UTAUT2. The main extension focus was to add additional factors to better explain and predict the acceptance. So, e.g., Venkatesh and Davis [18] introduced the factors subjective norm, image, (job) relevance, output quality, and result demonstrability that influence the factor perceived usefulness. Pavlou [12] introduced trust and perceived risk as additional factors that explain online shop usage. In Fig. 1, one of these factors adapted to TAM in an online shopping environment—shopping relevance—is integrated, following Venkatesh and Davis [18].

4 Empirical Application: From Idea Generation to Testing

In our empirical application, the online shop of a cooperating major German online fashion retailer (zalando.de) serves as demonstration object that needs improvement. There, at the time before our investigation, the category pages "fashion for women" and "fashion for men" were frequently used landing pages but also had high so-called bounce rates, i.e., high percentages of visits that immediately ended there without a goal achievement. Obviously, the two landing pages could not arouse the visitors' attention and interest, the visitor's expectations were not fulfilled, or trust, orientation, as well as call-to-action were missing (see the above discussion or Gofman et al. [8]; Ash et al. [1]). This assessment was confirmed by interviews of the authors with a small sample of customers confronted with these landing pages.

Consequently, market and technological scouting was performed which resulted in two improvement ideas: "integrating a heroshot in the navigation menu" and "adding a central navigation menu." A heroshot is a picture of an attractive member of the target segment that arouses the visitor's attention and interest (see Gofman et al. [8]; Ash et al. [1]). A central navigation menu is positioned in the middle of the screen and provides additional help to find interesting offers. The motivation for an additional central navigation menu comes from the observation that—on average—website visitors tend to look at the screen center first. This behavior is well known and seems even to have evolutionary reasons. Predators and preys look in the middle of a scene, maybe this is the best starting point to recognize actions and react quickly. Experiments in visual sociology support this observation. So, e.g., Tatler [17] showed 22 test persons 120 indoor, outdoor, and human-generated scenes with biased distributions of image features (image samples with bias to the left, bias to the right, unbiased samples). Eye tracking revealed that even with biased distributions, the test persons tended to look in the middle of the screen across the sample. Fehd and Seiffert [6] reported similar observations when altogether 65 test persons had to track 4–10 moving circles on the screen in a game setting. The test persons were asked to follow different strategies for keeping control (central looking, center-target switching, or target looking). The central looking respondents were the most successful in controlling the game.

Basing on these improvement ideas, two alternative variants were developed for the landing page "fashion for women" and two for the landing page "fashion for men": Two with an additional central menu below the usual teaser (variant 1) and two with a reduced teaser and the additional central menu combined with a heroshot (variant 2). It was assumed—as hypotheses for the following tests—that variant 2 would have highest conversion rates and the original landing page the lowest. Additionally, it was assumed that—if the visitors were asked to navigate the landing pages—original to variant 1 to variant 2 would reduce the time to fixate a navigation menu and that variant 2 would be superior to variant 1 w.r.t. perceived usability, perceived ease of use, usage intention, and usage behavior. In order to test these hypotheses, a field experiment in a user-lab was designed. The original and the two landing page variants were integrated into mock-ups of the online shop. An eye-tracking experiment was

prepared and a questionnaire according to the TAM model in Fig. 1 was developed. Additionally, at the online shop of the cooperating retailer, an A/B test was prepared to compare the three landing page versions (original, variant 1, variant 2) for women and for men across larger target segment samples.

5 Empirical Application: From Testing to Going Live

In the user-lab, where eye tracking and the TAM survey were conducted, altogether n = 93 respondents participated and filled out the questionnaires completely (n = 55 female, n = 38 male participants, all of them students at the local university). n = 32 participants evaluated the original and variant 1 of their gender-specific landing page (n = 18 female, n = 14 male participants). n = 61 participants evaluated the original and variant 2 of their gender-specific landing page (n = 37 female, n = 24 male participants). The higher number of participants who were asked to evaluate version 2 reflects the fact that version 2 was assumed to be the variant with higher conversion rates.

All participants in the user-lab received a short introduction into the context of the field experiment ("improvement of the online shop") and were made familiar with the eye-tracking system. Then, they were shown (in random order) their gender-specific original landing page and one of the two variants. In each case, they were asked to orientate themselves for 20–30 seconds on the landing page and then to navigate to prespecified trousers and shirts. During the visits of the landing pages, the eye-tracking system calculated the fixations and fixation durations across the landing pages. Figures 2 and 3 reflect the derived heat map for the original landing page "fashion for women" and variant 2 and the heat map for the original landing page "fashion for men" and variant 2.

The heat maps demonstrate that—across the samples—in variant 2 the participants preferred to orientate via the central menu. The fixations and fixation durations there were much higher than in the menu on the left which was alternatively offered to them. For further evaluations, the fixations and fixation durations were allocated to so-called areas of interest (AOIs). The original landing page contained the AOIs "left-side navigation," "top navigation," and "teaser," the variants 1 and 2 an additional AOI "central navigation." Table 1 reflects interesting performance measures of the three versions: "mean time to fixation (in seconds)," "mean number of fixations," "mean fixation duration (in seconds)," and "mean fixation duration per fixation (in seconds)."

Table 1 supports the findings from Figs. 2 and 3 but now additionally gives the results for variant 1. As expected, variant 2 outperforms variant 1 w.r.t. the important performance measures: mean time to fixation of the navigation menu and mean fixation duration of the central navigation (as a measure for fast orientation on the landing page). The original landing page even has a higher mean time to fixation of the left-side navigation.

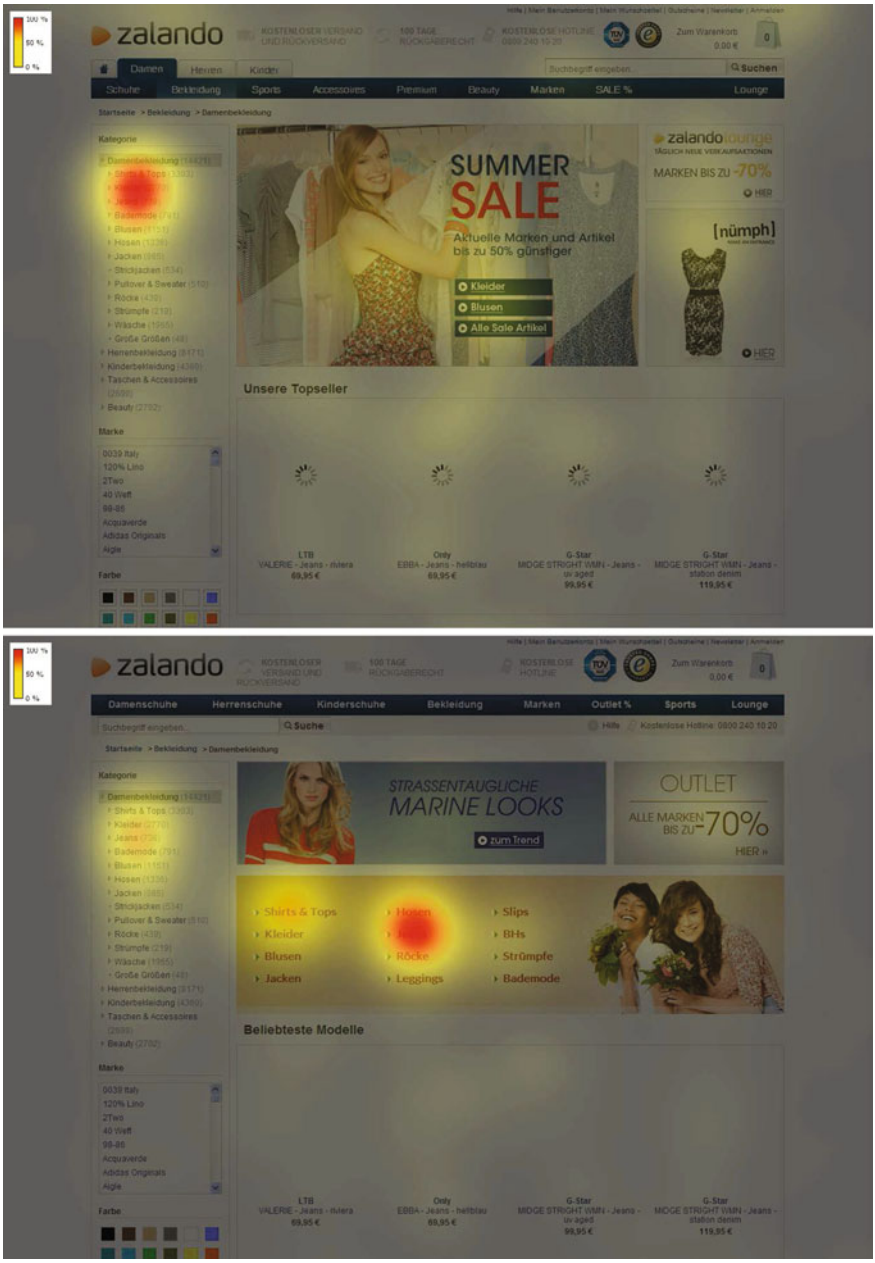

Fig. 2 Eye-tracking results: heat map for the original landing page "fashion for women" (above) and variant 2 with reduced teaser, additional central navigation menu, and a heroshot (below)

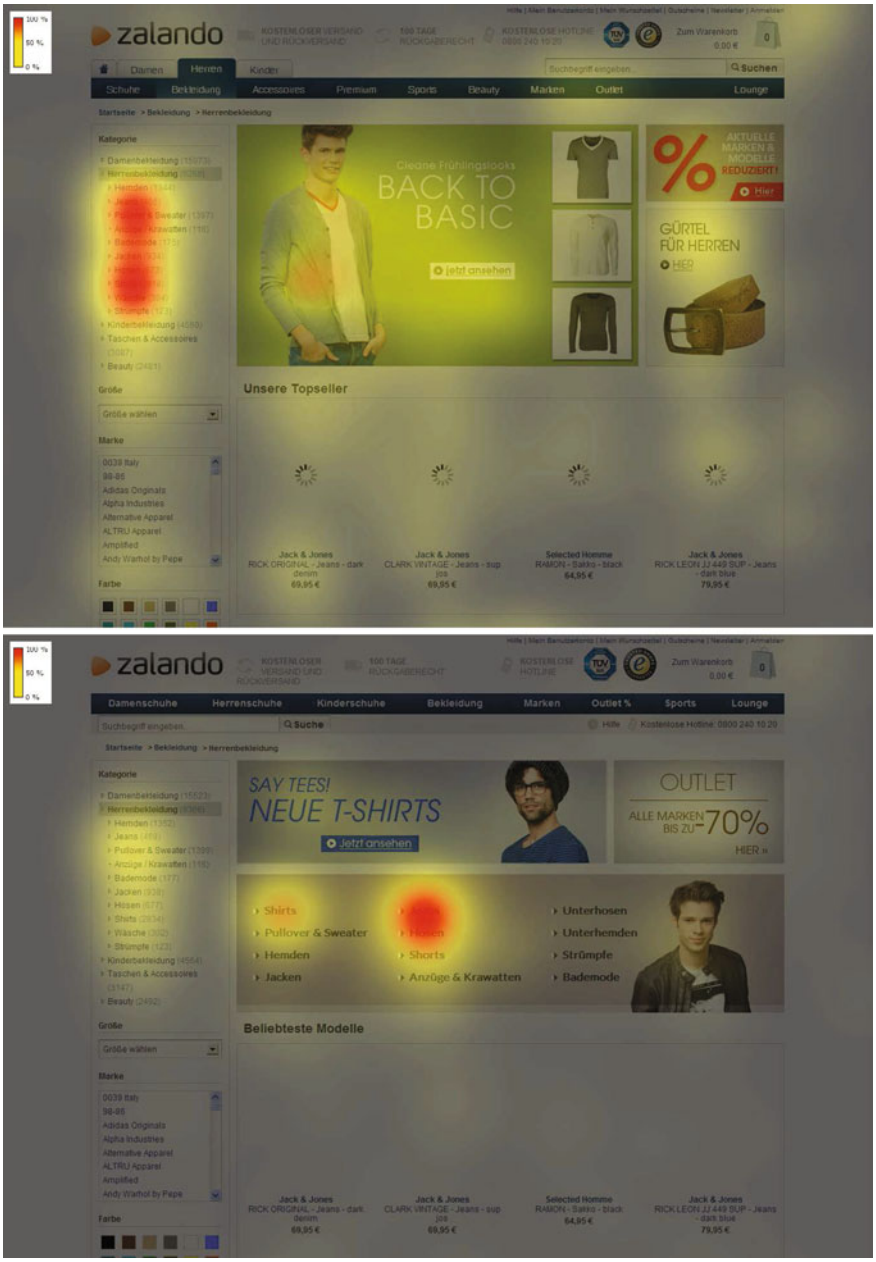

Fig. 3 Eye-tracking results: heat map for the original landing page “fashion for men” (above) and variant 2 with reduced teaser, additional central navigation menu, and a heroshot (below)

Table 1 Eye-tracking results: mean time to fixation, mean number of fixations, and mean fixation duration w.r.t. different areas of interest on the original website (all, n = 93)/variant 1 (n = 32)/variant 2 (n = 61)

Area of interest	Mean time to fixation (sec.)	Mean number of fixations	Mean fixation duration (sec.)	Mean fix. dur. per fix. (sec.)
Left-side nav.	10.54/7.23/5.22	10.96/13.00/9.53	4.45/3.89/3.96	0.43/0.29/0.42
Central nav.	–/6.01/2.44	–/18.37/25.85	–/5.77/8.92	–/0.30/0.35
Top nav.	10.23/11.82/9.62	4.99/4.08/2.55	1.19/1.00/0.51	0.23/0.23/0.21
Teaser	2.12/0.65/2.73	33.98/38.35/11.52	8.90/9.61/2.89	0.26/0.25/0.25

dur. = duration, fix. = fixation, nav. = navigation, sec. = in seconds

Table 2 TAM results: quality of measurement scales and construct values (1 = strongly disagree, …, 7 = strongly agree) for variant 1 (n = 32) and variant 2 (n = 61)

Construct (no. of items)	CA	CR	AVE	Mean constr. val. for variant 1 (std.)	Mean constr. val. for variant 2 (std.)
Shopping relevance (3)	0.824	0.894	0.739	3.490(1.661)	4.880(1.549)***
Perceived ease of use (3)	0.945	0.964	0.900	4.146(1.776)	4.443(1.842)
Perceived usefulness (5)	0.949	0.961	0.830	3.463(1.610)	4.230(1.822)**
Usage intention (4)	0.895	0.926	0.759	3.164(1.372)	4.021(1.645)**
Usage behavior (2)	0.905	0.955	0.913	1.969(1.722)	3.623(2.396)***

CA: Cronbach's α; CR: composite reliability; AVE: average variance extracted; constr. val. = construct values, std. = standard deviation; ***: Differences are significant at p = 0.01, **: at p = 0.05

When evaluating the filled out TAM questionnaires of the participants, as usual, the validity of the constructs and of the TAM model has to be checked. Table 2 reflects the usual information on the quality of the measurement scales and construct values. The five constructs were measured using two to five items, each on 7-point Likert scales (1=strongly disagree,...,7=strongly agree):

- Shopping relevance via three items ("I noticed the navigation in the middle of the screen.", "The location of the navigation in the middle of the screen was striking.", "I am very satisfied with the quality of the navigation centered in the middle of the screen."),
- perceived ease of use via three items ("Graphical navigations in the middle of the screen …make shopping easier.", "…make shopping more enjoyable.", "…help me to better orientate.),
- perceived usefulness via five items ("Placing the navigation in the middle of the screen facilitates orientation.", "By placing the navigation in the middle of the screen, I can shop more efficiently.", "Displaying an additional navigation in the middle of the screen makes shopping easier.", "By displaying the navigation in the middle the shopping experience can be improved.", "By displaying the navigation in the middle of the screen, the web page is clearer."),
- usage intention via four items ("I will use the navigation placed in the middle of the screen more often in the future.", "In the future I will regularly pay attention

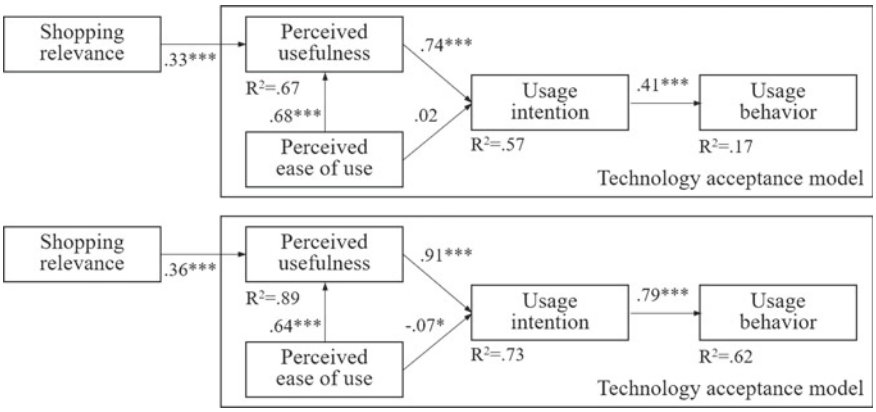

Fig. 4 TAM Results: estimated coefficients and variance explained for the structural model of variant 1 (above) and variant 2 (below)

to navigations placed in the middle of the screen.", "I will regard the navigation in the middle as assistance.", "I intend to use only centrally placed navigations."), and

- usage behavior via two items ("When shopping I was guided by the navigation placed in the middle of the screen.", "By using the navigation placed in the middle of the screen I would also have bought something.").

The validity measures (Cronbach's α, composite reliability, and average variance extracted) demonstrate overall good fit, as well as the estimated coefficients and variance explained for as well as the expected path coefficients and the explained variances of the structural model for variant 1 and variant 2 in Fig. 4. Moreover, shopping relevance, perceived usability, usage intention, and usage behavior of variant 2 are significantly higher than that of variant 1 which supports the hypotheses (with the exception of perceived ease of use) and gives again a strong support for the integration of variant 2.

The additionally performed A/B test with the three versions distributed among the target segment supports the findings. As a goal achievement, the filling of a shopping basket in the online shop was defined. The conversion rate was defined as the number of goal achievements divided through the number of visitors of the landing page. In order to receive stable results, each landing page version went 30 days live in the German online shop. The comparison of the calculated conversion rates for the three versions led to the following results: Concerning the "fashion for men" landing page, it was found out that variant 1 decreased the conversion rate from 2.37% (original) to 2.31% (variant 1), whereas variant 2 increased the conversion rate from 2.32% (original) to 2.48% (version 2). The improvement was even higher concerning the "fashion for women" landing page. Variant 1 increased the conversion rate from 2.56% (original) to 2.67% (version 1) and variant 2 from 2.35% (original) to 2.53% (version 2). The testing and tuning of the variants were so successful that the online

shop finally integrated variant 2 of both landing pages into the German online shop and even passed the results to the French online shop where similar landing pages were developed and integrated.

6 Conclusions and Outlook

To conclude: The proposed landing page modification leads to improved conversion rates. Most of the hypotheses could be supported. Due to overall positive results, the improvements were also communicated and integrated into online shops in neighbor markets (France). Even more interesting is the fact that, in this paper, the complete process from idea generation to integration in the online shop is discussed and proved to be successful. As the navigation and page layout of the landing pages as well as of the complete online shop with all elements need permanent improvement, the availability of such a cost-effective filtering and tuning process is promising. Maybe the next step for the authors could be to test the navigation improvements based on Okada and Imaizumi [11]'s asymmetric MDS that were mentioned by the authors in the introduction.

Acknowledgements The authors want to thank the whole team at the marketing chair for supporting this research, especially the former research assistant Dr. Eva Stüber and the cooperating partners at the online retailer. Also they want to thank Prof. Dr. Akinori Okada for his everlasting support, inspiration, and helpful suggestions in our research on asymmetric MDS and related methods and tools.

References

1. Ash, T., Ginty, M., & Page, R. (2012). *Landing page optimization: The definitive guide to testing and tuning for conversions* (2nd ed.). Wiley.
2. Baier, D., Rese, A., Nonenmacher, N., Treybig, S., & Bressem, B. (2019). Digital technologies for ordering and delivering fashion: How BAUR integrates the customer's point of view. In *Digitalization cases* (pp. 59–77). Springer.
3. Baier, D., Rese, A., & Röglinger, M. (2018). Conversational user interfaces for online shops? A categorization of use cases. In *Proceedings of the 39th International Conference on Information Systems (ICIS)*. Association of Information Systems.
4. Baier, D., & Stüber, E. (2010). Acceptance of recommendations to buy in online retailing. *Journal of Retailing and Consumer Services*, *17*(3), 173–180.
5. Davis, F. D. (1989). Perceived usefulness, perceived ease of use, and user acceptance of information technology. *MIS Quarterly*, 319–340.
6. Fehd, H. M., & Seiffert, A. E. (2010). Looking at the center of the targets helps multiple object tracking. *Journal of Vision*, *10*(4), 19.
7. Fishbein, M., & Ajzen, I. (1980). *Understanding attitudes and predicting social behavior*. Englewood Cliffs, NJ: Prentice-Hall.
8. Gofman, A., Moskowitz, H. R., & Mets, T. (2009). Integrating science into web design: Consumer-driven web site optimization. *Journal of Consumer Marketing*, *26*(4), 286–298.

9. Kim, J. B., Albuquerque, P., & Bronnenberg, B. J. (2011). Mapping online consumer search. *Journal of Marketing Research*, *48*(1), 13–27.
10. Meißner, M., Musalem, A., & Huber, J. (2016). Eye tracking reveals processes that enable conjoint choices to become increasingly efficient with practice. *Journal of Marketing Research*, *53*(1), 1–17.
11. Okada, A., & Imaizumi, T. (1997). Asymmetric multidimensional scaling of two-mode three-way proximities. *Journal of Classification*, *14*(2), 195–224.
12. Pavlou, P. (2001). Integrating trust in electronic commerce with the technology acceptance model: Model development and validation. In *Amcis 2001 Proceedings* (pp. 816–822).
13. Rese, A., Baier, D., Geyer-Schulz, A., & Schreiber, S. (2017). How augmented reality apps are accepted by consumers: A comparative analysis using scales and opinions. *Technological Forecasting and Social Change*, *124*, 306–319.
14. Rese, A., Schreiber, S., & Baier, D. (2014). Technology acceptance modeling of augmented reality at the point of sale: Can surveys be replaced by an analysis of online reviews? *Journal of Retailing and Consumer Services*, *21*(5), 869–876.
15. Ringel, D. M., & Skiera, B. (2016). Visualizing asymmetric competition among more than 1,000 products using big search data. *Marketing Science*, *35*(3), 511–534.
16. Schreiber, S., & Baier, D. (2015). Multivariate landing page optimization using hierarchical bayes choice-based conjoint. In *Data science, learning by latent structures, and knowledge discovery* (pp. 465–474). Springer.
17. Tatler, B. W. (2007). The central fixation bias in scene viewing: Selecting an optimal viewing position independently of motor biases and image feature distributions. *Journal of Vision*, *7*(14), 4.
18. Venkatesh, V., & Davis, F. D. (2000). A theoretical extension of the technology acceptance model: Four longitudinal field studies. *Management Science*, *46*(2), 186–204.
19. Venkatesh, V., Morris, M. G., Davis, G. B., & Davis, F. D. (2003). User acceptance of information technology: Toward a unified view. *MIS Quarterly*, 425–478.
20. Venkatesh, V., Thong, J. Y., & Xu, X. (2012). Consumer acceptance and use of information technology: Extending the unified theory of acceptance and use of technology. *MIS Quarterly*, *36*(1), 157–178.

Descriptive Analyses of Interrater Agreement for Ordinal Rating Scales

Giuseppe Bove and Alessio Serafini

Abstract A measure of interrater absolute agreement for ordinal rating scales that have advantages respect to intraclass correlation coefficients and other largely used measures is presented. Besides, some descriptive methods for analysing the dependence of the level of agreement by raters and targets are considered. In particular, biplot diagrams are proposed to detect differences in ratings the targets obtained by different raters, and multidimensional unfolding is suggested to display dependence of interrater agreement levels by targets. Finally, results of an application to data concerning the assessment of language proficiency are provided to highlight capabilities of the proposed procedures.

1 Introduction

Agreement among raters is relevant in many fields of application. For instance, in language studies the agreement of a group of raters who assess on a new rating scale (e.g. Likert scale) the language proficiency of a corpus of argumentative (written or oral) texts is analysed to test reliability of the scale. In medicine, agreement between diagnoses provided by more than one doctor (rater) is considered for identifying the best treatment for the patient. Similar situations can be found in organizational, educational, biomedical, social and behavioural research areas, where raters can be counsellors, teachers, clinicians, evaluators or consumers and targets can be organization members, students, patients, subjects or objects. A common feature of all these studies is that several 'raters' (or 'judges') evaluate a group of 'targets'. When each rater evaluates each target, the raters provide comparable categorizations of the targets. The extent to which the categorizations of raters coincide, the rating scale

G. Bove (✉)
Dipartimento di Scienze della Formazione, Università degli Studi Roma Tre, Rome, Italy
e-mail: giuseppe.bove@uniroma3.it

A. Serafini
Dipartimento di Economia, Università degli Studi di Perugia, Perugia, Italy
e-mail: alessio.serafini@unipg.it

T. Imaizumi et al. (eds.), *Advanced Studies in Behaviormetrics and Data Science*,
Behaviormetrics: Quantitative Approaches to Human Behavior 5,
https://doi.org/10.1007/978-981-15-2700-5_22

can be used with confidence without worrying about which raters produced those categorizations. So the main interest here is in analysing the extent that raters assign the same (or very similar) values on the rating scale (*interrater absolute agreement*), that is to establish to what extent raters' evaluations are close to an equality relation (e.g. in the case of only two raters, if the two sets of ratings are represented by x and y, the relation of interest is x = y). Several approaches to the statistical analysis of rater agreement are available (see, e.g. von Eye & Mun [20]). We focalize on the computation of coefficients that allow to summarize agreement in a single score. Cohen's *Kappa* (and extensions to take into account three or more raters, e.g. von Eye & Mun [20]) and intraclass correlations (Shrout & Fleiss [19]; McGraw & Wong [16]) seem appropriate for the analysis of absolute agreement in the case of nominal and numerical ratings, respectively. Some authors (e.g. LeBreton, Burgess, Kaiser, Atchley, & James [13]) have shown that the two indices are affected by the *restriction of variance problem* that consists in an attenuation of estimates of rating similarity caused by an artefact reduction of the between-targets variance in ratings. For instance, this happens in language studies when the same task is defined for native (L1) and non-native (L2) writers, and the analysis compares raters agreement in the two groups separately. Even in the presence of very good absolute agreement, Cohen's Kappa coefficient and intraclass correlations can assume low values, especially for L1 group, because the range of ratings provided by the raters is concentrated in one or two very high levels of the scale (a range restriction that determines a between-writers variance restriction). Measures like those proposed in LeBreton and Senter [14] overcome the restriction of variance problem because they measure the within-target variance of ratings (i.e. the between-raters variance) separately for each target and summarize the results in a final average index (usually normalized in the interval 0–1). In this approach, the influence of the low level of the between-targets variance is removed by the separate analysis of the ratings of each target. This group of measures reviewed in LeBreton and Senter [14] is defined only for interval data, and in some particular situations can assume negative values. Therefore, there is a lack of proposals for measures to deal with ratings at an ordinal scale level. For this reason, Bove, Nuzzo, and Serafini [3] and Bove, Conti, and Marella [4] proposed a new procedure to measure absolute agreement for ordinal rating scales, capitalizing on the dispersion index proposed by Leti [15] for ordinal variables.

When the interrater agreement is low, it is important to evaluate differences between raters and dependence of the level of agreement by targets features. Besides, rating scales frequently comprise subscales corresponding to different dimensions of the general construct measured, and interrater agreement can depend on the type of subscale considered. Moreover, when the rating scales assess some kind of proficiency (e.g. in language studies), they can be applied in different types of tasks, and agreement can depend on the characteristics of the task. In the following, it is shown how descriptive analyses of some of these kinds of dependencies can be performed by multivariate techniques like biplot (e.g. Gabriel [7]; Greenacre [9]; Gower, Lubbe, & Le Roux [8]) and multidimensional unfolding (e.g. Borg & Groenen [1]).

The paper is organized as follows. In Sect. 2, the measure of interrater absolute agreement for ordinal ratings proposed in Bove et al. [3] and its main properties

are presented. In Sect. 3, the bilinear model and the corresponding biplot diagram are proposed to perform analyses of differences in ratings the targets can obtain by different raters. In Sect. 4, the unfolding model is suggested as a tool for analysing by distances the dependence of the level of interrater agreement by targets. In Sect. 5, some results of a study on the assessment of language proficiency conducted at Roma Tre University in 2017 are provided to highlight the capabilities of the proposed procedures. Finally, Sect. 6 contains some remarks and tentative conclusions.

2 A Measure of Interrater Absolute Agreement for Ordinal Rating Scales

A data matrix $\mathrm{X} = (x_{ij})$ with each row corresponding to a target and each column to a rater is observed, the entry x_{ij} is the rating given by rater j to target i ($i = 1, 2, \ldots, n_T$; $j = 1, 2, \ldots, n_R$) on a K-point ordinal scale. According to Bove et al. [3], each row (target) of matrix X defines an ordinal categorical variable (the n_R ratings) whose dispersion can be measured by the index proposed in Leti [15], given by

$$D = 2 \sum_{k=1}^{K-1} F_k(1-F_k) \tag{1}$$

where K is the number of categories of the variable and F_k is the cumulative proportion associated to category k, for $k = 1, \ldots, K$. Index in (1) is non-negative and it is easy to prove that $D = 0$ if and only if all the observed categories are equal (absence of dispersion). The maximum value of the index (D_{max}) is obtained when all ratings are concentrated in the two extreme categories of the variable (maximum dispersion), and it is,

$$D_{max} = \frac{K-1}{2} \qquad \text{for } n_R \text{ even},$$

$$D_{max} = \frac{K-1}{2}\left(1 - \frac{1}{n_R^2}\right) \qquad \text{for } n_R \text{ odd}.$$

For n_R moderately large, the maximum of the index can be assumed equal to (K-1)/2. It is interesting to notice that D has properties of within and between dispersion decomposition analogous to the well-known variance decomposition (Grilli & Rampichini [11]).

Bove et al. [3] proposed to measure interrater agreement by the average of the n_T normalized values of index D obtained for the rows of the matrix X,

$$d = \frac{1}{n_T} \sum_{i=1}^{n_T} \frac{D_i}{D_{max}} \tag{2}$$

with D_i the value of index D for the *i-th* row of X. Index d is normalized in the interval [0, 1], and first empirical studies have shown that values below threshold 0.1 represent high levels of interrater agreement, values greater than 0.1 and below 0.2 represent moderate-low levels of agreement, and values greater than 0.2 represent disagreement. Bove et al. [4] explored sampling properties of d in order to construct confidence intervals.

3 Descriptive Analysis of Dependence of Agreement by Raters

Low levels of interrater absolute agreement suggest to perform analyses of the differences in ratings the targets obtained by the different raters. One way is to compare ratings in matrix X as values of numerical variables. Bilinear models (or inner product models) allow to perform these comparisons in geometric spaces, because it is possible to prove that any rectangular matrix may be represented choosing a vector for each row and a vector for each column in such a way that the elements of the matrix are the inner products of the vectors representing the corresponding rows and columns. The bilinear model for ratings in matrix X can be defined by

$$x_{ij}^t = \sum_{t=1}^{r} a_{it} b_{jt} + \varepsilon_{ij} \tag{3}$$

where x_{ij}^t is the value x_{ij} opportunely transformed (e.g. mean centred or standardized), a_{it} (component score) and b_{jt} (component loading) are the coordinates, respectively, of row (target) i and column (rater) j on dimension t in an *r-dimensional* space ($r \leq rank(\mathrm{X})$) and ε_{ij} is a residual term. Parameters in model (3) can be estimated by singular value decomposition (SVD). To make easier graphical interpretation, rows and columns are usually represented in two dimensions ($r = 2$). In order to render unique the bilinear decomposition of model (3), coordinates a_{it} and b_{jt} can be normalized in different ways. In the symmetric biplot normalization, row and column coordinates are scaled by the square roots of the singular values on respective dimensions. Each column (rater) is represented by a vector (arrow) that identifies a direction (or axis) in the plane. Points representing rows (targets) can be projected along that direction, and the product of the length of the column vector and the length of the obtained projection approximates the values x_{ij}^t in that column.

In order to simplify interpretation of diagrams, we can limit ourselves to compare point projections along column vector directions, because these projections are proportional (according to the vector length) to the corresponding values x_{ij}^t in the columns. The comparison of row point (targets) projections along the direction iden-

tified by column vector (rater) j provides an approximation of the rank order of values x_{ij}^t (or x_{ij}) in column j.

When the global scale is composed of several subscales, it is also worth to compare differences detected in correspondence to each subscale. After applying model (3) to each subscale separately, the comparison can be performed by the resulting diagrams.

4 Descriptive Analysis of Dependence of Agreement by Targets

The level of interrater agreement can depend on targets when raters tend to agree more on assigning rating to some groups of targets respect to other groups. When a global scale is composed of several subscales, target's dependence can change according to the subscale considered. For the analysis of these aspects, a matrix $\Delta = (\delta_{is})$ can be computed, in which each row corresponds to a target and each column corresponds to a subscale, and the entry δ_{is} is the [0, 1] normalized value of index D defined in (1) obtained for target i in the $(n_T \times n_R)$ matrix of ratings X_s corresponding to the subscale s. Entries of matrix Δ, considered as dissimilarities between targets and subscales, can be represented in a diagram obtained by multidimensional unfolding to help the analysis of the dependence of interrater agreement on targets and subscales.

The multidimensional unfolding model, originally proposed by Coombs [6] for rectangular matrices of preference scores, is given by

$$\delta_{is} = \sqrt{\sum_{t=1}^{r} (a_{it} - b_{st})^2} + \varepsilon_{is} \tag{4}$$

with δ_{is} dissimilarity between row (target) i and column (subscale) s in matrix Δ; a_{it} and b_{st} are the coordinates, respectively, of row i and column s on dimension t in an *r-dimensional* space ($r \leq rank(\Delta)$) and ε_{is} a residual term. We can consider model (4) as the distance version of model (3), with distances replacing inner products. It is worth to notice that the Euclidean distance model usually used in multidimensional scaling (MDS) for square dissimilarity matrices (e.g. Borg & Groenen [1]) is a constrained version of model (4), because for each s it is required $b_{st} = a_{st}$. Iterative algorithms, starting from initial estimates of a_{it}^0, b_{st}^0 (*initial configuration*), iteratively decrease a least squares loss function moving vectors $\boldsymbol{a}_i^0 = \left(a_{i1}^0,\ a_{i2}^0, \ldots, a_{ir}^0\right)$ and $\boldsymbol{b}_s^0 = (b_{s1}^0,\ b_{s2}^0, \ldots, b_{sr}^0)$, until convergence to a minimum value. An important point is picking a good initial configuration, in order to avoid the problem of *local minima* (that means the algorithm did not find the best possible choice for coordinate matrices). Available programmes for unfolding allow to start with many different configurations, so it is possible to check the stability of the estimates obtained, repeating their computations with different starting points.

For an easy visualization of dissimilarities, approximations in a planar display ($r = 2$) are usually computed. So, the distance between the point representing *i-th*

row (e.g. target) and the point representing *s-th* column (e.g. subscale) approximates the corresponding dissimilarity δ_{is} (e.g. interrater agreement for target i respect to subscale s). Hence, when model (4) is applied to a matrix of interrater agreement indices Δ, targets tend to be positioned far from a subscale if they obtained ratings with low levels of interrater agreement. On the contrary, targets are positioned close to a subscale if they obtained ratings with high levels of interrater agreement. Presence of clusters of targets located far from each other in the diagram indicates a possible dependence of interrater agreement by some target features. Subscales located far from each other present different patterns of interrater agreement. Notice that distances within each of the two sets of the row points and the column points are only implicitly defined and do not have corresponding observed entries in matrix Δ. The unfolding model has also been proposed for the analysis of asymmetric pairwise relationships in several fields of application (e.g. Bove & Okada [2]).

5 Application

Some descriptive analyses of interrater agreement are provided applying models (3) and (4) to data obtained in a research concerning the assessment of language proficiency, conducted at the Roma Tre University in 2017 (for details, see Nuzzo & Bove [17]). The main aim of the study was to investigate the applicability of a six-point Likert scale developed by Kuiken and Vedder [12] to texts produced by native and non-native writers, and to three different task types (narrative, instruction and decision-making tasks). The scale comprises four subscales, corresponding to the four dimensions of functional adequacy identified by the authors of the scale: content, task requirements, comprehensibility, coherence and cohesion (the reader is referred to Kuiken and Vedder 2017 for a detailed presentation of subscales and descriptors). Just to give a general idea of the scale, definitions of levels 1 and 6 for the content subscale are reported:

Level 1: 'The number of ideas is *not at all adequate* and insufficient and the ideas are unrelated to each other'.
Level 6: 'The number of ideas is *extremely adequate* and they are very consistent to each other'.

Twenty native speakers of Italian (L1) and twenty non-native speakers of Italian (L2) participated in the study as writers. The 20 native speakers were students of Foreign languages at Roma Tre University. The non-native speakers were 15 foreign students attending a course of history of Italian language at the University of Amsterdam and 5 foreign students of foreign languages at Roma Tre University. All the texts produced by L1 and L2 writers (120 texts in total for the three tasks) were assessed by 7 native speakers of Italian on the Kuiken and Vedder's six-point Likert scale. The raters were female university students of approximately the same age as the writers involved in the study, attending the same faculty (MA level).

Table 1 Values of the d index according to subscales and tasks

	Tasks					
Subscale	Task 1		Task 2		Task 3	
	N	d	N	d	N	d
Content	40	0.36	40	0.34	40	0.36
Task requirements	40	0.33	40	0.31	40	0.34
Comprehensibility	40	0.22	40	0.19	40	0.21
Coherence cohesion	40	0.35	40	0.36	40	0.33

In Table 1, the values of the index d are provided for each subscale in each of the three tasks (task 1—narrative, task 2—instruction, task 3—decision-making). All the subscales show low levels of interrater agreement, with the only exception of the comprehensibility subscale in the second task (instruction task). Hence, model (3) can be considered for analysing differences in rater evaluations in each subscale. The content subscale in the narrative task is considered as an example to show the type of analyses that can be performed.

An R (R Core Team [18]) programme was written to obtain component scores and component loadings of model (3). Figure 1 shows the diagram obtained approximating data in $r=2$ dimensions. The variance accounted for (VAF) by this solution is 75.5% of the total variance in the data matrix. As it was explained in Sect. 3, in the diagram, each writer is represented by a point and each rater is represented by a vector. Ratings x_{ij} are standardized for each rater, and coordinates of the projections of each writer on a rater vector provide the position of the ratings of the writers respect to the mean rating of the rater (that coincides with the origin in the diagram). Positive direction is identified by the arrow at the end of each vector, negative coordinates correspond to ratings less than the mean rating of the rater, positive coordinates correspond to ratings greater than the mean rating.

Besides, positions of projections along the axis generated by a rater vector provide an approximation of the rank order of the ratings that writers obtained by that rater. The approximation will be the more reliable the higher the value of VAF. The value 75.5% obtained for the VAF allows us to be quite confident in the analysis of the biplot diagram depicted in Fig. 1 (some rank order could be not exactly represented however).

To interpret the diagram in Fig. 1, we can consider, for instance, positions of writers labelled 40 and 32 respect to rater vector labelled R5. Projection of writer 32 on the axis generated by rater vector R5 falls far from the origin on the left side of the axis, and so represents one of the lowest rating of rater 5. Projection of writer 40 falls quite far on the right side of the same axis and so represent one of the highest ratings. Then, writer 40 is judged better than writer 32 by rater 5 respect to the subscale content in the narrative task, which means the text produced by writer 40 in the narrative task is considered by rater 5 more adequate and consistent than the text produced by writer 32. Rater 3 instead assigns the same rating to texts of writers 40

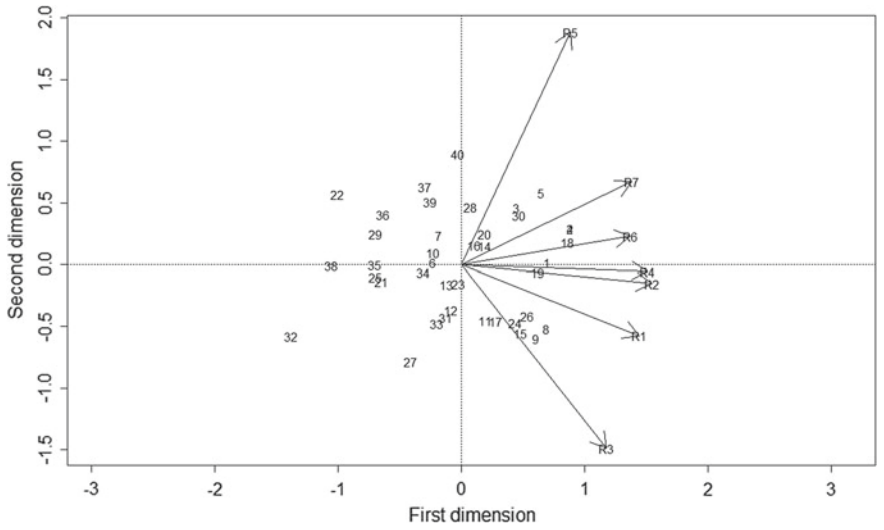

Fig. 1 Biplot of writers and raters for content subscale in the narrative task

and 32, so projections of writers 40 and 32 on the axis generated by rater vector R3 have coordinates very similar.

Overall, projections of writer 32 on the axes generated by the rater vectors have low coordinate values that indicate low ratings on the subscales. The opposite happens, for instance, for writer 18, with all projections having positive values, which means she is judged always better than the average of the writers group and better than many other writers.

Hence, the positions of vectors shown in Fig. 1 can be compared to analyse dependence of agreement by raters. Vectors labelled R2 and R4 are almost collinear, which means very similar ratings are provided by rater 2 and rater 4 for the writers on the content subscale (and so very high level of interrater agreement). This is not the case for rater 3 and rater 5 which, in many cases, provide different ratings for the same writers, as it was shown for writers 40 and 32, and provide different rank orders for the whole group of writers.

Diagram for subscale comprehensibility in the narrative task is provided in Fig. 2. VAF for this result was 83.4%. From Table 1, we can observe that interrater agreement is higher for this subscale ($d = 0.22$) than in the content subscale ($d = 0.36$), and this is reflected in the size of the angle determined by rater vectors in the extreme positions. In fact, the angle between R3 and R5 in Fig. 1 is a bit larger than the angle between R2 and R5 in Fig. 2. Besides, if we look for collinearity between vectors (remember that perfect interrater agreement means collinearity and same length of corresponding vectors), we find only vectors R2 and R4 almost collinear in Fig. 1, but we find two pairs of almost collinear vectors in Fig. 2 (R5–R6 and R3–R7).

For the analysis of the dependence of the level of interrater agreement on writers, for each task model (4) was applied to the dissimilarity matrix Δ of normalized

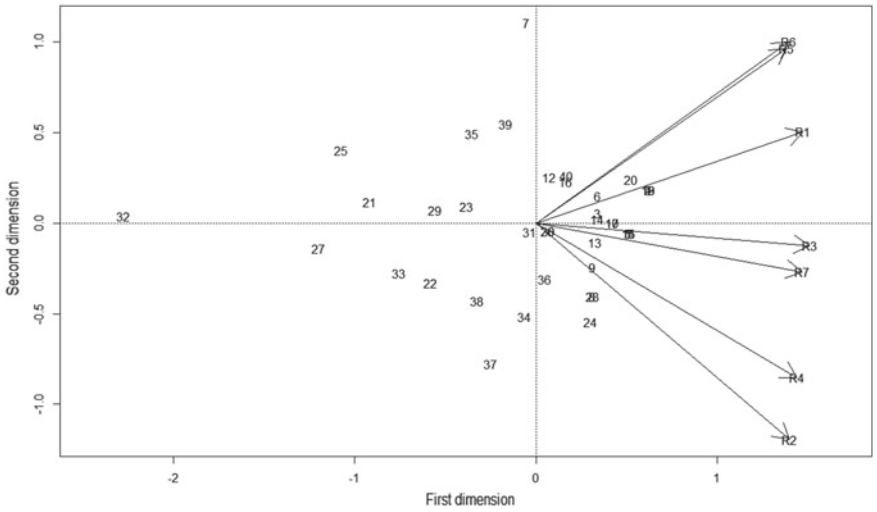

Fig. 2 Biplot of writers and raters for the comprehensibility subscale in the narrative task

value of index *D* defined in (1). The diagram obtained with PREFSCAL programme available in IBM-SPSS (see Busing, Groenen, & Heiser [5]; IBM Corp. Released [10]) is shown in Fig. 3, where numbers represent writers and letters represent the subscales (Stress-I = 0.16). Markers for each writer represent native (L1) or non-native (L2) category for the language variable. According to the unfolding model properties, the writers tend to be closer to the subscale for which they have higher level of interrater agreement in the task. For instance, writer 4 is close to comprehensibility subscale (COM) for which the normalized value of index *D* is zero (all the raters provide the same ratings to writer 4 on this subscale). On the contrary, writer 4 is positioned far from subscale coherence and cohesion (COE) because the normalized value of index *D* is high (0.37).

Comparing distances of writers from subscales content (CON), comprehensibility (COM) and task requirements (REQ), markers of native speakers of Italian (circles) result closer than markers of non-native speakers of Italian (squares). The contrary happens for the coherence and cohesion subscale (COE). This seems to indicate a certain dependence of agreement by writers language in the narrative task. Hence, a comparison of the level of dispersion of ratings of native and non-native speakers of Italian revealed that the scale was not very effective to differentiate proficiency levels among native speakers, especially for the comprehensibility subscale for which raters used only the higher two or three levels of the rating.

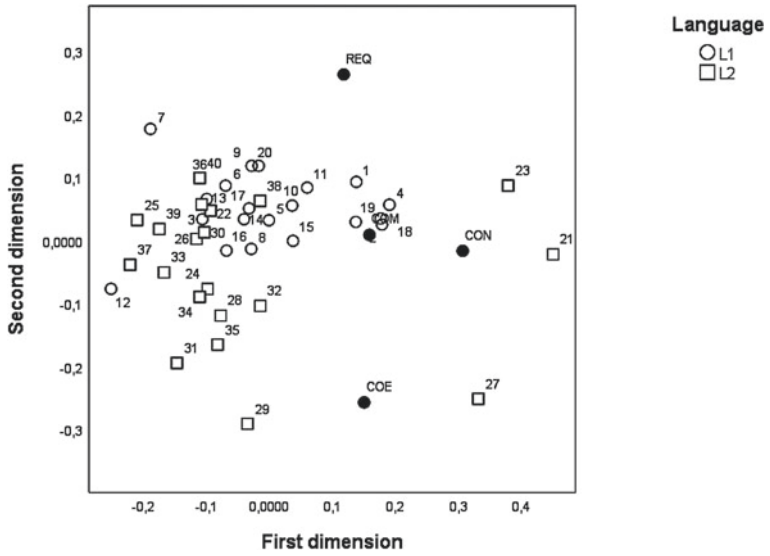

Fig. 3 Unfolding of the dissimilarity matrix of d indices for the narrative task

6 Conclusions

In this study, a measure of interrater absolute agreement for ordinal rating scales was presented capitalizing on the dispersion index for ordinal variables proposed by Leti [15]. The measure is not affected by the restriction of variance problem like intraclass correlation coefficients and other measures widely used. It was shown how descriptive analyses performed by multivariate techniques based on bilinear and multidimensional unfolding models can help to suggest possible explanations for low levels of interrater agreement found in the application. An application to data concerning the assessment of language proficiency allowed to highlight the capabilities of the proposed procedures. The biplot diagrams showed differences between raters respect to the subscales, and the dependence of the level of interrater agreement by the mother language of the writers was detected in the unfolding diagram. The level of interrater agreement was lower for non-native speakers than for native speakers in three subscales. The higher level of interrater agreement for native speakers was obtained with the comprehensibility subscale. For this subscale, the analysis of the dispersion of ratings showed that the scale was not effective to differentiate proficiency levels among native speakers because ratings were concentrated only on the higher levels of the scale. This result suggests that in order to gain a more balanced picture of the language proficiency, further investigations should take into account texts that are likely to be distributed along the whole scale for native speakers.

References

1. Borg, I., & Groenen, P. J. F. (2005). *Modern multidimensional scaling. Theory and applications* (2nd ed.). Springer.
2. Bove, G., & Okada, A. (2018). Methods for the analysis of asymmetric pairwise relationships. *Advances in Data Analysis and Classification*, *12*(1), 5–31.
3. Bove, G., Nuzzo, E., & Serafini, A. (2018). Measurement of interrater absolute agreement for the assessment of language proficiency. In S. Capecchi, F. Di Iorio, & R. Simone (Eds.),*ASMOD 2018: Proceedings of the Advanced Statistical Modelling for Ordinal Data Conference* (pp. 61–68). FedOAPress.
4. Bove, G., Conti, P. L., & Marella, D. (2019). Sampling properties of an ordinal measure of interrater absolute agreement. (submitted for publication). arXiv:1907.09756.
5. Busing, F. M. T. A., Groenen, P. J. F., & Heiser, W. J. (2005). Avoiding degeneracy in multidimensional unfolding by penalizing on the coefficient of variation. *Psychometrika*, *70*(1), 71–98.
6. Coombs, C. H. (1964). *A theory of data*. Wiley.
7. Gabriel, K. R. (1971). The biplot graphic display of matrices with application to principal component analysis. *Biometrika*, *58*(3), 453–467.
8. Gower, J. C., Lubbe, S., & Le Roux, N. (2011). *Understanding biplots*. Wiley.
9. Greenacre, M. J. (2010). *Biplots in practice*. BBVA Foundation.
10. IBM Corp. Released (2017). *IBM SPSS Statistics for Windows* Version 25.0. IBM Corp.
11. Grilli, L., & Rampichini, C. (2002). Scomposizione della dispersione per variabili statistiche ordinali [Dispersion decomposition for ordinal variables]. *Statistica*, *62*(1), 111–116.
12. Kuiken, F., Vedder, I. (2017). Functional adequacy in L2 writing. Towards a new rating scale. *Language Testing*, *34*(3), 321–336.
13. LeBreton, J. M., Burgess, J. R. D., Kaiser, R. B., Atchley, E. K., & James, L. R. (2003). The restriction of variance hypothesis and interrater reliability and agreement: Are ratings from multiple sources really dissimilar? *Organizational Research Methods*, *6*(1), 80–128.
14. LeBreton, J. M., & Senter, J. L. (2008). Answers to 20 questions about interrater reliability and interrater agreement. *Organizational Research Methods*, *11*(4), 815–852.
15. Leti, G. (1983). Statistica descrittiva [Descriptive Statistics]. *Il Mulino*.
16. McGraw, K. O., & Wong, S. P. (1996). Forming inferences about some intraclass correlation coefficients. *Psychological Methods*, *1*(1), 30–46.
17. Nuzzo, E., & Bove, G. (2019). Assessing functional adequacy across tasks: A comparison of learners' and native speakers' written texts. (submitted for publication).
18. R Core Team (2019). *R: A language and environment for statistical computing. R Foundation for Statistical Computing*. http://www.R-project.org/.
19. Shrout, P. E., & Fleiss, L. (1979). Intraclass correlations: Uses in assessing reliability. *Psychological Bullettin*, *86*(2), 420–428.
20. von Eye, A., & Mun, E. Y. (2005). *Analyzing rater agreement: Manifest variable methods*. Lawrence Erlbaum Associates.

The Globality of Brands—A Question of Methods?

Michael Löffler and Reinhold Decker

Abstract To develop a successful global brand strategy, a profound understanding of consumers' perceptions about the brand in the main markets or countries is needed. Measuring the image of global brands includes at least two challenges. First, the market researcher has to select an appropriate method, knowing that different methods may yield different outcomes. Second, measuring the image of global brands differs categorically from measuring the image of local ones, as the global perspective requires measuring the brand image in diverse markets that may differ according to various cultural and socioeconomic characteristics. To meet these challenges, this paper proposes a two-factor approach, including a combination of the factors "method" and "country." The data used for illustration purposes were collected in three leading target countries using a multi-method approach, including the free association method, the brand concept maps (BCM) method, and a user-generated content (UGC) method. Multiple correspondence analysis (MCA) shows how the two-factor approach enables the uncovering of method and country effects and how the suggested procedure leads to a holistic picture of the global brand image.

Keywords Brand associations · Brand image measurement · Correspondence analysis · Global brands · Multi-method approach

1 Introduction

In an increasingly dynamic world economy, many companies engage in global branding in order to reach new customers and, thereby, increase sales, profits, and market shares (Keegan & Green [31]). Especially in the automotive sector, nearly all premium brands, such as Audi, BMW, Jaguar, Lexus, and Porsche, act globally.

M. Löffler (✉)
Dr. Ing. h.c. F. Porsche AG, Porscheplatz 1, D-70435 Stuttgart, Germany
e-mail: michael.loeffler@porsche.de

R. Decker
Department of Business Administration and Economics, Bielefeld University, Universitätsstraße 25, D-33615 Bielefeld, Germany
e-mail: rdecker@uni-bielefeld.de

T. Imaizumi et al. (eds.), *Advanced Studies in Behaviormetrics and Data Science*,
Behaviormetrics: Quantitative Approaches to Human Behavior 5,
https://doi.org/10.1007/978-981-15-2700-5_23

Furthermore, competition among companies on a global scale has become increasingly intense with the growing pace of globalization (Chabowski & Mena [6]). In this highly competitive landscape, an understanding of consumers' thoughts and feelings about brands of interest in different target markets is needed to develop a successful strategy for building and managing a strong brand globally.

However, measuring brand image, in particular that of global brands, includes at least two challenges. First, the market researcher has to select from various options to measure brand image. In their extensive review of brand image measurement methods, Plumeyer, Kottemann, Böger, and Decker [52] identified 12 methods that were applied at least twice in prior studies and, beyond these, 18 additional methods. Accordingly, the methods to measure brand images have to be selected carefully. Second, measuring the image of global brands differs categorically from measuring the image of local brands. The global perspective requires measuring the brand image in diverse markets with different cultural and socioeconomic characteristics. Although prior research has suggested that consumer constructs across countries should be measured via methods that are not prone to country-dependent results (e.g., Löffler [43]), it is still unclear how to identify the country effects of brand perceptions.

To meet these challenges, this paper[1] proposes a two-factor approach, including a combination of the factors "method" and "country." More precisely, our approach comprises three well-established state-of-the-art methods for brand image measurement, namely, the free association method (e.g., Batra & Homer [1]), the brand concept maps (BCM) method (e.g., John, Loken, Kim, & Monga [30]), and a user-generated content (UGC) method (e.g., Gensler, Völckner, Egger, Fischbach, & Schoder [21]). In the present paper, we suggest a two-stage procedure, whereby the data are collected using a multi-method approach applied to different countries (i.e., the data collection stage) and are then aggregated to yield a holistic representation of the brand image (i.e., the data aggregation stage). This multi-method approach is in line with most recent suggestions in addressing complex research questions: In their paper about the meaning and the goals of data science, Emmert-Streib, Moutari, and Dehmer [19] emphasize that "there is not just one method that allows answering a complex, domain specific question," but in particular "the consecutive application of multiple methods allows achieving this." By using multiple methods and countries, this procedure can help to identify method and country effects of brand associations and, thus, determine whether varying brand image outcomes actually result from varying perceptions across countries.

In an empirical application, three measures were conducted in China, Germany, and the United States with 2,764 carefully selected respondents in total, resulting in nine empirical studies that share similarities as well as differences. While the methods share some core associations across countries, they complement each other by revealing additional associations that do not occur in all studies. Multiple correspondence analysis (MCA) is used in the second stage to show how the two-factor approach: (a) enables the uncovering of method and country effects of brand

[1]The authors would like to thank Dr. Anja M. Plumeyer for her valuable and comprehensive contribution to an earlier version of this paper.

associations; and (b) offers a holistic picture of the global brand, if existent. Thus, brand managers can direct their marketing efforts based on those associations that are, more or less, equally important for all target countries as part of a standardization strategy, and they can address country-specific associations if, for example, cultural differences require specific adjustments. The visual representation enabled by MCA allows marketers to identify important brand associations at a glance and to assess associations according to their appearance in methods and countries.

The remainder of the paper is organized as follows: In Sect. 2, the research background is presented, followed by a description of the two-factor approach in Sect. 3. Then, in Sect. 4, the usefulness of the suggested two-stage procedure is demonstrated in an empirical application. Finally, Sect. 5 provides concluding remarks and possible directions for future research.

2 Research Background on Brand Image Measures

Keller [32] defined "brand image" as consisting of consumers' perceptions about a brand, reflected by brand associations. As such, brand image is a key element of customer-based brand equity, and it is composed of specific types and dimensions of brand associations (in particular, favorability, strength, and uniqueness). Prior research features various methods for measuring brand image. For example, among others, Likert scales (e.g., Cretu & Brodie [9]), semantic differential scales (e.g., Hosany, Ekinci, & Uysal [26]), focus groups (e.g., Bian & Moutinho [3]), in-depth interviews (e.g., Thompson, Rindfleisch, & Arsel [59]), and projective techniques (e.g., Hogg, Cox, & Keeling [24]) have been used in studies measuring brand image (see Plumeyer et al. [52], for a recent overview).

Although in the last decades, many studies have investigated global brands, only some, such as Roth [54–56], Hsieh [27], Hsieh, Pan, and Setiono [28], and Park and Rabolt [51], have examined global brand images (see Table 1 for an overview). However, none of these studies focused on measuring brand images across countries but, instead, investigated the interplay of brand image and other variables. Moreover, they dealt with an aggregated form of brand image that was abstracted and usually limited to two or three dimensions. This might be highly suitable for experimental designs, but it does not fully reflect Keller's [32] conceptualization of brand image as brand associations that consumers have in mind. In contrast to the abovementioned studies, this paper focuses on brand image measurement in the global context by proposing a two-factor approach to capture the global brand image in a more holistic way.

To empirically compare the outcomes of brand image measurement methods, prior research has predominantly focused on the stability of brand associations. Table 2 provides a synoptic overview of corresponding research activities. In contrast to these previous studies, the current study indirectly compares the free association, the BCM method, and the UGC method by examining the method effects of brand associations in a two-stage procedure. The measures across countries do not rely on the same set of brand associations, as this proceeding is less suitable for depicting countries' distinctive perceptions.

Table 1 Overview of studies to investigate global brand image

Objective	Brand image measurement	Aggregation of brand associations	Direct country comparison
Roth [55] investigated the influence of brand image strategies on market shares in 10 countries and studied moderating effects on brand image strategy performance	Rating of brand image strategies (functional, social, sensory); no measurement of brand associations	Aggregated perspective	No
Hsieh [27] investigated, among other topics, whether the pattern of brand image dimensionality is similar across global markets (in 20 countries)	Focus groups identified 14 brand associations to be evaluated	Brand associations were aggregated into three dimensions (utilitarian, symbolic, sensory)	No
Hsieh et al. [28] investigated the effects of different dimensions of brand image on purchase behavior across 20 countries	Focus groups identified 17 brand associations to be evaluated via dichotomous measures	Brand associations were aggregated into three dimensions (utilitarian, symbolic, sensory)	No
Park and Rabolt [51] investigated cultural and consumption value as antecedents of global brand image in two countries	Semantic differential scaling based on 24 brand associations	Two factors of brand image (i.e., trendy, refined) were extracted after eliminating 11 associations	No
This paper proposes a two-stage procedure to measure global brand image and to draw a more holistic picture	Free association method, BCM method, and UGC method	Aggregation still differentiated 57 brand associations	Yes

Combining brand image measurement methods is not new (Plumeyer et al. [52]). The use of multi-methods can frequently be observed with studies integrating Likert scales and preceding methods for eliciting brand associations directly from consumers, such as the free association method (e.g., Danes, Hess, Story, & Vorst [11]; Lange & Dahlén [38]), focus groups (e.g., Bian & Moutinho [2]; Power, Whelan, & Davies [53]), and in-depth interviews (e.g., Cho, Fiore, & Russell [8]; Michel & Rieunier [46]). Semantic differential scales have similarly been used in combination with the free association method (e.g., Batra & Homer [1]; Low & Lichtenstein [44]). Scaling methods require predetermined brand associations, which makes the integration of preceding and subsequent procedures a natural consequence of the measurement task to be solved. However, to the best of the authors' knowledge, no study has previously combined brand image measurement methods as we do in the following.

Table 2 Overview of studies to compare brand image measures

Authors	Methods compared	Results	Same set of brand associations
Driesener and Romaniuk [18]	Rating, ranking, and free-choice measures	The three measures are highly correlated, and individuals utilize them in a consistent manner	Yes
Dolnicar and Rossiter [16]	Free-choice measures held one week apart	Low stability is partly caused by the prevailing methods used in market research, which can often lead consumers to construct temporary associations	Yes
Koll, von Wallpach, and Kreuzer [36]	Free association, storytelling, and collages	Each method is suitable for tapping and reproducing different aspects of brand knowledge	No
Dolnicar, Rossiter, and Grun [17]	Free-choice, forced-choice binary measures, semantic differential scales	The forced-choice measure is found to outperform the free-choice measure and the semantic differential scale measure due to its higher stability	Yes
This paper	Free association, BCM method, and UGC method conducted in three countries	Indirect comparison by detecting the method and country dependence of brand associations using MCA	No (in total, a set of 57 brand associations was considered)

3 Two-Factor Approach to Capture Global Brand Images

3.1 Overview

In the following, we suggest a two-factor approach to capture a holistic picture of the global brand image. The first factor is the method used to measure the brand image, and the second factor is the country in which the measurements are conducted. To adequately account for the global perspective of brand image, it is essential to measure brand image in the main target countries. Accordingly, this two-factor approach is embedded in a two-stage procedure: In the data collection stage, multiple methods

are used in different countries to collect a set of brand associations as complete as possible. In the subsequent data aggregation stage, the collected data are then aggregated by means of MCA to obtain a visual representation that reveals the method and country effects of brand associations.

3.2 Identification of Brand Image Measurement Methods

Brand image measurement methods can be classified, among others, according to data origin and association origin (Gensler et al. [21]). In this regard, both primary data (e.g., survey data) and secondary data (e.g., UGC) can be used to measure brand image. Especially when methods differ in the origin of their associations, they are likely to yield complementary outcomes in terms of whether and how often a certain association is mentioned. The methods focused on in this paper were selected because they cover a wide range of different aspects of brand image measurement.

The free association method is frequently used to measure brand image as it is "extremely powerful and provides insights beyond survey responses" (Danes et al. [11, p. 290]). Respondents are presented a stimulus (e.g., a brand name) and asked to name or write down everything that spontaneously comes to mind regarding it (Boivin [5]). Thus, the free association method has a remarkable tradition in research and applications (Levy [40]; Stern, Zinkhan, & Jajau [57]) and is a simple and straightforward method for eliciting consumers' easily accessible verbalized associations with brands.

John et al. [30] introduced the BCM method as a powerful tool for measuring brand images by identifying meaningful brand associations and revealing the underlying associative network structure. In general, the BCM method contains three subsequent steps: elicitation, mapping, and aggregation. First, a pre-test or previous research results are used to identify a list of salient brand associations. Then, respondents are requested to design individual brand maps for the brand of interest, using the predetermined brand associations. Finally, the individual brand maps can be aggregated into a so-called consensus map based on a set of standardized rules. The resulting consensus map shows which of the brand associations, on average, are the most salient ones. In the last decade, the BCM method has proven useful for measuring the images of different types of brands (see, e.g., French & Smith [20]; Kottemann, Plumeyer, & Decker [37]; Zenker & Beckmann [63]).

The increasing use of social media platforms has led to an enormous amount of content being shared every day (Chaffey [7]). By doing so, consumers are providing a new source of data that is easily accessible in real time and potentially relevant for measuring brand images. Brand-related UGC offers insights into what consumers think and feel about brands and provides the opportunity to "track the hearts and minds of [...] consumers" (Swaminathan [58, p. 37]). Up to now, several studies have concentrated on extracting brand associations from different types of UGC, including product reviews (Decker & Trusov [12]; Gensler et al. [21]; Lee & Bradlow [39]; Tirunillai & Tellis [60]), consumer messages from forums (Netzer, Feldman, Goldenberg, & Fresko [50]), social tags (Nam & Kannan [47]; Nam,

Table 3 Profile of brand image measurement methods

	Free association	BCM	UGC
Data origin	Survey data	Survey data	Web posts
Associations	Free	Predetermined	Extracted
Standardization	Low	High(er)	No

Joshi, & Kannan [48]), social connections on Twitter (Culotta & Cutle [10]), tweets (Liu, Burns, & Hou [42]), and Instagram posts (Klostermann, Plumeyer, Böger, & Decker [35]). The de facto availability of UGC-based brand information at any time enables the dynamic creation of brand images, which, in turn, enables continuous brand monitorings.

Since the three methods differ regarding their degree of standardization ("no standardization" with the UGC method, "low standardization" with the free association method, and "high(er) standardization" with the BCM method), they are likely to reveal outcomes that are potentially complementary. Table 3 summarizes the profile of the three methods selected in this paper.

3.3 Identification of Target Countries

While we propose three particular methods to be integrated into our two-factor approach, we cannot generally propose a particular set of countries, since the countries to be considered should be selected depending on the brand. Especially for target countries that differ according to important consumer characteristics, such as cultural dimensions (see, e.g., De Mooij & Hofstede [14]), an integrative consideration may yield interesting results.

4 Empirical Application

4.1 Stimulus and Country Selection

For this study, automobiles were selected as the research object for several reasons. Automobiles are highly engineered and sophisticated products, and they provide an emotional connection with image and fashion and offer experiential satisfaction (Lienert [41]). Furthermore, they require large expenditures by both agents, the customer and the company (Kirmani & Zeithaml [33]). In this risky environment, which usually involves extensive decision-making, understanding the brand image is important for automotive marketers, as it is a decisive purchasing factor for automobiles (De Mooij [13]). Moreover, automobiles have frequently been used as examples of high-involvement products in empirical studies, especially in cross-cultural studies (e.g., Löffler [43]). The premium brand Porsche was selected because it is glob-

ally well known (Interbrand [29]) and implements standardized marketing strategies across the global market. Focusing on a specific segment within the automotive sector follows the recommendation of Verhoef, Langerak, and Donkers [62], which is to consider the distinctness of different brand tiers (i.e., economy, volume, and premium brands). Geographically, Asia, North America, and Western Europe are the world's largest car markets. Within these areas, China, the United States, and Germany account for the highest numbers of car sales. Furthermore, according to Ueltschy, Laroche, Eggert, and Bindl [61], the cultural diversity of these countries allows for insightful cross-cultural research.

4.2 Respondents

Sampling has proven to be a serious challenge for conducting fieldwork, but it can lead to results that are more reliable (Hooghe, Stolle, Mahéo, & Vissers [25]). This is particularly true regarding premium brands in durable goods markets, such as the automotive market. To face this challenge, the respondents taking part in both the free association and the BCM methods were carefully recruited and were required to pass a comprehensive pre-study screening. Qualifying criteria included, among others, the ownership of a premium automobile brand to ensure respondents' first-hand experience. This is important, as prior research has shown that brand ownership can have an effect on brand evaluations (e.g., Kirmani, Sood, & Bridges [34]). Consequently, our empirical application relies on real premium car drivers instead of convenience samples. For the UGC method, such a criterion could not be examined, as typically no data exist concerning the characteristics of the authors of product reviews and chat posts. However, as reviews document real product experiences, it was assumed that their authors were either owners or had at least extensively tested a Porsche automobile.

4.3 Data Collection

According to our two-factor approach, a series of empirical studies was conducted using the three methods in three countries to capture the global brand image. Each method was carried out in China, Germany, and the United States, generating a 3 (free association method, BCM method, UGC method) x 3 (China, Germany, United States) design.

For the free association method, the data were collected through an online questionnaire. Respondents were asked to write down everything that came to mind when they thought about the Porsche brand.

The BCM method was implemented as described by John et al. [30], but an online application was used, since Meißner, Kottemann, Decker, and Scholz [45] recently emphasized the potential benefits of computer-based brand concept mapping. To identify predetermined brand associations for the mapping phase of the method, initial pre-tests were performed that included 1,642 respondents in the three countries

from the same population that took part in the main study. From this pre-test, the top 25 brand associations for each country were selected.

For the UGC method, online platforms for sporty automobiles were examined that enabled comparisons between China, Germany, and the United States. Consequently, product reviews were collected from three online platforms in China, Germany, and the United States. A team of three independent researchers examined the unstructured reviews and extracted the main brand associations that appeared within them. In contrast to the free association and the BCM methods, the data collected via the UGC method did not offer precise information on respondents' countries of origin. Therefore, it is assumed that the language spoken in the product reviews reflected the country of origin.

4.4 Descriptive Results

For the free association method, a final sample of N = 1,871 respondents was achieved (NCN = 587; NGER = 669; NUS = 615). The BCM method had a final sample of 156 respondents (NCN = 43; NGER = 47; NUS = 66), and for the UGC method, a final sample of 737 respondents was achieved (NCN = 498; NGER = 93; NUS = 146). To gain an overview of the outcomes of the three methods, Table 4 depicts the top 10 frequencies of brand associations mentioned for each method and each country.

Table 4 shows that isolated considerations across countries or across methods may lead to the conclusion that both country and method effects exist and, therewith, that the identification of the global brand image lying behind is hardly possible. However, at the same time, it also indicates that multiple methods are needed in order to uncover the obviously multifaceted set of relevant associations. Therefore, multiple correspondence analysis (MCA) (see, e.g., Nenadić & Greenacre [49] as well as Blasius & Greenacre [4] for methodological details) is used in the following to detect possible method and country effects. According to Di Franco [15, p. 1307], MCA "possesses excellent descriptive powers, since it allows one to examine the simultaneous interaction of many variables by exploring their direct links," taking advantage of the fact that (p. 1305) "the distance between two or more categories of different variables can be interpreted in terms of the associations existing between them."

4.5 Brand Image Representation Using MCA

Altogether, 57 brand associations, including all brand associations that made up the top 25 brand associations for the nine studies, are considered. The top 25 are chosen in order to depict a comprehensive image of the brand associations and because the BCM method, in line with common practice, comprised 25 predetermined brand associations.

Table 4 Top 10 brand associations

Free association		BCM		UGC	
Association	Ratio of mention	Association	Ratio of mention	Association	Ratio of mention
China					:
Classy/noble	0.36	Sports car	0.77	Design	0.38
Luxurious	0.25	911	0.67	Handling	0.28
Fashionable driver	0.18	High-priced	0.63	Convenience	0.27
Attractive design	0.17	Handling	0.63	Speedy	0.26
Sports car	0.16	Sportiness	0.60	Powerful	0.21
Speedy	0.13	Status symbol	0.60	Space (narrow)	0.20
Superior/premium	0.11	Performance	0.56	Sports car	0.19
Cool	0.08	Speedy	0.53	Economic efficiency	0.17
Good price-value	0.08	Made in Germany	0.51	Desirable	0.17
Desirable	0.07	Quality	0.51	911	0.15
Germany					:
Sporty	0.54	911	0.79	Mileage	0.51
Speedy	0.25	Sports car	0.70	Price	0.45
Design	0.20	Sportiness	0.68	Driving pleasure	0.32
Good price-value	0.20	High-priced	0.57	Performance	0.32
Quality	0.20	Prestige	0.53	Design	0.29
High-priced	0.19	Exclusiveness	0.53	Sound	0.28
Good brand image	0.13	Design	0.51	Processing	0.25
Brand tradition	0.11	Quality	0.51	Speedy	0.24
Exclusive	0.10	Good brand image	0.49	Quality	0.23
Reliability	0.10	Driving pleasure	0.49	Pract. for every day	0.18
United States					:
Design	0.31	High-priced	0.82	Handling	0.35
Quality	0.31	Performance	0.76	Design	0.24
Sporty	0.30	Sports car	0.74	Speedy	0.21
Speedy	0.28	Design	0.71	Driving pleasure	0.21
High-priced	0.23	Sportiness	0.70	Performance	0.20
Reliable engine	0.23	Quality	0.68	Powerful	0.20
Good price-value	0.20	Made in Germany	0.65	Price	0.18
Handling	0.17	Driving pleasure	0.65	Mileage	0.16
Reliability	0.13	Prestige	0.64	Love	0.16
Driving pleasure	0.11	Good brand image	0.61	Quality	0.16

4.5.1 Discussion of Results

Figure 1 depicts the two-dimensional MCA solution for the methods, countries, and brand associations (see, e.g., Hoffman & de Leeuw [23] for a comprehensive discussion on the interpretation of MCA maps). Each brand association is coded according to its presence and absence. MCA usually displays two label points for each association–one point for presence and one for absence. Figure 1, however, depicts label points for only the presence of brand associations, as the label points reflecting their absence accumulate around the origin and, thus, provide no meaningful information. The results describe two-way associations rather than one-way causality by positioning methods and countries relative to the associations and vice versa. The first principal axis explains 66.3% of the principal inertia, and the second principal axis explains 15.5%, leading to an acceptable 81.8% in total. Of the remaining principal axes, none explained more than 3.1%. These results indicate that a good approximation of the data is achieved by the two-dimensional MCA solution. Tendentially, the horizontal axis might be interpreted as reflecting method effects, and the vertical axis seemingly reflects country effects. However, the correspondence of methods and countries to the brand associations is more relevant.

Figure 1 reveals that the three methods have a larger deviation around the origin (indicated by the dashed line) than do the three countries (indicated by the solid line), which are positioned closer to the origin. This indicates a stronger relationship between methods and the mentioning of brand associations than between countries and the mentioning of brand associations. Some associations accumulate around the methods, indicating that these associations were exclusively mentioned in the corresponding method.

As can be seen, the associations “Cayenne,” “European brand,” “high-priced,” “made in Germany,” “Panamera,” and “Mission E” are placed close to the BCM label point at the top left. These brand associations were exclusively named in the BCM method. Associations predominantly mentioned in the UGC method (in particular, “classic,” “mileage,” “perfect,” “price,” “processing,” “sound,” “space,” and “defect”) are grouped around the UGC label point. Additionally, associations are spread among two or three methods to reflect in which methods the associations were mentioned. For instance, associations predominantly mentioned in the BCM and the UGC methods, such as “911,” “fascination,” “joy of living,” “performance,” and “sportiness,” are positioned between the BCM and the UGC methods. The three countries are portrayed closer to the origin, indicating that they do not discriminate as clearly as the methods do. Spreading along the vertical axis, the second dimension of the MCA reflects the country in which an association was mentioned. The countries Germany and the United States are arranged closely together, indicating a higher number of associations named in both countries. The positioning of China apart from Germany and the United States suggests that China has a smaller overlap of brand associations with the other two countries. This is confirmed by the brand image measures, where China received nine exclusively mentioned brand associations, while Germany and the United States each had three exclusively mentioned brand associations. All in all, this deduction should not be overrated, since only the

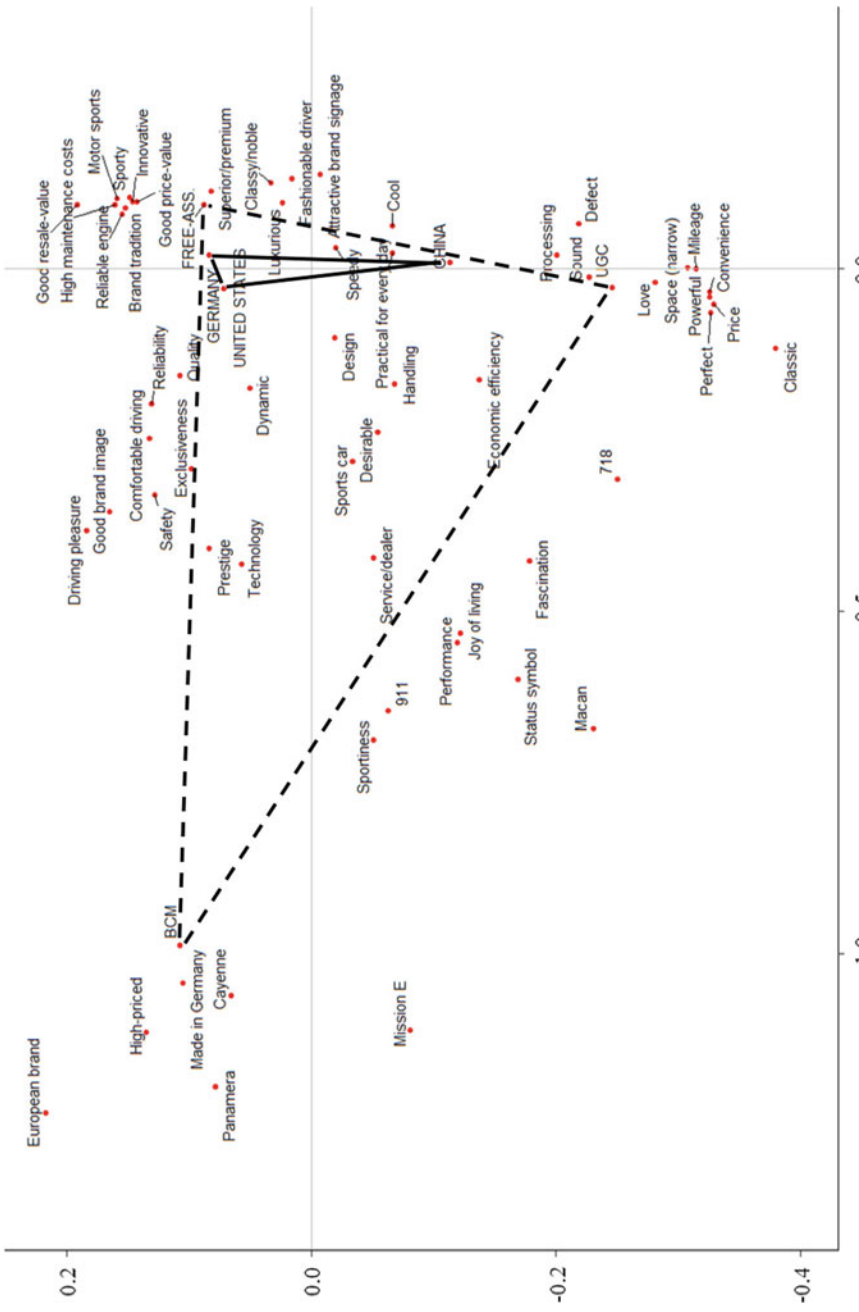

Fig. 1 Configuration of brand associations based on MCA

points lying away from the center of the map should be used as reference points for in-depth interpretations (Greenacre [22]).

In a nutshell, the MCA representation allows for concluding that the country effect can be neglected, with slight limitations with regard to China, whereas there seems to be a remarkable method effect. Accordingly, the "Porsche" brand can be rated as a global brand and, in turn, locality is not a real issue. The MCA shows in relation to which associations the method effect seemingly proves effective, in so far the convex hulls for the countries and the methods (i.e., the two triangles) in the MCA representation can serve as a kind of indicator of a brand's globality and as an indicator of possible methodological effects. The larger the convex hulls, the stronger the respective effect.

4.5.2 Practical Implications

The findings from an academic and rather methodological perspective summarized in Sect. 4.5.1 have been discussed with an international team of senior marketing executives of the automotive industry. The three markets together account for more than two-thirds of the annual sales volume of the underlying brand. The brand is consistently managed internationally following identical brand standards globally. Consistently, the three countries are positioned closely together in Fig. 1.

Some brand attributes have been found to be strongly linked to the underlying method. Most obvious is, for example, the mentioning of "Mission E" (the full-electric Porsche vehicle, later named "Taycan" and presented to the public first in September 2019) in the BCM setup only. From a practitioners' perspective, the finding underlines impressively the strong link between attribute selection and image measurement in the BCM approach. Carefully checking the attributes presented to the participants in advance again turns out to be necessary, and combining multiple approaches was revealed to be beneficial and insightful.

The attributes proprietarily mentioned in the UGC setting and grouped closely around the UGC method in Fig. 1 reflect the peculiarity of this method: the attributes together form less of a holistic brand image, but according to the senior managers, are more the outcome of specific usage, ownership, and driving situations. Among them are typically vehicle servicing, repairs, or classic car maintenance. The UGC method adds to the comprehensive understanding of the brand image but is less recommended as a sole method for brand image measurement.

4.5.3 Validity and Reliability

To gain insights into the suitability of the three data collection methods, we investigated two criteria as a follow-up analysis. On the one hand, we examined convergent validity to examine the degree to which the different methods for measuring the brand image construct provided consistent results. On the other hand, the robustness of the results as measured via split-half resampling was analyzed. The results of

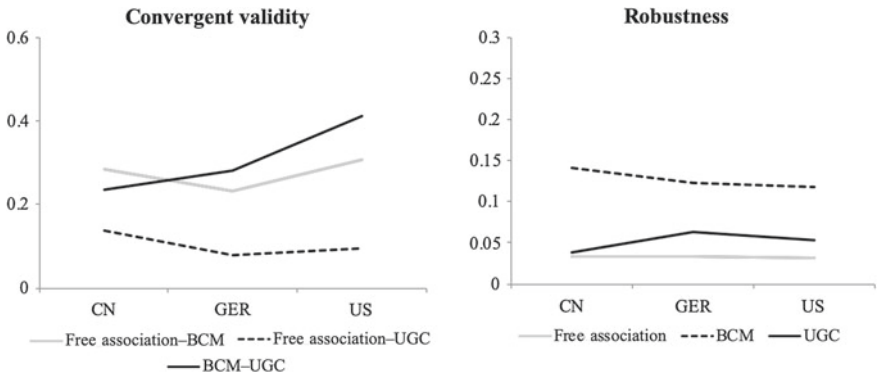

Fig. 2 Validity and robustness of results

each sample were randomly split, and mean correlations between the halves for each association were computed. Both convergent validity and the robustness of results are measured via Cramer's V.

Figure 2 depicts the measures for the convergent validity and the robustness. Concerning convergent validity, the brand images measured by the free association and UGC methods have the lowest measure of Cramer's V, taking the United States as an example. Consequently, the results provided by these methods feature the least differences (i.e., the most consistent results), reflecting an acceptable degree of convergent validity. Brand images measured via the BCM and UGC methods account for the biggest differences in terms of shared associations in the United States. Overall, the results indicate that the methods do not converge perfectly, which would render the multi-method approach redundant. Instead, they reveal differences between the methods that do not cast doubt on the validity of the individual measures but allow enough room to maneuver for a multi-method approach. Therewith, the present analyses confirm the impressions we already had from looking at Fig. 1 and the embedded triangles.

Concerning the robustness of the results, the three methods overall reveal encouraging results as they are characterized by relatively high levels of robustness. Additionally, the robustness appears to be fairly stable across all methods, independent of the country concerned. In sum, the analysis of additional criteria confirms the overall suitability of the multi-method approach.

5 Conclusion and Outlook

This paper proposed a two-factor approach, including a combination of the factors "method" and "country," to study the image of global brands. Using a large-scale empirical application, we demonstrated that only by combining complementary

methods in leading target countries a holistic picture of the global brand image, if it exists at all, can be drawn. The empirical findings have been discussed with an international team of marketing executives in the automotive industry and reveal that by carrying out a multi-method approach, both method and country effects, which are otherwise at risk of being overlooked, can be detected.

The first stage of our procedure (i.e., the data collection stage) requires the use of multiple methods to measure the brand image in the target countries. Three of the more current and frequently used brand image measurement methods—free association, BCM, and UGC—were used to capture Porsche's brand image in China, Germany, and the United States. In doing so, researchers and brand managers can uncover both the breadth and depth of associations connected with the brand of interest in different countries. It was shown that the use of complementary methods can reveal insights that would not have been obtained if a single method had been used.

The empirical example demonstrated that the methods can share core associations (i.e., associations that appear throughout all methods), but at the same time, further associations can be bound to just one method or to a combination of two methods. For example, the BCM method is highly standardized and, therefore, primarily focuses on a given set of brand associations. Thus, the BCM method is more likely to focus on strategic objectives defined, for example, by the brand management. In contrast, the UGC method enables the extraction of associations that refer to the actual use of the product. Moreover, measuring brand image in more than one country yields brand associations that are important across the considered countries, but it also uncovers associations that are predominant in one country. In sum, a high level of coverage regarding significant brand associations can be achieved in this way.

In the second stage (i.e., the data aggregation stage), the visual representation obtained by MCA enables the large variety of information from the nine studies to be managed and, thus, offers a holistic picture of how consumers think and feel about the brand. This holistic picture allows marketers to identify important brand associations at a glance and to assess associations according to their appearance in methods and countries. The empirical application showed that for the brand of interest, Porsche, method effects clearly dominate country effects. In addition to transnational core brand associations, market researchers can also identify desirable or undesirable brand associations for specific countries based on the identified country effects. In the present example, the association "cool" was exclusively mentioned in China (in the free association and UGC methods). By detecting country-dependent associations, the brand management can examine whether brand associations in particular countries go hand-in-hand with the intended positioning of the brand in the corresponding country.

Of course, our study is not free of limitations that directly suggest avenues for future research. As this paper solely demonstrated the usefulness of the two-stage procedure for one well-known brand from the automotive sector, future research should apply the procedure to other brands from this sector as well as to those from different sectors. Interesting findings could also result by switching from durable goods (like cars) to nondurable goods (such as soft drinks). Finally, the two-stage procedure presented does not provide self-explanatory results. The MCA represen-

tation always requires interpretation by persons who know both the target markets and the methods. An interesting alternative to MCA is joint correspondence analysis (JCA), that is, the joint analysis of the off-diagonal submatrices of the Burt matrix. Greenacre [22] discussed practical implications of using JCA instead of MCA, among others, with respect to geometric interpretations.

References

1. Batra, R., & Homer, P. M. (2004). The situational impact of brand image beliefs. *Journal of Consumer Psychology*, *14*(3), 318–330.
2. Bian, X., & Moutinho, L. (2009). An investigation of determinants of counterfeit purchase consideration. *Journal of Business Research*, *62*(3), 368–378.
3. Bian, X., & Moutinho, L. (2011). The role of brand image, product involvement and knowledge in explaining consumer purchase behaviour of counterfeits: Direct and indirect effects. *European Journal of Marketing*, *45*(1/2), 191–216.
4. Blasius, J., & Greenacre, M. (1998). *Visualization of categorical data*. San Diego: Academic Press.
5. Boivin, Y. (1986). A free response method to the measurement of brand perceptions. *International Journal of Research in Marketing*, *3*(1), 11–17.
6. Chabowski, B. R., & Mena, J. A. (2017). A review of global competitiveness research: Past advances and future directions. *Journal of International Marketing*, *25*(4), 1–24.
7. Chaffey, D. (2019). Global Social Media Research Summary 2019. Retrieved September 30, 2019, from https://www.smartinsights.com/social-media-marketing/social-media-strategy/new-global-social-media-research/.
8. Cho, E., Fiore, A. M., & Russell, D. W. (2015). Validation of a fashion brand image scale capturing cognitive, sensory, and affective associations: Testing its role in an extended brand equity model. *Psychology & Marketing*, *32*(1), 28–48.
9. Cretu, A. E., & Brodie, R. J. (2007). The influence of brand image and company reputation where manufacturers market to small firms: A customer value perspective. *Industrial Marketing Management*, *36*(2), 230–240.
10. Culotta, A., & Cutler, J. (2016). Mining brand perceptions from Twitter social networks. *Marketing Science*, *35*(3), 343–362.
11. Danes, J. E., Hess, J. S., Story, J. W.,& Vorst, K., (2012). On the validity of measuring brand images by rating concepts and free associations. *Journal of Brand Management*, *19*(4), 289–303.
12. Decker, R., & Trusov, M. (2010). Estimating aggregate consumer preferences from online product reviews. *International Journal of Research in Marketing*, *27*(4), 293–307.
13. De Mooij, M. (2010). *Consumer behaviour and culture*. London: Sage.
14. De Mooij, M., & Hofstede, G. (2010). The Hofstede model: Applications to global branding and advertising strategy and research. *International Journal of Advertising*, *29*(1), 85–110.
15. Di Franco, G. (2016). Multiple correspondence analysis: One only or several techniques? *Quality & Quantity*, *50*(3), 1299–1315.
16. Dolnicar, S., & Rossiter, J. R. (2008). The low stability of brand-attribute associations is partly due to market research methodology. *International Journal of Research in Marketing*, *25*(2), 104–108.
17. Dolnicar, S., Rossiter, J. R., & Grun, B. (2012). Pick-any measures contaminate brand image studies. *International Journal of Market Research*, *54*(6), 821–834.
18. Driesener, C., & Romaniuk, J. (2006). Comparing methods of brand image measurement. *International Journal of Market Research*, *48*(6), 681–698.

19. Emmert-Streib, F., Moutari, S., & Dehmer, M. (2016). The process of analyzing data is the emergent feature of data science. *Frontiers in Genetics*. Retrieved October 3, 2019, from https://doi.org/10.3389/fgene.2016.00012.
20. French, A., & Smith, G. (2013). Measuring brand association strength: A consumer based brand equity method. *European Journal of Marketing*, *47*(8), 1356–1367.
21. Gensler, S., Völckner, F., Egger, M., Fischbach, K., & Schoder, D. (2015). Listen to your customers: Insights into brand image using online consumer-generated product reviews. *International Journal of Electronic Commerce*, *20*(1), 112–141.
22. Greenacre, M. J. (1991). Interpreting multiple correspondence analysis. *Applied Stochastic Models and Data Analysis*, *7*, 195–210.
23. Hoffman, D. L., & de Leeuw, J. (1992). Interpreting multiple correspondence analysis as a multidimensional scaling method. *Marketing Letters*, *3*(3), 259–272.
24. Hogg, M. K., Cox, A. J., & Keeling, K. (2000). The impact of self-monitoring on image congruence and product/brand evaluation. *European Journal of Marketing*, *34*(5/6), 641–667.
25. Hooghe, M., Stolle, D., Mahéo, V. A., & Vissers, S. (2010). Why can't a student be more like an average person? Sampling and attrition effects in social science field and laboratory experiments. *The Annals of the American Academy of Political and Social Science*, *628*(1), 85–96.
26. Hosany, S., Ekinci, Y., & Uysal, M. (2006). Destination image and destination personality: An application of branding theories to tourism places. *Journal of Business Research*, *59*(5), 638–642.
27. Hsieh, M. H. (2002). Identifying brand image dimensionality and measuring the degree of brand globalization: A cross-national study. *Journal of International Marketing*, *10*(2), 46–67.
28. Hsieh, M. H., Pan, S. L., & Setiono, R. (2004). Product-, corporate- and country-image dimensions and purchase behavior: A multicountry analysis. *Journal of the Academy of Marketing Science*, *32*(3), 251–270.
29. Interbrand (2018). Best Global Brands 2018. Retrieved September 30, 2019, from https://www.interbrand.com/best-brands/best-global-brands/2018/ranking/.
30. John, D. R., Loken, B., Kim, K., & Monga, A. B. (2006). Brand concept maps: A methodology for identifying brand association networks. *Journal of Marketing Research*, *43*(4), 549–563.
31. Keegan, W. J., & Green, M. C. (2015). *Global marketing*. Upper Saddle River, NJ: Pearson.
32. Keller, K. L. (1993). Conceptualizing, measuring, and managing customer-based brand equity. *Journal of Marketing*, *57*(1), 1–22.
33. Kirmani, A., & Zeithaml, V. (1991). Advertising, perceived quality and brand image. In D. A. Aaker & A. L. Biel (Eds.), *Brand equity & advertising: Advertising's role in building strong brands* (pp. 143–161). Hillsdale, NJ: Lawrence Erlbaum Associates.
34. Kirmani, A., Sood, S., & Bridges, S. (1999). The ownership effect in consumer responses to brand line stretches. *Journal of Marketing*, *63*(1), 88–101.
35. Klostermann, J., Plumeyer, A., Böger, D., & Decker, R. (2018). Extracting brand information from social networks. Integrating image, text, and social tagging data. *International Journal of Research in Marketing*, *35*(4), 538–556.
36. Koll, O., von Wallpach, S., & Kreuzer, M. (2010). Multi-method research on consumer-brand associations: Comparing free associations, storytelling and collages. *Psychology & Marketing*, *27*(6), 584–602.
37. Kottemann, P., Plumeyer, A., & Decker, R. (2018). Investigating feedback effects in the field of brand extension using brand concept maps. *Baltic Journal of Management*, *13*(1), 41–64.
38. Lange, F., & Dahlén, M. (2003). Let's be strange: Brand familiarity and ad-brand incongruency. *Journal of Product & Brand Management*, *12*(7), 449–461.
39. Lee, T. Y., & Bradlow, E. T. (2011). Automated marketing research using online customer reviews. *Journal of Marketing Research*, *48*(5), 881–894.
40. Levy, S. J. (2006). History of qualitative research methods in marketing. In R. W. Belk (Ed.), *Handbook of Qualitative Research in Marketing* (pp. 3–17). Northampton: Edward Elgar.
41. Lienert, A. (1998). Brand management: At the big three. *Management Review*, *87*(5), 53–57.

42. Liu, X., Burns, A. C., & Hou, Y. (2017). An investigation of brand-related user-generated content on Twitter. *Journal of Advertising*, *46*(2), 236–247.
43. Löffler, M. (2015). Measuring willingness to pay: Do direct methods work for premium durables? *Marketing Letters*, *26*(4), 535–548.
44. Low, G. S., & Lichtenstein, D. R. (1993). Technical research note: The effect of double deals on consumer attitudes. *Journal of Retailing*, *69*(4), 453–466.
45. Meißner, M., Kottemann, P., Decker, R., & Scholz, S. W. (2015). The benefits of computer-based brand concept mapping. *Schmalenbach Business Review*, *67*(4), 430–453.
46. Michel, G., & Rieunier, S. (2012). Nonprofit brand image and typicality influences on charitable giving. *Journal of Business Research*, *65*(5), 701–707.
47. Nam, H., & Kannan, P. K. (2014). The informational value of social tagging networks. *Journal of Marketing*, *78*(4), 21–40.
48. Nam, H., Joshi, Y. V., & Kannan, P. K. (2017). Harvesting brand information from social tags. *Journal of Marketing*, *81*(4), 88–108.
49. Nenadić, O., & Greenacre, M. (2007). Correspondence analysis in R, with two- and three-dimensional graphics: The ca package. *Journal of Statistical Software*, *20*(3), 1–13.
50. Netzer, O., Feldman, R., Goldenberg, J., & Fresko, M. (2012). Mine your own business: Market-structure surveillance through text mining. *Marketing Science*, *31*(3), 521–543.
51. Park, H. J., & Rabolt, N. J. (2009). Cultural value, consumption value and global brand image: A cross-national study. *Psychology & Marketing*, *26*(8), 714–735.
52. Plumeyer, A., Kottemann, P., Böger, D., & Decker, R. (2019). Measuring brand image: A systematic review, practical guidance and future research directions. *Review of Managerial Science*, *13*(2), 225–265.
53. Power, J., Whelan, S., & Davies, G. (2008). The attractiveness and connectedness of ruth-less brands: The role of trust. *European Journal of Marketing*, *42*(5/6), 586–602.
54. Roth, M. S. (1992). Depth versus breadth strategies for global brand image. *Journal of Advertising*, *21*(2), 25–35.
55. Roth, M. S. (1995a). The effects of culture and socioeconomics on the performance of global brand image strategies. *Journal of Marketing Research*, *32*(2), 163–174.
56. Roth, M. S. (1995b). Effects of global market conditions on brand image customization and brand performance. *Journal of Advertising*, *24*(4), 55–74.
57. Stern, B. B., Zinkhan, G. M., & Jajau, A. (2001). Marketing images: Construct definition, measurement issues, and theory development. *Marketing Theory*, *1*(2), 201–224.
58. Swaminathan, V. (2016). Branding in the digital era: New directions for research on customer-based brand equity. *AMS Review*, *6*(1), 33–38.
59. Thompson, C. J., Rindfleisch, A., & Arsel, Z. (2006). Emotional branding and the strategic value of the doppelgänger brand image. *Journal of Marketing*, *70*(1), 50–64.
60. Tirunillai, S., & Tellis, G. J. (2014). Mining marketing meaning from online chatter: Strategic brand analysis of big data using latent Dirichlet allocation. *Journal of Marketing Research*, *51*(4), 463–479.
61. Ueltschy, L., Laroche, M., Eggert, A., & Bindl, U. (2007). Service quality and satisfaction: An international comparison of professional services perceptions. *Journal of Services Marketing*, *21*(6), 410–423.
62. Verhoef, P., Langerak, P., & Donkers, B. (2007). Understanding brand and dealer retention in the new car market: The moderating role of brand tier. *Journal of Retailing*, *83*(1), 97–113.
63. Zenker, S., & Beckmann, S. C. (2013). Measuring brand image effects of flagship projects for place brands: The case of Hamburg. *Journal of Brand Management*, *20*(8), 642–655.

Mapping Networks and Trees with Multidimensional Scaling of Proximities

Willem J. Heiser, Frank M. T. A. Busing and Jacqueline J. Meulman

Abstract Network methodology typically has two separate stages: (1) constructing a graph from relational data, and (2) drawing the graph on a map to comprehend its structure. Multidimensional scaling (MDS) is discussed as a distance-driven graph drawing method. It is shown that popular drawing methods in computer science that minimize the potential energy of a *spring model* are equivalent to a simple form of MDS without optimal transformation of the graphical distance. They share a weighted least squares loss function (Kruskal's stress). The best way to minimize Stress (Guttman's algorithm) is shown to be a particular force-directed updating scheme in terms of a spring model. With several analyses of two examples (a simple graph and an additive tree), it is shown that using shortest path distances in the graph as input to MDS gives better drawing results than just using its adjacency matrix. Inclusion of data weights in Stress to emphasize good fit of small distances turns out not to be essential. It may even be detrimental to correct representation of line length in a weighted graph.

W. J. Heiser (✉)
Faculty of Social and Behavioral Sciences and Mathematical Institute, Leiden University, Leiden, The Netherlands
e-mail: heiser@fsw.leidenuniv.nl

F. M. T. A. Busing
Faculty of Social and Behavioral Sciences, Leiden University, Leiden, The Netherlands
e-mail: busing@fsw.leidenuniv.nl

J. J. Meulman
Mathematical Institute, Leiden University, Leiden, The Netherlands

Department of Statistics, Stanford University, Stanford, CA, USA
e-mail: jmeulman@math.leidenuniv.nl; jmeulman@stanford.edu

T. Imaizumi et al. (eds.), *Advanced Studies in Behaviormetrics and Data Science*,
Behaviormetrics: Quantitative Approaches to Human Behavior 5,
https://doi.org/10.1007/978-981-15-2700-5_24

1 Introduction

Networks are discrete structures of relationships. Our dear friend and colleague Akinori Okada has made several original contributions to the study of structural characteristics of networks. In Okada [44], he provided an additive, ordinal model for interpersonal attraction in social networks, based on *expansiveness* and *popularity* of the actors. In Okada [45], he introduced multiple *measures of centrality* based on more than one eigenvector; and in Gaul, Klages, and Okada [22], we find an elegant procedure for *community structure discovery* in asymmetric relations, using the concept of *shortest walk length*. It inspired us to write here about the mapping of discrete relational structures into continuous spatial representations by multidimensional scaling. Out of respect for the Master of Asymmetry, we restrict ourselves to symmetric relations, using the concept of *shortest path distance*.

The utilization of multidimensional scaling (MDS) for displaying networks has a long history. The first example of an MDS mapping of a social network was the groundbreaking study by Klingberg [33] of the international relations among the Seven Great Powers in terms of their perceived relative friendliness or hostility. The data of this study were collected in March 1939—just before the start of World War II—using the opinions of 241 students of international affairs. Perceived distances among the nodes of the network were determined by the method of "multidimensional rank order". Those distances in turn were analyzed with what is known as *classical MDS*, proposed a few years earlier by Young and Householder [59]. It turned out that two dimensions did not fit well, and therefore, a photograph of a wax model with wooden connections was used to display the three-dimensional MDS solution.

Quite a different early example of the insights obtainable from network models in psychology was the study by Osgood and Luria [46], which concerned a blind analysis of a case of triple personality disorder, also known as "The Three Faces of Eve". Here, data were obtained from a single patient, who had to rate 15 "concepts" (roles, emotional problems, and significant persons, selected for their differentiating power) on 10 bipolar scales (such as valuable–worthless, active–passive, and strong–weak) in three different personality states ("Eve White", "Eve Black", and "Jane"). Profile distances among all concepts were calculated across the bipolar scales for each personality state. From these distances, three network models were constructed (with the same concepts as nodes), each representing a qualitatively different state of the patient. The models could be used to make inferences about her condition without any knowledge of the case history or prognosis. For a comprehensive description of the methodology to determine semantic networks of connotative meaning of concepts—called the *semantic differential*—see Osgood, Suci, and Tannenbaum [47].

It has to be noted that in the networks that were actually shown in the Osgood and Luria [46] paper, the nodes have on average a degree (number of incident lines) approximately equal to 3, which is a lot less than the number of possible connections with other nodes (14). What is the reason for the small number of lines, when in this case all distances were known? The paper does not tell us how the lines were selected; maybe only lines with length below a chosen threshold were retained, or perhaps lines

were omitted to keep the display transparent. More generally, it is remarkable that all subsequent early applications of MDS on network data show the nodes as points in a two-dimensional plane, but draw no lines between nodes at all. For example, Laumann and Guttman [40] studied the relative amount by which people of a given occupation share the same or one of the other 54 occupations with people to whom they are closely related, and discussed the structure of the occupations obtained by Guttman's [26] ordinal MDS technique. But even though they knew the strength of association between all pairs of occupations, they drew no lines whatsoever between strongly associated ones. The same thing is true for the Laumann and Pappi [41] study of connections between elite members of a community, the Romney and Faust [49] study of a communication network, and *virtually all* more recent studies of MDS on semantic or social network data. Apparently, the leading thought in this research tradition is: MDS gives us locations for the concepts or actors in a spatial model, and the distance between these locations represents the relative strength of their connections. So there is no need for adding any lines to the map.

For the network modeling paradigm in multivariate data analysis, however, the major mathematical model is the *graph*. A graph model forces us to make a distinction between pairs of nodes that are directly connected (or *adjacent*) and pairs of nodes that are *not adjacent*. Therefore, the process of displaying an empirical network in a spatial representation or a map can be divided into two stages:

1. Graph construction: Creating a graph model from relational or multivariate data. If dichotomous relational data are already available—for example, in case of a network of mutual friends—then the list of pairs of actors who are friends can easily be coded in an adjacency matrix with (0, 1) entries, which fully characterizes a *simple network graph*. If we have any other kind of information about the empirical network, we must first determine relational measures of association, correlation, dissimilarity or similarity—generically called *proximities* by Shepard [53]. Then we must somehow divide the proximities into two groups: pairs of nodes that are considered to be adjacent, and pairs of nodes that are not. Adjacent pairs give us a (possibly weighted) network graph.
2. Graph drawing: Creating a spatial representation of the graph. Given a simple network graph coded as an adjacency matrix, we can form a dissimilarity matrix in which adjacent pairs have a single value indicating the length of a line (e.g., one) and the nonadjacent pairs have an arbitrary single value strictly greater than that length. For a weighted network graph, we form a dissimilarity matrix in which the cells of adjacent pairs contain their weight (because in a graph the weight of a line corresponds to its length), and the cells of nonadjacent pairs contain a single value strictly greater than the largest weight.

To produce the spatial representation, we can use MDS or some other procedure for graphical display. There are two possibilities for the input of the graph drawing procedure:

(i) Using simply the adjacency matrix of the graph, with entries coded as dissimilarities;
(ii) Replacing the tied dissimilarities for all nonadjacent pairs by the *geodesic* or *shortest path* distances between any two nodes, which is the natural metric in a graph.

Let us illustrate the two stages with two well-known examples from the literature. The first one is the methodology of *Gaussian graphical modeling*, which started with Dempster [13]. It was already well developed in the eighties of the last century (*cf.* Whittaker [58]), and saw an upsurge more recently in wider communities, such as psychometrics (Epskamp, Waldorp, Möttus, & Borsboom [15]). Here the nodes of the graph are *variables*. Dempster introduced the idea that to reduce the number of parameters in the multivariate normal distribution, it would be of interest to restrict the elements of the *inverse of the covariance matrix* rather than the covariances through dimension reduction. The reason is that these elements involve the *partial correlation* of the two variables after elimination of the influence of all other variables. If the small partial correlations are forced to be equal to zero, then the remaining larger ones may be used to produce an *independence graph*, in which there is no line between two nodes whenever the pair of variables is independent given all other variables. Finding this graph constitutes Stage 1, which nowadays can be conveniently done with the graphical lasso (Friedman, Hastie, & Tibshirani [19]). Stage 2 of our two-stage process—drawing the independence graph—was usually done by hand in the older literature, and more recently with one of the *force-directed graph layout* methods (Brandes [1]).

The second example of a two-stage data analysis method that obeys the network modeling paradigm is *isometric feature mapping* or *Isomap* (Tenenbaum, de Silva, & Langford [56]). It was inspired by the aim of mapping data points on curved surfaces into a low-dimensional representation, and uses the *K-nearest neighbors* procedure for creating a weighted graph in Stage 1. Hence, it focuses on the local relations. Then in Stage 2, Isomap computes shortest path distances among the nonadjacent pairs of nodes and uses these—together with the original distances of the adjacent pairs—as input for classical MDS to create the low-dimensional representation. One might note that the graph construction stage is only instrumental in being able to "unfold" the curved surface and not of interest by itself. Then it should not be surprising that Isomap does not show the lines of the K-nearest neighbors graph. Nevertheless, it follows the network modeling paradigm; follow-up methods do explicitly address graph layout (e.g., Kruiger et al. [34]).

Because there are so many different contexts and considerations for Stage 1, we restrict ourselves in this paper to Stage 2, graph drawing. Section 2 will briefly discuss some technicalities of several graph drawing procedures, using a *weighted least squares* framework. Section 3 presents several analyses of a simple graph, coming from a classical data set about the marital relations between fifteenth-century Florentine families. Section 4 presents several analyses of a special type of (weighted) graph: an additive tree of the semantic relations between animal terms. In the analyses of these concrete network graphs, we try to shed some light on two questions. One

question concerns what the effect is of the relative weight that is given to different pairs of nodes in the weighted least squares loss function. Another question is: what differences arise (if any) between using only the adjacencies as input or including the shortest path distances among all pairs of nodes. We conclude with a discussion in Sect. 5.

2 Graph Drawing Procedures Based on Least Squares

Classical MDS has been propagated for graph drawing ever since Kruskal and Seery [39], in their pioneering paper on designing network diagrams, suggested: "for those who may want to write their own program, we describe very briefly the simplest method to program, namely the classical method of MDS, which was rescued from obscurity by Torgerson ([57], Chap. 11)". Classical MDS amounts to a projection of the high-dimensional data points into a space of lower dimensionality. It is based on a loss function in which the squared dissimilarities are approximated by squared Euclidean distances. Inherent to the concept of projection is that the approximation is "from below" (Meulman [43]), implying that large dissimilarities in high-dimensional space may become smaller or even arbitrarily small in the low-dimensional space, but never larger—not a desirable property in general. In addition, it assumes a linear relationship between dissimilarity and distance.

To circumvent the problems of classical MDS, Shepard [53] conceived a new approach that assumed only an ordinal relationship between distance and dissimilarity:

$$d_{ij} \leq d_{kl} \quad \text{whenever} \quad \delta_{ij} < \delta_{kl}, \tag{1}$$

where d_{ij} is the Euclidean distance between points i and j in the configuration, and δ_{ij} is the dissimilarity between nodes i and j in the graph, for $i, j = 1, \cdots, n$. Shepard used a heuristic iterative algorithm to obtain the locations for points with distances satisfying (1). Not much later, Kruskal [35] put the approach on a firm footing by defining a sum-of-squares measure that incorporated (1). He viewed the MDS problem as fitting a nonlinear regression model to a possibly nonlinear transformation of the data. Here we give his least squares loss function in its essential form. Let us first write the distances as an explicit function of the coordinate vectors $\mathbf{x}_i$ and $\mathbf{x}_j$ of length p, the dimensionality of the representation.

We have

$$d_{ij}(\mathbf{X}) = \left\| \mathbf{x}_i - \mathbf{x}_j \right\| \tag{2}$$

as the Euclidean distance between points $\mathbf{x}_i$ and $\mathbf{x}_j$, where $\mathbf{X}$ is an $n \times p$ matrix, the rows of which contain the coordinates of the points. The *least squares nonmetric MDS* loss function is

$$\sigma^2(\mathbf{X}, \varphi) = \frac{1}{S} \sum_{i<j}^{n} w_{ij} \left[\varphi\left(\delta_{ij}\right) - d_{ij}(\mathbf{X})\right]^2, \tag{3}$$

where S is a standardization factor to prevent the coordinates from becoming arbitrarily small, and φ is some monotonically nondecreasing function that is not prespecified but is part of the optimization problem. Kruskal called the square root of his criterion *Stress*. We will say more about the data weights w_{ij} shortly. The process of finding optimal φ only under restrictions (1) for given $\mathbf{X}$, and hence for fixed distances, is called *isotonic regression*, and finding an optimal $\mathbf{X}$ for given φ is a nonlinear regression problem. Minimizing Stress not only over $\mathbf{X}$ but also over transformations φ makes the results invariant under ordinal transformations of the dissimilarities, from which feature derives its name *nonmetric* MDS. Other classes of transformations φ can be incorporated, too. A simple example is the class of all *linear transformations* (which Kruskal & Seery [39] actually used in their examples of network layout, for which they also calculated shortest path distances among all nodes).

Before we give a few technical details about how to minimize least squares loss function (3), we briefly discuss the class of *physical spring models* that were developed for graph drawing in computer science. In the description of Brandes [1, p. 71],

> Their common denominator is that they liken the graph to a system of interacting physical objects, the underlying assumption being that relaxed (energy minimal) states of suitably defined systems correspond to readable and informative layouts.

In the spring model, the nodes of the graph are represented by physical objects behaving like charged *rings* (balls, particles) that spread well on the plane by *repelling electrical forces*. The lines between adjacent nodes are represented by *springs* that prevent the rings to drift too far apart by *attracting mechanical forces*. Depending on how these forces are formulated—according to criteria of aesthetics chosen, such as even node distribution in space, uniformity of line length, avoidance of line crossings, and preservation of symmetry—a different type of *force-directed graph drawing* method results. Pioneer in this area was Eades [14], whose model is known as the *spring embedder*. Several modifications of the spring embedder were proposed by Fruchterman and Reingold [20] to improve some of its shortcomings.

Then there is a second group of methods, introduced by Kamada and Kawai [32]. It is based on the idea that we can *minimize the potential energy* of a purely mechanical system without the need of repulsive electrical forces, if we use springs of different length and strength *for every pair of rings*. Also, they considered that the natural length of the spring connecting two rings is the desirable target distance for the corresponding lines in the drawing. They then chose the length of each spring as the length of the shortest path between two nodes in the graph. The potential energy E of a spring between a pair of rings located at positions $\mathbf{x}_i$ and $\mathbf{x}_j$, when stretched or compressed, is now equal to

$$E\left(\mathbf{x}_i, \mathbf{x}_j\right) = \frac{1}{2} k_{ij} \left(d_G(i, j) - \left\|\mathbf{x}_i - \mathbf{x}_j\right\|\right)^2, \tag{4}$$

where the natural length of the spring is $d_G(i, j)$, the shortest path distance in the graph, and its actual length is the distance between the locations of the pair of rings on the plane. The quantity k_{ij} is the *stiffness* or *strength* of the spring. Summing (4) over all springs gives us an objective function that is equivalent to Stress in (3), with the shortest path distances in the role of the dissimilarities. The data weights in Stress correspond to the strength of the springs, which can be chosen freely. Kamada and Kawai choose them proportional to the inverse of the *squared* shortest path distances. The motivation is that it will be easier for the system to relax if long springs are not too stiff. Note that ordinal or other transformations of spring length are not considered; apparently, there is no physical justification in the spring model for changing the natural length of a spring in relation to other springs. Cohen [7] recognized the strong connection between Energy and Stress minimization. He also introduced an *alternative distance function for graphs*, which would better reflect the presence of cliques (clusters).

The use of data weights is not very prominent in applications within the MDS tradition, although they were already available in the early versions of Kruskal's program MDSCAL5 (Kruskal & Carmone [37]) and its successor KYST-2A (Kruskal, Young, & Seery [38]). In a review of MDS programs devised at Bell Laboratories, we find:

> *Weighting of Data*—the MDSCAL5 and KYST programs allow for differential weighting of the original data values. This can be done either by supplying a matrix of weights in the same way as the data are laid out or by using a FORTRAN subroutine for generating weights internally. (Carroll [5])

After inspection of the code of these programs, we discovered that they contain the following *power family* formula for generating data weights internally:

$$w_{ij} = d + e(a + b\delta_{ij})^c, \tag{5}$$

where a, b, c, d, and e are user-provided parameters. Obviously, the Kamada and Kawai data weights belong to this family by choosing (0, 1, −2, 0, and 1). The same weighting function had been proposed by McGee [42], and the same function, but with $c = -1$, was used by Sammon [51] for nonlinear mapping of multivariate data, which became a seminal paper in the unsupervised machine learning literature. It is likely that Kruskal was aware of these papers and for this reason put (5) into updates of his original program; there was no mention of data weights in the Kruskal [36] paper, in which he described how he optimized Stress.

Kruskal [36] used a gradient method, in which he included his own carefully thought-out step size procedure, which nevertheless does not guarantee that the process always converges. Since the gradient of Stress has the distance between two points in its denominator, it was also not clear what to do whenever two points happen to coincide during the process. De Leeuw [9] solved these two difficulties by deriving an updating formula on the basis of a *majorization* principle that resolves both problems at the same time. It turned out that the resulting updating formula is equivalent to the *correction matrix* method used in Guttman [26], and for this reason,

it was called the *Guttman transform*. This transform is a special case of Kruskal's update, because it moves along the direction of the gradient with a fixed step size of one. Heiser and De Leeuw [28] implemented the majorization procedure in the first SMACOF program. In De Leeuw and Heiser [10], an important step was made by providing a unified framework for including the possibility of imposing constraints of different kinds on the configuration of points. For an up-to-date review of the majorization approach to MDS, with special attention to the use of data weights, we refer to Groenen and Van de Velden [24]. Stress majorization was introduced in the graph drawing community by Gansner, Koren, and North [21]. They also developed a number of useful extensions for graph layout that profited from the power and flexibility of majorization optimization.

We conclude this section by giving a formulation of the SMACOF algorithm that shows clearly how the update of one point depends on the (transformed) dissimilarities, the current distances, and the weights used in Stress. Suppose we have a current configuration of points $\mathbf{Y}$ and the distances $d_{ij}(\mathbf{Y})$ derived from it. On the basis of these distances we can also determine, if desired, conditionally optimal values of the transformation $\widehat{d}_{ij} = \widehat{\varphi}\left(\delta_{ij}\right)$ called *dhats*, to replace the δ_{ij}'s. Then the updating formula in the SMACOF algorithm for a single point $\mathbf{y}_i$ (keeping the other points fixed and denoting the update with $\overline{\mathbf{x}}_i$) is as follows:

$$\overline{\mathbf{x}}_i = \left[\frac{1}{\sum_{j\neq i} w_{ij}} \sum_{j\neq i}^{n} w_{ij} \frac{\widehat{d}_{ij}}{d_{ij}(\mathbf{Y})}\right] \mathbf{y}_i + \frac{1}{\sum_{j\neq i} w_{ij}} \sum_{j\neq i}^{n} w_{ij} \left(1 - \frac{\widehat{d}_{ij}}{d_{ij}(\mathbf{Y})}\right) \mathbf{y}_j. \quad (6)$$

The first term between brackets at the right side of (6) is a scalar: the weighted average of all correction factors $\widehat{d}_{ij}/d_{ij}(\mathbf{Y})$ for point $\mathbf{y}_i$ with respect to all other points $\mathbf{y}_j$. If on average all dhats are larger than the current distances, then this scalar will be larger than one, and the current point $\mathbf{y}_i$ will be pushed outward with respect to the origin—a direction forcing larger distances. Point $\mathbf{y}_i$ will be pulled inwards to the origin if the reverse holds. The second term in (6) adds to the first one a weighted average of directions of change toward or away from specific other points $\mathbf{y}_j$, depending on whether $\widehat{d}_{ij} < d_{ij}(\mathbf{Y})$ or the reverse. If $\widehat{d}_{ij} = d_{ij}(\mathbf{Y})$, point $\mathbf{y}_j$ does not contribute a pushing or pulling force to the final direction of change. We finally note that both terms do not at all take points $\mathbf{y}_j$ into account for which $w_{ij} = 0$.

3 Drawing a Simple Graph: Marital Relations Between Florentine Families

As an example for the effect of using shortest path distances rather than only using the adjacencies in a simple unweighted graph, and for exploring the effect of weighting, we are going to analyze a classic data set that was also analyzed in Okada [45]. In this paper, Okada was looking for (possibly overlapping) subgroups of actors in

a social network who show different types of centrality, and his example was the well-known symmetric graph of marital relations between 16 Florentine families in fifteenth-century Florence, Italy.

What do we know about the prospects of embedding an adjacency matrix in Euclidean space by MDS? Kruskal and Seery [39, p. 31] had a clear opinion:

> We also experimented with defining the distance [. . .] between two nodes to be either one (if they are adjacent) or "infinity" (if they are not directly connected) [. . .]. However, we found the method described above to give more desirable diagrams.

The "method described above" was calculating shortest path distances. Unfortunately, Kruskal and Seery did not tell the reader in what sense the MDS results on an adjacency matrix were less desirable. One possibility might have been that they used ordinal transformations. In a binary proximity matrix, there are only two tie blocks (sets of pairs with the same proximity value). In the so-called *primary approach to ties* (Kruskal [36]), the dhats will become equal to the corresponding distances in the block of nonadjacent pairs when they are larger than the largest distance in the block of adjacent pairs. According to update formula (6), these pairs will disappear as an acting force upon the current point. The same holds for the smallest distances in the block of adjacent pairs that do not overlap with the block of nonadjacent pairs. The implication is that there may not be enough constraints to steer away from undesirable solutions. However, there is positive theoretical evidence that using *linear transformations with intercept* can be a successful option for embedding an adjacency matrix in Euclidean space in such a way that adjacent nodes are located closer to each other than nonadjacent ones. In a very early paper on such an embedding, Guttman ([25], published in 1977) showed that it is always possible to locate the node points in less than $n - 1$ dimensions, provided that a suitably chosen *additive constant* is used. He also showed that it will be possible to draw a (hyper-)sphere (or circle) around any point, in such a way that its adjacent nodes are separated from the nonadjacent nodes. Of course, this result does not guarantee that a desirable diagram exists in two dimensions, but it does suggest that least squares MDS may work well for binary proximities. For an in-depth discussion of Guttman's type of graph embedding, we refer to Freeman [18].

A peculiarity of our example is that the Pucci family has no tie to any of the other Florentine families. Unconnected points or unconnected subgraphs cannot be accommodated in standard MDS techniques, so we continue with 15 families. In our analyses, we always use classical MDS as an initial configuration after estimation of the smallest additive constant that ensures a Euclidean representation (Cailliez [4]). In a large experimental study with graphs of different types, Brandes and Pich [2] confirmed that classical MDS followed by least squares MDS works particularly well for graph drawing. The software that we used for the SMACOF iterations and the type of plots made for the current paper is called PROXMAP.[1]

The three plots on the left of Fig. 1 give the results for the Florentine families graph, with as input one minus the adjacency matrix, and analyzed without any

[1] Available upon request from the second author.

transformation φ. The plot at the top gives the MDS drawing of the graph and shows a quite regular structure. The three families with largest node degree (6 for Medici, 4 for Strozzi, and 4 for Guadagni) form the center of three relatively dense areas, and the four families with node degree equal to one (Lamberteschi, Ginori, Acciaiuoli, and Pazzi) are located on the outside. The middle plot in the left column of Fig. 1 gives the result of *single-link hierarchical clustering* superimposed on the points in the MDS configuration. PROXMAP obtains the nested clusters by first calculating the minimum spanning tree (Prim [48]) based on the inter-point distances in the MDS solution, from which the single-link clusters can be easily derived, also for large networks (Gower & Ross [23]). The hierarchical clustering shows a major separation between the elongated 5-family group on the lower left side with the larger group on the right side around the central clique Medici–Ridolfi–Tornabuoni.

The third plot in this column contains circles around the family points, which indicate their contribution to the value of Stress in (3). The square root of (3) is usually reported and is called *Kruskal's Stress-1*. In this case, it equals 0.337, which is large—an effect due to the large tie blocks. Hence, the circles are relatively large—especially for the points in the center and the Barbadori node. Looking back at the graph in the top panel, we see that these points with large contributions to Stress have relatively long lines with other points, even though lines represent direct connections, and therefore should be relatively short.

In the right column of Fig. 1, we give the comparable results obtained when we add a constant equal to one to all cells of the (0, 1)-dissimilarity matrix, so that adjacent pairs of nodes now get a dissimilarity of one and nonadjacent pairs of nodes a dissimilarity of two. Kruskal's Stress-1 becomes lower (0.285), and the family locations are roughly the same. But note that some of the long lines between adjacent families have become shorter (e.g., between Strozzi and Ridolfi), and some of the short lines have become longer (e.g., between Strozzi and Peruzzi). More precisely, the coefficient of variation of the distances between adjacent pairs is reduced from 0.505 to 0.353 (30.1%). This effect of getting more homogeneous line lengths is also apparent in the single-link clustering plot: the big divide in two groups along the diagonal has become less wide, and the Medici family enters into a small cluster with the Acciaiuoli family. The circles in the Stress decomposition plot show that the reduction of Stress is especially due to the families in the middle. These effects remain totally unchanged if we include an optimal linear transformation φ in the analysis, or not (and either with or without optimal intercept).

We now turn to the MDS analyses using shortest path distances, calculated with Floyd's algorithm (Floyd [16]). The dissimilarities now range from 1 (for direct connections) to 5 (for the longest paths). We first look at the results of an *unweighted analysis*, with *ordinal transformation* and *primary approach to ties* (which means that ties may become untied in the dhats). They are displayed in the left column of Fig. 2. A first thing to note is that line length is now even more uniform than in the analysis of the adjacencies with the additive constant. Also, the graph is rotated counterclockwise with an angle of about 45°. Even though rotation is not a change affecting the distances, it does give an indication of change in the configuration, because PROXMAP rotates toward the principal axes. The longest paths are now

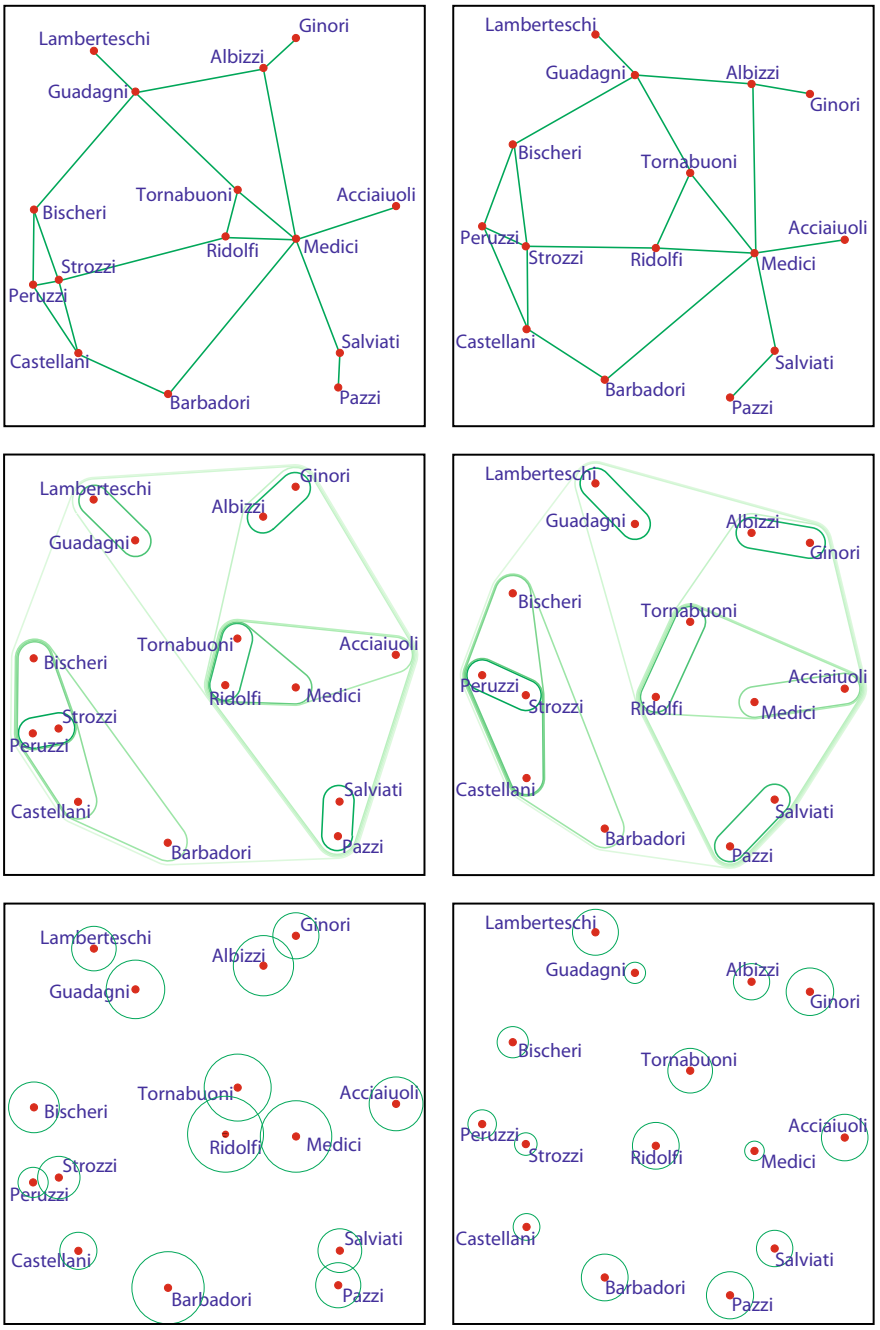

Fig. 1 MDS on adjacency matrix of Florentine families graph (for explanation, see the text)

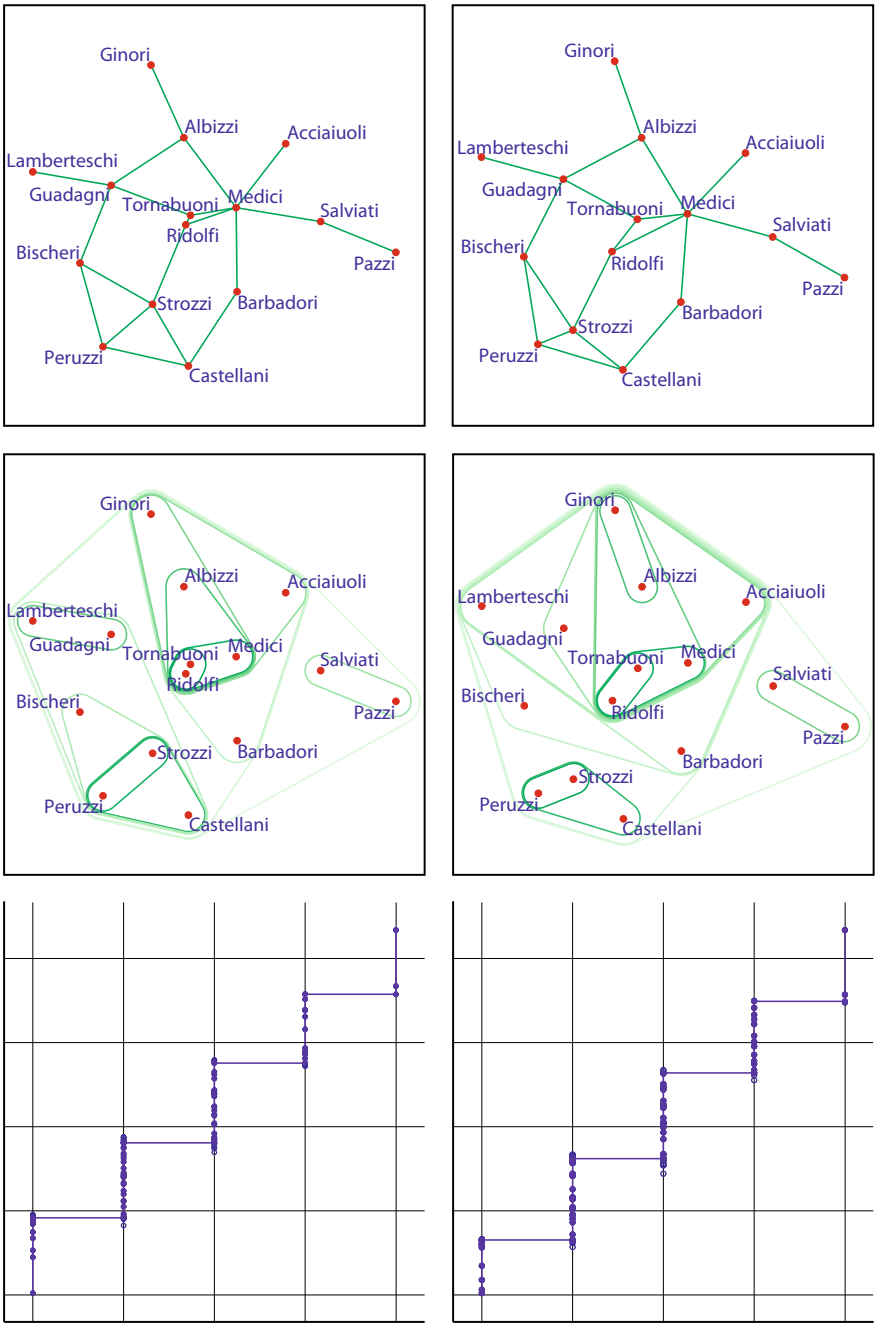

Fig. 2 MDS on the path distances of Florentine families graph (for explanation, see the text)

aligned horizontally (from Pazzi to Lamberteschi, from Pazzi to Bischeri, and from Pazzi to Peruzzi). The Medici–Tornabuoni–Ridolfi triangle moved to the center of the plot, and together with the Albizzi and Guadagni family, they have the highest loadings on *both* centrality measures of Okada [45]. The four families in the Strozzi group score high on Okada's *second* centrality measure, and also turn out to be the second most important cluster in the *additive clustering* analysis (Shepard & Arabie [55]) that he performed.

In the single-link hierarchical clustering, we see quite a few small changes, most likely due to the more homogeneous line lengths, which lead to a contraction of several points to the origin. The Barbadori family moved to an extended central cluster, while Salviati and Pazzi still form a small isolated cluster. Kruskal's Stress-1 equals 0.0112 for this analysis; the fit is very close to perfection. Stress decomposed by node, as in Fig. 1, would be invisible. So we give in the third plot of the left column in Fig. 2 the so-called *Shepard plot*, which has the shortest path distances on the x-axis and on the y-axis the fitted distances (labeled with open circles) and the optimally transformed data (labeled with closed circles). Almost all transformed data are equal to their corresponding distances spread out in the vertical direction within each tie block.

We see only a very few open circles in the first three steps of the step function, where some distances are a little bit too long or too short. Note that the step function suggests that a linear transformation would be an acceptable alternative in this case, and would give the same configuration of the nodes, with just a bit more Stress. When we checked this suggestion, we indeed obtained comparable results, with Kruskal's Stress-1 $= 0.134$.

Let us now compare these analyses with a *weighted* approach, where we have used the Kamada and Kawai [32] choice for the inverse of the *squared* shortest path distances (and where we note that the use of Sammon [51] weighting (not shown) did not make very much difference). The resulting graph representation, the single-link clusters, and the Shepard plot are shown in the right column of Fig. 2. Kruskal's Stress-1 moved from 0.0112 to 0.0121, just a little bit higher than the unweighted analysis. Nevertheless, the graph representations are very similar. In the single-link clustering, the Bischeri family became disconnected from the Strozzi group—a small change, and not in accordance with other evidence. In the Shepard plot, we see only very slight changes; the only noticeable one is that the distances in the first tie block are smaller and have less variation than the corresponding ones in the unweighted analysis.

Summarizing our results so far, we conclude that the unweighted analysis using shortest path distances is the one to be preferred. It has the lowest Stress, the graph representation is clearly interpretable, and the length of the lines (distances between adjacent pairs of nodes) has the least variation. But we have also seen that the results for the binary adjacency data are certainly acceptable, especially if we include an additive constant, either in the coding of the dissimilarities, or by choosing the option to transform them linearly with an intercept via the Stress algorithm.

4 Drawing a Weighted Graph: An Additive Tree of Animal Names

Trees are connected graphs with only one path between each pair of nodes, or alternatively, a tree is a graph without cycles and with $n - 1$ lines. Additive trees (or *phylogenetic trees*) are weighted graphs with these properties. But, in addition, they incorporate a distinction between *end nodes* (or terminal nodes), which have degree one and represent empirical objects or actors, and *internal nodes*, all of which except one have degree three and represent *nested clusters* of end nodes. If we have n end nodes, there will be $n - 1$ internal nodes and $2n - 2$ lines connecting all of them, provided that all branches of the tree are binary. The metric in a tree is just the graphical distance: the total length of the unique path between them. In a rooted additive tree, there is one distinguished internal node, called the *root*, which splits the total collection of end nodes into two or more groups. The other internal nodes in turn split these groups into subgroups until only single end nodes remain. An additive tree in which all end nodes are equidistant from the root is called an *ultrametric* tree.

The branches of an additive tree form long paths with additive segments from end nodes to the root, and both the number of branches and their length grows with n. It is known that an ultrametric tree can be embedded in a Euclidean space of $n - 1$ dimensions, but not in $n - 2$ dimensions (Holman [30]). This result supposes that we want to reproduce the ultrametric distances *exactly*. But it can also be shown that an ultrametric tree can be scaled in one dimension, provided that we are prepared to use optimal ordinal transformations with the primary approach to ties (Critchley & Heiser [8]). So it is not unreasonable to suppose that trees can be mapped by MDS *approximately* in *two* dimensions.

Our example is one of the data sets used by Sattath and Tversky [52] to illustrate their pioneering additive tree fitting algorithm, which is very closely related to the famous *neighbor-joining* method (Saitou & Nei [50]) for fitting phylogenetic trees in evolutionary biology. The data are from an experiment by Henley [29], who asked a homogeneous group of 18 students to rate the dissimilarity between all pairs of 30 animals on a scale from 0 to 10. We will use the adjacency characteristics and the weight parameters of the tree obtained by Sattath and Tversky with their ADDTREE program as input to our PROXMAP program. In Fig. 3, top panel, we first give the graph configuration computed by an MDS analysis with only the binary adjacency matrix as input and with transformation option "ordinal with primary approach to ties", which yielded a Kruskal's Stress-1 of 0.00575.

The first thing to notice about this configuration is that it has a lot more variance along the first (horizontal) dimension than along the second (vertical) dimension. The elongated configuration appears to be in accordance with the Critchley and Heiser [8] result on ultrametric trees. It should be noted, however, that their result does not apply completely here, because an additive tree does not have the restriction that all end nodes are equidistant from the root. There are some line crossings; see, for instance, the *pig*, the *chimp*, and the cluster of *chipmunk*, *squirrel*, *rat*, and *mouse*. Nevertheless, the MDS configuration certainly gives us some useful extra information about the

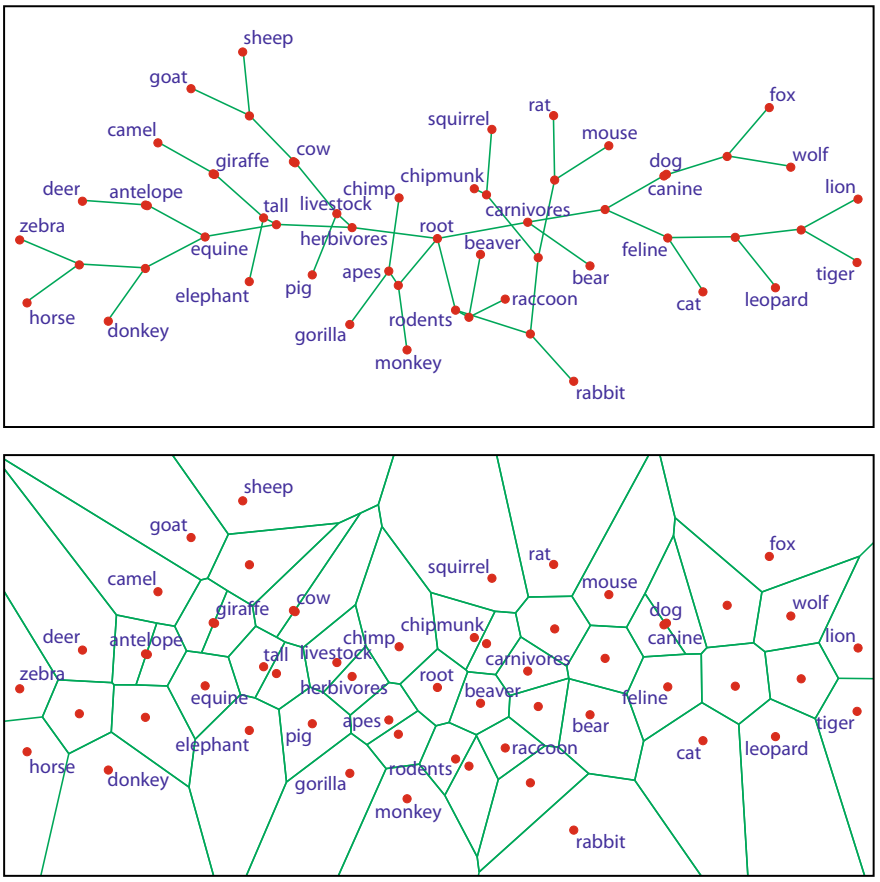

Fig. 3 Ordinal MDS on the adjacencies of the Animals tree (for explanation, see the text)

tree: the dominant distinction between the *carnivores* on the right and the *herbivores* on the left. That these groups form the strongest contrast cannot be easily detected in the traditional *dendrogram* representation of this tree in Sattath and Tversky [52], in which all branches point into the same direction. In the bottom panel of Fig. 3, we show the Voronoi diagram of this solution, which is a partitioning of the plane into regions of all points that are closer to the indicated node than to any other node. It gives an indication of how tightly constrained the location of each node is. It is clear that the end nodes, which all have degree one, have more freedom to move than the points in the middle.

Figure 4 gives the configuration of the tree obtained by analyzing the adjacencies with an optimal *linear* transformation *including an intercept*. Here, Kruskal's Stress-1 is 0.3817, which is relatively high, and normally an indication that we should seek a solution in higher dimensionality. However, we see only a little crossing of lines, and the full space is covered by the four major branches of the tree: starting with

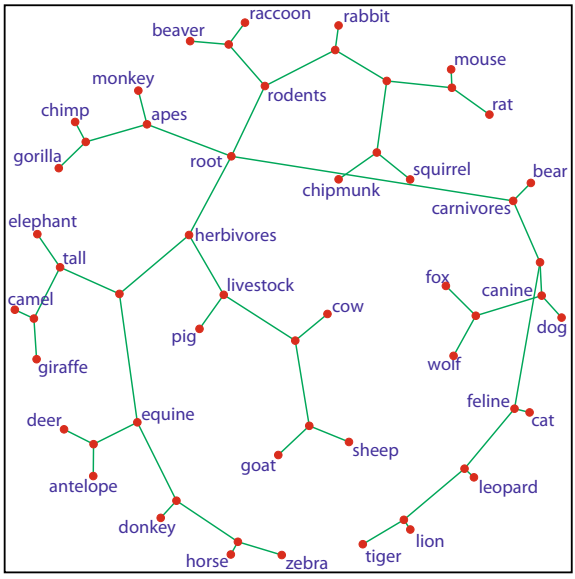

Fig. 4 Metric MDS on the adjacencies of the Animals tree (for explanation, see the text)

the *carnivores* on the right and going counterclockwise, we have the *rodents* on top, the *apes* in the left upper part, and the *herbivores* on the left lower part. Further subdivisions, such as *tall*, *equine*, and *livestock* for the herbivores, or *canine* and *feline* for the carnivores are clearly recognizable. So, at first sight, it looks like a good use of the available space.

However, from the point of view of distance approximation, this configuration is pretty bad, because the two major branches that formed the large contrast in Fig. 3 have been bent down in a horseshoe kind of shape. The effect is severe bias in the distances: for example, while the *lion* and the *tiger* are two steps apart from each other in the tree, like the *zebra* and the *horse*, we find that the tiger and the zebra are also close to each other in Euclidean distance, even though these two animals are *twelve steps apart* from each other in the tree. Similarly, the *chipmunk* appears to be close to the root, while it is five steps away from it in the tree. The fact that the points appear to be uniformly distributed within a circle can be attributed to a known phenomenon that occurs when *all dissimilarities are equal*. As noted by De Leeuw and Stoop [11, p. 397], optimal configurations minimizing metric Stress when all dissimilarities are equal (for sufficiently large n) must have this tendency (for less than 7 points they will all be on a circle). Buja, Logan, Reeds, & Shepp [3] called the equal dissimilarity case "totally uninformative" and gave a more detailed mathematical analysis. Although our example is not *totally* uninformative, it comes close. We have a first tie block of 56 dissimilarities for adjacent pairs and a second tie block of 1540 dissimilarities for nonadjacent pairs. So 96.5% of the dissimilarities are equal (to the larger value), which apparently is enough to cause a uniform distribution of points within the circle.

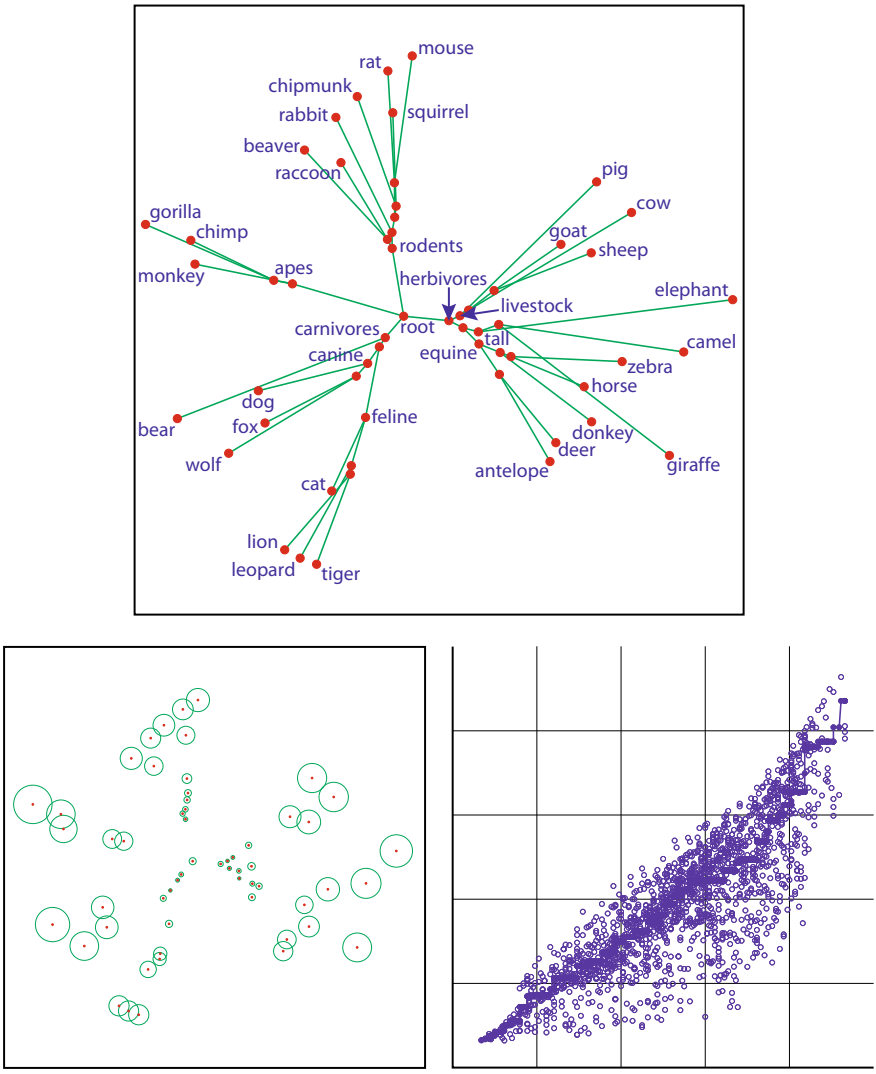

Fig. 5 Ordinal MDS with unweighted Stress on path distances of the Animals tree

Our last two analyses of the Animals example use path distances in the Sattath and Tversky additive tree, where the weight parameters (indicating line length) are incorporated. Both analyses have ordinal transformations with primary approach to ties. In Figs. 5 and 6, we give the tree configurations accompanied by Shepard plots and stress decomposition plots.

For the results of the analysis *without data weights* in the Stress function given in Fig. 5, Kruskal's Stress-1 is 0.2256. We find the *herbivores* on the right, with the

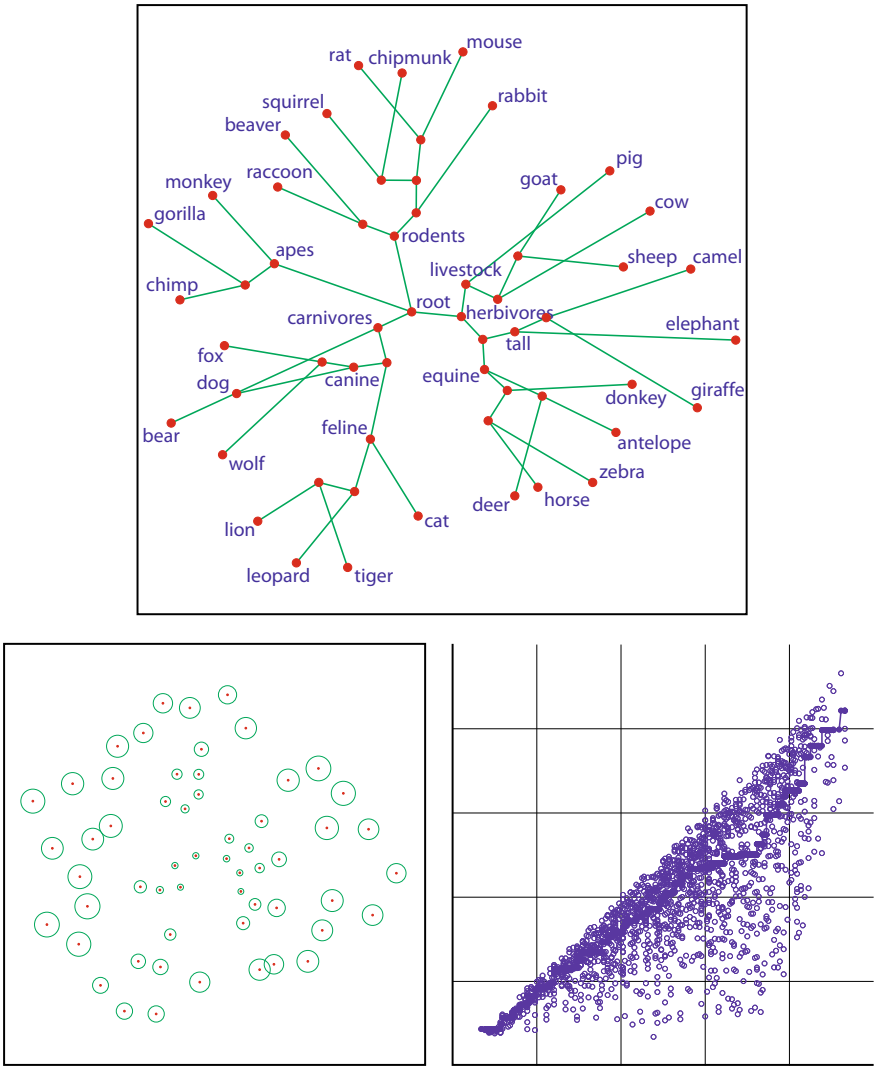

Fig. 6 Ordinal MDS with weighted Stress on path distances of the Animals tree

livestock clearly as a separate branch, while the *giraffe* from the tall group overlaps with the equine group. In the left upper part, we find the *rodents* and *apes*, and in the left lower part the *carnivores*, with separate branches for the *bear*, the *canines*, and the *felines*. The effect of the weight parameters of the tree is particularly visible in the different lengths of the lines to the end nodes. For instance: the *elephant*, the *giraffe*, and the *bear* have longer end lines in the tree than the *horse* and the *fox*.

In the Shepard plot on the right-hand side, we see a slightly accelerating nonlinear transformation and quite a lot of distances that are too small. It suggests that the tree, which has four main branches, will fit much better in three dimensions, allowing the branches to extend near the corners of a tetrahedron (but it would bring us outside the scope of this paper to pursue this suggestion). The Stress decomposition plot on the left-hand side shows a remarkable pattern that is the reverse of what we saw in the Florentine families example: the best fitting nodes are in the center, and the worst fitting nodes are on the outside. This effect is caused by the fact that for pairs in two different main branches located next to each other, the tree distances go via the root, while the Euclidean distances go directly to the neighboring branch.

For the ordinal analysis *with Kamada & Kawai data weights* in the Stress function, we see in Fig. 6 that the tree configuration shows more separation *within* branches and less differentiation in line length. Both effects are probably due to the emphasis on fitting the small tree distances right. Kruskal's Stress-1 is very slightly lower, 0.2206. However, using data weights in the fit function which are inversely proportional to the square of path distances does seem to eliminate the weight differentiation among lines in the weighted tree. Whenever such an effect occurs, it must be considered an undesirable feature. The Shepard plot in Fig. 6 has fewer distances that are larger than the transformed dissimilarities, compared to Fig. 5, and slightly more distances that are (much) smaller, except for the lower left corner of the plot. So the effect of Kamada & Kawai weighting shows up in the Shepard plot, too, and the Stress distribution over points has become slightly more even.

Summarizing our results of the Animals example, we believe that in this case, an ordinal analysis of the adjacency matrix does contribute to our understanding of the structure of the tree, by showing the major distinction between two of the four branches of the tree. We have shown that a metric analysis of the adjacencies can be misleading, due to the equal dissimilarity effect. Using path distances including the line length in the tree therefore is the best option. However, weighting the Stress function with the inverse of the squared path distances does not seem to be a good idea, because it tends to suppress the differentiation in line length.

5 Conclusions and Discussion

We have distinguished a two-stage network modeling paradigm for multivariate data analysis, with *graph construction* in the first stage and *graph drawing* in the second stage. Examples of graph construction were: making an independence graph, a K-nearest neighbors graph, or an additive tree graph. Many different graph construction methods have been proposed in the psychometrics and classification literature. We believe that least squares methods are preferable, in terms of generality and flexibility. Examples are least squares fitting of additive trees (De Soete [12]) and least squares fitting of intersection graphs defined on a *discrete feature space* (Heiser [27]; Frank & Heiser [17]). An overview of other structural models for proximity matrices, including appropriate software, is given in Hubert, Arabie, and Meulman [31]. For

graph drawing, there are two main types of methods: *force-directed* and *distance-driven* graph drawing. But it should be noted that there have also been proposals for a mixture of the two, for example by Chen and Buja [6], who proposed *local MDS*, and by Kruiger et al. [34], who proposed *tsNET*, a modification of *t-SNE*. Both papers use a modified objective function with terms based on a nonlinear dimension reduction technique and terms based on classical force-directed correction techniques.

We have restricted ourselves to distance-driven graph drawing by least squares MDS, on the basis of Kruskal's [35] Stress function, which accommodates the possibility of weighting the residuals differently and transforming the proximities optimally within a given class of functions. Two examples were presented to throw light on two questions. The first question was, what kind of graph characteristics would be best to use as input, adjacencies or shortest path distances? It turned out that shortest path distances were generally to be preferred, because they give a better fit, a representation that gives more valid information on the structure of the graph, and a portrayal of inter-node distance that more closely reproduces line length in the graph. Nevertheless, it also turned out that in the example of the tree an ordinal analysis of the adjacency matrix highlighted something that was not evident in the usual dendrogram representation: it showed which pair of main branches gives the largest contrast. However, metric analysis of the adjacency matrix is not recommended, because the dominance of equal distances between nonadjacent pairs tends to cause uniform distributions of points within a circle. The second question concerned the use of data weights in the Stress function to down-weight residuals related to large distances in the graph. In the first example of a simple graph, weighting did not make much difference. In the second example of an additive tree, weighting turned out to be detrimental to good differentiation of line length. So for weighted graphs, one has to be cautious with this kind of weighting of the residuals.

It is of interest to point out that the relation between an MDS and an additive tree representation for the Henley [29] data was also considered by Shepard [54] in his authoritative *Science* paper. He used an MDS configuration based on the original data and superimposed the Sattath and Tversky [52] tree on that solution. This kind of *parallel analysis* of MDS and clustering is the common thing to do in the MDS literature. What we did in the current paper, however, was either calculating a single-link clustering on distances fitted by MDS—to highlight features of the MDS configuration (in the first example)—or calculating an MDS configuration on distances fitted by hierarchical clustering—to highlight features of the tree (in the second example). When analyzing the data twice, it might be preferable to first select the model that produces a better fit, and then use the other method on the distances of the fitted model as an additional tool for interpretation.

In conclusion, we believe that there is much room for further action and development of multidimensional scaling in the network paradigm of multivariate data analysis. By exploiting the distinction between direct and indirect connections or influences, graphical models provide a conceptually interesting alternative to dimension reduction. But if—as is often the case—the structure of the fitted graph is high-dimensional, we still need nonlinear dimension reduction by multidimensional scaling to comprehend it.

References

1. Brandes, U. (2001). Drawing on physical analogies. In: M. Kaufman & D. Wagner (Eds.) *Drawing graphs* (Vol. 2025, pp. 71–86). Lecture notes in computer science. Berlin: Springer.
2. Brandes, U. & Pich, C. (2009). An experimental study on distance-based graph drawing. In: I. G. Tollis & M. Patrignani (Eds.) *Graph drawing (GD'08)* (Vol. 5417, pp. 218–229). Lecture notes in computer science. Berlin: Springer.
3. Buja, A., Logan, B. F., Reeds, J. A., & Shepp, L. A. (1994). Inequalities and positive-definite functions arising from a problem in multidimensional scaling. *Annals of Statistics*, *22*(1), 406–438.
4. Cailliez, F. (1983). The analytical solution of the additive constant problem. *Psychometrika*, *48*(2), 305–308.
5. Carroll, J. D. (1987). Some multidimensional scaling and related procedures devised at Bell Laboratories, with ecological applications. In P. Legendre & L. Legendre (Eds.), *Developments in numerical ecology* (pp. 65–138). New York: Springer.
6. Chen, L., & Buja, A. (2009). Local multidimensional scaling for nonlinear dimension reduction, graph drawing, and proximity analysis. *Journal of the American Statistical Association*, *104*(485), 209–219.
7. Cohen, J. D. (1997). Drawing graphs to convey proximity: An incremental arrangement method. *ACM Transactions on Computer-Human Interaction*, *4*(3), 197–229.
8. Critchley, F., & Heiser, W. J. (1988). Hierarchical trees can be perfectly scaled in one dimension. *Journal of Classification*, *5*(1), 5–20.
9. De Leeuw, J. (1977). Applications of convex analysis to multidimensional scaling. In J. R. Barra, F. Brodeau, G. Romier, & B. Van Cutsem (Eds.), *Recent developments in statistics* (pp. 133–146). Amsterdam: North Holland Publishing Company.
10. De Leeuw, J., & Heiser, W. J. (1980). Multidimensional scaling with restrictions on the configuration. In P. R. Krishnaiah (Ed.), *Multivariate analysis* (Vol. V, pp. 501–522). Amsterdam: North Holland Publishing Company.
11. De Leeuw, J., & Stoop, I. (1984). Upper bounds for Kruskal's Stress. *Psychometrika*, *49*(3), 391–402.
12. De Soete, G. (1983). A least squares algorithm for fitting additive trees to proximity data. *Psychometrika*, *48*(4), 621–626.
13. Dempster, A. P. (1972). Covariance selection. *Biometrics*, *28*(1), 157–175.
14. Eades, P. (1984). A heuristic for graph drawing. *Congressus Numerantium*, *42*, 149–160.
15. Epskamp, S., Waldorp, L. J., Möttus, R., & Borsboom, D. (2018). The Gaussian graphical model in cross-sectional and time series data. *Multivariate Behavioral Research*, *5*(4), 453–480.
16. Floyd, R. W. (1962). Algorithm 97: Shortest path. *Communications of the ACM*, *5*(6), 345.
17. Frank, L. E., & Heiser, W. J. (2008). Feature selection in feature network models: Finding predictive subsets of features with the Positive Lasso. *British Journal of Mathematical and Statistical Psychology*, *61*(1), 1–27.
18. Freeman, L. C. (1983). Spheres, cubes, and boxes: Graph dimensionality and network structure. *Social Networks*, *5*(2), 139–156.
19. Friedman, J., Hastie, T., & Tibshirani, R. (2008). Sparse inverse covariance estimation with the graphical lasso. *Biostatistics*, *9*(3), 432–441.
20. Fruchterman, T. M. J., & Reingold, E. M. (1991). Graph drawing by force-directed placement. *Software-Practice and Experience*, *21*(11), 1129–1164.
21. Gansner, E. R., Koren, Y., & North, S. (2005). Graph drawing by stress majorization. In: J. Pach (Ed.), *Graph drawing*: 12th *International Symposium GD 2004* (Vol. 3383, pp. 239–250). Lecture notes in computer science. Berlin: Springer.
22. Gaul, W., Klages, R., & Okada, A. (2013). Community structure discovery in directed graphs by asymmetric clustering. *Behaviormetrika*, *40*(1), 85–99.
23. Gower, J. C. & Ross, G. J. S. (1969). Minimum spanning trees and single linkage cluster analysis. *Journal of the Royal Statistical Society, Series C (Applied Statistics)*, *18*(1), 54–64.

24. Groenen, P. J. F., & Van de Velden, M. (2016). Multidimensional scaling by majorization: A review. *Journal of Statistical Software*, *73*(8), 1–26.
25. Guttman, L. (1965). A definition of dimensionality and distance for graphs. (Unpublished manuscript, published in: J. C. Lingoes (Ed., 1977), *Geometric representations of relational data: Readings in multidimensional scaling*, pp. 713-723. Ann Arbor, MI: Mathesis Press).
26. Guttman, L. (1968). A general nonmetric technique for finding the smallest coordinate space for a configuration of points. *Psychometrika*, *33*(4), 469–506.
27. Heiser, W. J. (1998). Fitting graphs and trees with multidimensional scaling methods. In C. Hayashi, K. Yajima, H.-H. Bock, N. Ohsumi, Y. Tanaka, & Y. Baba (Eds.), *Data science, classification, and related methods* (pp. 52–62). Tokyo: Springer.
28. Heiser, W. J., & De Leeuw, J. (1977). *How to Use SMACOF-I: A program for metric multidimensional scaling*. The Netherlands: Department of Data Theory, Leiden University.
29. Henley, N. M. (1969). A psychological study of the semantics of animal terms. *Journal of Verbal Learning and Verbal Behavior*, *8*(2), 176–184.
30. Holman, E. W. (1972). The relation between hierarchical and Euclidean models for psychological distances. *Psychometrika*, *37*(4), 417–423.
31. Hubert, L., Arabie, P., & Meulman, J. J. (2006). *The structural representation of proximity matrices with MATLAB*. Philadelphia, PA: SIAM.
32. Kamada, T., & Kawai, S. (1989). An algorithm for drawing general undirected graphs. *Information Processing Letters*, *31*(1), 7–15.
33. Klingberg, F. L. (1941). Studies in measurement of the relations among sovereign states. *Psychometrika*, *6*(6), 335–352.
34. Kruiger, J. F., Rauber, P. E., Martins, R. M., Kerren, A., Kobourov, S., & Telea, A. C. (2017). Graph layouts by t-SNE. *Computer Graphics Forum*, *36*(3), 283–294.
35. Kruskal, J. B. (1964a). Multidimensional scaling by optimizing goodness of fit to a nonmetric hypothesis. *Psychometrika*, *29*(1), 1–27.
36. Kruskal, J. B. (1964b). Nonmetric multidimensional scaling: a numerical method. *Psychometrika*, *29*(2), 115–129.
37. Kruskal, J. B. & Carmone, F. (1969). *How to use M-D-SCAL (version 5M) and other useful information*. Unpublished manuscript, Bell Laboratories, Murray Hill, NJ.
38. Kruskal, J. B., Young, F. W., & Seery, J. B. (1973). *How to use KYST-2A: A very flexible program to do multidimensional scaling and unfolding*. Unpublished manuscript, Bell Laboratories, Murray Hill, NJ.
39. Kruskal, J. B. & Seery, J. B. (2000). Designing network diagrams. In: *Proceedings of the First General Conference on Social Graphics* (pp. 22–50). Washington, DC: U.S. Bureau of the Census.
40. Laumann, E. O., & Guttman, L. (1966). The relative associational contiguity of occupations in an urban setting. *American Sociological Review*, *31*(2), 169–178.
41. Laumann, E. O., & Pappi, F. U. (1973). New directions in the study of community elites. *American Sociological Review*, *38*(2), 212–230.
42. McGee, V. E. (1966). The multidimensional scaling of "elastic" distances. *British Journal of Mathematical and Statistical Psychology*, *19*(2), 181–196.
43. Meulman, J. J. (1992). The integration of multidimensional scaling and multivariate analysis with optimal transformations. *Psychometrika*, *57*(4), 539–565.
44. Okada, A. (2003). Using additive conjoint measurement in analysis of social network data. In M. Schwaiger & O. Opitz (Eds.), *Exploratory data analysis in empirical research* (pp. 149–156). Berlin: Springer.
45. Okada, A. (2008). Two-dimensional centrality of a social network. In: C. Preisach, H. Burkhardt, Schmidt-Thieme L. & R. Decker (Eds.), *Data analysis, machine learning and applications* (pp. 381–388). Berlin: Springer.
46. Osgood, C. E., & Luria, Z. (1954). A blind analysis of a case of multiple personality using the semantic differential. *Journal of Abnormal and Social Psychology*, *49*(4), 579–591.
47. Osgood, C. E., Suci, G. J., & Tannenbaum, P. H. (1957). *The measurement of meaning*. Urbana, IL: University of Illinois Press.

48. Prim, R. C. (1957). Shortest connection networks and some generalizations. *Bell System Technical Journal*, *36*(6), 1389–1401.
49. Romney, A. K., & Faust, K. (1982). Predicting the structure of a communications network from recalled data. *Social Networks*, *4*, 285–304.
50. Saitou, N., & Nei, M. (1987). The neighbor-joining method: A new method for reconstructing phylogenetic trees. *Molecular Biology and Evolution*, *4*(4), 406–425.
51. Sammon, J. W. (1969). A nonlinear mapping for data structure analysis. *IEEE Transactions on Computers*, *C-18*(5), 401–409.
52. Sattath, S., & Tversky, A. (1977). Additive similarity trees. *Psychometrika*, *42*(3), 319–345.
53. Shepard, R. N. (1962). The analysis of proximities: Multidimensional scaling with an unknown distance function, *Psychometrika*, Part I: *27*(2), 125–140, Part II: *27*(3), 219–246.
54. Shepard, R. N. (1980). Multidimensional scaling, tree fitting, and clustering. *Science*, *210*, 390–398.
55. Shepard, R. N., & Arabie, P. (1979). Additive clustering: Representation of similarities as combinations of discrete overlapping properties. *Psychological Review*, *86*(2), 87–123.
56. Tenenbaum, J. B., de Silva, V., & Langford, J. C. (2000). A global geometric framework for nonlinear dimensionality reduction. *Science*, *290*(5500), 2319–2323.
57. Torgerson, W. S. (1958). *Theory and methods of scaling*. New York: Wiley.
58. Whittaker, J. (1990). *Graphical models in applied multivariate statistics*. Chichester, UK: Wiley.
59. Young, G., & Householder, A. S. (1938). Discussion of a set of points in terms of their mutual distances. *Psychometrika*, *3*(1), 19–22.

Pitfalls in the Construction of Response Scales in Cross-Cultural Surveys: An Example from East Asian Social Survey

Noriko Iwai and Satomi Yoshino

Abstract With an example from Japanese General Social Survey (JGSS) and East Asian Social Survey, this paper discusses difficulties in the construction of response scales in cross-cultural surveys. Issues on the cultural differences in response tendencies are examined with comparisons of response distributions from JGSS and EASS. Despite careful attempts to minimize biases, there can be problems in the instruments, which may influence the data quality. Challenges about the use of internationally validated scales are addressed with an example of EASS 2010 health nodule development.

1 Introduction

Due to the increasing popularity of cross-national survey research and the cross-cultural studies, there are a number of studies that examined issues in cross-national and cross-cultural surveys. Numerous findings have been reported on cultural differences in response tendencies across countries as well as within multicultural countries. For example, while there is a higher tendency for respondents to choose extreme responses in Western countries such as U.S. and Canada, U.K. and Germany, choosing midpoint responses is rather popular in East Asia (Chen, Lee, & Stevenson [2]; Si & Cullen [16]).

Different theories have been identified to explain these cultural differences. With respect to cultural differences in collectivistic versus individualistic culture, it had been identified that respondents from collectivistic culture value in group harmony and tend to choose midpoint responses, whereas those from individualistic culture do not afraid to speak their own mind and are likely to choose extreme responses

N. Iwai (✉) · S. Yoshino
JGSS Research Center, Osaka University of Commerce, 4-1-10 Mikuriyasakae-machi, Higashi-Osaka 577-8505, Japan
e-mail: n-iwai@tcn.zaq.ne.jp

S. Yoshino
e-mail: syoshino@daishodai.ac.jp

T. Imaizumi et al. (eds.), *Advanced Studies in Behaviormetrics and Data Science*,
Behaviormetrics: Quantitative Approaches to Human Behavior 5,
https://doi.org/10.1007/978-981-15-2700-5_25

(Behr & Shishido [1]; Harzing [5]; Takahashi, Ohara, Antonucci, & Akiyama [19]). As for differences in communication style, past research pointed out that in some culture people prefer to be seen as modest, while in other cultures, extreme response would be viewed as sincerity (Harzing [5]; Smith [17]).

Culture and country-level characteristics have been reported to explain the variance in response tendencies at a greater proportion as compared to socio-demographic characteristics (Roberts [13]; Van Vaerenbergh & Thomas [20]). As there is much to be learned from cross-cultural comparisons, construction of comparable measurements is essential. This paper discusses challenges in constructing response scales in cross-cultural surveys, using Japanese General Social Survey (JGSS) and East Asian Social Survey (EASS) as an example.

2 Development of Scales in JGSS and EASS Questionnaires

2.1 Development of JGSS Questionnaires

Japanese General Social Survey (JGSS) was modeled after the General Social Survey (GSS) in the United States (Iwai [9, 10]) . In the development of JGSS questionnaires, two pilot surveys were conducted in order to examine response tendencies among Japanese respondents, and how they might be different from those in the United States. The pilot studies used a split-ballot method with Questionnaire A including questions and response scales that are often used in the GSS. The other included the questions and scales which were common in Japanese surveys (Iwai [9, 11]; Sugita & Iwai [18]).

Specifically, the followings areas were tested to understand ways in which Japanese respondents answer to question: wording effect, characteristics of scales such as scales' polarity, symmetry, the number of categories, and inclusion of "Don't know" option (Iwai [9, 11]; Sugita & Iwai [18]). The examination of the results from the two pilot studies showed that among the eight common response styles identified by Roberts [13], Japanese respondents had midpoint response style as well as mild point response style. Therefore, a guideline for the JGSS questionnaire was made in the effort to minimize the bias (for details of the guidelines, see Iwai [9]).

Regarding the wording, JGSS had noticed that some of the Japanese translations in response categories for questions in the International Social Science Programme (ISSP) that have been conducted by The NHK Broadcasting Culture Research Institute were not exactly the same as the original wording in English. For example, in Gender Role Module (1994, 2002, 2012), a response category "strongly agree" was translated as "そう思う" which means "I think so" or "I agree" (Table 1). It is very interesting that a higher proportion of Japanese respondents chose "strongly disagree" to the statement, "A man's job is to earn money, a woman's job is to look after home and family (V11)" as compared to respondents from the United States in 2012 (Fig. 1). This result does not necessarily mean that Japanese had more liberal

Table 1 Comparison of translations of response categories between the United States and Japan for ISSP Gender Module

USA	Japan
Strongly agree	そう思う (Agree)
Agree	どちらかといえばそう思う (Somewhat agree)
Neither agree nor disagree	どちらともいえない (Neither agree nor disagree)
Diagree	どちらかといえばそうは思わない (Somewhat disagree)
Strongly disagree	そうは思わない (Disagree)

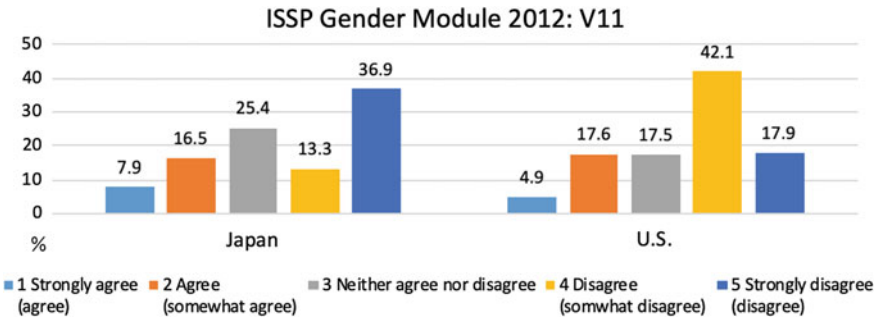

Fig. 1 Comparison of response distributions between Japan and the United States

gender role ideology than Americans in 2012. It was likely the result of translations in the response scale categories. In constructing JGSS questions and response categories, JGSS has been paying tremendous attention in wording and in translation of questions if they are originally made in English such as EASS module questions which will be described below.

2.2 Development of EASS Questioners

East Asian Social Survey (EASS) was launched to produce data on issues relevant to East Asian societies and is comprised with four teams, which conduct GSS-type national surveys in Japan (JGSS), China (Chinese GSS), Korea (Korean GSS), and

Taiwan (Taiwan Social Change Survey). EASS is not an independent survey, but the methodology was developed based on a pre-existing survey framework in each society, in which the EASS modules are incorporated into. Modules are developed in English first, and each team translates the modules into their own languages, followed by back translation into English for checking the accuracy of the translations.

EASS places emphasis on cultural comparability in data collections, and one of the central focuses of discussions for EASS modules development was the construction of response scales. As noted earlier, a number of previous studies illustrated cultural differences in response tendencies between respondents from Asia and Western cultures; they tend to report that Asians are likely to choose midpoint responses (Chen et al. [2]; Behr & Shishido [1]; Harzing [5]; Smith [17]). However, during the EASS module development, it became clear that there are also variations among the four societies and that issues on midpoint response style are not as problematic in China and Korea as they are in Taiwan and Japan (Shishido [14]; Shishido, Iwai, & Yasuda [15]). Variations can be observed in response patterns among Japanese, Chinese, Korean, and Taiwanese respondents (Behr & Shishido [1]). Figure 2 compares the distributions of 18 survey items for the four groups of respondents using the EASS 2006 family module, and the distinct patters of Japanese respondents are clearly displayed.

In Taiwan, in the face-to-face interview, respondents were first asked to choose "agree" or "disagree" to a question, followed by the degree to which they agree or disagree. Only when respondents refused to choose either an answer at the first step, they were given a choice for "neither agree nor disagree." This method is used to reduce the number of midpoint responses (Shishido et al. [15]) JGSS cannot adopt this method, since JGSS includes most of the EASS module questions into a self-administered questionnaire, not into an interview questionnaire.

During the discussions on EASS response scale development, while Japanese team was reluctant to include a midpoint in response scales due to tremendously high concentration of responses to the midpoint, other three teams requested to include it in order to make the scale comparable to other global surveys such as the ISSP (Behr & Shishido [1]). After a series of discussions and pre-tests in each society, EASS teams decided to adopt a 7-point scale with a midpoint (ranging from strongly agree to strongly disagree) in attitudinal questions (see (Shishido et al. [15]) for more details about the development of EASS response scales).

3 Inclusion of both EASS and JGSS Scales into JGSS Questionnaires

As described in the previous section, EASS scales put primary focus on the compatibility with other international surveys such as ISSP. At the same time, it was also critical for the JGSS to pursue the comparability with other Japanese surveys, in which intense adverb is generally avoided. Therefore, the JGSS team decided to

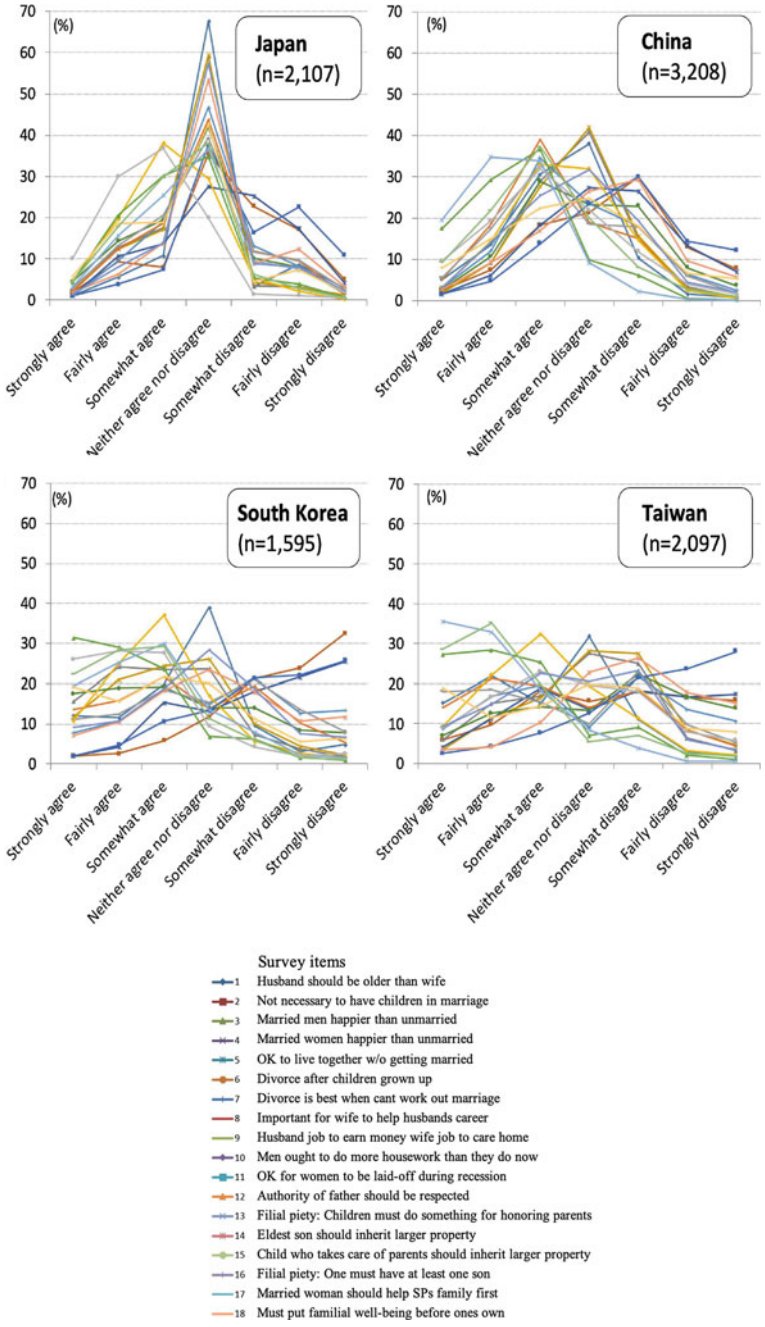

Fig. 2 Comparison of response distributions (Adopted from "Issues in cross sectional national surveys: Experience from JGSS and EASS projects," by Shishido [14])

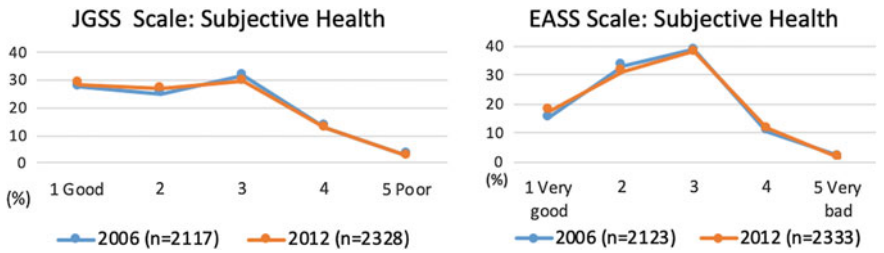

Fig. 3 Distributions of response on subjective health in JGSS-2006 and JGSS-2012

use the split-ballot method when possible in order to include two scales, the JGSS scale and the EASS scale, for some of the questions.

Subjective health is one of the questions that have been asked using two scales, while the JGSS scale ranges from 1 Good to 5 Poor, the EASS scale ranges from 1 Very good to 5 Very bad. The wording of the questions is exactly the same: "How would you rate your health condition?" Figure 3 shows the response distributions by each scale in JGSS-2006 and JGSS-2012. Though responses in both scales are concentrated on and around the midpoint, the concentrations are notably high in the EASS scale. Furthermore, in line with the previous findings and the results of JGSS pilot studies (Iwai [9]; Sugita & Iwai [18]), in the EASS scale, much less respondents chose the first category, which had the extreme adverb "very".

Table 2 Sample descriptions

	JGSS 2006				JGSS 2012			
Age (mean)	A		B		A		B	
	52.42		52.73		53.55		53.27	
T-test	t = −0.611, p = 0.541				t = 0.572, p = 0.568			
	N	%	N	%	N	%	N	%
Sex								
Male	1023	48.2	964	45.3	1060	45.5	1088	46.6
Female	1101	51.8	1166	54.7	1272	54.5	1247	53.4
Pearson chi-square	$\chi^2 = 3.607$, $p = 0.058$				$\chi^2 = 0.611$, $p = 0.434$			
Marital status								
Married/cohabitated/widowed	1739	81.9	1716	80.6	1847	79.2	1840	78.8
Divorced/separated/Never married	385	18.1	414	19.4	485	20.8	495	21.2
Pearson chi-square	$\chi^2 = 1.197$, $p = 0.274$				$\chi^2 = 0.113$, $p = 0.736$			
Education								
Less than high school	384	18.2	402	19	372	16	338	14.5
High school	1021	48.4	1045	49.3	1085	46.8	1071	46.0
Post-secondary school	704	33.4	672	31.7	863	37.2	917	39.4
Pearson chi-square	$\chi^2 = 1.412$, $p = 0.494$				$\chi^2 = 3.350$, $p = 0.187$			

As the respondents were randomly selected and randomly assigned to one of the two questionnaires, the observed differences in the distributions cannot be attributed to sampling selection bias. In addition, there were no significant differences in the sample characteristics between the two groups of respondents in the split-ballot for both JGSS 2006 and JGSS 2012 as summarized in Table 2. Therefore, there were no biases in the sample characteristics which might have influence on the observed differences in the two types of scales for subjective health.

The comparison of the two scales for subjective health highlights a pitfall in designing cross-country and cross-cultural surveys. While it is crucial to develop questions and response scales that are culturally appropriate for all the participating countries, it is also important to consider country-specific patterns, including response patterns and biases. Achieving cross-cultural comparability and pursuing for local validity can be incompatible at times (He & van de Vijver [6]).

Having two scales in one survey enables researchers to choose whichever scales that might be appropriate for their investigations; however, it is not always the option. Previous studies have pointed out the lack of attention to response scales among researchers who develop surveys (Shishido et al. [15]). Users of survey data need to make sure the details of the methodologies in the survey and be aware of the influence of response scales, which might have impact on their analysis.

4 Inclusion of Existing International Scales in EASS 2010 Health Module

The theme of the EASS 2010 module was health, and from an early stage of the module discussion, the EASS teams agreed to include internationally validated scales for health status of the respondents as it was the most fundamental questions for the module (Hanibuchi [4]). The EASS team decided to include the SF-12, which is a short version of the Medical Outcomes Study (MOS) 36-item Short-Form Health Survey SF-36 (Ware, Kosinski, Turner-Bowker, & Gandek [21]). The SF-12 was originally developed in English and translated to and validated in various other languages, including Japanese (Fukuhara & Suzukamo [3]) . Among the EASS teams, JGSS included the already validated version of questions in Japanese. In China, at the time of the EASS 2010 health module development, there was no Chinese version that has been validated, so CGSS purchased a copyright for the original English version and translated by themselves.

Although there was already validated version of SF-12 in Taiwan, the Taiwanese team (TSCS) decided not to include the SF-12 into their questionnaires for several reasons. TSCS was preparing for conducting the EASS 2010 health module along with the ISSP health module. Due to these reasons, TSCS chose not to include the SF-12, and included only a few basic measurements for respondents' health status.

Table 3 Comparison of the translations of the subjective health scale (SF-12) in the EASS 2010 module

EASS 2010		JGSS	CGSS	KGSS	TSCS
	SF-12				
1	Excellent	最高によい (Excellent)	很健康 (Very healthy)	매우 좋다 (Very good)	非常好 (Excellent)
2	Very good	とても良い (Very good)	比较健康 (Somewhat healthy)	다소 좋다 (Somewhat good)	很好 (Very good)
3	Good	良い (Good)	一般 (General)	좋지도 나쁘지도 않다 (Neither good nor bad)	好 (Good)
4	Fair	あまり良くない (Somewhat poor)	比较不健康 (Somewhat unhealthy)	다소 나쁘다 (Somewhat poor)	普通 (Fair)
5	Poor	良くない (Poor)	很不健康 (Very unhealthy)	매우 나쁘다 (Very poor)	不好 (Poor)

4.1 Translation Issues on Subjective Health in the EASS 2010 Health Module

Table 3 shows the comparison of literal translations of the response categories in Japanese, Chinese, Korean, and Taiwanese for the question on subjective health, which is one of the 12 questions in the SF-12. Parentheses under the translations in each language include the literal translations of the words back to English. As you can see, the table with back translations illustrates that the wording of the translations is not identical across four teams. Translations in Taiwanese are the most accurate among the four teams, and the rest of the teams had issues in the translations (Iwai [7]; Iwai & Yoshino [8]). For example, in Japan, the SF-12 had been validated in Japanese, and the Japanese version is copyrighted. Therefore, the JGSS team was unable to change any wordings in the scale.

As translations in the response scales for subjective health in the EASS 2010 health module were unequal across the four teams, there were notable variations in the response distributions among the respondents in the four societies Fig. 4. At first glance, Taiwanese respondents appear to be the least healthy with the highest proportion of respondents scoring 4. "Fair", and the less proportions of respondents reporting excellent to good health as compared to the other countries. However, when we compare the response distributions with Table 3, it became clear that the translation of the category 4. "Fair" was quite different in Taiwanese translation as they were in other languages. While the Taiwanese translation indicate 4. "Fair" as a middle point to slightly positive condition. translations in Japanese, Chinese, and Korean imply "somewhat poor". Thus, the observed differences in subjective health were likely to be attributed to the different connotations in the response categories.

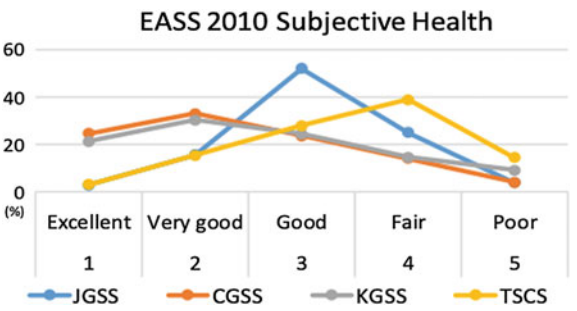

Fig. 4 Distributions of responses on subjective health in EASS 2010

Table 4 Proportions of not having chronic disease or longstanding health problem and their distributions of subjective health

	Japan	China	Korea	Taiwan
% not having any chronic disease or longstanding health problem	54.4	66.0	69.2	67.9
Subjective health				
Excellent	4.6	35.2	27.5	3.8
Very good	24.3	40.5	37.2	20.1
Good	60.2	19.3	25.6	31.2
Fair	10.3	4.2	8.2	36.7
Poor	0.5	0.7	1.5	8.2

There were not many objective measurements of health in the EASS 2010 health module, so it is difficult to clarify the influence of the translation problems on the response distributions for subjective health. However, it is possible to compare the response distributions of subjective health with self-reported presence of chronic conditions or longstanding health problem, which is the only quasi-objective health measurement.[1]

Table 4 shows the proportion of those who do not have any chronic disease or longstanding health problem and their distributions of subjective health. The proportion of respondents who do not have chronic health problems in China (66.0%), Korea (69.2%), and Taiwan (67.9%) was similar, yet the proportion of those who said their health to be excellent to very good were much lower in Taiwan compared to the other two countries (75.7% for Chinese, 64.7% for Korean, and 23.9% for Taiwanese). In fact, the number was the lowest for Taiwanese as it was even lower than Japanese (28.9%). As the response scale in Taiwanese was off balanced, the response distribution was notably skewed.

[1] As presence of chronic conditions was self-reported, it is called quasi-objective rather than objective Jürges [12].

Additionally, patterns in the response distributions for subjective health in EASS 2010 were also different from other modules. The next section compares the response distributions for subjective health between the EASS 2010 and the EASS 2012.

4.2 *Issues in the Distributions of Subjective Health in the EASS 2010 Health Module*

Figure 5 shows the comparison of the distributions of subjective health for Japanese, Chinese, Korean, and Taiwanese respondents in EASS 2010 and EASS 2012. As for Japanese respondents, the concentration at the midpoint is substantial in EASS 2010 compared to the response distributions in EASS 2012. As Japanese respondents have strong tendency to avoid extreme responses (Behr & Shishido [1]), having two

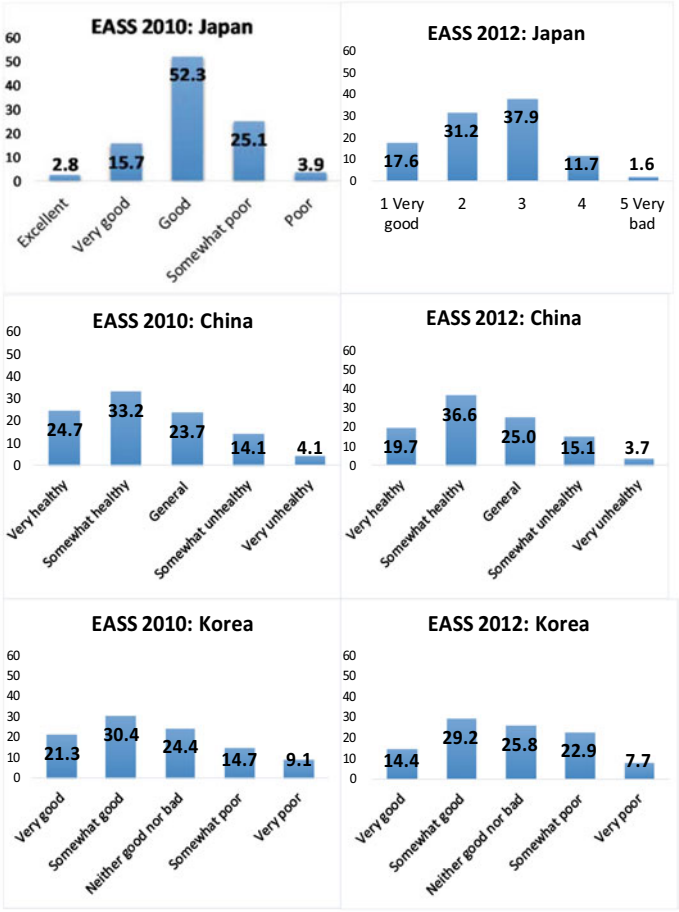

Fig. 5 Comparison of the distributions of subjective health in EASS 2010 and EASS 2012

Table 5 Comparison of the distributions of subjective health in EASS 2010 and EASS 2012

	Japan				Taiwan			
Age (mean)	2010		2012		2010		2012	
	53.7		53.3		46.8		45.81	
T-test	t = −0.888, p = 0.375				t = 1.836, p = 0.66			
	N	%	N	%	N	%	N	%
Sex								
Male	1154	46.2	1088	46.6	1086	49.4	1074	50.3
Female	1342	53.8	1247	53.4	1113	50.6	1060	49.7
Pearson chi-square	$\chi^2 = 0.063$, $p = 0.801$				$\chi^2 = 0.384$, $p = 0.535$			
Marital status								
Married/cohabitated/widowed	1805	72.3	1655	70.9	1309	59.7	1280	60
	203	8.1	185	7.9	173	7.9	166	7.8
Divorced/separated/Never married	99	4	127	5.4	99	4.5	106	5
	388	15.6	368	15.8	613	27.9	581	27.2
Pearson chi-square	$\chi^2 = 6.042$, $p = 0.110$				$\chi^2 = 0.706$, $p = 0.872$			
Education								
No formal education	0	0	0	0	140	6.4	114	5.9
Less than high school	396	15.9	338	14.5	593	27	551	26.4
High school	1157	46.6	1072	46.1	557	25.3	550	25.6
Post-secondary school	931	37.5	916	39.4	908	41.8	919	42.2
Pearson chi-square	$\chi^2 = 2.759$, $p = 0.0252$				$\chi^2 = 3.369$, $p = 0.338$			

categories with highly positive health status "excellent" and "very good" resulted in less variance.

Response distributions for Taiwanese respondents in EASS 2010 were also considerably different from those in EASS 2012. The highest point in the distributions in EASS 2010 was at "Fair", whereas in EASS 2012 the responses were peaked at the midpoint. This was likely because the wording of the translation used for "Fair" in EASS 2010 indicates the middle point. Response distributions for Chinese and Korean respondents in the two EASS modules were fairly similar as the response scales were exactly the same.

Table 5 shows some of the basic sample characteristics for respondents from Japan and Taiwan in EASS 2010 and EASS 2012. There were no significant differences between basic sample characteristics in EASS 2010 and EASS 2012, which might have influence on the observed differences in the distributions of subjective health, for both Japanese and Taiwanese respondents.

4.3 Issues in the Use of Existing Scales

Internationally developed and validated scales are of great use, which can provide opportunities for statistical comparisons. However, as shown in the example of the EASS 2010 health module, there might be inflexibility in the existing scales, which can be challenging when adding into cross-cultural survey. While translations and validations of scales into one language focus on cultural sensitivity in the country, cross-cultural survey needs to consider cultural sensitivity in all participating cultures. He and van de Vijver [6] pointed out the importance of instrument choices in cross-cultural surveys, highlighting the difficulties cultural-specific considerations may add to the methodology.

5 Conclusion

As cross-national and cross-cultural survey researches continue to gain attention from researchers in various disciplines, development of comparable measurements across cultures is important subject that needs further research. With an example from Japanese General Social Survey (JGSS) and East Asian Social Survey, this paper examined challenges regarding the construction of response scales in cross-cultural surveys.

Discussions on the development of the EASS scale highlight that there are variations in response style even among the four East Asian societies: Japanese and Taiwanese respondents tend to choose midpoint more than Chinese and Korean respondents. The comparison between the JGSS scale and the EASS scale on subjective health further illustrates the midpoint response style among the Japanese respondents.

As He and van de Vijver [6] point out, aiming for cross-cultural comparability might be incompatible with obtaining local validity when constructing measurements. In order to minimize the variations of response style among the four teams, EASS teams chose to use a 7-point scale in attitudinal questions as the 7-point scale works better than 5-point scale with regard to response variances. Similarly, in European Social Survey, there are various numbers of response options (up to 11 points) used depending on the types of questions. Choosing an appropriate response option based on results of pilot studies in each society is one way to minimize the influence of response styles in cross-cultural survey research.

Comparisons of response distributions for respondents' subjective health in EASS 2010 health module and translations in the four teams demonstrate the problems in cross-cultural survey data. As a part of the preparation for the EASS 2020 health module, the EASS teams had a number of discussions in order to solve the issues in the response scale. The four teams shared the difficulties and issues in the translation of the subjective health scale. While Taiwanese translation had no problem in the EASS 2010 health module, other three translations needed to be modified so that

the translations would be accurate and the data would be compatible across the four teams. There were concerns that needed to be considered, which include the comparability between the 2010 health module and the 2020 health module as well as the comparability with other EASS modules. The EASS teams agreed that the first priority should be achieving the equivalence in the translation of the response scale and that the wordings of the translation need to be changed accordingly. Specifically, Chinese and Korean scales would be changed from a balanced scale to an unbalanced scale, leaning toward positive, in order to make it equivalent with the original English scale (please refer to the Table 3 for details). As the Japanese translation is copyrighted and cannot be changed, the Japanese team decided to add another question to measure respondents' subjective health, in which the translation would be comparable with the other three teams.

While existing scales that have been validated in multiple languages can be a useful tool in cross-country survey research, there might be issues in comparability as the translation and validation are done in one country at a time. There are a number of other issues that can influence the comparability in cross-national survey research, such as sampling, survey mode, and response bias. For researchers to make accurate observations, examination of details in methodologies and basic data description are necessary before the analyses of any data.

Acknowledgements The Japanese General Social Surveys (JGSS) are designed and carried out by the JGSS Research Center at Osaka University of Commerce (Joint Usage/Research Center for Japanese General Social Surveys accredited by Minister of Education, Culture, Sports, Science and Technology). JGSS-2000 to 2012 had been conducted in collaboration with the Institute of Social Science at the University of Tokyo. The project is financially assisted by the Japanese Ministry of Education, Culture, Sports, Science and Technology and Osaka University of Commerce. East Asian Social Survey (EASS) is based on Chinese General Social Survey (CGSS), Japanese General Social Surveys (JGSS), Korean General Social Survey (KGSS), and Taiwan Social Change Survey (TSCS), and distributed by the EASSDA.

References

1. Behr, D., & Shishido, K. (2016). The translation of measurement instruments for cross-cultural surveys. In C. Wolf, D. Joye, T. W. Smith & Y. C. Fu (Eds.), *The SAGE handbook of survey methodology* (pp. 269–287). Sage.
2. Chen, C., Lee, S. Y., & Stevenson, H. W. (1995). Response style and cross-cultural comparisons of rating scales among East Asian and North American students. *Psychological Science*, *6*(3), 170–175.
3. Fukuhara, S., & Suzukamo, Y. (2004). *SF-8TM Nihongo manual*. [SF-8TM A Manual in Japanese]. iHope International.
4. Hanibuchi, T. (2009). Development of EASS 2010 health module: Results of JGSS pretest. *JGSS Research Series*, *6*, 211–242.
5. Harzing, A. W. (2006). Response style in cross-national survey: A 26-country study. *International Journal of Cross Cultural Management*, *6*(2), 243–266.
6. He, J., & van de Vijver, F. (2012). Bias and equivalence in cross-cultural research. *Online Readings in Psychology and Culture*, *2*(2), 8.

7. Iwai, N. (2017, September). *Effects of differences in response scale in cross-national surveys*. Paper presented at the 1st RC33 Regional Conference on Social Methodology, Taipei.
8. Iwai, N., & Yoshino, S. (2019, July). *The effects of differences in response scale in cross-national surveys*. Paper presented at the 2019 European Survey Research Association Conference, Zagreb.
9. Iwai, N. (2004a). Japanese general social survey: Beginning and development. *JGSS Monograph Series*, *3*, 241–271.
10. Iwai, N. (2004b). Japanese general social survey: Beginning and development. *ZA-Information*, *55*, 99–113.
11. Iwai, N. (2005). Japanese general social survey (2): Methodological experiments in administering the questionnaire, incentives, scales, and wording. *ZA-Information*, *57*, 83–102.
12. Jürges, H. (2006). *True Health vs. Response Styles: Exploring Crosscountry Differences in Self-reported Health*. DIW Discussion Papers, No. 588, Deutsches Institutfür Wirtschaftsforschung (DIW), Berlin.
13. Robert, C. (2016). Response styles in surveys: Understanding their causes and mitigating their impact on data quality. In C. Wolf, D. Joye, T. W. Smith & Fu, Y. C. (Eds.), *The SAGE handbook of survey methodology* (pp. 579–598). Sage.
14. Shishido, K. (2016, July). *Issues in cross sectional national surveys: Experience from JGSS and EASS projects*. Presented at Research Colloquium at Doshisha University, Kyoto.
15. Shishido, K., Iwai, N., & Yasuda, T. (2009). Designing response categories of agreement scales for cross-national surveys in East Asia: The approach of the Japanese general social surveys. *International Journal of Japanese Sociology*, *18*, 97–111.
16. Si, S. X., & Cullen, J. B. (1998). Response categories and potential cultural bias: Effects of an explicit middle point in cross-cultural surveys. *The International Journal of Organization Analysis, 6*(3), 218–230.
17. Smith, P. B. (2004). Acquiescent response bias as an aspect of cultural communication style. *Journal of Cross-Cultural Psychology*, *35*(1), 50–61.
18. Sugita, H., & Iwai, N. (2003). JGSS project (??) Sokutei shakudo to sentakushi [JGSS project (3) measurement and wording of questions]. *Statistics*, *12*, 49–56.
19. Takahashi, K., Ohara, N., Antonucci, T. C., & Akiyama, H. (2002). Commonalities and differences in close relationships among the Americans and Japanese: A comparison by the individualism/collectivism concept. *International Journal of Behavioral Development*, *26*(5), 453–465.
20. Van Vaerenbergh, Y., & Thomas, T. D. (2013). Response styles in survey research: A literature review of antecedents, consequences, and remedies. *International Journal of Public Opinion Research*, *25*(2), 195–217.
21. Ware, J. E, Jr., Kosinski, M., Turner-Bowker, D. M., & Gandek, B. (2002). *How to score version 2 of the SF-12R health survey (with a supplement documenting version 1)*. Lincoln, RI: QualityMetric Incorporated.

Japanese Women's Attitudes Toward Childrearing: Text Analysis and Multidimensional Scaling

Kunihiro Kimura

Abstract This study aimed to understand Japanese women's attitudes toward childrearing via text analysis. The text data were taken from the emails that readers had submitted to a magazine as a reply to the call for essays on the theme "Is Childrearing a Strain?" I hypothesized that Japanese women tended to attribute "failure" to external factors such as institutional flaws and "success" to internal factors such as their personal conditions. I employed an "appearance of strings" approach to natural language processing to map the keywords onto "topics." Based on the multiple classification of emails with respect to the topics referred, I calculated symmetric and asymmetric versions of Jaccard Similarity Coefficient and applied four multidimensional scaling models: Torgerson's method, SMACOF, slide vector model, and drift vector model. There was a contrast between positive and negative feelings. There were also personal, interpersonal, and societal facets. The emails expressing positive attitudes tended to refer to only personal topics, while those manifesting negative attitudes tended to refer to the topics in all the three facets. In the latter group of emails, reference to personal topics implied reference to interpersonal topics, and reference to interpersonal topics implied reference to societal topics.

1 Introduction

Text analysis, which is also called text mining or text analytics (Solka [22]; Brier & Hopp [5]), is helpful in exploring the structure of people's attitudes. In this paper, I will report the results of my study that employed text analysis to understand Japanese women's attitudes toward childrearing. The text data were taken from the emails that readers had submitted to a magazine as a reply to the call for essays on the theme "Is Childrearing a Strain?"

Although this study followed the orthodox procedure for text analysis that consists of two steps, that is, feature extraction and multivariate analysis (Solka [22]; Brier

K. Kimura (✉)
Tohoku University, 27-1 Kawauchi, Aoba-ku, Sendai 980-8576, Japan
e-mail: kkimura@tohoku.ac.jp

T. Imaizumi et al. (eds.), *Advanced Studies in Behaviormetrics and Data Science*,
Behaviormetrics: Quantitative Approaches to Human Behavior 5,
https://doi.org/10.1007/978-981-15-2700-5_26

& Hopp [5]), it had a distinctive characteristic in each step. In the first step of this study, it employed an "appearance of strings" approach to natural language processing in order to map the keywords and phrases that appeared in the documents onto "topics"[1] and thereby classify the documents. In the second step, it applied not only symmetric but also *asymmetric* multidimensional scaling (MDS) models to the data of the dissimilarity between topics.

I expected that these characteristics would contribute to elucidate the "implying–implied" relationship between the topics, and thereby enable us to examine a social–psychological hypothesis on the causal attribution in childrearing.

This study was also a reexamination of my previous study with my student (Hasegawa & Kimura [11]),[2] with the same dataset but different techniques. Hasegawa and Kimura [11] had adopted ALSCAL. In this study, I applied Torgerson's method, symmetric SMACOF, and the two asymmetric MDS models, that is, slide vector model and drift vector model.

2 Attribution of Success and Failure Hypothesis

Our previous study (Hasegawa & Kimura [11]) found the contrast between positive and negative feelings and that between personal and societal topics. It also found that personal topics had tended to be proximate to positive attitudes while societal topics had tended to be proximate to negative attitudes. We could interpret this pattern of association from a social–psychological perspective on the causal attribution of success and failure (Beckman [2]; Zuckerman [26]). People tend to attribute "success" to internal factors, while they tend to attribute "failure" to external factors. Although many scholars have used the term "self-serving bias" to describe these tendencies and assumed self-enhancement and self-protection motivations to explain them (Miller & Ross [16]; Böhm, & Pfister [3]), I would not like to delve into motivational processes or to examine whether they are a kind of error or not. Rather, I will simply hypothesize such tendencies and deduce predictions from the hypothesis.

Application of the idea of internal/external attribution to the case of Japanese women's experience in childrearing yields the following hypothesis:

– *Hypothesis*. Japanese women who have experienced strain in childrearing would believe that it was caused by external factors such as institutional flaws, while those who have not would believe that they are well-off owing to their personal conditions.

From the hypothesis, the two predictions will follow:

[1] Since I use the word "topic" in nontechnical terms, I would not refer to Topic Modeling or Latent Semantic Analysis.

[2] Hasegawa and Kimura [11] is a revised and abbreviated version of Hasegawa [10].

– *Prediction 1*. Configurations obtained by various multidimensional scaling (MDS) models will exhibit the contrast between positive and negative feelings and that between personal and societal topics.
– *Prediction 2*. In the configurations, personal topics are proximate to positive feelings while societal topics are proximate to negative feelings.

3 Method

The text data were taken from the emails that readers had submitted to a magazine. In the first step of text analysis, that is, in feature extraction, I used a text analytics software that is specialized to Japanese language and adopts an "appearance of strings" approach to natural language processing. I adopted the coding rules described in Hasegawa [10, Appendix] with some modification. These coding rules map the keywords or phrases that appeared in the emails onto topics.

The second step of text analysis is multivariate analysis. Multidimensional scaling (MDS) and correspondence analysis (CA) are often used to obtain a configuration of topics in documents. I used MDS because it is superior to CA in the visualization of data in the sense that a configuration plot obtained by MDS is much easier to interpret than graphical representation of a result obtained by CA.[3]

In order to apply MDS models to the data obtained by the multiple classification of emails with respect to the topics referred, we need to calculate a measure of similarity between the topics and transformed it to dissimilarity. I employed ordinary and asymmetric versions of Jaccard Similarity Coefficient to measure the similarity.

3.1 Data

I analyzed the same dataset as Hasegawa [10] and Hasegawa and Kimura [11] had used. The sample ($n = 102$) was taken from the emails published in *Is Childrearing a Strain? Emails from 2,118 Readers*, Special Issue of *AERA*, a Japanese magazine (AERA Editorial Office [1]). The editorial office of the magazine had asked the readers to submit their essays of this title via email. Hasegawa [10], considering the aim of her study, selected the 102 essays according to the following criteria: (1) the writer was female, (2) she voluntarily submitted her essay, and (3) it refers to the conditions of childrearing in Japan at that time. Essays that only referred to the conditions of childrearing in abroad or those that had been written at the request of the editorial office were excluded.

[3]For cautions in interpreting graphical representation of a result obtained by CA, see, for example, Brier and Hopp [5, p. 115]. For suggestions in interpreting a configuration plot obtained by MDS, see, for example, Borg, Groenen, and Mair [4, Chap. 7].

3.2 Classification of Documents According to Mapping of Keywords onto Topics

In order to map the keywords or phrases that appeared in the emails onto topics and classify the emails according to the mapping, I used AUTOCODE for Windows Ver. 1.03 (Sato [20, 21]), a text analytics software specialized to Japanese language. AUTOCODE adopts an "appearance of strings" approach to natural language processing. That is, it is only based on the appearance of strings (or sequences of characters). Although it requires preparing a dictionary, a set of coding rules that maps strings to topics, it does not involve morphological analysis, parsing, or machine learning.

The most important advantage of this approach is that it is easy to handle the expression of negation. For example, it is easy to distinguish between the four: happy, not happy, unhappy, and not unhappy. A disadvantage of this approach, however, lies in the fact that we need a dictionary customized to the specific data.

I used the coding rules described in Hasegawa [10, Appendix] with some modification for minimizing the errors in classification and thereby increasing the accuracy. Hasegawa [10] coded respondents' feelings by intensively reading the emails instead of using the results from AUTOCODE. In this study, I independently read them and reattached codes for feelings to each of them.

3.3 Measurement of Similarity Between Topics

Based on the multiple classification of emails with respect to the topics referred, I measured similarity between the topics, transformed it to dissimilarity, and applied multidimensional scaling (MDS) models to the dissimilarity matrix.

Although many similarity measures have been proposed (Gower [8]; van Eck & Waltman [24]), the most frequently used ones in text analysis are Jaccard Similarity Coefficient and Cosine (Solka [22]; Brier & Hopp [5]). Cosine is, however, mostly used to measure similarity between documents. We need to measure similarity between topics here. For this purpose, Jaccard Similarity Coefficient is more appropriate than Cosine.[4] Moreover, we can use a modified version of Jaccard Similarity Coefficient to measure asymmetric similarity.

Thus, I used ordinary Jaccard Similarity Coefficient (Jaccard [12–14]) to measure symmetric similarity between the topics appearing in the emails. Let $C = \{c_{ij}\}$ be a co-occurrence matrix, where c_{ij} stands for the entry to the cell of the ith row and the

[4] van Eck and Waltman [24] argued that for the purpose of normalization of occurrence, probabilistic measures of similarity, whose example is Association Strength, are more appropriate than set-theoretical measures such as Cosine, Inclusion Index, and Jaccard Similarity Coefficient. Lee, Pincombe, and Welsh [15] showed that the correlations predicted by the measures based on count similarity models of human similarity judgment between documents, such as Jaccard Similarity Coefficient and Cosine, tended to be lower than those predicted by LSA measures, that is, three local weighting functions used in Latent Semantic Analysis, and those achieved by human inter-rater correlation.

jth column in the matrix and represents the frequency of the documents that referred to both ith and jth topics. The coefficient for the topics i and j, denoted by s_{ij}, is defined as

$$s_{ij}=\frac{c_{ij}}{c_{ii}+c_{jj}-c_{ij}}$$

in terms of the entries in the co-occurrence matrix. We can interpret this coefficient as representing the conditional probability that both ith and jth topics appeared in a document given the appearance of one of these topics in it, that is,

$$s_{ij}=P\left(A_i\cap A_j \mid A_i\cup A_j\right)=\frac{P\left(A_i\cap A_j\right)}{P\left(A_i\cup A_j\right)}$$

where A_k represents the set of documents in which the kth topic appeared.

Dissimilarity between the topics, denoted by δ_{ij}, is defined as 1 minus Jaccard Similarity Coefficient, that is,

$$\delta_{ij}=1-s_{ij}$$

where the unity is equal to the theoretical maximum of the coefficient.

Similarly, I used Unilateral Jaccard Similarity Coefficient (Santisteban & Carcamo [19]) to measure *asymmetric* similarity between the topics. The coefficient, denoted by s^*_{ij}, is defined as

$$s^*_{ij}=\frac{c_{ij}}{c_{ii}}$$

Although Santisteban and Carcamo [19] presented an interpretation of this coefficient in terms of the number of edges (or ties) between two vertexes (or nodes) in a network, I prefer an alternative one. As in the case of original, symmetric Jaccard Similarity Coefficient, we can interpret the unilateral or asymmetric version as representing the conditional probability that both ith and jth topics appeared in a document given the appearance of the ith topic, that is,

$$s^*_{ij}=P\left(A_i\cap A_j \mid A_i\right)=\frac{P\left(A_i\cap A_j\right)}{P\left(A_i\right)}$$

In terms of this coefficient, I defined asymmetric dissimilarity as

$$\delta^*_{ij}=1-s^*_{ij}$$

3.4 Multidimensional Scaling

Hasegawa and Kimura [11] had adopted ALSCAL, a frequently used algorithm for multidimensional scaling (MDS), in SPSS. In this study, I applied four MDS models

to the data, using R packages and functions, instead. These models are Torgerson's method, symmetric SMACOF, slide vector model, and drift vector model.

Torgerson's [23] method is a classical, metric MDS model. On the assumption that the distance between a pair of objects is proportional to the similarity or dissimilarity between them and the dissimilarity satisfies the metric axioms, this model estimates the distances between all pairs of objects and obtains a configuration of the objects. This model is implemented in the R function **cmdscale**. In this study, its result was also used as the initial configuration in applying other three models that adopt SMACOF, the majorization approach.

SMACOF (de Leeuw & Mair [7]; Groenen & van de Velden [9]) is an approach to find an MDS solution by using majorization to minimize the loss function called *stress*, which summarizes the discrepancy between the estimated distance and the disparity, where a disparity is a monotonic transformation of the dissimilarity between a pair of objects. I applied simple, symmetric SMACOF model to the data, using the function **smacofSys** (or **mds**) in the R package "smacof."

Slide vector model and drift vector model are asymmetric MDS models. Both models assume decomposition of a dissimilarity matrix into a symmetric part and an asymmetric part. The symmetric part is scaled with SMACOF algorithm to give a configuration of points that represent the objects.

Slide vector model (Zielman & Heiser [25]) represents asymmetry in a dissimilarity matrix as one vector and locate it as an arrow in the configuration plot. Slide vector model would be most useful when there is a systematic and uniform trend or shift. I used the program **ssmacof. R** (de Leeuw [6]) instead of **slidevector** in the R package "asymmetry."

Drift vector model (Borg et al. [4, pp. 57–59]) uses the asymmetric part to attach an arrow on a point. The direction of an arrow is determined by the sign of the asymmetry between the point and another point. A drift vector is a resultant of all the arrows from a point. Drift vector model would be most useful when there is a systematic but not necessarily uniform trend. I used the function **driftVectors** in the R package "smacof."

I expected that these asymmetric MDS models would enable us to elucidate the "implying–implied" relationship between the topics and to examine the attribution of success and failure hypothesis and the predictions derived from it in detail.

4 Results

4.1 Frequency and Co-occurrence of Topics

Table 1 shows the 13 topics that I selected from the results of classification with AUTOCODE. Although our previous study (Hasegawa & Kimura [11]) had picked up 14 topics as variables from the results of classification, I selected 13 of them and

Table 1 Variables representing topics in the text

Variable name	Description
Pretty	"Children (or babies) are pretty"
Worklife	Work–Life balance
Workplac	Workplace system (e.g., childcare leave, reentry to employment)
Admin	Administrative agencies or policies; Governments
School	School; Kindergarten
Peer	Earwigging from peers or neighbors
Husband	Relationship with husband
Maturity	Matured or acquired a new perspective through childrearing
Help	Help or support from others
Captivit	Captivity; No freedom
Money	Money
Negative	Negative feelings for childrearing
Positive	Positive feelings for childrearing

dropped "society in general." This is because the topic was associated with other 13 topics in almost the same degree so that its distinctiveness was disputable.

The topic "workplac" refers to the workplace systems such as working hours, a salary system, childcare leave, or reentry to employment. The topic "maturity" refers to the respondent's belief that she matured or acquired a new perspective through the experience of childrearing.

Table 2 shows the co-occurrence matrix C for the 13 topics. The diagonal represents the number of the emails in which each topic appeared.

4.2 Similarity and Dissimilarity Between Topics

With the entries in the co-occurrence matrix, I calculated ordinary Jaccard Similarity Coefficient and Unilateral Jaccard Similarity Coefficient.[5] The observed values of the former are shown in Table 3, and those of the latter are shown in Table 4. These similarity matrices were transformed into dissimilarity matrices.

[5]Since I modified some of Hasegawa's [10, Appendix] coding rules and independently coded respondents' feelings, the co-occurrence matrix and the Jaccard Similarity Coefficient matrix differ in part from those that Hasegawa [10] and Hasegawa and Kimura [11] used. Although Hasegawa [10] did not show them, we can estimate them by referring to the frequency distribution for the topics [10, p. 30, Fig. 4.2] and the observed four-point correlation coefficients between the topics [10, p. 33, Table 4.1].

Table 2 Co-occurrence matrix (frequency, $n = 102$)

	Pretty	Worklife	Workplac	Admin	School	Peer	Husband	Maturity	Help	Captivit	Money	Negative	Positive
Pretty	14												
Worklife	3	28											
Workplac	3	6	18										
Admin	3	7	6	26									
School	1	7	9	11	21								
Peer	2	4	1	7	4	18							
Husband	5	9	8	2	5	7	29						
Maturity	7	3	0	4	3	3	5	18					
Help	3	10	5	6	4	4	8	5	23				
Captivit	2	4	4	1	2	4	7	2	5	14			
Money	3	6	4	9	6	4	6	5	7	5	20		
Negative	7	21	13	19	16	16	23	7	16	14	19	69	
Positive	11	11	4	6	5	5	12	15	9	3	4	17	42

Table 3 Jaccard similarity coefficient matrix

	Pretty	Worklife	Workplac	Admin	School	Peer	Husband	Maturity	Help	Captivit	Money	Negative	Positive
Pretty	1.000												
Worklife	0.077	1.000											
Workplac	0.103	0.150	1.000										
Admin	0.081	0.149	0.158	1.000									
School	0.029	0.167	0.300	0.306	1.000								
Peer	0.067	0.095	0.029	0.189	0.114	1.000							
Husband	0.132	0.188	0.205	0.038	0.111	0.175	1.000						
Maturity	0.280	0.070	0.000	0.100	0.083	0.091	0.119	1.000					
Help	0.088	0.244	0.139	0.140	0.100	0.108	0.182	0.139	1.000				
Captivit	0.077	0.105	0.143	0.026	0.061	0.143	0.194	0.067	0.156	1.000			
Money	0.097	0.143	0.118	0.243	0.171	0.118	0.140	0.152	0.194	0.172	1.000		
Negative	0.092	0.276	0.176	0.250	0.216	0.225	0.307	0.088	0.211	0.203	0.271	1.000	
Positive	0.244	0.186	0.071	0.097	0.086	0.091	0.203	0.333	0.161	0.057	0.069	0.181	1.000

Table 4 Unilateral Jaccard similarity coefficient matrix

	Pretty	Worklife	Workplac	Admin	School	Peer	Husband	Maturity	Help	Captivit	Money	Negative	Positive
Pretty	1.000	0.214	0.214	0.214	0.071	0.143	0.357	0.500	0.214	0.143	0.214	0.500	0.786
Worklife	0.107	1.000	0.214	0.250	0.250	0.143	0.321	0.107	0.357	0.143	0.214	0.750	0.393
Workplac	0.167	0.333	1.000	0.333	0.500	0.056	0.444	0.000	0.278	0.222	0.222	0.722	0.222
Admin	0.115	0.269	0.231	1.000	0.423	0.269	0.077	0.154	0.231	0.038	0.346	0.731	0.231
School	0.048	0.333	0.429	0.524	1.000	0.190	0.238	0.143	0.190	0.095	0.286	0.762	0.238
Peer	0.111	0.222	0.056	0.389	0.222	1.000	0.389	0.167	0.222	0.222	0.222	0.889	0.278
Husband	0.172	0.310	0.276	0.069	0.172	0.241	1.000	0.172	0.276	0.241	0.207	0.793	0.414
Maturity	0.389	0.167	0.000	0.222	0.167	0.167	0.278	1.000	0.278	0.111	0.278	0.389	0.833
Help	0.130	0.435	0.217	0.261	0.174	0.174	0.348	0.217	1.000	0.217	0.304	0.696	0.391
Captivit	0.143	0.286	0.286	0.071	0.143	0.286	0.500	0.143	0.357	1.000	0.357	1.000	0.214
Money	0.150	0.300	0.200	0.450	0.300	0.200	0.300	0.250	0.350	0.250	1.000	0.950	0.200
Negative	0.101	0.304	0.188	0.275	0.232	0.232	0.333	0.101	0.232	0.203	0.275	1.000	0.246
Positive	0.262	0.262	0.095	0.143	0.119	0.119	0.286	0.357	0.214	0.071	0.095	0.405	1.000

I will show the results of the application of four MDS models, that is, Torgerson's method, symmetric SMACOF, slide vector model, and drift vector model, to the dissimilarity matrices.

4.3 Torgerson's Method

The configuration obtained by the application of Torgerson's method, a classical metric MDS model, to the dissimilarity matrix, is shown in Fig. 1. The result was also used as the initial configuration in applying SMACOF, the majorization approach.

On the one hand, the configuration suggested that there was a contrast between positive feelings and negative feelings toward childrearing. This finding supported the first half of *Prediction 1*. On the other hand, it also suggested that there were three facets for the topics: that is, personal, interpersonal, and societal facets. The topics "pretty," "maturity," "husband," and "captivit" seem to belong to the personal facet. "Admin" and "school" seem to belong to the societal facet. The topics "help," "peer," "worklife," "workplac," and "money" seem to belong to the interpersonal facet, which had not been expected by *Prediction 1*.

We should also note that the positive feelings seemed only proximate to "pretty" and "maturity," which are in the personal facets, while the negative feelings seemed

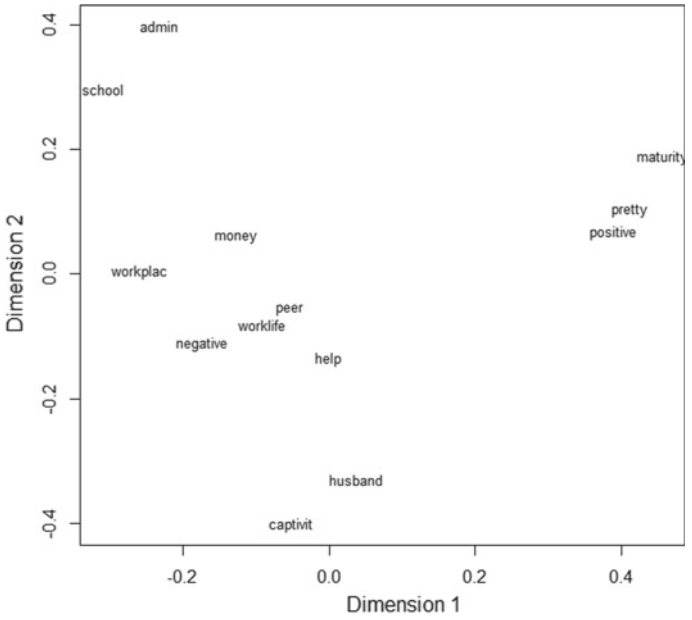

Fig. 1 Configuration plot by Torgerson's method

proximate to topics in all the three facets. The finding was more complicated than *Prediction 2*.

4.4 Symmetric SMACOF

Figure 2 shows the configuration plot of topics obtained by SMACOF with the initial configuration given by Torgerson's method. Compared with the result of Torgerson's method, the differences in distances between the topics were seemingly reduced. The overall pattern in positions of the topics, however, seemed almost preserved.

4.5 Slide Vector Model

Figure 3 shows the configuration plot of topics obtained by slide vector model with the initial configuration given by Torgerson's method. The magnitude of the slide vector was small. This suggested that there was not a uniform asymmetric trend between the topics.

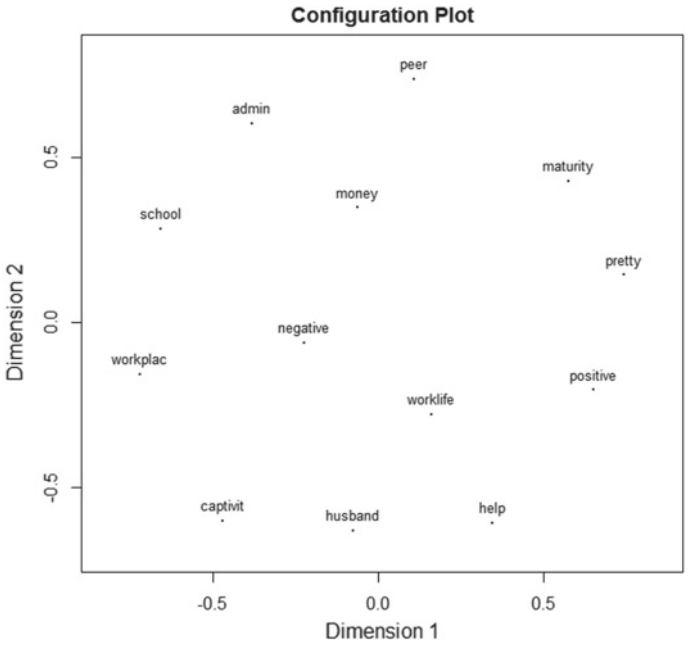

Fig. 2 Configuration plot by SMACOF (Stress = 7.406684)

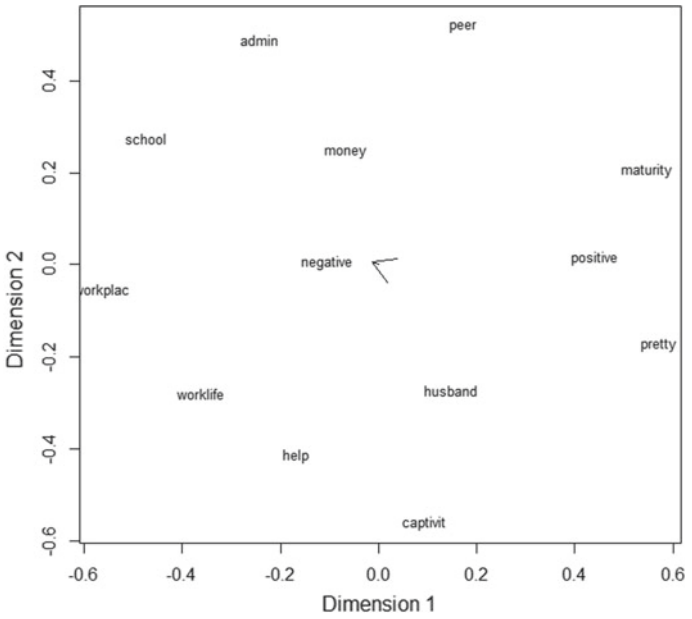

Fig. 3 Configuration plot by slide vector model (Stress = 8.128524, Slide-vector: (−0.013876473, 0.006437277))

4.6 Drift Vector Model

Figure 4 shows the configuration plot of topics obtained by drift vector model with the initial configuration given by Torgerson's method. An arrow from a point represents a drift vector defined as a resultant of all the vectors that represent asymmetry between a point and another point. We may think that a drift vector shows an "implying–implied" relationship between topics in the sense that the topic at its initial point tends to be implied by the topics near its terminal point.

The result of drift vector model suggested that the attribution of success and failure hypothesis and the predictions derived from it were only partly supported. We observed a clear bifurcation of attitudes into positive and negative ones. This was what I had expected in the first half of *Prediction 1*. The facets, their association with the feelings, and the relationship between the facets seemed, however, more complicated than I had predicted. It would be more appropriate to assume three facets or tiers, that is, personal, interpersonal, and societal ones, than to assume the dichotomy of personal/societal facets. Moreover, the emails expressing positive feelings toward childrearing tended to refer to only personal topics, while those manifesting negative attitudes tended to refer to personal, interpersonal, and societal topics. In the former group of emails, reference to "pretty" implied reference to the positive attitudes but not vice versa, and in turn, reference to the positive attitudes implied reference to perceived "maturity" but not vice versa. In the latter group, reference to personal

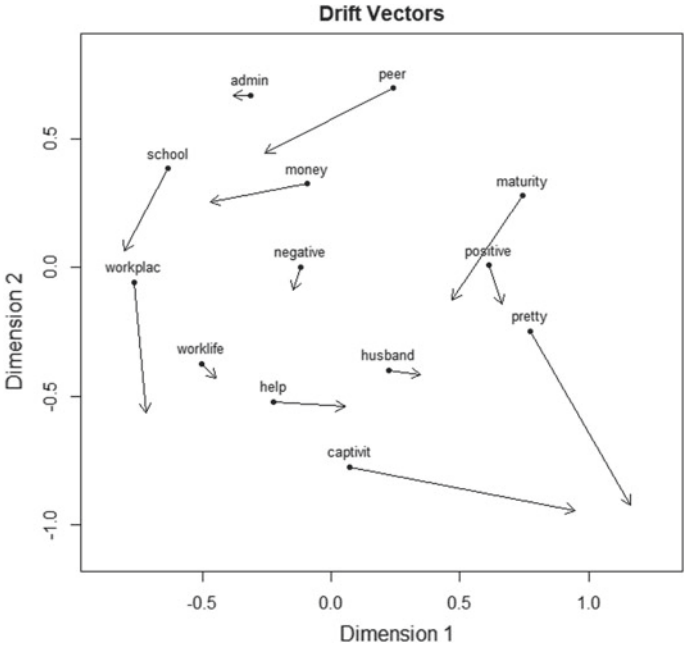

Fig. 4 Configuration plot by drift vector model (Stress = 0.266841)

topics such as "captivit" and "husband" implied reference to interpersonal topics such as "help" and "worklife," but not vice versa. In turn, reference to interpersonal topics implied reference to societal topics such as "school" and "admin," but not vice versa. Two topics, that is, "money" and "peer," might be exceptional in the sense that they seemed to belong to the interpersonal facet but the direction of the revealed implying–implied relationship did not seem congruent to the predictions from my hypothesis.

The resultant pattern of the vectors exhibited a "clockwise" flow of the implying–implied relationships. This pattern suggested that the directions of the asymmetric relationships are systematic but not uniform in the space. It is interesting to compare the pattern with the "systematic trend" that Borg et al. [4, pp. 58–59] found in their analysis of the Morse code confusion data provided by Rothkopf [18]. Their result showed that the directions of the arrows expressing drift vectors were almost the same, which means that the respondents in Rothkopf [18] failed to differentiate long signals from short ones more often than vice versa.

5 Concluding Remarks

The results of this study only partly supported the attribution of success and failure hypothesis and the predictions derived from it. Looking carefully at the configuration plots, however, I found that there might be three facets or tiers, that is, personal,

interpersonal, and societal ones. It seemed that the positive feelings toward childrearing were only proximate to topics in the personal facets, while the negative feelings were proximate to topics in all the three facets. Among the emails expressing negative feelings, reference to personal topics tended to imply reference to interpersonal topics, and in turn, reference to interpersonal topics tended to imply reference to societal topics.

There are limitations in this study. The sample size was small. The sample was possibly biased owing to readers' self-selection in their decision to submit an essay to the magazine or the editorial office's selection of essays to be published. We might need to conduct a survey with a large-scale random sample of Japanese women and ask the respondents to write an essay on the same theme to examine whether we can generalize the findings.

From a methodological point of view, this study could be regarded as an attempt to explore the applicability of various multidimensional scaling (MDS) models to sociological or social–psychological phenomena. Okada [17] observed that a limited number of MDS models had been used in sociological studies. As a reply to his observation, I tried to apply some MDS models with which sociologists might not be familiar. There is a lesson that the results taught us: Adopting an asymmetric MDS model in text analysis will contribute to our understanding of the structure of people's attitudes. Drift vector model may be especially useful when the directions of the asymmetric relationships between objects such as topics and concepts are systematic but not uniform.

Acknowledgements An earlier version of this paper was presented at the 16th Conference of the International Federation of Classification Societies (IFCS 2019), August 28, 2019, Thessaloniki, Greece. I appreciate comments from Akinori Okada and Boris Mirkin. I also thank the *AERA* editorial office for their granting permission to re-digitalize and analyze the 102 emails taken from *AERA* Editorial Office [1].

References

1. *AERA* Editorial Office. (2000). *Is childrearing a strain? Emails from 2,118 readers*, Special Issue of *AERA* (in Japanese). Tokyo: Asahi-shinbun.
2. Beckman, L. (1973). Teachers' and observers' perceptions of causality for a child's performance. *Journal of Educational Psychology*, *65*(2), 198–204.
3. Böhm, G., & Pfister, H.-R. (2015). How people explain their own and others' behavior: A theory of lay causal explanations. *Frontiers in Psychology*, *6*, 139–153.
4. Borg, I., Groenen, P. J. F., & Mair, P. (2018). *Applied multidimensional scaling and unfolding* (2nd ed.). Cham: Springer.
5. Brier, A., & Hopp, B. (2011). Computer assisted text analysis in the social sciences. *Quality & Quantity*, *45*, 103–128. https://doi.org/10.1007/s11135-010-9350-8.
6. de Leeuw, J. (2017). *Multidimensional scaling with anarchic distances*. https://doi.org/10.13140/RG.2.2.32075.39205.
7. de Leeuw, J., & Mair, P. (2009). Multidimensional scaling using majorization: The R package smacof. *Journal of Statistical Software*, *31*(3), 1–30. http://www.jstatsoft.org/v31/i03/.

8. Gower, J. C. (2006). Similarity, dissimilarity and distance, measures of. In: S. Kotz, C. B. Read, N. Balakrishnan, B. Vidakovic & N. L. Johnson (Eds.) *Encyclopedia of statistical sciences*. New York: Wiley. https://doi.org/10.1002/0471667196.ess1595.pub2.
9. Groenen, P. J. F., & van de Velden, M. (2016). Multidimensional scaling by majorization: A review. *Journal of Statistical Software*, *73*(8). https://doi.org/10.18637/jss.v073.i08.
10. Hasegawa, S. (2006). The structure of Japanese women's attitudes towards childrearing: An analysis of answers to an open-ended question (in Japanese). BA thesis, Department of Behavioral Science, Faculty of Arts and Letters, Tohoku University.
11. Hasegawa, S., & Kimura, K. (2006). The structure of Japanese women's attitudes towards childrearing: A quantitative analysis of answers to an open-ended question (in Japanese). In *Proceedings of the Annual Meeting of the Behaviormetric Society of Japan* (Vol. 34, pp. 178–181).
12. Jaccard, P. (1901). Étude comparative de la distribution flora dans une portion des Alpes et des Jura. *Bulletin de la Société Vaudoise des Sciences Naturelles*, *37*(2), 547–579.
13. Jaccard, P. (1907). La distribution de la flore dan la zone Alpine. *Revue générale des Sciences pures et appliquées*, *18*(23), 961–967.
14. Jaccard, P. (1912). The distribution of the flora in the Alpine zone. *New Phytologist*, *11*(2), 37–50. [English translation of Jaccard (1907)].
15. Lee, M. D., Pincombe, B., & Welsh, M. (2005). An empirical evaluation of models of text document similarity. In *Proceedings of the Annual Meeting of the Cognitive Science Society* (Vol. 27, pp. 1254–1259). Retrieved November 19, 2018 from https://escholarship.org/uc/item/48g155nq.
16. Miller, D. T., & Ross, M. (1975). Self-serving biases in the attribution of causality: Fact or fiction? *Psychological Bulletin*, *82*(2), 213–225.
17. Okada, A. (2002). A review of cluster analysis and multidimensional scaling research in sociology (in Japanese). *Sociological Theory and Methods*, *17*(2), 167–181.
18. Rothkopf, E. Z. (1957). A measure of stimulus similarity and errors in some paired-associate learning tasks. *Journal of Experimental Psychology*, *53*(2), 94–101.
19. Santisteban, J., & Carcamo, J. L. T. (2015). Unilateral Jaccard similarity coefficient. In O. Alonso, M. A. Hearst, & J. Kamps (Eds.) *CEUR Workshop Proceedings, GSB 2015 Graph Search and Beyond: Proceedings of the First International Workshop on Graph Search and Beyond co-located with the 38th Annual SIGIR Conference (SIGIR'15)*, Santiago, Chile, August 13th, 2015 (Vol. 1393, pp. 23–27). Published on CEUR-WS. Retrieved October 26, 2018 from http://ceur-ws.org/Vol-1393/.
20. Sato, Y. (1999). AUTOCODE. In A. Kawabata (Ed.), *Tools for the coding of atypical data* (in Japanese) (pp. 15–33). Osaka: Osaka University.
21. Sato, Y. (2000). AUTOCODE: A tool for coding answers to open-ended questions (in Japanese). Retrieved November 19, 2018 form http://www.hmt.u-toyama.ac.jp/socio/satoh/autocode/index.html.
22. Solka, J. L. (2008). Text data mining: Theory and methods. *Statistics Surveys*, *2*, 94–112. https://doi.org/10.1214/07-SS016.
23. Torgerson, W. S. (1952). Multidimensional scaling; I. theory and method. *Psychometrika*, *17*(4), 401–419.
24. van Eck, N. J., & Waltman, L. (2009). How to normalize cooccurrence data? An analysis of some well-known similarity measures. *Journal of the American Society for Information Science and Technology*, *60*(8), 1635–1651.
25. Zielman, B., & Heiser, W. J. (1993). Analysis of asymmetry by a slide-vector. *Psychometrika*, *58*(1), 101–114.
26. Zuckerman, M. (1979). Attribution of success and failure revisited, or: The motivational bias is alive and well in attribution theory. *Journal of Personality*, *47*(3), 245–287.

Consensus or Dissensus in Occupational Prestige Evaluation: A New Approach to Measuring Consensus and Inter-group Variations

Keiko Nakao

Abstract Numerous empirical studies of occupational prestige in the past several decades have accumulated a great deal of knowledge about the ways in which people evaluate the social standing of various occupations. One of the major findings is that individuals in different social locations were found to provide similar responses in their judgement about the occupational hierarchy in the society. At the same time, however, the individuals do vary in their responses to a certain degree and the level of agreement was found to be different in individuals with varying social status. In this paper, a recently developed theoretical model of cultural consensus and its related methods are shown to be useful in providing answers to whether the level of agreement is high enough to call the prestige hierarchy a consensus or a collective conscience. The application of these methods enables us to measure the portion of prestige perception that is commonly shared by all individuals relative to the amount of variation observed between subgroups and individuals.

Keywords Evaluation of occupational prestige · Consensus · Cultural consensus model · Inter-group variations

1 Introduction

Numerous empirical studies of occupational prestige in the past several decades have accumulated a great deal of knowledge about the ways in which people evaluate the social standing of various occupations. Prior studies not only produced widely used scales of prestige and the socioeconomic index (SEI) for various occupations, researchers have made efforts to investigate systematic properties of prestige scales as well as how people evaluate social standing of occupations. The general empirical findings point to that of stability. It is understood not only that different measuring instruments produce very similar results, but also that the prestige hierarchy is

K. Nakao (✉)
Tokyo Metropolitan University, Tokyo, Japan
e-mail: nakao@tmu.ac.jp

T. Imaizumi et al. (eds.), *Advanced Studies in Behaviormetrics and Data Science*,
Behaviormetrics: Quantitative Approaches to Human Behavior 5,
https://doi.org/10.1007/978-981-15-2700-5_27

remarkably stable over time (Hodge, Seigel, & Rossi [8]; Nakao & Treas [12]) and consistent across societies (Treiman [16]). These results were shown in analyses in which aggregated or constructed scales were compared. The consistency also has been observed at the individual level indicated by a strong agreement among individuals' ratings. Individuals in different social locations were found to provide similar responses in their judgement about the occupational hierarchy in the society. At the same time, however, the individuals do vary in their responses to a certain degree and the level of agreement was found to be different in individuals with varying social status. Thus, the question still remains as to whether the level of agreement is high enough to call the prestige hierarchy a consensus or a collective conscience. In this paper, a recently developed theoretical model of cultural consensus and its related methods are shown to be useful in providing answers to unresolved issues about the prestige consensus. The application of these methods enables us to measure the portion of prestige perception that is commonly shared by all individuals relative to the amount of variation observed between subgroups and individuals.

2 Occupational Prestige as a Collective Conscience

The discussions of consensus in prestige judgements took off when strong inter-rater correlations were found in several studies in the 1970s. For example, Balkwall, Bates, & Garbick [1, 2] reported 0.745 as the average correlation of individuals' judgements. While other researchers reported lower values of inter-rater correlations, from 0.42 to 0.48 (Jencks et al. [10]; Goldthorpe & Hope [5]), they were still regarded as indicating substantial agreement among the raters. Challenging such view of the prestige consensus, Guppy [6] argued that the degree of consensus varied according to the social strata, and thus no collective conscience can be claimed. He pointed out that the level of agreement is greater among higher status individuals than among those who are in lower strata. Guppy and Goyder [7] further reported the differences in the level of agreement based on education, occupation, and race of individuals. Acknowledging such variations in agreement, however, Hodge, Kraus, and Schild [9] contended that characteristics of evaluators never explain more than 25% of the variance in prestige ratings and that they would be far less than variations within subgroups. More recently, Wegener [17] reiterated the issue of prestige consensus and the importance of investigating individual differences. Using the psychological scaling techniques, Wegener found a polarization of judgments among higher status individuals, while a lack of discriminating responses was found in lower social strata. He suggested that this difference of variance in responses might attribute to the difference in the level of agreement between various social groups.

The objective of this paper is to clarify unresolved issues about consensus in occupational prestige evaluation. We adopted the conceptual basis of the cultural consensus model and its related statistical techniques recently developed in psychometrics and anthropology (Romney, Weller, & Batchelder [13]; Batchelder & Romney [3]; Romney, Moore, Batchelder, & Hsia [14]). The paper proceeds in the

following manner. First, after a brief explanation of the theory of cultural consensus and its analytical approach, we demonstrate the way to measure the degree of consensus in individuals' perceptions of occupational hierarchy. Second, in an attempt to assess the relative sizes of consensus versus dissensus, we measure the portion of their view shared by all individuals and compare it to the amount of variation that exist between subgroups based on some characteristics of individuals. Third, we investigate the differences in the level of agreement. The data used in analyses are from the occupational prestige module of the 1989 General Social Survey (GSS) (Davis & Smith [4]).

3 Theory of Cultural Consensus and Analytical Approach

The approach presented in this paper follows the theory of cultural consensus, the model first developed in the field of anthropology (Romney et al. [13]; Batchelder & Romney [3]). In the effort to objectively elicit an aspect of culture that is not directly observable, the theory of cultural consensus views culture (or an aspect of culture) as information shared and stored in the minds of the society's members. It assumes that the correspondence between any two informants in their responses is a function of the extent to which each shares the knowledge about the aspect of culture being investigated, an idea that traces back to Spearman's landmark 1904 article (Spearman [15]). The principle idea of this model, therefore, is to examine the pattern of agreement among informants' responses. It allows us to make inferences about how much each informant shares the knowledge of the information constituting culture, from which the aspect of the culture can be estimated.

We see occupational prestige similar to what anthropologists view an aspect of culture as above. The respondents' ratings of occupational status are subjective judgements based on their perceptions about how occupations are hierarchically located in the society. Like culture, occupational prestige ranking is an information shared in the minds of the members in a society, which is not directly observable. If all respondents rated the same way, i.e., in the case of a total consensus, we could say that their responses constitute the social reality about the society's occupational prestige hierarchy, and that every member of the society shares such knowledge and responds without error. In practice, of course, individuals' ratings are not all the same. Variation in individuals' responses could result from, aside from unavoidable response error, either one of the following situations: (1) there is no single prestige hierarchy on which the society's members agree; (2) there is a single hierarchy of prestige as a social reality that is commonly shared by the members of the society, but all members are not equal in the degree to which they share the knowledge about the common pattern. Disagreement between any two individuals' ratings could be attributed to the difference in their understanding or knowledge about the social reality. Likewise, the agreement between any two people's responses is a function of how much each shares the information about the society's prestige hierarchy. Based on this model of shared social reality and individuals' social knowledge about the social reality,

our approach is to examine the patterns of individuals' agreement with each other. Such information would lead us to find out (1) whether there is a single occupational prestige rankings that people agree on, and if so, (2) how much consensus there is.

4 Measuring Consensus

We applied the statistical techniques developed for the model of cultural consensus to the prestige ratings. The basis for the analysis is the inter-rater correlations, which contain the information about the patterns of individual agreement. We used the ratings of 40 occupations by 100 respondents randomly selected from the GSS sample, thus a 100 by 100 matrix of correlations between pairs of subjects based on their ratings of the 40 occupations. (See Appendix for 40 occupational titles.) Singular value decomposition was performed on this correlation matrix in order to extract the factors underlying the subject-by-subject correlation matrix. Eigenvalues for the first four factors are shown in Table 1.

As we observe in Table 1, the first eigenvalue is overwhelmingly greater than the rest of the eigenvalues. This is a strong indication of the existence of a single underlying factor in the matrix of subject-by-subject correlations. In other words, the respondents' judgements show a strong agreement such that a single prestige order of occupations can be elicited. This first factor alone accounts for 53% of variance in the respondents' ratings, while the other factors account for only 5% or less. To validate this single factor, we examined its correspondence with the prestige scores computed by the conventional manner, i.e., taking the mean of the ratings. The first factor scores correlated with the conventional prestige scores at 0.998.

As for the degree of collective consensus, the first factor accounts for more than half the variance—the remaining variance certainly contains measurement errors and individual differences. In the next section, we will examine whether any systematic rater's characteristics explain any of the patterns of agreement, by assessing inter-group variations.

Table 1 Singular value decomposition

Factor	Eigenvalues	%	Cumulative%
1	53.04	53.04	53.04
2	5.11	5.11	58.16
3	3.99	3.99	62.14
4	3.37	3.37	65.51

5 Measuring Inter-group Variations

In this section, an attempt is made to ascertain whether there are systematic differences among groups of individuals in their perceptions of occupational hierarchy. We do this by analyzing the subject-by-subject correlation matrix based on their ratings. The analytical methods we apply are based on the following assumptions. First, the mean of subject-by-subject correlations within a group of individuals indicates the extent to which a common shared pattern exists. Second, the correlation between two individuals is the product of the correlation of each individual with the shared societal pattern (Romney et al. [14]). These assumptions imply that the correlation between two individuals, i and j, r_{ij}, can be decomposed as a product of each individual's correlation with the collective pattern, $r_{ij} = r_{it}\, r_{jt}$, where t denotes the relevant shared pattern. An additional assumption is that there should be no negative correlation among subjects.

Based on the assumptions stated above, we assess the degree of variation among the groups of individuals sharing the same attributes. Here, we consider three characteristics of raters, i.e., sex, educational level, and occupation, that are thought to affect one's view of occupation. First, let us examine inter-subject agreement between and within groups of different sexes of raters. There are 51 male respondents and 49 females in our sample of 100. Table 2 shows the mean subject-by-subject correlation based on their ratings for male–male, female–female, and male–female raters.

The mean correlation among the male subjects is 0.422, while females show a mean of 0.457, slightly higher than that of males. Females agree among themselves more than the males do. The level of agreement as measured by the mean correlation within a group indicates the extent to which the group members conform to (or have the knowledge of) the society's collective view of the occupational hierarchy. Our data suggest that females seem to hold a slightly higher social knowledge about the occupational rankings than males. According to the process models of cultural consensus, the square root of the mean correlation within a group approximates the average knowledge of the collective view (Romney et al. [13]; Batchelder & Romney [3]). Thus, 0.650 for males and 0.676 for females would be the approximate estimate of the amount of social knowledge an average male or female would share with others of same sex.

Now we turn to analyze the between-group correlations, i.e., male–female correlations. The mean is 0.433. Following the decomposition of the correlation coefficient, $r_{ij} = r_{it}\, r_{jt}$, we can interpret the square root of 0.433, i.e., 0.658, as the approximate amount of social knowledge shared by both male and female groups. Comparing this value to what we obtained above would give us the relative portion that is specific to

Table 2 Mean Inter-subject correlation

	Male	Female	n
Male	0.422	0.433	51
Female		0.457	49

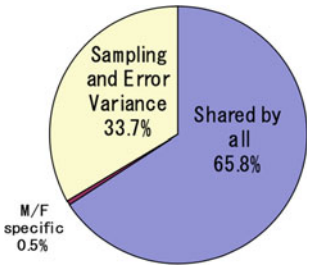

Fig. 1 Partitioning of the view of occupational prestige shared by males and females

the groups. From the above analysis, we obtained 0.422 and 0.457 as the means of subject-by-subject correlations within groups, male and females, respectively. Since we have different group sizes for males and females, we aggregate the two averages weighted by their group sizes, which equals to 0.439. The difference between the square root of this weighted mean, 0.663, and 0.658 obtained above would indicate the incremental portion that is specific to the groups. The difference is 0.005 ($= 0.663 - 0.658$), meaning that the group-specific portion is merely 0.5%. The rest, $1 - 0.658 - 0.005 = 0.337$, then make up for sampling and error variance. Figure 1 graphically displays how the view of occupational prestige hierarchy is shared (1) by all, (2) sex-specific, and (3) sampling and error variance.

The above partitioning helps us to evaluate the relative size of the inter-group variation compared to the amount that is commonly shared. While 65.8% is commonly shared by both males and females, only 0.5% is attributed to the difference in the raters' sex.

Using the same logic, the inter-group differences were examined in terms of groups based on the raters' educational levels and occupations. Individuals are grouped into three categories of educational levels (Less than High School, High School, More than High School) and two categories of occupations (White Collar and Blue Collar). The mean inter-subject correlations for within- and between-groups are shown in Table 3. Based on these mean inter-subject correlations, we calculated the relative amount of shared knowledge and they are summarized in Table 4.

Table 3 Mean inter-subject correlations

Education	Less than high school	High school	Above high school	n
LT high school	0.159	0.293	0.340	17
High school		0.451	0.518	55
Above high school			0.623	28
Occupation	Blue collar	White collar		n
Blue collar	0.387	0.428		39
White collar		0.470		58

Table 4 Partitioning of the shared perception about occupational prestige

	Sex	Education	Occupation
Share by all	0.658	0.646	0.654
Between group variation	0.005	0.035	0.013
Sampling and error variance	0.337	0.319	0.333

Table 5 Eigenvalues in % for different sample sizes

Factor	Sample size								
	100	90	80	70	60	50	40	30	20
1	52.52	53.73	50.24	53.67	53.62	49.67	54.68	44.28	56.94
2	6.56	5.02	5.16	6.05	5.60	8.38	6.01	7.64	7.15
3	3.74	4.01	4.56	5.15	4.74	4.60	5.13	6.03	6.29
4	3.32	3.52	4.24	3.66	4.31	4.43	4.65	5.71	5.21

Both Tables 3 and 4 confirm that the inter-group variation is quite small, compared to what is commonly shared by all. Sex and occupation (i.e., White collar vs. Blue collar) only accounts for less than 1% (0.5% and 0.7%, respectively). Education seems to make more difference than other two characteristics; however, its between-group variation is merely 2.4%. The portion commonly shared across groups is consistently high, all at the level around 65%. These results lead us to believe that these characteristics of raters do not account for the difference in their view of occupational prestige.

We notice in Table 3 that the average inter-subject correlation for the respondents with less than high school degree is a lot lower than those in other two groups (0.159 vs. 0.451 and 0.624).

6 On Sample Size

The analyses we have shown in the previous sections utilized a sample of 100 individuals randomly selected from 1166 respondents in the 1989 General Social Survey. We have chosen 100 for the sake of convenience in the calculation and we obtained a convincing evidence for (1) the existence of single occupational ranking underlying the agreement among individuals' responses, and (2) the negligible inter-group variations. We did, however, perform the same analyses even with smaller samples. Random samples of sizes from 20 to 100 were drawn for comparison (the sample of 100 here is different from the one used in the previous analyses). Table 5 shows the first four eigenvalues in percentages of explained variance resulted from the singular value decompositions for various sample sizes.

Table 6 Analysis of inter-subject correlations for different sample sizes

	Sample size								
Factor	100	90	80	70	60	50	40	30	20
Mean correlation									
Male–Male	0.431	0.431	0.394	0.381	0.560	0.343	0.426	0.321	0.077
Female–Female	0.444	0.448	0.493	0.524	0.447	0.457	0.502	0.338	0.626
Male–Female	0.434	0.436	0.441	0.439	0.495	0.389	0.463	0.337	0.263
# of males	48	44	39	32	27	24	14	15	8
# of females	50	46	39	38	32	24	25	14	11
Commonly shared	0.659	0.660	0.664	0.663	0.691	0.624	0.680	0.580	0.513
Sex-specific	0.003	0.003	0.002	0.019	0.000	0.008	0.015	−0.007	0.151
Error variance	0.339	0.337	0.334	0.318	0.309	0.368	0.304	0.427	0.336

We note from Table 5 that the dominance of the first eigenvalue is consistently observed for all samples of various sizes. This is a strong evidence of the existence of single ranking underlying people's perceptions about occupational prestige hierarchy. To validate those extracted underlying factors, factor scores were computed from each sample of various sizes and they were compared. The computed factor scores correlated very highly among all nine samples of various sizes. For example, the correlation between the factor scores from the sample of 100 and those of 20 was 0.980. The mean of correlations between all samples is 0.985, ranging from 0.964 to 0.997. They also correspond with the prestige scores computed from all 1166 subjects, the mean correlation = 0.992, ranging from 0.977 to 0.996. These results indicate the high degree of consensus and robustness in the responses.

Table 6 displays results of the analysis of inter-group (males vs. females) variation. We observe that for smaller samples (i.e., $n = 20$ and $n = 30$), the pattern of within- versus between-group mean correlations is not consistent with the larger samples. The mean is affected by a few outliers, and the smaller the sample and group sizes, the greater the effect of the outlier values on the mean. We would also expect greater sampling error for smaller samples. For the sample of size 60, we notice that the males have higher agreement with each other than females, which is the opposite of the patterns of the rest. In terms of the pattern of partitioning of shared knowledge, samples of 80, 90, and 100 show a very similar pattern, two-thirds are commonly shared, less than 1% is group-specific, and the rest is error. As expected, the portion attributed to sampling and error variance is greater for the two smallest samples. The negative value of sex-specific portion in the sample of 30 (−0.0065) would be attributed to the violation of assumptions about negative inter-subject correlations. Few cases of negative inter-subject correlations produced a noticeable effect on small samples.

7 Differences in the Level of Agreement

Previous empirical studies found that the level of agreement differs according to the social status of the respondents. Higher status individuals agree more to each other than those of lower status. Our analysis confirms such phenomena. If we measure individual's social status by his/her educational level and occupation, the results shown in Table 3 concur this difference in the level of agreement. Those who hold less than high school degree correlates with each other on the average of 0.1593, while those with high school diploma agrees at 0.4508, and the mean of those with higher education is 0.6230. Similarly, individuals with blue-collar occupations show a lower mean correlation (0.3867) than those who hold white-collar jobs (0.4701).

One of the explanations for this difference was offered by Wegener [17]. He suggested that higher status individuals tend to polarize the difference in occupational status, while those with lower status do not differentiate statuses of various occupations. This polarization tendency would possibly be responsible for higher correlation observed among high-status individuals. As Table 7 shows, however, our data did not confirm his proposition. Standard deviation and range, both of which are measures of variation in individuals' ratings of 40 occupations, were higher for lower status individuals than those of higher status, the opposite of what Wegener's hypothesis would predict. (The differences in means were statistically significant at 1% for educational level, while differences between occupational categories were not significant even at the 5% level).

We offer an alternative interpretation. The difference in the level of agreement between groups is related to the difference in the level of social knowledge of the respective group members about the relevant issue in question. According to the model of consensus on which our analyses are based, a correlation between two subjects, i and j, is a product of two components: how much i shares the society's collective view and how much j shares it. Therefore, if a certain social group, Group A, produces higher inter-subject correlations than another social group, Group B, then members of Group A tend to have higher level of social knowledge than member of Group B.

In the model of cultural consensus, each individual's level of cultural knowledge can be estimated from the loading on the first factor. Though our data do not strictly satisfy all the assumptions for the mathematical model of consensus to apply, we

Table 7 Standard deviation and range of 40 ratings

	Mean S.D.	Mean range
LT high school	2.27	7.59
High school	2.07	7.27
Above high school	1.79	6.32
Blue collar	2.12	7.33
White collar	1.95	6.83

Table 8 Association with the measure of individuals' social knowledge

	Correlation	Sig.	n
Education in years	0.303	0.002	100
Occupational prestige	0.206	0.043	97
Respondent's income	−0.074	0.538	72
Family income	0.100	0.328	98
	Mean	S.D.	n
LT high school	0.434	0.482	17
High school	0.672	0.255	55
Above high school	0.784	0.143	28
Blue collar	0.625	0.300	39
White collar	0.689	0.310	58
Male	0.648	0.283	51
Female	0.678	0.325	49

feel that the data conform to the model satisfactorily enough to assume the loading on the first eigenvector is a good approximation of individuals' social knowledge about occupational status. Table 8 describes the association between the loading and selected characteristics of individual.

The loading on the first eigenvector correlates positively with individual's educational level. Individuals with more education tend to have higher social knowledge about the occupational hierarchy than those with less education. Individual's occupational status does seem to relate to his/her social knowledge, as indicated by a significant correlation with occupational prestige; however, the association is not as strong as that with education. Individual's economic status (both his/her own income and family income) as well as sex did not differentiate the level of social knowledge.

When three variables (sex, education, and occupation) were considered simultaneously, controlling for age, to predict the values of the loading, they were all shown to have independent effects (significant at 5%). This is consistent with our previous findings shown in Tables 2 and 3. Inter-subject correlations are higher among females than males, among more educated individuals than less educated, and among those with white-collar than blue-collar jobs. Thus, the mean inter-subject correlation can also be seen as an indication of the level of social knowledge among a group of individuals.

The above results suggest that the difference in the level of agreement between groups of varying social status might be attributed to the difference in the level of social knowledge they share. Individuals with higher education tend to have higher level of social knowledge about the structure of occupational status in the society.

In order to substantiate the validity of the index of social knowledge, we performed the following analysis. In the occupational prestige module of the 1989 General Social Survey, two fictitious titles were included; "Persologist" and "Fooser". It was an experiment to find out to what extent people use "guessing" when they were asked

to rate the status of an occupation which does not exist. Of 98 respondents who were asked to rate "Persologist", 46.9% gave a rating, and 52.9% of 119 respondents rated "Fooser". Regardless of the ratings given, if they rated at all, they were incorrect answers indicating the lack of knowledge about the existence of such occupations. Not giving an answer could mean either (1) the respondent knew such an occupation does not exist in the society (i.e., correct answer), or (2) he/she is not sure if it existed, but certainly does not know the social status of such an occupation. Thus, not giving an answer does not necessarily mean having the correct knowledge; however, the giving an answer does indicate the lack of knowledge.

In the GSS, these fictitious titles were not rated by all respondents in the sample, but each was rated by a different subsample of respondents, who also rated a set of 40 titles we used in our analyses in the previous sections. We applied the same methods as above and analyzed the ratings of the 40 occupations and examined whether the index of social knowledge derived from the analyses would be related to their answers on the fictitious titles. For both subsamples, we found a single factor structure underlying the pattern of agreement among the subjects, confirming the consensus (the first eigenvalues account for 54.04 and 52.87%). The mean value of the first factor loadings, the index of social knowledge, was found lower for those who rated the fictitious titles (i.e., incorrect answer) than for those who did not, both for "Persologist" and "Fooser". The loading on the first vector was also associated with the respondent's educational level and occupation. It was greater for more educated and for those with white-collar occupations. (The associations were all statistically significant at the 5% level, except the significance level was 6% for the association between the loading and the educational level for "Fooser".) These results provide an additional validation of the index of social knowledge as derived in our analyses.

8 Summary and Discussion

In this paper, we applied a theory of cultural consensus in conceptualizing the collective conscience of occupational prestige. Applying the statistical methods developed for the cultural consensus model and its related methods enabled us to clarify some unresolved issues about consensus in occupational prestige evaluations. The analyses focused on investigating the patterns of agreement among individuals' ratings.

Our analyses found the following. First, it showed that there is a single occupational status ranking underlying people's perception about occupational prestige. The extracted single factor corresponds to the widely used conventional prestige scores, confirming the validity of the underlying factor. Furthermore, a single underlying factor is found even from small samples, as small as 20, that are randomly drawn. This suggests that the level of consensus is high enough that only a small sample is needed to elicit the aggregate view of the occupational hierarchy.

Second, variations between groups based on the raters' characteristics are negligible, compared to how much they share in their view of occupational prestige hierarchy. Our analyses showed that less than 1% was attributed to the difference

between groups based on sex and occupation. Groups of different educational levels account for only 2.4%. On the other hand, the portion of shared view by all subgroups of individuals is shown to be around 65%. Since one's location in the social structure as well as one's sex has been shown to influence so many other attitudes and behaviors of individuals, this is a remarkable level of agreement between groups. In fact, people are shown to have about the same level of agreement on their cognition of semantic structures, such as colors and emotion terms. By comparing different cultures (U.S. and Japan), Romney et al. [14] found that 63% of semantic structure is universally shared in emotional terms and 15% is culture-specific. For the semantic domain of colors, Moore, Romney, and Hsia [11] found 70% being universally shared and only 1% language-specific. The view of the social order, i.e., occupational prestige, is shared by all members of the society as much as people share such cognitive domain of semantic structures.

Our third finding is that the level of social knowledge is related to the level of his/her education, where social knowledge is defined as the degree to which an individual shares the knowledge of the collective view of the society. Our method allowed us to estimate each individual's level of social knowledge, and it was shown positively related to his/her educational level. Individuals with higher educational level have more knowledge about the social order than those with lower education do. Based on our model, this offers an explanation for the prior empirical observations, i.e., the degree of consensus is higher among individuals of higher social status than among those in lower level of social strata.

As summarized above, the facts that there is a single ranking extracted, and that little variation was found between social groups, lead us to believe that the occupational prestige hierarchy is a collective conscience. If we conceptualize social reality to be something that is created in the minds of the members of the society collectively, then occupational ranking extracted by the above methods may be called a social reality. The difference in the level of agreement found between individuals can be attributed to the difference in individuals' social knowledge about such reality collectively created by the members of the society.

The theory of cultural consensus and its related statistical techniques that we used in this paper can be useful in investigating various social views that is not directly measurable. When this model was applied to the situations in which correct answers are known to the researchers, but not to the subjects, the answers that were estimated from the inter-subject agreements were found to closely approximate the correct answers (Romney et al. [13]). Sociologists often conduct surveys to find out what individuals' perceptions are about various social phenomena. Applying these analytical approach and the methods shown here would allow us to measure the degree of consensus and variations among groups and one can determine whether such views can be considered as a collective conscience created in the minds of members of the society.

Appendix: Occupational Titles and Their Prestige Scores

	Occupational title	Prestige score
1	Accountant	65.38
2	Airplane mechanic	52.86
3	Assembly line worker	34.74
4	Bartender	24.53
5	Bill collector	24.3
6	Baker	34.86
7	Banker	63.25
8	Bus driver	32.07
9	Bank teller	43.28
10	Barber	35.71
11	Chemist	73.33
12	Cook in a restaurant	34.28
13	Clergyman	67.13
14	Cashier in a supermarket	32.56
15	Department head in a state government	75.55
16	Farm owner and operator	52.76
17	Filling station attendant	21.36
18	Gardener	28.57
19	General manager of a manufacturing plant	62.42
20	House painter	33.91
21	Housekeeper in a private home	33.93
22	Insurance agent	46.37
23	Janitor	22.33
24	Lawyer	74.77
25	Locomotive engineer	48.13
26	Lunchroom operator	27.06
27	Logger	31.10
28	Manager of a supermarket	48.31
29	Medical technician	68.40
30	Musician in a symphony orchestra	58.90
31	Public Grade School teacher	64.08
32	Policeman	59.16
33	Post office clerk	42.20
34	Superintendent of a construction job	57.32
35	Shipping clerk	32.71
36	Secretary	46.08
37	Saw sharpener	22.75
38	Telephone solicitor	21.54
39	Travel agent	41.26
40	Welder	41.89

Source Nakao and Treas [12]

References

1. Balkwell, J. W., Bates, F. L., & Garbick, A. P. (1980). On the intersubjectivity of occupational status evaluations: A test of a key assumption underlying the "Wisconsin Model" of status attainment. *Social Forces*, *58*, 865–81.
2. Balkwell, J. W., Bates, F. L., & Garbick, A. P. (1982). Does the degree of consensus on occupational status evaluations differ by socioeconomic stratum? Response to Guppy. *Social Forces*, *60*, 1183–9.
3. Batchelder, W. H., & Romney, A. K. (1988). Test theory without and answer key. *Psychometrika*, *53*, 71–92.
4. Davis, J. A. & Smith, T. W. (1999). *General social surveys, 1972–1998: [cumulative file]* [Computer file]. Chicago, IL: National Opinion Research Center [producer], Ann Arbor, MI: Inter-university Consortium for Political and Social Research [distributor].
5. Goldthorpe, J. H., & Hope, K. (1974). *The social grading of occupations. A new scale and approach*. Oxford: Clarendon.
6. Guppy, L. N. (1982). On intersubjectivity and collective conscience in occupational prestige research: A comment on Balkwell-Bates-Garbin and Kraus-Schild-Hodge. *Social Forces*, *60*, 1178–82.
7. Guppy, L. N., & Goyder, J. C. (1984). Consensus on occupational prestige: A reassessment of the evidence. *Social Forces*, *62*, 709–25.
8. Hodge, R. W., Siegel, P. M., & Rossi, P. H. (1964). Occupational prestige in the United States: 1925–1963. *American Journal of Sociology*, *70*, 286–302.
9. Hodge, R. W., Kraus, V., & Schild, E. O. (1982). Consensus in occupational prestige ratings: Response to Guppy. *Social Forces*, *60*, 1190–96.
10. Jencks, C. M., Acland, H., Bane, M. J., Cohen, D., Gintis, H., Heyns, B., et al. (1972). *Inequality: A reassessment of the effect of family and schooling in America*. New York: Basic Books.
11. Moore, C. C., Romney, A. K., & Hsia, T. (2000). Shared cognitive representations of perceptual and semantic structures of basic colors in Chinese and English. *Proceedings of the National Academy of Sciences*, *97*, 5007–10.
12. Nakao, K., & Treas, J. K. (1994). Updating occupational prestige and socioeconomic scores: How the new measures measure up. *Sociological Methodology*, *24*, 1–72.
13. Romney, A. K., Weller, S. C., & Batchelder, W. H. (1986). Culture as consensus: a theory of culture and informant accuracy. *American Anthropologist*, *88*, 313–38.
14. Romney, A. K., Moore, C. C., Batchelder, W. H., & Hsia, T. (2000). Statistical methods for characterizing similarities and differences between semantic structures. *Proceedings of the National Academy of Sciences*, *97*, 518–23.
15. Spearman, C. (1904). 'General Intelligence', objectively determined and measured. *American Journal of Psychology*, *15*, 201–93.
16. Treiman, D. J. (1977). *Occupational prestige in comparative perspective*. New York: Academic Press.
17. Wegener, B. (1992). Concepts and measurement of prestige. *Annual Review of Sociology*, *18*, 253–80.

People and Trust

Ryozo Yoshino

Abstract This chapter introduces a study of peoples' sense of trust in a paradigm of longitudinal and cross-national comparative survey, called CULMAN (Cultural Manifold Analysis). Firstly, I explain a history of the survey paradigm developed in the Japanese National Character Survey (JNCS) and the related cross-national survey for more than the past six decades. Secondly, fundamental social values of the Japanese and interpersonal trust as identified in the JNCS are summarized. Thirdly, a cross-national analysis of interpersonal trust and institutional trust is presented. Finally, I present some comments for future research.

Keywords Cultural Manifold Analysis (CULMAN) · Science of Data · Sense of trust · Japanese National Character Survey · Asia-Pacific Values Survey

1 Introduction: Longitudinal and Cross-National Surveys of National Character by ISM

This chapter introduces a study on longitudinal and cross-national comparative surveys by the Institute of Statistical Mathematics (ISM) over the past 65 years (see Table 1). The survey research covers many theoretical and methodological issues. Here I focus on peoples' sense of trust. The background and the significance of this study are as follows.

The ISM has been conducting a longitudinal nationwide social survey called the Japanese National Character Survey (JNCS) every 5 years since 1953 (Mizuno et al.

This chapter is a shorter version of Yoshino [32] adapted for this book, with some updated data. See Yoshino [32], Yoshino et al. [36] and their references for detailed data with the following websites. http://www.ism.ac.jp/ism_info_e/kokuminsei_e.html (Surveys) http://www.ism.ac.jp/~yoshino/index_e.html (Cross-national Surveys) http://www.ism.ac.jp/editsec/kenripo/contents_e.html (Survey Research Report).

R. Yoshino (✉)
Graduate School of Culture and Information Science, Doshisha University, Kyoto, Japan
e-mail: yoshino-8@ma.scn-net.ne.jp

T. Imaizumi et al. (eds.), *Advanced Studies in Behaviormetrics and Data Science*,
Behaviormetrics: Quantitative Approaches to Human Behavior 5,
https://doi.org/10.1007/978-981-15-2700-5_28

Table 1 List of Main Surveys on National Character Conducted by ISM

1953–present	*Japanese National Character Survey (every 5 years)* (The most recent survey has been conducted in 2018.)
1971	Japanese Americans in Hawaii
1978	Honolulu residents and mainland Americans
1983	Honolulu residents
1988	Honolulu residents
1987–1993	*Seven-Country Survey*
	UK, FRG (West Germany) and France (1987), USA and Japan (1988), Italy (1992) and The Netherlands (1993)
1991	Japanese Brazilians in Brazil
1998	Americans of Japanese ancestry on the US West Coast (Seattle and Sant Clara)
1999	Honolulu Residents in Hawaii
2002–2005	*East Asia Values Survey (EAVS)*
	Japan, China (Beijing and Shanghai) and Hong Kong (2002), Taiwan and South Korea (2003), and Singapore (2004)
2004–2009	*Pacific Rim Values Survey (PRVS)*
	Japan, China (Beijing and Shanghai) and Hong Kong (2005), Taiwan and South Korea and USA (2006), Singapore and Australia (2007), and India (2008)
2010–2014	*Asia-Pacific Values Survey (APVS)*
	Japan and USA (2010), China (Beijing, Shanghai), Hong Kong and Taiwan (2011), South Korea, Singapore and Australia (2012), and India and Vietnam (2013)

(See http://www.ism.ac.jp/ism_info_e/kokuminsei_e.html for the ISM Surveys)

[16]). By the term "national character," we refer to characteristics reflected in peoples' response patterns in questionnaire surveys (cf. Inkeles [13]). The survey covers various aspects of people's attitudes and opinions in their daily lives. This research was closely related to the establishment of a scientific system of public opinion polling for the development of post-World War II democracy in Japan (Yoshino [32, 33]; Yoshino, Hayashi, & Yamaoka [35]). Stimulated by this survey, the now well-known surveys such as ALLBUS in Germany, the European Values Survey and the Eurobarometer in the EU, and the General Social Survey (GSS) in the USA have been initiated.

Since 1971, the JNCS has been expanded to cross-national surveys for a more advanced understanding of the Japanese national character in the context of comparative study. Our final goal is to develop a statistical study of civilizations that will give us fundamental information for the peaceful development of the world, under the paradigm of "Science of Data" (Yoshino & Hayashi [34]). Here, the Science of Data means a data-based exploratory and wholistic approach by which we overview a survey process starting from a survey design, preliminary survey, data collection based on statistical sampling survey, data analysis, to final report for policymaking. And, if necessary, we repeat the process and extend it to longitudinal survey or cross-national survey. Collecting data, we try to present multifaced survey data in order to facilitate

the understanding of the reality. This is closely related Tukey [24]'s "Exploratory Data Analysis" or Benzecri [2]'s "Correspondence Data Analysis", although these three were independently developed.

Cross-national survey must overcome multi-faceted methodological problems involving, e.g., different languages, different statistical sampling methods, and different peoples' general response tendencies. There is no a priori knowledge regarding how these varying conditions influence peoples' responses even in the cases where there is no substantive difference between the peoples. Thus, an important task for our study is to investigate those conditions under which meaningful cross-national comparability of social survey data is guaranteed. Many findings have been reported in our past publications (Hayashi [7]; Hayashi et al. [9]; Kuroda [15]; Yoshino [27–33]; Yoshino & Hayashi [34]; Yoshino, Hayashi, & Yamaoka [35]).

In our search for conditions that could assure meaningful cross-national comparability of social survey data, we decided at the onset that a comparison of two nations (or groups) with some similarities (e.g., the Japanese in Japan and Hawaii residents with Japanese ancestry) would be more meaningful than attempting to compare two totally different nations (or groups). Some nations (or groups) share certain common features such as race or language. Therefore, they provide meaningful links for comparison. Extending these links may eventually create a chain for global cross-national comparison. By developing the idea of spatial comparison in relation to temporal and thematic comparisons, we eventually have formulated our methodology called Cultural Linkage Analysis (CLA) which incorporates (1) spatial linkages of cross-national comparison; (2) temporal linkages inherent in longitudinal analysis; and (3) item-structure linkages inherent in the commonalities and differences in item response patterns within and across different cultures (e.g., on modernization, religious attitudes, work values, etc.) (see Fig. 1). Furthermore, this has been developed as a paradigm of Cultural Manifold Analysis (CULMAN), which introduces hierarchical structures into the three types of linkages within the CLA framework (Yoshino [28]). For cross-national comparison, a global map consisting of a set of local charts (corresponding to links of CLA) may be constructed. Each local chart covers a particular area or region, and some of these may partially overlap. The whole set of charts covers the globe. The set of charts may compose a sort of hierarchical structure, where each level of charts may correspond to a certain expanse of coverage (e.g., Japan, Asia, Eurasia, or the world), and the larger chart corresponds to the higher level. Furthermore, the larger chart may be associated with the less restricted cross-national scalability. In this approach, the concept of a spatial chart can be extended to both the temporal and item-structure links.[1]

As for the study of trust, although there are various definitions of "trust," they may be roughly classified as "trust in transactions" or "trust in normative philosophy"

[1] This approach may be contrasted to Inglehart's World Values Survey that covers culturally diverse countries worldwide, using a single set of question items. There are some significant differences between his model and CULMAN. For example, (1) Inglehart's cultural map classifies the world by a set of clearly classified cultural zones with definite boundaries, but a cultural manifold may consist of overlapping charts with a hierarchical structure and each chart may expand or shrink or merged with the others over time.

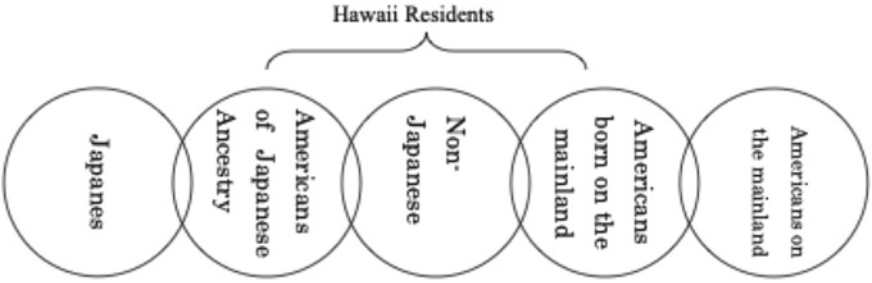

Fig. 1 Cultural Linkage Analysis (CLA). An example of spatial linkage. Extension of comparisons of local pairs will lead to a global comparison. Each neighboring (overlapping) pair of charts corresponds to a certain questionnaire (a set of question items). Longitudinal Survey: Japanese National Character Survey(JNCS) ("Nihon-jin no Kokkumin-sei Chosa")

(Hosmer [12]). These may be closely related to Uslaner [25]'s distinction between "strategic trust" and "moralistic trust." Zucker [41] points out three methods for the production of trust: (1) process-based trust tied to past exchanges; (2) characteristic-based trust tied to personal characteristics, such as family background and ethnicity; and (3) institution-based trust tied to formal societal structures. Shapiro [22] criticizes the third category because he believes that trust cannot be institutionalized. Further, Zucker [41] claims that trust is not directly measurable.

Although the Zucker's three categories of trust are mutually interrelated, my focus in this study is mainly on the second, i.e., trust based on personal characteristics. Besides, I pay much attention to the ways people's trust appears in social survey data under the influences of culture and general social values as well as general response tendencies due to gender or ethnic differences. See Yoshino [33] for more explanation on background of our research.

2 Social Values and Interpersonal Trust

Some researchers say that "trust" is not directly measurable. Fukuyama [5], for example, suggests to use a measure of distrust such as rates of divorce or murderer which are directly measurable. There may be no universal scale on sense of trust beyond differences in cultures and time. Or even if there is such a scale, it may not be linear with respect to various factors (cf., Yoshino [27]; Yoshino & Tsunoda [39]). I believe, however, that people's responses in questionnaire surveys can reveal certain aspects of their sense of trust, if we can adequately analyze the following: (1) the time series patterns or cross-national patterns of responses, (2) possibility of nonlinear correlations between "trust" and other social variables (e.g., class, education, income, subjective health, etc.), and (3) general response tendencies associated with genders, nations, and personality types.

2.1 Fundamental Dimensions of Japanese Social Values

Hayashi [7] and Hayashi and Hayashi [8] show that three dimensions underlie the Japanese national character: (1) "Giri-Ninjyo" interpersonal relationship, (2) contrast between the modern versus tradition in their way of thinking, and (3) religious attitudes (or heart/mind). Here "Giri" represents the obligation to uphold social duties and "Ninjyo" represents the more visceral warm-heartedness.

The Japanese shows a particular attitude distressed in balancing "Giri" and "Ninjyo" on the Giri–Ninjyo continuum in their interpersonal relationships. Overall, basic Japanese interpersonal attitudes have been stable, at least over the last six decades, and probably much longer. Most likely, the basic interpersonal attitudes concerning human bonds, sense of happiness, life satisfaction, optimism, etc. tend to be stable in any country over time (Yoshino & Osaki [38]). On the other hand, certain aspects are sensitive to changes in economic or political conditions and more or less vary in the short term in most countries. In the study of JNCS data of 1953–2008, Sakamoto [21] points out remarkable changes of the response patterns in the periods of 1973–78, 1988–93, and 1998–2003. In all those periods, we have seen sudden changes of economic conditions due to, respectively, the oil shock, the collapse of bubbling economy, and the Asia Financial Crisis.

As for the second dimension, the Japanese had long been facing a sort of emotional and institutional conflicts between the modernization (effectively Westernization or Americanization) and the maintenance of Japanese tradition since the Meiji Restoration of 1868. In those days, the Japanese faced a situation necessarily to master Western science and technology and to adapt it into a Japanese style for national survival (security and prosperity). This situation was called as "Wakon–Yousai" (i.e., Use Western technology with Japanese spirit). This enduring effort had underlined the dimension of the traditional versus modern orientation in the Japanese way of thinking, at least, until the early 1970s or so. The then younger generation born more than 10 years after the end of World War II started to show some significant change. Their response patterns looked conservative on nature, science, and technology, so some people called it "the return to tradition." The conservative attitudes looked a reaction to rapid industrial development and environmental changes in the 1970s or so.

Since signs of generational changes appeared around 1978, the Japanese ways of thinking became more complicated than ever. Since the early 1990s, Japan has been in a period of transition from the established social system to a system of a highly advanced information age. Parallel to the world order change after the end of cold war, this situation brought disruption not only to the fields of science and technology but also to the fields of economics and politics under the name of "globalization." In this period of confusion, the majority of Japanese people came to distrust traditional systems such as banking and bureaucracy as well as the legislature, police, etc. (Yoshino [27]).

As for religion, about one-third of the Japanese have religious faith but most of the Japanese think that religious heart/mind is important (Hayashi & Nikaido [10]; Mizuno et al. [16]). In the world-wise secularization after the WWII up to the end of

cold war, the Japanese is not an exception on this trend, but their religious heart/mind seems not much changed. For more advanced arguments, we may need to face some significant differences of religion between the East and the West (Hayashi & Nikaido [10]).

2.2 *Interpersonal Trust of the Japanese*

The past decades have developed psychological studies of measures of interpersonal trust. Among others, a set of three items from the GSS has been used to measure people's sense of trust (Uslaner [25, 26]; Yoshino & Osaki [38]). Although the GSS started as a sort of American version of the JNCS, we have adopted the three items from the GSS for our survey since 1978. They are stated as follows (for the Japanese questionnaire, see http://www.ism.ac.jp/kokuminsei/index.html[2]).

Q36. Would you say that, most of the time, people try to be helpful, or that they are mostly just looking out for themselves?

1. Try to be helpful, 2. Look out for themselves.

Q37. Do you think that most people would try to take advantage of you if they got the chance, or would they try to be fair?

1. Take advantage, 2. Try to be fair.

Q38. Generally speaking, would you say that most people can be trusted or that you can't be too careful in dealing with people?

1. Can be trusted, 2. Can't be too careful.

The source of these items was obtained by Rosenberg [20] selecting five items among hundreds of items when he constructed a Guttmann scale called "Faith-in-People Scale" with a regeneration rate of 92% in a student survey. The items were on trustworthiness, honesty, goodness, genericity, and brotherliness. These items were used for research by Almond and Verba [1] and others, and then the ISR survey (the Survey Research Center, the University of Michigan) and the GSS (NORC, the University of Chicago). In the process, those items have been gradually modified and the abovementioned three items with binary response scales are survived (Uslaner [26]).

Each of the three items is supposed to capture somewhat different aspects of trust. That is, Q36 is related to trust in neighbors (or the norm of reciprocity), Q38 is related to general interpersonal trust, and Q37 is concerned with something in between the other two items. Our data repeatedly demonstrate that Q37 and Q38 are more correlated for the Japanese, whereas Q36 and Q37 are more correlated for

[2]Throughout this paper, codes such as Q36 correspond to the common item code of the APVS questionnaire. For the exact wording of items and the precise data, see http://www.ism.ac.jp/editsec/kenripo/contents_e.html or http://www.ism.ac.jp/ism_info_e/kokuminsei_e.html. As for Q38, there are slight differences in wording between our cross-national Japan survey and the Japanese National Character Survey. In the process of translation and back-translation check to make a Japanese version of the cross-national survey questionnaire, we ended up with these two versions. This difference may produce some percentage differences in the response distributions, but the overall pattern is stable.

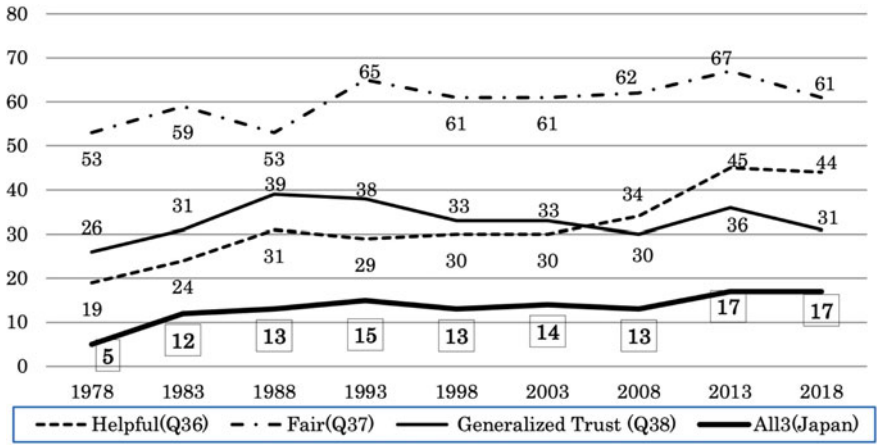

Fig. 2 Percentages of positive responses of GSS trust items (Q36, Q37, and Q38) and percentage of positive response to all the three items in Japan. The data are from the Japanese National Character Survey, except the 1988 data from the Seven-Country Survey. *Note* Some papers, such as Yoshino [30, Fig. 1] and Yoshino [31, Fig. 7.3], included an error in the 1978 data, but it has been corrected here

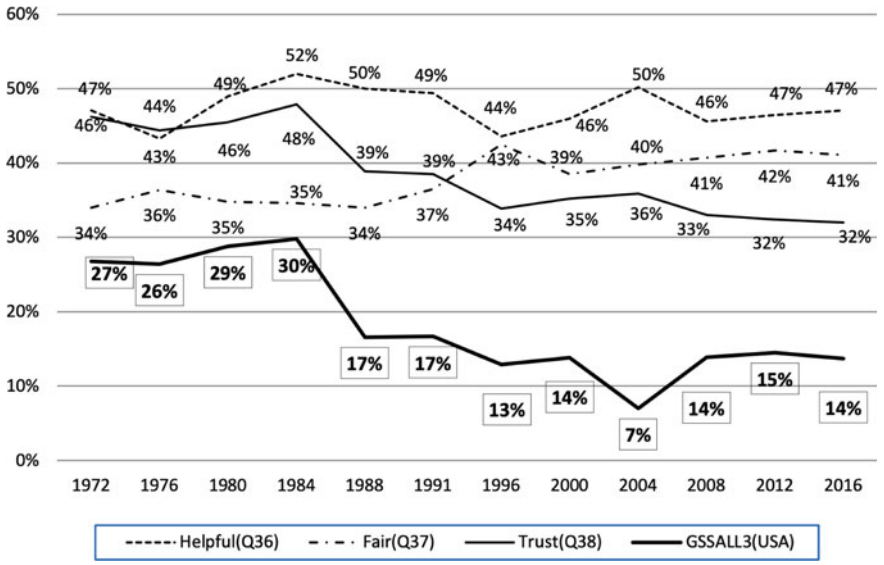

Fig. 3 Percentages of positive responses of GSS trust items (Q36, Q37, and Q38) and percentage of positive response to all the three items in USA. The data are from the SPSS format of GSS (downloaded from the website on May 23, 2019)

Americans. Some countries such as India may consistently show unique patterns of correlations, whereas other countries such as South Korea may show less-stable patterns over years. Yoshino [32] gives more details of cross-national differences on the three pairs of correlations between the three items.

The response distribution for the Japanese over the past decades (1978–2018) is shown in Fig. 2. As a measure on a sort of "total interpersonal trust," I often use the percentage of those who choose positive categories to all of Q36, Q37, and Q38. (Because Q36 was missing in some of our past surveys, I sometimes use also the percentage of those who gave positive answers to both Q36 and Q38. The rankings on the two items and on the three items are mostly consistent over the countries/areas where the three items were used (See Fig. 4).

On the measure of "total interpersonal trust," both the Japanese and Americans (Fig. 3) have been fairly stable but the Japanese may be more stable than Americans, at least during 1983–2008. We need to pay attention to the changes in 1978 and in 2013. The Japanese experienced a nationwide panic trying to hoard necessities for their daily lives after the oil crisis and the Nixon shock (i.e., the unilateral cancellation of the direct international convertibility of the US dollar to gold) around 1973. Necessarily, this would have downgraded mutual trust. On the other hand, in the disaster of the Great East Japan Earthquake of 2011, people run to the devastated area from all over Japan to help the suffered people. Still under the lasting economic depression, many people considered how they could contribute to recovery of the area. Comparing to those suffered in the great disaster of earthquake and the succeeding nuclear plant accidents, all the Japanese must have felt that they must be satisfied with their lives and have to appreciate mutual assistances. Naturally, this would have raised mutual trust.[3] If Q36, Q37, and Q38 are separately studied, the Japanese data also show more changes over the years. The changes may confirm that the economic and political structural reformation damaged the Japanese sense of trust, roughly, during 1993–2008. Since the postwar time of WWII, the life-long employment system of Japan provided for better job security—workers' salaries may become lower, but they can't be so easily fired. This may explain the higher levels of trust (i.e., the relative stability of response patterns on Q36, Q37, and Q38) found in the Japanese samples than among the American ones, at least during 1983–2008.

But, in the early 1990s, the reformation under "globalization" started to force the Japanese to change economic, political, and social systems, looking for efficiency or internationalization disregarding of the Japanese structures rooted in historical background or culture. The change of the social systems attacked even interpersonal systems of family, school, and workplace, disturbing people's heart and mind. The "lost two decades" since the collapse of bubbling economy around 1991, after all,

[3]For the study of longitudinal survey data, as well as cross-national surveys, we need to be careful of changes of valid questionnaire returns over decades. Generally, respondents who participated in a survey might be biased to be more trustful than refusers. Thus, we tend to get more trustful respondents in surveys of the lower response rates. For the change of response rates of the JNCS over six decades, see: https://www.ism.ac.jp/kokuminsei/en/page9/page13/index.html. Also see Yoshino [33] for possible misunderstanding of longitudinal data on Japanese high school students' happiness.

resulted in confusions and failures not only in the Japanese systems but also in foreign banks and commercial companies which attempted to take advantage of the opportunities in Japan. Meanwhile, the government has lost people's trust in the national pension system. Senior people rely on younger people for future financial support, but the population of younger generations has been decreasing, and the younger are less motivated to pay pension costs, in consideration of the balance. These situations, originally due to distrust on governmental institution, have necessarily led to a gap of consciousness on social institutions between the young and the senior people.

Incidentally, the new graduates during, roughly, 1993–2004 are called "Syusyoku Hyoga-ki Sedai" (Ice Age Generation of Job Market) or "lost generation" because they faced remarkable difficulties to get regular job positions under the rapid recession. They are now in their 30s or 40s, but still face difficulties of getting positions of regular employees, in spite of recent economic recovery. Because Japanese job market is mainly for new graduates, those of Ice Age Generation meet much more disadvantages than younger graduates. At last, the government started amending the situation, demanding the Japanese business world to employ them as regular employees.

Looking back over the last 30 years, during the prosperity of the 1980s, there was a shift of young men's social values toward individualism and then personal preference (give priority on personal matters). But the structural reforms of the 1990s led to the economic recession and the departure from lifetime employment. As a reaction, human relationships in the workplace seem reconsidered (regression to tradition), among others, in young people.

Yoshino [27] discussed several aspects of trust, such as trust in politics, science, and technology, as well as the work ethic of the Japanese. He concluded that some aspects of trust may be variable according to economic and political conditions, whereas some others may be more stable. Although the world used to have a stereotype of the Japanese workers called the "economic animal" in the 1980s, their attitudes and ethic toward work seem to be influenced by economic and political conditions.

3 Cross-National Surveys on Trust

3.1 Sense of Interpersonal Trust

Our cross-national surveys also included the three items on interpersonal trust from the GSS. Table 2 is the data from the Asia-Pacific Values Survey (APVS) (2010–2014). Yoshino [32] and Yoshino, Shibai, and Nikaido [36] show the response distributions for most of the countries/areas that we have surveyed over the past four decades. See Figs. 2 and 3 also.

Miyake ([9], Chap. 7) presented an analysis on our Seven-Country Survey. He concluded that the trust scale had correlations with gender and religion and stronger

Table 2 Percentages of positive responses to three GSS items on trust in the Asia-Pacific Values Survey (APVS)

Year	2011	2011	2011	2011	2012	2012	2013	2012	2010	2010
	Beijing	Shanghai	Hong Kong	Taiwan	South Korea	Singapore	India	Australia	USA	Japan
Q36	72	66	43	46	52	50	55	59	51	41
Q37	57	58	40	53	53	49	34	63	53	57
Q38	42	36	21	21	32	34	45	45	31	44

Q36 "People are always trying to be helpful to others."
Q37 "People are trying to be fair."
Q38 "People can be trusted"

correlations with family income, educational level, and social class. On this scale, West Germany, the UK, and the USA scored higher than Japan and the Netherlands, but the difference was small. The French and Italians clearly scored lower than in other countries. In addition, those who had religious faith gave more positive response rate ("try to be helpful") to item Q36, irrespective of their religious affiliation. For Q37, women gave more optimistic answers ("they would try to be fair") than men. As for item Q38, there was a clear difference between social classes in all seven countries. That is, the higher the social class, the more trustful the respondents were. The difference between classes was remarkably large in France and the USA. Observing that the higher level of education was associated with the greater trust, Miyake suspected that the association was caused by the correlation between education and social class. (Although there was a relatively strong correlation between education and social class, and between education and income in the USA, this was not necessarily the case for other countries.) Using the same data, Yoshino [27] showed positive correlations between trust and social class or income in the USA and the UK but nonlinear correlations in the other five countries, including Japan and West Germany (i.e., the middle social class shows the higher trust rate than the lower or the higher). Incidentally, Yoshino and Tsunoda [39] suggested nonlinear relationship between subjective health and sense of trust.

Figure 4 shows the ranking of the percentages in each country of those who gave positive answers to both Q36 and Q38. The measure seems fairly stable within the countries/ areas when repeatedly surveyed over years. Interestingly, the Japanese immigrants in the USA and Brazil are ranked, respectively, as the highest and the lowest. That is, JAWCS (Japanese Americans on the West Coast) is higher than the general Americans, whereas JB (Japanese Brazilian) is lower than the Latin countries (France and Italy). The percentages of positive response in the USA and the UK were high, whereas those in Italy and France were low. This may be consistent with Fukuyama's [5] theory contrasting Japan, the USA, and Germany as highly trustful countries with China and Italy as less trustful countries. His arguments are based on the assumption that the former countries have well-developed intermediate civic organizations between the government and families, whereas the latter have established atmosphere of strict political centralization in the past long histories.

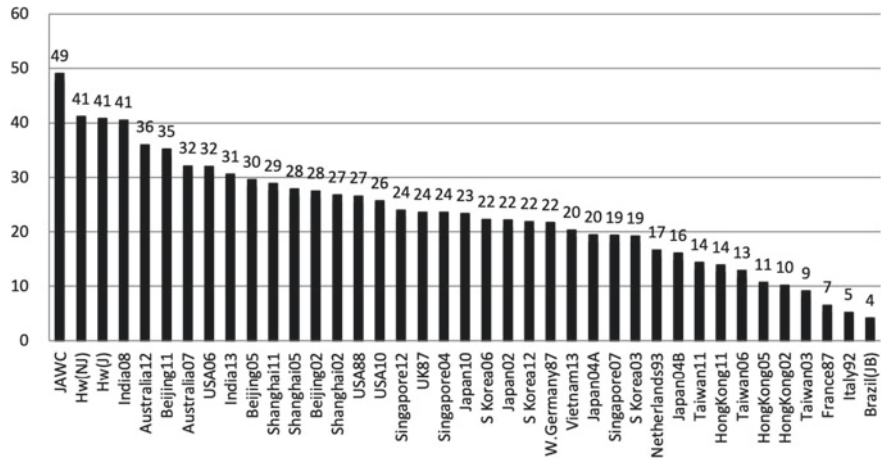

Fig. 4 The percentages of positive responses to both Q36 and Q38 (GSS) Abbreviation: JAWCS: Japanese Americans on the West Coast (USA), HW(J) or (NJ): Hawaii Residents (Japanese) or (Non-Japanese), Brazil (JB): Japanese Brazilian in Brazil. Numbers (e.g., 88 or 03) show the survey years (e.g., 1988 or 2003). *Note* Fig. 2 of Yoshino [30] included an error of Australia 2012, but corrected in the figure above

A close look at this figure, however, shows a more complicated reality because the percentages of positive responses of Mainland China (Beijing and Shanghai) were higher than might have been expected by the Fukuyama's argument. There may be several possible explanations for this. First, the data really do indicate that the Chinese have a higher sense of interpersonal trust. (Probably they may be focusing on in-group relationships when responding to those items). Second, the Chinese respondents might have tried to show a higher sense of interpersonal trust because they were sensitive to their international reputation, such as Fukuyama's contention. Third, the questionnaire items were constructed as a trust scale for Americans, so they may not be suitable for the measurement of trust in other nations. Fourth, we need to be careful about the political and sociological implications of the trust scale. For example, Dogan ([3, p. 258]) states, "Erosion of confidence is first of all a sign of political maturity. It is not so much that democracy has deteriorated, but rather the critical spirit of most citizens has improved." This suggests that we need to distinguish between the face value of a scale and its implications. In this context, trust and distrust may not be opposite on a unidimensional scale but instead may be closely related in a sort of multidimensional mind structure. Furthermore, people may give the same response for different reasons or different responses for the same reason. Therefore, for a more meaningful comparison of countries, it is necessary to consider peoples' responses with objective measures on, e.g., economics and politics, as well as general response tendencies of those peoples. As such, I may in this study give some interpretations of response patterns on certain items, but they should necessarily be considered tentative.

Lastly, I note on general response tendencies (Yoshino, Hayashi, & Yamaoka [35]). Yoshino and Osaki [38] reviewed our past surveys on trust and subjective well-beingness, and concluded that the long-term tendency is relatively stable over time regardless of objective economic or political conditions (cf. Hofstead, Hofstead, & Minkov [11]) although a serious incident or disaster perturbs the stability.

As for general response tendency of each nation, for example, the Japanese tend to avoid polar answers and prefer intermediate response categories (or "Don't Know"), the French tend to choose critical categories, and the Indians tend to choose optimistic categories. Furthermore, as to gender differences, women show stronger self-disclosure than men (Yoshino [30, Sect. 2]; Yoshino et al. [35, pp. 109–111]). This may lead a superficial contradiction, e.g., the women show higher sense of satisfaction when asked about their satisfaction, whereas they show higher sense of dissatisfaction when asked about their dissatisfaction.

3.2 Trust of Social Institutions and Systems

The questionnaires of the APVS included the same items on institutional trust used in the World Values Survey, with an additional item on trust in science and technology. The items are stated as in Table 3.

Table 4 shows the response distribution of the APVS. (Yoshino et al. [36] show all data from most of countries that we surveyed, which would be helpful to read the following explanation with them.) To reduce the effects of general response tendencies particular to individuals or countries, Yoshino [29] transformed the response data from the East Asia Values Survey (EAVS) (2002–2005) into standardized scores

Table 3 Q.52. How much confidence do you have in the following? Are you very confident, somewhat confident, not confident, or not confident at all?

	Very confident	Somewhat confident	Not confident	Not confident at all
a. Religious organizations	1	2	3	4
b. The law and the legal system	1	2	3	4
c. The press and television	1	2	3	4
d. The police	1	2	3	4
e. Federal bureaucracy	1	2	3	4
f. Congress	1	2	3	4
g. NPO/NGO (nonprofit and nongovernmental organization)	1	2	3	4
h. Social welfare facilities	1	2	3	4
i. The United Nations	1	2	3	4
j. Science and technology	1	2	3	4

Table 4 Institutional Trust of WVS Items

	Item	2011	2011	2011	2011	2010	2012	2012	2012	2013	2010	2013
		Beijing	Shanghai	Hong Kong	Taiwan	USA	South Korea	Singapore	Australia	India	Japan	Vietnam
Q 52a	Religious organization	27	36	58	75	58	41	82	44	87	13	79
Q 52b	The law and the legal system	85	82	86	53	56	51	83	78	78	72	94
Q 52c	The press and television	68	64	56	44	21	63	78	33	70	70	80
Q 52d	The police	75	72	69	59	65	46	92	89	59	70	85
Q 52e	Federal bureaucracy	83	77	50	46	26	34	89	47	49	38	93
Q 52f	Congress	83	75	53	38	22	17	88	46	55	25	95
Q 52g	NPO/NGO	41	45	64	56	51	42	80	74	61	49	86
Q 52h	Social welfare facilities	78	70	81	69	48	59	83	79	75	71	88
Q 52i	The United Nations	59	54	70	61	40	68	82	63	60	59	90
Q 52j	Science and technology	95	89	85	86	76	75	91	92	90	83	95

The figures show percentages of sum of positive categories “1. very much confident” and “2. confident somewhat.” APVS

country by country. Here "general response tendencies" mean, e.g., the Japanese tend to avoid polar responses than the Americans (a sort of variances of the range of responses). But let us use an easier way that Yoshino [30] used for the Pacific Rim Values Survey (PRVS) (2004–2009). First, the original response categories are re-categorized to sum up the percentage of responses to positive categories ("1" and "2"). Second, the percentages of positive responses are compared item by item within each country. This yields a rank order of items in each country. Third, the rank orders of all countries involved are compared. This procedure results in the loss of some information from the original data, but it may provide more stable cross-national comparability (unless the rank orders are unstable). Yoshino [32, Table 3a, 3b, and 3c] confirms the generally consistent patterns in the countries or areas participating in all three surveys of APVS, PRVS, and the East Asia Values Survey (EAVS). For example, the item-by-item differences of percentages between the Japan surveys in 2002 (EAVS), 2004 (PRVS), and 2010 (APVS) were almost within the margin of the sampling error. The maximum difference was about 10%, for example, on NPO/NGO (Nonprofit Organization/Nongovernmental Organization). (The percentage on NPO/NGO changed from 55% in 2002 to 45% in 2004 and then up to 49% in 2010. NPO/NGO activities had been increasing and some disguised NPO/NGOs had managed illegal businesses in the early 2000s. This was one of the reasons that the Japanese laws on registered organizations were substantially revised in 2008.)

In Table 4, except for India, Singapore, Vietnam, the USA, and Hong Kong, in all the studied countries or areas, there was a low degree of confidence in religious organizations. Even in these five countries or area, the relative degrees of confidence were not very high compared with all the other items for each country, except for India. Japan and Mainland China indicated remarkably negative attitudes toward religious organizations. The percentage of positive responses among the Japanese was lower than among the Chinese. However, of the 10 items on Q50, the percentage of positive responses was the lowest for religious organization among Chinese. Most of the Japanese respect religions or the "religious heart/mind" even when they do not have religious faith (Hayashi & Nikaido [10]). However, they may keep cautious about "religious organizations" because some religious groups, such as the "Aum Shinrikyo" (a religious cult), caused disasters in the 1990s. In China, the government is very sensitive toward religious groups because, in the long history of China, religious groups frequently overthrew governments. In some countries, some religious groups are closely linked to terrorism.

The percentages of responses that show confidence in authority such as the "police," "government," and "Congress" may represent various patterns of attitudes; these are likely concerned with democracy. Because free criticism is allowed in democracy, a negative attitude does not necessarily mean the negation of such authority, and it may reflect a mature democracy in some countries (Dogan [3, p. 258]). Thus, the percentage of positive (or negative) responses may not be linearly proportional to the degree of political maturity. Table 4 shows, for example, the USA's lower degrees of confidence in the press and TV and in Congress. This may be a critical attitude of matured democracy, or it may be a reflection of current confusions of democracy, or both.

As for science and technology, all the countries or areas showed a high degree of confidence. Hayashi [7] and Zheng and Yoshino [40] presented cross-national analyses of data on science and technology from our seven-country survey. Hayashi [7] concluded that the Japanese generally have positive attitudes toward science. They were, however, negative regarding scientific approaches toward the understanding of the human heart and mind ("kokoro" in Japanese), solving social and economic problems, and the possibility of living in space stations in the near future (at the time of the survey in 1988). The response pattern of West Germans in 1987 was similar to that of Japanese in the sense that they were also more negative about science and technology than those in other Western countries. However, they were not so negative toward the applications of science and technology to social problems as well as psychological problems of individuals as the Japanese were. This might be related to that the theories of Hegel and Marx and the psychological theories of Freud originated in the German culture area.

As for data from the APVS, all of the countries or areas were highly positive toward science and technology, with rates of positivity for that item being the highest among all items. In particular, the rates for Mainland China were remarkably close to 100% in both the PRVS and the EAVS, although the rates were slightly down in the APVS. There may be several possible explanations for this. On the one hand, the high rates may represent the fact that, since the late 1970s, China has been emphasizing the scientific reformation of government agencies, military systems, and social systems as a priority in their social planning. On the other hand, until recently, they had placed priority on economic development and they had not paid much attention to the negative impact of science and technology that advanced industrial countries have experienced in the past. After the Beijing Olympics in 2008 or even slightly earlier, the Chinese government started paying attention to the negative side of rapid economic and industrial development and began planning to improve environmental conditions, including serious air, soil, and water pollution. Incidentally, they started also paying attention to political issues, such as the social inequality between urban and rural areas. They are struggling to deal with these domestic problems, but complete solutions seem still far away to many observers' eyes (Reuters [18, 19]), despite their rising power in international politics. Furthermore, under the recent slowdown of economic development, environmental improvement may not be on the government top priority. And serious pollutions in the urban areas sometimes go over to the neighboring areas and countries. More recently, however, certain steady environment improvements in some rural areas are reported [Y. Chen, personal communication, August 17, 2019].

As a final comment in this section, it should be noted that Sasaki and Suzuki [23, Chap. 11] concluded that "a single scale is not adequate to measure people's sense of trust in science and technology because people's attitudes differ from one issue to another within the fields of science and technology." This is also the case with our study on people's sense of trust. Note that we have Japanese Nobel Prize Laureates in the 1990s–2010s more than the past. The JNCS (Nakamura, Yoshino, Maeda, Inagaki & Shibai [17, p. 15]), however, shows a clear decrease of self-confidence in science and technology during "the lost decade (1993–2003 or so)." Thus, some

aspects of confidence are more variable due to economic or political conditions, whereas generalized interpersonal trust is more stable.

Incidentally, Yoshino [32] gives a summary on regional and generational differences among Japanese immigrants in Hawaii, Brazil, and the U.S. West Coast. It touches also ethnic differences (Chinese, Malays, and Indians) in Singapore, and between indigenous Taiwanese and Chinese mainlanders in Taiwan. Domestic ethnic differences on trust are often linked with domestic and international political issues. Mutual trust is a key for peace.

4 For Future Research—Universal Values of Human Bonds

This chapter has shown a longitudinal and cross-national study of peoples' sense of trust. As mentioned, however, we need to be cautious in interpreting the results because survey data on trust are often a compound of many variables, including general response tendencies and respondent biases on participation of survey.[4] Issues on cross-national comparability might never be completely solved because of significant differences of infrastructures on survey conditions unique to each country. But I believe that elucidations of those differences themselves reveal each country's situation on economy, politics, and social conditions, beyond superficial comparison of survey data. I present several comments for our future research as follows.

First, for mutual understanding between East and West, we need to pay much attention to methodological issues in measuring social values. Scaling of trust may caution us on the applicability of a certain "single" scale invented in Western cultures for Eastern cultures, or vice versa. Gallup ([6], p. 461) reported that, in their global survey, they could not find a very poor but still happy people. Later studies, however, have found examples not consistent with the pattern of Gallup report. For example, Brazilians were very optimistic even when Brazil was the worst debtor nation in the 1980s (Inkeles [13]). Inglehart reported a positive correlation between economic development and life satisfaction for some 20 countries in the 1980s (Inkeles [13, pp. 366–371]). However, life satisfaction of Japan in the 1980s was lower than it was in 2003 or in 2018, although Japan was prosperous in the 1980s but struggled with a recession in the 2000s–2010s. Thus, we need to be careful regarding peoples' general response tendencies in the measurement of social values.

Second, people's negative responses may not necessarily mean a lack of a sense of trust. As Dogan [3, p. 258] suggested, some people express distrust or complaint toward the government or political leaders, not because they lack trust, but because they know that it is a way to improve their own country and eventually our world in a democratic way.

Third, I give a comment on the CULMAN framework. The last century was the time of the expansion of Western civilization, and this century is said to be the time of Asian revival. Differences between cultures or civilizations occasionally

[4] See Footnote 3.

prevent us from deeply understanding each other. In this time of globalization, world leaders should be knowledgeable about world geography and history, and sensitive to peoples' social values if they wish to take seriously their responsibility to develop and maintain world peace. In studying world history, we should remember that there are various ways of successful social development.

Some institutional systems or customs are changing, converging toward more universal ones under the influence of transnational exchange or trade. Other systems are, however, becoming more sensitive to cultural differences as a reaction to globalization. The last three decades has shown that, at least for the foreseeable future, globalization will not lead us to a single unified global culture. This is consistent with a theory of Cultural Evolution that more variations enhance chance of survival. (cf. Inglehart [14, p. 42] presents a theory of cultural evolution that the value systems of different cultures may not be converging but changing in the same direction on "self-expressive values.") I think CULMAN can be utilized to develop a framework of policymaking for the gradual development of, so to speak, a global cultural man-

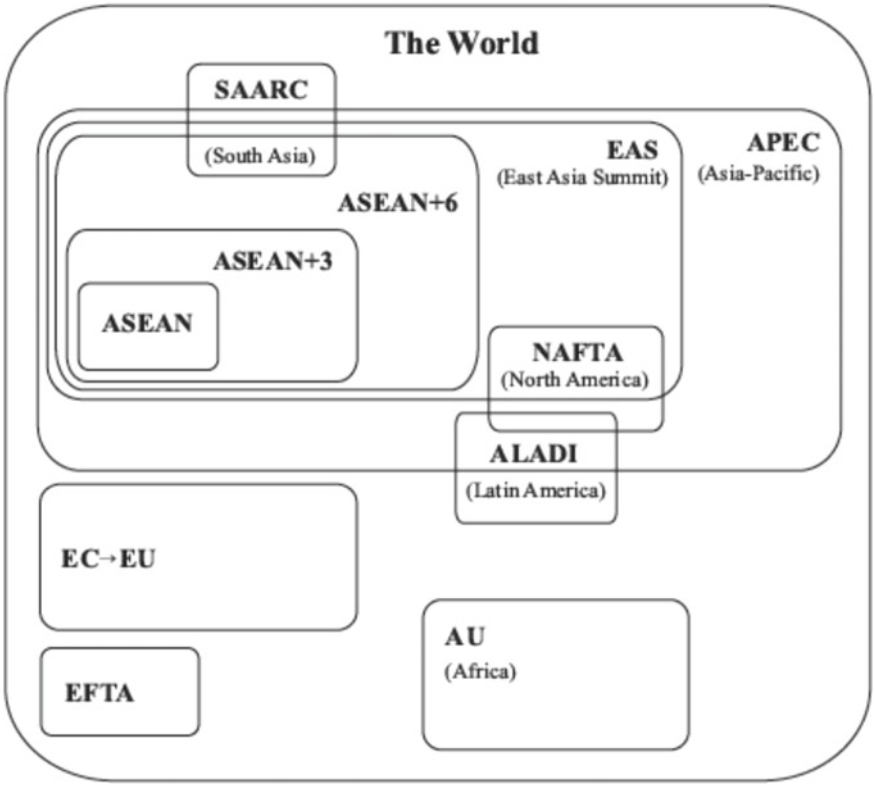

Fig. 5 A manifold of communities in the World. In order to have a steady, peaceful, and prosperous development, we may need a set of "soft" regulations to connect pairs of communities rather than a single restrictive global standard

ifold (GCM) (Fujita & Yoshino [4]; Yoshino [32, 33]; Yoshino et al. [36]; Yoshino, Shibai Nikaido, & Fujita [37]) (see Fig. 5).

The GCM is a set of hierarchical overlapping local charts, and each chart covers a certain area (region, country, national groups, civilization, etc.). In each chart, we may assume that people share a certain culture or social values; the larger chart corresponds to the less restrictive but more universal culture or social values. Together, the charts may comprise a sort of hierarchy. According to the size of the chart (area, region, or social group), people may be able to assess the degree to which decision-making or the extent of regulations concerning various types of exchanges (e.g., international trade within the members of the region) ought to be rigidly enforced. GCM charts are dynamic, so each chart may be enlarged, be shrunk, be split into two, or disappear over time. Some overlapping charts may be assimilated to make a larger chart. And a new chart may appear. For peaceful and steady integration and expansion of charts, a set of soft local rules to connect neighboring charts would be more effective, rather than a single strict global regulation. The set of local rules may make a hierarchical structure with respect to its coverage and strictness.

The history of the EU may exemplify the concept of GCM. Currently, the East Asia and the Asia-Pacific area may be presenting other examples. More than two decades ago, many people doubted such a unification in the East Asia as in the EU because the East Asia is too complicated on races, languages, religions, and political systems even in a country. Now, one could see a slow but a steady unification such as ASEAN, contrasted with the current confusion in the EU. There must be various ways to achieve successful developments. On March 11, 2011, the Great East Japan earthquake caused a huge tsunami and resulted in the Fukushima nuclear power plant disaster. The world media, however, reported the calm attitudes of the Japanese even in the tragedy. The devastated yet surviving Japanese kept an orderly line in front of grocery stores waiting to buy food. Many Japanese had a chance to reconsider the value of their own lives and works and to think of various ways of contributing to the people and area damaged by the quake. Many news, stories, and surveys reported on the human bond and the importance of family, relatives, and friends, not only on a domestic but also a worldwide scale. We have confirmed that the differences in ideology or religions are minor compared to the universal importance of human bonds and trust between peoples.

It is my sincere hope that mutual understanding among the various cultures and civilizations will prevent serious conflicts between nations and cultures and will lead us to a peaceful and prosperous world in the twenty-first century.

References

1. Almond, G. A., & Verba, S. (1963). *Civic culture*. Boston: Little Brown.
2. Benzecri, J.-P. (1992). *Correspondence analysis handbook*. NY: Marcel Dekker Inc.
3. Dogan, M. (2000). Deficit of confidence within European democracies. In M. Haller (Ed.), *The making of the European Union* (pp. 243–261). Paris: Springer.

4. Fujita, T., & Yoshino, R. (2009). Social values on international relationships in the Asia-Pacific region. *Behaviormetrika*, *36*(2), 149–166.
5. Fukuyama, F. (1995). Trust. NY: Free Press.
6. Gallup, G. H. (1977). Human needs and satisfactions: a global survey. *Public opinion quarterly*, winter, 459–467.
7. Hayashi, C. (1993). Nihon-jin no kokuminnsei [Japanese national character]. *Phase'93*, 64–96.
8. Hayashi, C., & Hayashi, F. (1995). Kokumin-sei no kokusai-hikaku [Cross-national comparison of national character]. In *Proceedings of Institute of Statistical Mathematics*, *43*(1), 27–80.
9. Hayashi, C., Yoshino, R., Suzuki, T., Hayashi, F., Kamano, S., Miyake, I., et al. (1998). *Kokuminsei nanaka-koku hikaku [cross-national comparison of seven nations]*. Tokyo: Idemitsu-syoten.
10. Hayashi, F., & Nikaido, K. (2009). Religious faith and religious feelings in Japan: Analyses of cross-cultural and longitudinal surveys. *Behaviormetrika*, *36*(2), 167–180.
11. Hofstead, G., Hofstead, G. J., & Minkov, M. (2010). *Culture and organizations-software of the mind* (3rd ed.). NY: McGraw-Hill.
12. Hosmer, L. T. (1995). Trust: The connecting link between organizational theory and philosophical theory. *Academy of Management Review*, *20*(2), 379–403.
13. Inkeles, A. (1997). *National character*. New Brunswick: Transaction Publishers.
14. Inglehart, R. D. (2018). *Cultural evolution: People's motivations are changing, and reshaping the world*. London: Cambridge University Press.
15. Kuroda, Y. (2002). The rainbow model of American ethnic groups. *Behaviormetrika*, *30*(1), 39–62.
16. Mizuno, K., Suzuki, T., Sakamoto, Y. Murakami, M., Nakamura, T., Yoshino, R., et al. (1992). *Dai 5 Nihon-jin no Kokuminsei [the fifth volume Japanese National Character Survey]*. Tokyo: Idemitsu-syoten.
17. Nakamura, T., Yoshino, R., Maeda, T., Inagaki, Y., & Shibai, K. (Eds.). (2017). A study of the Japanese national character–The thirteenth nationwide survey (2013)–English Edition. *ISM Survey Research Report*, No. 119. Tokyo: The Institute of Statistical Mathematics.
18. Reuters. (2013). China struggling to meet 2011-2015 environment goals (December 25, 2013). Retrieved March 14, 2015, from http://www.reuters.com/article/2013/12/25/china-environment-idUSL3N0K40YK20131225.
19. Reuters. (2015). China orders two local governments to punish polluting steel mills. (March 2, 2015). Retrieved March 14, 2015, from http://www.reuters.com/article/2015/03/02/us-china-steel-environment-idUSKBN0LY0C120150302.
20. Rosenberg, M. (1956). Misanthropy and political ideology. *American Sociological Review*, *21*(6), 690–695.
21. Sakamoto, Y. (2010). Memories of a statistical study on the Japanese national character: Looking back on 36 years of being a researcher at the Institute of Statistical Mathematics [in Japanese]. *Proceedings of the Institute of Statistical Mathematics*, *58*(1), 61–82.
22. Shapiro, S. (1987). The social control of interpersonal trust. *American Journal of Sociology*, *93*, 623–658.
23. Sasaki, M., & Suzuki, T. (2000). *Social attitudes in Japan*. Boston: Brill.
24. Tukey, J. W. (1977). *Exploratory data analysis*. Massachusetts: Addison Wesley Publishing Company (Re-published by Pearson, 2019).
25. Uslaner, E. M. (2011). Measuring generalized trust: in defense of the 'standard' question. In F. Lyon, G. Moellering, & M. N. K. Saunders (Eds.), *Handbook of methods on trust*, Chapter 7.
26. Uslaner, E. M. (2018). *The Oxford handbook of social and political trust*. Chapter 2. Oxford University Press.
27. Yoshino, R. (2002). A time to trust-a study on peoples' sense of trust from a viewpoint of cross-national and longitudinal study on national character. *Behaviormetrika*, *29*(2), 231–260.
28. Yoshino, R. (2013). On the trust of nations: The world as a hierarchical cultural manifold. In N. I. Dryakhlov, et al. (Eds.), *Japan-Russia conference on trust in society, business and organization* (pp. 213–250). Moscow: National Research University.

29. Yoshino, R. (2005). A time to trust in the East Asia—A Behaviormetric study on the sense of trust in the East Asia Values Survey [in Japanese]. *Japanese Journal of Behaviormetrics, 32*(2), 147–160.
30. Yoshino, R. (2009). Reconstruction of trust on a cultural manifold: Sense of trust in longitudinal and cross-national surveys of national character. *Behaviormetrika, 36*(2), 115–147.
31. Yoshino, R. (2014). Trust of nations on cultural manifold analysis (CULMAN): sense of trust in our longitudinal and cross-national surveys of national character. In M. Sasaki (Ed.), *Cross-national studies on sense of trust*, Ch. 7. Tokyo: Chuo-University Press.
32. Yoshino, R. (2015a). Trust of nations: Looking for more universal values for intrapersonal and international relationships. *Behaviormetrika*, *42*(2), 131–166.
33. Yoshino, R. (2015b). Cultural manifold analysis CULMAN as a paradigm of cross-national comparative surveys on national character [in Japanese]. *Proceedings of the Institute of Statistical Mathematics*, *63*(2), 203–228.
34. Yoshino, R., & Hayashi, C. (2002). An overview of cultural link analysis of national character. *Behaviormetrika*, *29*(2), 125–142.
35. Yoshino, R., Hayashi, F., & Yamaoka, K. (2010). *Kokusai- hikaku deta no kaiseki [Analysis of cross-national comparative survey data]*. Tokyo: Asakura-syoten.
36. Yoshino, R., Shibai, K., & Nikaido, K. (Eds.). (2015). The Asia-Pacific Values Survey—Cultural Manifold Analysis (CULMAN) on People's Sense of Trust: Summary Report. *ISM Survey Research Report*, No. 117.
37. Yoshino, R., Shibai, K., Nikaido, K., & Fujita, T. (2015). The Asia-Pacific values survey 2010–2014-cultural manifold analysis (CULMAN) of national character. *Behaviormetrika*, *42*(2), 99–130.
38. Yoshino, R., & Osaki, H. (2013). Subjective social class, sense of satisfaction, and sense of trust-a note on psychological scales of social surveys [in Japanese]. *Japanese Journal of Behaviormetrics*, *40*(2), 97–114.
39. Yoshino, R., & Tsunoda, H. (2010). A note on social capital—from a viewpoint of cross-national comparative methodology [in Japanese]. *Japanese Journal of Behaviormetrics*, *37*(1), 3–17. Retrieved January 11, 2016, from https://www.jstage.jst.go.jp/article/bhmk/42/2/42_99/_article.
40. Zheng, Y., & Yoshino, R. (2003). Diversity patterns of attitudes toward nature and environment in Japan, USA, and European nations. *Behaviormetrika*, *30*(1), 21–37.
41. Zucker, L. G. (1986). Production of trust: institutional sources of economic structure. 1840–1920. *Research in Organizational Behavior*, *8*, 53–111.